frontiers | Research Topics

Microbiota in skin inflammatory diseases

Edited by
Hariom Yadav, Eun Jeong Park and Tej Pratap Singh

Published in
Frontiers in Immunology
Frontiers in Cellular and Infection Microbiology

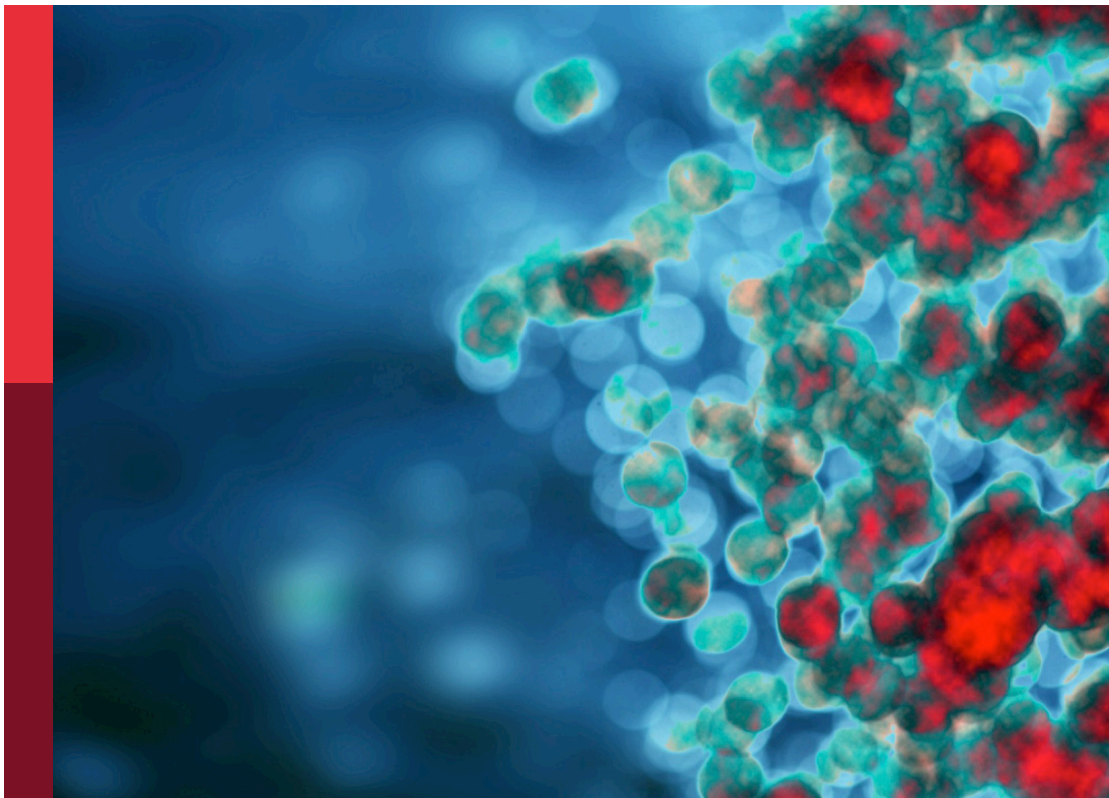

ISSN 1664-8714
ISBN 978-2-8325-2858-7
DOI 10.3389/978-2-8325-2858-7

About Frontiers

Frontiers is more than just an open access publisher of scholarly articles: it is a pioneering approach to the world of academia, radically improving the way scholarly research is managed. The grand vision of Frontiers is a world where all people have an equal opportunity to seek, share and generate knowledge. Frontiers provides immediate and permanent online open access to all its publications, but this alone is not enough to realize our grand goals.

Frontiers journal series

The Frontiers journal series is a multi-tier and interdisciplinary set of open-access, online journals, promising a paradigm shift from the current review, selection and dissemination processes in academic publishing. All Frontiers journals are driven by researchers for researchers; therefore, they constitute a service to the scholarly community. At the same time, the *Frontiers journal series* operates on a revolutionary invention, the tiered publishing system, initially addressing specific communities of scholars, and gradually climbing up to broader public understanding, thus serving the interests of the lay society, too.

Dedication to quality

Each Frontiers article is a landmark of the highest quality, thanks to genuinely collaborative interactions between authors and review editors, who include some of the world's best academicians. Research must be certified by peers before entering a stream of knowledge that may eventually reach the public - and shape society; therefore, Frontiers only applies the most rigorous and unbiased reviews. Frontiers revolutionizes research publishing by freely delivering the most outstanding research, evaluated with no bias from both the academic and social point of view. By applying the most advanced information technologies, Frontiers is catapulting scholarly publishing into a new generation.

What are Frontiers Research Topics?

Frontiers Research Topics are very popular trademarks of the *Frontiers journals series*: they are collections of at least ten articles, all centered on a particular subject. With their unique mix of varied contributions from Original Research to Review Articles, Frontiers Research Topics unify the most influential researchers, the latest key findings and historical advances in a hot research area.

Find out more on how to host your own Frontiers Research Topic or contribute to one as an author by contacting the Frontiers editorial office: frontiersin.org/about/contact

Microbiota in skin inflammatory diseases

Topic editors

Hariom Yadav — USF Center for Microbiome Research, United States

Eun Jeong Park — Mie University, Japan

Tej Pratap Singh — University of Pennsylvania, United States

Citation

Yadav, H., Park, E. J., Singh, T. P., eds. (2023). *Microbiota in skin inflammatory diseases*. Lausanne: Frontiers Media SA. doi: 10.3389/978-2-8325-2858-7

Table of contents

frontiers | Frontiers in Immunology

TYPE Editorial
PUBLISHED 15 June 2023
DOI 10.3389/fimmu.2023.1235314

OPEN ACCESS

EDITED AND REVIEWED BY
Francesca Granucci,
University of Milano-Bicocca, Italy

*CORRESPONDENCE
Eun Jeong Park
epark@med.mie-u.ac.jp
Hariom Yadav
hyadav@usf.edu
Tej Pratap Singh
tpsingh6@hotmail.com

RECEIVED 06 June 2023
ACCEPTED 06 June 2023
PUBLISHED 15 June 2023

CITATION
Park EJ, Yadav H and Singh TP (2023) Editorial: Microbiota in skin inflammatory diseases.
Front. Immunol. 14:1235314.
doi: 10.3389/fimmu.2023.1235314

Editorial: Microbiota in skin inflammatory diseases

Eun Jeong Park[1]*, Hariom Yadav[2]* and Tej Pratap Singh[3]*

[1]Department of Molecular Pathobiology and Cell Adhesion Biology, Mie University Graduate School of Medicine, Tsu, Japan, [2]Center for Microbiome Research, Microbiomes Institute, Morsani College of Medicine, University of South Florida, Tampa, FL, United States, [3]Department of Pathobiology, University of Pennsylvania, Philadelphia, PA, United States

KEYWORDS

skin, microbiota, inflammation, metagenomics, psoriasis, atopic dermatitis

Editorial on the Research Topic
Microbiota in skin inflammatory diseases

Mammalian skin furnishes a niche habitat to diverse microorganisms. The skin contains hair follicles or appendages that provide the home presumably favorable for microbial accessibility (1). Various microbes, including fungi, bacteria, and viruses, inhabit the interface between the skin and external area to constitute the microbiota (2). This microbiota of skin is quite analogous to that of the gut in terms of developing homeostasis and the immune system (3). Microbiota interactions with epithelial or immune cells play critical roles in wound healing, barrier restoration, or pathogenic protection (4). The quantitative and qualitative changes in skin microbiota, such as dysbiosis, may closely associate with the dysfunction of the host immune system, possibly leading to the induction of inflammatory disorders. Although the skin microbiota might play crucial roles in remodeling host immune and inflammatory responses, the exact mechanisms by which the alterations in skin microbiota induce inflammatory disorders need to be defined. Thus, it is imperative to systemically explore the etiologic factors in charge of compositional changes in skin microbiota. For instance, as for the approach to uncover the unknown mechanisms responsible for these changes, it is essential to validate cellular and molecular interactions between skin microbiota and host cells, which are helpful to better understand the cause and effect of the pathogenesis of skin inflammations such as psoriasis and atopic dermatitis (AD). Such approaches may provide insight into further developing diagnostics and therapeutics for skin inflammations. The current Research Topic encompasses some recent findings related to the roles of cutaneous microbiota in affecting the pathophysiology of inflammatory diseases. In a comprehensive review, Chen et al. overviewed methodological advances in analyzing the skin microbiome, significant challenges in systemically substantiating the skin microbial communities, and current knowledge of skin microbiome in health and disease. Moreover, the authors comprehensively discussed the reports examining the microbiome characteristic of diverse skin diseases.

A recent study highlighted the roles played by the skin-resident immune cells in modifying the progression of microbiota-involved infectious diseases. Park et al. have

shown that the gut microbiota is critical in the induction of $CD169^+$ skin macrophages associated with the signaling of type I interferon. This cutaneous macrophage subset, relying on the gut microbiota, can protect mice from *Staphylococcus aureus* skin infection. This protective function required the recruitment and activation of dermal γδ T cells *via* interleukin (IL)-23. Park et al.'s study has provided a molecular basis for a better understanding of the potential role of gut microbiota in the induction of remote $CD169^+$ skin macrophages to affect bacterial skin infection. Pemphigus vulgaris (PV) is an autoimmune disease characterized by blisters and erosions on the skin and mucous membranes (5, 6). A recent study reported the alterations in gut microbiota composition and plasma cytokine levels in PV (7), which may require subsequent studies for validation. Wang et al. have examined the changes in gut microbiota and metabolites on the onset and treatment of PV using metagenomics and metabolomic tools. The increase in the pathogenic bacteria and decrease in the probiotics producing short chain fatty acids (SCFA) were shown to correlate with PV onset.

From a possible genetic contribution to AD onset, examining the associations between gut microbiota compositions and maternal influences on developing AD in children is essential. Fan et al. found that pediatric AD development correlated with the enrichment or reduction of particular microbes in mothers' gut during pregnancy. Thus, Fan et al.'s research offers a possible way to manipulate gut microbiota in pregnant mothers possibly to prevent AD in their offspring. Environmental factors are the driver in modifying the skin microbial composition, possibly through eliciting dysbiosis of particular bacteria. Some pollutants can restrict ceramide production mediated by skin *Roseomonas mucosa* and thus drive its dysbiosis during atopic dermatitis (8). Gough et al. investigated the effects of *R. mucosa* in psoriasis-like skin inflammation. Treatment of this microbe affected tumor necrosis factor signaling in cultured keratinocytes and alleviated symptoms in a mouse model of psoriasis. The authors further observed a dependable correlation between psoriatic severity and the influence of environmental factors such as carbon monoxide. Gough et al.'s works show a potential benefit of microbial manipulation and ecological mitigation for reducing the inflammatory responses, presumably in AD and psoriasis. Head and neck dermatitis (HND), a phenotypic variant of AD, often accompanied with facial erythema, remains therapeutically challenging (9). Due to more sensitivity to *Malassezia furfur* than other AD patients, HND patients showed improved symptoms upon antifungal treatment (10). Chu et al. examined the underlying mechanisms by which the pathogenesis of HND is associated with *M. furfur*. The levels of ceramide were reduced, while the proinflammatory mediators and T-helper 2 type cytokines were increased with *M. furfur*, revealing the effects of this fungal microbe on contributing to HND pathogenesis.

Tissue-specific microbiota contributes to intrinsic tissue homeostasis. Schwarz et al. have demonstrated the potential roles of the skin microbiota in controlling inflammation in a mouse model of psoriasis. The effect of topical treatment with SCFA on ameliorating inflammatory responses in psoriasis can be derived from the signaling of SCFA across hydroxycarboxylic acid receptor 2 (HCA2). Schwarz et al. sought to elucidate the role of HCA2 in inducing regulatory T (Treg) cells to downregulate skin inflammation. The HCA2-knockout (KO) mice showed an exaggerated inflammation due to a decline of Treg cells from a remarkable change in skin microbiota. The HCA2-KO mice recovered functional activity of the Treg cells to suppress inflammatory responses in psoriasis, upon being co-housed with WT mice, due to the restoration of the skin microbiota in the KO mice. This study gave us insight into the potential impacts of modifying the skin microbial composition on alleviating cutaneous inflammations. Luo et al. shed light on the novel roles of butyrate produced by *Staphylococcus epidermidis* in alleviating inflammatory symptoms aggravated by infection with *S. aureus* in an established AD-like model. Specifically, butyrate can downregulate dermal IL-33 expression and leukocyte infiltration and attenuate skin inflammation by inhibiting histone deacetylase 3. Thus, this study provides scientific evidence on butyrate as a potential agent to treat skin inflammations in AD patients. Joshi et al. discussed potential AD therapeutics of microbe-derived antimicrobial peptides (AMP). Because the reduced AMP levels in AD patients derived from the increased colonization of *S. aureus*, the authors pointed out the significance of the selective killing of *S. aureus* without impairment of the commensal microbiome as a therapeutic future avenue. *S. epidermidis* is an abundant bacterium that inhabits healthy human skin, but *S. epidermidis* can also be harmful to the skin, for example inducing AD, depending on the strains (11). Landemaine et al. characterized 12 strains of *S. epidermidis* isolated from healthy and AD skin. The strains from AD skin displayed three functional features: i) structural modification of the epidermis in a model of a 3D reconstructed skin; ii) no induction of aryl hydrocarbon receptor/ovo-like1 pathway to limit production of indole metabolites in co-cultures with normal human epidermal keratinocytes; and consequently, iii) alteration in skin differentiation markers such as desmoglein-1 and filaggrin. This study offers insight into how *S. epidermidis* communicates with the skin in health and disease.

Narrowband ultraviolet-B (nbUVB) phototherapy has been broadly utilized as a dermatological therapy effective in psoriasis, AD, and other inflammatory dermatitis (12–14). Hooper et al. performed a longitudinal analysis of skin microbiota in cutaneous T-cell lymphoma (CTCL) patients treated with nbUVB. The authors probed changes in skin microbiota composition *via* 16S rRNA sequencing analysis. The nbUVB treatment increased the microbial complexity and decreased two pathogens *S. aureus* and *S. lugdunensis*, in the skin of CTCL patients. This study provides a global implication to gauge a biological assessment of nbUVB-induced changes in the skin microbiome. On the other hand, radiation-induced skin injury (RISI) can occur after radiotherapy. Huang et al. investigated the composition and function of skin microbiota changed by RISI. Although further validation requires

identifying its interactive functions with skin, the phylum Firmicutes, considered active for wound healing, was predominantly upregulated in RISI. This study proposes the microbiota and metabolites as potential targets for RISI therapeutics.

We have cited and summarized just a part of the papers chosen depending on the intent of the Research Topic. Thus, we earnestly apologize that a majority of original and review articles are not included in the references due to the restricted capacity of this Editorial.

Author contributions

All authors listed conceived the idea, contributed to preparing the draft, edited the manuscript, and approved the work for publication.

Conflict of interest

The authors declare that the research was conducted in the absence of any commercial or financial relationships that could be construed as a potential conflict of interest.

Publisher's note

References

1. Gallo RL. Human skin is the largest epithelial surface for interaction with microbes. *J Invest Dermatol* (2017) 137:1213–4. doi: 10.1016/j.jid.2016.11.045

2. Byrd AL, Belkaid Y, Segre JA. The human skin microbiome. *Nat Rev Microbiol* (2018) 16:143–55. doi: 10.1038/nrmicro.2017.157

3. Coates M, Lee MJ, Norton D, Macleod AS. The skin and intestinal microbiota and their specific innate immune systems. *Front Immunol* (2019) 10:2950. doi: 10.3389/fimmu.2019.02950

4. Tomic-Canic M, Burgess JL, O'neill KE, Strbo N, Pastar I. Skin microbiota and its interplay with wound healing. *Am J Clin Dermatol* (2020) 21:36–43. doi: 10.1007/s40257-020-00536-w

5. Amagai M, Klaus-Kovtun V, Stanley JR. Autoantibodies against a novel epithelial cadherin in pemphigus vulgaris, a disease of cell adhesion. *Cell* (1991) 67:869–77. doi: 10.1016/0092-8674(91)90360-B

6. Bhol K, Natarajan K, Nagarwalla N, Mohimen A, Aoki V, Ahmed AR. Correlation of peptide specificity and IgG subclass with pathogenic and nonpathogenic autoantibodies in pemphigus vulgaris: a model for autoimmunity. *Proc Natl Acad Sci U.S.A.* (1995) 92:5239–43. doi: 10.1073/pnas.92.11.5239

7. Huang S, Mao J, Zhou L, Xiong X, Deng Y. The imbalance of gut microbiota and its correlation with plasma inflammatory cytokines in pemphigus vulgaris patients. *Scand J Immunol* (2019) 90:e12799. doi: 10.1111/sji.12799

8. Zeldin J, Chaudhary PP, Spathies J, Yadav M, D'souza BN, Alishahedani ME, et al. Exposure to isocyanates predicts atopic dermatitis prevalence and disrupts therapeutic pathways in commensal bacteria. *Sci Adv* (2023) 9:eade8898. doi: 10.1126/sciadv.ade8898

9. Maarouf M, Saberian C, Lio PA, Shi VY. Head-and-neck dermatitis: diagnostic difficulties and management pearls. *Pediatr Dermatol* (2018) 35:748–53. doi: 10.1111/pde.13642

10. Guglielmo A, Sechi A, Patrizi A, Gurioli C, Neri I. Head and neck dermatitis, a subtype of atopic dermatitis induced by malassezia spp: clinical aspects and treatment outcomes in adolescent and adult patients. *Pediatr Dermatol* (2021) 38:109–14. doi: 10.1111/pde.14437

11. Brown MM, Horswill AR. Staphylococcus epidermidis-skin friend or foe? *PloS Pathog* (2020) 16:e1009026. doi: 10.1371/journal.ppat.1009026

12. Reynolds NJ, Franklin V, Gray JC, Diffey BL, Farr PM. Narrow-band ultraviolet b and broad-band ultraviolet a phototherapy in adult atopic eczema: a randomised controlled trial. *Lancet* (2001) 357:2012–6. doi: 10.1016/S0140-6736(00)05114-X

13. Dawe RS. A quantitative review of studies comparing the efficacy of narrowband and broad-band ultraviolet b for psoriasis. *Br J Dermatol* (2003) 149:669–72. doi: 10.1046/j.1365-2133.2003.05498.x

14. Ibbotson SH, Bilsland D, Cox NH, Dawe RS, Diffey B, Edwards C, et al. An update and guidance on narrowband ultraviolet b phototherapy: a British photodermatology group workshop report. *Br J Dermatol* (2004) 151:283–97. doi: 10.1111/j.1365-2133.2004.06128.x

frontiers | Frontiers in Immunology

ORIGINAL RESEARCH
published: 09 June 2022
doi: 10.3389/fimmu.2022.799598

A Microbiota-Dependent Subset of Skin Macrophages Protects Against Cutaneous Bacterial Infection

Young Joon Park[1,2], *Byeong Hoon Kang*[1], *Hyun-Jin Kim*[1], *Ji Eun Oh*[1] *and Heung Kyu Lee*[1*]

[1] *Graduate School of Medical Science and Engineering, Korea Advanced Institute of Science and Technology (KAIST), Daejeon, South Korea,* [2] *Department of Dermatology, Ajou University School of Medicine, Suwon, South Korea*

Microbiota is essential to the development and functional maturation of the immune system. The effects of the gut microbiota on myeloid cells remote from the gut, especially the skin remain unclear. Transcriptomic analysis revealed that type I interferon (IFN) signaling was down-regulated in the skin of germ-free mice compared to that in specific pathogen-free mice. The decrease in type I IFN signaling was closely related to the presence of microbiota and macrophage-specific marker CD169. The absence of $CD169^+$ macrophages resulted in increased bacterial burden and impaired immune responses against Staphylococcus aureus skin infection. $CD169^+$ macrophages mediated the recruitment of γδ T cells as well as the activation of γδ T cells via interleukin (IL)-23. Our findings demonstrate the role of the microbiota in establishment of a specific myeloid cell subset expressing CD169 in the skin and provide evidence of a specific mechanism by which this subset protects against bacterial skin infection.

Keywords: microbiota, Siglec-1, CD169, macrophages, interferon, γδ T cells, IL-17, *S. aureus*

OPEN ACCESS

Edited by:
Laurel L. Lenz, University of Colorado, United States

Reviewed by:
Tao Jin, Sahlgrenska University Hospital, Sweden
Mathieu Paul Rodero, UMR8601 Laboratoire de Chimie et Biochimie Pharmacologiques et Toxicologiques, France

***Correspondence:**
Heung Kyu Lee
heungkyu.lee@kaist.ac.kr
orcid.org 0000-0002-3977-1510

Specialty section:
This article was submitted to Microbial Immunology, a section of the journal Frontiers in Immunology

Received: *21 October 2021*
Accepted: *06 May 2022*
Published: *09 June 2022*

Citation:
Park YJ, Kang BH, Kim H-J, Oh JE and Lee HK (2022) A Microbiota-Dependent Subset of Skin Macrophages Protects Against Cutaneous Bacterial Infection. Front. Immunol. 13:799598. doi: 10.3389/fimmu.2022.799598

INTRODUCTION

The microbiome actively affects the host's immune system in several ways. Commensals residing in the gastrointestinal tract regulate immune responses in the gut and across distal sites other than the gut (1). There are three major mediators of microbiota affecting remote tissues: microbes, microbial products (metabolites), and circulating immune cells (2, 3). These mediators translocate from the intestines *via* circulations and affect immune responses at distal sites. Recently, the gut microbiota was found to influence type I IFN signaling at the remote tissues such as the lung, lymph nodes, and spleen (4, 5).

Type I IFNs and interferon stimulated genes (ISGs) protect the host against viral pathogens, bacteria and parasites (6, 7). Aberrantly expressed type I IFNs and/or ISGs are linked to autoimmune disorders and cancers (8, 9). Type I IFNs are constitutively secreted at low amounts in various organs (10), and the tonic IFN signaling maintains homeostasis of resident immune cells and primes cells to mount a rapid and robust immune response when challenged (4, 10).

Our analysis of a published data suggested that type I IFN signaling increases in the skin of specific pathogen free (SPF) mice compared to germ-free (GF) mice (11). Higher expression of genes related to multiple monocyte/macrophage lineage were also noted in SPF mice. Therefore, in this study, we

investigated the possible relationship between increased type I IFN signaling and monocyte/macrophage lineage in the skin. We show that CD169 expression in skin macrophages is regulated by microbiota-dependent type I IFN signaling. Furthermore, we comprehensively explored the characteristics and roles of skin CD169 expressing cells in host defense.

RESULTS

Reduced Type I IFN Signaling in GF Skin Alters Expression of the Macrophage-Specific Marker, CD169

We mined the data of a previous study on genes differentially expressed in the skin between GF and SPF mice using the GEO database (11). We pre-ranked 15,448 featured genes using log2FC values and analyzed them using GSEA. GSEA showed increase in type I IFN signature in the skin of SPF mice (**Figure 1A**). Gene Ontology (GO) analysis of the top 100 genes highly expressed in SPF mice revealed an increase in pathways related to type I IFN signaling (**Figure 1B**). There was also selective enrichment of tissue-resident macrophage markers, and monocytes in SPF condition (**Figure S1**). Thus, we hypothesized that there might be a relationship between type I IFN signaling and monocyte/macrophage lineage cells. Macrophage markers were investigated in *Ifnar* KO mice for evidence of this relationship. Mannose receptor CD206 is a well-known macrophage marker of the skin and is important for wound healing (12). CD169$^+$ macrophages have been described in skin (13, 14), although their features are not identical to those of CD169$^+$ cells in other tissues (15). Both CD206 and CD169,

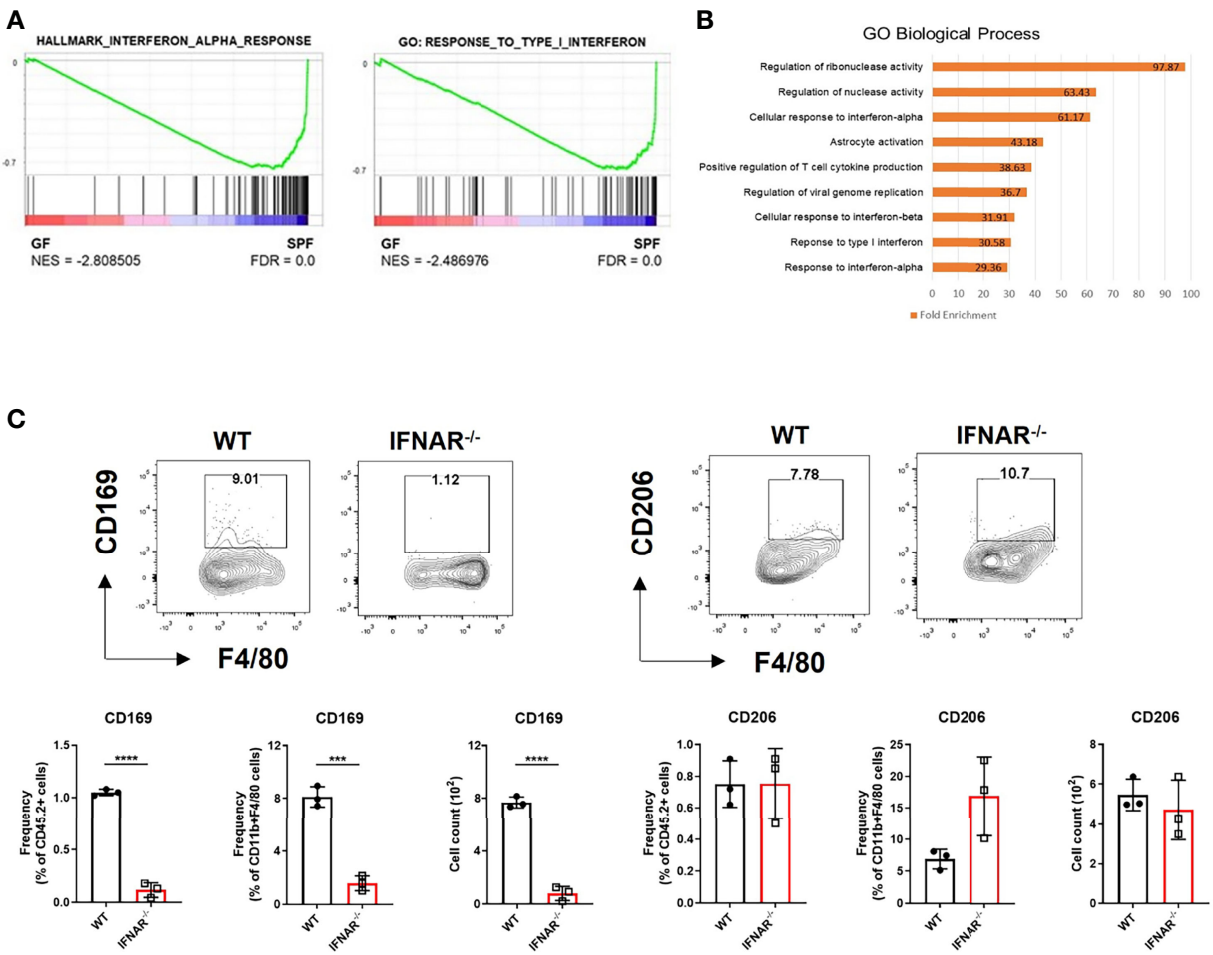

FIGURE 1 | Diminished type I IFN signaling in germ-free skin alters expression of macrophage-specific marker, CD169. **(A)** Gene set enrichment analysis (GSEA) enrichment plots performed on two gene set collections (h.all.v7.2.symbols.gmt and c5.all.v7.2.symbols.gmt) in germ-free (GF) and specific pathogen-free (SPF) mice from data published in Meisel et al., 2018 (GSE98877 from GEO database). GSEA performed 1000 permutations. **(B)** Gene Ontology analysis of GSE98877. **(C)** Representative FACS plot and graphs showing frequency and cell counts of CD169$^+$ and CD206$^+$ myeloid cells in skin of WT and Ifnar KO mice (n = 3 per group). The cells were gated on FSC/SSC, PI$^-$, singlet, CD45.2$^+$, CD11b$^+$, F4/80$^+$ cells. Data represent two independent experiments. Data are expressed as means ± SEM. Horizontal lines above bars indicate statistical comparisons with statistical differences between categories (***p < 0.001, ****p < 0.0001).

are ISGs, as queried using the Interferome database (16). We speculated that the decrease in type I IFN signaling would affect myeloid cells and result in decreased CD206 and/or CD169 expression. Flow cytometry data showed that CD169 expression was dramatically reduced in $CD11b^+$ $F4/80^+$ skin cells of *Ifnar* KO mice, but CD206 expression was not (**Figure 1C**).

$CD169^+$ Cells Are Skin Macrophages With Unique Characteristics and Less Frequent in GF Skin

We found $CD169^+$ cells primarily in the margins of the lower dermis and subcutaneous fat, otherwise termed dermal white adipose tissue (DWAT) (**Figure 2A**). The cells also overlapped with some $F4/80^+$ cells, a marker of myeloid cells. In the horizontal sections, $CD169^+$ cells were abundant in the lower dermis and were also mainly perivascular (**Figure 2B**). Most $CD11b^+/CD169^+$ cells were not $Ly6c^{hi}$ monocytes or $CD11c^{hi}/MHCII^{hi}$ dendritic cells, but were macrophages, defined by their expression of F4/80 and CD64 (**Figure 2C**). We also found $CD169^+$ macrophages in the lower dermis and DWAT of human skin (**Figure 2D**). We presumed that the CD169+ macrophages would be less frequent in skin of GF mice due to its decreased type I IFN signaling. Our confocal microscope images showed lack of $CD169^+$ cells in GF skin compared to substantial amount of $CD169^+$ cells in SPF skin, as expected (**Figure 2E**). These cells were mostly bone marrow-derived (BMD), as confirmed by domination of $CD45.1^+$ and $CD169^+$ expressing cells in CD45.1/CD45.2 chimeric mice (**Figure S2A**). High C-X3-C motif chemokine receptor 1 (CX3CR1) expression accounts for tissue-residency and self-renewal with minimal contribution from blood monocytes (17–19). $CX3CR1^{hi}$ macrophages did not overlap with $CD169^+$ cells in $Cx3cr1^{+/gfp}$ mice (**Figure S2B**). Nearly all $CD169^+$ macrophages were $CX3CR1^{lo}$ (**Figure S2C**). These results indicate that $CD169^+$ macrophages were replenished from BMD monocytes.

Type I IFN Signaling Dictates $CD169^+$ Expression in BMDMs and Skin Macrophages

We investigated whether CD169 expression was induced by type I IFN in BMDMs. IFNα and IFNβ induced higher CD169 expression than media and lipopolysaccharide (LPS) (**Figures 3A, B**). Low levels of type I IFNs was capable of inducing CD169 expression, which was higher at 6 hours post stimulation and decreased after 24 hours. A challenge with a various dose of LPS (10 ng/mL and 100 ng/mL) or *S. aureus* also did not change CD169 expression (**Figure S3A**). The results demonstrate that type I IFN signaling in macrophages might specifically alter CD169 expression, but may not be dose-dependent, due to the change in type I IFN receptor (IFNAR) expression (**Figure S3B**). Our flow cytometry data was in accordance with image data (**Figure 2E**), as CD169 expression was diminished in $F4/80^+$ cells of GF mice compared to SPF mice (**Figure 3C**). We speculated that antibiotic treatment might cause a similar decrease in CD169 expression, and we confirmed, albeit statistically insignificant ($p=0.09$), the decrease in skin macrophages ($CD11b^+/CD64^+$ cells) (**Figure S3C**). Finally, fecal transplantation, not topical *S. epidermis* application, was capable of partially restoring CD169 expression in skin macrophages (**Figure 3D**), possibly suggesting the importance of gut microbiota, rather than skin microbiota in CD169 expression.

$CD169^+$ Cell-Deficient Mice Have an Impaired Immune Response Against *S. aureus* Skin Infection

To address whether such decrease of CD169+ macrophages might affect host immune response against pathogens, we measured the dermonecrotic area after intradermal challenge with methicillin-resistant *S. aureus* (MRSA) on SPF and GF mice. The size of the skin lesion was significantly larger in GF mice (**Figures 4A, B**). We presumed that the result might, at least in part, be due to decrease of CD169+ macrophages. To further elucidate the role of $CD169^+$ macrophages, we used CD169-DTR mice, which have a diphtheria toxin (DT) receptor (DTR) on all cells expressing CD169, and $CD169^+$ cells are readily depleted upon administration of DT (20, 21). Mice were treated with DT (25 ng/g bodyweight) on 3 days (D-3) and 1 day (D-1) before *S. aureus* infection. The dermonecrotic area caused by *S. aureus* was significantly larger in CD169-DTR mice compared to WT mice (**Figures 4C, D**). There were significantly more bacteria on day 7 (but not on day 4) in skin of deficient mice of $CD169^+$ cells (**Figure 4E**). Taken together, the immune response against *S. aureus* was impaired in absence of $CD169^+$ cells. To discern the cause of underlying the difference in immune response, we analyzed isolated immune cells ($CD45^+$ cells) on day 0, day 2, and day 5 of *S. aureus* skin infection using scRNA-seq. Using UMAP and conventional cell markers, we determined the lineages of several immune cell clusters (**Figure S4A** and **Figure 5A**). The identified clusters contained fewer infiltrated immune cells in GF mice, confirming the impairment of the local immune reaction (**Figure S4B**).

γδ T Cell Recruitment Is Impaired in GF and $CD169^+$ Cell-Deficient Mice

We analyzed the difference in monocyte/macrophage cluster at each time points with scRNA-seq. The monocyte/macrophage cluster was identified using markers *Ly6c2, Fcgr1*, and *Adgre1*. WT and CD169-deficient mice differed in a number of DEGs on day 2, which included multiple cytokines and chemokines (*Ccl4*, *Ccl3*, *Il1a*, *Cxcl3, Cxcl2, and Cxcl1*) critical to leukocyte recruitment (**Figure 5B** and **Figure S5A**). On day 5, monocyte/macrophage cluster of WT mice did not show any differences between these cytokines and chemokines (**Figure S5B**). *Cxcl10* and *Vegfa* were the only DEGs noted on day 5 (**Figure 5C**). There were no differences in neutrophil number between the two groups on day 6 (**Figure 5D**), but significantly impaired recruitment of γδ T cells (**Figure 5E**), which are known for their involvement in *S. aureus* skin infection (22, 23). Similar significant compromise in recruitment of dermal γδ T cells was noted in GF mice challenged with *S. aureus*, which also did not

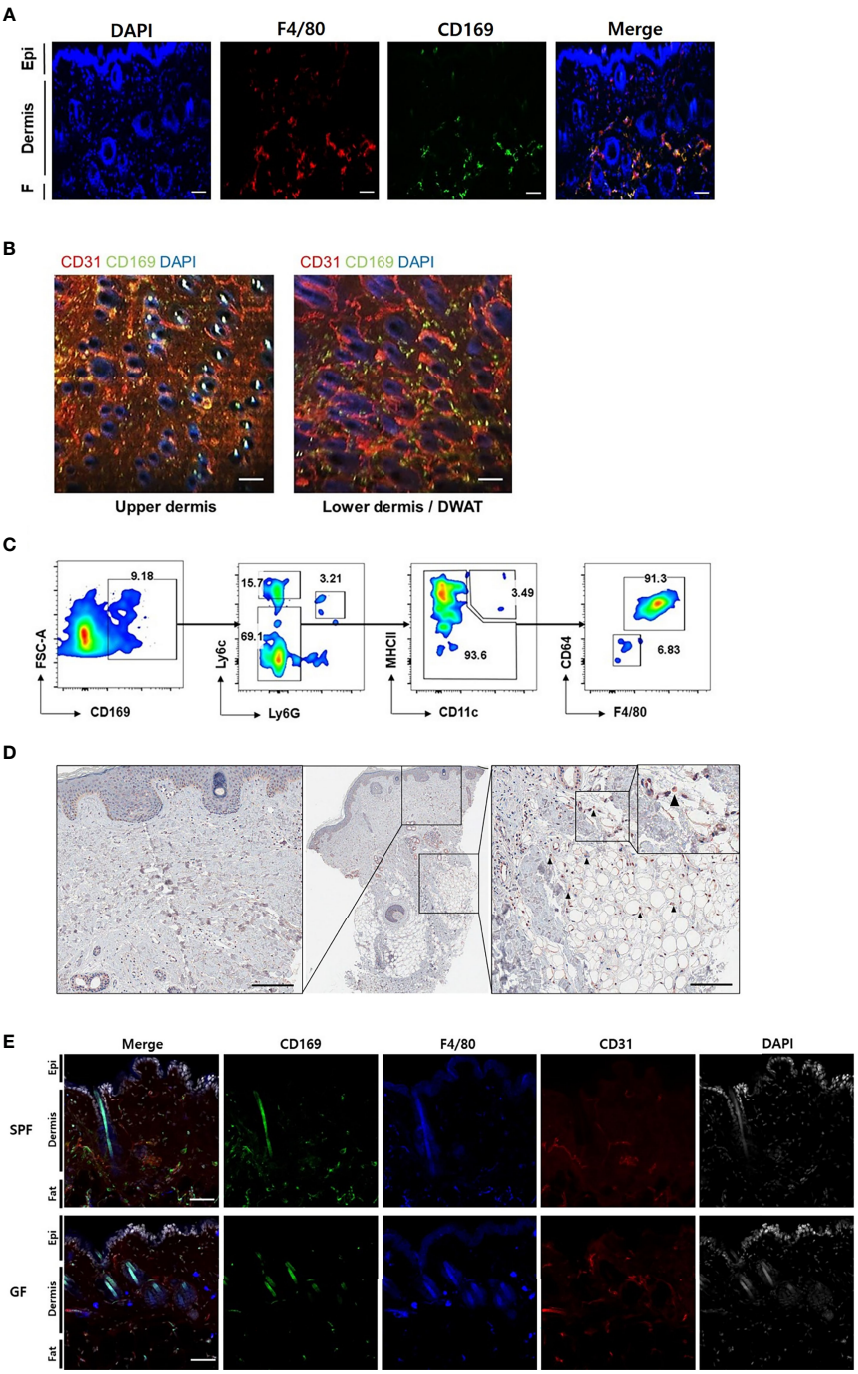

FIGURE 2 | CD169+ cells are detectable in the skin of mouse and human, and less frequent in skin of germ-free mice compared to specific-pathogen-free mice. **(A)** Orthogonal projected image of a vertical skin section (100 μm) using confocal microscopy (F4/80-red, CD169-green, DAPI-blue color). Scale bar indicates 100 μm (Epi: epidermis, F: subcutaneous fat). **(B)** Merged images from a horizontal section (CD31-red, CD169-green, DAPI-blue color) of dermis and dermal white adipose tissue (DWAT) from WT mice. White spots indicate auto fluorescent hair shafts. Scale bar, 100 μm. Images represent three **(A)** and two **(B)** independent experiments. **(C)** Representative gating strategy and features of FACS-sorted CD169$^+$ cells in skin. Gated on FSC/SSC, PI$^-$, CD45.2 and CD11b. Plots represent two independent experiments. **(D)** Representative human skin sample immunostained with CD169 (black arrows indicate CD169$^+$ cells). **(E)** Orthogonal projected images of vertical skin sections (100 μm) from SPF and GF mice (CD169-green, F4/80-blue, CD31-red, DAPI-white color). Scale bar indicates 100 μm. Images represent three independent experiments.

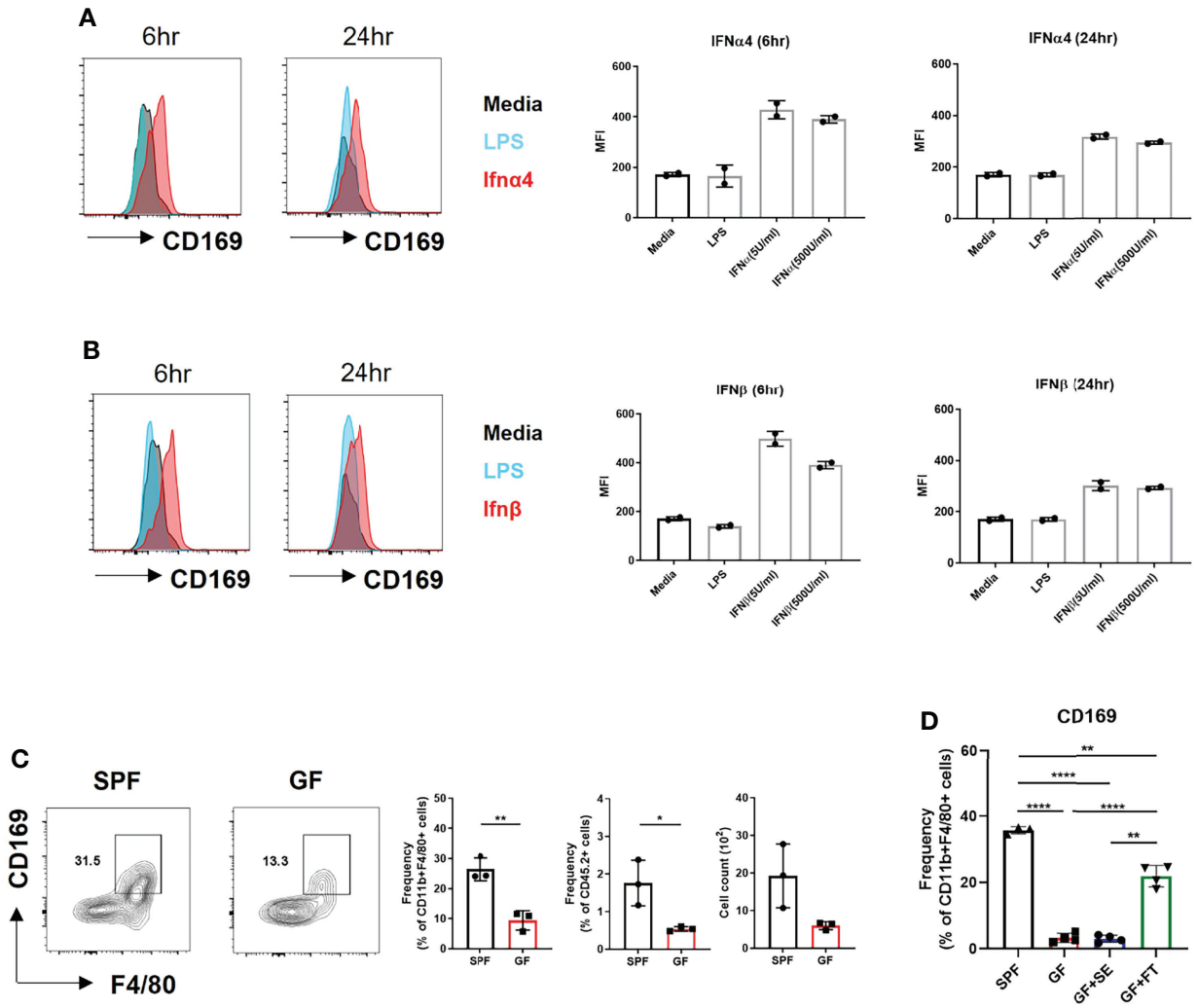

FIGURE 3 | Microbiota-induced type I Interferon signaling dictates CD169$^+$ expression in BMDMs and skin macrophages. **(A)** Representative FACS plot and bar graphs showing mean fluorescence intensity (MFI) of CD169 in BMDMs challenged with various doses of recombinant IFNα4 (5 U/mL and 500 U/mL) and **(B)** recombinant IFNβ (5 U/mL and 500 U/mL) at different time points (6 hours and 24 hours). Data represent two independent experiments. **(C)** Representative FACS plot showing frequency and cell counts of F4/80$^+$ CD169$^+$ cells in skin of SPF and GF mice (n = 3 per group). Gated on FSC/SSC, PI$^-$, singlet, CD45.2$^+$, CD11b$^+$ cells. Data are expressed as means ± SEM (*p<0.05, **p<0.01). Data represent three independent experiments. **(D)** Frequency of CD169$^+$ macrophages in skin of SPF mice (n = 3) with DPBS oral gavage (SPF), GF mice (n = 3) with DPBS oral gavage (GF), GF mice (n = 3) with *S. epidermis* topical application (GF+SE) and GF mice (n = 3) with fecal transplantation (GF+FT). The cells were gated on FSC/SSC, PI$^-$, singlet, CD45.2$^+$, CD11b$^+$, F4/80$^+$ cells. Combined data of three independent experiments are shown. Data are expressed as means ± SEM (**p < 0.01, ***p < 0.001, ****p < 0.0001).

show differences between SPF mice in neutrophil number on day 6 (**Figures 5F, G**). There were no other significant differences in skin T cells, except decreased frequency of dendritic epidermal γδ T cells (**Figures S5C, D**).

Activation of γδ T Cells by CD169$^+$ Macrophages

Local activation of γδ T cells was suspected from GSEA of γδ T cells on day 2 (**Figure 6A**) and larger number of IL-17A+ γδ T cells in SPF mice compared to GF mice, despite statistically insignificant (**Figure S6A**). As γδ T cells can be activated without T cell receptor signaling, we investigated whether differences in IL-1β and IL-23 expression by CD169$^+$ macrophages resulted in local activation of IL-17-producing γδ T cells. Interestingly, using scRNA-seq analysis, we found that monocyte/macrophage cluster was the most popular source of *Il23a* in myeloid clusters, whereas DCs expressed more *Il12b* (**Figure 6B**). Using BMDMs, we were able to detect IL-23p19 production from macrophages challenged with *S. aureus* and confirmed that CD169$^+$ macrophages were the major IL-23p19 producers (**Figure 6C**). Intracellular staining (ICS) of skin immune cells on day 1 post infection revealed that CD169$^+$ macrophages mostly produced IL-23p19 production *in vivo* (**Figure 6D**). The absence of CD169$^+$ cells resulted in a decrease of IL-17-

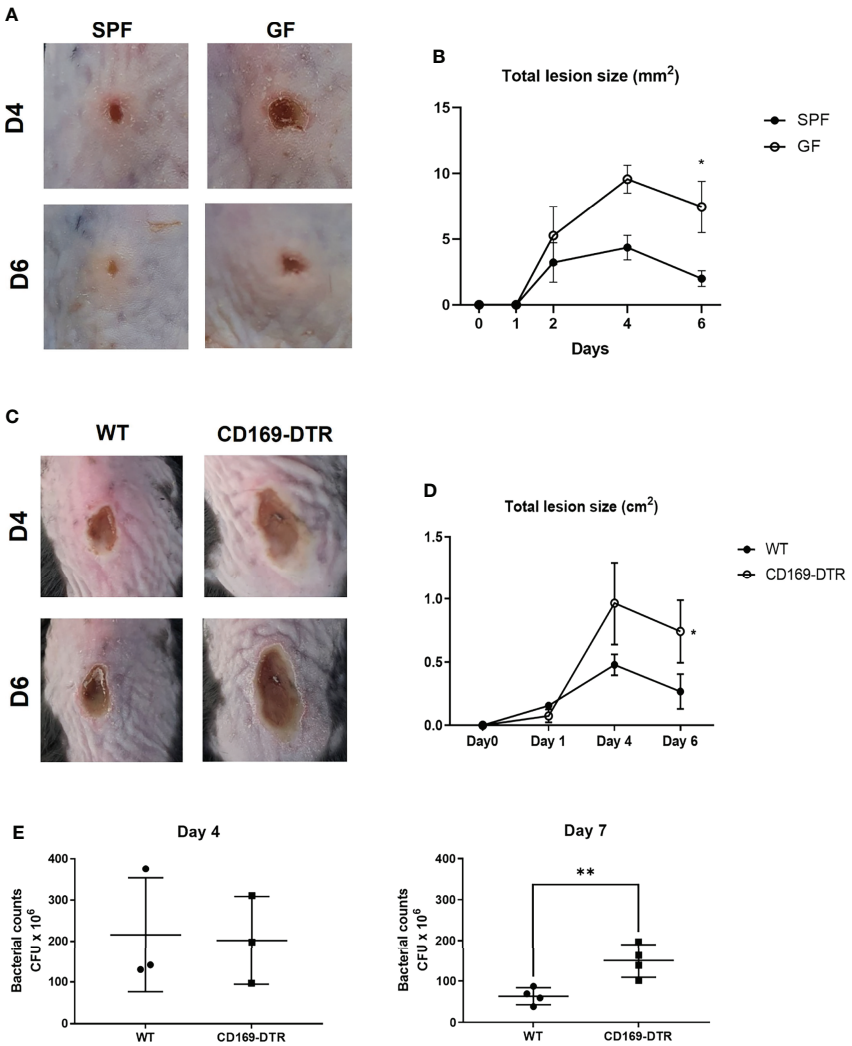

FIGURE 4 | Impairment of immune response in germ-free and CD169$^+$ cell-deficient mice against *Staphylococcus aureus* skin infection. **(A)** SPF and GF mice (n = 3 per group) were intradermally challenged with 2×10^7 CFUs of CA-MRSA (USA300). Representative pictures of skin lesions on day 4 (D4) and day 6 (D6) post infection. **(B)** Total lesion size of SPF and GF mice (n = 3 per group) over-time calculated by ImageJ program. The Images and data represent two independent experiments. **(C)** Representative pictures of skin lesions in WT and CD169-DTR mice (n = 3 per group) after intradermal *S. aureus* infection on D4 and D6 post infection. **(D)** Total lesion size of WT and CD160-DTR mice over-time. The Images **(C)** and data **(D)** represent three independent experiments. **(E)** CFU counts in skin lesion homogenates of WT and CD169-DTR mice after *S. aureus* intradermal infection on day 4 (n = 3 per group) and day 7 (n = 4 per group). Data represent three independent experiments. Data are expressed as means ± SEM (*p < 0.05, **p < 0.01).

producing γδ T cells on day 6 (**Figure 6E**). The number of IFN-γ producing T cells was minimal and was not altered in absence of CD169$^+$ macrophages (**Figure S6B**). Taken all together, we assumed that the absence of CD169$^+$ macrophages result in the decreased number of IL-17-producing γδ T cells, which lead to the impairment of host defense response, as observed from the high CFU counts and a larger area of dermonecrosis.

DISCUSSION

CD169$^+$ macrophages have been studied primarily in lymphoid organs due to their location, for example subcapsular sinus and medullary macrophages in lymph nodes (LNs) and marginal metallophilic macrophages in the marginal zone of the spleen (24, 25). In LNs, the presence of B cells is necessary to generate CD169$^+$ macrophages, mediated by their production of lymphotoxin alpha beta (LTα1β2) (26, 27). CD169$^+$ macrophages also reside in various peripheral tissues, such as the brain, gastrointestinal tract, liver, lung, kidney, and skin (13, 15, 21). CD169 expression in these tissues is possibly not due to B cells, as peripheral B cells are more infrequent and generally not adjacent to macrophages. Our results suggest that local tonic IFN signaling induced by microbiota might be a factor governing CD169 expression of macrophages in these tissues and yield additional interesting findings. First, CD169-expressing macrophages were present in the lower dermis and within

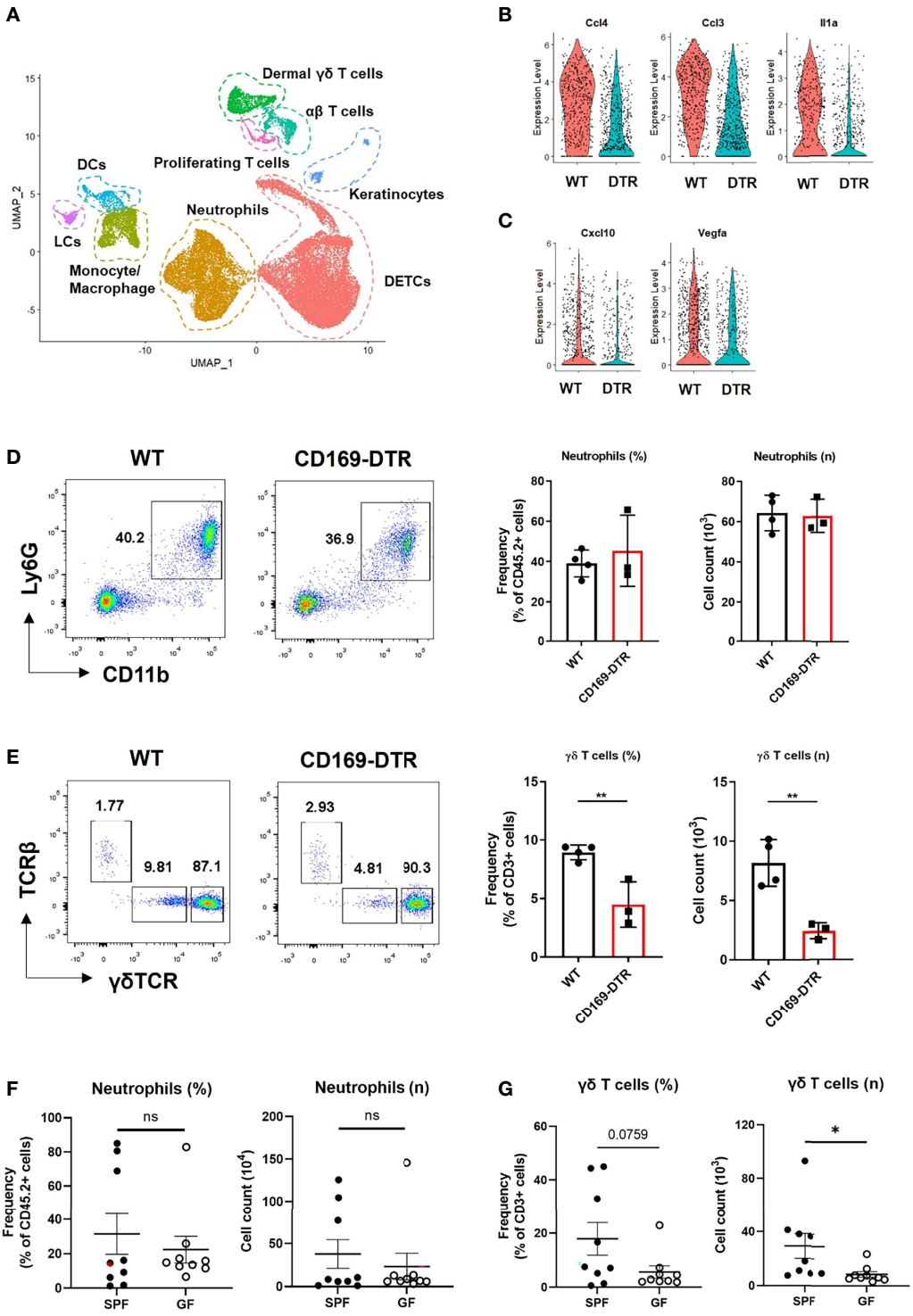

FIGURE 5 | γδ T cells, not neutrophils, are affected by an absence of CD169+ cells at late time points. **(A)** UMAP projections of all skin-infiltrating immune cells. **(B, C)** Violin plot showing DEGs between WT and CD169-DTR of monocyte/macrophage cluster on day 2 **(B)** and day 5 **(C)**. **(D, E)** Flow cytometry analysis of neutrophils **(D)** and dermal γδ T cells **(E)** in WT (n = 4) and CD169-DTR (n = 3) mice skin at day 6 post infection. The cells are gated on FSC/SSC, singlet, PI^-, $CD45.2^+$ **(D)** and FSC/SSC, singlet, PI^-, $CD45.2^+$, $CD3^+$, $CD11b^{-to lo}$ **(E)** cells. Data are representative of three experiments. **(F, G)** Flow cytometry analysis of neutrophils **(F)** and dermal γδ T cells **(G)** in SPF (n = 9) and GF (n = 9) mice skin at day 6 post infection. The cells are gated on FSC/SSC, singlet, PI^-, $CD45.2^+$ **(F)** and FSC/SSC, singlet, PI^-, $CD45.2^+$, $CD3^+$, $CD11b^{-to lo}$ **(G)** cells. Representative data of two independent experiments are shown. Data are expressed as means ± SEM (*$p < 0.05$, **$p < 0.01$, ns, not significant).

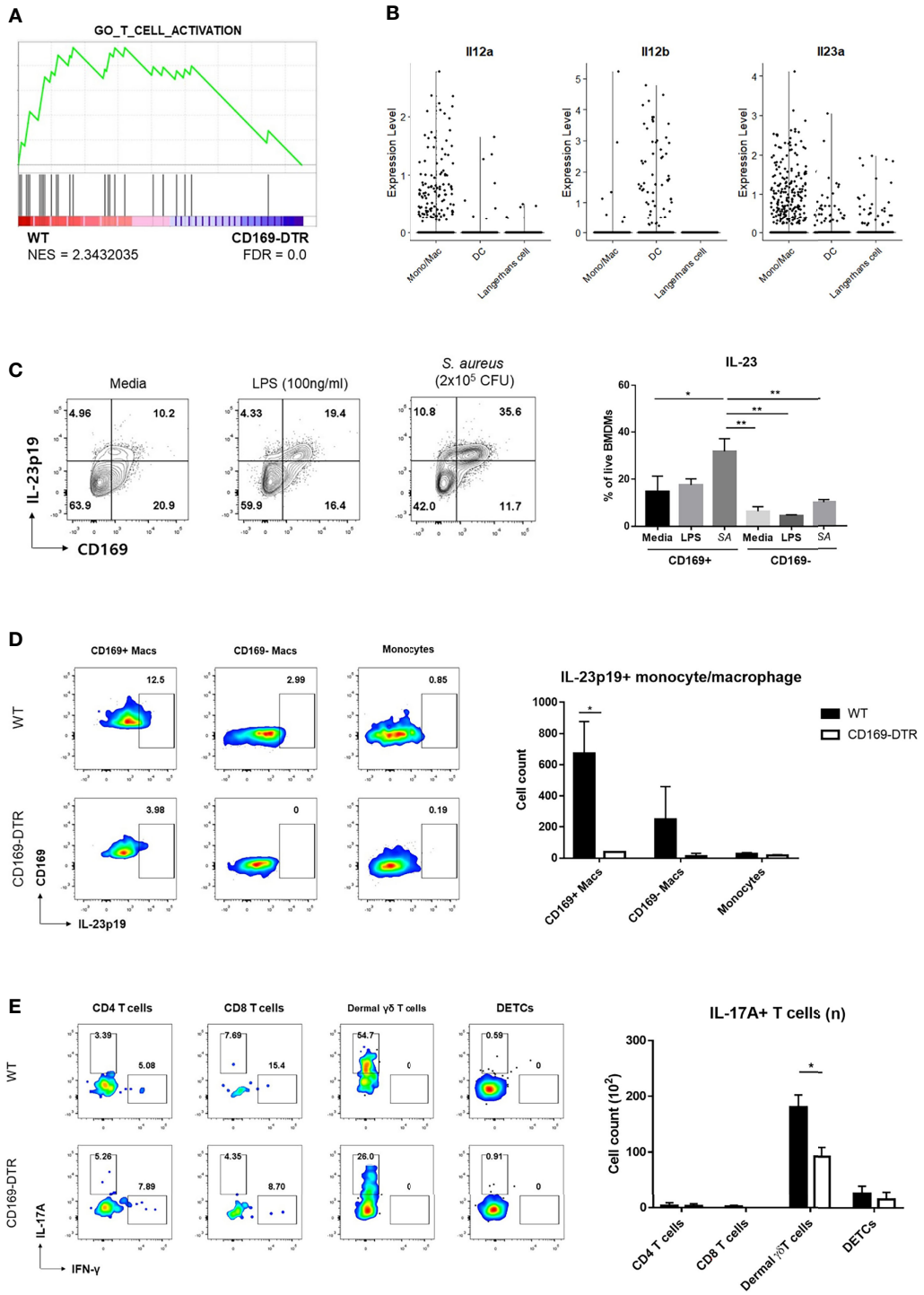

FIGURE 6 | Activation of γδ T cells by CD169+ macrophages. **(A)** GSEA of DEGs from dermal γδ T cells of WT mice compared to CD169-DTR mice. **(B)** Violin plots of Il12a, Il12b, and Il23a expression in monocyte/macrophage, dendritic cell (DCs) and Langerhans cell clusters from scRNA-seq analysis data. **(C)** Representative flow cytometry plots and bar graph of BMDMs challenged with LPS (100 ng/mL) and S. aureus (SA, $2x10^5$ CFU). **(D)** Representative plots and bar graph of IL-23p19 production by $CD169^+$ macrophages (Macs), $CD169^-$ macrophages and monocytes on day 1 post skin *S. aureus* infection. Single-cell suspensions from two mice were pooled for both WT and CD169-DTR group. $CD169^{+/-}$ Macs were gated on FSC/SSC, PI^-, singlet, $CD45.2^+$, $CD11b^+$, $EpCAM^-$, $Ly6c^{-to lo}$, $Ly6G^-$, $F4/80^+$ cells. Monocytes are gated on FSC/SSC, PI^-, singlet, $CD45.2^+$, $CD11b^+$, $EpCAM^-$, $Ly6c^{hi}$ cells. **(E)** Representative plots and bar graph of IL-17A-producing T cells in skin 6 days post infection. T cells are gated on FSC/SSC, singlet, PI^-, $CD45.2^+$, $CD3^+$, $CD11b^{-to lo}$ cells. Single-cell suspensions from two mice were pooled for both WT and CD169-DTR group. Data are representative of three independent experiments. Error bars show mean ± SEM (*$p < 0.05$; **$p < 0.01$).

DWAT. Second, these cells are replenished by monocytes. Third, the selective depletion of CD169$^+$ macrophages resulted in increased bacterial burden and impaired immune response. This phenotype was possibly due to an impaired ability to recruit γδ T cells. The CD169$^+$ macrophages also were capable of γδ T cell activation, which resulted in IL-17 production by γδ T cells. Based on these findings, we concluded that CD169$^+$ cells are an indispensable for combating intradermal *S. aureus* infection.

Surprisingly low levels of type I IFNs were sufficient to induce CD169 in BMDMs, while a high amount and/or prolonged type I IFN did not upregulate CD169 expression. CD169 expression might be under the control of type I IFN receptor (IFNAR) expression, which is affected by the strength of type I IFN signaling. Our results, in part, support the notion that a specific tone of type I IFNs is required for homeostatic CD169 expression by macrophages (4, 28). Furthermore, we present the novel mechanism of how microbiota-induced tonic type I IFN signaling affects monocyte/macrophage lineage cells. However, we also found that CD169 expression of skin macrophages *in vivo* is not strictly consistent, which might suggest a possibility of other factors affecting the CD169 expression in more precise manner.

Without CD169$^+$ cells, the skin was more susceptible to *S. aureus* infection, as shown by larger dermonecrotic areas and higher CFU counts in CD169$^+$ cell-deficient mice than in WT mice. Also, the WT monocyte/macrophage cluster expressed more *Cxcl10* and *Vegfa*, both chemokines important in proliferation phase and remodeling phase of wound healing (29), compared to the CD169-DTR monocyte/macrophage cluster at day 5. We speculated that the lesions of WT mice more successfully eliminated *S. aureus* and were heading towards resolution phase, whereas the CD169$^+$ cell-deficient mice remained in the active inflammatory phase. Early excessive neutrophil accumulation, however, might also result in tissue damage and dermonecrosis (30). The area of dermonecrosis should be interpreted along with the data on bacterial burden.

Intradermal injection results in involvement of the whole skin layer including DWAT (31). In this regard, CD169$^+$ can act as the initiator of immune responses in intradermal infection, although they are located distantly from the epidermis. A similar role was proposed in a dextran sulfate sodium-induced colitis model, as the colitis symptoms decreased in the absence of CD169$^+$ cells (20). The number of RORγt$^+$ cells (Th17, γδ T17, LTi, and ILC3) did not change in that study but showed diminished IL-17 and IL-22 mRNA expression. Our data suggested that the skin CD169$^+$ macrophages not only affected the recruitment of IL-17A-producing γδ T cells, but also acted as activators of γδ T cells *via* local IL-23 production.

Our study has multiple limitations. First, we did not evaluate the phagocytic activity or previously reported antigen presentation activity of CD169$^+$ macrophages (32). It is unlikely, however, that the possible increase in phagocytic activity of CD169$^+$ macrophages resulted in such a difference in the phenotype, as the number of resident immune cells were much lower than those of infiltrating neutrophils, monocytes, and T cells. CD169$^+$ can also cross-prime CD8 T cells or transfer antigens to CD8a$^+$ DCs (32, 33), but acute *S. aureus* infection mostly involves IL-17-producing γδ T cells, in which the activation of the T cells do not require antigen presentation. Consequently, CD8 T cells are likely to have minimal effects on *S. aureus* infection. Second, we were not able to fully elucidate h microbiota enhance type I IFN signaling in skin remain to be elucidated. Previous research suggested that the lung stromal cells (28) and plasmacytoid DCs in lymphatic organs as the source of tonic type I IFN signals (4). These studies indicated that the gut microbiota was involved in the process of tonic signaling, while it is not clear where and how the cells received microbiota signals. We showed that gut microbiota is important in CD169 expression using the fecal transplantation experiment. However, we cannot be completely sure that gut microbiota is entirely responsible for CD169 expression, as not only did we not address the possibility of the act of oral gavage being an inducer of CD169, but also because we were not able to address specific microbiota signals. We also cannot fully exclude the possibility of skin commensals being involved in local type I IFN signaling, as *S. epidermidis* cannot represent the plethora of commensal microorganism skin harbors. Future work will need to explore the exact source and nature of signals leading to enhanced type I IFN and ISG signatures.

MATERIALS AND METHODS

Ethics Statement

All animal experiments in this study were in accordance with the legal and ethical requirements and the guidelines and protocols for rodent research were approved by the institutional animal care and use committee of Korea Advance Institute Science and Technology (KAIST, KA2017-40).

Mice

SPF male C57BL/6 mice were purchased from the KAIST (Daejeon, Korea) or DBL Co. Ltd (Eumseong, Korea). *Ifnar* knock-out (KO) mice (stock number: 028288, B6(Cg)-Ifnar1$^{tm1.2Ees}$/J) and CX3CR1-GFP (B6.129P2(Cg)-Cx3cr1tm1Litt/J, Stock number: 005582) were purchased from the Jackson Laboratory (Bar Harbor, ME, USA). CD169-DTR (Siglec1<tm1 (HBEGF) Mtka>) mice were purchased from RIKEN BioResource Research Center with the permission of Dr. Masato Tanaka of the Tokyo University of Pharmacy and Life Sciences (Tokyo, Japan). GF mice were obtained from animal care facility of Microbiome Core Research Support Center at Pohang University of Science and Technology (POSTECH, Pohang, Korea). All mice used in this study were maintained in a SPF facility at the KAIST Laboratory Animal Resource Center.

Bacteria Preparation

Community-associated methicillin-resistant *Staphylococcus aureus* (CA-MRSA) strain USA300 (ATCC® BAA-1717) and *Staphylococcus epidermidis* (ATCC®12228) were purchased from the ATCC (ATCC, Manassas, VA, USA) and Korean Collection

for Type Cultures (KCTC), respectively. Overnight cultures of a single bacteria colony were pelleted and resuspended in a 15% glycerol solution, aliquoted and stored at -80°C. One hundred microliters of aliquoted bacteria were defrosted and grown overnight in tryptic soy broth (TSB) at 37°C in a shaking incubator (200 rpm). A 2-h subculture (1:20 dilution) was made subsequently. The bacteria were pelleted and resuspended in phosphate-buffered saline (PBS). Optical Density was measured to estimate the colony forming units (CFUs), which was verified after overnight culture on tryptic soy agar (TSA) plates.

Mouse *S. aureus* Skin Infection Model And Treatments

Mice were anesthetized with 2% isoflurane, and their backs were shaved and depilated a day before *S. aureus* injection. A suspension of 1–2 × 10^7 CFUs/100μL PBS was injected intradermally using a 29-gauge insulin syringe. Digital photographs of the backs of the injected mice and total lesion size (cm^2) measurements were analyzed using the image analysis software program ImageJ (https://imagej.nih.gov/ij/). For additional mice treatments, please see the **Supplementary Data**.

Generation of Bone Marrow Chimeras

C57BL/6 CD45.2 recipient mice were irradiated with 600cGy twice and reconstituted with 5 × 10^6 BM cells from C57BL/6 CD45.1 donor mice *via* tail vein injection. Chimeric mice were supplied with antibiotic containing water. The transplanted mice were analyzed after 6 weeks.

Bone Marrow-Derived Macrophage Preparation

Cells were prepared by flushing the femurs and tibiae of mice and were cultured in RPMI-1640 medium supplemented with 10% fetal bovine serum (FBS) (HyClone, Logan, USA), 1% penicillin/streptomycin, and 30% macrophage colony stimulating factor (M-CSF) conditional medium (supernatants of M-CSF from L929 cell cultures). After 7 days, adherent bone marrow derived macrophages (BMDMs) were collected *via* pipetting.

Enumeration of *S. aureus* CFU

Skin specimens were obtained from the center of lesions using an 8mm-disposable punch (Kai Industries, Seki city, Japan), and homogenized in 1mL PBS using a TissueRuptor II (Qiagen, Germantown, MD, USA). The homogenates were passed through 100-μm cell strainers and plated at serial dilution onto TSA plates. The number of CFU was determined after overnight incubation at 37°C.

Single Cell Preparation From Skin

Whole skin cells were prepared from mouse back skin. 4 cm^2 of back skin tissue were harvested. The skin tissue was minced by blade and treated with 2 mg/mL Dispase II (Roche, Basel, Switzerland) for 1 h at 37°C. The skin was further minced into small pieces using scissors and digested with DMEM containing 1% FBS, 1 mg/mL Collagenase IV (Worthington Biochemical Corp., NJ, USA), 0.1 mg/mL DNase I (Roche), and 1.2 mg/ml hyaluronidase (Sigma-Aldrich, St Louis, MO, USA) for 30 minutes at 37°C. The digested skin tissues were then plunged through 70 μm cell strainers. The cells were resuspended on a Percoll gradient (70%/30%) (GE Healthcare, Chicago, IL, USA) and centrifuged at 2000 rpm for 20 min at 25°C. Cells were treated with ACK lysis buffer for 5 min at RT to remove red blood cells.

Flow Cytometry

Single-cell suspensions were pretreated with anti-CD16/32 (clone 2.4G2; TONBO Biosciences, CA, USA) antibody to block Fc receptors. For additional flow cytometry methods, please see the **Supplementary Data**.

Single-Cell Transcriptomic Analysis

At 2 days (48 hours) and 5 days (128 hours) after intradermal injection of *S. aureus*, single-cell suspensions were obtained from skin as described above. Cells were treated with anti-CD16/32 to neutralize Fc receptors. Cells then were stained with anti-CD45.2. and 7-AAD, and live leukocytes were isolated using a FACS Aria II cell sorter (BD Biosciences). Single-cell RNA sequencing was performed using a Chromium Single Cell 3' V3 Reagent kit (10X Genomics, Pleasanton, CA, USA) according to the manufacturer's protocol. For additional information on single-cell RNA sequencing and its analysis methods, please see the **Supplementary Data**.

Histological Analysis and Image Acquisition

Skin samples were obtained from the center of the dorsal skin using an 8 mm-disposable biopsy punch (Kai Industries). Samples were fixed in 4% paraformaldehyde (Duksan General Science, Seoul, Korea) and dehydrated in a 30% sucrose solution for 24 h at 4°C. Tissues were embedded in OCT compound (4538, Sakura Finetek, Alphen aan den Rijin, South Holland, Netherlands). Frozen blocks were cut into 100-μm thick sections using a cryostat (Microm HM525, Thermo Fisher Scientific). For detailed information on immunofluorescence staining methods and image acquisition, please check the **Supplementary Data**.

Analysis of Publicly Curated Gene Expression Dataset

The gene datasets deposited by Grice and Meisel in 2018 were accessed from the Gene Expression Omnibus database (NCBI GEO database, accession GSE98877) (11). The functional classification for the previously published results was analyzed according to their functional similarity based on PANTHER (v15.0, www.pantherdb.org). For GSEA (34), 15,448 differentially expressed genes were annotated to the reference gene set based on MSigDB 7.2.

Statistical Analysis

All data are presented as means with standard deviations. Statistical analyses were performed using GraphPad Prism 9 (GraphPad Software, Inc., La Jolla, CA, USA) and R statistical program where relevant. An unpaired Student's t-test was used for analysis between two groups with Welch's correction when

necessary, and unpaired one-way analysis of variance was used for multiple comparisons. A difference between groups was considered significant: *, $P < 0.05$; **, $P < 0.01$; ***, $P < 0.001$.

DATA AVAILABILITY STATEMENT

Publicly available datasets were analyzed in this study. This data can be found here: https://www.ncbi.nlm.nih.gov/geo/query/acc.cgi?acc=GSE98877.

ETHICS STATEMENT

The studies involving human participants were reviewed and approved by Ajou University Hospital (AJIRB-MED-KSP-21-376). The patients/participants provided their written informed consent to participate in this study. The animal study was reviewed and approved by The institutional animal care and use committee of Korea Advance Institute Science and Technology.

AUTHOR CONTRIBUTIONS

YJP, BHK and H-JK conducted the experiments. YJP, JEO and HKL analyzed the data. YJP and HKL wrote the manuscript. HKL supervised the project. All authors contributed to the article and approved the submitted version.

FUNDING

This study was supported by the National Research Foundation of Korea (NRF-2021M3A9D3026428 and NRF-2021M3A9H3015688) funded by the Ministry of Science and ICT of Korea.

ACKNOWLEDGMENTS

The authors would like to thank the members of the Laboratory of Host Defenses for their helpful advice and discussions. The authors thank Ji Ye Kim at the BioMedical Research Center for technical service.

SUPPLEMENTARY MATERIAL

The Supplementary Material for this article can be found online at: https://www.frontiersin.org/articles/10.3389/fimmu.2022.799598/full#supplementary-material

REFERENCES

1. Molloy MJ, Bouladoux N, Belkaid Y. Intestinal Microbiota: Shaping Local and Systemic Immune Responses. *Semin Immunol* (2012) 24:58–66. doi: 10.1016/j.smim.2011.11.008
2. Constantinides MG, Link VM, Tamoutounour S, Wong AC, Perez-Chaparro PJ, Han SJ, et al. MAIT Cells are Imprinted by the Microbiota in Early Life and Promote Tissue Repair. *Science* (2019) 366. doi: 10.1126/science.aax6624
3. Zheng D, Liwinski T, Elinav E. Interaction Between Microbiota and Immunity in Health and Disease. *Cell Res* (2020) 30:492–506. doi: 10.1038/s41422-020-0332-7
4. Schaupp L, Muth S, Rogell L, Kofoed-Branzk M, Melchior F, Lienenklaus S, et al. Microbiota-Induced Type I Interferons Instruct a Poised Basal State of Dendritic Cells. *Cell* (2020) 181:1080–96.e19. doi: 10.1016/j.cell.2020.04.022
5. Steed AL, Christophi GP, Kaiko GE, Sun L, Goodwin VM, Jain U, et al. The Microbial Metabolite Desaminotyrosine Protects From Influenza Through Type I Interferon. *Science* (2017) 357:498–502. doi: 10.1126/science.aam5336
6. Kovarik P, Castiglia V, Ivin M, Ebner F. Type I Interferons in Bacterial Infections: A Balancing Act. *Front Immunol* (2016) 7:652. doi: 10.3389/fimmu.2016.00652
7. McNab F, Mayer-Barber K, Sher A, Wack A, O'Garra A. Type I Interferons in Infectious Disease. *Nat Rev Immunol* (2015) 15:87–103. doi: 10.1038/nri3787
8. Jiang J, Zhao M, Chang C, Wu H, Lu Q. Type I Interferons in the Pathogenesis and Treatment of Autoimmune Diseases. *Clin Rev Allergy Immunol* (2020) 59:248–72. doi: 10.1007/s12016-020-08798-2
9. Trinchieri G. Type I Interferon: Friend or Foe? *J Exp Med* (2010) 207:2053–63. doi: 10.1084/jem.20101664
10. Gough DJ, Messina NL, Clarke CJ, Johnstone RW, Levy DE. Constitutive Type I Interferon Modulates Homeostatic Balance Through Tonic Signaling. *Immunity* (2012) 36:166–74. doi: 10.1016/j.immuni.2012.01.011
11. Meisel JS, Sfyroera G, Bartow-McKenney C, Gimblet C, Bugayev J, Horwinski J, et al. Commensal Microbiota Modulate Gene Expression in the Skin. *Microbiome* (2018) 6:20. doi: 10.1186/s40168-018-0404-9
12. Hesketh M, Sahin KB, West ZE, Murray RZ. Macrophage Phenotypes Regulate Scar Formation and Chronic Wound Healing. *Int J Mol Sci* (2017) 18. doi: 10.3390/ijms18071545
13. Thornley TB, Fang Z, Balasubramanian S, Larocca RA, Gong W, Gupta S, et al. Fragile TIM-4-Expressing Tissue Resident Macrophages are Migratory and Immunoregulatory. *J Clin Invest* (2014) 124:3443–54. doi: 10.1172/JCI73527
14. Yanagihashi Y, Segawa K, Maeda R, Nabeshima YI, Nagata S. Mouse Macrophages Show Different Requirements for Phosphatidylserine Receptor Tim4 in Efferocytosis. *Proc Natl Acad Sci U S A* (2017) 114:8800–5. doi: 10.1073/pnas.1705365114
15. Sheng J, Chen Q, Soncin I, Ng SL, Karjalainen K, Ruedl C. A Discrete Subset of Monocyte-Derived Cells Among Typical Conventional Type 2 Dendritic Cells Can Efficiently Cross-Present. *Cell Rep* (2017) 21:1203–14. doi: 10.1016/j.celrep.2017.10.024
16. Rusinova I, Forster S, Yu S, Kannan A, Masse M, Cumming H, et al. Interferome V2.0: An Updated Database of Annotated Interferon-Regulated Genes. *Nucleic Acids Res* (2013) 41:D1040–6. doi: 10.1093/nar/gks1215
17. Chorro L, Geissmann F. Development and Homeostasis of 'Resident' Myeloid Cells: The Case of the Langerhans Cell. *Trends Immunol* (2010) 31:438–45. doi: 10.1016/j.it.2010.09.003
18. Burgess M, Wicks K, Gardasevic M, Mace KA. Cx3CR1 Expression Identifies Distinct Macrophage Populations That Contribute Differentially to Inflammation and Repair. *Immunohorizons* (2019) 3:262–73. doi: 10.4049/immunohorizons.1900038
19. Kolter J, Feuerstein R, Zeis P, Hagemeyer N, Paterson N, d'Errico P, et al. A Subset of Skin Macrophages Contributes to the Surveillance and Regeneration of Local Nerves. *Immunity* (2019) 50:1482–97.e7. doi: 10.1016/j.immuni.2019.05.009
20. Asano K, Takahashi N, Ushiki M, Monya M, Aihara F, Kuboki E, et al. Intestinal CD169(+) Macrophages Initiate Mucosal Inflammation by Secreting CCL8 That Recruits Inflammatory Monocytes. *Nat Commun* (2015) 6:7802. doi: 10.1038/ncomms8802
21. Gupta P, Lai SM, Sheng J, Tetlak P, Balachander A, Claser C, et al. Tissue-Resident CD169(+) Macrophages Form a Crucial Front Line Against Plasmodium Infection. *Cell Rep* (2016) 16:1749–61. doi: 10.1016/j.celrep.2016.07.010
22. Cho JS, Pietras EM, Garcia NC, Ramos RI, Farzam DM, Monroe HR, et al. IL-17 Is Essential for Host Defense Against Cutaneous Staphylococcus Aureus Infection in Mice. *J Clin Invest* (2010) 120:1762–73. doi: 10.1172/JCI40891

23. Marchitto MC, Dillen CA, Liu H, Miller RJ, Archer NK, Ortines RV, et al. Clonal Vgamma6(+)Vdelta4(+) T Cells Promote IL-17-Mediated Immunity Against Staphylococcus Aureus Skin Infection. *Proc Natl Acad Sci USA* (2019) 116:10917–26. doi: 10.1073/pnas.1818256116
24. Saunderson SC, Dunn AC, Crocker PR, McLellan AD. CD169 Mediates the Capture of Exosomes in Spleen and Lymph Node. *Blood* (2014) 123:208–16. doi: 10.1182/blood-2013-03-489732
25. Uchil PD, Pi R, Haugh KA, Ladinsky MS, Ventura JD, Barrett BS, et al. A Protective Role for the Lectin CD169/Siglec-1 Against a Pathogenic Murine Retrovirus. *Cell Host Microbe* (2019) 25:87–100.e10. doi: 10.1016/j.chom.2018.11.011
26. Moseman EA, Iannacone M, Bosurgi L, Tonti E, Chevrier N, Tumanov A, et al. B Cell Maintenance of Subcapsular Sinus Macrophages Protects Against a Fatal Viral Infection Independent of Adaptive Immunity. *Immunity* (2012) 36:415–26. doi: 10.1016/j.immuni.2012.01.013
27. Xu HC, Huang J, Khairnar V, Duhan V, Pandyra AA, Grusdat M, et al. Deficiency of the B Cell-Activating Factor Receptor Results in Limited CD169+ Macrophage Function During Viral Infection. *J Virol* (2015) 89:4748–59. doi: 10.1128/JVI.02976-14
28. Bradley KC, Finsterbusch K, Schnepf D, Crotta S, Llorian M, Davidson S, et al. Microbiota-Driven Tonic Interferon Signals in Lung Stromal Cells Protect From Influenza Virus Infection. *Cell Rep* (2019) 28:245–56.e4. doi: 10.1016/j.celrep.2019.05.105
29. Ridiandries A, Tan JTM, Bursill CA. The Role of Chemokines in Wound Healing. *Int J Mol Sci* (2018) 19. doi: 10.3390/ijms19103217
30. Castleman MJ, Febbraio M, Hall PR. CD36 Is Essential for Regulation of the Host Innate Response to Staphylococcus Aureus Alpha-Toxin-Mediated Dermonecrosis. *J Immunol* (2015) 195:2294–302. doi: 10.4049/jimmunol.1500500
31. Yasuda T, Ura T, Taniguchi M, Yoshida H. Intradermal Delivery of Antigens Enhances Specific IgG and Diminishes IgE Production: Potential Use for Vaccination and Allergy Immunotherapy. *PLoS One* (2016) 11:e0167952. doi: 10.1371/journal.pone.0167952
32. Bernhard CA, Ried C, Kochanek S, Brocker T. CD169+ Macrophages are Sufficient for Priming of CTLs With Specificities Left Out by Cross-Priming Dendritic Cells. *Proc Natl Acad Sci USA* (2015) 112:5461–6. doi: 10.1073/pnas.1423356112
33. van Dinther D, Veninga H, Iborra S, Borg EGF, Hoogterp L, Olesek K, et al. Functional CD169 on Macrophages Mediates Interaction With Dendritic Cells for CD8(+) T Cell Cross-Priming. *Cell Rep* (2018) 22:1484–95. doi: 10.1016/j.celrep.2018.01.021
34. Subramanian A, Tamayo P, Mootha VK, Mukherjee S, Ebert BL, Gillette MA, et al. Gene Set Enrichment Analysis: A Knowledge-Based Approach for Interpreting Genome-Wide Expression Profiles. *Proc Natl Acad Sci USA* (2005) 102:15545–50. doi: 10.1073/pnas.0506580102

Conflict of Interest: The authors declare that the research was conducted in the absence of any commercial or financial relationships that could be construed as a potential conflict of interest.

Publisher's Note: All claims expressed in this article are solely those of the authors and do not necessarily represent those of their affiliated organizations, or those of the publisher, the editors and the reviewers. Any product that may be evaluated in this article, or claim that may be made by its manufacturer, is not guaranteed or endorsed by the publisher.

frontiers | Frontiers in Immunology

TYPE Original Research
PUBLISHED 29 July 2022
DOI 10.3389/fimmu.2022.886468

OPEN ACCESS

EDITED BY
Marcello Chieppa,
University of Salento, Italy

REVIEWED BY
Carlo De Salvo,
Case Western Reserve University, United States
Alessandro Miraglia,
University of Salento, Italy

*CORRESPONDENCE
Amedeo Amedei
amedeo.amedei@unifi.it

SPECIALTY SECTION
This article was submitted to Mucosal Immunity, a section of the journal Frontiers in Immunology

RECEIVED 30 March 2022
ACCEPTED 30 June 2022
PUBLISHED 29 July 2022

CITATION
Russo E, Cinci L, Di Gloria L, Baldi S, D'Ambrosio M, Nannini G, Bigagli E, Curini L, Pallecchi M, Andrea Arcese D, Scaringi S, Malentacchi C, Bartolucci G, Ramazzotti M, Luceri C, Amedei A and Giudici F (2022) Crohn's disease recurrence updates: first surgery *vs.* surgical relapse patients display different profiles of ileal microbiota and systemic microbial-associated inflammatory factors. *Front. Immunol.* 13:886468. doi: 10.3389/fimmu.2022.886468

Crohn's disease recurrence updates: first surgery *vs.* surgical relapse patients display different profiles of ileal microbiota and systemic microbial-associated inflammatory factors

Edda Russo[1], Lorenzo Cinci[2], Leandro Di Gloria[3], Simone Baldi[1], Mario D'Ambrosio[2,4], Giulia Nannini[1], Elisabetta Bigagli[2], Lavinia Curini[1], Marco Pallecchi[2], Donato Andrea Arcese[1], Stefano Scaringi[1], Cecilia Malentacchi[3], Gianluca Bartolucci[2], Matteo Ramazzotti[3], Cristina Luceri[2], Amedeo Amedei[1]* and Francesco Giudici[1]

[1]Department of Experimental and Clinical Medicine, University of Florence, Florence, Italy, [2]Department of Neurosciences, Psychology, Drug Research and Child Health (NEUROFARBA), University of Florence, Florence, Italy, [3]Department of Biomedical, Experimental and Clinical Sciences "Mario Serio", University of Florence, Florence, Italy, [4]Enteric Neuroscience Program, Department of Medicine, Section of Gastroenterology and Hepatology, Mayo Clinic, Rochester, MN, United States

Background and aims: Crohn's disease (CD) pathogenesis is still unclear. Remodeling in mucosal microbiota and systemic immunoregulation may represent an important component in tissue injury. Here, we aim to characterize the ileal microbiota in both pathological and healthy settings and to evaluate the correlated systemic microbial-associated inflammatory markers comparing first-time surgery and relapse clinical conditions.

Methods: We enrolled 28 CD patients at surgery; we collected inflamed and non-inflamed mucosa tissues and blood samples from each patient. Bacterial wall adherence was observed histologically, while its composition was assessed through amplicon sequencing of the 16S rRNA gene. In addition, we evaluated the systemic microRNA (miRNA) using quantitative real-time PCR amplification and free fatty acids (FFAs) using gas chromatography–mass spectroscopy.

Results: The total number of mucosal adherent microbiota was enriched in healthy compared to inflamed mucosa. In contrast, the phylum *Tenericutes*, the family *Ruminococcaceae*, and the genera *Mesoplasma* and *Mycoplasma*

were significantly enriched in the pathological setting. Significant microbiota differences were observed between the relapse and first surgery patients regarding the families *Bacillaceae 2* and *Brucellaceae* and the genera *Escherichia/Shigella*, *Finegoldia*, *Antrobacter*, *Gemmatimonas*, *Moraxella*, *Anoxibacillus*, and *Proteus*. At the systemic level, we observed a significant downregulation of circulating miR-155 and miR-223, as well as 2-methyl butyric, isobutyric, and hexanoic (caproic) acids in recurrence compared to the first surgery patients. In addition, the level of hexanoic acid seems to act as a predictor of recurrence risk in CD patients (OR 18; 95% confidence interval 1.24–261.81; p = 0.006).

Conclusions: We describe a dissimilarity of ileal microbiota composition comparing CD and healthy settings, as well as systemic microbial-associated inflammatory factors between first surgery and surgical relapse. We suggest that patterns of microbiota, associated with healthy ileal tissue, could be involved in triggering CD recurrence. Our findings may provide insight into the dynamics of the gut microbiota–immunity axis in CD surgical recurrence, paving the way for new diagnostics and therapeutics aimed not only at reducing inflammation but also at maintaining a general state of eubiosis in healthy tissue.

KEYWORDS

Crohn's disease, recurrence, microbiota, miRNA, free fatty acids, SCFA

Introduction

Inflammatory bowel disease (IBD), which includes Crohn's disease (CD) and ulcerative colitis (UC), is defined by intermittent chronic inflammation of the gastrointestinal system, resulting in bowel damage. CD, a multifactorial disorder that causes significant life-long impairment, commonly begins in young adulthood and is accompanied by periods of remission and recurrence (1). Nevertheless, surgical recurrence, or the necessity for a further operation, has been reported in 25% to 45% of patients within 10 years following the initial bowel resection (2). The transmural and segmental inflammation in CD is typically concentrated in the terminal ileum, but the pathophysiology remains unknown. Moreover, the drivers of recurrence following ileocolonic resection (ICR) remain hypothetical and challenging.

Current data have suggested that a complex interplay of genetic, epigenetic, microbial, metabolic, and environmental factors promotes, at the gut level, aberrant innate immune responses, as reviewed in Zheng et al. (3). In fact, mucosal immunoregulation dysfunctions may play a role in the etiology of chronic intestinal inflammation and tissue damage (4). Moreover, several reports have shown that the multifaceted regulatory mechanisms linked with mucosal immunity against microbial flora, epithelial barrier dysfunction, and environmental influences can cause an abnormal inflammatory response, contributing to CD pathogenesis (5–7). Furthermore, in CD patients, the richness of mucosal microbiota (and its metabolites) was strongly linked with disease activity or exacerbations (8).

Increasing data point to the importance of gut microbiota (GM) alterations in CD pathogenesis (9), involving decreased abundance of *Bacteroides*, *Firmicutes*, *Clostridia*, and *Lactobacillus*, *Ruminococcaceae* and increased abundance of *Gammaproteobacteria* and *Enterobacteriaceae* (10). Some studies have examined the gut microflora at surgery to find microbial profiles associated with remission or recurrence (11). It has been observed that ileal mucosa–associated microflora changed significantly after surgery, including variations between patients with and without recurrence (12, 13). Through a comprehensive analysis of ileal tissue layers, inflammatory response, and microbiota composition, we have recently reported that the phylum *Tenericutes* and the genera *Mesoplasma* and *Mycoplasma* were significantly augmented in the inflamed tissues (14). Moreover, we reported different and significant cytokine levels at the three tissue layers (mucosa, submucosa, and serosa) and differences in bacterial flora composition between the relapse and first surgery patients (14).

Other key factors acting as regulators of inflammatory responses and metabolic pathways are free fatty acids (FFAs),

classified into short–chain fatty acids (SCFAs), medium–chain fatty acids (MCFAs), and long–chain fatty acids (LCFAs). SCFAs are produced as a result of bacterial and host metabolism. Recent studies have shown that SCFAs and LCFAs play a vital role in CD pathophysiology and development by various mechanisms, i) affecting pro– and anti–inflammatory mediators, ii) maintaining intestinal homeostasis, and iii) regulating gene expression. In particular, SCFAs and LCFAs activate signaling cascades that control immune functions through interaction with cell surface free fatty acid receptor, while SCFAs are crucial to maintaining the host's normal gut physiology and metabolic functions and that a part of them enters the systemic circulation (15).

Additionally, several studies suggest that the GM may interact also with microRNAs (miRNAs) in regulating host pathophysiology and many immune processes. However, how miRNA circuits orchestrate aberrant intestinal inflammation during inflammatory CD and recurrence phenomena is poorly defined. Furthermore, miRNAs can regulate bacterial composition by specifically targeting bacterial genes, and they can be used as markers of microbial fluctuations in intestinal pathologies (16). In addition, the GM has been found to regulate the host miRNA expression, primarily through the GM metabolites, such as lipopolysaccharide (LPS) and SCFAs such as butyrate (17, 18). Specific miRNAs are related to microbiome and inflammatory processes, including miR–223 and miR–155 (19). Chief among these, miR–223 is emerging as an important regulator of the innate immune system and the response to bacterial stimulation (20, 21), the upregulation of miR–223 is reported as a novel biomarker in subsets of IBD patients (22) as well as in preclinical models of intestinal inflammation (19, 23). miR–155 influences numerous biological functions including inflammatory response, intracellular signaling cascades, regulation of cytokine production, and response to microbiota (24–27). miR–423 is also a pro–inflammatory miRNA, tightly controlled by IL–21 in IBD. It directly targets claudin–5, a critical family member in the maintenance of normal intestinal barrier property, and regulates the NF–κB/MAPK/JNK signaling pathway (28).

This emerging evidence suggests that "taking an instant picture" of all the above mentioned microbial, metabolic, and epigenetic factors, involved in the intricate transmural and systemic inflammatory process, might be useful to deepen our understanding of the CD recurrence dynamics.

Starting from these premises, through a holistic and innovative analysis of ileal microbiota composition, circulating FFAs, and miRNAs, we investigated the mutual dialogue between CD microbial and inflammatory factors, comparing healthy and pathological tissues as well as first surgery and relapse conditions.

Our results showed a different regulation of the gut microbiota–immunity axis, corroborating our previous results (14) and expanding them with new details and perspectives on circulating microbiota–related factors (SCFAs and miRNAs), at first surgery time and relapse conditions. Moreover, we observed a potential involvement of microbiome patterns, associated to healthy ileal tissue, in triggering recurrence–linked determinants, suggesting that not only anti–inflammatory therapies but also GM eubiosis maintenance may be crucial for early treatment adjustments.

Materials and methods

Patients

We enrolled 28 adult patients (16 men and 12 women, mean age 46.82 years, age range 19–72 years) affected by ileal CD (Table 1) at "Careggi University Hospital" (Florence, Italy) between 2018 and 2019, after obtaining informed consent and approval of the local ethics committee (study no. 2016.0842). Among these 28 patients, the clinical and anamnestic data, as well as the ileal microbiome sequences from 10 patients, were previously included in a study already published by our group (14) describing the interplay between ileal cytokines at three different tissue layers (mucosa, submucosa, and serosa) and mucosal microbiota, in first surgery and relapse CD.

As reported in our previous study (14), ileal CD diagnosis had been performed by clinical/endoscopic criteria and confirmed by histological analysis. The inclusion criteria were as follows: i) diagnosis of IBD for at least 3 months according to the standard Montreal classification (29), ii) patients with IBD with ileocolic localization, and iii) patients aged 25–70 years. The exclusion criteria include the following: i) use of antibiotics or any other probiotic bacterial supplement in the previous 1 month, ii) use of non–steroidal anti–inflammatory drugs (NSAIDs) in the previous 1 month, iii) reported recent diagnosis (less than 3 months) of bacterial or parasitic infections of the gastrointestinal tract, and iv) trip to exotic areas in the last 5 years. Patients have not been treated with antibiotics, aminosalicylates or immunosuppressants, biological therapy, and steroids for at least 3 weeks before the ICR.

Bacterial wall adherence

Samples of affected (based on visual expert inspection) and apparently normal mucosa, harvested at surgery, were fixed in Carnoy's solution and embedded in paraffin. Sections (4 μm) were stained with 2.5 ng/ml of ethidium bromide and observed with an Olympus BX63 microscope equipped with a metal halide lamp (Prior Scientific Instruments Ltd., Cambridge, United Kingdom) and a digital camera (Olympus XM10, Olympus, Milan, Italy).

Ten photomicrographs were randomly taken for each section at ×400 magnification, and the number of adherent

10.3389/fimmu.2022.886468

TABLE 1 Clinical features of the enrolled patients.

No.	Sex[a]	CD site[b]	Age of CD onset	Surgery	Disease behavior[c]	Smoking status[d]	Familiarity	BMI	Malnutrition according to ESPEN 2015	CD duration (years)	Age at surgery (years)	Period from previous surgery (years)	Comorbidities[e]	CD therapies
1	M	L2	27	First surgery	B2	No	No	22.4	No	4	31	–	–	Infliximab, methylprednisolone
2	M	L2	23	First surgery	B2, B4	No	No	17.4	Yes	11	27	–	–	Methylprednisolone
3	M	L2	18	First surgery	B2, B3	No	No	20.7	No	1	19	–	–	–
4	M	L2	11	First surgery	B2, B3	No	No	22.1	No	1	30	–	–	Adalimumab
5	M	L2	16	Relapse	B3	Cur	No	16.8	Yes	29	45	4	–	Azathioprine, vedolizumab
6	M	L1	37	First surgery	B2	Ex	No	32.8	No	13	50	–	BS, H, OSAS	Mesalamine, omeprazole, prednisone
7	M	L1	17	Relapse	B3	Ex	No	20.1	No	23	40	9	O	Risedronate
8	F	L2	40	First surgery	B2	No	No	30.5	No	1.5	41	–	A, AS	Beclomethasone
9	F	L1	63	First surgery	B2	No	No	24.2	No	7	70	–	–	Mesalamine, sulfasalazine
10	F	L2	40	First surgery	B2, B3	No	No	18.7	No	10	50	–	–	Mesalamine
11	M	L2	24	Relapse	B2	No	No	23.3	No	16	40	16	–	Mesalamine
12	M	L2	28	Relapse	B2, B3	No	No	27.9	No	33	61	19	AS	–
13	F	L2	37	Relapse	B2	No	No	21.6	No	12	49	12	–	Prednisone
14	M	L2	40	Relapse	B2	No	No	20.1	No	12	53	0.5	–	Mesalamine
15	F	L2	42	Relapse	B2	No	No	16.6	Yes	29	71	21	MD	Prednisone
16	F	L2	64	First surgery	B2	Yes	Yes	21.3	Yes	5	69	–	H	–
17	M	L1	62	First surgery	B2	No	No	23.9	Yes	2	64	–	DM, GA, HHG	Allopurinol, budesonide, mesalamine
18	F	L2	21	Relapse	B3, B4	No	No	23.5	No	36	57	36	EA, H	Mesalamine, ranitidine
19	M	L1	36	First surgery	B2	Ex	No	22,2	No	4	40	–	–	Budesonide
20	F	L1	17	Relapse	B2, B3	No	No	21	No	1	17	1	–	Budesonide
21	M	L2	47	First surgery	B2	No	No	20.9	No	12	60	12	–	Mesalamine, prednisone
22	F	L2	29	First surgery	B2	Yes	No	22.8	No	28	57	–	–	–
23	F	L2	32	Relapse	B2	Yes	No	21.5	No	13	45	13	–	–
24	F	L2	21	First surgery	B2	No	No	20	No	1 month	21	–	–	Methylprednisolone, piperacillin/ tazobactam
25	M	L1	13	First surgery	B2	Yes	No	27.8	No	13	26	–	HZ	Adalimumab
26	M	L1	49	First surgery	B2	Yes	No	21.1	No	5	54	–	P	–
27	M	L1	37	First surgery	B3	No	No	19.1	No	6	43	–	–	Mesalamine
28	M	L1	34	Relapse	B3	Yes	No	18.8	No	13	47	13	–	Prednisone

[a]Sex: M, male, F, female. [b]CD site: L1, terminal ileum, L2, ileum colon. [c]Disease behavior: B1, non–stricturing, non–penetrating, B2, stricturing, B3, penetrating, B4, perianal disease. [d]Smoking status: No, non–smoker, Ex, ex–smoker, Cur, current smoker. [e]Comorbidities: A, asthma, AS, ankylosing spondylitis, BS, Brown–Sequard syndrome, DM, Dupuytren's morbus, EA, enteropathic arthritis, GA, gouty arthritis, H, hypertension, MD, major depression, NHG, non–Hodgkin lymphoma, O, osteoporosis, OSAS, obstructive sleep apnea syndrome, HZ, herpes zoster, P, psoriasis.

bacteria was evaluated using ImageJ 1.33 image analysis software (http://rsb.info.nih.gov/ij).

Characterization of paraffin–embedded tissue microbiota

The microbiota of paraffin–embedded tissue was assessed as described in our previous study (14). In detail, for each sample, the first few scrolls from the paraffin–embedded blocks were discarded and then eight 10–µm scrolls were cut and placed into sterile 2–ml centrifuge tubes. For deparaffinization, we used xylene (Sigma–Aldrich, MO, USA) for all extractions. DNA was extracted using the QIAamp DNA FFPE tissue kit (Qiagen, CA, USA) according to the manufacturer's protocol. Nucleic acids were eluted in a 50–µl elution buffer following a 5–min column incubation at room temperature. The microtome was cleaned with DNA AWAY (Thermo Scientific, MA, USA) between each sample, and the equipment was regularly tested using sterile swabs that also underwent sequencing as controls. The quality and quantity of extracted DNA were assessed using the NanoDrop ND–1000 (Thermo Fisher Scientific, Waltham, MA, USA) and the Qubit Fluorometer (Thermo Fisher Scientific), respectively. Then, genomic DNA was frozen at −20°C.

The extracted DNA samples were sent to IGA Technology Services (Udine, Italy) where amplicons of the variable V3–V4 region of the bacterial 16S rRNA gene were sequenced in paired–end (2 × 300 cycles) on the Illumina MiSeq platform, according to the Illumina 16S rRNA amplicon.

The bioinformatic analysis of ileal microbiome sequences was performed following the methods already described in our previous studies (14, 30). In detail, regarding the sequencing library preparation protocol (31), raw sequences were processed following the software pipeline MICCA (32). Paired–end reads were assembled using the "mergepairs" command, maintaining a minimum overlap of 100 bp and an edit distance in the maximum overlap of 32 bp. Subsequently, the sequences were cut with the "trim" command in order to remove the primers and eventually eliminate the reads with imperfections in primer sequences. All the reads with a length lower than 350 bp and with an error rate higher than or equal to 0.5 were removed with the "filter" command. The cleaned reads were eventually merged into a single file with the "merge" command and transformed into a fasta file. The operational taxonomic units (OTUs) were generated using the "out" command in "denovo_greedy" mode, setting a 97% identity and performing an automatic removal of chimeras with the "–c" option. The longest sequence of each OTU was used for the taxonomic assignment using the "classify" command in "rdp" mode, i.e., using the RDP Bayesian classifier that is able to obtain classification and confidence for taxonomic ranks up to genus.

Statistical analyses on the bacterial community were performed in R (R Core Team, 2014) with the help of the packages phyloseq 1.26.1 (33), DESeq2 1.22.2 (34), breakaway 4.6.16 (35), and other packages satisfying their dependencies, particularly vegan 2.5–5 (35). Rarefaction analysis on OTUs was performed using the function rarecurve (step 50 reads), further processed to highlight saturated samples (arbitrarily defined as saturated samples with a final slope in the rarefaction curve with an increment in OTU number per reads <1e–5). For the cluster analysis (complete clustering on Euclidean distance) of the entire community, the OTU table was first normalized using the total OTU counts of each sample and then adjusted using square root transformation. The coverage was calculated by Good's estimator using the formula: $(1 - n/N) \times 100$, where n is the number of sequences found once in a sample (singletons), and N is the total number of sequences in that sample.

Richness, Shannon, Chao 1, and evenness indices were used to estimate bacterial diversity in each sample using the function estimate_richness from phyloseq (33). The evenness index was calculated using the formula $E = S/\log(R)$, where S is the Shannon diversity index and R is the number of OTUs in the sample. Differences in all indices between CD and healthy tissues were tested using a paired Wilcoxon signed–rank test. Sample richness was further measured using the estimator and its associated error was introduced in the breakaway package (35). The function betta_random of breakaway was further used to evaluate the statistical differences in richness between paired–by–patient samples. The differential analysis of abundance at the OTUs as well as at the different taxonomic ranks (created using the tax_glom function in phyloseq) was performed with DESeq2 (34) using two groups blocked by patient design in order to perform a paired test when needed (14).

miRNA analyses

Total RNA was extracted from 200 µl of plasma by using TRIzol (Invitrogen, Life Technologies, Carlsbad, CA, USA), according to the instructions provided by the manufacturer.

For miRNA–specific cDNA synthesis, total RNA was reverse–transcribed using the miRCURY LNA RT kit (Qiagen). Quantitative real–time PCR amplification and analysis were performed using the Rotor–Gene Q thermal cycler (Qiagen, Hilden, Germany), the miRCURY LNA SYBR® Green PCR kit, and the specific miRCURY LNA miRNA PCR Assay for miR–423, miR–223–3p, and miR–155–3p. RNU–6B was used as endogenous control and relative expression levels among miRNAs and RNU–6B were calculated using the 2^{-dCT} method.

Evaluation of FFAs by GC–MS analysis

Analysis of the FFAs was performed using an Agilent GC–MS system composed of an HP 5971 single quadrupole mass

spectrometer, an HP 5890 gas chromatograph, and an HP 7673 autosampler, according to previously described protocols (36). Briefly, just before the analysis, each sample was thawed and the FFAs were extracted as follows: an aliquot of 300 µl of serum sample was added to 10 µl of ISTD mixture, 100 µl of tert–butyl methyl ether, and 20 µl of 6 M HCl + 0.5 M NaCl solution in a 0.5–ml centrifuge tube. Afterward, each tube was stirred in a vortex for 2 min and centrifuged at 10,000 rpm for 5 min, and finally, the solvent layer was transferred to a vial with a microvolume insert and analyzed.

Statistical analysis

The software GraphPad Prism 7.00 and Statgraphics Centurion XVI were used for statistical data analysis. Categorical variables were expressed as frequency with proportions and compared by chi–square or Fisher's exact test, when necessary. Continuous data were presented as mean ± standard deviation (SD) or median with interquartile range (IQR) and compared using the Mann–Whitney/Kruskal–Wallis test or *t*–test/one–way ANOVA, depending on data distribution. Linear regression was applied to identify the correlation between two variables.

The odds ratio and 95% confidence intervals for recurrence risk were calculated using logistic regression analysis. p <0.05 was considered statistically significant.

Correlations between FFAs and taxonomies that varied significantly between the first operation and surgery relapse patients (both in CD tissue and healthy tissue) were evaluated using Spearman's rank correlation analysis, under the assumption that there is a non–linear relationship between the examined variables. Correlations with adjusted *p*–value lower than 0.05 were considered significant.

Results

Microbiota analysis in CD *vs*. healthy ileal mucosa

Distinct bacterial wall adherence in CD *vs*. healthy ileal mucosa

In the first part of the study, we investigated bacterial wall adherence in healthy and CD mucosal paraffin–embedded tissues, collected at the time of ICR from 24 out of 28 patients. In detail, using a microscope, we evaluated the number of total adherent bacteria and we were able to perform a morphological distinction between cocci and bacilli. The number of observed total bacteria was enriched in healthy *vs*. CD tissues (p = 0.03) (Figure 1) suggesting a dysbiotic condition. Moreover, bacteria having bacillus morphology were significantly enriched in healthy *vs*. CD tissues (p = 0.021) (Figure 1), while a trend was observed in the number of cocci (p = 0.057) (Figure 1). As the most represented ileal bacteria having bacillus morphology are *lactobacilli* and *bifidobacteria*, known to be inflammation–suppressing taxa, their depletion in the CD setting suggests a loss of microbial defense against tissue inflammation. Representative images of bacterial wall adherence are shown in Figure 1 (a and b).

Dysbiotic variation of the ileal microbiota

Since we detected significant total bacterial count variations between the affected and healthy mucosa tissues, we deeply characterized the resident ileal microbial communities of retrospectively diagnostic paraffin–embedded sections in 23 CD (of the 28 samples, 5 showed insufficient amount for analysis) patients using 16S rRNA amplicon sequencing.

We obtained a total of 4,051,315 reads, and after all the steps of preprocessing (pair merging, trimming, quality filtering, and chimera detection), a total of 2,325,681 (57.4%) were available for further analysis. The samples showed a Good's coverage ranging from 99.90% to 99.98% indicating that less than 1% of the reads in a given sample came from OTUs that appear only once in that sample.

The alpha diversity of the samples displayed significant differences between CD and healthy tissues for the Chao (p = 0.014) and Shannon indexes (p = 0.045) (Supplementary Figure 1), while no differences were observed for the evenness index. The differences in the Chao index may evidence that rare OTUs are enriched in healthy *vs*. CD tissues. The analysis of the taxonomic composition revealed that more than 89% of the sequences collected were classified into five phyla: *Proteobacteria* (50.6%), *Firmicutes* (14.1%), *Actinobacteria* (9.5%), *Cyanobacteria* (10.6%), and T*enericutes* (6.1%). The relative abundance of the five most represented microbial phyla in CD and healthy tissues is reported in Figure 2.

In detail, in the affected tissue, we observed a particular enrichment of the *Tenericutes* phylum which is relatively absent in healthy tissue (Figure 2). In addition, we also explored any genus differences between the two considered settings, and the relative abundance of the five most represented microbial genera in CD and healthy tissues is reported in Supplementary Figure 2. Notably, we observed a particular enrichment of the *Mesoplasma* genus (belonging to the *Tenericutes* phylum) which is relatively absent in non–inflamed tissue.

Moreover, PCoA analysis revealed significant differences between healthy *vs*. inflamed tissues (Figure 3), and it was possible to detect a clear clustering between the two groups. Finally, the paired comparison of the abundance of single OTUs revealed significant [$p < 0.05$, abs (logFC) ≥ 1] differences between the two sample groups.

In detail, the phylum *Tenericutes*, the class *Mollicutes*, the orders *Entomoplasmatales* and *Mycoplasmatales*, the families *Entomoplasmataceae* and *Mycoplasmataceae*, and the genera *Mesoplasma*, *Mycoplasma*, *Anoxibacillus*, *Ralstonia*, and

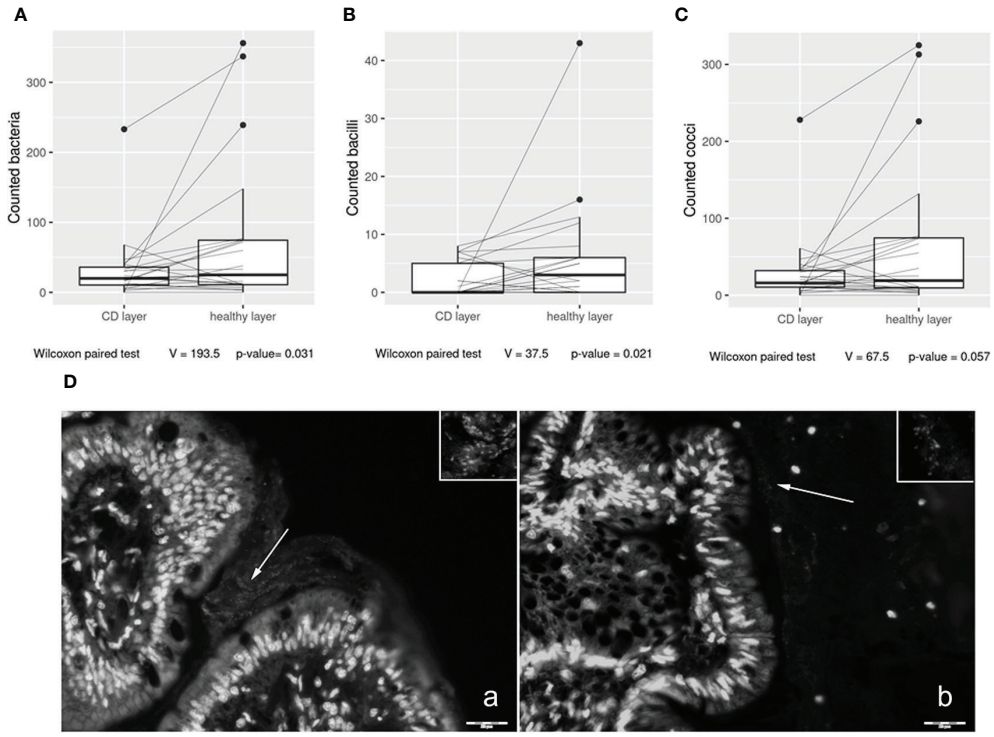

FIGURE 1
Box plot distribution of adherent bacteria counts **(A)**, bacilli **(B),** and cocci **(C)** identified in healthy tissues and Crohn's disease (CD) samples. Analyses were assessed using the paired Wilcoxon signed–rank test, and *p*–values less than 0.05 were considered statistically significant. Mucosa–associated bacteria in histological samples **(D)**. Images collected at ×400 magnification indicate **(A)** H mucosa sample and **(B)** CD sample. White arrows: bacteria present in the mucus contiguous to the mucosa. Insert magnification: bacteria. Scale bar: 20 μm.

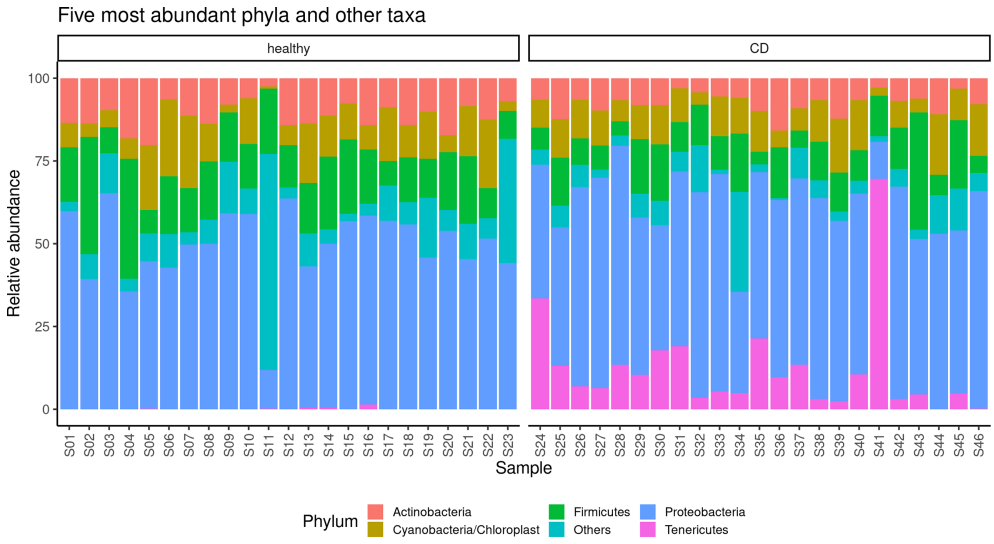

FIGURE 2
Taxonomic composition of the paraffin–embedded ileal samples in ileal and CD tissues. The stacked bar plot shows the relative abundance of the five more abundant bacterial phyla in each sample, the "Others" group contains phyla with ranks below five.

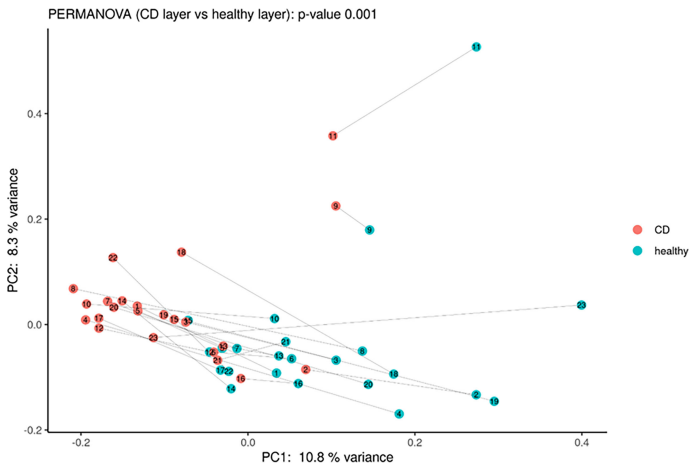

FIGURE 3
Principal coordinate analysis using Bray–Curtis dissimilarity as a distance metric on square root–transformed percent abundance of identified OTUs showing permuted *p*–value of general β dispersion and pairwise β dispersion of CD and healthy groups. The lines connect the samples from the same patient.

Tepidimonas were significantly higher in CD tissue (Figure 4). On the contrary, the class *Negativicutes*, the orders *Pasteurellales*, *Rodospirillales*, and *Selenomonadals*, the families *Prevotellaceae*, *Flavobacteriaceae*, *Fusobacteriaceae*, *Pasteurellaceae*, *Caulobacteriaceae*, *Veillonellaceae*, and *Staphylococcaceae*, and the genera *Fusobacterium*, *Prevotella*, *Neisseria*, and *Gemella* were significantly lower in CD tissue (Figure 4). This result indicates a different regulation of the mucosal microbial population in the two different settings, possibly due to the different inflammatory environment that guides the selection of certain bacterial populations over others. The graphical results of the differential analysis of all taxonomic ranks are available in Figures 4B.

Differences between first surgery *vs*. surgical relapse

Dissimilar composition of the ileal microbiota

Based on clinical characteristics, we divided the patients into two groups (a: first surgery and b: relapse) and compared the respective microbial patterns in CD and healthy tissues. Starting from the different comparisons, we have documented some significant variations.

In the healthy tissue, we observed a trend ($p = 0.06$) in the number of observed total bacteria and cocci, enriched in the first surgery patients (Figures 5A, B), while in the affected tissue, no significant differences were detected (data not shown).

The alpha diversity of the samples displayed no significant differences for Chao, Shannon, and evenness indexes (Supplementary Figures 3A) in CD and healthy tissues for both patient groups (Supplementary Figures 3A). In addition, beta diversity displayed no significant clustering in CD and healthy tissues for both subsets of patients (Supplementary Figures 4A).

However, the differential abundance analysis revealed significant differences. In detail, regarding the CD tissue, the family *Bacillaceae 2* and the genus *Nocardioides* were significantly higher in the first surgery compared to the relapse patients, on the contrary, the family *Brucellaceae* and the genera *Escherichia/Shigella*, *Finegoldia*, and *Kocura* were significantly enriched in the relapse condition (Figure 6).

The analysis of the healthy tissue revealed that all differences were focused on several genera: in particular, *Antrobacter*, *Capnocytophaga*, *Gemmatimonas*, *Moraxella*, and *Novosphingobium* were all significantly augmented in the first surgery patients, while *Acholeplasma*, *Anoxibacillus*, *Cloacibacterium*, and *Proteus* were decreased (Figure 6). The meaning of these data may be linked to a perturbation of ileal microbiota architecture at surgery time, with a consequent different microbiota recolonization after ICR.

Discrepancies in the plasma levels of miR–155, miR–223, and miR–423

Supposing that significant variations in ileal microbial architecture could be mirrored in circulating factors, associated with GM composition and expression, we selected three specific circulating miRNAs related to GM activity and the regulation of inflammation (37). In detail, we measured miR–155, miR–223, and miR–423. We observed significant differences between the first surgery and relapse patients in terms of miR–223 ($p = 0.0273$) and miR–155 ($p = 0.0413$), both being downregulated in recurrence patients compared to

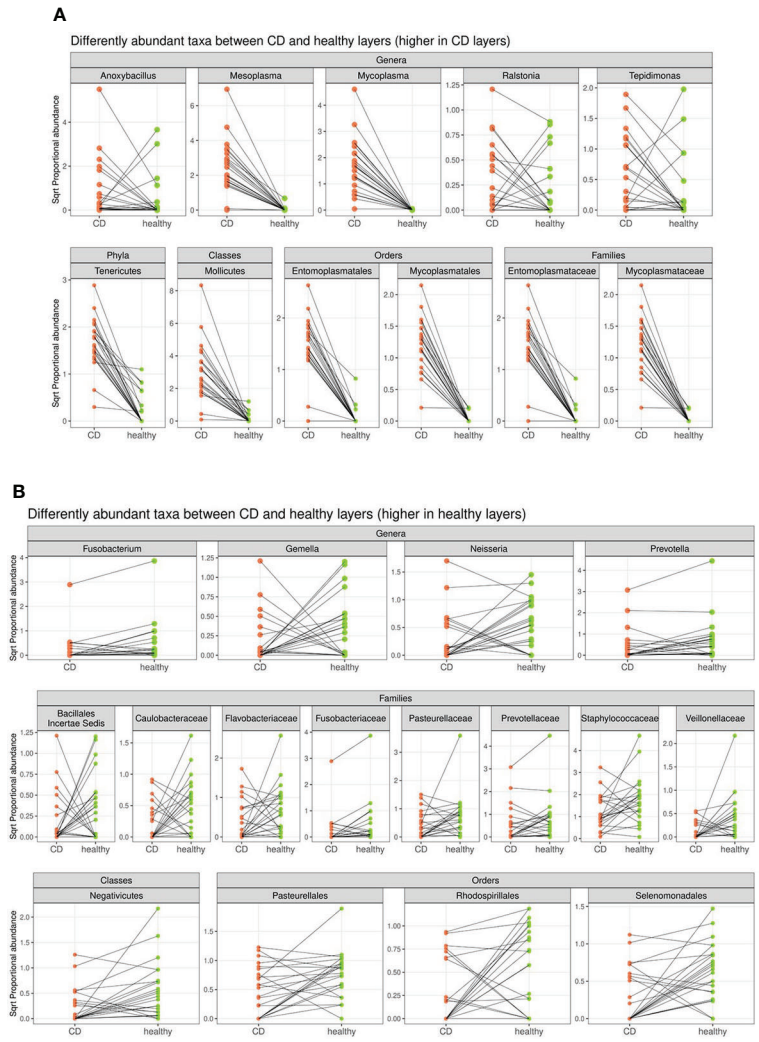

FIGURE 4
Segment plot depicting significantly different taxa (phylum, classes, families, orders, and genera) between CD **(A)** and healthy tissues **(B)**. Lines connect paired samples and highlight the differences in normalized abundance for the indicated rank. Red or blue colors highlight a decrease or increase in CD *vs.* healthy tissues, respectively. Numbers on the top–left corner represent counts of decreased (red) and increased (blue) measurement for paired samples. Plot titles report the shrunken log2 fold change between inflamed and non–inflamed tissues (according to the DESeq2 function lfcShrink). All taxa tested have a *p*–value <0.05.

patients at first surgery (Figures 7A). miR–423 exhibited a similar trend without reaching statistical significance (Figure 7). This result suggested the activation of different signaling pathways in relapse patients compared to those at first surgery. In addition, this outcome may also indicate a dissimilar regulation of the activated inflammatory pathways involved in CD recurrence compared to first surgery.

Different serum FFA profiles

The production of SCFAs, the major bacterial fermentative end–products, reflects the intestinal microbiota composition and especially its function. In addition, given that SCFAs are crucial to health, maintaining the host gut physiology, and that a part of them enters the systemic circulation (15), it is tempting to speculate that GM composition could be also related to FFA levels. We then performed qualitative and quantitative analyses of serum FFAs, namely, linear SCFAs (acetic, propionic, butyric, and valeric acids), branched SCFAs (isobutyric, isovaleric, 2–ethylhexanoic, 2–methylbutyric, and cyclohexanoic acids), MCFAs (hexanoic, heptanoic, octanoic, nonanoic, decanoic, and dodecanoic acids), and LCFAs (tetradecanoic, hexadecenoic, and octadecanoic acids), between the first surgery and relapse patients. We observed significantly higher levels of two branched SCFAs, notably 2–methyl butyric

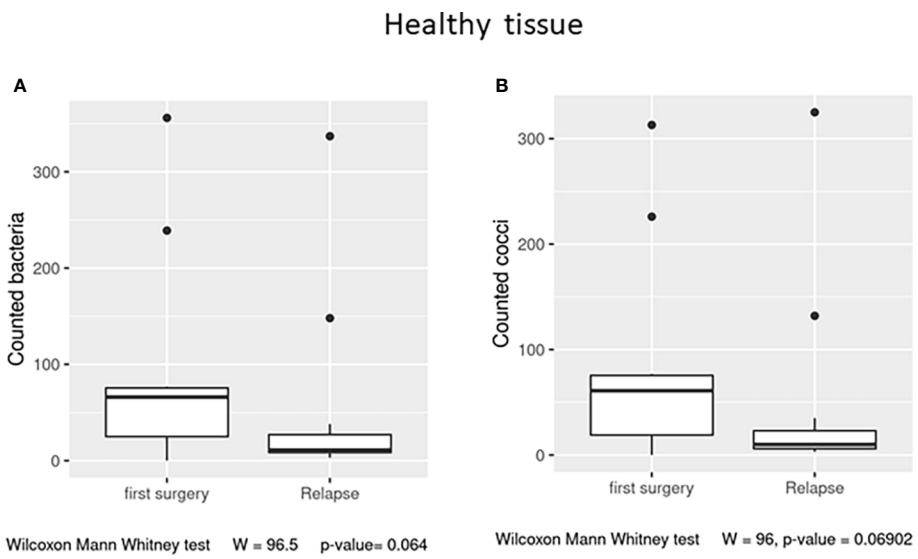

FIGURE 5
Box plot distribution of adherent bacteria counts **(A)** and cocci **(B)** identified in healthy samples from the first surgery and relapse patients. Analyses were assessed using the Mann–Whitney paired test, and *p*–values less than 0.05 were considered statistically significant.

(p = 0.0380) and isobutyric acids (p = 0.0245), and one MCFA, namely, hexanoic acid (p = 0.0492), in relapse patients (Figure 8). The meaning of this result may be connected to a different expression of GM functionality between the first surgery and relapse patients.

Correlation between miRNA profile, FFAs, and ileal microbiota

Firstly, we correlated the levels of miR–155, miR–223, and miR–423 with FFA profiles. Among all the correlations, we identified only a negative association between miR–423 and the total amount of SCFA in the serum (p = 0.0463) (Figure 7).

Next, in order to assess particular associations between bacterial composition in ileal tissue and circulating bacterial metabolites, as well as miRNAs, we correlated the levels of the two SCFAs that were significantly changed between the first surgery and relapse patients (2–methyl butyric and isobutyric acids) with clades significantly altered in the same conditions (both CD and healthy settings). In addition, we also assessed the associations with hexanoic acid.

We documented the significant association only in the healthy setting, notably, the genus *Anoxybacillus* (greatly enriched in the healthy ileal tissue of relapse patients) was negatively correlated ($p < 0.05$) with circulating 2–methyl butyric and hexanoic acids (both reduced in the serum of relapse patients). The correlation heatmap in CD and healthy tissues is shown in Figure 9, and it is relevant because it compares the obtained Spearman correlations in the two analyzed settings, thus suggesting a potential involvement of healthy tissue microbiota in the regulation of circulating serum inflammatory markers.

In the same way, we correlated the significantly changed miRNAs between the first surgery and relapse patients (miR–223 and miR–155) with the abovementioned selected genera. However, any significant correlation was found (data not shown).

Risk factors for recurrence

By logistic regression analysis, among all the considered parameters, we identified only the serum hexanoic acid as the significant independent risk factor for surgical recurrence: patients with hexanoic acid <1.4 μM (median value) were at increased risk of recurrence compared to patients exhibiting higher serum level of this MCFA (OR 18, 95% confidence interval 1.24–261.81, p = 0.006). If confirmed by future validated data, this outcome suggests that monitoring of hexanoic acid level might be useful as a potential strategy for recurrence predictor.

Discussion

A deeper understanding of CD recurrence mechanisms may help clinicians refine treatment and improve outcomes. Recent evidence supports the key role of an aberrant immune response to the microbiota in the development of gut mucosal

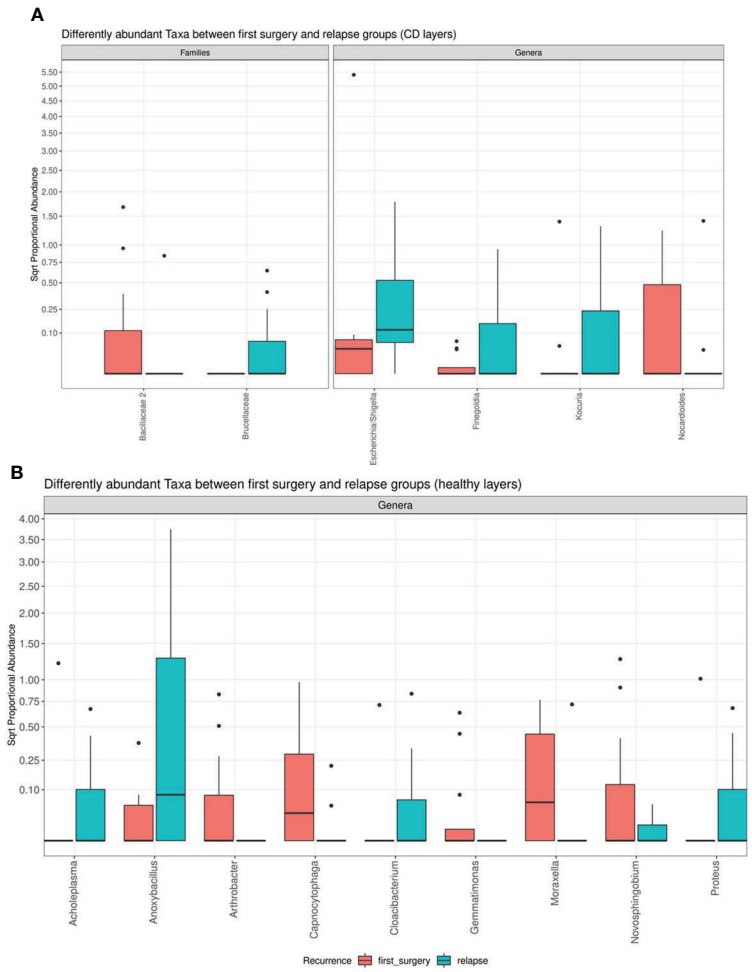

FIGURE 6
Box plot showing the results of taxa differential abundance analysis between the first surgery and relapse patients, respectively, in CD **(A)** and healthy tissues **(B)**. The *y*–axis has been scaled to improve the readability of values. All results have an adjusted *p*–value <0.05.

inflammation, in both CD pathogenesis and recurrence. However, the mechanisms regulating the interplay between the host immune system and ileal microbiota, as well as the specific changes occurring in GM composition and functionality, remain to be defined. To shed light on these intricate relationships between the actors of the "microbiota–immunity" axis, in our previous pilot study, we explored this connection at the tissue level, analyzing the molecular immune response distribution within the ileal layers and evaluating the correlated mucosal microbiota in pathological/healthy settings and in the first surgery/relapse clinical conditions (14). Having observed a dissimilarity of ileal cytokine distribution and mucosal microbiota composition in the first surgery and relapse patients, we wondered if even at the systemic level the microbiota–immunity axis could be differently regulated, leading to new possible recurrence circulating biomarkers' detection (such as miRNAs and FFAs).

To this aim, in this study, we explored the microbiome–immunity axis at the systemic level, in a larger number of patients (10 of the 28 patients were shared between the two studies). In detail, we assessed ileal microbiota composition, systemic functionality, and immunoregulation at the gene expression level in the first surgery and recurrence conditions and at the two different inflammatory tissue settings.

Firstly, the GM composition of CD patients was evaluated in paraffin–embedded materials. Several findings suggest that GM changes in CD, including decreased microbial diversity and relative abundance, particularly of bacteria (38). CD clinical lesions are usually seen in the distal ileum and colon, both of which have significant microbial concentrations. We investigated the bacterial wall adherence in healthy and CD ileal tissues, in line with previous results (38), we reported enrichment of total bacteria count in healthy tissue, with an increase in bacillus morphology. On the other

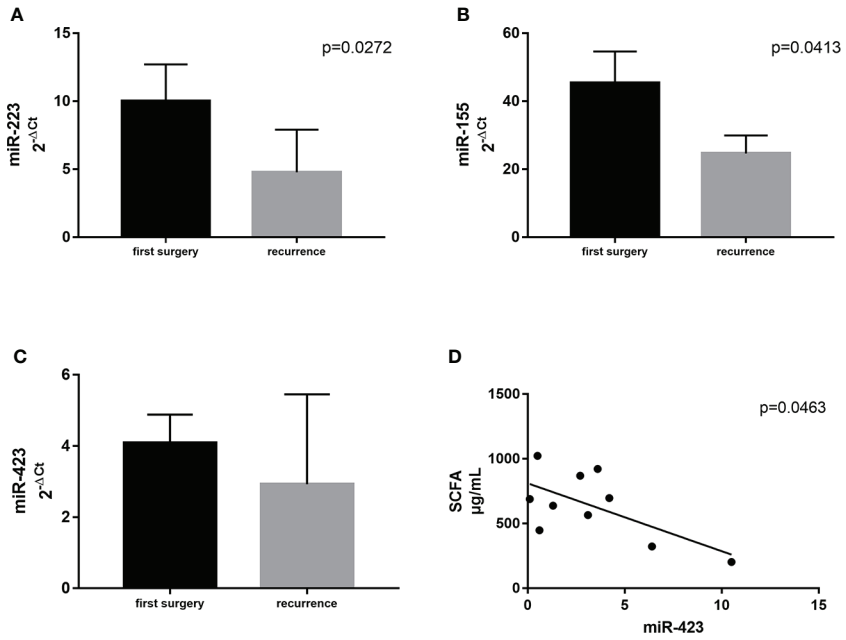

FIGURE 7
Expression levels of miR−223 **(A)** and miR−155 **(B)** in plasma samples from CD patients with surgical recurrence (*n* = 12) compared to those at first surgery (*n* = 16). Correlation between plasma levels of miR−423 and the total amount of SCFA in the serum of the same patient **(C)**. **(D)** Correlation between SCFA and miR−423. Data are expressed as mean ± SD.

hand, the pathological tissue appeared depleted of bacteria, suggesting a dysbiotic condition. Indeed, CD patients usually present dysbiosis and reduced biodiversity in the GM composition, linked to an increase in pro−inflammatory bacteria and a decrease in anti−inflammatory bacteria (39). So, in order to explore the taxonomy and, consequently, the inflammatory nature of adherent GM, we performed an in−depth taxonomic analysis. According to our previous pilot results (14), the majority of the sequences collected in both tissues (affected and healthy) were classified into five phyla: *Proteobacteria* (50.6%), *Firmicutes* (14.1%), *Actinobacteria* (9.5%), *Cyanobacteria* (10.6%), and T*enericutes* (6.1%). In general, CD patients usually show a decreased number of *Firmicutes* (40), on the other hand, the *Proteobacteria* phylum has a well−preserved ecological pattern associated with inflammation (41). Nevertheless, we are aware that the quantity of *Pseudomonas*, a typical paraffin−embedded contaminant genus, may have an effect on the amounts of *Proteobacteria* detected (42), as we also reported in our previous study (14).

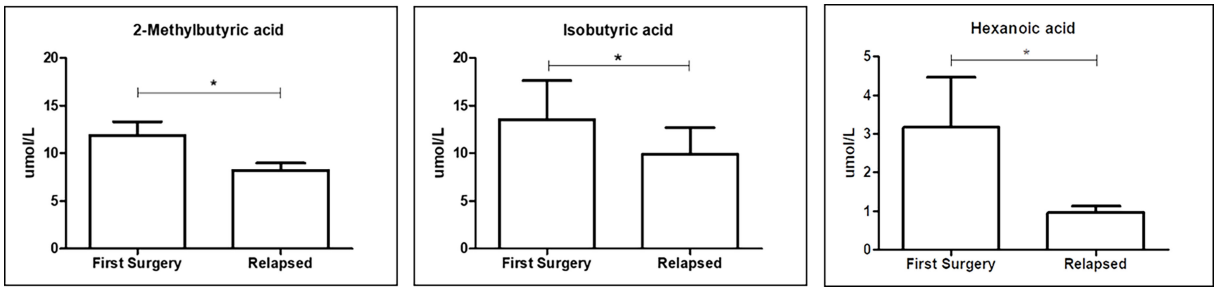

FIGURE 8
Box plot reporting the statistically significantly different FFAs between the first surgery and relapse patients. Analyses were assessed using the Mann−Whitney test, and *p*−values less than 0.05 were considered statistically significant. The asterisks (*) represent p−values: *p < 0.05.

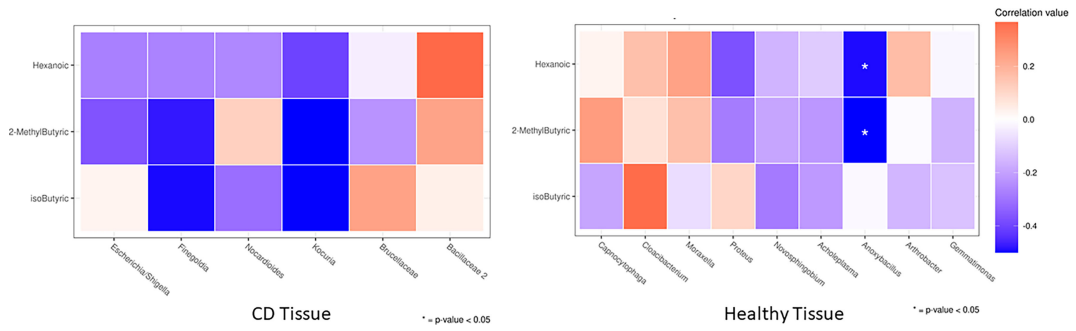

FIGURE 9
Heatmap of the Spearman correlation values between significantly changed FFAs (rows) and taxa that were differently abundant in DESeq2 analyses (columns) between the first surgery and relapse patients. As it is an explorative analysis, non–adjusted *p*–values lower than 0.05 are marked with an asterisk.

Successively, we compared the bacterial architecture between the two examined settings (CD *vs.* healthy), finding significant differences in alpha diversity expressed through the Chao and Shannon indexes. Confirming our previous pilot outcomes (14), the principal coordinate analysis documented different microbial distribution between the two evaluated tissues. In detail, we verified an increase of the *Tenericutes* phylum, comprising *Mycoplasma*, in CD tissue. From a biological point of view, *Mycoplasma* has a role in promoting inflammation, indeed, lipopeptides from mycoplasmal membranes have been postulated to promote chronicity and higher immune responses than other bacteria [as reviewed in (43)]. Additionally, the *Prevotella* genus was lower in CD tissue. *Prevotella* prevalence is related to increased Th17–mediated mucosal inflammation, which is consistent with the capacity shown by *Prevotella* to drive Th17 immunological responses *in vitro*. In line with our result, a study indicated reduced *Prevotella* in pediatric Crohn's disease (44). Furthermore, the most comprehensive study to date found no association between *Prevotella* and new-onset Crohn's disease before treatment (45).

Previous studies documented that distinct profiles of mucosa–associated microbiota at the ICR and postoperatively are associated with disease recurrence and remission, respectively (46). On these premises, as well as based on our previous pilot study (14), we performed a differential abundance analysis between the relapse and first surgery patients. We did not observe significant alterations between the two conditions at the microscopy levels for both CD and healthy settings, nevertheless, significant differences in microbiota signatures, mostly at the genus level, were detected with NGS, pointing to a different microbiota recolonization after ICR, as evidenced by a recent study (47). However, compared to our pilot study, due to the higher number of samples, we were able to further find different taxa (Figures 6A). Indeed, regarding the affected tissue, the family *Bacillaceae* was significantly higher in the first surgery patients compared to the relapse patients. An increase in *Bacillaceae* was recently observed in UC patients, in relation to healthy controls (48). This family is composed of aerobic spore–formers, and their presence in the gut is related to the ingestion of food and water. *Bacillaceae* is one of the rare *Firmicutes* families that share a specific LPS, being highly immunogenic. Indeed, it has recently been suggested that the efficiency of the immune system may depend on the immunogenicity of microbiota lipopolysaccharides (49). On the contrary, the family *Brucellaceae* and the genera *Escherichia/Shigella*, *Finegoldia*, and *Kocura* were significantly increased in the relapse condition. *Brucellaceae* is a family of Gram–negative bacteria involved in the progression of diseases of the central nervous system, including those of affective and psychiatric nature (50). Moreover, *Escherichia/Shigella* is a pro–inflammatory genus related to intestinal inflamed conditions, as it was previously found enriched in CRC patients (30, 51).

In healthy tissue, we observed that *Antrobacter*, *Capnocytophaga*, *Gemmatimonas*, *Moraxella*, and *Novosphingobium* were all significantly augmented in the first surgery patients, while *Acholeplasma*, *Anoxibacillus*, *Cloacibacterium*, and *Proteus* were decreased. In particular, *Proteus* belonging to Gram–negative facultative anaerobic bacilli has been recently linked to CD recurrence after surgery (52). We hypothesized an ICR influence on microbiota architecture based on our observations of substantial variations between the first surgery and recurrence patients, possibly due to the removal of the ileocecal valve (ICV) as discussed in our previous work (14).

Bacterial dysbiosis in CD patients increases intestinal barrier permeability, which explains the pathophysiology of luminal translocation of bacteria and their products (SCFAs) at the systemic level, a common occurrence in CD, which promotes a persistent inflammatory response in these patients. Many recent studies have suggested that bacterial product translocation causes uncontrolled systemic inflammation in CD patients, due to the host's circulating epigenetic fragments

(miRNAs), which are gut bacteria–associated. In detail, the circulating miRNAs are attractive non–invasive biomarkers with promising clinical values (53). However, few studies have been performed on the relationship between miRNAs and the different clinical CD conditions.

While in our previous pilot study we focused only on the interplay of microbiota and immune response at the tissue level, here, we studied also some microbial aspects of systemic inflammation. miR–155 is a multifunctional miRNA, involved in several biological processes such as hematopoiesis, inflammation, and immunity, its putative targets include several molecules of NF–κB signaling and the suppressor of cytokine signaling (SCS1). miR–155 is reported to be upregulated in the inflamed colonic mucosa of patients with active UC (54–56). However, it plays both positive and negative regulatory roles in immune responses, and it was hypothesized that miR–155 is part of a negative feedback loop to dampen inflammatory responses (57). Here, we reported a significant decrease in the level of miR–155 in the plasma of patients with surgical recurrence compared to those at the first surgery, suggesting the activation of different signaling pathways among these patients that deserve to be explored, to identify the molecular mechanisms underlying the recurrent relapses observed only in a subgroup of CD patients. We also observed the same significant decrease for miR–223, a potent regulator of some inflammatory responses. Its altered expression has been linked to several immune disorders, including rheumatoid arthritis and type 2 diabetes mellitus. It is differentially expressed during macrophage polarization, and miR–223–deficient macrophages were hypersensitive to LPS stimulation and exhibited delayed responses to IL–4 (58).

Regarding miR–423, we did not observe a significant difference between the first surgery and recurrence patients, however, we detected a negative correlation with hexanoic acid. In other words, when the hexanoic level is low (a risk factor for recurrence), miR–423 increases. This is an intriguing result as in a recent work, miR–423, inserted in a specific miRNA signature, has shown a strong capacity to confirm the presence of recurrence within 1 year of surgery, which could also help spare patients from colonoscopies (59). It has been observed that this miRNA appears with the establishment of recurrence and could therefore be participating in the development of active lesions in CD (59).

In addition, it has been reported in the literature that there were differences in the GM and in microbial metabolism depending on CD disease activity (60). We observed a significant decrease of two circulating branched–chain fatty acids (BCFAs), 2–methylbutyric and isobutyric acids, in recurrence conditions. It is known that BCFAs are mainly produced during the fermentation of branched–chain amino acids, such as valine, leucine, and isoleucine, by the GM (61). In the human intestine, the fermentation of BCFAs is carried out mainly by the genera *Bacteroides* and *Clostridium* (62). Moreover, in our study, recurrence patients exhibited diminished levels of hexanoic (caproic) acid, an MCFA whose metabolic fate is β–oxidation to acetyl–CoA, oxidized in the tricarboxylic acid cycle or converted to ketone bodies. Hexanoic acid reduces the colonization and dysbiotic expansion of potentially pathogenic bacteria in the gut (63). Even more recently, MCFAs have been shown to support the differentiation of some T helper (Th) lymphocytes, specifically Th1 and Th17, and to suppress the development of regulatory T cells (Tregs) (64). Hexanoic acid, in particular, seems to be prototypically endowed with such pro–inflammatory properties, which result from the activation of p38 MAPK signaling (64). Notably, it can also be directly produced by some of the microbiota bacteria such as *Prevotella*. In line with our result, fecal levels of hexanoic acid were recently shown to be inversely correlated with CD activity (65). In addition, our logistic regression analysis identified serum hexanoic acid as a significant independent risk factor for surgical recurrence. However, we are aware of the limitation of this result, and to translate these functional data into a more profound biological disease understanding, more knowledge of the relevance of this metabolite modulation is needed.

So far, FFA profiling mainly detects associations between profiles and specific phenotypes, which may not always be meaningful. In addition, we have to explore further whether changes in metabolites are the cause or consequence of particular CD conditions. Integration of other "omics" may enable a further understanding of IBD–related pathophysiological processes.

Finally, in order to explore a possible different regulation of GM functionality at the first surgery and recurrence conditions, we evaluated the potential associations between significantly changed clades and FFAs in CD vs. healthy settings in two clinical conditions (Figure 9).

We observed a particular negative association of *Anoxybacillus* (a bacillus significantly increased in healthy tissue of recurrence patients) with 2–methyl butyric and hexanoic acids, both reduced in the serum of recurrence patients. The genus *Anoxybacillus* is composed of 22 species, and it is interesting to highlight that some of them showed immunomodulatory and immunostimulatory properties due to the production of specific metabolites (66, 67). Our outcome may suggest a direct association of this microbial pattern in CD recurrence, however, we are not yet able to give mechanistic explanations, which require a study on cellular or *in–vivo* models.

Interestingly, in a previous study on CRC, according to the bacterial driver–passenger model put forward by Tjalsma et al. (68), *Anoxybacillus* was included in the group of driver bacteria for CRC, being away from the tumor sites (i.e., adjacent non–malignant tissue) (69). This model states that CRC development is triggered by local mucosal colonization of drivers that cause changes in the tumor microenvironment allowing for colonization by opportunistic (passenger) bacteria or their by–

products, i.e., metabolites, to pass through the epithelium, easing disease progression (70). Each bacterium contributes to carcinogenesis by a distinct microbial signature, such as the production of deleterious metabolites or by–products, stimulation or inhibition of local immune responses, or modulation in gene expression. Making a parallelism with the CRC bacterial driver–passenger model, we may speculate that the microbial patterns that lead to the onset of recurrent inflammation could be triggered by particular "driver" bacteria that reside in healthy tissue. They may activate an aberrant local immune response, leading to an increase in gut permeability and translocation of microbial products in the systemic circulation, promoting a vicious cycle with the production of epigenetic regulators at the systemic level acting as inflammation amplifiers. To corroborate this hypothesis, it is important to notice that there is a recognized increased risk for CRC in patients with IBD due to the extent of inflammatory change.

Even so, due to the small number of samples and the use of paraffin–embedded methods (which are prone to biases introduced by the embedding process and tissue archiving time), such analyses should be improved in future studies to adequately describe the complex scenario of the relationship between circulating pro– and anti–inflammatory factors and intestinal microbiota composition. Nonetheless, we are conscious that more human and animal model studies will be required to reinforce our results, but there is no dispute about the study's innovativeness.

Conclusion

To sum up, this study was proposed as a continuation and expansion of our previous pilot study (14) in which we examined the relationships between immune response elements (represented by cytokine levels in the serosa, submucosa, and mucosa) and microbiota at the tissue level, in the first surgery and relapse CD patients, demonstrating a different regulation among the examined clinical conditions. We therefore studied the architecture of mucosal GM in the same conditions as the pilot study (14) but in a greater number of patients, confirming a different ileal microbiota composition and abundance.

Unlike our previous study, in this research, we explored further the differences at the systemic level, observing for the first time a dissimilar regulation of ileal microbiota and circulating microbial–associated inflammatory factors (SCAFs, BCFAs, and miRNAs) between the first surgery and relapse CD patients, suggesting a different involvement of the gut microbiota–immunity axis in the two clinical conditions. Moreover, we also detected an association between the serum hexanoic acid and recurrence risk that needs to be further explored with prospective studies. Indeed, a comprehensive and accurate analysis is imperative to identify biomarkers of recurrence, performing targeted therapies in CD. Finally, we observed for the first time on healthy ileal tissue the potential involvement of the microbiome pathways in triggering recurrence determinants, pointing out that also GM eubiosis maintenance may be crucial for CD early treatment adjustments. Nonetheless, further mechanistic studies evaluating cellular and humoral immune responses, GM alterations, and epigenetic predisposition will help clinicians to better control and personalize the management of patients with CD, thus avoiding future post–surgery recurrences.

Data availability statement

The microbial–related data (raw reads, OTU tables, and taxonomic assignments) are freely available at NCBI Gene Expression Omnibus under the series accession GSE162844 and GSE198329, and the analysis scripts (in 263 R) are available at GitHub (https://github.com/matteoramazzotti/papers/tree/main/2022IBD).

Ethics statement

The studies involving human participants were reviewed and approved by Careggi University Hospital. The patients/participants provided their written informed consent to participate in this study. Written informed consent was obtained from the individual(s) for the publication of any potentially identifiable images or data included in this article.

Author contributions

ER, AA, and FG designed the study. ER, MD, and CL revised the literature on this topic. MD, ER, SB, LaC, GN, and Arcese D.A. collected the samples. LoC, MD, ER, SB, MP, and EB performed the experiments. ER, CL, LoC, MD, EB, and SB analyzed the data. LG and MR performed the microbiota analysis. ER wrote the manuscript. ER edited the manuscript. ER, FG, and AA supervised the preparation of the manuscript. AA, FG, ER, SS, GB, CM, and CL revised the manuscript. FG, ER, CL, and AA were responsible for funding acquisition. All authors contributed to the article and approved the submitted version.

Funding

This work was supported by Fondazione Cassa di Risparmio di Firenze (CRF2018, Number 2016.0842) and was funded by ECCO Grant 2020 to FG. Moreover, this project received funding from MUR under the umbrella of the European Joint Program Initiative "A Healthy Diet for a Healthy Life" (JPI–HDHL) and of the ERA–NET Cofund ERA–HDHL, ID: 1523 (GA N 696295 of the EU HORIZON 2020 Research and Innovation Programme).

Acknowledgments

We thank Professor Marcus J. Claesson for critically reading the manuscript. We also sincerely thank the patients for their willingness to participate in the study.

Conflict of interest

The authors declare that the research was conducted in the absence of any commercial or financial relationships that could be construed as a potential conflict of interest.

Publisher's note

All claims expressed in this article are solely those of the authors and do not necessarily represent those of their affiliated organizations, or those of the publisher, the editors and the reviewers. Any product that may be evaluated in this article, or claim that may be made by its manufacturer, is not guaranteed or endorsed by the publisher.

Supplementary material

The Supplementary Material for this article can be found online at: https://www.frontiersin.org/articles/10.3389/fimmu.2022.886468/full#supplementary-material

SUPPLEMENTARY FIGURE 1
Box-plots showing alpha diversity indices (Chao1 index, Shannon index, Evenness) in CD and healthy samples. Statistical differences were evaluated using paired Wilcoxon signed-rank test for Chao, Shannon and Evenness indices. P-values less than 0.05 were considered statistically significant.

SUPPLEMENTARY FIGURE 2
Taxonomic composition of paraffin-embedded ileal samples in ileal and CD tissue. The stacked bar plot shows the relative abundance of the five more abundant bacterial genus in each sample, The "Others" group contains genus with ranks below five.

SUPPLEMENTARY FIGURE 3
Box-plots reporting alpha diversity indices (Chao1, Shannon and Eveness index) in first surgery and relapse patients, for both CD **(A)** and Healthy tissues **(B)**. P-values less than 0.05 were considered statistically significant.

SUPPLEMENTARY FIGURE 4
Principal Coordinate Analysis using Bray-Curtis dissimilarity as a distance metric on square root transformed percent abundance of identified OTUs showing permuted p-value of general β dispersion and pairwise β dispersion of CD and healthy groups. The lines connect the samples from the same patient.

References

1. Orlando A, Mocciaro F, Renna S, Scimeca D, Rispo A, Lia Scribano M, et al. Early post–operative endoscopic recurrence in crohn's disease patients: data from an Italian group for the study of inflammatory bowel disease (IG–IBD) study on a large prospective multicenter cohort. *J Crohns Colitis* (2014) 8(10):1217–21. doi: 10.1016/j.crohns.2014.02.010

2. Bernell O, Lapidus A, Hellers G. Risk factors for surgery and recurrence in 907 patients with primary ileocaecal crohn's disease. *Br J Surg* (2000) 87(12):1697–701. doi: 10.1046/j.1365–2168.2000.01589.x

3. Zheng D, Liwinski T, Elinav E. Interaction between microbiota and immunity in health and disease. *Cell Res* (2020) 30(6):492–506. doi: 10.1038/s41422–020–0332–7

4. Romagnani P, Annunziato F, Baccari MC, Parronchi P. T Cells and cytokines in crohn's disease. *Curr Opin Immunol* (1997) 9(6):793–9. doi: 10.1016/s0952–7915(97)80180–x

5. Imhann F, Vich Vila A, Bonder MJ, Fu J, Gevers D, Visschedijk MC, et al. Interplay of host genetics and gut microbiota underlying the onset and clinical presentation of inflammatory bowel disease. *Gut* (2018) 67(1):108–19. doi: 10.1136/gutjnl–2016–312135

6. Yue B, Luo X, Yu Z, Mani S, Wang Z, Dou W. Inflammatory bowel disease: A potential result from the collusion between gut microbiota and mucosal immune system. *Microorganisms* (2019) 7(10):440. doi: 10.3390/microorganisms7100440

7. Amoroso C, Perillo F, Strati F, Fantini MC, Caprioli F, Facciotti F. The role of gut microbiota biomodulators on mucosal immunity and intestinal inflammation. *Cells* (2020) 9(5):1234. doi: 10.3390/cells9051234

8. Swidsinski A, Ladhoff A, Pernthaler A, Swidsinski S, Loening–Baucke V, Ortner M, et al. Mucosal flora in inflammatory bowel disease. *Gastroenterology* (2002) 122(1):44–54. doi: 10.1053/gast.2002.30294

9. Ryan FJ, Ahern AM, Fitzgerald RS, Laserna–Mendieta EJ, Power EM, Clooney AG, et al. Colonic microbiota is associated with inflammation and host epigenomic alterations in inflammatory bowel disease. *Nat Commun* (2020) 11(1):1512. doi: 10.1038/s41467–020–15342–5

10. Kostic AD, Xavier RJ, Gevers D. The microbiome in inflammatory bowel disease: current status and the future ahead. *Gastroenterology* (2014) 146(6):1489–99. doi: 10.1053/j.gastro.2014.02.009

11. Mondot S, Lepage P, Seksik P, Allez M, Treton X, Bouhnik Y, et al. Structural robustness of the gut mucosal microbiota is associated with crohn's disease remission after surgery. *Gut* (2016) 65(6):954–62. doi: 10.1136/gutjnl–2015–309184

12. Sokol H, Brot L, Stefanescu C, Auzolle C, Barnich N, Buisson A, et al. Prominence of ileal mucosa–associated microbiota to predict postoperative endoscopic recurrence in crohn's disease. *Gut* (2020) 69(3):462–72. doi: 10.1136/gutjnl–2019–318719

13. Yilmaz B, Juillerat P, Oyas O, Ramon C, Bravo FD, Franc Y, et al. Microbial network disturbances in relapsing refractory crohn's disease. *Nat Med* (2019) 25(2):323–36. doi: 10.1038/s41591–018–0308–z

14. Russo E, Giudici F, Ricci F, Scaringi S, Nannini G, Ficari F, et al. Diving into inflammation: A pilot study exploring the dynamics of the immune–microbiota axis in ileal tissue layers of patients with crohn's disease. *J Crohns Colitis* (2021) 15(9):1500–16. doi: 10.1093/ecco–jcc/jjab034

15. den Besten G, van Eunen K, Groen AK, Venema K, Reijngoud DJ, Bakker BM. The role of short–chain fatty acids in the interplay between diet, gut microbiota, and host energy metabolism. *J Lipid Res* (2013) 54(9):2325–40. doi: 10.1194/jlr.R036012

16. Moloney GM, Viola MF, Hoban AE, Dinan TG, Cryan JF. Faecal microRNAs: indicators of imbalance at the host–microbe interface? *Benef Microbes* (2018) 9(2):175–83. doi: 10.3920/BM2017.0013

17. Hu S, Liu L, Chang EB, Wang JY, Raufman JP. Butyrate inhibits pro–proliferative miR–92a by diminishing c–myc–induced miR–17–92a cluster transcription in human colon cancer cells. *Mol Cancer* (2015) 14:180. doi: 10.1186/s12943–015–0450–x

18. Peck BC, Mah AT, Pitman WA, Ding S, Lund PK, Sethupathy P. Functional transcriptomics in diverse intestinal epithelial cell types reveals robust MicroRNA sensitivity in intestinal stem cells to microbial status. *J Biol Chem* (2017) 292(7):2586–600. doi: 10.1074/jbc.M116.770099

19. Zhou H, Xiao J, Wu N, Liu C, Xu J, Liu F, et al. MicroRNA–223 regulates the differentiation and function of intestinal dendritic cells and macrophages by targeting C/EBPbeta. *Cell Rep* (2015) 13(6):1149–60. doi: 10.1016/j.celrep.2015.09.073

20. O'Connell RM, Rao DS, Chaudhuri AA, Baltimore D. Physiological and pathological roles for microRNAs in the immune system. *Nat Rev Immunol* (2010) 10(2):111–22. doi: 10.1038/nri2708

21. Dorhoi A, Iannaccone M, Farinacci M, Fae KC, Schreiber J, Moura–Alves P, et al. MicroRNA–223 controls susceptibility to tuberculosis by regulating lung neutrophil recruitment. *J Clin Invest* (2013) 123(11):4836–48. doi: 10.1172/JCI67604

22. Polytarchou C, Oikonomopoulos A, Mahurkar S, Touroutoglou A, Koukos G, Hommes DW, et al. Assessment of circulating MicroRNAs for the diagnosis and disease activity evaluation in patients with ulcerative colitis by using the nanostring technology. *Inflammation Bowel Dis* (2015) 21(11):2533–9. doi: 10.1097/MIB.0000000000000547

23. Schaefer JS, Montufar–Solis D, Vigneswaran N, Klein JR. Selective upregulation of microRNA expression in peripheral blood leukocytes in IL–10–/– mice precedes expression in the colon. *J Immunol* (2011) 187(11):5834–41. doi: 10.4049/jimmunol.1100922

24. Iborra M, Bernuzzi F, Invernizzi P, Danese S. MicroRNAs in autoimmunity and inflammatory bowel disease: crucial regulators in immune response. *Autoimmun Rev* (2012) 11(5):305–14. doi: 10.1016/j.autrev.2010.07.002

25. Chen WX, Ren LH, Shi RH. Implication of miRNAs for inflammatory bowel disease treatment: Systematic review. *World J Gastrointest Pathophysiol* (2014) 5 (2):63–70. doi: 10.4291/wjgp.v5.i2.63

26. Whiteoak SR, Felwick R, Sanchez–Elsner T, Fraser Cummings JR. MicroRNAs in inflammatory bowel diseases: paradoxes and possibilities. *Inflammation Bowel Dis* (2015) 21(5):1160–5. doi: 10.1097/MIB.0000000000000288

27. Raisch J, Darfeuille–Michaud A, Nguyen HT. Role of microRNAs in the immune system, inflammation and cancer. *World J Gastroenterol* (2013) 19 (20):2985–96. doi: 10.3748/wjg.v19.i20.2985

28. Wang M, Guo J, Zhao YQ, Wang JP. IL–21 mediates microRNA–423–5p /claudin–5 signal pathway and intestinal barrier function in inflammatory bowel disease. *Aging (Albany NY)* (2020) 12(16):16099–110. doi: 10.18632/aging.103566

29. Satsangi J, Silverberg MS, Vermeire S, Colombel JF. The Montreal classification of inflammatory bowel disease: controversies, consensus, and implications. *Gut* (2006) 55(6):749–53. doi: 10.1136/gut.2005.082909

30. Niccolai E, Russo E, Baldi S, Ricci F, Nannini G, Pedone M, et al. Significant and conflicting correlation of IL–9 with prevotella and bacteroides in human colorectal cancer. *Front Immunol* (2020) 11:573158. doi: 10.3389/fimmu.2020.573158

31. Pagliai G, Russo E, Niccolai E, Dinu M, Di Pilato V, Magrini A, et al. Influence of a 3–month low–calorie Mediterranean diet compared to the vegetarian diet on human gut microbiota and SCFA: the CARDIVEG study. *Eur J Nutr* (2020) 59(5):2011–24. doi: 10.1007/s00394–019–02050–0

32. Albanese D, Fontana P, De Filippo C, Cavalieri D, Donati C. MICCA: a complete and accurate software for taxonomic profiling of metagenomic data. *Sci Rep* (2015) 5:9743. doi: 10.1038/srep09743

33. McMurdie PJ, Holmes S. Phyloseq: an r package for reproducible interactive analysis and graphics of microbiome census data. *PLoS One* (2013) 8(4):e61217. doi: 10.1371/journal.pone.0061217

34. Love MI, Huber W, Anders S. Moderated estimation of fold change and dispersion for RNA–seq data with DESeq2. *Genome Biol* (2014) 15(12):550. doi: 10.1186/s13059–014–0550–8

35. Willis A, Bunge J. Estimating diversity *via* frequency ratios. *Biometrics* (2015) 71(4):1042–9. doi: 10.1111/biom.12332

36. Baldi S, Menicatti M, Nannini G, Niccolai E, Russo E, Ricci F, et al. Free fatty acids signature in human intestinal disorders: Significant association between butyric acid and celiac disease. *Nutrients* (2021) 13(3):742. doi: 10.3390/nu13030742

37. Bi K, Zhang X, Chen W, Diao H. MicroRNAs regulate intestinal immunity and gut microbiota for gastrointestinal health: A comprehensive review. *Genes (Basel)* (2020) 11(9):1075. doi: 10.3390/genes11091075

38. Hedin CR, McCarthy NE, Louis P, Farquharson FM, McCartney S, Taylor K, et al. Altered intestinal microbiota and blood T cell phenotype are shared by patients with crohn's disease and their unaffected siblings. *Gut* (2014) 63(10):1578–86. doi: 10.1136/gutjnl–2013–306226

39. Manichanh C, Borruel N, Casellas F, Guarner F. The gut microbiota in IBD. *Nat Rev Gastroenterol Hepatol* (2012) 9(10):599–608. doi: 10.1038/nrgastro.2012.152

40. Erickson AR, Cantarel BL, Lamendella R, Darzi Y, Mongodin EF, Pan C, et al. Integrated metagenomics/metaproteomics reveals human host–microbiota signatures of crohn's disease. *PLoS One* (2012) 7(11):e49138. doi: 10.1371/journal.pone.0049138

41. Winter SE, Baumler AJ. Why related bacterial species bloom simultaneously in the gut: principles underlying the 'Like will to like' concept. *Cell Microbiol* (2014) 16(2):179–84. doi: 10.1111/cmi.12245

42. Pinto–Ribeiro I, Ferreira RM, Pereira–Marques J, Pinto V, Macedo G, Carneiro F, et al. Evaluation of the use of formalin–fixed and paraffin–embedded archive gastric tissues for microbiota characterization using next–generation sequencing. *Int J Mol Sci* (2020) 21(3):1096. doi: 10.3390/ijms21031096

43. Roediger WE. Intestinal mycoplasma in crohn's disease. *Novartis Found Symp* (2004) 263:85–93. doi: 10.1002/0470090480.ch7

44. Lewis JD, Chen EZ, Baldassano RN, Otley AR, Griffiths AM, Lee D, et al. Inflammation, antibiotics, and diet as environmental stressors of the gut microbiome in pediatric crohn's disease. *Cell Host Microbe* (2017) 22(2):247. doi: 10.1016/j.chom.2017.07.011

45. Gevers D, Kugathasan S, Denson LA, Vazquez–Baeza Y, Van Treuren W, Ren B, et al. The treatment–naive microbiome in new–onset crohn's disease. *Cell Host Microbe* (2014) 15(3):382–92. doi: 10.1016/j.chom.2014.02.005

46. De Cruz P, Kang S, Wagner J, Buckley M, Sim WH, Prideaux L, et al. Association between specific mucosa–associated microbiota in crohn's disease at the time of resection and subsequent disease recurrence: a pilot study. *J Gastroenterol Hepatol* (2015) 30(2):268–78. doi: 10.1111/jgh.12694

47. Machiels K, Pozuelo Del Rio M, Martinez–De la Torre A, Xie Z, Pascal Andreu V, Sabino J, et al. Early postoperative endoscopic recurrence in crohn's disease is characterized by distinct microbiota recolonization. *J Crohns Colitis* (2020) 14(11):1535–46. doi: 10.1093/ecco–jcc/jjaa081

48. Zakerska–Banaszak O, Tomczak H, Gabryel M, Baturo A, Wolko L, Michalak M, et al. Dysbiosis of gut microbiota in polish patients with ulcerative colitis: a pilot study. *Sci Rep* (2021) 11(1):2166. doi: 10.1038/s41598–021–81628–3

49. Vatanen T, Kostic AD, d'Hennezel E, Siljander H, Franzosa EA, Yassour M, et al. Variation in microbiome LPS immunogenicity contributes to autoimmunity in humans. *Cell* (2016) 165(4):842–53. doi: 10.1016/j.cell.2016.04.007

50. Schwarz E, Maukonen J, Hyytiainen T, Kieseppa T, Oresic M, Sabunciyan S, et al. Analysis of microbiota in first episode psychosis identifies preliminary associations with symptom severity and treatment response. *Schizophr Res* (2018) 192:398–403. doi: 10.1016/j.schres.2017.04.017

51. Wang T, Cai G, Qiu Y, Fei N, Zhang M, Pang X, et al. Structural segregation of gut microbiota between colorectal cancer patients and healthy volunteers. *ISME J* (2012) 6(2):320–9. doi: 10.1038/ismej.2011.109

52. Zhang J, Hoedt EC, Liu Q, Berendsen E, Teh JJ, Hamilton A, et al. Elucidation of Proteus mirabilis as a key bacterium in crohn's disease inflammation. *Gastroenterology* (2021) 160(1):317–30.e11. doi: 10.1053/j.gastro.2020.09.036

53. Kalla R, Ventham NT, Kennedy NA, Quintana JF, Nimmo ER, Buck AH, et al. MicroRNAs: new players in IBD. *Gut* (2015) 64(3):504–17. doi: 10.1136/gutjnl–2014–307891

54. Takagi T, Naito Y, Mizushima K, Hirata I, Yagi N, Tomatsuri N, et al. Increased expression of microRNA in the inflamed colonic mucosa of patients with active ulcerative colitis. *J Gastroenterol Hepatol* (2010) 25 Suppl 1:S129–33. doi: 10.1111/j.1440–1746.2009.06216.x

55. Valmiki S, Ahuja V, Paul J. MicroRNA exhibit altered expression in the inflamed colonic mucosa of ulcerative colitis patients. *World J Gastroenterol* (2017) 23(29):5324–32. doi: 10.3748/wjg.v23.i29.5324

56. Guz M, Dworzanski T, Jeleniewicz W, Cybulski M, Kozicka J, Stepulak A, et al. Elevated miRNA inversely correlates with e–cadherin gene expression in tissue biopsies from crohn disease patients in contrast to ulcerative colitis patients. *BioMed Res Int* (2020) 2020:4250329. doi: 10.1155/2020/4250329

57. Ceppi M, Pereira PM, Dunand–Sauthier I, Barras E, Reith W, Santos MA, et al. MicroRNA–155 modulates the interleukin–1 signaling pathway in activated human monocyte–derived dendritic cells. *Proc Natl Acad Sci U.S.A.* (2009) 106 (8):2735–40. doi: 10.1073/pnas.0811073106

58. Zhuang G, Meng C, Guo X, Cheruku PS, Shi L, Xu H, et al. A novel regulator of macrophage activation: miR–223 in obesity–associated adipose tissue inflammation. *Circulation* (2012) 125(23):2892–903. doi: 10.1161/CIRCULATIONAHA.111.087817

59. Moret–Tatay I, Cerrillo E, Hervas D, Iborra M, Saez–Gonzalez E, Forment J, et al. Specific plasma MicroRNA signatures in predicting and confirming crohn's disease recurrence: Role and pathogenic implications. *Clin Transl Gastroenterol* (2021) 12(10):e00416. doi: 10.14309/ctg.0000000000000416

60. Forbes JD, Van Domselaar G, Bernstein CN. Microbiome survey of the inflamed and noninflamed gut at different compartments within the gastrointestinal tract of inflammatory bowel disease patients. *Inflammation Bowel Dis* (2016) 22(4):817–25. doi: 10.1097/MIB.0000000000000684

61. Russo E, Giudici F, Fiorindi C, Ficari F, Scaringi S, Amedei A. Immunomodulating activity and therapeutic effects of short chain fatty acids and tryptophan post–biotics in inflammatory bowel disease. *Front Immunol* (2019) 10:2754. doi: 10.3389/fimmu.2019.02754

62. Macfarlane S, Macfarlane GT. Regulation of short–chain fatty acid production. *Proc Nutr Soc* (2003) 62(1):67–72. doi: 10.1079/PNS2002207

63. Van Immerseel F, De Buck J, Boyen F, Bohez L, Pasmans F, Volf J, et al. Medium–chain fatty acids decrease colonization and invasion through hilA suppression shortly after infection of chickens with salmonella enterica serovar enteritidis. *Appl Environ Microbiol* (2004) 70(6):3582–7. doi: 10.1128/AEM.70.6.3582–3587.2004

64. Haghikia A, Jorg S, Duscha A, Berg J, Manzel A, Waschbisch A, et al. Dietary fatty acids directly impact central nervous system autoimmunity *via* the small intestine. *Immunity* (2015) 43(4):817–29. doi: 10.1016/j.immuni.2015.09.007

65. De Preter V, Machiels K, Joossens M, Arijs I, Matthys C, Vermeire S, et al. Faecal metabolite profiling identifies medium–chain fatty acids as discriminating compounds in IBD. *Gut* (2015) 64(3):447–58. doi: 10.1136/gutjnl–2013–306423

66. Wang GX, Wang Y, Wu ZF, Jiang HF, Dong RQ, Li FY, et al. Immunomodulatory effects of secondary metabolites from thermophilic anoxybacillus kamchatkensis XA–1 on carp, cyprinus carpio. *Fish Shellfish Immunol* (2011) 30(6):1331–8. doi: 10.1016/j.fsi.2011.03.011

67. Liu J, Lei Y, Wang F, Yi Y, Liu Y, Wang G. Immunostimulatory activities of specific bacterial secondary metabolite of anoxybacillus flavithermus strain SX–4 on carp, cyprinus carpio. *J Appl Microbiol* (2011) 110(4):1056–64. doi: 10.1111/j.1365–2672.2011.04963.x

68. Tjalsma H, Boleij A, Marchesi JR, Dutilh BE. A bacterial driver–passenger model for colorectal cancer: beyond the usual suspects. *Nat Rev Microbiol* (2012) 10(8):575–82. doi: 10.1038/nrmicro2819

69. Geng J, Fan H, Tang X, Zhai H, Zhang Z. Diversified pattern of the human colorectal cancer microbiome. *Gut Pathog* (2013) 5(1):2. doi: 10.1186/1757–4749–5–2

70. Russo E, Taddei A, Ringressi MN, Ricci F, Amedei A. The interplay between the microbiome and the adaptive immune response in cancer development. *Therap Adv Gastroenterol* (2016) 9(4):594–605. doi: 10.1177/1756283X16635082

frontiers | Frontiers in Immunology

TYPE Original Research
PUBLISHED 11 November 2022
DOI 10.3389/fimmu.2022.1022093

OPEN ACCESS

EDITED BY
Eun Jeong Park,
Mie University, Japan

REVIEWED BY
Sunita Keshari,
University of Texas MD Anderson Cancer Center, United States
Wei Li,
Fudan University, China

*CORRESPONDENCE
Xiaolong A. Zhou
alan.zhou@northwestern.edu

†These authors share first authorship

‡These authors share senior authorship

SPECIALTY SECTION
This article was submitted to Molecular Innate Immunity, a section of the journal Frontiers in Immunology

RECEIVED 18 August 2022
ACCEPTED 19 October 2022
PUBLISHED 11 November 2022

CITATION
Hooper MJ, Enriquez GL, Veon FL, LeWitt TM, Sweeney D, Green SJ, Seed PC, Choi J, Guitart J, Burns MB and Zhou XA (2022) Narrowband ultraviolet B response in cutaneous T-cell lymphoma is characterized by increased bacterial diversity and reduced *Staphylococcus aureus* and *Staphylococcus lugdunensis*. *Front. Immunol.* 13:1022093. doi: 10.3389/fimmu.2022.1022093

Narrowband ultraviolet B response in cutaneous T-cell lymphoma is characterized by increased bacterial diversity and reduced *Staphylococcus aureus* and *Staphylococcus lugdunensis*

Madeline J. Hooper[1†], Gail L. Enriquez[2†], Francesca L. Veon[1], Tessa M. LeWitt[1], Dagmar Sweeney[3], Stefan J. Green[4], Patrick C. Seed[5], Jaehyuk Choi[1], Joan Guitart[1], Michael B. Burns[2‡] and Xiaolong A. Zhou[1*‡]

[1]Department of Dermatology, Northwestern University, Feinberg School of Medicine, Chicago, IL, United States, [2]Department of Biology, Loyola University Chicago, Chicago, IL, United States, [3]Genome Research Core, University of Illinois at Chicago, Chicago, IL, United States, [4]Genomics and Microbiome Core Facility, Rush University Medical Center, Chicago, IL, United States, [5]Division of Pediatric Infectious Diseases, Ann & Robert H. Lurie Children's Hospital of Chicago, Chicago, IL, United States

Skin microbiota have been linked to disease activity in cutaneous T-cell lymphoma (CTCL). As the skin microbiome has been shown to change after exposure to narrowband ultraviolet B (nbUVB) phototherapy, a common treatment modality used for CTCL, we performed a longitudinal analysis of the skin microbiome in CTCL patients treated with nbUVB. 16S V4 rRNA gene amplicon sequencing for genus-level taxonomic resolution, *tuf2* amplicon next generation sequencing for staphylococcal speciation, and bioinformatics were performed on DNA extracted from skin swabs taken from lesional and non-lesional skin of 25 CTCL patients receiving nbUVB and 15 CTCL patients not receiving nbUVB from the same geographical region. Disease responsiveness to nbUVB was determined using the modified Severity Weighted Assessment Tool: 14 (56%) patients responded to nbUVB while 11 (44%) patients had progressive disease. Microbial α-diversity increased in nbUVB-responders after phototherapy. The relative abundance of *Staphylococcus*, *Corynebacterium*, *Acinetobacter*, *Streptococcus*, and *Anaerococcus* differentiated nbUVB responders and non-responders after treatment ($q<0.05$). Microbial signatures of nbUVB-treated patients demonstrated significant post-exposure depletion of *S. aureus* ($q=0.024$) and *S. lugdunensis* ($q=0.004$) relative abundances. Before nbUVB, responder lesional skin harboured higher levels of *S. capitis* ($q=0.028$) and *S. warneri* ($q=0.026$) than non-responder lesional skin. *S. capitis* relative abundance increased in the lesional skin of responders ($q=0.05$) after phototherapy; a similar upward trend was observed in non-responders ($q=0.09$). Post-

treatment skin of responders exhibited significantly reduced *S. aureus* (q=0.008) and significantly increased *S. hominis* (q=0.006), *S. pettenkoferi* (q=0.021), and *S. warneri* (q=0.029) relative abundances compared to that of no-nbUVB patients. *Staphylococcus* species abundance was more similar between non-responders and no-nbUVB patients than between responders and no-nbUVB patients. In sum, the skin microbiome of CTCL patients who respond to nbUVB is different from that of non-responders and untreated patients, and is characterized by shifts in *S. aureus* and *S. lugdunensis*. Non-responsiveness to phototherapy may reflect more aggressive disease at baseline.

KEYWORDS

cutaneous T-cell lymphoma, microbiome, phototherapy, cancer, oncology, dermatology

Introduction

Cutaneous T-cell lymphoma (CTCL) is a rare non-Hodgkin's lymphoma in which malignant T-cells infiltrate the skin. Although the etiology of CTCL remains unexplained, bacteria inhabiting the skin are understood to drive disease flares and the pathophysiology therein – specifically, *S. aureus* enterotoxin and alpha-toxin are tied to pronounced oncogenesis in CTCL (1–4). Additionally, CTCL patients have an increased risk of skin infections compared to the general population and such infections tend to be associated with disease progression (5). Influenced by local physiochemical properties and adjacent physical, autoimmune, and infectious trauma, the skin comprises a site-specific microbial niche rich with therapeutic and prognostic utility in cutaneous disease (6–8). Commensal skin bacteria play important roles in immune education and skin barrier homeostasis, and with dysbiosis comes disruption of these essential mechanisms (9). Mirroring this observation, specific changes in the skin microbiome have been associated with immune-mediated inflammatory skin conditions, including atopic dermatitis (AD) (10, 11), psoriasis (12, 13), hidradenitis suppurativa (14, 15), and vitiligo (16, 17). Nasal and gut dysbiosis have also been linked to these same diseases (15, 18). Considering recent research demonstrating CTCL patients harbor altered nasal and gut microbiota, and data revealing distinct bacterial communities distinguish healthy from lesional skin, CTCL may be a disease of global dysbiosis (19–25). While direct causality between dysbiosis and disease progression remains to be demonstrated, these findings are highly anticipated as they may precipitate innovative management strategies for CTCL patients.

Narrowband ultraviolet B (nbUVB) phototherapy is a common treatment modality for CTCL with an overall response rate of 89% in early-stage disease (26). Notably effective for skin-limited CTCL, nbUVB has been shown to shape the skin microbiome in association with disease improvement in AD and vitiligo (10, 11, 16). Interestingly, nbUVB in AD was observed to decrease lesional skin *Staphylococcus* abundance, induce clinical improvement, and enhance the anti-*S. aureus* activity and treatment effects of topical corticosteroids (11). *In vitro* studies have demonstrated ultraviolet light can suppress *S. aureus* superantigen production (27). Furthermore, excimer laser-mediated increases of *Cyanobacterium* in AD skin may reflect improved skin water content (10), thereby supporting the hypothesis that non-*Staphylococcus* taxa also play an important role in the homeostasis of skin health and disease.

We conducted a longitudinal study of the bacterial communities populating the lesional and non-lesional skin of CTCL patients treated with nbUVB phototherapy. This early effort to detail a therapeutic-microbial relationship in CTCL achieves two aims: first, to assess the impact of nbUVB on the CTCL skin microbiome; and second, to provide a comprehensive framework for evaluating the biological relevance of the microbial differences separating healthy and diseased skin.

Materials and methods

Participants

Ethical approval was obtained from the Northwestern University Institutional Review Board (STU00209226). In compliance with the Declaration of Helsinki, 40 patients with clinically- and biopsy-confirmed CTCL, as reviewed by an expert dermatopathologist (JG), were consented and enrolled in the study between 2019 and 2021. Specimen and data collection were performed at the Northwestern University Cutaneous Lymphoma specialty clinic. Clinical staging and modified

Severity Weighted Assessment Tool (mSWAT) were assessed by the principal investigator (XAZ) at sample collection.

Figure 1 illustrates the study design. Twenty-five patients were prescribed a treatment regimen involving nbUVB phototherapy; the remaining 15 participants used non-nbUVB standard-of-care treatments. In total, 28 patients used topical treatments, of which 89% (n=25) were using topical corticosteroid monotherapy, 14 patients used systemic treatments, and 8 were treatment naïve. The great majority of patients (85%) had been stable on these therapies for minimum 24 months prior to study enrollment. Patients who used antibiotics in the 4 weeks prior to sample collection were excluded.

16S rRNA amplification and sequencing

Genomic DNA was prepared for sequencing using a two-stage amplicon sequencing workflow, as described previously (28). Genomic DNA was PCR-amplified using primers targeting the V4 region of microbial 16S rRNA genes. The primers, 515F modified and 806R modified, contained 5' linker sequences compatible with Access Array primers for Illumina sequencers (Fluidigm; South San Francisco, CA) (29). PCRs were performed in a total volume of 10µL using MyTaq™ HS 2X Mix (Bioline; Memphis, TN), primers at 500nM concentration, and approximately 1,000 copies per reaction of a synthetic double-stranded DNA template (described below). Thermocycling conditions were 95°C for 5' (initial denaturation), followed by 28 cycles of 95°C for 30 sec, 55°C for 45 sec, and 72°C for 30 sec. The second-stage PCR reaction contained 1µL of PCR product from each reaction and a unique primer pair of Access Array primers. Thermocycling conditions were 95°C for 5' (initial denaturation), followed by 8 cycles of 95°C for 30 sec, 60°C for 30 sec, and 72°C for 30 sec. Libraries were pooled and sequenced on an Illumina MiniSeq sequencer (Illumina; San Diego, CA) with 15% phiX spike-in and paired-end 2x153 base sequencing reads.

A synthetic double-stranded DNA spike-in was created as a gBLOCK by Integrated DNA Technologies (IDT; Coralville, IA). The design basis was a 999 base pair (bp) region of the 16S rRNA gene of *Rhodanobacter denitrificans* strain 2APBS1^T (NC_020541) (30). Portions of V1, V2, and V4 variable regions were replaced by eukaryotic mRNA sequences (*Apostichopus japonicus* glyceraldehyde-3-phosphate dehydrogenase mRNA, HQ292612 and *Strongylocentrotus intermedius* glyceraldehyde-3-phosphate dehydrogenase mRNA, KC775387). Primer sites were preserved, and the overall length of the synthetic DNA did not differ from the equivalent *R. denitrificans* fragment. PCR amplicons generated from this synthetic DNA do not differ in size from bacterial amplicons and can only be identified and removed through post-sequencing bioinformatics analysis. The sequence can be accessed *via* GenBank (OK324963).

Basic processing

Sequencing resulted in a total of 23,825,736 reads with an average of 42,698 reads per sample. Forward (F) and reverse (R)

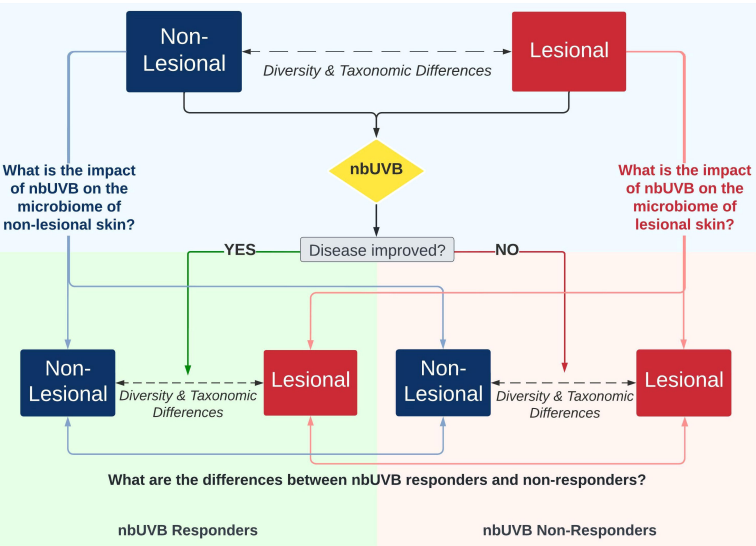

FIGURE 1
Investigational schemata for evaluating the skin microbiome of lesional and non-lesional cutaneous T-cell lymphoma (CTCL) skin in response to narrowband ultraviolet B (nbUVB) phototherapy. Differences in microbial community diversity and taxonomic abundance between responders and non-responders are illustrated in Figures 2–5.

reads were trimmed using cutadapt v3.5 to remove primer sequences (31). All reads were trimmed and filtered based on quality using the default parameters within dada2 v1.22 (32) with the following modification: the truncLen parameter was disabled, and maxEE for all reads was set to 1,1. The error models were initiated using $5x10^8$ randomized bases for the F and R sets. Following subsequent denoising with dada2's divisive partitioning machine learning approach, F and R amplicon sequence variant (ASV) read pairs were merged with a maxMismatch of 0 and a minOverlap of 8 bases. Merged pairs that did not fall within the expected length window of 252-254 bases were removed. Chimeric sequences were identified and removed using a *de novo* approach within dada2 assessing the entire sequence pool as a whole. ASVs were assigned taxonomy using DECIPHER v2.22 with the SILVA v138 training set (33, 34). The synthetic spike-in sequences were then removed from the dataset. The decontam R package v1.14 was used to identify potentially contaminating sequences, using environmental control samples collected at experimental sample collection (35). Suspected contaminant ASVs above the default prevalence threshold of 0.1 were classified as potential environmental artifacts and removed from the dataset. An abundance filter of 0.1% and a prevalence filter of 10% were applied. Following QC processing, decontamination, and filtering, there were a total of 5,862,546 merged read pairs with an average of 17,042 per sample. To maximize data retention, while removing uninformative patient samples, only samples with minimum 1000 reads following processing were retained. Patient samples were paired across disease status (lesional, non-lesional) and time (pre-nbUVB, post-nbUVB). Only complete patient-matched sets were retained for analysis.

Tuf2 amplicon next generation sequencing

Genomic DNA was PCR amplified with primers CS1_tuf2-F (ACACTGACGACATGGTTCTACAACAGGCCGTGTTGAACGTG) and CS2_tuf2-R (TACGGTAGCAGAGACTTGGTCTACAGTACGTCCACCTTCACG) (36, 37) targeting the *Staphylococcus tuf* gene. Amplicons were generated using a two-stage PCR amplification protocol, as previously described (28). First stage PCR amplifications were performed in 10µL reactions in 96-well plates, using MyTaq HS 2X mastermix (Bioline). PCR conditions were 95°C for 5 min, followed by 28 cycles of 95°C for 30 sec, 55°C for 30 sec and 72°C for 60 sec. Second-stage reactions using Access Array primers were performed as described above. Samples were pooled, purified, and sequenced on an Illumina MiSeq with 10% phiX spike-in and paired-end 2x300 base sequencing reads (*i.e.*, V3 chemistry). Library preparation, pooling, and sequencing were performed at the Genome Research Core within the Research Resources Center at the University of Illinois at Chicago.

Tuf2 amplicon processing

Tuf2 sequencing generated a total of 27,022,394 reads with an average of 57,372 raw reads per sample. Primer trimming and denoising were accomplished using the same procedure as above for the 16S amplicon data with the following modifications: during filtering and trimming, the maxEE for all reads was set to 3,3 due to their increased length, read merging used default parameters, and the read length cutoff window range was 400-500 nucleotides for merged read pairs. Following processing there were a total of 4,496,566 reads retained for an average sample read count of 9,547. ASVs were taxonomically annotated using BLASTn alignments against NCBI prokaryotic (nr) refseq database (online access 14 June 2022). Only taxa that were within the *Staphylococcus* genus were retained.

Statistical analyses

The samples in the cleaned ASV table were visually evaluated using phyloseq v1.38 (38). α-diversity metrics were generated using the ASV table rarefied to 1000 sequences. Differences in α-diversity (Observed OTUs, Chao1, Shannon, and Simpson indices) between patient sets were calculated using Wilcoxon rank-sum non-paired tests from the stats R package (39) while differences within patient-matched samples were calculated using Pairwise Wilcoxon rank-sum tests. β-diversity metrics were generated using the rarefied ASV table. Principal coordinate analysis (PCoA) with Bray-Curtis dissimilarity was performed to identify β-diversity using an ADONIS2 method (permutations = 500) of vegan v2.5.7 (40). To verify the PCoA findings, "createDataPartition" function from the Caret package v6.0.93 was used to split the data into training and test sets (41) and a supervised machine-learning algorithm Random Forest from the random Forest package v 4.7.1.1 was applied for a 10-fold cross-validation in R. The model was created using 1500 trees (42). To evaluate the model, receiver operating characteristic curves and area under the curve (AUC) values were generated using the "roc" function of the R pROC package v1.18.0 (43). Differential abundance analysis was conducted by metagenomeSeq v1.36 (44) using the non-rarefied ASV table, with ASVs removed if they had less than 4 counts or a prevalence below 10% across the sample set. A zero-inflated Gaussian (ZIG) log-normal model was implemented using the "fitFeatureModel" function of the metagenomeSeq R package to compare abundance of taxa among different groups. To further refine the differential taxa results and to reduce the likelihood of false positives, a second method, edgeR v3.36 (45), was applied to the same ASV table. For both the metagenomeSeq and edgeR results, significant ASVs were only considered if they achieved a false discovery rate (FDR)-adjusted p-value of <0.05 (q-value) by both methods.

The post-process *tuf2* ASV and taxa table was filtered using phyloseq v1.38 (38). To identify the most abundant *Staphylococcus* species, filters of minimum 20% prevalence and

10.3389/fimmu.2022.1022093

4 ASVs were applied. After centered log-ratio (CLR) transformation, the final ASV table including only the *Staphylococcus* species present at 20% abundance or greater was used for statistical analysis. Differences in abundance between patient groups were calculated using Wilcoxon rank-sum non-paired tests from the stats R package (39) while Pairwise Wilcoxon rank-sum tests were used to calculate differences between patient-matched samples. Differential abundance analysis was conducted using the CLR transformed abundance table. A ZIG log-normal model as described above was implemented to compare abundance of the top 8 *Staphylococcus* species among different groups. Significant ASVs were only considered if they achieved a FDR of <0.05.

Results

Patient characteristics

Table 1 summarizes patient characteristics. Of the 25 CTCL patients treated with nbUVB, 20 were diagnosed with mycosis fungoides, 2 with Sézary syndrome, and 3 with other CTCL subtypes. The patients were predominately male (n=17, 68.0%) and Caucasian (n=19, 76.0%). Fifteen sex-, age-, and race-matched patients who were not treated with nbUVB phototherapy (NT) were also included (Table 2). On average, nbUVB-treated participants were evaluated after 6.2 months (range 1.6-14.7) of treatment, at which time 14 patients (56.0%) had improved disease (Responders [R]; mean mSWAT change -18.5) and 11 (44.0%) had progressive disease (Non-Responders [NR]; mean mSWAT change +11.4). There were no significant differences in demographic or clinical characteristics between R and NR (p>0.05).

Treated patients were prescribed nbUVB two or three times per week. All patients endorsed using standard-of-care topical (n=31) and systemic (n=14) CTCL treatments (Supplemental Table S1). Hypercholesterolemia (n=21) and hypertension (n=17) were the most common comorbidities across the entire cohort. There were no significant differences in treatment profiles or comorbidity prevalence amongst R, NR, and NT groups (p=0.822 and p=0.656, respectively).

TABLE 1 Patient demographic and clinical characteristics.

	Responders	Non-responders	*p-value*
N	14	11	
Mean age (range), years[†]	58 (35-78)	57 (36-72)	0.857
Sex (%)[‡]			1.000
Male	10 (71.4)	7 (63.6)	
Female	4 (28.6)	4 (36.4)	
Race (%)[‡]			0.333
White	11 (78.6)	8 (72.7)	
African American	1 (7.1)	3 (27.3)	
Other	2 (14.3)	0 (0.0)	
FST (%)[‡]			0.623
Light (I-III)	12 (85.7)	8 (72.7)	
Dark (IV-VI)	2 (14.3)	3 (27.3)	
CTCL Subtype (%)[‡]			0.774
Mycosis fungoides	12 (85.7)	8 (72.7)	
Sézary syndrome	1 (7.1)	1 (9.1)	
Other CTCL	1 (7.1)	2 (18.2)	
Stage (%)[‡]			0.115
Early (IA-IIA)	11 (78.6)	5 (45.5)	
Late (IIB-IVB)	3 (21.4)	6 (54.5)	
Non-nbUVB treatments (%)[‡]			0.927
Skin-directed only	7 (50.0)	4 (36.4)	
Systemic only	1 (7.1)	1 (0.1)	
Skin-directed and systemic	3 (21.4)	4 (36.5)	
None	3 (21.4)	2 (18.2)	
Mean change in mSWAT, pre- versus post-nbUVB (range)	-18.5 (-52 - -1)	11.4 (2-79)	0.002[†]

CTCL, cutaneous T-cell lymphoma; FST, Fitzpatrick skin phototype; mSWAT, modified Severity Weighted Assessment Tool; nbUVB, narrowband ultraviolet B.
[†]Independent T-test, [‡]Fisher exact test.

TABLE 2 Demographic and clinical characteristics of patients not treated with nbUVB (NT) compared to nbUVB responders (R) and non-responders (NR).

	No nbUVB (NT)	R vs NT, *p-value*	NR vs NT, *p-value*
N	15		
Mean age (range), years[†]	64 (37-83)	0.307	0.188
Sex (%)[‡]		1.000	1.000
Male	10 (66.7)		
Female	5 (33.3)		
Race (%)[‡]		0.791	0.279
White	13 (86.7)		
African American	0 (0.0)		
Other	2 (13.3)		
FST (%)[‡]		0.598	0.279
Light (I-III)	14 (93.3)		
Dark (IV-VI)	1 (6.7)		
CTCL Subtype (%)[‡]		1.000	1.000
Mycosis fungoides	11 (73.4)		
Sézary syndrome	2 (13.3)		
Other CTCL	2 (13.3)		
Stage (%)[‡]		0.009	0.419
Early (IA-IIA)	4 (26.6)		
Late (IIB-IVB)	11 (73.4)		
Treatments (%)[‡]		0.884	0.925
Skin-directed only	7 (46.7)		
Systemic only	0 (0.0)		
Skin-directed and systemic	5 (33.3)		
None	3 (20.0)		
Mean change in mSWAT, pre- versus post-nbUVB (range)[†]	3.2 (-10 - 37)	0.807	

CTCL, cutaneous T-cell lymphoma; FST, Fitzpatrick skin phototype; mSWAT, modified Severity Weighted Assessment Tool; nbUVB,narrowband ultraviolet B.
[†]Independent T-test, [‡]Fisher exact test.

Biodiversity and community richness modulated by nbUVB

The pre-nbUVB microbial communities of R and NR were distinct in both lesional (Bray-Curtis index; $R^2 = 0.049$, p=0.012; AUC=0.852) and non-lesional skin ($R^2 = 0.077$, p=0.004; AUC=0.796) (Figure 2A). After phototherapy, R and NR non-lesional microbiota remained distinct ($R^2 = 0.030$, p=0.045; AUC=0.852), but lesional communities became non-distinct ($R^2 = 0.031$, p=0.089; AUC=0.759) (Figure 2B). As expected, the PCoA plots show between-group overlap because the samples are all from the same microbial niche.

Phylogenetic diversity increased in all treated patients' skin after phototherapy (observed p=0.009; Chao1 p=0.016) (Figure 2C). Post-nbUVB, lesional α-diversity was significantly greater in R than in NR (Shannon p=0.0024; Simpson p=0.0093) (Figure 2D). This difference corresponded to a significant increase in α-diversity after nbUVB in R skin (lesional: observed p=0.007, Chao1 p=0.002; non-lesional: observed p=0.001, Chao1 p=0.002) (Figures 2E, F) while no significant changes were noted in NR skin (lesional: observed p=0.160, Chao1 p=0.260; non-lesional: observed p=0.640, Chao1 p=0.330) (Figures 2G, H).

Decreased *Staphylococcus*, increased *Acinetobacter* differentiate nbUVB responsiveness after phototherapy

The genera *Staphylococcus*, *Corynebacterium*, and *Acinetobacter* predominated all analyzed specimens (Figure 3A). Differential analyses revealed significant genus-level shifts that distinguished R and NR, and lesional and non-lesional skin in response to phototherapy (q<0.05). In addition to genus-level taxonomic shifts, several specific ASVs within these genera provided opposing abundance shifts across the patient sample set. Figure 4 summarizes these genus-level taxon-by-taxon differences with specific reference to the unique ASV shifts, as appropriate.

10.3389/fimmu.2022.1022093

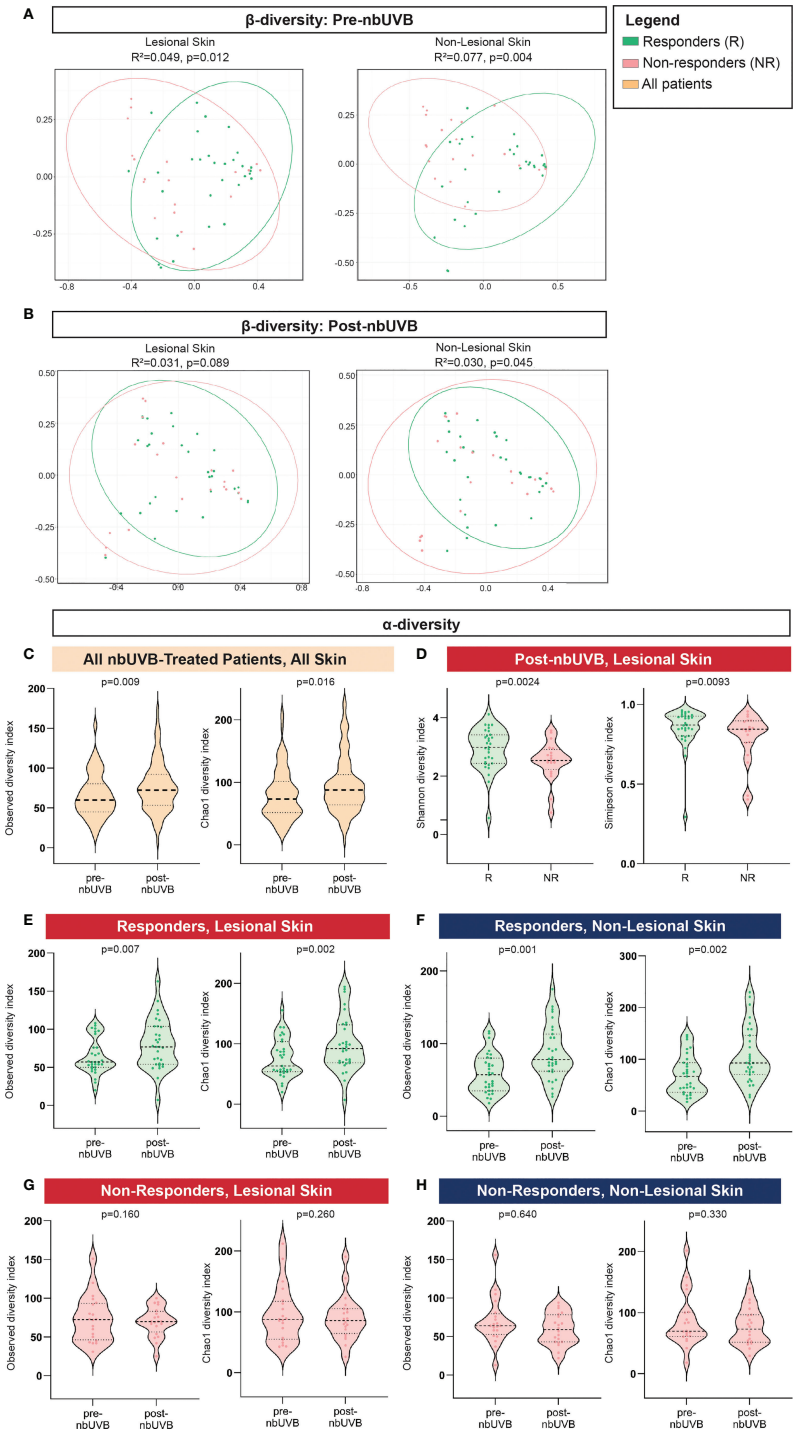

FIGURE 2
Distinct microbial communities comprise the skin microbiota of nbUVB responders and non-responders before and after nbUVB. **(A)** Bray-Curtis dissimilarity indices demonstrated Responder (R) and Non-Responder (NR) bacterial skin communities were distinct prior to nbUVB in lesional and non-lesional skin. **(B)** R versus NR post-nbUVB community differences approached significance in lesional skin, but reached significance in non-lesional skin. **(C)** Amongst all nbUVB-treated patients, α-diversity increased after phototherapy. **(D)** Following nbUVB, α-diversity of lesional skin was higher in R than NR. **(E)** α-diversity of R lesional skin and **(F)** non-lesional skin significantly increased after phototherapy. **(G)** No pre- versus post-nbUVB α-diversity differences were noted in NR lesional or **(H)** non-lesional skin. Thick dashed horizontal black lines indicate group median; thin dashed lines indicate 1st and 3rd quartiles.

10.3389/fimmu.2022.1022093

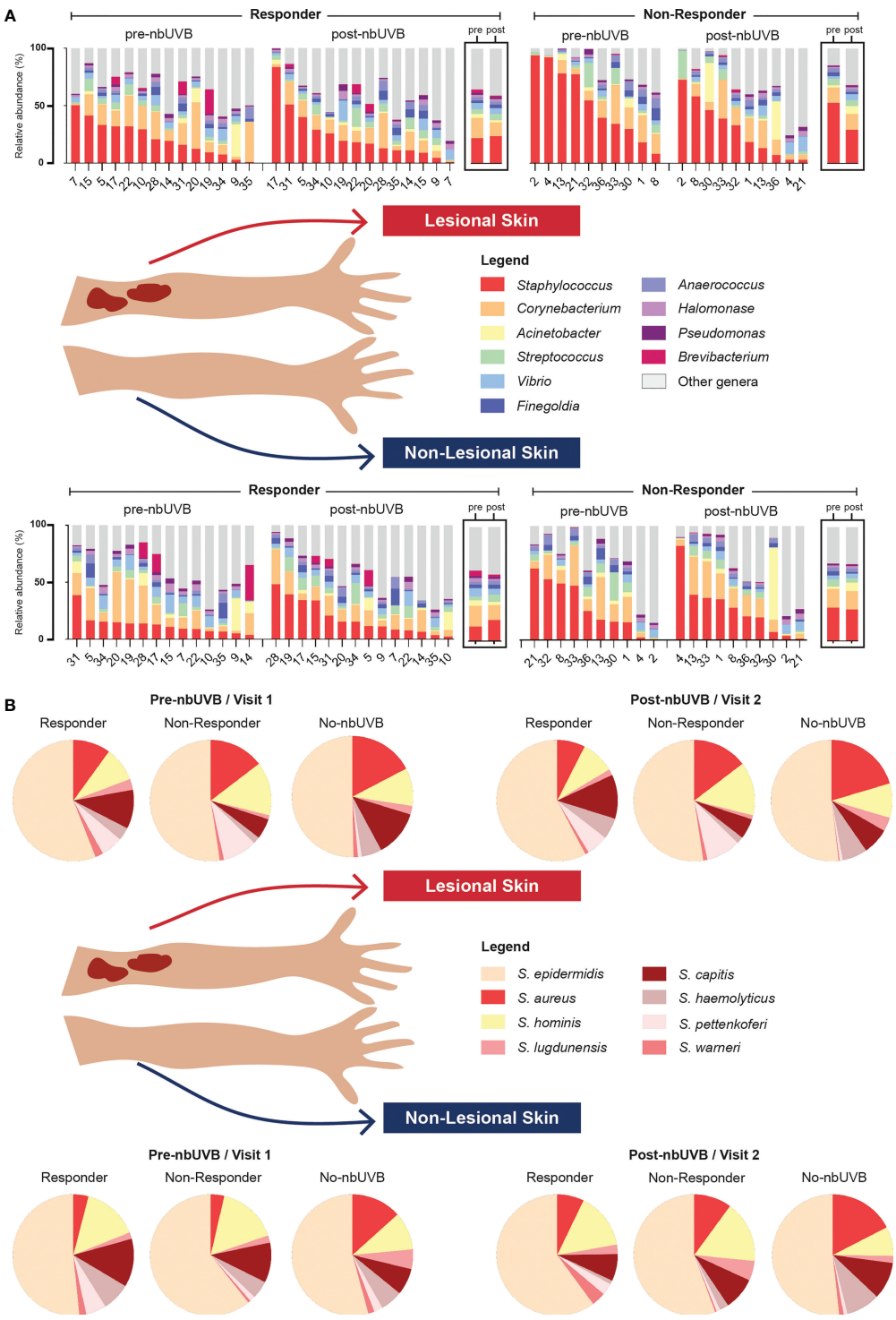

FIGURE 3
Microbial communities of CTCL lesional and non-lesional skin are predominated by different taxa. **(A)** At the taxonomic level of genus, *Staphylococcus*, *Corynebacterium*, and *Acinetobacter* were the most prevalent and abundant genera present in all treated samples. Bar charts indicate relative abundance (%) of the 10 most abundant genera populating the skin of each patient; boxed graphs reflect group mean relative abundance at pre-nbUVB (left) and post-nbUVB (right). Subject IDs are indicated along the x-axis and ordered to best visualize the distribution of relative abundances in descending order. Of note, this figure is not intended to illustrate statistically significant differences. **(B)** Staphylococcal speciation across all samples revealed a majority presence of *S. epidermidis*, *S. aureus*, and *S. hominis*. Pie charts reflect mean relative abundance of each species identified across R, NR, and no-nbUVB patient groups.

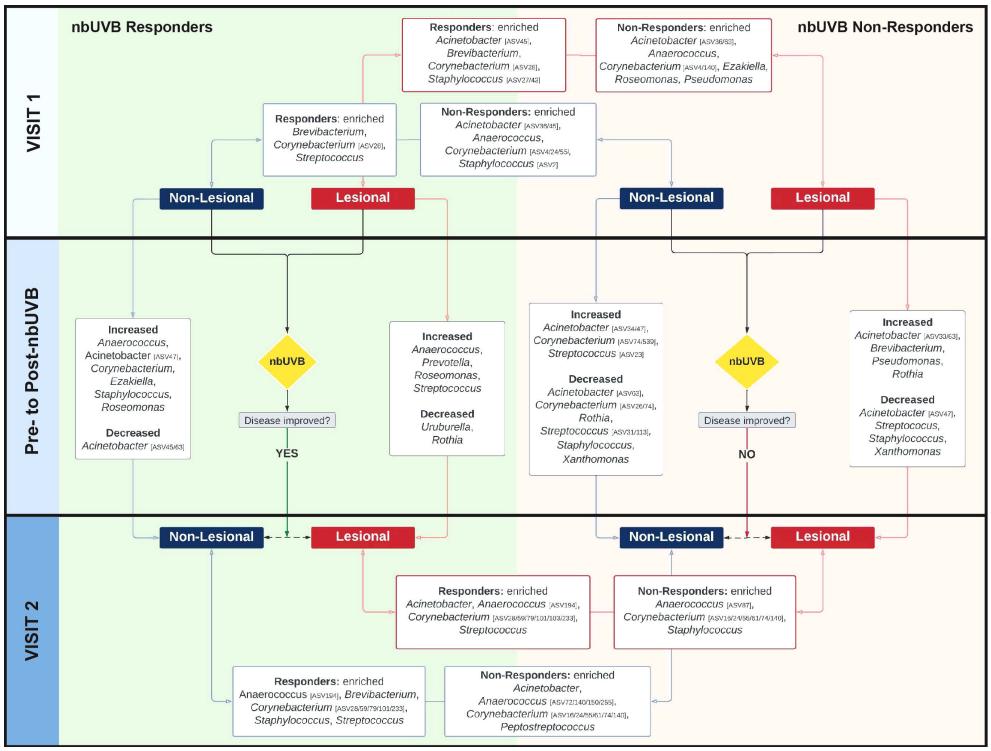

FIGURE 4
The skin microbiome changes after exposure to nbUVB phototherapy, as demonstrated by shifts at the taxonomic level of genus. Map of genus-level taxa abundances differentiating responders (R) and non-responders (NR) at lesional and non-lesional sites. Panels represent specific analyses: pre-nbUVB (top panel), pre- versus post-nbUVB (middle panel), and post-nbUVB (bottom panel). In cases of mixed responses at the genus level, specific ASVs identified on differential analysis are noted. Bidirectional arrows indicate the skin sites being compared at the same time point (e.g., R/lesional skin/pre-nbUVB versus NR/lesional skin/pre-nbUVB); unidirectional arrows indicate longitudinal shifts (e.g., R/lesional skin/pre-nbUVB versus R/lesional skin/post-nbUVB).

Pre-nbUVB treatment

Before phototherapy, *Brevibacterium*, *Staphylococcus* ASV27, and *Staphylococcus* ASV43 were significantly more abundant in eventual R relative to eventual NR across both lesional and non-lesional sites. Comparing non-lesional samples, *Streptococcus* was more abundant in R and *Staphylococcus* ASV2 was more abundant in NR. Mixed responses among several *Corynebacterium* ASVs were observed: ASV28 was more abundant in R, while ASV4 was more abundant in NR. At lesional sites, *Acinetobacter* ASV45 was greater in R than NR while *Acinetobacter* ASV36 was depleted in R; at non-lesional sites, both *Acinetobacter* ASV45 and ASV36 were more abundant in R.

Comparing pre- and post-nbUVB treatment

Pre- versus post-phototherapy comparisons of R lesional skin showed increased abundance of *Streptococcus*, *Anaerococcus*, and *Prevotella* after nbUVB treatment (Figure 4). In contrast, NR lesional skin demonstrated a reduction of *Streptococcus*, *Staphylococcus*, and *Acinetobacter*. R and NR shared some non-lesional genus-level similarities: mixed changes were observed amongst *Acinetobacter* ASVs (decreased ASV63; increased ASV47) and several *Corynebacterium* ASVs were more abundant (ASV16/233 in R, ASV74/539 in NR). While R patient samples revealed increased relative abundance of lesional *Streptococcus* ASV31, NR lesional skin exhibited a loss of this ASV.

Post-nbUVB treatment

Finally, post-nbUVB R lesional skin was differentiated from NR lesional skin by greater relative abundance of *Acinetobacter* and *Streptococcus*, and lower relative abundance of *Staphylococcus*. A mixed abundance distribution across several *Corynebacterium* ASVs was observed in R compared to NR skin: increased ASV101/103/233/28/59/79, and decreased ASV140/16/24/55/61/74. The pre-nbUVB differences in *Brevibacterium* and *Corynebacterium* identified between R and NR non-lesional skin persisted after nbUVB.

With ASVs collapsed by genus, taxon-by-taxon analysis revealed *Streptococcus* comprised a larger relative abundance in R than NR lesional skin (p=0.008, q=0.08) after phototherapy; this comparison approached significance in non-lesional skin (p=0.047, q=0.260). In the pre- versus post-nbUVB analysis, loss

of *Corynebacterium* across all lesional sites trended towards significance (p=0.033, q=0.330).

Genus-level differences distinguishing nbUVB-treated patients from no-nbUVB patients

No pre- versus post-nbUVB changes in NT α- or β-diversity were observed (Shannon p=0.51; Bray-Curtis R^2 = 0.007, p=0.425). Differential analysis of microbial profiles at the genus level between treated and NT patients revealed phototherapy has similar effects on the skin microbiota regardless of disease response. Comparison of R and NT at visit 2 demonstrated *Acinetobacter* and *Corynebacterium* (ASV24/55) were more abundant in NT, whereas *Corynebacterium* ASV233 and *Streptococcus* were more abundant in R. Similarly, NR versus NT analysis indicated *Acinetobacter* and *Corynebacterium* (ASV16) were more abundant in NT. *Peptostreptococcus* and *Anaerococcus* were more abundant in NR.

Shifts in *Staphylococcus* species abundance are associated with nbUVB responsiveness

Given the changes in relative abundance of *Staphylococcus* at the genus level and considering the importance of these species to skin health, we next assessed *Staphylococcus* species-level relative abundance within our samples using tuf amplicon sequencing. The most prevalent and abundant species were *S. epidermidis*, *S. aureus*, and *S. hominis* (Figure 3B).

Analysis of pre-nbUVB R versus NR revealed greater relative abundances of *S. capitis* (q=0.028) and *S. warneri* (q=0.026) characterized R lesional skin (Figure 5A). Pre-treatment non-lesional skin also exhibited greater relative abundance of *S. warneri* in R than NR (q=0.032), while *S. hominis* relative abundance trended higher in NR than R (q=0.084) (Figure 5A). Pre- versus post-nbUVB assessment demonstrated *S. capitis* communities were significantly more abundant in R lesional skin (q=0.05) and trended higher in NR lesional skin (q=0.09) after phototherapy (Figure 5B). Across all sites, relative abundance of *S. aureus* (q=0.024) and *S. lugdunensis* (q=0.004) significantly decreased after phototherapy in R while *S. warneri* increased in NR (q=0.032). Lastly, post-nbUVB *S. haemolyticus* relative abundance trended higher in R compared to NR lesional skin (q=0.081) (Figure 5C). Post-treatment R versus NT analysis revealed R skin was characterized by significantly less abundant *S. aureus* (q=0.008) and significantly more abundant *S. hominis* (q=0.006), *S. pettenkoferi* (q=0.021), and *S. warneri* (q=0.029). NR versus NT comparisons revealed *S. capitis* relative abundance was greater in NR (q=0.004) while *S. haemolyticus* was more abundant in NT (q=0.037).

Discussion

The antigenic stimulation provided by skin microbiota and bacterial toxins is likely one of several phenomena that, in concert with chronic skin inflammation, drives CTCL progression. Our observations suggest that successful treatment with phototherapy is associated with a microbial signature unique from that of untreated disease and phototherapy-refractory disease. This finding could suggest skin microbiota may play a role in nbUVB-responsiveness; conversely, improved disease may be characterized by a distinct microbial signature outside of any nbUVB-related effects. The increased α-diversity of nbUVB responders' skin also supports the hypothesis that phototherapy helps recoup microbial richness that may be lost in CTCL. This change could be explained by targeted attenuation of abundant taxa, such as *S. aureus* and *S. lugdunensis*, as seen in this dataset. Because the influence of cutaneous microbes on skin health is manifold, these findings underscore the potential role of commensal skin bacteria in CTCL pathogenesis and the therapeutic applications therein.

The current literature strongly supports a key role for *S. aureus* in CTCL progression (2, 3, 46); however, little is known about the influence of other staphylococcal species. We noted baseline genus-level *Staphylococcus* and species-level *S. capitis* and *S. warneri* abundances were higher in patients that eventually responded to phototherapy. These findings suggest commensal staphylococci abundance could help prognosticate disease responsiveness to phototherapy. Patient heterogeneity may limit the applicability of this theory, which warrants further study. Moreover, fewer significant differences were found between the species-level *Staphylococcus* profiles of non-responders and no-nbUVB patients than responders and no-nbUVB patients. This observation could indicate that the benefit of phototherapy in CTCL may be derived from the modulation of non-*S. aureus* species. Similarly, *S. epidermidis* trended higher in R after phototherapy across lesional and non-lesional skin. While the importance of coagulase-negative staphylococci to CTCL disease activity has yet to be determined, quorum sensing – as has been discussed in AD – could explain this finding (47). Further, very recent research revealed *S. warneri* exhibits methicillin-resistant *S. aureus* quorum sensing activity that helps protect skin from atopic and necrotic damage (48). Lastly, *S. epidermidis* – a very common commensal coagulase-negative staphylococcal species – contributes to skin microbial homeostasis through its ability to inhibit *S. aureus* growth *via* the production of antimicrobial peptides (49) and interfering with *S. aureus* biofilm production (50). Additionally, *S. epidermidis* has been shown to have anti-tumor properties in UV-induced skin cancers (51) and can suppress cutaneous inflammation by activating regulatory T-cells (52).

Other notable genera from this analysis included *Acinetobacter*, *Corynebacterium*, *Brevibacterium*, and *Streptococcus*. As *in vitro* studies have demonstrated *Acinetobacter* can induce anti-

10.3389/fimmu.2022.1022093

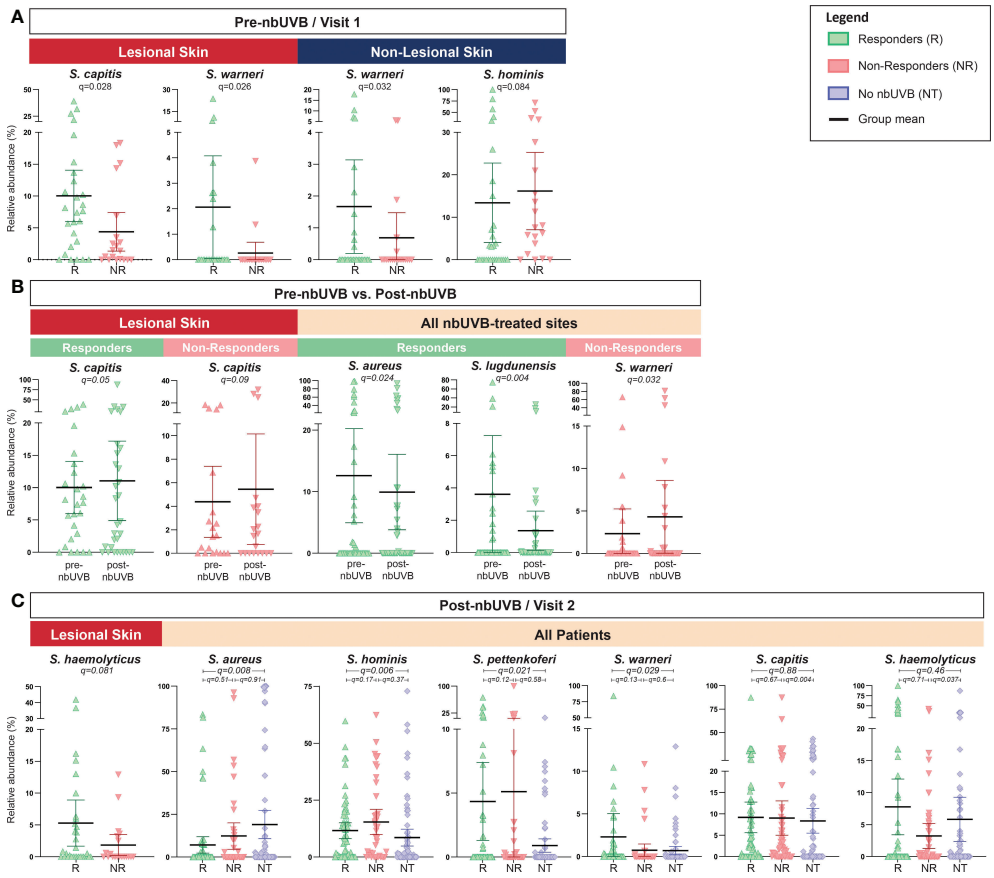

FIGURE 5
Staphylococcus species abundance differentiates nbUVB responders, nbUVB non-responders, and no-nbUVB patients. Differential analysis demonstrated significant shifts in various staphylococcal species including *S. aureus*, *S. lugdunensis*, *S. hominis*, and *S. haemolyticus* characterize R, NR, and no-nbUVB (not treated; NT) skin **(A)** pre-nbUVB, **(B)** pre- versus post-nbUVB, and **(C)** post-nbUVB. Black horizontal bars indicate group means with 95% confidence interval.

inflammatory IL-10 expression in both monocytes and keratinocytes (53), our observation that *Acinetobacter* abundance was greater in responder than non-responder lesional skin after phototherapy suggests direct linkages exist between skin microbiota and the local inflammatory microenvironment in CTCL. Moreover, little is known about the effect of nbUVB on skin microbiota. Increased abundance of healthy skin commensal flora (e.g., *Anaerococcus*, *Streptococcus*, and *Acinetobacter*) in lesional skin after phototherapy may reflect the reconstitution of a balanced skin microbiome. Increased *Streptococcus* abundance has been associated with successful treatment of AD and recovery of disease-related skin dysbiosis (54). Our data also mirrored previous research demonstrating nbUVB treatment is associated with increased *Corynebacterium* abundance (11). In addition to its potent anti-staphylococcal powers (55), this genus may influence CTCL skin activity depending on disease stage. As *Corynebacterium*-induced skin inflammation is contextually influenced by the host's overall metabolic state and gut dysbiosis severity is tied to more advanced CTCL, further study of the *gut-skin* axis and *Corynebacterium* in CTCL is warranted (19, 56). Our findings clearly demonstrated a deep and unexplored network of ASVs arising from *Corynebacterium* genera, each with specific responses among the research interrogations performed longitudinally here. This strongly suggests that there is an as-yet unexplored diversity of responses to clinically-relevant interventions that manifest as changes at the sub-genus level.

Ours is the largest evaluation of the skin microbiota in CTCL to date and the first to evaluate the impact of a therapy on this microcosm within CTCL. The novel identification of genus-level shifts in the microbiome of non-lesional skin introduces the idea that the microbial profiles of these sites could be utilized to anticipate nbUVB responsiveness. While our study is limited by the heterogeneity and distribution of disease stage within our cohort, capturing the larger shifts in the microbiome across disease stage in CTCL has yet to be thoroughly documented. Just as transcriptional heterogeneity has been associated with CTCL

(57), we expect the influence of the microbiome may vary on both inter- and intra-patient bases. Larger datasets may provide greater statistical power for conducting multivariate analyses. Furthermore, the likelihood that multiple bacterial species influence CTCL substantiate why shifts in some genera were identified in our cohort while others (e.g., *Bacillus*) were not found in our samples, despite their potential connection to CTCL tumorigenesis (24). Future analysis accounting for geographical variations in human microbiota composition is also warranted (58).

Microbes contribute to the impaired skin barrier integrity and altered local immune activity known of CTCL (59) and the extent of skin dysbiosis has been associated with disease stage (22). Here, we establish that the skin microbiome could also involve microbial biomarkers that predict nbUVB response, such as greater *Staphylococcus* relative abundance, yet we also recognize that patient heterogeneity will require further assessment in this research area. Larger and ideally multicenter analyses will validate these observations and expand upon their clinical translation.

Data availability statement

The datasets presented in this study can be found in online repositories. The names of the repository/repositories and accession number(s) can be found below: https://www.ncbi.nlm.nih.gov/bioproject/PRJNA853302.

Ethics statement

The studies involving human participants were reviewed and approved by the Northwestern University Institutional Review Board (STU00209226). The patients/participants provided their written informed consent to participate in this study.

Author contributions

Conceptualization: XZ; Data Curation: XZ, TL, MH, and FV; Formal Analysis: GE, MB, DS, and SG; Funding Acquisition: XZ; Investigation: XZ, TL, MH, and FV; Methodology: SG, XZ, and PS; Project administration: XZ and JG; Resources: XZ, JG, SG, and MB; Software: MB and SG; Supervision: XZ, PS, and JG; Validation: XZ, MB, and SG; Visualization: MH and GE; Writing – original draft: MH and XZ; Writing – review and editing: MH, XZ, JG, MB, JC, SG, GE, FV, and TL. All authors contributed to the article and approved the submitted version.

Funding

Supported by a Dermatology Foundation Medical Dermatology Career Development Award, Cutaneous Lymphoma Foundation Catalyst Research Grant, American Cancer Society Institutional Research Grant, and an institutional grant from the Northwestern University Clinical and Translational Sciences Institute (NUCATS) and the National Institutes of Health (NIH) (GRANT KL2TR001424).

Acknowledgments

The authors would like to thank the patients who contributed to the study.

Conflict of interest

The authors declare that the research was conducted in the absence of any commercial or financial relationships that could be construed as a potential conflict of interest.

Publisher's note

Supplementary material

The Supplementary Material for this article can be found online at: https://www.frontiersin.org/articles/10.3389/fimmu.2022.1022093/full#supplementary-material

References

1. Willerslev-Olsen A, Krejsgaard T, Lindahl LM, Bonefeld CM, Wasik MA, Koralov SB, et al. Bacterial toxins fuel disease progression in cutaneous T-cell lymphoma. *Toxins* (2013) 5(8):1402–21. doi: 10.3390/toxins5081402

2. Blümel E, Willerslev-Olsen A, Gluud M, Lindahl LM, Fredholm S, Nastasi C, et al. Staphylococcal alpha-toxin tilts the balance between malignant and non-malignant Cd4(+) T cells in cutaneous T-cell lymphoma. *Oncoimmunology* (2019) 8(11):e1641387–e. doi: 10.1080/2162402X.2019.1641387

3. Blümel E, Munir Ahmad S, Nastasi C, Willerslev-Olsen A, Gluud M, Fredholm S, et al. Staphylococcus aureus alpha-toxin inhibits Cd8+ T cell-mediated killing of cancer cells in cutaneous T-cell lymphoma.

Oncoimmunology (2020) 9(1):1751561. doi: 10.1080/2162402X.2020.1751561

4. Lindahl LM, Willerslev-Olsen A, Gjerdrum LMR, Nielsen PR, Blümel E, Rittig AH, et al. Antibiotics inhibit tumor and disease activity in cutaneous T-cell lymphoma. *Blood* (2019) 134(13):1072–83. doi: 10.1182/blood.2018888107

5. Axelrod PI, Lorber B, Vonderheid EC. Infections complicating mycosis fungoides and sézary syndrome. *JAMA J Am Med Assoc* (1992) 267(10):1354–8. doi: 10.1001/jama.1992.03480100060031

6. Patra V, Laoubi L, Nicolas J-F, Vocanson M, Wolf P. A perspective on the interplay of ultraviolet-radiation, skin microbiome and skin resident memory tcrαβ+ cells. *Front Med* (2018) 5:166. doi: 10.3389/fmed.2018.00166

7. Silva SH, Guedes ACM, Gontijo B, Ramos AMC, Carmo LS, Farias LM, et al. Influence of narrow-band uvb phototherapy on cutaneous microbiota of children with atopic dermatitis. *J Eur Acad Dermatol Venereology* (2006) 20(9):1114–20. doi: 10.1111/j.1468-3083.2006.01748.x

8. Mukherjee S, Mitra R, Maitra A, Gupta S, Kumaran S, Chakrabortty A, et al. Sebum and hydration levels in specific regions of human face significantly predict the nature and diversity of facial skin microbiome. *Sci Rep* (2016) 6(1):36062. doi: 10.1038/srep36062

9. Chen YE, Fischbach MA, Belkaid Y. Skin microbiota–host interactions. *Nature* (2018) 553(7689):427–36. doi: 10.1038/nature25177

10. Kurosaki Y, Tsurumachi M, Kamata Y, Tominaga M, Suga Y, Takamori K. Effects of 308 nm excimer light treatment on the skin microbiome of atopic dermatitis patients. *Photodermatology photoimmunology photomedicine* (2020) 36(3):185–91. doi: 10.1111/phpp.12531

11. Kwon S, Choi JY, Shin J-W, Huh C-H, Park K-C, Du M-H, et al. Changes in lesional and non-lesional skin microbiome during treatment of atopic dermatitis. *Acta dermato-venereologica* (2018) 99(3):284–90. doi: 10.2340/00015555-3089

12. Wang W-M, Jin H-Z. Skin Microbiome: An actor in the pathogenesis of psoriasis. *Chin Med J* (2018) 131(1):95–8. doi: 10.4103/0366-6999.221269

13. Liang X, Ou C, Zhuang J, Li J, Zhang F, Zhong Y, et al. Interplay between skin microbiota dysbiosis and the host immune system in psoriasis: Potential pathogenesis. *Front Immunol* (2021) 12:764384. doi: 10.3389/fimmu.2021.764384

14. Lam SY, Radjabzadeh D, Eppinga H, Nossent YRA, van der Zee HH, Kraaij R, et al. A microbiome study to explore the gut-skin axis in hidradenitis suppurativa. *J Dermatol Sci* (2021) 101(3):218–20. doi: 10.1016/j.jdermsci.2020.12.008

15. McCarthy S, Barrett M, Kirthi S, Pellanda P, Vlckova K, Tobin AM, et al. Altered skin and gut microbiome in hidradenitis suppurativa. *J Invest Dermatol* (2022) 142(2):459–68.e15. doi: 10.1016/j.jid.2021.05.036

16. Yuan X, Wang L, Meng D, Wu L, Wang X, Zhang D, et al. The impact of nbuvb on microbial community profiling in the lesional skin of vitiligo subjects. *Microbial pathogenesis* (2020) 140:103943–. doi: 10.1016/j.micpath.2019.103943

17. Bzioueche H, Simonyté Sjödin K, West CE, Khemis A, Rocchi S, Passeron T, et al. Analysis of matched skin and gut microbiome of patients with vitiligo reveals deep skin dysbiosis: Link with mitochondrial and immune changes. *J Invest Dermatol* (2021) 141(9):2280–90. doi: 10.1016/j.jid.2021.01.036

18. Olesen CM, Ingham AC, Thomsen SF, Clausen ML, Andersen PS, Edslev SM, et al. Changes in skin and nasal microbiome and staphylococcal species following treatment of atopic dermatitis with dupilumab. *Microorganisms* (2021) 9(7):1487. doi: 10.3390/microorganisms9071487

19. Hooper MJ, LeWitt TM, Pang Y, Veon FL, Chlipala GE, Feferman L, et al. Gut dysbiosis in cutaneous T-cell lymphoma is characterized by shifts in relative abundances of specific bacterial taxa and decreased diversity in more advanced disease. *J Eur Acad Dermatol Venereology* (2022) 36(9):1552–63. doi: 10.1111/jdv.18125

20. Hooper MJ, LeWitt TM, Veon FL, Pang Y, Chlipala GE, Feferman L, et al. Nasal dysbiosis in cutaneous T-cell lymphoma is characterized by shifts in relative abundances of non-staphylococcus bacteria. *JID Innovations* (2022) 2(5):100132. doi: 10.1016/j.xjidi.2022.100132

21. Harkins CP, MacGibeny MA, Thompson K, Bubic B, Huang X, Brown I, et al. Cutaneous T-cell lymphoma skin microbiome is characterized by shifts in certain commensal bacteria but not viruses when compared with healthy controls. *J Invest Dermatol* (2021) 141(6):1604–8. doi: 10.1016/j.jid.2020.10.021

22. Salava A, Deptula P, Lyyski A, Laine P, Paulin L, Väkevä L, et al. Skin microbiome in cutaneous T-cell lymphoma by 16s and whole-genome shotgun sequencing. *J Invest Dermatol* (2020) 140(11):2304–8.e7. doi: 10.1016/j.jid.2020.03.951

23. Zhang Y, Seminario-Vidal L, Cohen L, Hussaini M, Yao J, Rutenberg D, et al. Tcl-036: Alternations in the skin microbiota are associated with symptom severity in mycosis fungoides. *Clin lymphoma myeloma leukemia* (2021) 21:S409–S. doi: 10.1016/S2152-2650(21)01922-4

24. Dehner CA, Ruff WE, Greiling T, Pereira MS, Redanz S, McNiff J, et al. Malignant T cell activation by a bacillus species isolated from cutaneous T-cell lymphoma lesions. *JID Innov* (2022) 2(2):100084. doi: 10.1016/j.xjidi.2021.100084

25. Jost M, Wehkamp U. The skin microbiome and influencing elements in cutaneous T-cell lymphomas. *Cancers* (2022) 14(5):1324. doi: 10.3390/cancers14051324

26. Phan K, Ramachandran V, Fassihi H, Sebaratnam DF. Comparison of narrowband uv-b with psoralen–uv-a phototherapy for patients with early-stage mycosis fungoides: A systematic review and meta-analysis. *JAMA Dermatol* (2019) 155(3):335–41. doi: 10.1001/jamadermatol.2018.5204

27. Yoshimura-Mishima M, Akamatsu H, Namura S, Horio T. Suppressive effect of ultraviolet (Uvb and puva) radiation on superantigen production by staphylococcus aureus. *J Dermatol Sci* (1999) 19(1):31–6. doi: 10.1016/S0923-1811(98)00046-2

28. Naqib A, Poggi S, Wang W, Hyde M, Kunstman K, Green SJ. Making and sequencing heavily multiplexed, high-throughput 16s ribosomal rna gene amplicon libraries using a flexible, two-stage pcr protocol. *Gene Expression Anal* (2018) 1783:149–69. doi: 10.1007/978-1-4939-7834-2_7

29. Walters W, Hyde ER, Berg-Lyons D, Ackermann G, Humphrey G, Parada A, et al. Improved bacterial 16s rrna gene (V4 and V4-5) and fungal internal transcribed spacer marker gene primers for microbial community surveys. *mSystems* (2016) 1(1):e00009-15. doi: 10.1128/mSystems.00009-15

30. Prakash O, Green S, Jasrotia P, Overholt W, Canion A, Watson DB, et al. Description of rhodanobacter denitrificans sp. nov., isolated from nitrate-rich zones of a contaminated aquifer. *Int J systematic evolutionary Microbiol* (2012) 62(10):2457–62. doi: 10.1099/ijs.0.035840-0

31. Martin M. Cutadapt removes adapter sequences from high-throughput sequencing reads. *EMBnet.journal* (2011) 17(1):3. doi: 10.14806/ej.17.1.200

32. Callahan BJ, McMurdie PJ, Rosen MJ, Han AW, Johnson AJA, Holmes SP. Dada2: High-resolution sample inference from illumina amplicon data. *Nat Methods* (2016) 13(7):581–3. doi: 10.1038/nmeth.3869

33. Quast C, Pruesse E, Yilmaz P, Gerken J, Schweer T, Yarza P, et al. The Silva ribosomal rna gene database project: Improved data processing and web-based tools. *Nucleic Acids Res* (2012) 41(D1):D590–D6. doi: 10.1093/nar/gks1219

34. Murali A, Bhargava A, Wright ES. Idtaxa: A novel approach for accurate taxonomic classification of microbiome sequences. *Microbiome* (2018) 6(1):140. doi: 10.1186/s40168-018-0521-5

35. Davis NM, Proctor DM, Holmes SP, Relman DA, Callahan BJ. Simple statistical identification and removal of contaminant sequences in marker-gene and metagenomics data. *Microbiome* (2018) 6(1):226. doi: 10.1186/s40168-018-0605-2

36. Ahle CM, Stødkilde K, Afshar M, Poehlein A, Ogilvie LA, Söderquist B, et al. Staphylococcus saccharolyticus: An overlooked human skin colonizer. *Microorganisms* (2020) 8(8):1105. doi: 10.3390/microorganisms8081105

37. Ahle CM, Stødkilde-Jørgensen K, Poehlein A, Streit WR, Hüpeden J, Brüggemann H. Comparison of three amplicon sequencing approaches to determine staphylococcal populations on human skin. *BMC Microbiol* (2021) 21(1):221. doi: 10.1186/s12866-021-02284-1

38. McMurdie PJ, Holmes S. Phyloseq: An r package for reproducible interactive analysis and graphics of microbiome census data. *PLoS One* (2013) 8(4):e61217. doi: 10.1371/journal.pone.0061217

39. R Core Team.. R: A language and environment for statistical computing. Vienna, Austria: Vienna, Austria (2022). Available at: https://ww.R-project.org.

40. Okansen J, Guillaume Blanchet F, Kindt R, Legendre P, Minchin P, O'Hara R, et al. Vegan: Community ecology. *R Package Version* (2018) 2:4–6. Avalibale at: https://github.com/vegandevs/vegan.

41. Kuhn M. The caret package. *J Stat Software* (2012) 28(5):1–26. doi 10.18637/jss.v028.i05.

42. Ho TK. (1995). Random decision forests, in: *Proceedings of the Third International Conference on Document Analysis and Recognition*, Montreal, (14-16) 278–82.

43. Robin X, Turck N, Hainard A, Tiberti N, Lisacek F, Sanchez J-C, et al. Proc: An open-source package for r and s+ to analyze and compare roc curves. *BMC Bioinf* (2011) 12(1):77. doi: 10.1186/1471-2105-12-77

44. Paulson JN, Stine OC, Bravo HC, Pop M. Differential abundance analysis for microbial marker-gene surveys. *Nat Methods* (2013) 10(12):1200–2. doi: 10.1038/nmeth.2658

45. Robinson MD, McCarthy DJ, Smyth GK. Edger: A bioconductor package for differential expression analysis of digital gene expression data. *Bioinformatics* (2010) 26(1):139–40. doi: 10.1093/bioinformatics/btp616

46. Krejsgaard T, Willerslev-Olsen A, Lindahl LM, Bonefeld CM, Koralov SB, Geisler C, et al. Staphylococcal enterotoxins stimulate lymphoma-associated immune dysregulation. *Blood* (2014) 124(5):761–70. doi: 10.1182/blood-2014-01-551184

47. Williams MR, Costa SK, Zaramela LS, Khalil S, Todd DA, Winter HL, et al. Quorum sensing between bacterial species on the skin protects against epidermal

injury in atopic dermatitis. *Sci Transl Med* (2019) 11(490):eaat8329. doi: 10.1126/scitranslmed.aat8329

48. Severn MM, Cho YK, Manzer HS, Bunch ZL, Shahbandi A, Todd DA, et al. The commensal staphylococcus warneri makes peptide inhibitors of mrsa quorum sensing that protect skin from atopic or necrotic damage. *J Invest Dermatol* (2022) S0022-202X(22)01646-3. doi: 10.1016/j.jid.2022.05.1092

49. Nakatsuji T, Chen TH, Narala S, Chun KA, Two AM, Yun T, et al. Antimicrobials from human skin commensal bacteria protect against staphylococcus aureus and are deficient in atopic dermatitis. *Sci Transl Med* (2017) 9(378):eaah4680. doi: 10.1126/scitranslmed.aah4680

50. Glatthardt T, Campos JCM, Chamon RC, de Sá Coimbra TF, Rocha GA, de Melo MAF, et al. Small molecules produced by commensal staphylococcus epidermidis disrupt formation of biofilms by staphylococcus aureus. *Appl Environ Microbiol* (2020) 86(5):e02539-19. doi: 10.1128/aem.02539-19

51. Nakatsuji T, Chen TH, Butcher AM, Trzoss LL, Nam SJ, Shirakawa KT, et al. A commensal strain of staphylococcus epidermidis protects against skin neoplasia. *Sci Adv* (2018) 4(2):eaao4502. doi: 10.1126/sciadv.aao4502

52. Laborel-Préneron E, Bianchi P, Boralevi F, Lehours P, Fraysse F, Morice-Picard F, et al. Effects of the staphylococcus aureus and staphylococcus epidermidis secretomes isolated from the skin microbiota of atopic children on Cd4+ T cell activation. *PLoS One* (2015) 10(10):e0141067–e. doi: 10.1371/journal.pone.0141067

53. Fyhrquist N, Ruokolainen L, Suomalainen A, Lehtimäki S, Veckman V, Vendelin J, et al. Acinetobacter species in the skin microbiota protect against allergic sensitization and inflammation. *J Allergy Clin Immunol* (2014) 134 (6):1301–9.e11. doi: 10.1016/j.jaci.2014.07.059

54. Kong HH, Oh J, Deming C, Conlan S, Grice EA, Beatson MA, et al. Temporal shifts in the skin microbiome associated with disease flares and treatment in children with atopic dermatitis. *Genome Res* (2012) 22(5):850–9. doi: 10.1101/gr.131029.111

55. Flowers L, Grice EA. The skin microbiota: Balancing risk and reward. *Cell Host Microbe* (2020) 28(2):190–200. doi: 10.1016/j.chom.2020.06.017

56. Ridaura VK, Bouladoux N, Claesen J, Chen YE, Byrd AL, Constantinides MG, et al. Contextual control of skin immunity and inflammation by corynebacterium. *J Exp Med* (2018) 215(3):785–99. doi: 10.1084/jem.20171079

57. Licht P, Mailänder V. Transcriptional heterogeneity and the microbiome of cutaneous T-cell lymphoma. *Cells* (2022) 11(3):328. doi: 10.3390/cells11030328

58. Gupta VK, Paul S, Dutta C. Geography, ethnicity or subsistence-specific variations in human microbiome composition and diversity. *Front Microbiol* (2017) 8:1162. doi: 10.3389/fmicb.2017.01162

59. Suga H, Sugaya M, Miyagaki T, Ohmatsu H, Kawaguchi M, Takahashi N, et al. Skin barrier dysfunction and low antimicrobial peptide expression in cutaneous T-cell lymphoma. *Clin Cancer Res* (2014) 20(16):4339–48. doi: 10.1158/1078-0432.Ccr-14-0077

frontiers | Frontiers in Cellular and Infection Microbiology

TYPE Original Research
PUBLISHED 14 November 2022
DOI 10.3389/fcimb.2022.1029592

OPEN ACCESS

EDITED BY
Hariom Yadav,
USF Center for Microbiome Research, United States

REVIEWED BY
E Xiao,
Peking University, China
Michael Bording-Jorgensen,
University of Alberta, Canada

*CORRESPONDENCE
Biao Huang
hbcd1997@163.com
Haifang Zhang
haifangzhang@sina.com
Dao-Jiang Yu
ydj51087@163.com

SPECIALTY SECTION
This article was submitted to Extra-intestinal Microbiome, a section of the journal Frontiers in Cellular and Infection Microbiology

RECEIVED 02 September 2022
ACCEPTED 19 October 2022
PUBLISHED 14 November 2022

CITATION
Huang B, An L, Su W, Yan T, Zhang H and Yu D-J (2022) Exploring the alterations and function of skin microbiome mediated by ionizing radiation injury.
Front. Cell. Infect. Microbiol. 12:1029592.
doi: 10.3389/fcimb.2022.1029592

Exploring the alterations and function of skin microbiome mediated by ionizing radiation injury

Biao Huang[1,2*], Lu An[3], Wenxing Su[1,2], Tao Yan[4], Haifang Zhang[5*] and Dao-Jiang Yu[1,2,4*]

[1]Department of Plastic and Burn Surgery, The Second Affiliated Hospital of Chengdu Medical College, China National Nuclear Corporation 416 Hospital, Chengdu, China, [2]Department of Clinical Medicine, Chengdu Medical College, Chengdu, China, [3]Transformation Center of Radiological Medicine, The Second Affiliated Hospital of Soochow University, Suzhou, China, [4]West China School of Basic Medical Sciences and Forensic Medicine, Sichuan University, Chengdu, China, [5]Department of Clinical Laboratory, The Second Affiliated Hospital of Soochow University, Suzhou, China

Background: Radiation-induced skin injury (RISI) is still the most common and severe side effect of radiotherapy. The role of the skin's microbial barrier in the pathogenesis and progression of RISI needs to be fully investigated.

Methods: This study aimed to explore the alterations in and functions of the skin microbiota in RISI. We applied the unculturable approach to characterize the cutaneous microbiomes of a radiation-induced animal model by sequencing the V1–V3 regions of the 16S ribosomal RNA (rRNA) gene. Combined with the downloaded clinical data of patients, a comprehensive analysis was performed to identify potential radioprotective species and metabolic pathways.

Results: There were no significant differences in the alpha diversity indices (Sobs, Shannon, Simpson, Ace, and Chao) between the acute radiation injury and control groups. Phylum-level analysis of the RISI microbiomes exhibited significant predominance of Firmicutes (mean abundance = 67%, corrected p = 0.0035). The high abundance of Firmicutes was significantly associated with rapid healing of RISI (average relative abundance = 52%; Kruskal–Wallis: p = 5.7E–4). Among its members, *Streptococcus*, *Staphylococcus*, *Acetivibrio ethanolgignens group*, *Peptostreptococcus*, *Anaerofilum*, and *UCG-002* [linear discriminant analysis (LDA) > 3, $p < 0.05$] were identified as the core genera of Firmicutes. In addition, Lachnosiraceae and *Lactobacillus* occupied an important position in the interaction network ($r > 0.6$, $p < 0.05$). The differential metabolic pathways of RISI were mainly associated with carbohydrate metabolism (butanoate and propanoate metabolism), amino acid metabolism (tryptophan and histidine metabolism), energy metabolism, and lipid metabolism (fatty acid degradation and biosynthesis).

Conclusion: This study provides new insights into the potential mechanism and skin microbial changes in the progression of RISI. The overwhelming

predominance of members of Firmicutes, including Streptococcaceae, Staphylococcaceae, Lachnospiraceae, and *Lactobacillus*, is potentially related to rapid healing of RISI. The microbiota–metabolite axis plays a critical role in RISI and provides promising therapeutic targets for the treatment of adverse side effects.

KEYWORDS

skin microbiome, radiation-induced skin injury, 16S rRNA, radiation protection, microbial metabolism

Introduction

Radiation-induced skin injury (RISI) is defined as cutaneous and includes deep tissue damage (Akh et al., 2022). It usually occurs following nuclear accidents, occupational exposure, and radiation therapy (Drozdovitch et al., 2022). According to research statistics, nearly 50% of patients with cancer receive radiotherapy, and 95% of them develop varying degrees of skin damage impacted by their age, physical condition, skin type, and the location of the tumor (Steinert et al., 2003). RISI is an irreversible and progressive condition that seriously deteriorates patients' quality of life, even leading to the termination of therapy. On the whole, RISI is of two types: acute and chronic. Acute RISI includes dry and wet desquamation, skin necrosis, ulcers, and bleeding. Chronic RISI covers chronic ulcers, radiation-induced keratosis, telangiectasias, fibrosis, and skin cancer. RISI is a common and dose-limiting reaction. Following a cumulative radiation dose exceeding 10 Gy, the exposed skin often develops an intense local inflammatory reaction within 2 days to 1 week. The reaction peaks at 48 h, then subsides, only to be followed by a second phase of intense erythema with edema and vesiculation beginning 1 week after exposure and lasting up to 1 month. Erosions, pustule, and ulcerations may also develop with secondary infection. The mechanism of RISI is mainly related to skin cell senescence, fibrosis, vascular injury, radiation-induced reactive oxygen species (ROS) damage, and other signaling pathways (Wei et al., 2021; Yadav et al., 2022). Multiple therapeutic methods such as physical therapy, external dressing, and surgery have not been fully successful in the treatment of RISI and the prevention of damage to the adjacent tissue (Rosenthal et al., 2019).

As the largest organ of the human body, the skin structure forms a protective barrier against external invasion (Persinal-Medina et al., 2022). It is well known that the skin barrier functions as a microbial barrier, physical barrier, chemical barrier, and an immune barrier. Based on their integral collaboration, these barriers maintain the metabolic and immune homeostasis of the human skin (Celebi Sozener et al., 2022). As the outermost barrier against the external environment, the unique ecosystem constituted by colonizing microbiota has gradually been found to play an important role in the occurrence and progression of various inflammatory skin diseases. Factors affecting skin microbial colonization include lifestyle, systemic host factors, and environmental factors such as ionizing radiation damage (Luna, 2020). Although the skin microbiota has been intensely investigated regarding its significance in several diseases (atopic dermatitis, psoriasis, diabetic foot, and burns) in the past few years, research has been mainly based on the culture method (Alam et al., 2022; Durand et al., 2022). The role of skin microbiomes in the pathogenesis and prognosis of RISI remains to be fully studied, and the use of the unculturable approach helps provide a holistic view of the entire community (Wensel et al., 2022).

Our study provides insights into the alterations of the microbial barrier in RISI and identifies the core bacteria that may serve as potential targets for protection from and treatment of RISI.

Materials and methods

Ethics statement

The protocols for experiments involving animals were approved by the Animal Experimentation Ethics Committee at China National Nuclear Corporation 416 Hospital (Chengdu, China; reference no. SYXK2020-196).

Animal model construction

A total of 29 male Sprague–Dawley rats (7–8 weeks old) were purchased from the Shanghai SLAC Laboratory Animal Co., Ltd.

(Shanghai, China). These animals were housed in a pathogen-free environment at the facilities of the Medical College of Soochow and provided standard chow and water *ad libitum*.

Before irradiation, we collected skin samples from the gluteal region of 29 rats, which represents the control site. Subsequently, irradiated skin samples from the same site were taken as the treatment group.

For irradiation, the rats were anesthetized with an intraperitoneal injection of 10% chloral hydrate (10 mg/kg), and the hair on the gluteal region was shaved. The animals were immobilized using an adhesive tape on a plastic plate to minimize their motion during irradiation. A 3-cm-thick piece of lead was used to shield the animals and localize the radiation field (4 cm × 4.5 cm). The rats received a 40-Gy dose of radiation to the treatment area at a rate of 500 cGy/min using a 6-MeV electron beam accelerator (Clinac 2100EX; Varian Medical Systems, Palo Alto, CA, USA) for the construction of an acute skin radiation damage model. After irradiation, the exposed skin showed erythema and high temperature at around 10 days. After about 2 weeks, a large area of wet desquamation and superficial ulcers were formed, and the skin samples were collected at the same time.

Sample collection

Defatted cotton swabs were pre-moistened in ST solution (0.15 M NaCl with 0.1% Tween-20). Thereafter, an area of 4 cm × 4.5 cm in the irradiated gluteal region was rubbed for 30 s for sample collection. A similar gluteal region before irradiation, which represents the control site, was swabbed to collect specimens from healthy subjects. Two to three swabs were saved per sample. After sampling, the cotton swab head was cut into a sterilized frozen tube, quickly frozen with liquid nitrogen, and stored at −80°C.

DNA extraction and 16S rRNA gene sequencing

Skin sample preparation and 16S ribosomal RNA (rRNA) sequencing were conducted as previously described (Ellison et al., 2021; Olesen et al., 2022). Genomic DNA was extracted using Wizard® Genomic DNA Purification Kit (Promega, Madison, WI, USA) according to the manufacturer's protocol. Purified genomic DNA was quantified with a TBS-380 fluorometer (Turner BioSystems Inc., Sunnyvale, CA, USA). High-quality DNA [optical density $(OD)_{260/280}$ = 1.8–2.0, >20 μg] was used for further analysis. The genome was sequenced using a combination of the PacBio RS II Single-Molecule Real-Time (SMRT) (PacBio, Menlo Park, CA, USA) and Illumina (San Diego, CA, USA) sequencing platforms. The Illumina data were used to evaluate the complexity of the genome. For Illumina sequencing, at least 1 μg genomic DNA was used for each strain to construct the sequencing library. The complete genome sequence was assembled using both the PacBio and Illumina reads. The original imaging data were converted into sequencing data *via* base calling, defined as the raw data or raw reads and saved as FASTQ files. These FASTQ files are the original data provided for users, which included the read sequences and quality information. A statistic of quality information was applied for quality trimming, by which low-quality data can be removed to obtain clean data. The reads were then assembled into a contig using Unicycler. The last circular step was checked and manually finished, generating a complete genome with seamless chromosomes and plasmids. Finally, error correction of the PacBio assembly results was performed using the Illumina reads with Pilon.

Patient clinical data

Patient clinical data were from NCBI under accession no. PRJNA665254 (http://www.ncbi.nlm.nih.gov/bioproject/665254). Patients were included if they were newly diagnosed with grade 2 RISI. The exclusion criterion was systemic topical application of corticosteroids and antibiotics (Ramadan et al., 2021). The clinical characteristics of patients including age, sex, cancer type, and concomitant diseases are shown in Table 1.

TABLE 1 Clinicopathological characteristics of patients with radiation-induced dermatitis (RID).

Characteristics	RID cohort (*N* = 78)	Healthy cohort (*N* = 20)
Age (years)	49.42 ± 8.79	36.35 ± 13.46
Gender, *n* (%)		
Male	35 (45)	10 (50)
Female	43 (55)	10 (50)
Site of RISI, *n* (%)		
Chest	41 (53)	NA
Sacrum	13 (17)	NA
Pelvis	12 (15)	NA
Leg	3 (4)	NA
Head	5 (6)	NA
Neck	4 (5)	NA
Systemic disease, *n* (%)		
Diabetes	36 (46)	NA
Hypertension	21 (27)	NA
Clinical prognosis, *n* (%)		
Rapidly recovery	33(42)	NA
Delayed recovery	24(31)	NA
Chronic ulcer	21(27)	NA

RID, radiation-induced dermatitis; NA, not available.

Bioinformatics analysis

The paired-end (PE) reads obtained with MiSeq sequencing were first spliced according to the overlap relationship, and the sequence quality was controlled and filtered at the same time. After distinguishing the samples, operational taxonomic unit (OTU) clustering analysis and species taxonomic analysis were carried out.

Non-repetitive sequences were extracted from optimized sequences to reduce the number of redundant computations (http://drive5.com/usearch/manual/dereplication.html). Single sequences without repetitions were removed, while the non-repetitive sequences (excluding single sequences) were clustered into OTUs according to 97% similarity, with the chimera removed in the clustering process to obtain the representative sequences of the OTUs.

Taxonomic analysis of the OTU representative sequences with 97% similarity was performed using the RDP classifier Bayesian algorithm. The community species composition of each sample was calculated at eight taxonomic levels: domain, kingdom, phylum, class, order, family, genus, and species. SILVA (http://www.arb-silva.de) and RDP (http://rdp.cme.msu.edu/) were used to compare databases.

Bacterial diversity was estimated using QIIME 2 for the entire dataset without subsampling (Callahan et al., 2016), and the alpha diversity was determined using two approaches: richness (number of observed species and Chao1 index) and evenness (Shannon diversity index) of communities. Unpaired Wilcoxon rank-sum test was used to assess the statistical significance between two groups. Principal coordinates analysis (PCoA) based on unweighted UniFrac distance matrix was used to calculate the similarities or differences of the community composition between two groups.

Based on the community abundance data in the sample, the Wilcoxon rank-sum test was used to detect species with significant differential abundance. The non-parametric factorial Kruskal–Wallis rank-sum test was used to determine the characteristics of the significant abundance differences and the group differences. Finally, linear discriminant analysis (LDA) effect size (LEfSe) was used to estimate the effect of the abundance of each component (species) (Segata et al., 2011).

Network analysis was conducted to obtain the coexistence relationship of species in the environment. The top 50 species based on the total abundance at the genus level were selected, and the Spearman's correlation coefficients of these species were calculated. The size of the node represented species abundance, while the thickness of the line represented the correlation coefficient.

To predict the functional profile of cutaneous microbiota, the Greengenes database (v.13.8) at a 97% identity used a closed-reference script for OTU picking in QIIME (McDonald et al., 2012). The functional potential of cutaneous microbiomes was predicted using PICRUSt (http://picrust.github.io/picrust/) (Langille et al., 2013).

Statistical analysis

Analyses of bacterial diversity, species differences, LEfSe, and PICRUSt were all performed and visualized using R software. A $p < 0.05$ or a false discovery rate (FDR) < 0.05 was considered as the statistical significance cutoff in all tests.

Results

Optimization of the 16S rRNA sequence

In total, the PE reads of 58 samples were input into QIIME 2 for merging, quality control and filtering, and correcting the direction of the sequences. The results revealed an optimized number of sequences of 3,842,947, optimized number of sequence bases of 1,614,133,683, and an average length of 420 bp.

Species annotation and evaluation

According to the optimized sequence, the 16S rRNA reads were taxonomically assigned to 1 domain, 1 kingdom, 42 phyla, 108 classes, 254 orders, 424 families, 914 genera, 1,699 species, and 9,614 OTUs. There were no significant differences in the alpha diversity indices (Sobs, Shannon, Simpson, Ace, and Chao) between the acute radiation injury and control groups ($Q > 0.05$) (Figures 1A, C). In addition, the structure and composition of the bacterial communities significantly distinguished the classification of cutaneous microbiomes into RISI and healthy skin. PCoA based on unweighted UniFrac metrics sorted the samples into two particular clusters ($R = 0.4138$, $p = 0.001$) (Figure 1B).

Composition differences between RISI and normal skin

In general, acute radiation injury-induced skin microbiome alterations showed remarkable differences in certain bacterial taxa at several classification levels compared with the healthy control. Phylum-level analyses of the RISI microbiomes exhibited alternately significant predominance of Firmicutes (mean abundance = 67%, corrected $p = 0.0035$) (Figures 2A, B, E). In contrast, the proportions of Proteobacteria (mean abundance = 19%, corrected $p = 0.0029$), Bacteroidetes (mean abundance = 6%, corrected $p = 0.02$), and Actinobacteria (mean abundance = 5%, corrected $p = 0.0029$) decreased significantly in RISI. In addition, Verrucomicrobia (mean abundance = 0.1%) showed a relatively constant proportion. Family-level analyses revealed that the abundances of Streptococcaceae (mean abundance = 26%, corrected $p = 4.435E{-}5$) (Figures 2C, D)

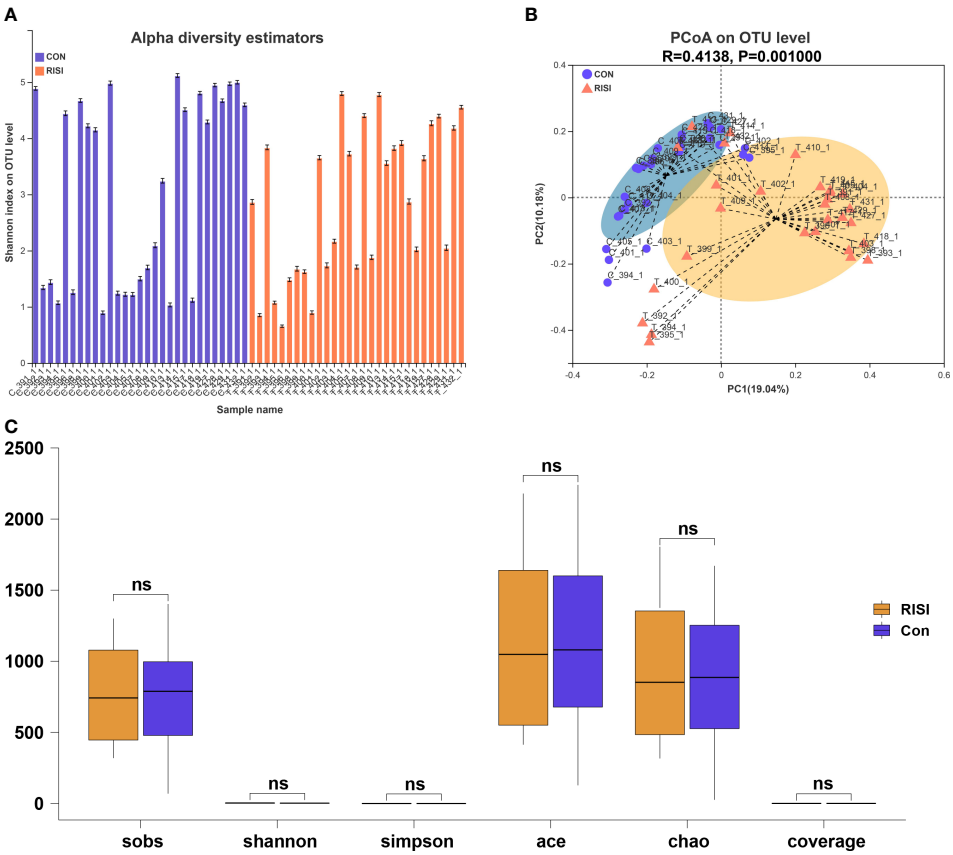

FIGURE 1
Diversity analysis of cutaneous microbiomes. **(A)** Alpha diversity bar charts between the radiation-induced skin injury (*RISI*) group and healthy controls (*CON*). **(B)** Beta diversity estimation. Principal coordinates analysis (PCoA) of RISI and CON based on unweighted UniFrac distance matrices. **(C)** Box plot of the comparison of the alpha diversity indices. ns: not sinificant.

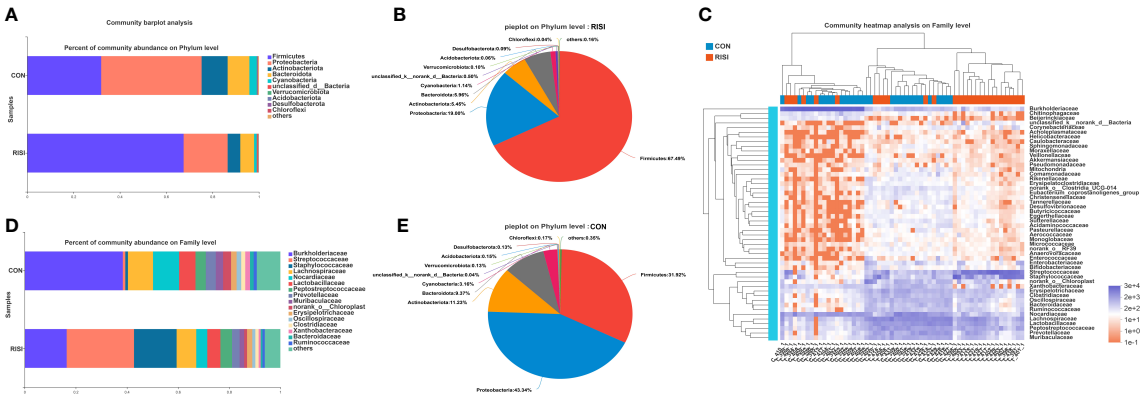

FIGURE 2
Species composition analysis. **(A)** Phylum-level analysis of the skin microbiota. *Bar charts* illustrate the relative proportions of dominant phyla across all study groups. **(B)** Pie chart illustrating the proportions of species at the phylum level in healthy skin. **(C)** Community heatmap. **(D)** Family-level analysis of the skin microbiota using bar charts. **(E)** Pie chart illustrating the proportions of species at the phylum level in radiation-induced skin injury (RISI).

and Staphylococcaceae (mean abundance = 17%, corrected p = 0.0004) significantly increased in RISI. In contrast, the proportions of Burkholderiaceae (mean abundance = 16%, corrected p = 0.0058), and Nocardiaceae (mean abundance = 4%, corrected p = 0.0007) significantly decreased in RISI.

Differential species analysis of RISI

LEfSe was used to discover high-dimensional biomarkers and determine their genomic characteristics (Figures 3A, B). LDA can estimate the effect of abundance of each component (species) on the difference effect. Phylum-level analyses of the RISI microbiomes revealed the significant effect of Firmicutes (LDA = 5.223, p = 2.42E−5) on RISI, while order-level analyses revealed that Lactobacillales (LDA = 5.07, p = 7.79E−06) and Staphylococcales (LDA = 4.89, p = 2.75E−06) were the significant orders. We did a further analysis to determine the core species that play key roles in Firmicutes. The results identified *Streptococcus* (genus of Streptococcaceae; LDA = 5.10, p = 1.0E−07), *Staphylococcus* (genus of Staphylococcaceae; LDA = 4.89, p = 1.0E−06), *Acetivibrio ethanolgignens group* (genus of Lachnosiraceae; LDA = 3.51, p = 0.02), *Peptostreptococcus* (genus of *Peptostreptococcaceae*; LDA = 3.35, p = 0.04), *Anaerofilum* (genus of *Ruminococcaceae*; LDA = 3.48, p = 0.04), and *UCG-002* (genus of Oscillospiraceae; LDA = 2.59, p = 0.03) as the core genera of Firmicutes. In addition, *Ralstonia* (genus of Burkholderiaceae) was significantly decreased in RISI (LDA = 4.98, p = 8.50E−04) (Figure 3C).

Interaction network analysis

As expected, the members of Firmicutes had the closest interaction with other species in the network. Among these, multiple members of Lachnospiraceae, such as *unclassified_f_Lachnospiraceae*, *norank_f_Lachnospiraceae*, *Lachnoclostridium*, *Blautia*, and *Lachnospiraceae_NK4A136_group*, were found positively correlated with other Firmicutes species (r > 0.6, p < 0.05) (Figure 4B). Additionally, Streptococcaceae and *Staphylococcus* showed a close correlation with each other (r = 0.79, p = 2.45E−13) (Figure 4B). *Lactobacillus* also occupied an important position in this network, and the average correlation coefficient between *Lactobacillus* and the members of Lachnospiraceae was greater than 0.9 (Figure 4A). Moreover, *Hydrotalea* and *Ralstonia* showed a significant correlation with each other (r = 0.74, p = 2.8E−11), but were negatively correlated with members of Firmicutes.

Function prediction of cutaneous microbiomes

The overall function of cutaneous microbiomes may be related to the pathogenesis of RISI, providing a number of potential targets for its prevention and treatment. The differential metabolic pathways were mainly associated with carbohydrate metabolism [butanoate, glyoxylate, dicarboxylate, and propanoate metabolism and citrate cycle—tricarboxylic acid (TCA) cycle], amino acid metabolism (phenylalanine, tryptophan, and histidine metabolism), energy metabolism (oxidative phosphorylation, sulfur metabolism, and carbon fixation pathways in prokaryotes), and lipid metabolism (fatty acid degradation and biosynthesis). In addition, membrane transport [ATP-binding cassette (ABC) transporters], nucleotide metabolism (purine metabolism), endocrine system [peroxisome proliferator-activated receptor (PPAR) signaling pathway], and cell motility (bacterial chemotaxis) may contribute to the progression of RISI (Figures 5A–C).

Alterations in clinical patients

According to the patient data from BioProject 665254, the adverse effects of undergoing radiotherapy can lead to significant changes in the skin microbiomes (Figure 6). Overall, radiotherapy induced a significant reduction in bacterial diversity (Shannon and Chao: p < 0.001) (Figure 6C). The microbiome associated with the rapid healing of RISI (2–4 weeks) was significantly related to the predominance of Firmicutes (average relative abundance = 52%; Kruskal–Wallis: p = 5.7E−4) (Figure 6A). In contrast, the microbiota of chronic ulcers was clearly dominated by Proteobacteria and the low abundance of Firmicutes (average relative abundance = 74% and 18%, respectively; Kruskal–Wallis: p = 8.3E−4). LEfSe revealed the significant enrichment of *Klebsiella* (LDA = 3.27, p = 0.0078), *Pseudomonas* (LDA = 3.45, p = 6.23E-04), and *Staphylococcus* (LDA = 3.69, p = 0.0004) in RISI compared with healthy subjects (Figure 6E).

The differential metabolic pathways were mainly associated with epidermal integrity, alteration in pH, lipid metabolism (fatty acid metabolism), amino acid metabolism, histidine metabolism, membrane transport (ABC transporters), Hedgehog signaling pathway, nitrogen metabolism, and peptidases (Figure 6D).

Discussion

With the wide application of radiological instruments and radioactive materials in medicine and industry, radiation-induced injury is still a serious concern in nuclear safety (Rios et al., 2020; Ashack et al., 2020). RISI, the most common type of injury, has progressed to some form of radio lesions, including erythema, desquamation, ulceration, and cutaneous tumor. According to statistics, almost 50% of patients eventually died of skin wound events from the Chernobyl nuclear accident (Steinert et al., 2003). RISI can seriously affect the quality of life of patients. It represents a challenge for clinicians and is

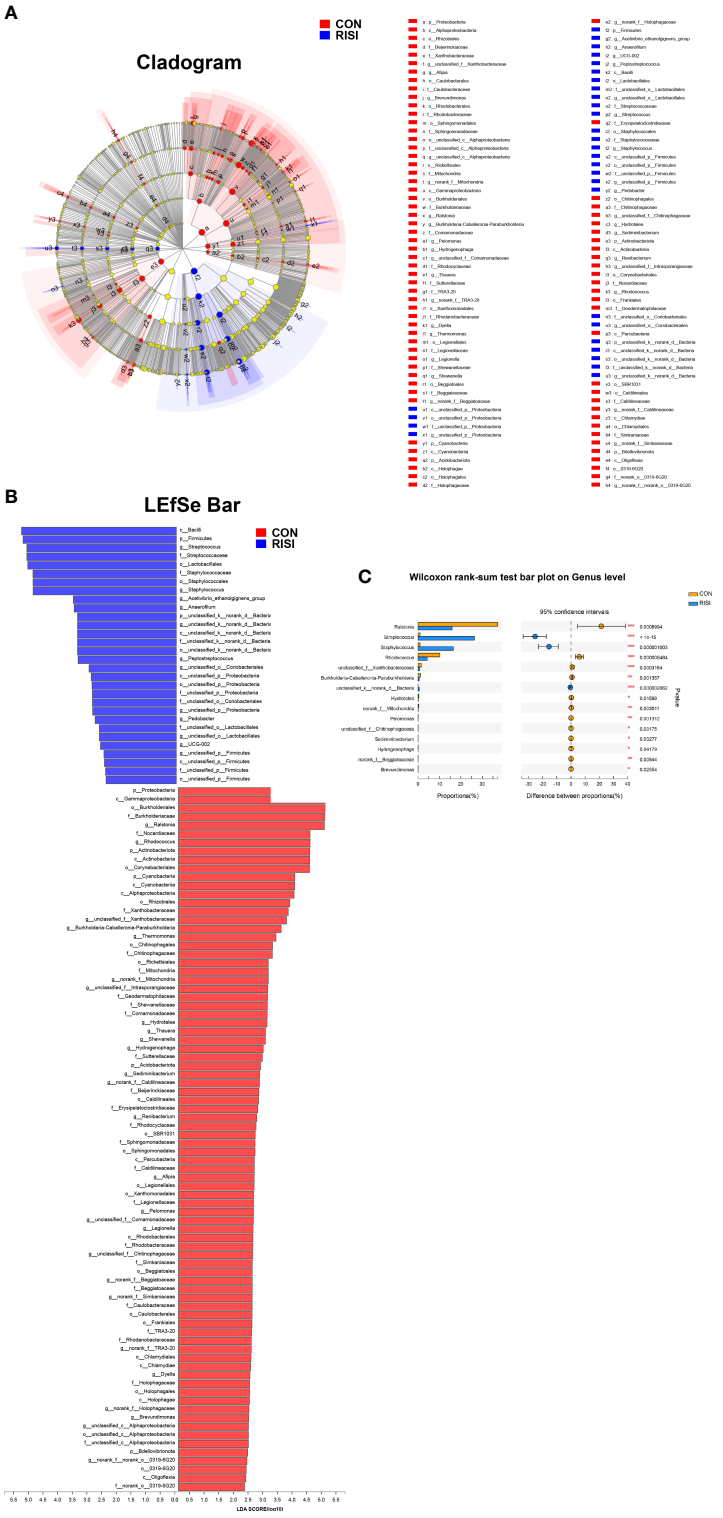

FIGURE 3
Results of linear discriminant analysis (LDA) effect size (LEfSe). **(A)** Hierarchical tree map of multilevel species. **(B)** LDA histogram showing the microbial groups that play significant roles in several groups. The LDA scores obtained by linear regression analysis showed that the higher the score, the greater the effect of species abundance on the difference. **(C)** Relative abundance of the most predominant genera in cutaneous microbiomes of radiation-induced skin injury (RISI) and healthy controls.

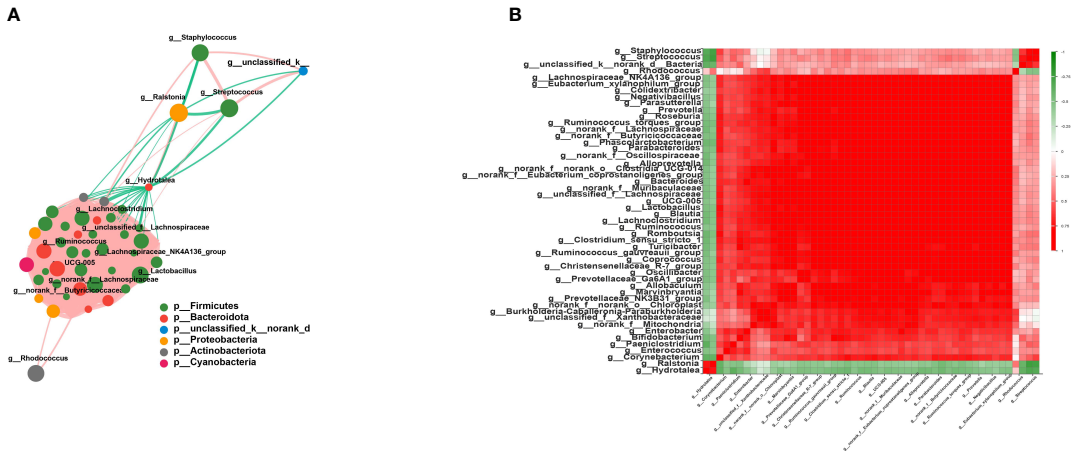

FIGURE 4
Interaction network and correlation analysis. **(A)** Interaction network of the top 50 species in total abundance. The *size of the nodes* represents the abundance of species, while *different colors* represent different species. The *color of the connecting lines* represents positive and negative correlations: *red lines* denote positive correlation, while *green lines* indicate negative correlation. The *thickness of the line* represents the magnitude of the correlation coefficient. **(B)** Correlation coefficient heatmap. Both the *x*- and *y*-axes indicate the species, with *red* denoting positive correlation and *green* indicating negative correlation.

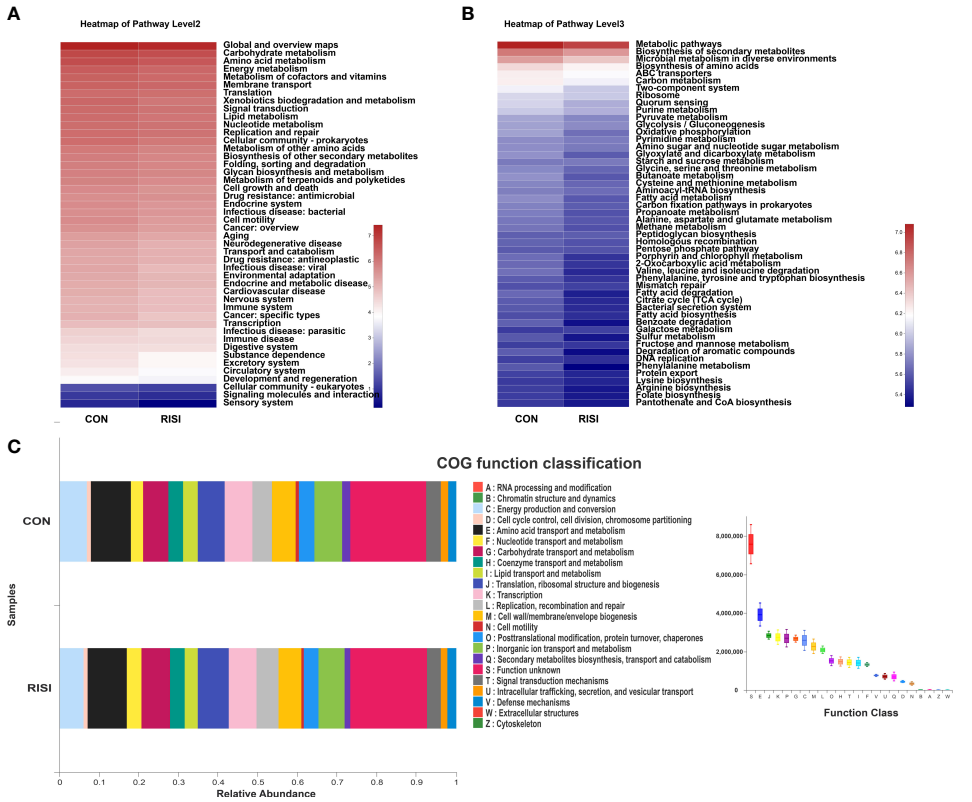

FIGURE 5
Differentially abundant metabolic pathways between radiation-induced skin injury (RISI) and healthy controls. **(A)** Kyoto Encyclopedia of Genes and Genomes (KEGG) pathways at level 2. **(B)** KEGG pathways at level 3. **(C)** Clusters of Orthologous Genes (COG) function.

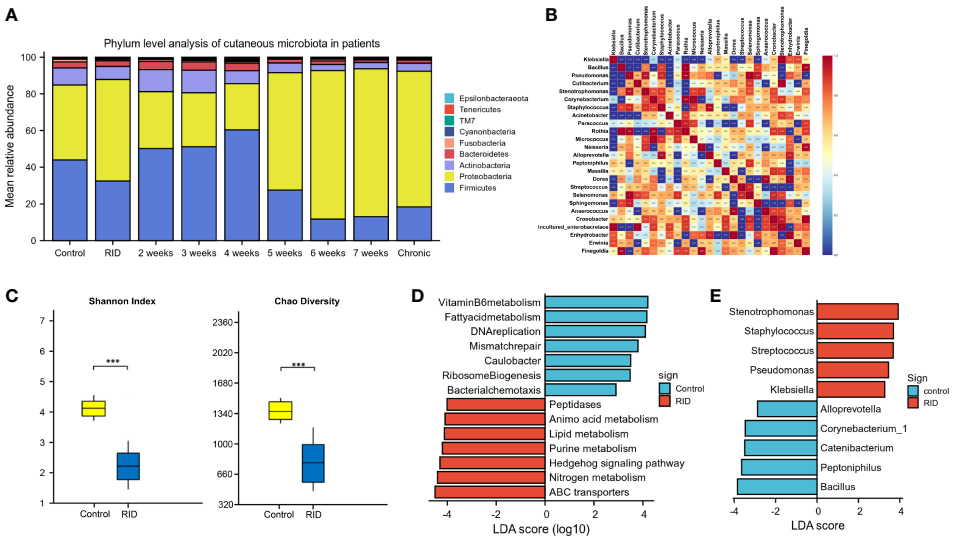

FIGURE 6
Alterations in patients with radiotherapy-induced dermatitis. **(A)** Changes in the microbial structure of patients with radiation-induced dermatitis (RID) with different prognosis. **(B)** Heatmap of the correlation coefficients. **(C)** Change of species diversity. **(D)** Differential metabolic pathways. **(E)** Linear discriminant analysis effect size (LEfSe) in patients with radiation-induced skin injury (RISI) compared with healthy subjects. *p < 0.05; **p < 0.01; ***p < 0.001.

regarded as an additional burden in the healthcare expenditure (Yao et al., 2021; Xie et al., 2021; Hao et al., 2022). However, the exact pathogenic molecular mechanism of RISI is still unclear.

The skin microbiota itself is a barrier against environmental invasion (radiation, climate, or pollution) and infection by multiple pathogenic microbes (Uberoi et al., 2021; Harris-Tryon and Grice, 2022). The culture-based approaches used in the clinic have not been able to determine the integral role of the entire community. Therefore, the application of culture-independent techniques, such as metagenomics and 16S rRNA, to characterize microbial communities provides important new insights into the diversity of the microbial world and its role in dermatological health (Yadav et al., 2022; Liu et al., 2022).

Disruption to the structural integrity of skin microbes is often associated with the progress of disease (Byrd et al., 2017). It has been reported that the alpha diversity was significantly reduced in dermatological disorders such as atopic dermatitis and psoriasis (Ramadan et al., 2019; Elsherbiny et al., 2020). In our animal study, the differences in the alpha diversity indices were not significant between the acute radiation injury and control groups. Subsequent data analysis of clinical patients found that radiotherapy induced a significant reduction in the bacterial diversity (Shannon and Chao: $p < 0.001$). This result was due to a large proportion of the clinical cohort comprising patients with chronic ulcers and lesions with delayed healing whose microbiome structure has been severely damaged. This is similar to the results showing that radiotherapy can significantly reduce the diversity of the digestive tract microbiome (Kumpitsch et al., 2020). The pathophysiology mechanism of RISI was mainly associated with epidermal disturbances, fibrosis, vascular injury, ROS damage, and immune disorder, leading to the lack of oxygen and nutrients in the skin. These factors explain the radiation-induced reduction in microbial diversity. In addition, the injury recovery process can be accelerated by activating the aryl hydrocarbon receptor (AhR) in keratinocytes and restoring the skin microbiome on the wound (Uberoi et al., 2021; Marvasi et al., 2022). This reflects the protective role of cutaneous microbiota in the maintenance of the epidermis.

Taxonomic analysis of the skin microbiota associated with acute radiation injury highlighted the high prevalence of Firmicutes. The results of clinical patients revealed that rapid healing of RISI (2–4 weeks) was significantly accompanied by the predominance of Firmicutes (abundance = 52.2%). In contrast, chronic ulcers were significantly related to the low abundance of Firmicutes (18.36%). It has been reported that Firmicutes can mediate intestinal radioprotection in mice by alleviating the effects of DNA damage. The expression levels of the DNA damage-related markers (gH2AX, p53, and 53BP1) were reduced in the Firmicutes- and short-chain fatty acid (SCFA)-treated groups compared with the controls. We speculated that the predominance of Firmicutes is a stress response of the skin flora to resist external radiation injury. Several members of the Firmicutes phylum are probiotics that can resist dehydration and extreme environments (Wozniak et al., 2022). When bacteria (*Lactobacillus* and *Lachnospira*) ferment carbohydrates, they produce metabolites, including vitamins and SCFAs such as butyrate and lactate (Li et al., 2022). Butyrate helps prevent inflammation and maintains the

intestinal epithelial stability. *Lactobacillus* and its lysate reduce the pro-inflammatory cytokines interleukin 6 (IL-6) and IL-8 and enhance the levels of laminin A/B in the human epidermis, suggesting a positive impact on the skin barrier (Khmaladze et al., 2019). Therefore, we regard Firmicutes as the core phylum of early radiation protection.

LEfSe identified several species that have a significant impact on RISI. *Streptococcus* is a genus of Streptococcaceae belonging to the order Lactobacillales. According to relevant reports, *Streptococcus salivarius K12* can alleviate radiation-induced oral mucositis in mice by decreasing the abundance of oral anaerobes, inhibiting NI1060 in *Pasteurella* and downregulating the expression of nitrate reductase (Wang et al., 2021). *Staphylococcus* is a member of the healthy skin microbiota, but it can also cause disease (Williams et al., 2021). Although *Staphylococcus* was significantly enriched in RISI microbiomes, it was overrepresented in patients with rapidly healed RISI. This is consistent with the results of our animal experiments in which the stress of acute radiation injury induced a high abundance of *Staphylococcus*. There is increasing evidence that *Staphylococcus epidermidis* downregulates the pro-inflammatory cytokine IL-6 *via* its metabolite butyric acid and the SCFA receptor (Keshari et al., 2019). Peptides and other metabolites produced by *S. epidermidis* might also contribute to normal defense on the surface of human skin (Cogen et al., 2010; Oliveira et al., 2021). Additionally, previous studies have reported that *Staphylococcus aureus* infection is associated with limited exacerbation and short hospital stay (Armbruster et al., 2016). One of the interesting findings is the significant positive association between *Streptococcus* and *Staphylococcus* in RISI (r = 0.79, p = 2.45E−13). Notably, *Klebsiella* was considered as a core species that was significantly overrepresented in RISI patients with chronic ulcer and diabetes. However, both of *Streptococcus* (r = −0.66, $p < 0.05$) and *Staphylococcus* (r = −0.89, $p < 0.05$) were significantly negatively correlated with *Klebsiella*. These observations matched the protective roles of probiotics by secreting antimicrobials and metabolites that resist pathogenic microbial invasion and maintain epidermal integrity (Kazemi et al., 2022). It must be pointed out that several risk factors can influence the incidence and severity of RISI. These risk factors may be intrinsic, including age, ethnicity, gender, malnutrition, location and stage of the tumor, and concomitant diseases such as systemic inflammation and diabetes mellitus. In our study, some of the included clinical patients had systemic diseases such as diabetes, which affected the process of RISI development and healing and the skin microbiota.

In the univariate network analysis, Lachnospiraceae and *Lactobacillus* occupied important positions and were positively correlated with multiple members of Firmicutes. Lachnospiraceae is known for its ability to synthesize SCFAs through the fermentation of dietary carbohydrates (Hexun et al., 2022). SCFAs are crucial substrates of the skin microbiota and epithelium cells that could maintain the acid–base balance, inhibit the growth of harmful pathogens, and regulate the immune system and inflammatory responses (Arpaia et al., 2013; Agus et al., 2021). *Lactobacillus* can ferment carbohydrates to lactic acid, which can also be regarded as a type of SCFA. By investigating the gut microbiome of mice that survived a high dose of radiation, Lachnospiraceae and Enterococcaceae were found to be the most enriched bacteria in these elite survivors (Guo et al., 2020). After bacterial reconstitution, the grouped mice received a high-dose radiation. Mice inoculated with Lachnospiraceae showed the greatest improvement in survival rate and clinical score, while those given *Lactobacillus rhamnosus* showed a 40%–60% increase in the survival rate.

The differential metabolic pathways of RISI were mainly associated with carbohydrate metabolism (butanoate and propanoate metabolism), amino acid metabolism (tryptophan and histidine metabolism), energy metabolism, endocrine system (PPAR signaling pathway), and lipid metabolism (fatty acid degradation and biosynthesis). An untargeted metabolomics study revealed that tryptophan metabolism selectively increased in the elite survivors affected by radiation (Guo et al., 2020). It was also found that tryptophan metabolites, including I3A and KYNA, significantly increased the survival rates and decreased the clinical scores of radiation-treated mice. Butyrate and propionate mediate radioprotection by alleviating the levels of the DNA damage-related proteins and reducing the ROS levels by 50%–60% (Guo et al., 2020; Liu et al., 2021). Interestingly, a report illustrated the effect of ionizing radiation on skin lipid metabolism. The function of adipose tissue has traditionally been understood as energy storage, physical buffering, temperature regulation, and thermal insulation (Wrba et al., 2022). Xiao et al. revealed that radiation modulates the skin lipid mass and profiles and downregulates multiple lipid metabolism pathways, including PPAR signaling. Rats fed with a high-fat diet with increased fat accumulation were found resistant to RISI (Xiao et al., 2020). It has been shown that PPAR alpha (PPARα) activation can significantly ameliorate RISI (Liu et al., 2022). PPARα is a member of the PPAR nuclear hormone receptor superfamily, which can be activated by a variety of ligands including fatty acids (Bougarne et al., 2018; Takada and Makishima, 2020). It has been reported that SCFAs can induce the expression of PPARα in a time- and concentration-dependent manner in the intestinal epithelial cell line (Higashimura et al., 2015). This is a potential molecular mechanism of radiation protection mediated by cutaneous microbiomes, which influence skin metabolism through their metabolite fatty acids and SCFAs.

This study has some limitations. Firstly, we focused solely on the unculturable approach. In further mechanism research, the culturable approach should also be combined to isolate the probiotics and causative agents in order to define their virulence characteristics, including the antimicrobial resistance patterns. In addition, there is still a lack of microbiome characterization at different sampling times. Moreover, microbial communities in the human skin are distinct and significantly less diverse than those in animal models. To better understand the mechanism of RISI, we combined the results from animal models and human data to identify some common changes. This study provides data on potential core microbes and metabolic pathways for further

mechanism research and treatment development. However, further functional validation is required to elucidate their roles in RISI.

Conclusion

We have investigated the alterations and functions of cutaneous microbiomes mediated by RISI. Our study provides new insights into the potential mechanism and microbial changes in the progression of RISI. The overwhelming predominance of members of Firmicutes, such as Streptococcaceae, Staphylococcaceae, Lachnospiraceae, and *Lactobacillus*, potentially help promote rapid healing in RISI. The microbiota–metabolite axis plays a critical role in RISI and provides promising therapeutic targets for the treatment of adverse side effects.

Data availability statement

The datasets presented in this study can be found in online repositories. The names of the repository/repositories and accession number(s) can be found in the article/Supplementary Material.

Ethics statement

The animal study was reviewed and approved by the Animal Experimentation Ethics Committee at China National Nuclear Corporation 416 Hospital. Written informed consent was obtained from the individual(s) for the publication of any potentially identifiable images or data included in this article.

Author contributions

BH designed and carried out the bioinformatics analyses and animal experiment and drafted the manuscript. LA, WS, and TY helped with drawing the figures and with the animal experiment. D-JY and HZ initiated the study. All authors contributed to the article and approved the submitted version.

Funding

This work was supported by China National Nuclear Corporation Medical Department "Nuclear Medicine Technology Innovation" Project (ZHYLYB2021009) and the National Natural Science Foundation of China (32071238 and 82073477). The Fundamental ResearchFunds for the Central Universities andYoung Talent Program of China National Nuclear Corporation (CNNC2021136). TheScience and Technology Program of Suzhou (SKY2021007) , Discipline Construction of The Second Affiliated Hospital of Soochow University (XKTJ-TD202001).

Conflict of interest

BH, WS, and D-JY were employed by China National Nuclear Corporation 416 Hospital.

The remaining authors declare that the research was conducted in the absence of any commercial or financial relationships that could be construed as a potential conflict of interest.

Publisher's note

Supplementary material

The Supplementary Material for this article can be found online at: https://www.frontiersin.org/articles/10.3389/fcimb.2022.1029592/full#supplementary-material

References

Agus, A., Clément, K., and Sokol, H. (2021). Gut microbiota-derived metabolites as central regulators in metabolic disorders. *Gut* 70 (6), 1174–1182. doi: 10.1136/gutjnl-2020-323071

Akh, L., Ishak, M., Harris, J., Glaros, T., Sasiene, Z., Mach, P., et al. (2022). -omics potential of *in vitro* skin models for radiation exposure. *Cell. Mol. Life Sci. CMLS* 79 (7), 390. doi: 10.1007/s00018-022-04394-z

Alam, M., Xie, L., Yap, Y., Marques, F., and Robert, R. (2022). Manipulating microbiota to treat atopic dermatitis: Functions and therapies. *Pathogens* 11 (6), 642. doi: 10.3390/pathogens11060642

Armbruster, C., Wolter, D., Mishra, M., Hayden, H., Radey, M., Merrihew, G., et al. (2016). Staphylococcus aureus protein a mediates interspecies interactions at the cell surface of pseudomonas aeruginosa. *mBio* 7 (3), e00538–16. doi: 10.1128/mBio.00538-16

Arpaia, N., Campbell, C., Fan, X., Dikiy, S., van der Veeken, J., deRoos, P., et al. (2013). Metabolites produced by commensal bacteria promote peripheral regulatory T-cell generation. *Nature* 504 (7480), 451–455. doi: 10.1038/nature12726

Ashack, K., Kuritza, V., Visconti, M., and Ashack, L. (2020). Dermatologic sequelae associated with radiation therapy. *Am. J. Clin. Dermatol.* 21 (4), 541–555. doi: 10.1007/s40257-020-00519-x

Bougarne, N., Weyers, B., Desmet, S., Deckers, J., Ray, D., Staels, B., et al. (2018). Molecular actions of PPARα in lipid metabolism and inflammation. *Endocr. Rev.* 39 (5), 760–802. doi: 10.1210/er.2018-00064

Byrd, A., Deming, C., Cassidy, S., Harrison, O., Ng, W., Conlan, S., et al. (2017). Staphylococcus aureus and strain diversity underlying pediatric atopic dermatitis. *Sci. Trans. Med.* 9 (397), eaal4651. doi: 10.1126/scitranslmed.aal4651

Callahan, B., McMurdie, P., Rosen, M., Han, A., Johnson, A., and Holmes, S. (2016). DADA2: High-resolution sample inference from illumina amplicon data. *Nat. Methods* 13 (7), 581–583. doi: 10.1038/nmeth.3869

Celebi Sozener, Z., Ozdel Ozturk, B., Cerci, P., Turk, M., Gorgulu Akin, B., Akdis, M., et al. (2022). Epithelial barrier hypothesis: Effect of the external exposome on the microbiome and epithelial barriers in allergic disease. *Allergy* 77 (5), 1418–1449. doi: 10.1111/all.15240

Cogen, A., Yamasaki, K., Sanchez, K., Dorschner, R., Lai, Y., MacLeod, D., et al. (2010). Selective antimicrobial action is provided by phenol-soluble modulins derived from staphylococcus epidermidis, a normal resident of the skin. *J. Invest. Dermatol.* 130 (1), 192–200. doi: 10.1038/jid.2009.243

Drozdovitch, V., Chizhov, K., Chumak, V., Bakhanova, E., Trotsyuk, N., Bondarenko, P., et al. (2022). Reliability of questionnaire-based dose reconstruction: Human factor uncertainties in the radiation dosimetry of Chernobyl cleanup workers. *Radiat. Res.* 198 (2), 172–180. doi: 10.1667/RADE-21-00207.1

Durand, B., Yahiaoui Martinez, A., Baud, D., François, P., Lavigne, J., and Dunyach-Remy, C. (2022). Comparative genomics analysis of two helcococcus kunzii strains co-isolated with staphylococcus aureus from diabetic foot ulcers. *Genomics* 114 (3), 110365. doi: 10.1016/j.ygeno.2022.110365

Ellison, A., Wilcockson, D., and Cable, J. (2021). Circadian dynamics of the teleost skin immune-microbiome interface. *Microbiome* 9 (1), 222. doi: 10.1186/s40168-021-01160-4

Elsherbiny, N., Rammadan, M., Hassan, E., Ali, M., El-Rehim, A., Abbas, W., et al. (2020). Autoimmune hepatitis: Shifts in gut microbiota and metabolic pathways among Egyptian patients. *Microorganisms* 8 (7), 1011. doi: 10.3390/microorganisms8071011

Guo, H., Chou, W., Lai, Y., Liang, K., Tam, J., Brickey, W., et al. (2020). Multi-omics analyses of radiation survivors identify radioprotective microbes and metabolites. *Science* 370 (6516), eaay9097. doi: 10.1126/science.aay9097

Hao, J., Sun, M., Li, D., Zhang, T., Li, J., and Zhou, D. (2022). An IFI6-based hydrogel promotes the healing of radiation-induced skin injury through regulation of the HSF1 activity. *J. Nanobiotechnol.* 20 (1), 288. doi: 10.1186/s12951-022-01466-x

Harris-Tryon, T., and Grice, E. (2022). Microbiota and maintenance of skin barrier function. *Science* 376 (6596), 940–945. doi: 10.1126/science.abo0693

Hexun, Z., Miyake, T., Maekawa, T., Mori, H., Yasukawa, D., Ohno, M., et al. (2022). High abundance of lachnospiraceae in the human gut microbiome is related to high immunoscores in advanced colorectal cancer. *Cancer Immunol. Immunother. CII*. doi: 10.1007/s00262-022-03256-8

Higashimura, Y., Naito, Y., Takagi, T., Uchiyama, K., Mizushima, K., and Yoshikawa, T. (2015). Propionate promotes fatty acid oxidation through the up-regulation of peroxisome proliferator-activated receptor α in intestinal epithelial cells. *J. Nutr. Sci. Vitaminol.* 61 (6), 511–515. doi: 10.3177/jnsv.61.511

Kazemi, A., Ataellahi Eshkoor, P., Saeedi, P., and Halabian, R. (2022). Evaluation of antioxidant and antibacterial effects of lactobacilli metabolites- preconditioned bone marrow mesenchymal stem cells in skin lesions amelioration. *Bioorg. Chem.* 124, 105797. doi: 10.1016/j.bioorg.2022.105797

Keshari, S., Balasubramaniam, A., Myagmardoloonjin, B., Herr, D., Negari, I., and Huang, C. (2019). Staphylococcus epidermidisButyric acid from probiotic in the skin microbiome down-regulates the ultraviolet-induced pro-inflammatory IL-6 cytokine via short-chain fatty acid receptor. *Int. J. Mol. Sci.* 20 (18), 4477. doi: 10.3390/ijms20184477

Khmaladze, I., Butler, É., Fabre, S., and Gillbro, J. (2019). Lactobacillus reuteri DSM 17938-a comparative study on the effect of probiotics and lysates on human skin. *Exp. Dermatol.* 28 (7), 822–828. doi: 10.1111/exd.13950

Kumpitsch, C., Moissl-Eichinger, C., Pock, J., Thurnher, D., and Wolf, A. (2020). Preliminary insights into the impact of primary radiochemotherapy on the salivary microbiome in head and neck squamous cell carcinoma. *Sci. Rep.* 10 (1), 16582. doi: 10.1038/s41598-020-73515-0

Langille, M., Zaneveld, J., Caporaso, J., McDonald, D., Knights, D., Reyes, J., et al. (2013). Predictive functional profiling of microbial communities using 16S rRNA marker gene sequences. *Nat. Biotechnol.* 31 (9), 814–821. doi: 10.1038/nbt.2676

Li, J., Su, S., Xu, Z., Zhao, L., Fan, R., Guo, J., et al. (2022). Potential roles of gut microbiota and microbial metabolites in chronic inflammatory pain and the mechanisms of therapy drugs. *Ther. Adv. Chronic Dis.* 13, 20406223221091177. doi: 10.1177/20406223221091177

Liu, S., Moon, C., Zheng, N., Huws, S., Zhao, S., and Wang, J. (2022). Opportunities and challenges of using metagenomic data to bring uncultured microbes into cultivation. *Microbiome* 10 (1), 76. doi: 10.1186/s40168-022-01272-5

Liu, P., Wang, Y., Yang, G., Zhang, Q., Meng, L., Xin, Y., et al. (2021). The role of short-chain fatty acids in intestinal barrier function, inflammation, oxidative stress, and colonic carcinogenesis. *Pharmacol. Res.* 165, 105420. doi: 10.1016/j.phrs.2021.105420

Liu, P., Yu, D., Sheng, W., Geng, F., Zhang, J., and Zhang, S. (2022). PPARα activation by fenofibrate ameliorates radiation-induced skin injury. *J. Eur. Acad. Dermatol. Venereol. JEADV* 36 (3), e207–e210. doi: 10.1111/jdv.17745

Luna, P. (2020). Skin microbiome as years go by. *Am. J. Clin. Dermatol.* 21, 12–17. doi: 10.1007/s40257-020-00549-5

Marvasi, M., Monici, M., Pantalone, D., and Cavalieri, D. (2022). Exploitation of skin microbiota in wound healing: Perspectives during space missions. *Front. Bioeng. Biotechnol.* 10, 873384. doi: 10.3389/fbioe.2022.873384

McDonald, D., Price, M., Goodrich, J., Nawrocki, E., DeSantis, T., Probst, A., et al. (2012). An improved greengenes taxonomy with explicit ranks for ecological and evolutionary analyses of bacteria and archaea. *ISME J.* 6 (3), 610–618. doi: 10.1038/ismej.2011.139

Olesen, C., Clausen, M., Agner, T., Asplund, M., Rasmussen, L., Yüksel, Y., et al. (2022). Altered maturation of the skin bacterial communities in infants with atopic dermatitis. *Acta Dermato-Venereol.* doi: 10.2340/actadv.v102.2275

Oliveira, F., Rohde, H., Vilanova, M., and Cerca, N. (2021). Staphylococcus epidermidisFighting biofilm-associated infections: Can iron be the key to success? *Front. Cell. Infect. Microbiol.* 11, 798563. doi: 10.3389/fcimb.2021.798563

Persinal-Medina, M., Llames, S., Chacón, M., Vázquez, N., Pevida, M., Alcalde, I., et al. (2022). Polymerizable skin hydrogel for full thickness wound healing. *Int. J. Mol. Sci.* 23 (9), 4837. doi: 10.3390/ijms23094837

Ramadan, M., Hetta, H., Saleh, M., Ali, M., Ahmed, A., and Salah, M. (2021). Alterations in skin microbiome mediated by radiotherapy and their potential roles in the prognosis of radiotherapy-induced dermatitis: a pilot study. *Sci. Rep.* 11 (1), 5179. doi: 10.1038/s41598-021-84529-7

Ramadan, M., Solyman, S., Yones, M., Abdallah, Y., Halaby, H., and Hanora, A. (2019). Skin microbiome differences in atopic dermatitis and healthy controls in Egyptian children and adults, and association with serum immunoglobulin e. *Omics* 23 (5), 247–260. doi: 10.1089/omi.2019.0011

Rios, C., DiCarlo, A., and Marzella, L. (2020). Cutaneous radiation injuries: Models, assessment and treatments. *Radiat. Res.* 194 (3), 310–313. doi: 10.1667/RADE-20-00132.1

Rosenthal, A., Israilevich, R., and Moy, R. (2019). Management of acute radiation dermatitis: A review of the literature and proposal for treatment algorithm. *J. Am. Acad. Dermatol.* 81 (2), 558–567. doi: 10.1016/j.jaad.2019.02.047

Segata, N., Izard, J., Waldron, L., Gevers, D., Miropolsky, L., Garrett, W., et al. (2011). Metagenomic biomarker discovery and explanation. *Genome Biol.* 12 (6), R60. doi: 10.1186/gb-2011-12-6-r60

Steinert, M., Weiss, M., Gottlöber, P., Belyi, D., Gergel, O., Bebeshko, V., et al. (2003). Delayed effects of accidental cutaneous radiation exposure: fifteen years of follow-up after the Chernobyl accident. *J. Am. Acad. Dermatol.* 49 (3), 417–423. doi: 10.1067/S0190-9622(03)02088-7

Takada, I., and Makishima, M. (2020). Peroxisome proliferator-activated receptor agonists and antagonists: a patent review (2014-present). *Expert Opin. Ther. Pat.* 30 (1), 1–13. doi: 10.1080/13543776.2020.1703952

Uberoi, A., Bartow-McKenney, C., Zheng, Q., Flowers, L., Campbell, A., Knight, S., et al. (2021). Commensal microbiota regulates skin barrier function and repair via signaling through the aryl hydrocarbon receptor. *Cell Host Microbe* 29 (8), 1235–1248.e8. doi: 10.1016/j.chom.2021.05.011

Wang, Y., Li, J., Zhang, H., Zheng, X., Wang, J., Jia, X., et al. (2021). Streptococcus salivariusProbiotic K12 alleviates radiation-induced oral mucositis in mice. *Front. Immunol.* 12, 684824. doi: 10.3389/fimmu.2021.684824

Wei, J., Zhao, Q., Zhang, Y., Shi, W., Wang, H., Zheng, Z., et al. (2021). Sulforaphane-mediated Nrf2 activation prevents radiation-induced skin injury through inhibiting the oxidative-Stress-Activated DNA damage and NLRP3 inflammasome. *Antioxidants* 10 (11), 1850. doi: 10.3390/antiox10111850

Wensel, C., Pluznick, J., Salzberg, S., and Sears, C. (2022). Next-generation sequencing: insights to advance clinical investigations of the microbiome. *J. Clin. Invest.* 132 (7), e154944. doi: 10.1172/JCI154944

Williams, S., Frew, J., and Krueger, J. (2021). A systematic review and critical appraisal of metagenomic and culture studies in hidradenitis suppurativa. *Exp. Dermatol.* 30 (10), 1388–1397. doi: 10.1111/exd.14141

Wozniak, H., Beckmann, T., Fröhlich, L., Soccorsi, T., Le Terrier, C., de Watteville, A., et al. (2022). The central and biodynamic role of gut microbiota in critically ill patients. *Crit. Care* 26 (1), 250. doi: 10.1186/s13054-022-04127-5

Wrba, L., Halbgebauer, R., Roos, J., Huber-Lang, M., and Fischer-Posovszky, P. (2022). Adipose tissue: a neglected organ in the response to severe trauma? *Cell. Mol. Life Sci. CMLS* 79 (4), 207. doi: 10.1007/s00018-022-04234-0

Xiao, Y., Mo, W., Jia, H., Yu, D., Qiu, Y., Jiao, Y., et al. (2020). Ionizing radiation induces cutaneous lipid remolding and skin adipocytes confer protection against radiation-induced skin injury. *J. Dermatol. Sci.* 97 (2), 152–160. doi: 10.1016/j.jdermsci.2020.01.009

Xie, J., Zhao, M., Wang, C., Yong, Y., Gu, Z., and Zhao, Y. (2021). Rational design of nanomaterials for various radiation-induced diseases prevention and treatment. *Adv. Healthc. Mater.* 10 (6), e2001615. doi: 10.1002/adhm.202001615

Yadav, K., Nimonkar, Y., Poddar, B., Kovale, L., Sagar, I., Shouche, Y., et al. (2022). Two-dimensional cell separation: a high-throughput approach to enhance the culturability of bacterial cells from environmental samples. *Microbiol. Spectr.* 10 (3), e0000722. doi: 10.1128/spectrum.00007-22

Yadav, H., Sharma, R., and Singh, R. (2022). Immunotoxicity of radiofrequency radiation. *Environ. pollut.* 309, 119793. doi: 10.1016/j.envpol.2022.119793

Yao, C., Zhou, Y., Wang, H., Deng, F., Chen, Y., Zhu, X., et al. (2021). Adipose-derived stem cells alleviate radiation-induced dermatitis by suppressing apoptosis and downregulating cathepsin f expression. *Stem Cell Res. Ther.* 12 (1), 447. doi: 10.1186/s13287-021-02516-1

frontiers | Frontiers in Immunology

TYPE Original Research
PUBLISHED 17 November 2022
DOI 10.3389/fimmu.2022.1038876

OPEN ACCESS

EDITED BY
Stéphane Ranque,
Aix-Marseille Université, France

REVIEWED BY
Joana Vitte,
INSERM UMRUA11 Institut Desbrest d'Épidémiologie et de Santé Publique (IDESP), France
Kirsi Jarvinen-Seppo,
University of Rochester, United States
Carina Venter,
University of Colorado, United States

*CORRESPONDENCE
Yanqun Liu
liuyanqun1984@163.com

SPECIALTY SECTION
This article was submitted to Microbial Immunology, a section of the journal Frontiers in Immunology

RECEIVED 07 September 2022
ACCEPTED 03 November 2022
PUBLISHED 17 November 2022

CITATION
Fan X, Zang T, Dai J, Wu N, Hope C, Bai J and Liu Y (2022) The associations of maternal and children's gut microbiota with the development of atopic dermatitis for children aged 2 years.
Front. Immunol. 13:1038876.
doi: 10.3389/fimmu.2022.1038876

The associations of maternal and children's gut microbiota with the development of atopic dermatitis for children aged 2 years

Xiaoxiao Fan[1], Tianzi Zang[1], Jiamiao Dai[1], Ni Wu[1], Chloe Hope[2], Jinbing Bai[2] and Yanqun Liu[1]*

[1]Wuhan University School of Nursing, Wuhan University, Wuhan, China, [2]Emory University Nell Hodgson Woodruff School of Nursing, Atlanta, GA, United States

Background: It is critical to investigate the underlying pathophysiological mechanisms in the development of atopic dermatitis. The microbiota hypothesis suggested that the development of allergic diseases may be attributed to the gut microbiota of mother-offspring pairs. The purpose of this study was to investigate the relationship among maternal-offspring gut microbiota and the subsequent development of atopic dermatitis in infants and toddlers at 2 years old.

Methods: A total of 36 maternal-offspring pairs were enrolled and followed up to 2 years postpartum in central China. Demographic information and stool samples were collected perinatally from pregnant mothers and again postpartum from their respective offspring at the following time intervals: time of birth, 6 months, 1 year and 2 years. Stool samples were sequenced with the 16S Illumina MiSeq platform. Logistic regression analysis was used to explore the differences in gut microbiota between the atopic dermatitis group and control group.

Results: Our results showed that mothers of infants and toddlers with atopic dermatitis had higher abundance of *Candidatus_Stoquefichus* and *Pseudomonas* in pregnancy and that infants and toddlers with atopic dermatitis had higher abundance of *Eubacterium_xylanophilum_group* at birth, *Ruminococcus_gauvreauii_group* at 1 year and *UCG-002* at 2 years, and lower abundance of *Gemella* and *Veillonella* at 2 years. Additionally, the results demonstrated a lower abundance of *Prevotella* in mothers of infants and toddlers with atopic dermatitis compared to mothers of the control group, although no statistical difference was found in the subsequent analysis.

Conclusion: The results of this study support that gut microbiota status among mother-offspring pairs appears to be associated with the pathophysiological development of pediatric atopic dermatitis.

KEYWORDS

gut microbiota, atopic dermatitis, eczema, pregnancy, offspring

Introduction

There has been an increased incidence in allergic diseases, including allergic asthma, allergic rhinitis, and food allergies in the last 40 years (1). Atopic dermatitis is defined as chronic inflammatory disease of the integumentary system characterized by recurring symptoms, including pruritus, dryness, peeling, blistering, bleeding, and risk for secondary bacterial infection (2). Epidemiological survey has reported 60% of atopic dermatitis occurs in the first year of life (infantile eczema) (3). Previous study (4) indicated that the prevalence of atopic dermatitis in children was as high as 30%. In China, the prevalence of atopic dermatitis in infants was estimated as 64.8% (5). Furthermore, the literature indicated that atopic dermatitis may present as an initial manifestation of an underlying allergic disease process in infants and toddlers. Of note, up to 80% of infants and toddlers diagnosed with atopic dermatitis eventually develop allergic rhinitis or asthma later in childhood (6). Therefore, it is imperative to identify factors that may influence the pathophysiological development of pediatric atopic dermatitis.

Epidemiological studies have identified a number of environmental risk factors that may play a role in the development of atopic dermatitis, such as mode of delivery, breastfeeding status, urban living factors, pet exposure, tobacco exposure, antibiotic therapy and dietary habits (7). Recent research surrounding the "microbiota hypothesis" has acquired increased attention suggesting that allergic processes may stem from an underlying imbalance within the gut microbiota (8). Prior studies indicated that the composition of the gut microbiota was an important factor in the normal development of immune system functioning (9) and that certain gut microbiota and microbial metabolites may promote the production of regulatory peripheral T cells, providing a protective effect against inflammatory processes that drive allergic and autoimmune disease processes (10–12). Moreover, these studies indicate that gut microbiota is an important regulator in the pathogenesis of atopic dermatitis (13–15).

Low diversity of gut microbiota and alternative gut microbial composition were associated with the development of atopic dermatitis in infants and toddlers compared to healthy children (16). Children with atopic dermatitis exhibit a higher abundance of *Bacillariophyceae, Clostridium* and *Enterobacteriaceae*, and a lower relative abundance of *Bifidobacterium and Lactobacillus* (16). Wang et al. (15) found that a decrease in gut microbiota diversity at one week of age was strongly associated with developing atopic dermatitis within the first 18 months of life postpartum. Recently, studies (17–19) also revealed that the maternal gut microbiota during pregnancy was crucial in the development of healthy infantile immune system functioning. Lange et al. (20) reported that higher counts of maternal total *aerobes* and *Enterococci* were associated with an increased risk for asthma-like symptoms among infants. Comprehensive analysis of both the maternal and offspring's gut microbiota may provide insight into establishing key biomarkers for the prediction of subsequent pediatric allergic disease states, including atopic dermatitis, within the first two years of life postpartum. Interpretation of these results may provide a fulcrum on which the development of target-specific pharmaceutical therapies and interventions hinge upon.

However, some inconsistencies were noted regarding the role of gut microbiota in the development of atopic dermatitis in infants and toddlers, which may be explained by time discrepancies in stool sample collection, variable microbiological profiling methods, and poor control of potential confounding variables that may indirectly affect gut microbiota composition (8, 16). Currently, many studies exploring the relationship between gut microbiota and atopic dermatitis are cross-sectional studies with a tendency toward reverse causality, including changes in microbiota composition due to disease manifestations. Few studies have included longitudinal cohort studies linking infant microbiota status to the subsequent development of pediatric atopic dermatitis (21). Additionally, previous literature on the gut microbiota and allergic diseases have solely focused on the postnatal period, but recent findings suggest that maternal gut microbiota status during pregnancy plays a pivotal role in fetal immune development (22, 23) and may drive the evolution of allergic diseases in respective offspring (20, 24).

There remain few relevant population studies to investigate the important relationship between maternal gut microbiota during pregnancy and the risk for infantile atopic dermatitis.

Therefore, this study was a 2-year prospective cohort study to investigate the relationships between maternal-offspring's gut microbiota during pregnancy and the subsequent risk for development of atopic dermatitis in offspring up to two years postpartum.

Materials and methods

Study design and participants

This was a prospective cohort study. Sixty-two pregnant women were recruited from March 2017 to November 2017 in Central China and followed until two years of age. The inclusion criteria were (1): pregnant women in the third trimester, (2) pregnant women who planned to give birth in a tertiary hospital in central China, and (3) pregnant women without pregnancy complications. The exclusion criteria were: (1) pregnant women receiving antibiotic treatment, and (2) those with cognitive impairment. A total of 62 pregnant women were recruited in our study, and 21 mother-offspring pairs could not be reached by phone or email at follow-up, leaving 41 mother-offspring pairs in this cohort. Of these 41 mother-offspring pairs, one infant had asthma and four participants of sample were not collected at 6 months, 1 year, or 2 years, therefore, 36 participants were included in the final analysis of this study. This study was approved by the Research Ethics Boards of Medical School of Wuhan University (JKHL2017-03-03). Informed consent was obtained for all participants.

Variables and measures

At the time of recruitment, pregnant women in the third trimester completed a demographic questionnaire and diet questionnaire. Newborn general demographic data, including gender, height, weight, and mode of delivery, were obtained *via* hospital medical records at the time of birth. Moreover, data collection was performed regarding pertinent perinatal and postnatal environmental exposures, including alcohol exposure, pet dander exposure, feeding modalities, and use of antibiotics up to postpartum two years.

Stool samples were collected perinatally from pregnant women in the third trimester and again postpartum from their respective offspring at the following time intervals: time of birth, 6 months, 1 year, and 2 years. Sample collection was performed by trained personnel at the participant's home. Samples obtained consisted of formed stool or residual fecal matter collected from infant diapers in accordance to the Human Microbiota Project (HMP) protocol. Following immediate collection, all stool samples were transported to the laboratory in an incubator (+4 °C) and then were stored at -80 °C in a freezer at our laboratory. DNA extraction, polymerase chain reaction (PCR) amplification, and Illumina MiSeq sequencing about stool samples have been elaborated on our previous study (25). The V3-V4 highly variable region of the bacterial 16S rRNA gene was amplified with primers 338F (5'-ACTCCTACGGGAGGCAGCAG-3') and 806R (5' - ggactachvgggtwtctaat -3') by a thermocycling PCR system (GeneAmp 9700, ABI, Walthma, MA, USA).

In this study, pediatrician used the Williams' criteria (26) for the diagnosis of atopic dermatitis in infants and toddlers between the ages of 1 and 2 years. The Williams' criteria were as follows: primary criteria: pruritus; secondary criteria: (1) history of flexor side dermatitis eczema, including elbow fossa, rouge fossa, anterior ankle, and neck (children under 10 years old including buccal rash); (2) history of asthma or allergic rhinitis (or history of atopic disease in first-degree relatives of children under 4 years of age); (3) history of dry skin all over the body in recent years; (4) presence of flexor side eczema (eczema of the cheeks/forehead and extremities in children under 4 years of age); (5) onset before 2 years of age (for patients over 4 years of age). Atopic dermatitis was diagnosed when there was pruritus with three or more secondary criteria in infants and toddlers.

Statistical analysis

Descriptive statistics were used to summarize the general demographic characteristics of all participants. Mean (standard deviation [SD]) was used for continuous variables and frequency (%) was implemented for categorical variables. Independent t-tests, Mann-Whitney U test, Chi-square test and Fisher exact tests were utilized to compare the relationship between variables, including demographics, environmental factors and diet during pregnancy and the subsequent risk for development of atopic dermatitis in infants and toddlers.

For the microbiota data, raw 16S rRNA sequencing data were spliced together, with quality control and filtering conducted by FLASH (https://ccb.jhu.edu/software/FLASH/index.shtml). The UPARSE version 7.0.1090 (http://drive5.com/uparse/) was used to cluster the smallest operational classification units (OTUs) based on highly similar sequences (>97%). Chimeric sequences were identified and removed using UCHIME in the process of clustering. The RDP classifier bayesian algorithm version 2.11 (http://sourceforge.net/projects/rdp-classifier/) was used on the QIIME (QIIME version 1.9.1) platform for classification analysis of representative sequences of OTUs from the sliva138/16S bacterial classification database with a default confidence threshold of 0.7. Core species analysis was used to indicate that the sample size was sufficient (27). The fecal alpha diversity among the two groups was evaluated *via* Sobs, Shannon and Simpson indices. Principal coordinates analysis (PCoA) based on Bray-Curtis distance matrix was used to evaluate the beta

diversity at the OTU level, and analysis of similarities (ANOSIM) was used to compare differences in beta diversity between groups. Wilcoxon rank-sum test was used to analyze the difference between the two groups for phylum and genus. After adjusting confounders (mothers: maternal age, mother's educational level, alcohol intake during pregnancy and frequency of maternal soy products consumption; infants and toddlers: mode of delivery, breastfeeding mode, maternal alcohol intake during breastfeeding, antibiotics exposure and pet exposure), logistics regression analysis was used to further explore the differential genera among atopic dermatitis and control groups.

The p-values for multiple analyses were adjusted using the Benjamini-Hochberg false discovery rate (FDR). The significant level and FDR threshold were both at 0.05. SPSS 23.0 (IBM, Chicago, IL, USA) and R 4.0.2. were used for all data analyses.

Results

General characteristics and factors affecting the development of atopic dermatitis

Characteristics and medical history of the mother and offspring pairs were displayed in Table 1. Mean age of the pregnant women was 29.83 (SD = 3.14) years. More than half of the pregnant women for both groups had a bachelor's degree or higher. Infants of both groups were full-term with a mean weight of 3.40 (SD = 0.36) kg and a mean height of 50.41 (SD = 1.35) cm. The cesarean delivery rate was 61.1%, with a breastfeeding rate of 58.3% for the first 6 months postpartum. Comparatively, although there was no significant different of breastfeeding between control group and the atopic dermatitis group, the breastfeeding rate for the atopic dermatitis group was lower than that of the control group (30.8% vs. 69.2%). There were no statistical differences in baseline characteristics of the mother and offspring among atopic dermatitis and control groups. The results did not demonstrate any significant associations between environmental variables, diet during pregnancy, and subsequent risk of atopic dermatitis in infants and toddlers (Table 1 and Supplemental Table 1).

Descriptions of the gut microbiota and changes of maternal and children's gut microbiota

In total, 7,976,645 high-quality reads were obtained from the 169 stool samples. These reads were clustered into 2,673 OTUs. The flatness of the core species curve indicated that the sequencing sample size was sufficient (Supplemental Figure 1).

We conducted a within-group comparison of alpha diversity and beta diversity in infants and toddlers and their mothers in the atopic dermatitis groups and control group, respectively. The results showed that alpha diversity (Sobs, Shannon and Simpson indices) of infants and toddlers increased with age and the trends were similar in both groups (Figure 1 and Supplementary Figure 2). It was found that in the control group, Sobs index was higher in infants at birth and lower at 6 months and 1 year in infants and toddlers compared to maternal Sobs index (Figure 1A). In addition, in the atopic dermatitis group, Sobs index was higher at birth and lower at 6 months compared to maternal Sobs index (Figure 1B). The results also revealed significant differences in beta diversity in the control group (Figure 1C) or in the atopic dermatitis group (Figure 1D) among different ages, and the maternal community composition was similar to the infants' community composition at birth, while the maternal community composition was significantly different from that of infants and toddlers at 6 months, 1 year and 2 years (Figure 1).

In addition, we compared the differences in maternal alpha diversity and beta diversity between high or low frequency of different foods consumption (more than 3 days or 3 days/week vs less than 3 days/week). Our results didn't find the difference in maternal alpha diversity (Shannon and Simpson indices) and beta diversity between high or low frequency of different foods consumption (Supplemental Table 2 and Supplemental Table 3). However, our results found mothers who consumed soy products less than 3 days/week had higher Sobs index (Supplemental Table 2).

Associations between maternal gut microbiota and atopic dermatitis of infants and toddlers

We compared the diversity and composition of the gut microbiota perinatally in mothers of both groups. Surprisingly, this study indicated that the alpha diversity of maternal gut microbiota in control groups was higher than that of atopic dermatitis groups (Sob and Shannon indices all $p < 0.05$, Figure 2). It was noted that the Shannon index of maternal gut microbes between the atopic dermatitis group and control group was not statistically significant after controlling confounding factors (mother's age, mother's educational level, alcohol intake during pregnancy and frequency of maternal soy products consumption); however, the Sobs index still retains statistical significance. Based on the PCoA plot, there were no significant differences in the beta diversity of maternal gut microbiota between the atopic dermatitis group and control group (R=-0.0706, p=0.799, Figure 3).

Compositions of maternal gut microbiota at the phylum and genus level were displayed in Supplemental Figure 3A and Supplemental Figure 3B. The predominant phyla in the atopic dermatitis group and control group were Firmicutes (59.94% vs. 59.74%) and Bacteroidetes (35.10% vs. 35.97%), respectively. Twenty-two genera accounting for more than 0.01% were identified in each group with the top five genera as follows: *Bacteroides* (26.9% vs. 18.9%), *Faecalibacterium* (11.36% vs.

TABLE 1 Demographic and environmental variables characteristics of the participants.

Characteristics		Atopic dermatitis		P value
	All	No (n=26)	Yes (n=10)	
Demographic variables				
Mother's age (years)*	29.83 ± 3.14	29.42 ± 2.64	30.90 ± 4.15	0.211
Mother's educational level				1.000
college degree or below	12 (33.3%)	8 (34.8%)	4 (40.0%)	
bachelor's degree	20 (55.6%)	14 (60.9%)	6 (60.0%)	
master degree or above	1 (2.8%)	1 (4.3%)	0 (0%)	
Gestational age (weeks)*	39.4 ± 0.914	39.40 ± 0.87	39.40 ± 1.08	1.000
Gender of the infant				0.454
Female	25 (69.4%)	19 (73.1%)	6 (60.0%)	
Male	11 (30.6%)	7 (26.9%)	4 (40.0%)	
Birth Weight of the infant (kg)*	3.40 ± 0.36	3.38 ± 0.39	3.47 ± 0.27	0.481
Birth Height of the infant (cm)*	50.41 ± 1.35	50.50 ± 1.44	50.20 ± 1.13	0.565
The infant is the first child				0.673
Yes	25 (69.4%)	18 (78.3%)	7 (70.0%)	
No	8 (22.2%)	5 (21.7%)	3 (30.0%)	
Environmental variables				
Mode of delivery				0.462
Cesarian section	22 (61.1%)	17 (65.4%)	5 (50.0%)	
Vaginal	14 (38.9%)	9 (34.6%)	5 (50.0%)	
Breastfeeding in first 6 months				0.058
Yes	21 (58.3%)	18 (69.2%)	3 (30.0%)	
No	15 (41.7%)	8 (30.8%)	7 (70.0%)	
Alcohol intake during pregnancy				0.193
Yes	9 (25.0%)	5 (19.2%)	4 (40.0%)	
No	27 (75.0%)	21 (80.8%)	6 (60.0%)	
Alcohol intake during breastfeeding				0.658
Yes	8 (22.2%)	5 (19.2%)	3 (30.0%)	
No	28 (77.8%)	21 (80.8%)	7 (70.0%)	
Antibiotics using in the first 6 months				0.269
Yes	8 (22.2%)	7(26.9%)	1 (10.0%)	
No	28 (77.8%)	19 (73.1%)	9(90.0%)	
Antibiotics using in the first 1 years				0.092
Yes	19 (52.8%)	16 (61.5%)	3 (30.0%)	
No	17 (47.2%)	10 (38.5%)	7 (70.0%)	
Antibiotics using in the first 2 years				0.269
Yes	26 (72.2%)	20 (76.9%)	6 (60.0%)	
No	10 (27.8%)	6 (23.1%)	4 (40.0%)	

Data marked with * are presented as mean (standard deviation), all others are presented as frequency (%);
Continuous and categorical variables were compared between the two groups using independent t-test and chi-square test or Fisher's exact test, respectively.

14.45%), *Prevotella* (3.75% vs. 13.73%), *Agathobacter* (4.49% vs. 4.51%) and *Phascolarctobacterium* (4.53% vs. 3.15%). Following the interpretation of the aforementioned results, we discovered that the abundance of *Bacteroides* was higher in the atopic dermatitis group, while the abundance of *Prevotella* was higher in the control group, although no statistical difference was found in the subsequent analysis.

Wilcoxon rank-sum test was used to further investigate the differences in maternal gut microbiota composition between the atopic dermatitis group and the control group. The results found that at the phylum level, mothers in the atopic dermatitis group exhibited a lower abundance of *Fusobacteriota* compared to mothers in the control group, while *Acidobacteriota* was significantly higher in mothers of the atopic dermatitis group versus

10.3389/fimmu.2022.1038876

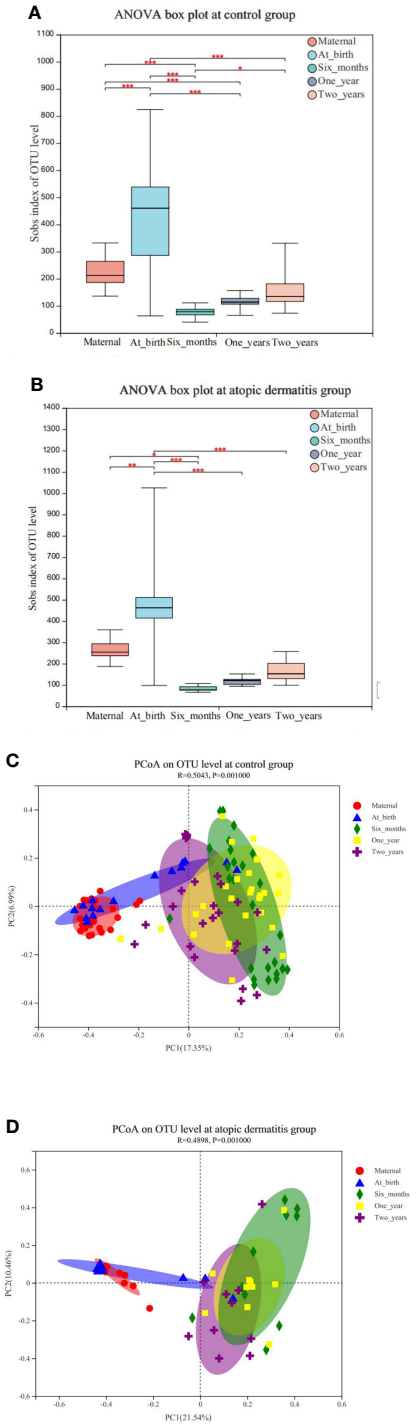

FIGURE 1
(A) Changes of maternal and infant and toddler's microbial alpha diversity of in control group. **(B)** Changes of maternal and infant and toddler's microbial alpha diversity in atopic dermatitis group. **(C)** Principal coordinate analysis (PCoA) analysis of the OTU level at maternal and infants and toddlers in control group. **(D)** Principal coordinate analysis (PCoA) analysis of the OTU level at maternal and infants and toddlers in atopic dermatitis group. **(A, B)** P value for alpha diversity differences at atopic dermatitis groups and control group was determined by one-way ANOVA (analysis of variance) after adjusting for subject. The 95% confidence interval around the mean is displayed by the boxplots. **(C, D)** The X-axis and Y-axis in Figure 1 represent the two selected principal axes, and the percentage represents the explanatory degree value of the principal axes to the sample composition difference; The scale of X axis and Y axis is relative distance and has no practical significance. Points with different colors or shapes represent samples of different groups. The more scattered the two sample points are, the greater the difference in species composition between the two samples. *0.01<P≤0.05, **0.001<P≤0.01, ***P≤0.001.

10.3389/fimmu.2022.1038876

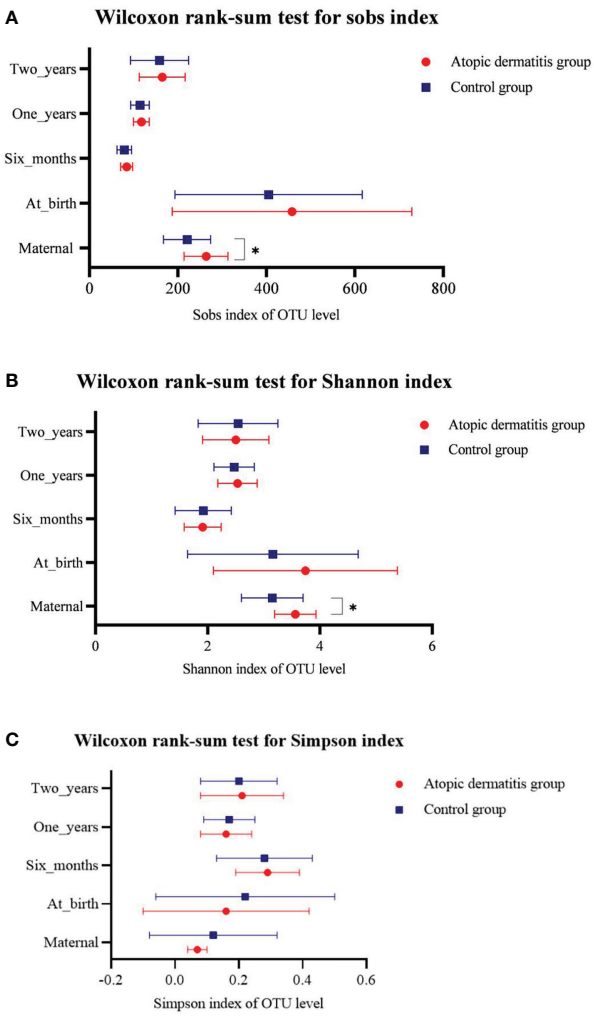

FIGURE 2
Differences of maternal and offspring's microbial alpha diversity between Atopic dermatitis group and Control group. **(A)** Wilcoxon rank-sum text for sobs index. **(B)** Wilcoxon rank-sum text for Shannon index. **(C)** Wilcoxon rank-sum text for Simpson index.

mothers in the control group (all $p<0.05$, Supplemental Figure 3C). In addition, maternal gut microbiota at the genus level in the atopic dermatitis group had higher abundance of *Bacteroides, Megasphaera, Hungatella, Butyricimonas, Eisenbergiella, Acinetobacter, norank_f_Xanthobacteraceae, Paenarthrobacter, unclassified_o_Veillonellales-Selenomonadales, Candidatus_Stoquefichus, norank_f_Mitochondria, Anaerofilum, Pseudomonas, Dielma, norank_f_Xanthobacteraceae* and *Candidatus_Solibacter* organisms than those in control group (Figure 4).

Associations between children's gut microbiota and atopic dermatitis of infants and toddlers

We performed group comparisons for infant and toddler microbial alpha diversity and beta diversity in both the atopic dermatitis group and the control group. This study did not demonstrate the difference in alpha diversity and beta diversity between the two groups in different ages (Figure 2 and Supplemental Figure 4).

The overall trend of change for each dominant gut microbiota in atopic dermatitis and control groups was similar from 0-2 years at the phylum level (Supplemental Figure 5). To further investigate the differences in gut microbiota composition between atopic dermatitis and control groups, we performed analyses based on the Wilcoxon rank-sum test. At the phylum level, the results revealed that the abundance of *Proteobacteria* was significantly lower in the atopic dermatitis group than in the control group of infants aged 1 year ($p < 0.05$). The results of the study revealed that the abundance of *norank_f_norank_o_Clostridia_UCG-014, unclassified_o_Coriobacteriales, Aliterella, Eubacterium_xylanophilum_group, Defluviitaleaceae_UCG-011, unclassified_*

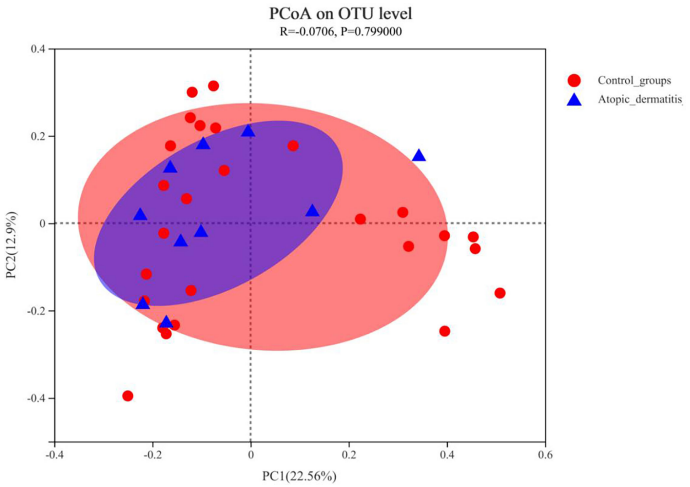

FIGURE 3
Principal coordinate analysis (PCoA) analysis of the OTU level at mother in atopic dermatitis group and control group. The X-axis and Y-axis in Figure 1 represent the two selected principal axes, and the percentage represents the explanatory degree value of the principal axes to the sample composition difference; The scale of X axis and Y axis is relative distance and has no practical significance. Points with different colors or shapes represent samples of different groups. The more scattered the two sample points are, the greater the difference in species composition between the two samples.

o_Bacteroidales and Meiothermus were significantly higher in the atopic dermatitis group than in the control group at birth ($p < 0.05$). The results of the study also revealed a higher abundance of *Klebsiella, Helicobacter, norank_f_ML635J-40_aquatic_group, Faecalibaculum, Anaeroglobus, UBA1819 and norank_f_norank_o_MBA03* in the atopic dermatitis group than the control group in infants aged 6 months ($p < 0.05$). The atopic dermatitis group of infants at 1 year demonstrated a significantly higher abundance of *Parabacteroides, Anaerostignum, UBA1819, unclassified_o_Bacteroidale, Dialister and Ruminococcus_gauvreauii_group* compared to the control group. Toddlers aged 2 years of the atopic dermatitis group demonstrated significantly

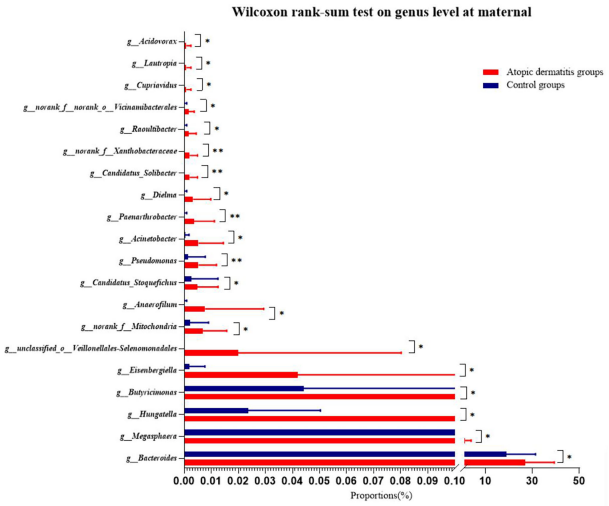

FIGURE 4
Differences of maternal gut microbiota of atopic dermatitis group and control group on genus level. Wilcoxon rank-sum test bar plot shows the differences of gut microbial composition between two groups on the genus level. The Y-axis represents different genera groupings, boxes of different colors represent two different groupings, and the X-axis represents the average relative abundance of genera in different groupings. * 0.01<P⩽0.05, **0.001 <P⩽0.01.

higher levels of *Eubacterium_siraeum_group, Candidatus_Soleaferrea, unclassified_f_Ruminococcaceae and Frisingicoccus*, but exhibited lower levels of *Veillonella, UCG-002* and *Gemella* compared to the control group ($p < 0.05$). Other relevant results are detailed in Figure 5.

Impacts of maternal and offspring's gut microbiota on atopic dermatitis

To further clarify the effect of differential genera on the development of atopic dermatitis in infants and toddlers, we classified the above differential genera into high and low abundance models based on the median of the total sample. These findings were then included in the logistic regression model. After adjusting for relevant covariates (mothers: maternal age, mother's educational level, alcohol intake during pregnancy and frequency of maternal soy products consumption; infants and toddlers: mode of delivery, breastfeeding mode, maternal alcohol intake during breastfeeding, antibiotics exposure and pet exposure), this study revealed that mothers in the atopic dermatitis group exhibited a higher abundance of *Pseudomonas and Candidatus_Stoquefichus*. Meanwhile, findings suggest that infants and toddlers in the atopic dermatitis group demonstrated a higher abundance of *Eubacterium_xylanophilum_group* at birth, *Ruminococcus_gauvreauii_group* at 1 year and *UCG-002* at 2 years, while exhibiting a lower abundance of *Gemella* and *Veillonella* at 2 years (Table 2).

Discussion

This was the first study to explore the effects of involving maternal-offspring microbiota status on the subsequent risk for development of atopic dermatitis in infants and toddlers up to two years. Our findings suggested that the enrichment and reduction of certain gut microbiota were strongly associated with the development of atopic dermatitis in infants and toddlers. These findings provide a basis for the development of interventions in the risk reduction and treatment of atopic dermatitis in infants and toddlers.

Our results indicated that there was a lower abundance of *Prevotella* in mothers assigned to the atopic dermatitis group versus the control group. But no statistical difference was noted in the subsequent analysis, likely due to the small sample size. However, these results reflected to some extent that the enrichment of *Prevotella* during pregnancy may serve as a protective factor against the development of pediatric allergic diseases. Vuillermin et al. (24) discovered that an increased abundance of *Prevotella* in pregnant women was associated with a decreased risk for the development of food allergies in respective offspring. *Prevotella* is a gram-negative anaerobic bacterium that ferments dietary fiber to produce metabolites, including short-chain fatty acids (SCFAs) and succinic acid (28, 29). SCFAs demonstrate significant anti-inflammatory effects and may influence fetal immune development through the production of interleukin-10 (IL-10) producing regulatory T cells (11). Additionally, succinic acid can stimulate the development, migration, and function of innate immune cells (30). In addition, *Prevotella* produces endotoxins that negatively affect fetal immune development and increase the risk for allergic outcomes *via* toll-like receptor-4-dependent pathways (31).

Previous work (32) indicated that an increased abundance of *Bacteroides*, an anaerobic bacterium belonging to the *Bacteroidaceae*, promoted the secretion of IL-6 and IL-23 in dendritic cells. IL-6 and IL-23 can promote the differentiation of Th17 cells and the secretion of IL-17. Th17 cells trigger inflammatory pathways that increase the risk for development of chronic autoimmune and allergic disease states (33). Therefore, the association between increased *Bacteroides* and the risk for atopic dermatitis is further understood by *Bacteroides*-associated cytokine production with notable systemic downstream effects. Our study further supports this finding in that a higher abundance of *Bacteroides* was noted in mothers of infants with atopic dermatitis, without adjusting for covariates. Our results also revealed maternal carrier with the higher abundance of *Pseudomonas* and *Candidatus Stoquefichus* during pregnancy was risk factor for atopic dermatitis in infants and toddlers after the adjustment of potential covariates. *Pseudomonas* belonging to the *Proteobacteria* phylum is an opportunistic pathogen, it has been shown to induce a type 2 immune response leading to the production of mucin, which is used as an energy source by pathogens (34, 35). *Candidatus Stoquefichus* belongs to the class of *Bacilli*. Notably, there was limited data regarding the biological implications of these genera in atopic dermatitis. Further investigation of these genera as it relates to human application involving the gut microbiota should be considered in future studies.

Initially, our findings indicated a higher alpha diversity of the gut microbiota in mothers of the atopic dermatitis group compared to mothers in the control group. However, the relationship between maternal Shannon index and infantile atopic dermatitis was not significant after controlling for relevant covariates, consistent with findings of previous work (36). Hiromi Tanabe et al. (36) reported an increase in the total diversity of maternal gut microbiota during pregnancy in the atopic dermatitis group compared to mothers in control group, however, this difference was not statistically significant. Although the relationship between maternal gut microbiota during pregnancy, and the risk for development of atopic dermatitis in respective offspring remains controversial, our results indicated that enrichment and reduction of certain maternal gut microbiota during pregnancy were associated with the subsequent development of atopic dermatitis in infants and toddlers. This data provided a new perspective for

10.3389/fimmu.2022.1038876

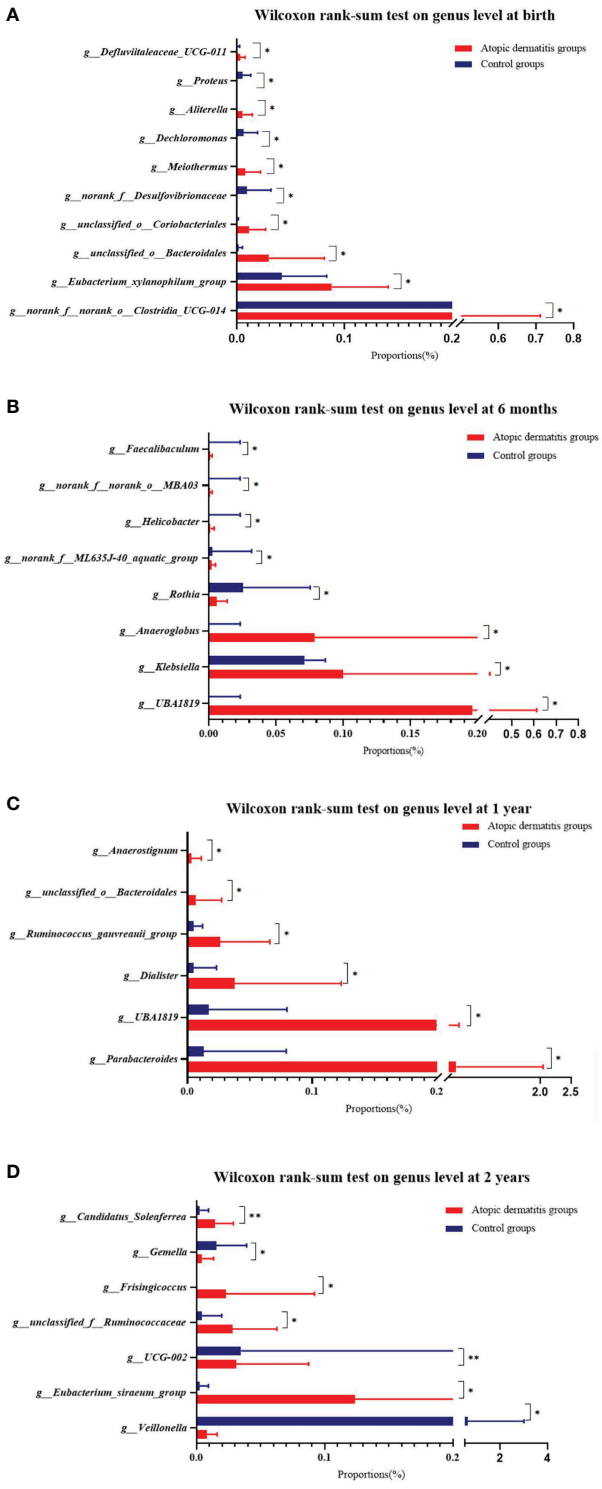

FIGURE 5
Difference of infant and toddler's gut microbiota of atopic dermatitis group and control group on genus level. **(A)** Wilcoxon rank-sum test on genus level at birth. **(B)** Wilcoxon rank-sum test on genus level at 6 months. **(C)** Wilcoxon rank-sum test on genus level at 1 year. **(D)** Wilcoxon rank-sum test on genus level at 2 years. Note: Wilcoxon rank-sum test bar plot shows the differences of gut microbial composition between two groups on the genus level. The Y-axis represents different genera groupings, boxes of different colors represent two different groupings, and the X-axis represents the average relative abundance of genera in different groupings. *0.01<P≤0.05, **0.001<P≤0.01.

TABLE 2 Logistics regression analysis to explore the impacts of maternal and offspring's gut microbiota on atopic dermatitis after controlling for confounding factors.

	β	S.E.	Wald	P value
Gut microbiota in Pregnancy women[a]				
Candidatus_Stoquefichus				
Low (ref)				
High	2.842	1.158	6.025	0.014
Pseudomonas				
Low (ref)				
High	3.127	1.124	7.736	0.005
Gut microbiota in infants and toddlers				
Eubacterium_xylanophilum_group (at birth) [b]				
Low(ref)				
High	2.041	0.966	4.462	0.035
Ruminococcus_gauvreauii_group (one year) [c]				
Low(ref)				
High	2.051	0.832	6.073	0.014
Gemella (two years) [d]				
Low(ref)				
High	-2.644	1.211	4.762	0.029
UCG-002 (two years) [d]				
Low(ref)				
High	3.006	1.453	4.278	0.039
Veillonella (two years) [d]				
Low(ref)				
High	-3.175	1.351	5.522	0.019

Ref, Reference group of the categorical variable.
[a]Logistics regression analysis Model 1, adjusting covariates (mother's age, mother's educational level, alcohol intake during pregnancy and frequency of maternal soy products consumption).
[b]Logistics regression analysis Model 2; adjusting covariates (mode of delivery).
[c]Logistics regression analysis Model 3; adjusting covariates (mode of delivery, maternal alcohol intake during breastfeeding, breastfeeding in first 6 months, antibiotics using in the first 6 months and pet exposure).
[d]Logistics regression analysis Model 3; adjusting covariates (mode of delivery,maternal alcohol intake during breastfeeding, breastfeeding in first 6 months, antibiotics using in the first 6 months and pet exposure).

preventative and interventional measures to minimize the development of allergic diseases in infants and toddlers.

Our study included postpartum analysis involving the examination of offspring gut microbiota status up to two years of age, and the potential pathophysiological impact involving the microbiota-immune axis and risk for pediatric atopic dermatitis. Hong et al. (2) noted a higher abundance of *Klebsiella* in infants with documented atopic dermatitis (2). Rhoads et al. (37) reported a higher abundance of *Klebsiella* in infants with colic, further substantiating the potential systemic inflammatory effects of *Klebsiella*. A prior study (38) demonstrated an increased abundance of *Parabacteroides* in infants presenting with atopic dermatitis. Our study further supports this finding in that a higher abundance of *Parabacteroides* and *Klebsiella* was noted in infants with atopic dermatitis, without adjusting for covariates. Our results showed that infants and toddlers in the atopic dermatitis group presented with a higher abundance of *Eubacterium xylanophilum group* at birth, *Ruminococcus gauvreauii group* at 1 year *and UCG-002* at 2 years after adjusting for covariates. *Eubacterium xylanophilum group* and *Ruminococcus gauvreauii group* belong to the family of *Lachnospiraceae*. Previous study (39) noted a significant increase in the abundance of *Lachnospiraceae* in infants and toddlers presenting with atopic dermatitis. Additionally, Xu et al. (40) discovered that *Ruminococcus gauvreauii group* was positively associated with systemic immune response mechanisms mediated *via* pro-inflammatory cytokines including tumor necrosis factor-α (TNF-α), IL-1β, and IL-6. Therefore, *Ruminococcus gauvreauii group* can initiate an inflammatory signaling cascade that may facilitate the pathophysiological development of allergic disease processes, including pediatric atopic dermatitis. However, there was no direct association between the above genera and risk for the development of atopic dermatitis in infants and toddlers in previous study (16). Particularly, the role of the genus *UCG-002* in the development of atopic dermatitis in infants and toddlers was unclear. Further studies involving the above three genera

would be needed to explore its role in mechanisms of allergic disease.

Our study demonstrated an important association involving reduced abundance of *Gemella* and *Veillonella* with an increased risk for atopic dermatitis in infants and toddlers. However, it is important to note that our findings were not entirely consistent with previous studies. Los-R et al. (41) discovered a positive correlation between the development of allergic disease in infants and presence of *Gemella*. Moreover, Huang et al. (42) noted a higher abundance of *Gemella* in infants presenting with asthma, while Simonyte et al. (43) indicated that reduced abundance of *Veillonella* in infancy was associated with an increased risk of asthma. Despite the notable discrepancies in previous literature findings, the anti-allergic effects of *Gemella* and *Veillonella* should be explored and considered in future applications. *Veillonella*, an anaerobic gram-negative coccus, can ferment lactic acid to propionate and acetate (44). *Gemella* is obligatory fermentative, producing either a mixture of acetic and lactic acids or an equimolar molar mixture of acetic acid and CO_2 depending on the abundance of oxygen (45). Therefore, both *Gemella* and *Veillonella* can produce SCFAs. SCFAs, such as butyrate, propionate, and acetate, are primary energy sources with anti-inflammatory and immunomodulatory effects (46). Previous studies also found lower levels of fecal SCFAs (i.e., acetate, butyrate and valerate) were associated with the development of atopic dermatitis in infants (47, 48). These findings cannot be generalized at this time as they require further investigation in studies involving larger sample sizes.

Our findings couldn't determine significant differences in the gut microbiota diversity between atopic dermatitis and control children involving infants and toddlers at different ages, inconsistent with other relevant studies (16, 21). We suspected that these inconsistencies may be a result of variable dietary habits of both maternal and infant origin. Differences in breastfeeding rates and maternal diet may affect the gut microbiota composition of infants and toddlers across different populations. Other plausible causes of discrepancy include individual environmental influences and underreported perinatal/postnatal factors. Therefore, a comprehensive analysis of all potential variables must be considered when exploring the complex relationship between gut microbiota and the development of pediatric atopic dermatitis.

While our findings did not indicate an association between exogenous influences and subsequent development of atopic dermatitis in infants and toddlers, prior studies have indicated otherwise (49, 50). A possible limitation influencing the overall results of our study includes our small sample size, which proved to be insufficient in detecting any statistical significance in exogenous influence and the development of pediatric atopic dermatitis. Therefore, it is imperative that we consider a larger sample size to control for these variables in an effort to elucidate the relationship among exogenous influences that may pose an indirect effect on infantile gut-microbiota status in the development of atopic dermatitis and other allergic processes.

Our study presents with strengths and weaknesses. Our study was a longitudinal cohort study allowing us to explore the relationship between gut microbiota in the first two years of life and risk for pediatric atopic dermatitis. Additionally, this served as a pilot study to investigate the relationship between changes in maternal gut microbiota during pregnancy and the development of atopic dermatitis in infants and toddlers, closing the gap in current research on maternal gut microbiota and subsequent atopic dermatitis of infants and toddlers in China. However, there were some distinct limitations of our study that require rectification for future applications. Principally, the sample size was insufficient for generalization of the data obtained. Moreover, we did not collect a complete medical history of both maternal and paternal subjects which is necessary for determining additional genetic components that may contribute to the development of pediatric atopic dermatitis. 16S rRNA sequencing was also a limitation of this study as it cannot provide sequences in a resolution like shotgun sequencing and provides no information about the functional capacity of the gut microbiota. Additionally, a further genetic function prediction or the measurements of SCFAs are suggested to be conducted to explore the clinical relevance to the changes in fecal microbiota in future studies.

Results of this study supported that enrichment and reduction of certain gut microbiota in mother-offspring pairs were associated with an increased risk of atopic dermatitis in infants and toddlers. The enrichment of *Gemella* and *Veillonella* in the microbiota of offspring appear to exhibit protective properties against the development of atopic dermatitis. Moreover, the results indicated that the enrichment of *Prevotella* during pregnancy may serve as a protective factor in the development of allergic diseases in offspring. The enrichment of *Pseudomonas*, *Candidatus Stoquefichus* during pregnancy and *Ruminococcus gauvreauii group*, *Eubacterium xylanophilum group* and *UCG-002* in offspring were risk factors for the development of atopic dermatitis in the offspring. Collectively, these findings provide a basis for continued research involving the gut-microbiota-immune axis and for the development of target-specific interventions in the prevention of pediatric atopic dermatitis.

Data availability statement

The datasets presented in this study can be found in online repositories. The names of the repository/repositories and accession number(s) can be found below: https://www.ncbi.nlm.nih.gov/, PRJNA482931.

Ethics statement

The studies involving human participants were reviewed and approved by the Research Ethics Boards of Medical School of Wuhan University (JKHL2017-03-03). Written informed

consent to participate in this study was provided by the participants' legal guardian/next of kin.

Author contributions

XF wrote all sections of the manuscript and performed the analysis. XF and YL contributed to the conception and design of the study. TZ, JD, and NW contributed to data collection. CH, JB, and YL contributed to the manuscript revisions. All authors contributed to the article and approved the submitted version.

Funding

This work was supported by the National Natural Science Foundation of China (grant number 81903334).

Acknowledgments

We were grateful for the technical support from Shanghai Majorbio Bio-pharm Technology Co., Ltd.

Conflict of interest

The authors declare that the research was conducted in the absence of any commercial or financial relationships that could be construed as a potential conflict of interest.

Publisher's note

All claims expressed in this article are solely those of the authors and do not necessarily represent those of their affiliated organizations, or those of the publisher, the editors and the reviewers. Any product that may be evaluated in this article, or claim that may be made by its manufacturer, is not guaranteed or endorsed by the publisher.

Supplementary material

The Supplementary Material for this article can be found online at: https://www.frontiersin.org/articles/10.3389/fimmu.2022.1038876/full#supplementary-material

References

1. Platts-Mills T. The allergy epidemics: 1870-2010. *J Allergy Clin Immunol* (2015) 136(1):3–13. doi: 10.1016/j.jaci.2015.03.048

2. Hong P, Lee B, Aw M, Shek L, Yap G, Chua K, et al. Comparative analysis of fecal microbiota in infants with and without eczema. *PloS One* (2010) 5(4):e9964. doi: 10.1371/journal.pone.0009964

3. Bieber T. Mechanisms of disease: Atopic dermatitis. *N Engl J Med* (2008) 358 (14):1483–94. doi: 10.1056/NEJMra074081

4. Myers JMB, Hershey GKK. Eczema in early life: Genetics, the skin barrier, and lessons learned from birth cohort studies. *J Pediatr* (2010) 157(5):704–14. doi: 10.1016/j.jpeds.2010.07.009

5. Mei F, Yizhu X, Xiaoyan L, Yan H. Investigation of environmental risk factors of eczema in different genetic background infants. *Chinese Journal of Child Health Care* (2015) 23(10):1070–3. doi: 10.11852/zgetbizz2015-23-10-19

6. Plötz S, Wiesender M, Todorova A, Ring J. What is new in atopic dermatitis/eczema? *Expert Opin emerging Drugs* (2014) 19(4):441–58. doi: 10.1517/14728214.2014.953927

7. Flohr C, Mann J. New insights into the epidemiology of childhood atopic dermatitis. *Allergy* (2014) 69(1):3–16. doi: 10.1111/all.12270

8. Penders J, Stobberingh E, van den Brandt P, Thijs C. The role of the intestinal microbiota in the development of atopic disorders. *Allergy* (2007) 62(11):1223–36. doi: 10.1111/j.1398-9995.2007.01462.x

9. Belkaid Y, Hand TW. Role of the microbiota in immunity and inflammation. *Cell* (2014) 157(1):121–41. doi: 10.1016/j.cell.2014.03.011

10. Arpaia N, Campbell C, Fan X, Dikiy S, van der Veeken J, deRoos P, et al. Metabolites produced by commensal bacteria promote peripheral regulatory T-cell generation. *Nature* (2013) 504(7480):451–5. doi: 10.1038/nature12726

11. Furusawa Y, Obata Y, Fukuda S, Endo T, Nakato G, Takahashi D, et al. Commensal microbe-derived butyrate induces the differentiation of colonic regulatory T cells. *Nature* (2013) 504(7480):446–50. doi: 10.1038/nature12721

12. Trompette A, Gollwitzer E, Yadava K, Sichelstiel A, Sprenger N, Ngom-Bru C, et al. Gut microbiota metabolism of dietary fiber influences allergic airway disease and hematopoiesis. *Nat Med* (2014) 20(2):159–66. doi: 10.1038/nm.3444

13. Forno E, Onderdonk A, McCracken J, Litonjua A, Laskey D, Delaney M, et al. Diversity of the gut microbiota and eczema in early life. *Clin Mol Allergy* (2008) 6:11. doi: 10.1186/1476-7961-6-11

14. Sjögren Y, Jenmalm M, Böttcher M, Björkstén B, Sverremark-Ekström E. Altered early infant gut microbiota in children developing allergy up to 5 years of age. *Clin Exp Allergy* (2009) 39(4):518–26. doi: 10.1111/j.1365-2222.2008.03156.x

15. Wang M, Karlsson C, Olsson C, Adlerberth I, Wold A, Strachan D, et al. Reduced diversity in the early fecal microbiota of infants with atopic eczema. *J Allergy Clin Immunol* (2008) 121(1):129–34. doi: 10.1016/j.jaci.2007.09.011

16. Zimmermann P, Messina N, Mohn W, Finlay B, Curtis N. Association between the intestinal microbiota and allergic sensitization, eczema, and asthma: A systematic review. *J Allergy Clin Immunol* (2019) 143(2):467–85. doi: 10.1016/j.jaci.2018.09.025

17. Jenmalm M. Childhood immune maturation and allergy development: regulation by maternal immunity and microbial exposure. *Am J Reprod Immunol* (2011) 66(suppl.1):75–80. doi: 10.1111/j.1600-0897.2011.01036.x

18. Jenmalm M. The mother-offspring dyad: microbial transmission, immune interactions and allergy development. *J Intern Med* (2017) 282(6):484–95. doi: 10.1111/joim.12652

19. West C, Jenmalm M, Prescott S. The gut microbiota and its role in the development of allergic disease: a wider perspective. *Clin Exp Allergy* (2015) 45 (1):43–53. doi: 10.1111/cea.12332

20. Lange N, Celedón J, Forno E, Ly N, Onderdonk A, Bry L, et al. Maternal intestinal flora and wheeze in early childhood. *Clin Exp Allergy* (2012) 42(6):901–8. doi: 10.1111/j.1365-2222.2011.03950.x

21. Stokholm J, Blaser M, Thorsen J, Rasmussen M, Waage J, Vinding R, et al. Maturation of the gut microbiome and risk of asthma in childhood. *Nat Commun* (2018) 9(1):141. doi: 10.1038/s41467-017-02573-2

22. Gao Y, Nanan R, Macia L, Tan J, Sominsky L, Quinn T, et al. The maternal gut microbiome during pregnancy and offspring allergy and asthma. *J Allergy Clin Immunol* (2021) 148(3):669–78. doi: 10.1016/j.jaci.2021.07.011

23. Vuillermin P, Macia L, Nanan R, Tang M, Collier F, Brix S. The maternal microbiome during pregnancy and allergic disease in the offspring. *Semin Immunopathol* (2017) 39(6):669–75. doi: 10.1007/s00281-017-0652-y

24. Vuillermin P, O'Hely M, Collier F, Allen K, Tang M, Harrison L, et al. Maternal carriage of prevotella during pregnancy associates with protection against food allergy in the offspring. *Nat Commun* (2020) 11(1):1452. doi: 10.1038/s41467-020-14552-1

25. Wang Y, Liu Y, Bai J, Chen X. The effect of maternal postpartum practices on infant gut microbiota: A Chinese cohort study. *Microorganisms* (2019) 7 (11):511. doi: 10.3390/microorganisms7110511

26. Williams H, Burney P, Hay R, Archer C, Shipley M, Hunter J, et al. The U.K. working party's diagnostic criteria for atopic dermatitis. i. derivation of a minimum set of discriminators for atopic dermatitis. *Br J Dermatol* (1994) 131(3):383–96. doi: 10.1111/j.1365-2133.1994.tb08530.x

27. Zhang XX, Zou Y, Zou X, Xu ZG, Nan XN, Han CX. DNA Metabarcoding uncovers the diet of subterranean rodents in China. *PloS One* (2022) 17(4): e0258078. doi: 10.1371/journal.pone.0258078

28. Franke T, Deppenmeier U. Physiology and central carbon metabolism of the gut bacterium prevotella copri. *Mol Microbiol* (2018) 109(4):528–40. doi: 10.1111/mmi.14058

29. Kovatcheva-Datchary P, Nilsson A, Akrami R, Lee Y, De Vadder F, Arora T, et al. Dietary fiber-induced improvement in glucose metabolism is associated with increased abundance of prevotella. *Cell Metab* (2015) 22(6):971–82. doi: 10.1016/j.cmet.2015.10.001

30. Rubic T, Lametschwandtner G, Jost S, Hinteregger S, Kund J, Carballido-Perrig N, et al. Triggering the succinate receptor GPR91 on dendritic cells enhances immunity. *Nat Immunol* (2008) 9(11):1261–9. doi: 10.1038/ni.1657

31. Gomez de Agüero M, Ganal-Vonarburg S, Fuhrer T, Rupp S, Uchimura Y, Li H, et al. The maternal microbiota drives early postnatal innate immune development. *Sci (New York NY)* (2016) 351(6279):1296–302. doi: 10.1126/science.aad2571

32. Kamada N, Seo S, Chen G, Núñez G. Role of the gut microbiota in immunity and inflammatory disease. *Nat Rev Immunol* (2013) 13(5):321–35. doi: 10.1038/nri3430

33. Yurkovetskiy L, Pickard J, Chervonsky A. Microbiota and autoimmunity: exploring new avenues. *Cell Host Microbe* (2015) 17(5):548–52. doi: 10.1016/j.chom.2015.04.010

34. Agaronyan K, Sharma L, Vaidyanathan B, Glenn K, Yu S, Annicelli C, et al. Tissue remodeling by an opportunistic pathogen triggers allergic inflammation. *Immunity* (2022) 55(5):895–911.e10. doi: 10.1016/j.immuni.2022.04.001

35. Caminero A, Galipeau H, McCarville J, Johnston C, Bernier S, Russell A, et al. Duodenal bacteria from patients with celiac disease and healthy subjects distinctly affect gluten breakdown and immunogenicity. *Gastroenterology* (2016) 151(4):670–83. doi: 10.1053/j.gastro.2016.06.041

36. Tanabe H, Sakurai K, Kato T, Kawasaki Y, Nakano T, Yamaide F, et al. Association of the maternal microbiome in Japanese pregnant women with the cumulative prevalence of dermatitis in early infancy: A pilot study from the Chiba study of mother and child health birth cohort. *World Allergy Organ J* (2019) 12 (10):100065. doi: 10.1016/j.waojou.2019.100065

37. Rhoads J, Fatheree N, Norori J, Liu Y, Lucke J, Tyson J, et al. Altered fecal microflora and increased fecal calprotectin in infants with colic. *J pediatr* (2009) 155(6):823–8.e1. doi: 10.1016/j.jpeds.2009.05.012

38. Ye S, Yan F, Wang H, Mo X, Liu J, Zhang Y, et al. Diversity analysis of gut microbiota between healthy controls and those with atopic dermatitis in a Chinese population. *J Dermatol* (2021) 48(2):158–67. doi: 10.1111/1346-8138.15530

39. Zheng H, Liang H, Wang Y, Miao M, Shi T, Yang F, et al. Altered gut microbiota composition associated with eczema in infants. *PloS One* (2016) 11(11): e0166026. doi: 10.1371/journal.pone.0166026

40. Xu T, Ge Y, Du H, Li Q, Xu X, Yi H, et al. Berberis kansuensis extract alleviates type 2 diabetes in rats by regulating gut microbiota composition. *J Ethnopharmacol* (2021) 273:113995. doi: 10.1016/j.jep.2021.113995

41. Los-Rycharska E, Golebiewski M, Sikora M, Grzybowski T, Gorzkiewicz M, Popielarz M, et al. A combined analysis of gut and skin microbiota in infants with food allergy and atopic dermatitis: A pilot study. *Nutrients* (2021) 13(5):1682. doi: 10.3390/nu13051682

42. Huang C, Yu Y, Du W, Liu Y, Dai R, Tang W, et al. Fungal and bacterial microbiome dysbiosis and imbalance of trans-kingdom network in asthma. *Clin Transl Allergy* (2020) 10:42. doi: 10.1186/s13601-020-00345-8

43. Simonyte Sjodin K, Vidman L, Ryden P, West CE. Emerging evidence of the role of gut microbiota in the development of allergic diseases. *Curr Opin Allergy Clin Immunol* (2016) 16(4):390–5. doi: 10.1097/ACI.0000000000000277

44. van den Bogert B, Erkus O, Boekhorst J, de Goffau M, Smid EJ, Zoetendal EG, et al. Diversity of human small intestinal streptococcus and veillonella populations. *FEMS Microbiol Ecol* (2013) 85(2):376–88. doi: 10.1111/1574-6941.12127

45. Constantinos M, Marios S. Gemella morbillorum tricuspid valve endocarditis resulting in septic pulmonary emboli in a patient with intracranial hemorrhage. *Int J Cardiol* (2015) 184:769–71. doi: 10.1016/j.ijcard.2015.02.094

46. Smith PM, Howitt MR, Panikov N, Michaud M, Gallini CA, Bohlooly YM, et al. The microbial metabolites, short-chain fatty acids, regulate colonic treg cell homeostasis. *Science* (2013) 341(6145):569–73. doi: 10.1126/science.1241165

47. Park YM, Lee SY, Kang MJ, Kim BS, Lee MJ, Jung SS, et al. Imbalance of gut streptococcus, clostridium, and akkermansia determines the natural course of atopic dermatitis in infant. *Allergy Asthma Immunol Res* (2020) 12(2):322–37. doi: 10.4168/aair.2020.12.2.322

48. Kim HK, Rutten NB, Besseling-van der Vaart I, Niers LE, Choi YH, Rijkers GT, et al. Probiotic supplementation influences faecal short chain fatty acids in infants at high risk for eczema. *Benef Microbes* (2015) 6(6):783–90. doi: 10.3920/BM2015.0056

49. Chan CWH, Leung TF, Choi KC, Tsui SKW, Wong CL, Chow KM, et al. Association of early-life gut microbiome and lifestyle factors in the development of eczema in Hong Kong infants. *Exp Dermatol* (2021) 30(6):859–64. doi: 10.1111/exd.14280

50. Chan CWH, Yuet Wa Chan J, Leung TF, Choi KC, Tsui SKW, Wong CL, et al. Altered gut microbiome and environmental factors associated with development of eczema in Hong Kong infants: A 4-month pilot study. *Int J Environ Res Public Health* (2020) 17(20):7634. doi: 10.3390/ijerph17207634

frontiers | Frontiers in Immunology

TYPE Brief Research Report
PUBLISHED 20 December 2022
DOI 10.3389/fimmu.2022.1094376

OPEN ACCESS

EDITED BY
Eun Jeong Park,
Mie University, Japan

REVIEWED BY
Tara Chand Yadav,
Indian Institute of Technology Roorkee, India
Shuo Yan Gau,
Chung Shan Medical University, Taiwan

*CORRESPONDENCE
Ian A. Myles
mylesi@niaid.nih.gov

†These authors have contributed equally to this work

SPECIALTY SECTION
This article was submitted to Molecular Innate Immunity, a section of the journal Frontiers in Immunology

RECEIVED 10 November 2022
ACCEPTED 07 December 2022
PUBLISHED 20 December 2022

CITATION
Gough P, Zeldin J and Myles IA (2022) Assessing microbial manipulation and environmental pollutants in the pathogenesis of psoriasis. *Front. Immunol.* 13:1094376. doi: 10.3389/fimmu.2022.1094376

Assessing microbial manipulation and environmental pollutants in the pathogenesis of psoriasis

Portia Gough†, Jordan Zeldin† and Ian A. Myles*

Epithelial Therapeutics Unit, National Institute of Allergy and Infectious Disease, National Institutes of Health, Bethesda, MD, United States

The cutaneous microbiome is increasingly recognized as a contributor to skin diseases like atopic dermatitis (AD) and psoriasis. Although traditionally AD and psoriasis have been viewed as having opposing immunologic findings, recent evidence suggests an overlap in ceramide-family lipid production in the protection against symptoms. We recently identified that specific environmental pollutants may drive dysbiosis through direct suppression of ceramide-family lipids produced by health-associated skin bacteria in atopic dermatitis (AD). We further demonstrated that one such bacteria, *Roseomonas mucosa*, generated significant clinical improvement in AD lasting beyond active treatment *via* lipid-mediated modulation of tumor necrosis factor (TNF) signaling. To assess the potential preclinical benefit of *R. mucosa* in psoriasis we assessed for direct effects on surface TNF signaling in cell cultures and identified direct effects on the TNF axis. We also identified preclinical efficacy of *R. mucosa* treatment in the imiquimod mouse model of psoriasis. Finally, we expanded our previous environmental assessment for psoriasis to include more traditional markers of air quality and found a strong association between disease rates and ambient carbon monoxide (CO), nitrogen dioxide (NO_2), and particulate matter (PM). At the current stage this work is speculative but does support consideration of further preclinical models and/or clinical assessments to evaluate any potential for therapeutic benefit through microbial manipulation and/or environmental mitigation.

KEYWORDS

psoriasis, microbiome, *Roseomonas*, atopic dermatatis, pollution

1 Introduction

The cutaneous microbiome is increasingly recognized as a contributor to skin disease. Although the literature is less robust for the skin microbiome in psoriasis as it is for related gut dysbiosis or dysbiosis in diseases like atopic dermatitis (AD), both microbial signatures and therapeutic targeting have been described (1–3). We recently suggested that environmental pollutants may drive dysbiosis through direct effects on cutaneous

commensal bacteria (4). Furthermore, we have reported that use of topical *Roseomonas mucosa* generated significant clinical improvement in AD lasting beyond active treatment (4, 5). These lasting effects were likely related to colonization with the treatment strains whose modeled mechanism involves the production of amine-containing lipids (such as ceramides) which potentiated tumor necrosis factor (TNF) receptor 2 (TNFR2) signaling to drive epithelial repair (5, 6). For AD, these lipids appeared to be directly depleted by exposure to the isocyanate containing air and may suggest a mechanism for the association between industrial environments and AD-linked dysbiosis (4).

However, unlike psoriasis (7, 8), TNF has not classically been considered a central mediator in AD. Yet, psoriasis and AD have both been linked to a reduction in cutaneous ceramide levels (9). Furthermore, epidemiologic features that argue for a potential environmental contributor to psoriasis include: finding that the rates in the US have increased 1.75 fold since 1974 (10); urban living carries an odds ratio of 3.61 compared to rural (11); tobacco, alcohol, and change in work or family conditions increase risk of psoriasis (11); and rates are higher in high income countries (although data in many nations are lacking) (12). Although our preliminary screen of pollutants that may contribute to psoriasis failed to identify any strong candidates (4), we hypothesized that *R. mucosa* treatment could benefit psoriasis through impacts on TNFR2 signaling and/or production of therapeutic lipids.

Due to the shared pathology of TNF and ceramide family lipids, we thus aimed to assess if R. mucosa directly influences the TNF axis *in vitro* and models of psoriasis *in vivo*. Furthermore, given the associations between industrialization and psoriasis, we aimed to perform an untargeted assessment of Environmental Protection Agency (EPA) monitored pollutants versus the rate of clinical visits for psoriasis by US zip codes. Herein we describe that *R. mucosa* directly influences surface TNF, TNFR2, and TNF alpha converting enzyme (TACE, aka ADAM17) in cell culture models and influenced soluble TNFR2 in patients with AD. *R. mucosa* improved outcomes in the imiquimod (IMQ) model of murine psoriasis, a model known to be dependent on TNFR signaling balance (7). Finally, we expanded our previous environmental assessment for psoriasis to include more traditional markers of air quality and found a strong association between disease rates and ambient carbon monoxide (CO), nitrogen dioxide (NO2), and particulate matter (PM). Overall, our findings support the consideration of clinical trials using *R. mucosa* for psoriasis as well as further *in vitro* modeling for a role of air pollution in psoriasis pathogenesis.

2 Methods

2.1 Cell culture and staining

Primary Neonatal keratinocytes (HEKn, ATCC) were seeded at 1.5x10^5 cells/well in 24 well plates that were coated with 10 µg/mL human fibronectin (Millipore). The cells were allowed to settle for 1 hour. RmHV1 were added at MOI 10, and cells were incubated at 37°C and 5% CO2 for 12 hours. Cells were fixed in 4% PFA, blocked with 10% normal goat serum, and labeled with antibodies for TNFR2 (Sigma, SAB4502989, 1:100), TACE/ADAM17 (ThermoFisher, 3H46L1, 1:200), or TNF (Abcam, ab1793, 1:100) overnight at 4°C. Cells were washed and secondary antibodies (anti-rabbit AlexaFluor 488 or anti-mouse AlexaFluor 594, ThermoFisher, 1:1000) were added and incubated for 1 hour at room temperature. Cells were washed and DAPI was added as counterstain (ThermoFisher). Cells were imaged in 4 different areas of well using a Cytation5, and image analysis was performed by Gen5 software as follows: each cell was identified based on nuclear stain, and fluorescence intensity was measured for each cell in image and was divided by total number of cells to obtain the mean fluorescence intensity (MFI) value for each image.

2.2 Patients

Patients were recruited and enrolled at the NIH under the IRB approved clinical trial NCT03018275 (Beginning Assessment of Cutaneous Treatment Efficacy of *Roseomonas* in Atopic Dermatitis, Phase I/II; BACTERiAD I/II). Enrollment criteria, treatment formulation, and clinical scoring were all as previously described (5).

2.3 Serum analysis

Serum samples were analyzed for sTNFR1 and sTNFR2 using the BioPlex system (BioRad, Hercules, CA) per manufacture instructions and as previously described (5).

2.4 Mice

Male and female C57BL/6 mice aged 6-12 weeks were purchased from Jackson Labs (Bar Harbor, MA). All mice were age and sex matched within each experiment. Imiquimod modeling of psoriasis was performed as previously described (13). Briefly, IMQ was applied to each ear daily for 5 days, then either 10mcL of 10% sucrose or 10^5 CFU of *R. mucosa* in 10mcL of 10% sucrose was applied daily for 3 days. Ear thickness was monitored, and ears collected for histology analysis at day 11. Ear mounting to slides and H&E staining was performed by Historserv (Germantown, MD). Images of slides were collected as previously described (5). A histologic comparison of the ear pinna between the diluent-treated, RnAD-treated, and RmHV-treated mice (i.e. 3 total) was made based solely on the submitted microscopic image from each animal. Animal work was approved by an IACUC and followed the guidelines and basic

principles in the United States Public Health Service Policy on Humane Care and Use of Laboratory Animals, and the Guide for the Care and Use of Laboratory Animals by certified staff in an Association for Assessment and Accreditation of Laboratory Animal Care (AAALAC) International accredited facility.

2.5 Pollution analysis

As detailed previously (4), data on pollution was derived from the Environmental Protection Agency's Risk-Screening Environmental Indicators (RSEI) system from 2015-2019 was contrasted against the Definitive Health database, which contains 1.2 billion diagnostic billing codes per year from 2019 across 20,000 zip codes in the United States, including Hawaii, Alaska, and U.S. territories for ICD-10 code L40.9. Additional data on air pollution in 2015 from Center for Air, Climate, and Energy Solutions (CACES) was used to incorporate CO, NO_2, particulate matter of 2.5 microns or less (PM2.5), PM10, and SO_2 (14). For each zip code tabulation area where ICD codes are aggregated, the concentration of pollution from the surrounding census tracts within a 50-mile radius were averaged. Weights were based on the population in the census tract and the proximity to the zip code centroid. Other covariates included the population density, bracketed age ranges [from American Community Survey), the Area Deprivation Index (from Neighborhood Atlas (15)], and the proportion of visits to specialists (i.e., rheumatologists, dermatologists). The spatially lagged y autocovariate was constructed with inverse distance weights. Poisson regression lasso was implemented with the glmnet package using spatial folds created with 10 k-means clusters. Random forest regression was implemented with the ranger package, with case weights equal to the total number of visits, mtry untuned to $1/3^{rd}$ the number of features, and 1000 trees.

3 Results

3.1 *R. mucosa* directly influences cell surface TNF in keratinocytes

We previously demonstrated the modeled activity of *R. mucosa* was dependent upon TNFR signaling, but such analysis could not discriminate if the bacteria directly impacted surface expression of TNF signaling or if the activity was intra-cellular. To assess this, we stained human primary keratinocytes for surface TNFα, TNFα converting enzyme (TACE), and TNFR2. After 12 hours of co-culture, the expression for each of these markers was significantly reduced by exposure to *R. mucosa*. (Figures 1A–E).

3.2 *R. mucosa* induced reduction of soluble TNFR2 associated with clinical improvement

We previously reported the impact of topical *R. mucosa* treatment on select serum cytokines in an open-label clinical protocol for patients with AD (5). In that initial report we identified reductions in serum TNF was associated with clinical improvement (5) but had not evaluated the balance of TNF receptor expression. Analysis of the samples revealed that treatment was associated with a significant reduction in soluble TNFR2 (sTNFR2) but not sTNFR1 (Figures 1F, G). Like TNF, reductions in sTNFR2 significantly associated with improvement in AD as measured by SCORing Atopic Dermatitis (SCORAD) metric (a metric which combines clinical scores for itch, rash, and sleep disturbance) (Figure 1H). Together, these data suggest that *R. mucosa* may have a direct impact on the cell surface TNF axis.

3.3 *R. mucosa* treatment improved outcomes in the IMQ murine model of psoriasis

Given that the IMQ model of psoriasis is dependent on TNFR signaling balance (7) and cutaneous ceramide levels (9) we hypothesized that *R. mucosa* treatment may improve outcomes. All groups presented with the expected histopathologic features of IMQ exposure (16) including epidermal hyperplasia and hyperkeratosis. Compared to 10% sucrose diluent, treatment with *R. mucosa* from healthy volunteers (RmHV) significantly reduced the resultant swelling (Figure 2A) as well as the acanthosis and dermal thickening (Figure 2B). We further compared RmHV to isolates taken from patients with AD (RmAD); although these were not cultured from psoriasis patients, these isolates lack the beneficial lipid production and TNFR2 activity seen in RmHV (5). Treatment with RmAD did not produce any improvement in swelling or histologic abnormalities and interestingly induced an increase in the size and number of sebocytes (sebaceous hyperplasia) that was not seen in the diluent treated mice (Figures 2A, B); this suggests both a specific benefit of the health-associated isolates and a potential harm from AD-associated *R. mucosa*.

3.4 Psoriasis associated with carbon dioxide pollution by US zip code

Similar to our previous work in AD (4), we performed an untargeted comparison between the pollution reported to the EPA under the Risk-Screening Environmental Indicators (RSEI) system. This system collates mandatory self-reporting of air

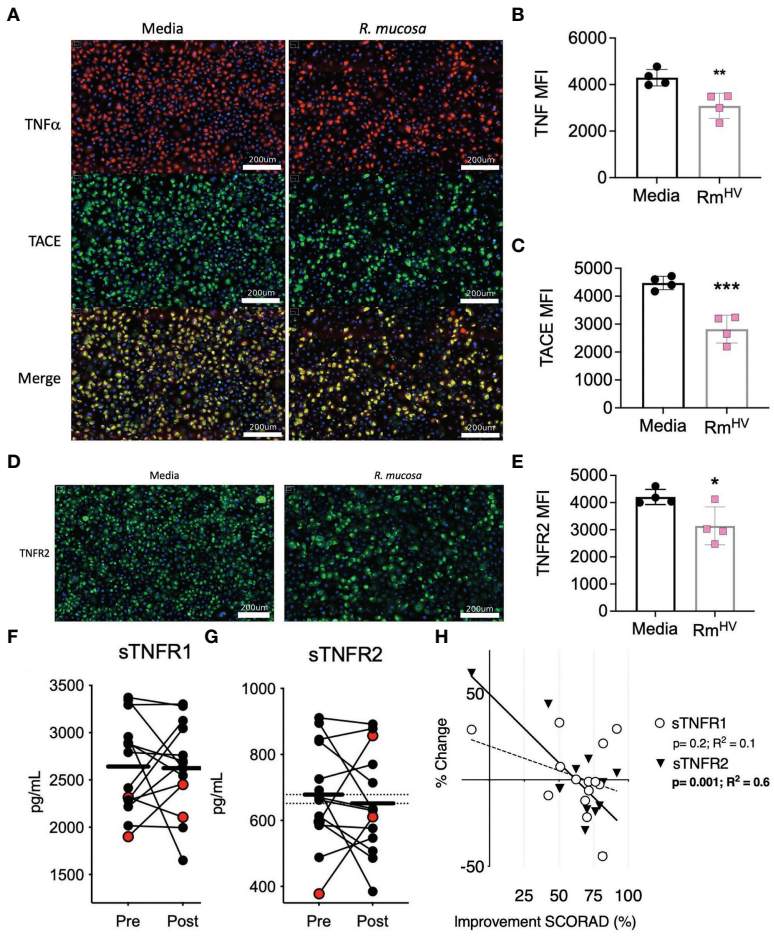

FIGURE 1
R. mucosa alters surface TNF-related marks in human keratinocyte cultures and patients with AD. **(A)** Representative images for immunofluorescent staining of tumor necrosis factor alpha (TNFα; red), TNFα converting enzyme (TACE; green) and both (merge; yellow) for human primary keratinocytes stimulated with *R. mucosa* from healthy volunteers or media alone. White lines represent scale of 200 micrometers. **(B, C)** Quantification of signal for indicated marker in replicate wells. **(D, E)** Representative image **(D)** and quantification in replicate wells **(E)** for immunofluorescent staining of tumor necrosis factor receptor 2 (TNFR2). White lines **(D)** represent scale of 200 micrometers. **(F–H)** 14 pediatric patients with atopic dermatitis (AD) were treated with topical *R. mucosa* for a total of four months. **(F, G)** Levels of soluble tumor necrosis factor receptor 1 (sTNFR1) and sTNFR2 in the serum at enrollment (Pre) or after 16 weeks of active treatment (Post) are shown. Red dots indicate the two patients that did not achieve at least a 50% improvement in symptoms during treatment. **(H)** Percent change in sTNFR1 and sTNFR2 levels are contrasted against improvement in SCORing AD are shown along with a simple linear regression line. Data represent three independent experiments and are displayed as mean ± SEM. ***p<0.001, **p<0.01, *p<0.05 as determined by Student T test.

pollution from facilities in the US and incorporates information about facility transfers, stack height, and wind dispersion to calculate their likely concentration across the US. In addition to the RSEI, we considered variables from the Center for Air Climate and Energy Solutions, which enriches our analysis for more common air pollutants that comprise the more familiar air quality scores. Further variables accounted for include demographic and age information from the American Community Survey (ACS) and local deprivation from the Neighborhood Atlas. Contrasting aggregate exposures from 2015-2019 against the rates of billing visits for psoriasis to medical providers in 2019 (Figure 3A) demonstrated a consistent association between carbon monoxide (CO) exposure and the rate of clinic visits for psoriasis as detected with a non-spatial lasso regression (Figure 3B), spatial lasso regression with spatially lagged y autocovariate and spatial folds (Figure 3C), and when visualized by pollution percentile (Figure 3D). Isopropyl alcohol, allylamine, and dimethyl phthalate were the other selected chemicals however quantile plots did not suggest a clear independent dose-response relationship (Figures 3E, F).

Consistent with the literature (11, 15), there was strong co-linearity between CO and other pollutants typically associated with automobile exhaust, especially NO_2, but also PM2.5 and

10.3389/fimmu.2022.1094376

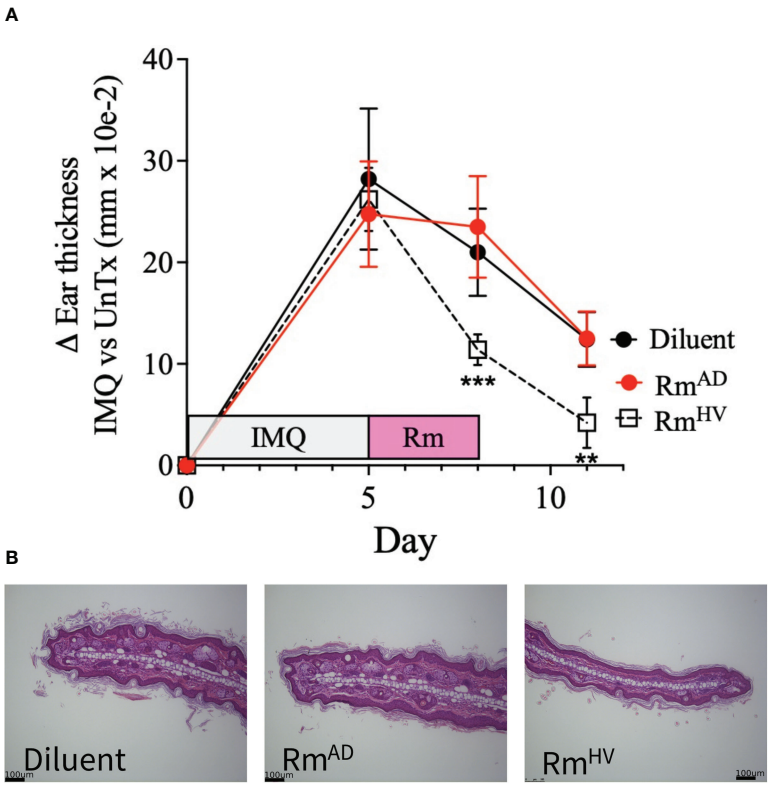

FIGURE 2
Topical *R. muocsa* improves mouse models of psoriasis. Mice (N = 5 per group) were treated with imiquimod (IMQ) daily for 5 days on one ears before topical treatment with 10^6 colony forming units of R. mucosa from a healthy volunteer (Rm^{HV}), a patients with atopic dermatitis (Rm^{AD}), or diluent control were applied with the same ear for 3 days. **(A)** Differences between the unperturbed and treated ear are shown. **(B)** Representative images for one treated ear from each group are shown. Black bars indicate 100um scale. Data represent two independent experiments and displayed as mean ± SEM. ***p<0.001, **p<0.01.

PM10 (Figure 4A). Furthermore, when a random forest model was used, which flexibly models nonlinear relationships and potentially complex interactions between exposures, NO_2 was the top variable selected, along with barium (Figure 4B). Like CO, an independent dose-response curve was evident for both NO_2 and barium (Figures 4C, D).

4 Discussion

TNFα has a well-established role in the pathogenesis of psoriasis. In this study, we found that *R. mucosa* had a direct effect on levels of TNFα, TACE and TNFR2 on the cell surface of primary human keratinocytes. The significant reduction of these targets on the surface of human keratinocytes can be a result of either receptor internalization or receptor shedding, either of which can occur following activation of TNFR2 (17). Further experimentation in this model will be needed to determine whether the changes in surface expression is due to shedding or internalization, but the data point to *R. mucosa* causing activation of TNFR2 signalling.

While some of the cell culture findings will require additional inquiry, direct observation of TNFR impact was seen in our clinical trial of topical *R. mucosa* for AD. However, the clinical data is limited by the small sample size and lack of placebo. Furthermore, comparison between *R. mucosa* treatment and established treatment modalities will be needed to elucidate if reductions in sTNFR2 is generally related to clinical improvement or specific to responses to *R. mucosa*. One study indicated that sTNFR levels were each associated with severity but did not assess if levels changed with clinical treatment (18).

These preclinical findings suggest that the benefit of *R. mucosa* in mouse models of psoriasis would most likely operate through either modulating TNF signalling or non-specific pathways that aide in tissue repair. Although resent evidence suggests a bidirectional association between AD and psoriasis (19), traditionally they have been viewed as having opposing immunologic findings (20) and thus finding improvement in

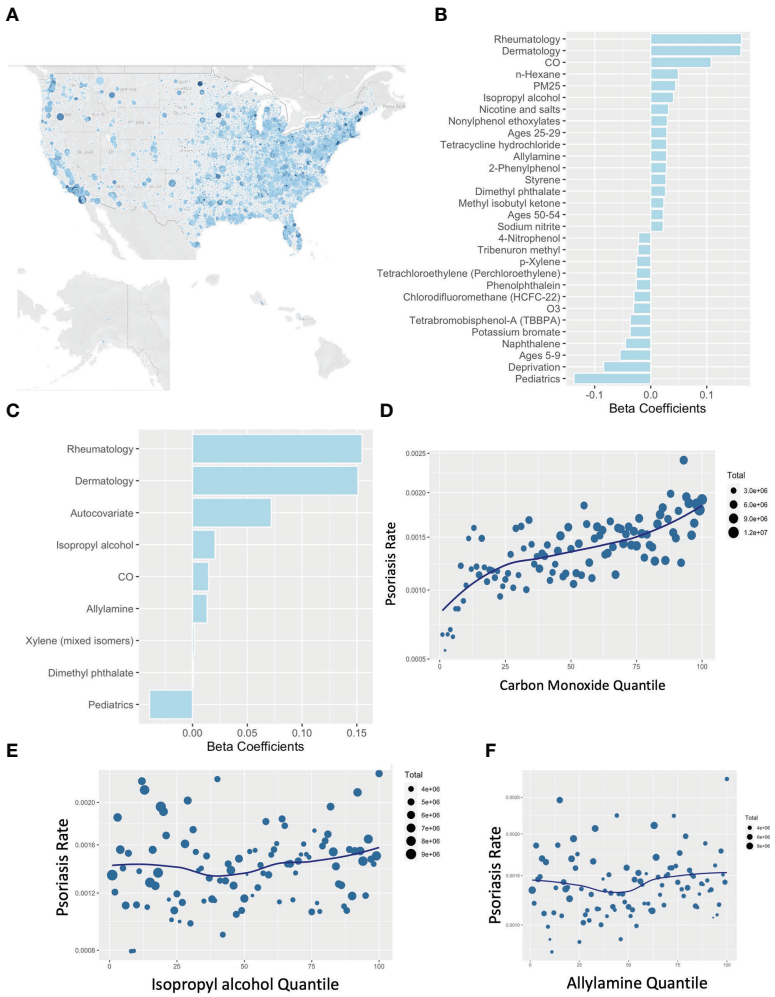

FIGURE 3
Rates of psoriasis associate with carbon monoxide by US zip code. **(A)** Map of rates of psoriasis (clinical visits billing for psoriasis divide by total billable visits) by US zip code. **(B, C)** Lasso Poisson regression models using non-spatial **(B)** or spatial **(C)** assessments pollutants associated with psoriasis. **(D–F)** Percentile plots for concentration of CO **(D)**, isopropyl alcohol **(E)**, and allylamine **(D)** against rates of psoriasis.

mouse models of both diseases may be somewhat unexpected. However, the importance of both TNF and skin lipid biology have been established in the pathogenesis of psoriasis (8, 9). Therefore, even if *R. mucosa* is unlikely to specifically modulate each of the immunologic pathways that distinguish the AD and psoriasis, modulation of TNF signalling along with increased ceramide-family lipids would be expected to provide utility to any inflammatory skin disease. Therefore, our models suggest that a clinical trial using *R. mucosa* in patients with psoriasis may be worthy of consideration. In addition, our mouse models should be repeated using commensal isolates taken from patients with psoriasis as comparisons, in addition to the *Rm*AD used in our work thus far.

R. mucosa is not the only skin organism capable of modulating ceramide-family lipid production. For example, *Staphylococcus epidermidis* has recently been shown to enhance host production of ceramides and thus may also offer therapeutic benefit (21). While commensal influence over cutaneous TNF signalling is less well established in the literature, future work could screen isolates for impact on TNF and/or the TNF receptors. As recently well reviewed (22), microbes which as over-represented in lesional skin in psoriasis compared to controls and/or unaffected skin include *Corynebacterium* spp., *S. pyogenes*, *Neisseria* spp., and *Propionibacterium* spp. If these organisms contribute to symptom severity, then strategies which target these organisms may also provide benefit to patients.

Furthermore, the pathophysiology of psoriasis goes beyond this manuscripts TNF focus. Numerous other cytokines and chemokines are involved in the pathogenesis of psoriasis including but not limited to interleukin (IL-) 1β, IL-17, IL-23,

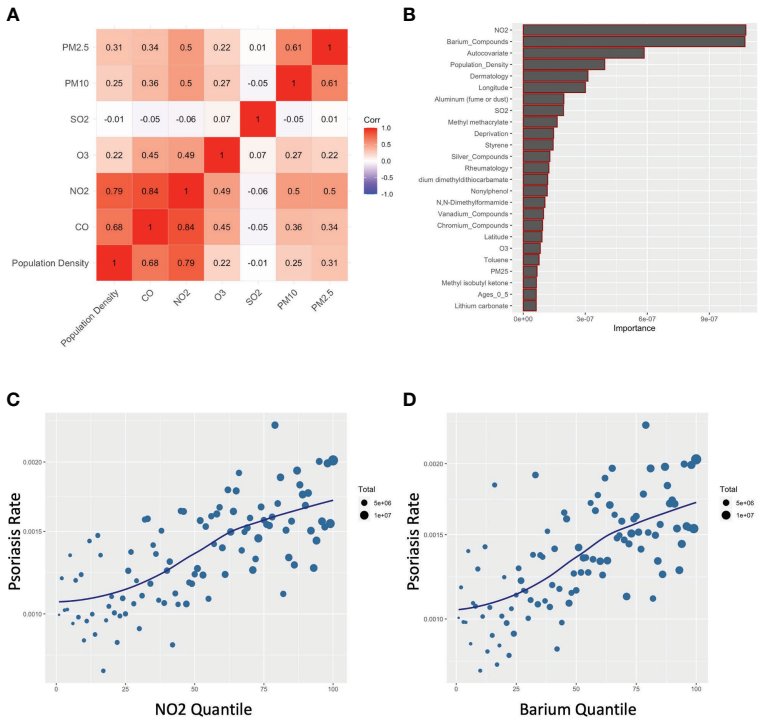

FIGURE 4
Carbon monoxide associates with other common air pollutants for psoriasis. **(A)** Correlogram for indicated pollutants. **(B)** Random forest assessment accounting for non-linearities and complex interactions **(C, D)** Percentile plots for concentration of NO2 **(C)** and barium **(D)** against rates of psoriasis.

and CXCL1 (22). *In vitro* screening for commensals which modulate any of these additional immunologic markers might identify viable probiotic options that may offer more targeted benefit and/or synergize with *R. mucosa*. However, one thing to be mindful of in researching diseases like psoriasis is the challenge presented by the potential for delayed onset of symptoms. Microbial disruption in the gut or skin present in childhood could generate disease later in life and thus there is a risk that the most valuable dysbiotic insights could fade from detection by the time of disease onset.

We used multiple models to query for psoriasis-associated pollutants. CO was ranked most important by our penalized regression models, though it may only be a marker of vehicle exhaust, urbanicity, or often-associated pollutants like NO_2. A previous study reported that subacute exposure to pollutants often found in vehicle exhaust, including CO, NOx, PM2.5, PM10, and benzene, are associated with psoriasis flares (15). Select studies have linked CO with autoimmunity in general (23) and psoriasis in specific (15). Although average CO levels in the US have been declining during the era of rising rates of psoriasis (24), increased population growth in urban areas could still present a means for increased overall exposure to CO (11, 25). Isopropyl alcohol and allylamine were weakly associated with psoriasis, but neither have reported links to psoriasis in the literature. The permutation importance rankings from the random forest regression model, which is flexible to non-linearities and complex interactions, suggested NO_2 (Figure 4B), which is highly correlated with CO (Figure 4A).

Thus, similar to our clinical modelling, our assessment of psoriasis-associated toxins is limited by its current speculative stage. The literature suggests possible mechanisms for CO induced inflammation through feedback loops with the host enzyme heme oxygenase 1, which is elevated in the plaques and serum of psoriasis patients and associated with metabolic syndrome (26–28). Additionally, bacterial ATP activation of the host inflammasome can be mediated by CO signalling from macrophages (29). However, given the high correlation between CO and general industrialization, and because our psoriasis database represents visits to providers aggregated by zip code rather than individual-level data, it may be plausible to conclude that the correlation with psoriasis and CO in our databases may be partly representative of the ease with which patients can transit to their providers in urbanized settings. Other researchers may also need to consider the possibility that correlations in measured CO and NO_2 may be nonspecific associations with population density rather than a biologic mechanism of disease. Therefore, directed investigation will be needed to test if these reported findings are relevant in psoriasis. For example, patient registries containing

both location and severity could be compared in a cross-sectional and/or longitudinal study against measured CO levels in the surrounding geography. If our findings can be validated, the clinical implications include the potential for improving outcomes in and/or prevention of psoriasis *via* microbial manipulation and targeted environmental mitigation. In conclusion, our findings suggest that while AD and psoriasis represent distinct pathologies, they may share a potential for future therapeutic benefit through microbial manipulation of the TNF axis and/or through environmental mitigations.

Data availability statement

The raw data supporting the conclusions of this article will be made available by the authors, without undue reservation.

Ethics statement

The studies involving human participants were reviewed and approved by IRB of the National Institutes of Health. Written informed consent to participate in this study was provided by the participants' legal guardian/next of kin. The animal study was reviewed and approved by Animal Care Board for National Institutes of Health.

Author contributions

PG performed all studies involving cell culture staining and wrote the manuscript. JZ performed the assessments for pollutants associated with psoriasis. IM performed serum and murine studies and wrote the manuscript. All authors contributed to the article and approved the submitted version.

Funding

This work was supported by the Intramural Research Program of the National Institute of Allergy and Infectious Diseases (NIAID) and the National Institutes of Health (NIH).

Acknowledgments

We would like to thank the patients and families enrolled in the clinical trial. The manuscript was reviewed in consultation with NIAID's Infectious Disease Pathogenesis Section.

Conflict of interest

The authors declare that the research was conducted in the absence of any commercial or financial relationships that could be construed as a potential conflict of interest.

Publisher's note

References

1. Tao R, Li R, Wan Z, Wu Y, Wang R. Skin microbiome signatures associated with psoriasis and seborrheic dermatitis. *Exp Dermatol* (2022) 31:1116–8. doi: 10.1111/exd.14618

2. Habeebuddin M, Karnati RK, Shiroorkar PN, Nagaraja S, Asdaq SMB, Khalid Anwer M, et al. Topical probiotics: More than a skin deep. *Pharmaceutics* (2022) 14 (3):557. doi: 10.3390/pharmaceutics14030557

3. Langan EA, Kunstner A, Miodovnik M, Zillikens D, Thaci D, Baines JF, et al. Combined culture and metagenomic analyses reveal significant shifts in the composition of the cutaneous microbiome in psoriasis. *Br J Dermatol* (2019) 181:1254–64. doi: 10.1111/bjd.17989

4. Zeldin J, Chaudhary PP, Spathies J, Yadav M, D'Souza BN, Alishahedani ME, et al. Exposure to isocyanates predicts atopic dermatitis prevalence and disrupts therapeutic pathways in commensal bacteria. *Sci Adv In Press* (2022).

5. Myles IA, Castillo CR, Barbian KD, Kanakabandi K, Virtaneva K, Fitzmeyer E, et al. Therapeutic responses to roseomonas mucosa in atopic dermatitis may involve lipid-mediated TNF-related epithelial repair. *Sci Transl Med* (2020) 12 (560). doi: 10.1126/scitranslmed.aaz8631

6. Myles IA, Earland NJ, Anderson ED, Moore IN, Kieh MD, Williams KW, et al. First-in-human topical microbiome transplantation with roseomonas mucosa for atopic dermatitis. *JCI Insight 3* (2018). doi: 10.1172/jci.insight.120608

7. Chen S, Lin Z, Xi L, Zheng Y, Zhou Q, Chen X. Differential role of TNFR1 and TNFR2 in the development of imiquimod-induced mouse psoriasis. *J Leukoc Biol* (2021) 110:1047–55. doi: 10.1002/JLB.2MA0121-082R

8. Mylonas A, Conrad C. Psoriasis: Classical vs. *Paradoxical Yin-Yang TNF Type I Interferon Front Immunol* (2018) 9:2746. doi: 10.3389/fimmu.2018.02746

9. Cho Y, Lew BL, Seong K, Kim NI. An inverse relationship between ceramide synthesis and clinical severity in patients with psoriasis. *J Korean Med Sci* (2004) 19:859–63. doi: 10.3346/jkms.2004.19.6.859

10. Icen M, Crowson CS, McEvoy MT, Dann FJ, Gabriel SE, Maradit Kremers H. Trends in incidence of adult-onset psoriasis over three decades: A population-based study. *J Am Acad Dermatol* (2009) 60:394–401. doi: 10.1016/j.jaad.2008.10.062

11. Jankovic S, Raznatovic M, Marinkovic J, Jankovic J, Maksimovic N. Risk factors for psoriasis: A case-control study. *J Dermatol* (2009) 36:328–34. doi: 10.1111/j.1346-8138.2009.00648.x

12. Parisi R, Iskandar IYK, Kontopantelis E, Augustin M, Griffiths CEM, Ashcroft DM, et al. National, regional, and worldwide epidemiology of psoriasis: Systematic analysis and modelling study. *BMJ* (2020) 369:m1590. doi: 10.1136/bmj.m1590

13. Singh TP, Zhang HH, Hwang ST, Farber JM. IL-23- and imiquimod-induced models of experimental psoriasis in mice. *Curr Protoc Immunol* (2019) 125:e71. doi: 10.1002/cpim.71

14. Kim S-Y, Bechle M, Hankey S, Sheppard L, Szpiro AA, Marshall JD. Concentrations of criteria pollutants in the contiguous U.S., 1979 – 2015: Role of prediction model parsimony in integrated empirical geographic regression. *PLos One* (2020) 15:e0228535. doi: 10.1371/journal.pone.0228535

15. Bellinato F, Adami G, Vaienti S, Benini C, Gatti D, Idolazzi L, et al. Association between short-term exposure to environmental air pollution and psoriasis flare. *JAMA Dermatol* (2022) 158:375–81. doi: 10.1001/jamadermatol.2021.6019

16. van der Fits L, Mourits S, Voerman JS, Kant M, Boon L, Laman JD, et al. Imiquimod-induced psoriasis-like skin inflammation in mice is mediated *via* the IL-23/IL-17 axis. *J Immunol* (2009) 182:5836–45. doi: 10.4049/jimmunol.0802999

17. Fischer R, Maier O, Naumer M, Krippner-Heidenreich A, Scheurich P, Pfizenmaier K. Ligand-induced internalization of TNF receptor 2 mediated by a di-leucin motif is dispensable for activation of the NFkappaB pathway. *Cell Signal* (2011) 23:161–70. doi: 10.1016/j.cellsig.2010.08.016

18. Lopatnikova JA, Alshevskaya AA, Krugleeva OL, Nepomnyschih VM, Gladkikh VS, Lukinov VL, et al. Expression of TNFalpha receptors on immunocompetent cells is increased in atopic dermatitis. *Int Arch Allergy Immunol* (2017) 174:151–60. doi: 10.1159/000481135

19. Dai YX, Tai YH, Chang YT, Chen TJ, Chen MH. Bidirectional association between psoriasis and atopic dermatitis: A nationwide population-based cohort study. *Dermatology* (2021) 237:521–7. doi: 10.1159/000514581

20. Guttman-Yassky E, Krueger JG. Atopic dermatitis and psoriasis: two different immune diseases or one spectrum? *Curr Opin Immunol* (2017) 48:68–73. doi: 10.1016/j.coi.2017.08.008

21. Zheng Y, Hunt RL, Villaruz AE, Fisher EL, Liu R, Liu Q, et al. Commensal staphylococcus epidermidis contributes to skin barrier homeostasis by generating protective ceramides. *Cell Host Microbe* (2022) 30:301–313 e9. doi: 10.1016/j.chom.2022.01.004

22. Hsu DK, Fung MA, Chen H-L. Role of skin and gut microbiota in the pathogenesis of psoriasis, an inflammatory skin disease. *Med Microecol* (2020) 4:100016. doi: 10.1016/j.medmic.2020.100016

23. Huang CC, Ho CH, Chen YC, Hsu CC, Lin HJ, Wang JJ, et al. Autoimmune connective tissue disease following carbon monoxide poisoning: A nationwide population-based cohort study. *Clin Epidemiol* (2020) 12:1287–98. doi: 10.2147/CLEP.S266396

24. EPA. Global greenhouse gas emissions data, greenhouse gas emissions. (2021).

25. Wang Y, Li C, Ruan Z, Ye R, Yang B, Ho HC. Effects of ambient exposure to nitrogen dioxide on outpatient visits for psoriasis in rapidly urbanizing areas. *Aerosol Air Qual* (2022) 22(8). doi: 10.4209/aaqr.220166

26. Campbell NK, Fitzgerald HK, Dunne A. Regulation of inflammation by the antioxidant haem oxygenase 1. *Nat Rev Immunol* (2021) 21:411–25. doi: 10.1038/s41577-020-00491-x

27. Jais A, Einwallner E, Sharif O, Gossens K, Lu TT, Soyal SM, et al. Heme oxygenase-1 drives metaflammation and insulin resistance in mouse and man. *Cell* (2014) 158:25–40. doi: 10.1016/j.cell.2014.04.043

28. Wojas-Pelc A, Marcinkiewicz J. What is a role of haeme oxygenase-1 in psoriasis? *Curr concepts pathog Int J Exp Pathol* (2007) 88:95–102. doi: 10.1111/j.1365-2613.2006.00505.x

29. Wegiel B, Larsen R, Gallo D, Chin BY, Harris C, Mannam P, et al. Macrophages sense and kill bacteria through carbon monoxide-dependent inflammasome activation. *J Clin Invest* (2014) 124:4926–40. doi: 10.1172/JCI72853

frontiers | Frontiers in Immunology

TYPE Perspective
PUBLISHED 25 January 2023
DOI 10.3389/fimmu.2023.1125635

OPEN ACCESS

EDITED BY
Tej Pratap Singh,
University of Pennsylvania, United States

REVIEWED BY
Ian Antheni Myles,
National Institutes of Health (NIH),
United States

*CORRESPONDENCE
Vijaykumar Patra
vijaykumar.patra@gmail.com

†PRESENT ADDRESS
Vijaykumar Patra,
L'Oréal Research and Innovation,
Aulnay-sous-Bois, France

SPECIALTY SECTION
This article was submitted to
Molecular Innate Immunity,
a section of the journal
Frontiers in Immunology

RECEIVED 16 December 2022
ACCEPTED 09 January 2023
PUBLISHED 25 January 2023

CITATION
Joshi AA, Vocanson M, Nicolas J-F, Wolf P and Patra V (2023) Microbial derived antimicrobial peptides as potential therapeutics in atopic dermatitis.
Front. Immunol. 14:1125635.
doi: 10.3389/fimmu.2023.1125635

Microbial derived antimicrobial peptides as potential therapeutics in atopic dermatitis

Aaroh Anand Joshi [1], Marc Vocanson [2], Jean-Francois Nicolas [2,3], Peter Wolf [1,4] and Vijaykumar Patra [1,2*†]

[1]Department of Dermatology and Venereology, Medical University of Graz, Graz, Austria, [2]Centre International de Recherche en Infectiologie, Institut National de la Santé et de la Recherche Médicale, U1111, Université Claude Bernard Lyon 1, Centre National de la Recherche Scientifique, UMR 5308, Ecole Normale Supérieure de Lyon, Université de Lyon, Lyon, France, [3]Department of Allergology & Clinical Immunology, Lyon-Sud University Hospital, Lyon, France, [4]BioTechMed Graz, Graz, Austria

Atopic dermatitis (AD) is a common chronic inflammatory skin disease that significantly affects the patient's quality of life. A disrupted skin barrier, type 2 cytokine-dominated inflammation, and microbial dysbiosis with increased *Staphylococcus aureus* colonization are critical components of AD pathogenesis. Patients with AD exhibit decreased expression of antimicrobial peptides (AMPs) which is linked to increased colonization by *Staphylococcus aureus*. The skin microbiome itself is a source of several AMPs. These host- and microbiome-derived AMPs define the microbial landscape of the skin based on their differential antimicrobial activity against a range of skin microbes or their quorum sensing inhibitory properties. These are particularly important in preventing and limiting dysbiotic colonization with *Staphylococcus aureus*. In addition, AMPs are critical for immune homeostasis. In this article, we share our perspectives about the implications of microbial derived AMPs in AD patients and their potential effects on overlapping factors involved in AD. We argue and discuss the potential of bacterial AMPs as therapeutics in AD.

KEYWORDS

antimicrobial peptides, atopic dermatitis, autoinducing peptides, bacteriocins, skin microbiome, *Staphylococcus aureus*

Abbreviations: AD, atopic dermatitis; AMP, antimicrobial peptides; *S.aureus*, *Staphylococcus aureus;* CC, clonal complex; MIC, minimum inhibitory concentration; agr, accessory gene regulator; HDP, host defence peptides; PLE, Polymorphous light eruption; SPB, short peptide bacteriocins; RiPPs, Ribosomally synthesized and post translationally modified peptides; NRPs, Peptide bacteriocins synthesized by non-ribosomal synthetases; QS, quorum sensing; AIP, autoinducing peptide; Mrgprb2, mas-related G-protein coupled receptor member B2; MRGPRX2, Mas-related G-protein coupled receptor member X2.

1 Atopic dermatitis and its features

Atopic dermatitis (AD), also called atopic eczema, is one of the most common skin diseases in humans (1). The prevalence of AD ranges from 15% to 25% in children and from 7% to 10% in adults (2). AD shows remarkable heterogeneity in clinical presentation, but in most patients, the disease manifests as a condition with extensive eczematous lesions with red, dry, scaly patches that are intensely itchy. Patients with AD often suffer from sleep deprivation and depression, which significantly affects their quality of life (3, 4). The prevalence of AD varies by geographic location and has nearly doubled to tripled in developed countries in recent decades. One explanation for it is provided by the "biodiversity hypothesis", i.e., that a reduced contact to natural environments in early life does lead to a failure of enrichment in the human microbiome, disturbs immune balance and leads in turn to allergy and inflammatory disorders (5–7).

Although the pathogenesis of AD is complex and not fully understood, three key features are involved in its development. These include (i) disruption of epidermal barrier function, (ii) an excessive immune response mediated by type 2 cells, including Th2, and innate lymphoid cells (ILCs) cells, and (iii) skin microbial dysbiosis with excessive growth of *Staphylococcus aureus* (*S. aureus*). AD patients exhibit altered stratum corneum lipids composition, decreased moisture content, and increased permeability to environmental molecules in both lesional and nonlesional skin (8, 9). Defects in structural barrier proteins (e.g., filaggrin) and the itch-scratch cycle are among the major causes of the observed barrier deficiencies in AD (10, 11). Epidermal barrier disruption leads to excessive secretion of damage-associated molecular patterns (DAMPs) and alarmins such as thymic stromal lymphopoietin (TSLP), IL-1ß, IL-25, and IL-33. Alarmins promote the secretion of cytokines IL-13 and IL-5 by immune cells such as dendritic cells and ILCs, which further promote a type 2 cell-mediated immune response (12). Increased allergen permeation, along with a Th2-cell mediated immune response lead IgE isotype switching (13); a hallmark of chronic recurring AD. Skin microbiome, the third feature involved in the pathogenesis of AD will be discussed in detail in the next sections.

2 Skin microbiome in AD

The skin harbours millions of bacteria, fungi, viruses, archaea, and skin mites that together form the skin microbiome. Bacteria constitute the most abundant kingdom in the skin microbiome with the major genera being *Cutibacterium*, *Corynebacterium*, and *Staphylococcus* (14, 15). The composition and abundance of these genera depend upon the skin site, physiology, and microenvironments (sebaceous, dry, and moist). Skin microbiome is now known to be an imperative component of skin homeostasis maintenance, which includes development of skin's barrier functions (16), immune system, breakdown of natural products and protection against invading pathogens (14, 17).

2.1 Role of *S. aureus* in AD

The implications of microbial shifts correlate with several dermatological diseases most notably, AD (18). The prevalence of *S. aureus* in patients with AD is approximately 20 times higher than the skin of healthy controls. The lesional skin of AD patients shows higher prevalence of *S.aureus* (up to 70%) than nonlesional skin of the same patients (39%) (19). A positive correlation was found between *S. aureus* density on lesional and nonlesional skin and disease severity (20). Moreover, the higher abundance of *S. aureus* in AD patients is independent of age group, ethnicity, and geographic location (21, 22).

S. aureus secretes several metabolites, also known as virulence factors, which are responsible in part for the proinflammatory activity and barrier destruction in AD lesions (Figure 1). The enzyme ceramidase secreted by *S. aureus* lowers lipid and fatty acid levels

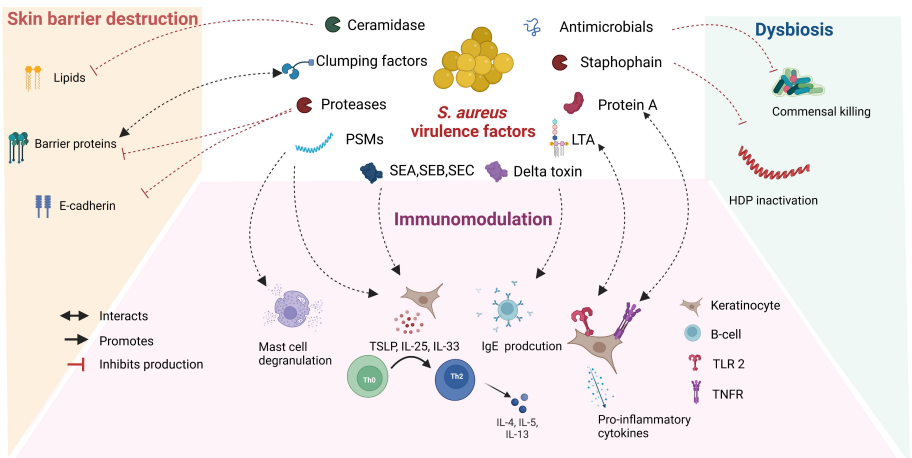

FIGURE 1
Role of *S. aureus* secreted virulence factors in the pathogenesis of atopic dermatitis: *S. aureus* secretes several virulence factors, which interact with overlapping features involved in the pathogenesis of AD. Abbreviations: VF: virulence factors, PSMs: Phenol soluble modulins, SE: staphylococcal enterotoxins, LTA: Lipoteichoic acid, HDP: Host defence peptide, TSLP: Thymic stromal lymphopoietin, TLR: Toll like receptor, TNFR: Tumor necrosis factor receptor.

and makes the skin permeable to allergens (23). Lower fatty acid levels also lead to decreased formation of phospholipid hydrolysis products in sebum and sweat, which increase skin surface pH and further promote *S. aureus* growth. Cell surface proteins of *S. aureus* such as clumping factors A and B and fibronectin-binding proteins support attachment to the uppermost skin, the stratum corneum (24, 25). *S. aureus* is known to secrete several proteases and is also able to induce protease secretion from host (26). Staphophain, inactivates host defence peptides, thus promoting *S. aureus* colonization (27). Proteases also promote the permeation of allergens through the stratum corneum by acting on barrier proteins and tight junctions (28). Alpha toxin secreted by *S. aureus* is cytotoxic to keratinocytes and alters the integrity of E-cadherin, compromising barrier function (29). Staphylococcal enterotoxins (SE) (SEA, SEB, and SEC), phenol-soluble modulins, and lipoproteins target key immune pathways and create a pro-inflammatory environment characteristic of patients with AD (29). The mechanisms of virulence factors secreted by *S. aureus* that play a role in the pathogenesis of AD have been described in detail elsewhere (30–32).

So far, there appears to be no evidence linking the presence of a single virulence factor to AD severity. *S. aureus* strains isolated from AD skin differ from those isolated from healthy individuals (33). Fleury et al. showed that the frequency of isolation of *S. aureus* strains belonging to clonal complex (CC) 1 is higher than that of strains isolated from the nasal cavity of healthy children, which have a higher frequency of isolation of CC30 (24). Byrd et al. performed shotgun metagenome sequence analysis of the skin microbiome at the strain level in patients with AD throughout the disease course. They found that the severity of AD is strain-specific, with isolated strains from severe AD lesions being phylogenetically similar. This suggests that specific combinations of virulence factors expressed by certain strains may be responsible for the pathogenicity of *S. aureus* observed in AD (34).

S. aureus modulates the production of virulence factors necessary for its survival by sensing environmental factors such as cell density. This phenomenon is known as quorum sensing. The accessory gene regulator (agr) quorum sensing system is one of the best studied quorum sensing systems in *S. aureus*. The agr quorum sensing system recognizes cognate autoinducing peptides which are short peptides of 7-12 amino acids containing a cyclic thiolactone at the C- terminus (35). Interestingly, several virulence factors such as superantigens, lipases, and proteases involved in the pathogenesis of AD are also controlled by the agr quorum-sensing system (35, 36). Nakamura et al. demonstrated that agr virulence is essential for the epithelial degradation observed in AD. Moreover, the probability of developing AD is higher when *S. aureus* with a functional agr virulence system is present in childhood (37). These studies suggest that inhibition of agr quorum-sensing in addition to inhibition of *S. aureus* growth may be a promising therapeutic target in AD.

2.2 Role of commensal microbiome in AD

AD skin has lower microbial diversity compared to healthy individuals. This is associated with a lower abundance of the genera *Streptococcus*, *Corynebacterium*, and *Cutibacterium*, as well as members of the commensal *Staphylococci* with anti-*S. aureus* activity (38, 39). These bacterial communities play a critical role in the immune response to pathogens. Ridaura et al. showed that the genus *Corynebacterium* can promote IL-23 signalling and induce IL-17A γδT cells in the dermis, which recruit immune cells (40). At the species level, *Cutibacterium acnes* associated with healthy skin were shown to activate the release of extracellular traps from specialized Th17 subsets (41). Coagulase negative *Staphylococci* (CoNS) such as *Staphylococcus cohnii* activate the host steroid pathway and promote immunosuppression (42), while application of *Staphylococcus epidermidis* to mouse skin showed enhanced innate protection against *Candida albicans* by upregulating Th17 immune mediators such as S100A8 and S100A9 (43). Commensal microbes also play a critical role in epidermal barrier development and surface pH regulation (16, 44). For example, *Roseomonas mucosa* secretes glycerophospholipids which induce host epithelial repair by enhancing the cholinergic activation *via* TNFR2 signalling and *Staphylococcus epidermidis* increases the production of skin ceramides (45, 46), while *Cutibacterium acnes* secretes a lipase that converts triacylglycerols contained in sebum to propionic acid, which contributes to the acidification of the skin surface; a factor that limits the growth of *S. aureus* (47). Notably, commensals directly provide colonization resistance to pathogenic bacteria including *S. aureus* by secreting certain metabolites that inhibit their growth or virulence factor production. The most promising of these metabolites are bacterial-derived AMPs and are discussed in detail in later sections. Additionally, the host-derived AMPs also play a significant role in defining the skin microbiome composition and are discussed briefly as well.

3 Host-derived AMPs/host defence peptides in AD

Host-derived AMPs, also known as host defence peptides (HDPs), are mostly cationic peptides with a molecular weight of less than 10 kDa (48–51) but also include a few classes with larger molecules than 10 kDa (52, 53). These peptides are present on epithelial surfaces such as the oral mucosa, vaginal epithelia, skin etc. HDPs are either constitutively produced by keratinocytes and immune cells or induced in response to stimuli such as pathogen-associated molecular patterns (PAMPs) or inflammatory cytokines. Some important classes of HDPs include RNases, defensins, cathelicidins, dermcidin, and S100 class peptides (51, 54, 55).

HDPs show broad-spectrum but variable antimicrobial activity against different pathogens and members of the commensal microbiome. For example, RNAse7 showed higher inhibitory activity against *E. Coli* and *Cutibacterium acnes* compared to *S. aureus* (56). Interestingly, in the context of the vaginal microbiome, certain commensal bacteria have been shown to use constitutively expressed peptides (S100A7 and Elafin) as amino acid sources to ensure their survival (57). This phenomenon is most likely also found in skin epithelia but has not yet been studied. HDPs are well-known for their immunomodulatory and barrier-improving properties and play a critical role in the pathogenesis of diseases such as psoriasis and polymorphic light eruption underscoring the versatile role of HDPs in skin physiology (58–60).

Atopic skin exhibits lower levels of certain HDPs such as dermcidin, human beta-defensin-2 (hBD-2), human beta-defensin-3 (hBD-3), and cathelicidin, as well as increased expression of RNase7 and S100A7 (61–64). Moreover, a higher abundance of *S. aureus* in atopic skin and during disease flare-ups has also been linked to defective HDP expression (18, 65). Th2 cytokine activity and lower vitamin D levels are thought to be responsible for the altered HDP expression observed in AD (66–68). Interestingly, AD treatments such as UVB phototherapy improve expression of certain HDPs which has led researchers to question whether HDPs could potentially be used as a therapy in AD (69–71). This potential was recently indicated by Peng et.al, who showed that subcutaneous injection of hBD-3 in mice with AD alleviated inflammation through its barrier-improving properties (72). Several detailed reviews on host defence peptides are published during the last five years (58, 71, 73, 74).

4 Bacterial AMPs in AD

Bacterial AMPs are small peptide substances usually restricted to short peptide bacteriocins that inhibit microorganisms by physically disrupting the cell membrane or interact with the intracellular components crucial for bacterial survival (75). Recently, bacteriocins and peptide molecules that inhibit the quorum-sensing activity of competing bacteria have gained increasing attention. The inhibitory effect on the quorum-sensing activity of effector bacteria results in reduced virulence, giving the producer a competitive advantage. These peptides are known as heterologous autoinducing peptides (AIPs) and are considered a class of bacterial AMPs in this review (Figure 2).

4.1 Short peptide bacteriocins and their clinical potential

Bacteriocins are structurally diverse, and there are several classification systems that make them difficult to follow. Many authors restrict the term bacteriocin to ribosomally synthesized peptide antimicrobials with a molecular weight of less than 10 kDa (76, 77). They further divide bacteriocins into class I bacteriocins, which are post-translationally modified, and class II bacteriocins, which are unmodified. These class I bacteriocins are also referred to as ribosomally synthesized and post translationally modified peptides (RiPPs). Recently, however, the term bacteriocin has also been used to refer those AMPs generated by non-ribosomal synthetases (78–80). In the following, we will only discuss about the peptides with a molecular weight of less than 5 kDa, belonging to the group of RiPPs, and those peptides with a molecular weight of less than 5 kDa generated by non-ribosomal synthetases (NRPs). They are collectively known/described as short peptide bacteriocins (SPBs) (Figure 2).

Members of SPBs possess potent narrow spectrum antibacterial activity at nanomolar concentrations, and have lower chances of resistance development (81). The important classes belonging to SPB group, and their structural details are shown in Figure 2. SPBs inhibit bacterial growth by several mechanisms. For example, the lantibitoic nisin binds to the lipid II, which is responsible for peptidoglycan synthesis, thus interfering with cell wall biosynthesis of target

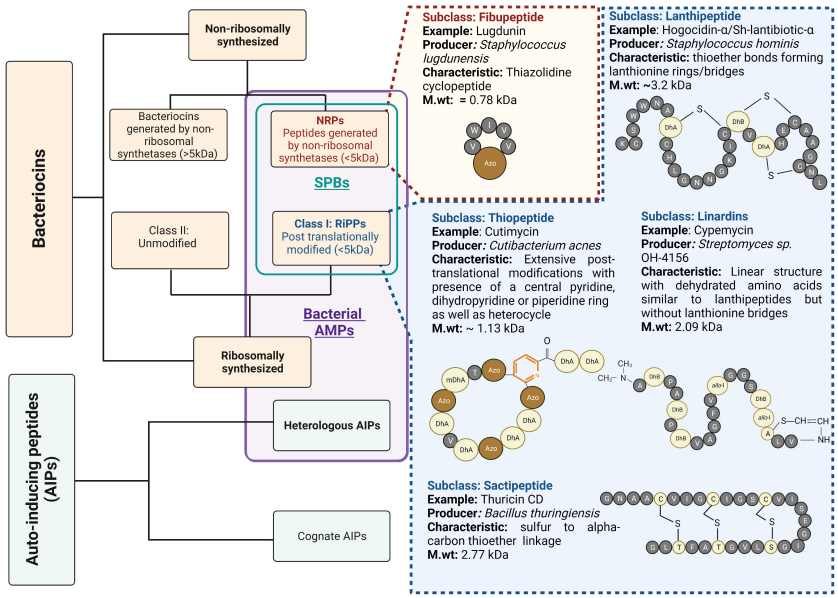

FIGURE 2
Bacterial AMPs and structural variety of short peptide bacteriocins: Bacterial AMPs include Short Peptide Bacteriocins (SPBs) with molecular weight less than 5kDa and Quorum quenching peptides, which are heterologous autoinducing peptides. The subcategory SPBs also includes the class I bacteriocins which undergo post-translational modifications of amino acids, also known as RiPPs, and the peptides synthesized by non-ribosomal synthetases (NRPs) with molecular weight less than 5kDa. SPBs constitute several subclasses based on their structural characteristics. The figure enlists some important classes with examples. Standard amino acids are described as single letter code with grey colour balls. The colour light yellow represents post-translationally modified amino acids. The prefix "Dh" stands for Dehydro and prefix "allo" represents stereo isomer of amino acid. The pyridine ring is coloured in orange. The azole moieties are indicated by abbreviation "Azo" and brown colour balls.

bacteria. In addition, its C-terminal region leads to the formation of pores that result in membrane disruption and efflux of bacterial metabolites necessary for growth (82, 83). Bottoromycins and Thiopeptides such as thiostrepton and micrococcin inhibit bacterial protein synthesis by binding to the 50s ribosomal subunit. Glycocins (e.g., sublancin 168) bind to and inhibit the function of the glucose phosphotransferase system and mechanosensitive channel (MscL) while Sactipeptides e.g., Ruminococcin C inhibits RNA polymerase (84).

The antimicrobial activity of SPBs is mainly directed against closely related bacteria (85). Moreover, not all susceptible members of the microbiome are equally targeted by SPBs; rather, certain species are more sensitive than others. For example, Subtilosin A, a RiPP produced by *Bacillus subtilis*, had a minimum inhibitory concentration (MIC) of 1.25 µg/ml against *Streptococcus pyogens*, but a MIC of 83.25 µg/ml against *Streptococcus gordonii*, a member of the same genus (86). This property makes SPBs an interesting therapeutic candidate for AD, in which dysbiotic colonization with single bacterial species is present.

SPBs are widely used in food and veterinary medicine. Medical applications in humans have experienced low growth due to insufficient investment. Today, however, there is growing interest in the potential of SPBs (76). A suitable example is *Clostridium difficile*-associated diarrhea (CDAD). It is well known that broad-spectrum antibiotic treatment for *Clostridium difficile* intestinal infections provides acute relief to patients but disrupts the gut microbiome with long-term use by depleting commensal bacteria necessary to control *Clostridium difficile* growth. This altered environment contributes to the thriving of *Clostridium difficile* and the secretion of toxins that cause diarrheal disease (87). In this case, the search for narrow spectrum bacteriocins from the commensal microbiome led to the discovery of a SPB of class RiPP- sactibitoic called thuricin CD, which showed potent inhibition of *Clostridium difficile* without affecting the commensal gut microbiome (88). In addition, the semisynthetic thiopeptide LEF571 has been tested in clinical trials for the treatment of CDAD but showed lower narrow spectrum activity compared with thuricin CD (89). Interestingly, NAI003, a derivative of thiopeptide GE2270A, showed selective activity against *Cutibacterium acnes* over the skin commensals. This thiopeptide has already completed a phase 1 clinical trial for the topical treatment of acne and provides evidence of use of SPBs as topical treatments for skin conditions (90). *Lactocillin*, a thiopeptide SPB isolated from a vaginal commensal *lactobacillus* was shown to inhibit several pathogens colonising skin or vagina and showed no antimicrobial activity against other lactobacilli species (91). Despite increasing research into how SPBs work, the exact reason for their selectivity is still not clear (92). However, this can be attributed to a combination of their properties such as amphipathicity, conformation, charge, hydrophilicity, and secondary structure.

4.2 Short peptide bacteriocins in skin microbiome modulation

Metagenomic analyses revealed that biosynthetic gene clusters encoding bacteriocins are ubiquitous in microbes associated with humans (91). O'Sullivan et al. further demonstrated that the human skin microbiome provides colonization resistance to pathogens by secreting a variety of novel bacteriocins (93). Within the skin microbiome, an inter-genera competition exists (Figure 3); for example, *Cutibacterium acnes* secretes a thiopeptide RiPP called cutimycin that inhibits members of *Staphylococcus* but does not affect the members of the genera *Corynebacterium* and *Cutibacterium* (94). However, the mechanism of action remains unknown. Similarly, RiPPs from *lactobacilli* have shown to inhibit members of *Staphylococci*, *Cutibacterium* and *Corynebacterium* (91, 95).

The chances of obtaining bacteriocins with a narrow spectrum of activity are greater if isolated from a phylogenetically similar species or a species that cohabits with the target species. Several staphylococcal-derived bacteriocins exhibit antimicrobial activity against *S. aureus* (96). Known SPBs are epidermin from *Staphylococcus epidermidis* (97), hominicin from *Staphylococcus hominis* (98), lugdunin from *Staphylococcus lugdunensis* (99), BacSp22 from *Staphylococcus Pseudintermedius* (100) and capidermicin *and* nisin J *from* *Staphylococcus capitis* (101, 102). An approach used by Nakatsuji et al. showed that several CoNS isolated from healthy skin inhibited

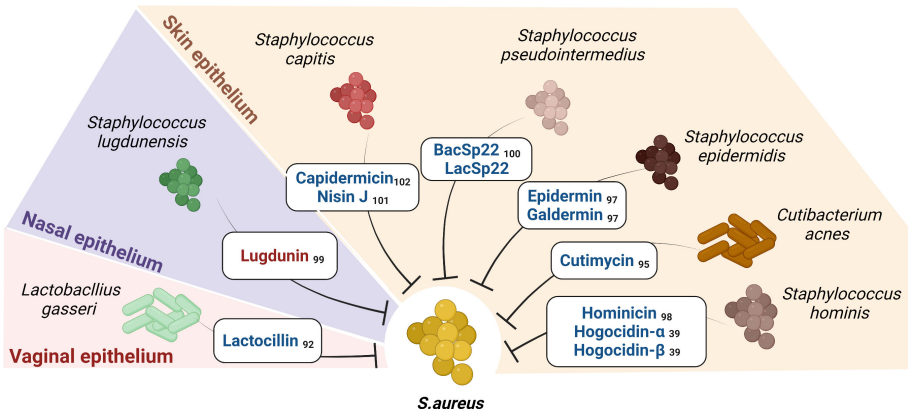

FIGURE 3
Short Peptide Bacteriocins (SPBs) secreted by certain commensals on human epithelia inhibit *S.aureus*: The figure enlists the SPBs isolated from human epithelial residing commensal bacteria known to possess narrow spectrum activity against *S. aureus* and sparing certain commensals (the color red represents NRPs, and color blue represents RiPPs). Subscripts denote references.

S. aureus. In addition, they isolated and identified the *S. hominis* A9-derived RiPPs *Sh*-lantibiotic-alpha (Hogocidin-α) and *Sh*-lantibiotic-beta (Hogocidin-β), which inhibited *S. aureus* but showed no antimicrobial activity against commensal bacteria namely *Staphylococcus epidermidis* and *Staphylococcus hominis* (39).

4.3 Short peptide bacteriocins as immunomodulators

Reports indicate that several SPBs modulate the host immune response (103). In bovine gut epithelium, oral administration of nisin for a short period resulted in an increased accumulation of $CD4^+$ and $CD8^+$ T lymphocytes (LT) and a decrease in B lymphocytes (104). However, it remains to be determined whether Nisin has as direct effect on epithelial or immune cells or an indirect effect mediated by gut microbiome changes. Interestingly, a higher concentration of nisin was shown to activate extracellular trap release (NETs) and increased intracellular superoxide levels in human neutrophils *in-vitro* (105). In contrast, in another study nisin showed high biological compatibility with explant cultures of rabbit vaginal tissue and did not exhibit immunomodulatory effects (106). This suggests that the immunomodulatory activities of SPBs may be dependent on the epithelia or the tissue under consideration. *Lactobacilli* are endogenous inhabitants of healthy skin. Hemert et al. investigated the immunomodulatory effects of *Lactobacillus Plantarum* (*L. plantarum*) by evaluating its ability to stimulate cytokine production in PBMCs. They found that *L. plantarum* strains stimulated the secretion of the anti-inflammatory cytokines IL -10 and IL -12 more than 10-fold. They moreover identified genetic loci responsible for immunomodulatory capabilities involving components of the bacteriocin biosynthesis and transport pathways (107), suggesting an anti-inflammatory effect of bacteriocins. Interestingly, Thiostrepton an SPB belonging to the thiopeptide RiPP class, was able to inhibit psoriasis-like inflammation induced by TLR7, TLR8, and TLR9 (108). Additionally, Lugdunin, an SPB belonging to the NRP class and produced by the nasal commensal *Staphylococcus lugdunensis*, provided multilevel protection against *S. aureus*. In addition to directly inhibiting *S. aureus*, it also enhanced the innate immune response by recruiting neutrophil granulocytes and monocytes in a mouse model of *S. aureus* infection. Similarly, BacSp222, a RiPP produced by a common skin colonizer, *Staphylococcus pseudintermedius*, showed immunomodulatory and cytotoxic properties apart from its antimicrobial activity (101).

4.4 Quorum quenching AMPs against *S. aureus*

As mentioned earlier, the agr quorum-sensing system of *S. aureus* plays a significant role in the secretion of virulence factors observed in AD (Figure 4). The system kicks in when cognate autoinducing peptides bind to a kinase receptor called AgrC. AgrC activates the downstream regulator AgrA, which triggers transcription of the agrBDCA operon and regulatory small RNA called RNAIII by binding to promoter regions P2 and P3. While agrBDCA is responsible for the production of quorum sensing machinery the RNAIII induces transcription of several virulence factors associated to the pathogenesis of AD (35).

The ability of certain bacterial supernatants to modulate the *S. aureus* agr system led to an interest in discovering the metabolites responsible for this phenomenon, which later became known as heterologous AIPs. These heterologous AIPs had similar structures to cognate AIPs (cyclic 7-12 amino acid long with a thiolactone group). This phenomenon is also referred to as quorum quenching and can be used as a therapeutic target in AD (109). Williams et al. identified and isolated an AIP from *S. hominins* with a potent inhibitory effect on the *S. aureus* quorum sensing (110). This AIP successfully inhibited

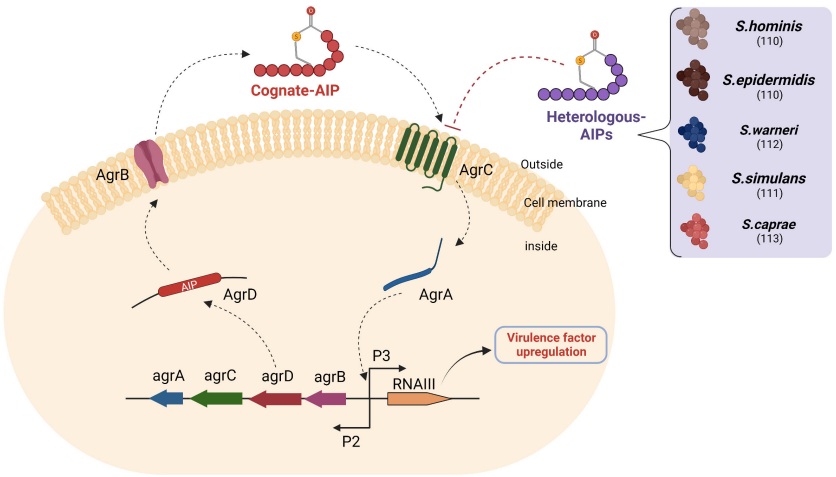

FIGURE 4
Heterologous AIPs inhibit agr quorum sensing of *S. aureus*: AIPs secreted by *S. aureus* (Cognate AIPs) and recognized *via* the AgrC receptor of the same species activate AgrA-mediated transcription of two divergent transcripts under the control of promoters (P), namely P2 and P3. The P2 promoter encodes the quorum-sensing machinery, while the P3 promoter encodes RNAIII. The RNAIII transcript is responsible for the expression of exoprotein virulence factors. AgrD is a precursor of autoinducing peptide, which is processed by AgrB and then exported to the extracellular space. Several heterologous AIPs secreted by CoNS compete with cognate AIP for binding to AgrC and inhibit downstream Agr signalling. The numbers in brackets denote references. Abbreviations: agr- accessory gene regulation, P2: Promoter region 2, P3: Promoter region 3.

S. aureus-mediated epidermal proteolysis and inflammation in mouse skin. Another study showed that synthetic heterologous AIPs identified from *Staphylococcus simulans* isolated from humans and cattle were able to reduce dermonecrotic and epicutaneous skin lesions in mouse models of methicillin-resistant *S. aureus* (MRSA) skin infections by inhibiting all agr quorum sensing signalling subtypes (111). Similarly, several peptide quorum quenchers, including those from *Staphylococcus warneri*, *Staphylococcus capitis*, and *Staphylococcus epidermidis*, have potential as therapeutic agents in AD (110, 112, 113). Interestingly, apicidin, a cyclic fungal tetrapeptide, also inhibited all agr QS systems in methicillin-resistant *S. aureus* (MRSA), suggesting that there is competition within kingdoms that can be exploited in the discovery of new quorum quenching AMPs (114).

The therapeutic potential of quorum quenching molecules is attributed in part to indirect immunomodulatory effects by quorum quenching, i.e., inhibition of Agr-associated virulence factors that interact with immune cells. However, in a recent publication by Pundir et al, many Gram-positive bacterial AIPs were shown to be recognized by the mast cell-specific receptor in humans and mice (Mrgprb2 and MRGPRX2). Among these AIPs, they found that the competence-stimulating peptide secreted by *Streptococcus pneumoniae* (CSP)-1 strongly activated Mrgprb2 and MRGPRX2 and induced effective mast cell degranulation that inhibited bacterial growth and biofilm formation (115).

5 Perspectives and challenges

Despite intensive research, a cure for AD is not yet possible. Currently, there are several treatment options for AD but due to the heterogeneous course of the disease, not all patients respond well, therefore there is an urgent need to develop novel treatment strategies. Topical antibiotics have shown little promise as the sole treatment for AD unless secondary infections are involved (116). In addition, treatment guidelines discourage the use of topical antibiotics (117). This is due to the broad-spectrum activity of marketed antibiotics, which not only inhibit *S. aureus* but also kill commensal bacteria, which, as mentioned earlier, are critical for homeostasis and resistance to *S.aureus* colonization. Recently, ATx201 (Niclosamide), a small molecule, was introduced as a promising AD therapy (118). The therapeutic potential was attributed to ATx201's narrow spectrum activity against *S. aureus* without causing damage to the commensal microbiome (119). Interestingly, inhibition of *S. aureus* growth by live bacteriotherapy in AD has also shown promising results (120, 121). The mediators responsible for this effect were bacterial AMPs of class SPBs with a narrow spectrum of activity. Bacteriotherapy, while promising, also presents some challenges, e.g., we currently lack an understanding of the metabolism and interactions of individual bacteria when exposed to a complex microbial environment, as well as their long-term safety. This is especially true for the changes that result from interactions with mobile genetic elements. Long-term culture of bacteria can lead to spontaneous mutations that result in the loss or gain of undesirable functions. In addition, it is difficult to assess the purity and composition of live bacterial products compared to chemical components.

An alternative strategy is to use well-characterized bacterial metabolites, such as bacterial AMPs, to treat AD. Many SPBs have shown that they can be used in clinical practice (76). To date, however, most of them have been limited to use in animals. Certain patented SPBs, namely lugdunin, Hogocidin-α, and Hogocidin-ß, have already shown narrow-spectrum activity against *S. aureus*, but their therapeutic potential in AD remains uninvestigated. Further research is needed to explore and characterize the vast pool of undiscovered SPBs from the skin microbiome. Inadequate investment and lengthy identification and isolation procedures have severely hindered the development of SPBs as therapeutics. Technological advances in genomics have recently enabled the use of metagenome databases and the identification of novel bacteriocins from biosynthetic gene clusters using genome mining tools (122, 123). Mass spectrometry-assisted peptidomics is another popular technology commonly used to identify novel biomarkers from clinical blood samples for a variety of diseases. Recently, more robust techniques have enabled the application of this approach to a range of biological tissues (124). For example, Azkargorta et al. performed a differential peptidomic analysis of the natural peptide content of the endometrium and demonstrated the presence and activity of antimicrobial peptides *in situ* (125). Whether a similar approach can be used to identify novel bacterial AMPs from skin remains to be investigated but sounds promising.

Several SPBs are active against multidrug-resistant *S. aureus* and are also less likely to develop resistance compared with conventional antibiotics (81). For example, Oyama et al. identified two antimicrobial peptides from the rumen microbiome metagenome data set that are active against multidrug-resistant *S. aureus*. When they examined the likelihood of resistance development after exposure to sub-MIC levels of these peptides, they found that the AMPs did not generate resistant mutants for 20 days. Moreover, the MIC remained within a 1-2-fold increase compared with mupirocin, a marketed topical antibiotic that had a 32-fold MIC increase (126). Nevertheless, there are reports of the development of resistance to the antimicrobial activity of HDPs (127, 128), so the possibility of resistance developing in SPBs cannot be excluded. Therefore, it is important to study the long-term development of resistance of *S. aureus* to SPBs before considering them for therapeutic use. It is known that the addition of SPBs to conventional antibiotics can have a synergistic effect against multidrug-resistant pathogens and also reduces the likelihood of resistance development (129, 130). This raises the likelihood that the use of multiple narrow-spectrum SPBs targeting different mechanisms could have synergistic and favorable microbial killing profiles and reduce the likelihood of resistance development. Some recent studies suggest this phenomenon (131, 132). Alternatively, a combination of bacterial AMPs with HDPs could also show synergistic activities and provide a favorable microbial killing profile, as recently shown by Bitschar et al. (99).

Certain bacterial AMPs have the potential to modulate skin immunity and possess cytotoxic activity (99, 100, 108, 115). On the one hand, this property makes bacterial AMPs of interest to AD, as there is evidence that an inadequate immune response due to a type 2 inflammatory environment and the absence of immune-enhancing cues from the commensal microbiome is a feature of AD (38, 133). On the other hand, it also raises the question of a possible cytotoxic effect of bacterial AMPs on the host. However, it should be kept in mind that bacterial AMPs derived from the human skin microbiome are ubiquitous on the skin and therefore may be better tolerated (91). NAI003, a derivative of a thiopeptide SPB, has completed a phase 1

clinical trial for acne treatment, providing evidence that SPBs can be safely used as topical agents (90). However, it will be extremely important to investigate the chronic effects of such bacterial AMPs at therapeutic concentrations on the skin and their potential to trigger inflammation.

Antimicrobial screening campaigns from the microbiome have so far focused only on the inhibition of pathogens; however, further research should also highlight the ability of bacteriocins to protect commensals. Targeted delivery of antimicrobials and the use of bacteriophages are other promising tools that can be used to kill specific microbes without harming commensals (134, 135).

Another way to render *S. aureus* ineffective is to affect its quorum sensing by bacterial AMPs. Studies targeting quorum sensing of *S. aureus* with synthetic AIPs have shown improved outcomes in AD mouse models and *S. aureus*-associated infections following the reduction of virulence factors. Inhibition of quorum sensing could reduce the production of proteases by *S. aureus* that are responsible for inactivating bacteriocins. This leads us to an interesting question: can a combination of SPBs and a heterologous AIP result in a better therapeutic outcome and a lower risk of resistance development in AD?

It is also important to note that *S. aureus* associated with AD, is non-communicable. This is because the conditions for *S. aureus* colonization and establishment of AD requires (I) altered barrier function (24, 136) or (II) loss of the commensal microbiota necessary to limit *S. aureus* (39), or (III) an inadequate immune response (66, 137) or their combination; all of which are normally intact in healthy individuals.

6 Limitations of targeted control of *S. aureus* and its virulence in AD

Several authors have put forward the idea that skin microbiome manipulation with targeted control of *S. aureus* colonization is a therapeutic aim in AD (30, 32, 38), and recent findings strongly support this idea (39, 110, 118, 121). However, it should be noted that not all patients with AD are colonized with *S. aureus*. This suggests that the disease is caused by multiple factors and their interaction with each other. It appears that certain commensal microbes which tend to act as pathobionts can take over the role of *S. aureus* in its absence. For example, *Staphylococcus epidermidis*, a skin commensal, has been shown to colonize the skin of AD and produce proteases that damage the host and induce expression of AD-associated proinflammatory cytokines in human primary keratinocytes (138, 139). However, further research is required to elucidate the fate and role of pathobionts like *Staphylococcus epidermidis* in AD. In addition, host gene defects, e.g., filaggrin, lower HDP expression owing to type 2 cytokine action (66, 140), and environmental factors may play an exacerbating role in AD. Whether therapies targeting *S. aureus* have any effect when *S. aureus* is not involved in AD remains to be determined but seems unrealistic. In such cases, it is important that the microbial AMPs used also target pathogenic *Staphylococcus epidermidis*, possess additional immunomodulatory activities and/or be supplemented with therapeutics that improve the skin barrier or immune system, or both.

In addition, studies using biologics targeting the immune system in AD patients show decreased *S. aureus* abundance after treatment (137, 141), suggesting the bidirectional nature of the disease and supporting the proposition that *S. aureus* is not the initiator of AD but rather a mediator that exacerbates the disease. This also leads to the question if microbial AMPs alone can lead to therapeutic efficacy equal to baseline level, which remains to be investigated.

7 Conclusion

Selective killing or virulence inhibition of *S. aureus* without damage to the commensal microbiome is an important therapeutic approach in AD. Evidence suggests that certain bacterial AMPs, which include short peptide bacteriocins and heterologous autoinducing peptides isolated from commensal microbiome, have the potential to treat AD by selectively inhibiting *S. aureus* or its virulence and/or by immunomodulation. This warrants the discovery of novel bacterial AMPs from members of the commensal microbiome of skin surface for the treatment of AD.

Data availability statement

The original contributions presented in the study are included in the article/supplementary material. Further inquiries can be directed to the corresponding author.

Author contributions

VP and AJ conceived the ideas. AJ drafted the manuscript and figures. All authors critically revised the manuscript to provide important intellectual content. All authors contributed to the article and approved the submitted version.

Funding

This work was supported by Sanofi Regeneron Type2 innovation grant and funding from City of Graz to VP; FWF (I 4939-B) -ANR (ANR-20-CE91-0002) International joint project to PW, J-FN, MV and VP. PhD student AJ was supported by Medical University of Graz, and PhD program MolMed. The funders had no role in study design, data collection and interpretation, or the decision to submit the work for publication.

Acknowledgments

The authors would like to thank Dr. Thomas Eichmann, from CF mass spectrometry, Medical University of Graz, 8010, Graz, Austria for his feedback on the peptide structures in Figure 2. Figures created using Biorender.com.

Conflict of interest

The authors declare that the research was conducted in the absence of any commercial or financial relationships that could be construed as a potential conflict of interest.

Publisher's note

References

1. Langan SM, Irvine AD, Weidinger S. Atopic dermatitis. *Lancet* (2020) 396 (10247):345–60. doi: 10.1016/s0140-6736(20)31286-1

2. Weidinger S, Beck LA, Bieber T, Kabashima K, Irvine AD. Atopic dermatitis. *Nat Rev Dis Primers* (2018) 4(1):1. doi: 10.1038/s41572-018-0001-z

3. Fishbein AB, Mueller K, Kruse L, Boor P, Sheldon S, Zee P, et al. Sleep disturbance in children with Moderate/Severe atopic dermatitis: A case-control study. *J Am Acad Dermatol* (2018) 78(2):336–41. doi: 10.1016/j.jaad.2017.08.043

4. Chatrath S, Lei D, Yousaf M, Chavda R, Gabriel S, Silverberg JI. Longitudinal course and predictors of depressive symptoms in atopic dermatitis. *J Am Acad Dermatol* (2022) 87(3):582–91. doi: 10.1016/j.jaad.2022.04.061

5. Narla S, Silverberg JI. The role of environmental exposures in atopic dermatitis. *Curr Allergy Asthma Rep* (2020) 20(12):74. doi: 10.1007/s11882-020-00971-z

6. Haahtela T, Holgate S, Pawankar R, Akdis CA, Benjaponpitak S, Caraballo L, et al. The biodiversity hypothesis and allergic disease: World allergy organization position statement. *World Allergy Organ J* (2013) 6(1):3. doi: 10.1186/1939-4551-6-3

7. Haahtela T. A biodiversity hypothesis. *Allergy* (2019) 74(8):1445–56. doi: 10.1111/all.13763

8. Janssens M, van Smeden J, Gooris GS, Bras W, Portale G, Caspers PJ, et al. Increase in short-chain ceramides correlates with an altered lipid organization and decreased barrier function in atopic eczema patients. *J Lipid Res* (2012) 53(12):2755–66. doi: 10.1194/jlr.P030338

9. Celebi Sozener Z, Ozdel Ozturk B, Cerci P, Turk M, Gorgulu Akin B, Akdis M, et al. Epithelial barrier hypothesis: Effect of the external exposome on the microbiome and epithelial barriers in allergic disease. *Allergy* (2022) 77(5):1418–49. doi: 10.1111/all.15240

10. Irvine AD, McLean WH, Leung DY. Filaggrin mutations associated with skin and allergic diseases. *N Engl J Med* (2011) 365(14):1315–27. doi: 10.1056/NEJMra1011040

11. Mack MR, Kim BS. The itch-scratch cycle: A neuroimmune perspective. *Trends Immunol* (2018) 39(12):980–91. doi: 10.1016/j.it.2018.10.001

12. Hammad H, Lambrecht BN. Barrier epithelial cells and the control of type 2 immunity. *Immunity* (2015) 43(1):29–40. doi: 10.1016/j.immuni.2015.07.007

13. Geha RS, Jabara HH, Brodeur SR. The regulation of immunoglobulin e class-switch recombination. *Nat Rev Immunol* (2003) 3(9):721–32. doi: 10.1038/nri1181

14. Byrd AL, Belkaid Y, Segre JA. The human skin microbiome. *Nat Rev Microbiol* (2018) 16(3):143–55. doi: 10.1038/nrmicro.2017.157

15. Grice EA, Segre JA. The skin microbiome. *Nat Rev Microbiol* (2011) 9(4):244–53. doi: 10.1038/nrmicro2537

16. Harris-Tryon TA, Grice EA. Microbiota and maintenance of skin barrier function. *Science* (2022) 376(6596):940–5. doi: 10.1126/science.abo0693

17. Schommer NN, Gallo RL. Structure and function of the human skin microbiome. *Trends Microbiol* (2013) 21(12):660–8. doi: 10.1016/j.tim.2013.10.001

18. Kong HH, Oh J, Deming C, Conlan S, Grice EA, Beatson MA, et al. Temporal shifts in the skin microbiome associated with disease flares and treatment in children with atopic dermatitis. *Genome Res* (2012) 22(5):850–9. doi: 10.1101/gr.131029.111

19. Totté JE, van der Feltz WT, Hennekam M, van Belkum A, van Zuuren EJ, Pasmans SG. Prevalence and odds of staphylococcus aureus carriage in atopic dermatitis: A systematic review and meta-analysis. *Br J Dermatol* (2016) 175(4):687–95. doi: 10.1111/bjd.14566

20. Tauber M, Balica S, Hsu CY, Jean-Decoster C, Lauze C, Redoules D, et al. Staphylococcus aureus density on lesional and nonlesional skin is strongly associated with disease severity in atopic dermatitis. *J Allergy Clin Immunol* (2016) 137(4):1272–4.e3. doi: 10.1016/j.jaci.2015.07.052

21. Katsarou A, Armenaka M. Atopic dermatitis in older patients: Particular points. *J Eur Acad Dermatol Venereol* (2011) 25(1):12–8. doi: 10.1111/j.1468-3083.2010.03737.x

22. Ndhlovu GON, Abotsi RE, Shittu AO, Abdulgader SM, Jamrozy D, Dupont CL, et al. Molecular epidemiology of staphylococcus aureus in African children from rural and urban communities with atopic dermatitis. *BMC Infect Dis* (2021) 21(1):348. doi: 10.1186/s12879-021-06044-4

23. Ohnishi Y, Okino N, Ito M, Imayama S. Ceramidase activity in bacterial skin flora as a possible cause of ceramide deficiency in atopic dermatitis. *Clin Diagn Lab Immunol* (1999) 6(1):101–4. doi: 10.1128/cdli.6.1.101-104.1999

24. Fleury OM, McAleer MA, Feuillie C, Formosa-Dague C, Sansevere E, Bennett DE, et al. Clumping factor b promotes adherence of staphylococcus aureus to corneocytes in atopic dermatitis. *Infect Immun* (2017) 85(6):e00994-16. doi: 10.1128/iai.00994-16

25. Leung DY. New insights into atopic dermatitis: Role of skin barrier and immune dysregulation. *Allergol Int* (2013) 62(2):151–61. doi: 10.2332/allergolint.13-RAI-0564

26. Pietrocola G, Nobile G, Rindi S, Speziale P. Staphylococcus aureus manipulates innate immunity through own and host-expressed proteases. *Front Cell Infect Microbiol* (2017) 7:166. doi: 10.3389/fcimb.2017.00166

27. Sonesson A, Przybyszewska K, Eriksson S, Mörgelin M, Kjellström S, Davies J, et al. Identification of bacterial biofilm and the staphylococcus aureus derived protease, staphopain, on the skin surface of patients with atopic dermatitis. *Sci Rep* (2017) 7 (1):8689. doi: 10.1038/s41598-017-08046-2

28. Nakatsuji T, Chen TH, Two AM, Chun KA, Narala S, Geha RS, et al. Staphylococcus aureus exploits epidermal barrier defects in atopic dermatitis to trigger cytokine expression. *J Invest Dermatol* (2016) 136(11):2192–200. doi: 10.1016/j.jid.2016.05.127

29. Seiti Yamada Yoshikawa F, Feitosa de Lima J, Notomi Sato M, Álefe Leuzzi Ramos Y, Aoki V, Leao Orfali R. Exploring the role of staphylococcus aureus toxins in atopic dermatitis. *Toxins (Basel)* (2019) 11(6):321. doi: 10.3390/toxins11060321

30. Geoghegan JA, Irvine AD, Foster TJ. Staphylococcus aureus and atopic dermatitis: A complex and evolving relationship. *Trends Microbiol* (2018) 26(6):484–97. doi: 10.1016/j.tim.2017.11.008

31. Kim J, Kim BE, Ahn K, Leung DYM. Interactions between atopic dermatitis and staphylococcus aureus infection: Clinical implications. *Allergy Asthma Immunol Res* (2019) 11(5):593–603. doi: 10.4168/aair.2019.11.5.593

32. Koh LF, Ong RY, Common JE. Skin microbiome of atopic dermatitis. *Allergol Int* (2022) 71(1):31–9. doi: 10.1016/j.alit.2021.11.001

33. Simpson EL, Villarreal M, Jepson B, Rafaels N, David G, Hanifin J, et al. Patients with atopic dermatitis colonized with staphylococcus aureus have a distinct phenotype and endotype. *J Invest Dermatol* (2018) 138(10):2224–33. doi: 10.1016/j.jid.2018.03.1517

34. Byrd AL, Deming C, Cassidy SKB, Harrison OJ, Ng W-I, Conlan S, et al. *Staphylococcus aureus* and *Staphylococcus epidermidis* strain diversity underlying pediatric atopic dermatitis. *Sci Trans Med* (2017) 9(397):eaal4651. doi: 10.1126/scitranslmed.aal4651

35. Jenul C, Horswill AR. Regulation of staphylococcus aureus virulence. *Microbiol Spectr* (2019) 7(2). doi: 10.1128/microbiolspec.GPP3-0031-2018

36. Lomholt H, Andersen KE, Kilian M. Staphylococcus aureus clonal dynamics and virulence factors in children with atopic dermatitis. *J Invest Dermatol* (2005) 125(5):977–82. doi: 10.1111/j.0022-202X.2005.23916.x

37. Nakamura Y, Takahashi H, Takaya A, Inoue Y, Katayama Y, Kusuya Y, et al. Staphylococcus agr virulence is critical for epidermal colonization and associates with atopic dermatitis development. *Sci Transl Med* (2020) 12(551). doi: 10.1126/scitranslmed.aay4068

38. Paller AS, Kong HH, Seed P, Naik S, Scharschmidt TC, Gallo RL, et al. The microbiome in patients with atopic dermatitis. *J Allergy Clin Immunol* (2019) 143(1):26–35. doi: 10.1016/j.jaci.2018.11.015

39. Nakatsuji T, Chen TH, Narala S, Chun KA, Two AM, Yun T, et al. Antimicrobials from human skin commensal bacteria protect against staphylococcus aureus and are deficient in atopic dermatitis. *Sci Transl Med* (2017) 9(378). doi: 10.1126/scitranslmed.aah4680

40. Ridaura VK, Bouladoux N, Claesen J, Chen YE, Byrd AL, Constantinides MG, et al. Contextual control of skin immunity and inflammation by corynebacterium. *J Exp Med* (2018) 215(3):785–99. doi: 10.1084/jem.20171079

41. Thiboutot DM, Nelson AM. Keeping the peace: Commensal cutibacterium acnes trains Cd4+ Th17 cells to trap and kill. *J Clin Invest* (2021) 131(2). doi: 10.1172/jci145379

42. Ito Y, Sasaki T, Li Y, Tanoue T, Sugiura Y, Skelly AN, et al. Staphylococcus cohnii is a potentially biotherapeutic skin commensal alleviating skin inflammation. *Cell Rep* (2021) 35(4):109052. doi: 10.1016/j.celrep.2021.109052

43. Agak GW, Mouton A, Teles RM, Weston T, Morselli M, Andrade PR, et al. Extracellular traps released by antimicrobial Th17 cells contribute to host defense. *J Clin Invest* (2021) 131(2). doi: 10.1172/jci141594

44. Uberoi A, Bartow-McKenney C, Zheng Q, Flowers L, Campbell A, Knight SAB, et al. Commensal microbiota regulates skin barrier function and repair *Via* signaling through the aryl hydrocarbon receptor. *Cell Host Microbe* (2021) 29(8):1235–48.e8. doi: 10.1016/j.chom.2021.05.011

45. Zheng Y, Hunt RL, Villaruz AE, Fisher EL, Liu R, Liu Q, et al. Commensal staphylococcus epidermidis contributes to skin barrier homeostasis by generating protective ceramides. *Cell Host Microbe* (2022) 30(3):301–13.e9. doi: 10.1016/j.chom.2022.01.004

46. Myles IA, Castillo CR, Barbian KD, Kanakabandi K, Virtaneva K, Fitzmeyer E, et al. Therapeutic responses to roseomonas mucosa in atopic dermatitis may involve lipid-mediated tnf-related epithelial repair. *Sci Transl Med* (2020) 12(560). doi: 10.1126/scitranslmed.aaz8631

47. Danby SG, Cork MJ. Ph in atopic dermatitis. *Curr Probl Dermatol* (2018) 54:95–107. doi: 10.1159/000489523

48. Hill CP, Yee J, Selsted ME, Eisenberg D. Crystal structure of defensin hnp-3, an amphiphilic dimer: Mechanisms of membrane permeabilization. *Science* (1991) 251 (5000):1481–5. doi: 10.1126/science.2006422

49. Li X, Li Y, Han H, Miller DW, Wang G. Solution structures of human ll-37 fragments and nmr-based identification of a minimal membrane-targeting antimicrobial and anticancer region. *J Am Chem Soc* (2006) 128(17):5776–85. doi: 10.1021/ja0584875

50. Nguyen VS, Tan KW, Ramesh K, Chew FT, Mok YK. Structural basis for the bacterial membrane insertion of dermcidin peptide, dcd-1l. *Sci Rep* (2017) 7(1):13923. doi: 10.1038/s41598-017-13600-z

51. Harder J, Gläser R, Schröder JM. Review: Human antimicrobial proteins — effectors of innate immunity. *J Endotoxin Res* (2007) 13:317 – 38. doi: 10.1177/0968051907088275

52. Singh P, Ali SA. Multifunctional role of S100 protein family in the immune system: An update. *Cells* (2022) 11(15). doi: 10.3390/cells11152274

53. Zasloff M. Antimicrobial rnases of human skin. *J Invest Dermatol* (2009) 129 (9):2091–3. doi: 10.1038/jid.2009.216

54. Yamasaki K, Gallo RL. Antimicrobial peptides in human skin disease. *Eur J Dermatol* (2008) 18(1):11–21. doi: 10.1684/ejd.2008.0304

55. Oppenheim JJ, Biragyn A, Kwak LW, Yang D. Roles of antimicrobial peptides such as defensins in innate and adaptive immunity. *Ann Rheum Dis* (2003) 62 Suppl 2(Suppl 2):ii17–21. doi: 10.1136/ard.62.suppl_2.ii17

56. Harder J, Schroder JM. Rnase 7, a novel innate immune defense antimicrobial protein of healthy human skin. *J Biol Chem* (2002) 277(48):46779–84. doi: 10.1074/jbc.M207587200

57. Lebeau A, Bruyere D, Roncarati P, Peixoto P, Hervouet E, Cobraiville G, et al. Hpv infection alters vaginal microbiome through down-regulating host mucosal innate peptides used by lactobacilli as amino acid sources. *Nat Commun* (2022) 13(1):1076. doi: 10.1038/s41467-022-28724-8

58. Takahashi T, Gallo RL. The critical and multifunctional roles of antimicrobial peptides in dermatology. *Dermatol Clin* (2017) 35(1):39–50. doi: 10.1016/j.det.2016.07.006

59. Patra V, Mayer G, Gruber-Wackernagel A, Horn M, Lembo S, Wolf P. Unique profile of antimicrobial peptide expression in polymorphic light eruption lesions compared to healthy skin, atopic dermatitis, and psoriasis. *Photodermatol Photoimmunol Photomed* (2018) 34(2):137–44. doi: 10.1111/phpp.12355

60. Kiatsurayanon C, Niyonsaba F, Smithrithee R, Akiyama T, Ushio H, Hara M, et al. Host defense (Antimicrobial) peptide, human B-Defensin-3, improves the function of the epithelial tight-junction barrier in human keratinocytes. *J Invest Dermatol* (2014) 134 (8):2163–73. doi: 10.1038/jid.2014.143

61. Hata TR, Kotol P, Boguniewicz M, Taylor P, Paik A, Jackson M, et al. History of eczema herpeticum is associated with the inability to induce human B-defensin (Hbd)-2, hbd-3 and cathelicidin in the skin of patients with atopic dermatitis. *Br J Dermatol* (2010) 163(3):659–61. doi: 10.1111/j.1365-2133.2010.09892.x

62. Mallbris L, Carlén L, Wei T, Heilborn J, Nilsson MF, Granath F, et al. Injury downregulates the expression of the human cathelicidin protein Hcap18/Ll-37 in atopic dermatitis. *Exp Dermatol* (2010) 19(5):442–9. doi: 10.1111/j.1600-0625.2009.00918.x

63. Rieg S, Steffen H, Seeber S, Humeny A, Kalbacher H, Dietz K, et al. Deficiency of dermcidin-derived antimicrobial peptides in sweat of patients with atopic dermatitis correlates with an impaired innate defense of human skin in vivo. *J Immunol* (2005) 174 (12):8003–10. doi: 10.4049/jimmunol.174.12.8003

64. Harder J, Dressel S, Wittersheim M, Cordes J, Meyer-Hoffert U, Mrowietz U, et al. Enhanced expression and secretion of antimicrobial peptides in atopic dermatitis and after superficial skin injury. *J Invest Dermatol* (2010) 130(5):1355–64. doi: 10.1038/jid.2009.432

65. Miller LS, Sørensen OE, Liu PT, Jalian HR, Eshtiaghpour D, Behmanesh BE, et al. Tgf-B regulates tlr expression and function on epidermal keratinocytes. *J Immunol* (2005) 174(10):6137–43. doi: 10.4049/jimmunol.174.10.6137

66. Hönzke S, Wallmeyer L, Ostrowski A, Radbruch M, Mundhenk L, Schäfer-Korting M, et al. Influence of Th2 cytokines on the cornified envelope, tight junction proteins, and ß-defensins in filaggrin-deficient skin equivalents. *J Invest Dermatol* (2016) 136(3):631–9. doi: 10.1016/j.jid.2015.11.007

67. Albenali LH, Danby S, Moustafa M, Brown K, Chittock J, Shackley F, et al. Vitamin d and antimicrobial peptide levels in patients with atopic dermatitis and atopic dermatitis complicated by eczema herpeticum: A pilot study. *J Allergy Clin Immunol* (2016) 138 (6):1715–9.e4. doi: 10.1016/j.jaci.2016.05.039

68. Searing DA, Leung DY. Vitamin d in atopic dermatitis, asthma and allergic diseases. *Immunol Allergy Clin North Am* (2010) 30(3):397–409. doi: 10.1016/j.iac.2010.05.005

69. Vieyra-Garcia PA, Wolf P. A deep dive into uv-based phototherapy: Mechanisms of action and emerging molecular targets in inflammation and cancer. *Pharmacol Ther* (2021) 222:107784. doi: 10.1016/j.pharmthera.2020.107784

70. Suwanchote S, Waitayangkoon P, Chancheewa B, Inthanachai T, Niwetbowornchai N, Edwards SW, et al. Role of antimicrobial peptides in atopic dermatitis. *Int J Dermatol* (2021) 61(5):532–40. doi: 10.1111/ijd.15814

71. Mookherjee N, Anderson MA, Haagsman HP, Davidson DJ. Antimicrobial host defence peptides: Functions and clinical potential. *Nat Rev Drug Discovery* (2020) 19 (5):311–32. doi: 10.1038/s41573-019-0058-8

72. Peng G, Tsukamoto S, Ikutama R, Le Thanh Nguyen H, Umehara Y, Trujillo-Paez JV, et al. Human-B-Defensin-3 attenuates atopic dermatitis-like inflammation through autophagy activation and the aryl hydrocarbon receptor signaling pathway. *J Clin Invest* (2022) 132(17). doi: 10.1172/jci156501

73. Hancock RE, Haney EF, Gill EE. The immunology of host defence peptides: Beyond antimicrobial activity. *Nat Rev Immunol* (2016) 16(5):321–34. doi: 10.1038/nri.2016.29

74. Nguyen HLT, Trujillo-Paez JV, Umehara Y, Yue H, Peng G, Kiatsurayanon C, et al. Role of antimicrobial peptides in skin barrier repair in individuals with atopic dermatitis. *Int J Mol Sci* (2020) 21(20):7607. doi: 10.3390/ijms21207607

75. Cotter PD, Hill C, Ross RP. Bacteriocins: Developing innate immunity for food. *Nat Rev Microbiol* (2005) 3(10):777–88. doi: 10.1038/nrmicro1273

76. Cotter PD, Ross RP, Hill C. Bacteriocins - a viable alternative to antibiotics? *Nat Rev Microbiol* (2013) 11(2):95–105. doi: 10.1038/nrmicro2937

77. Soltani S, Hammami R, Cotter PD, Rebuffat S, Said LB, Gaudreau H, et al. Bacteriocins as a new generation of antimicrobials: Toxicity aspects and regulations. *FEMS Microbiol Rev* (2021) 45(1). doi: 10.1093/femsre/fuaa039

78. Lewis BB, Pamer EG. Microbiota-based therapies for clostridium difficile and antibiotic-resistant enteric infections. *Annu Rev Microbiol* (2017) 71(1):157–78. doi: 10.1146/annurev-micro-090816-093549

79. Wexler AG, Goodman AL. An insider's perspective: Bacteroides as a window into the microbiome. *Nat Microbiol* (2017) 2:17026. doi: 10.1038/nmicrobiol.2017.26

80. Otto M. Staphylococci in the human microbiome: The role of host and interbacterial interactions. *Curr Opin Microbiol* (2020) 53:71–7. doi: 10.1016/j.mib.2020.03.003

81. van Heel AJ, Montalban-Lopez M, Kuipers OP. Evaluating the feasibility of lantibiotics as an alternative therapy against bacterial infections in humans. *Expert Opin Drug Metab Toxicol* (2011) 7(6):675–80. doi: 10.1517/17425255.2011.573478

82. Breukink E, de Kruijff B. The lantibiotic nisin, a special case or not? *Biochim Biophys Acta* (1999) 1462(1-2):223–34. doi: 10.1016/s0005-2736(99)00208-4

83. Chatterjee C, Paul M, Xie L, van der Donk WA. Biosynthesis and mode of action of lantibiotics. *Chem Rev* (2005) 105(2):633–84. doi: 10.1021/cr030105v

84. Acedo JZ, Chiorean S, Vederas JC, van Belkum MJ. The expanding structural variety among bacteriocins from gram-positive bacteria. *FEMS Microbiol Rev* (2018) 42 (6):805–28. doi: 10.1093/femsre/fuy033

85. Hatakka K, Saxelin M. Probiotics in intestinal and non-intestinal infectious diseases–clinical evidence. *Curr Pharm Des* (2008) 14(14):1351–67. doi: 10.2174/138161208784480162

86. Shelburne CE, An FY, Dholpe V, Ramamoorthy A, Lopatin DE, Lantz MS. The spectrum of antimicrobial activity of the bacteriocin subtilosin a. *J Antimicrob Chemother* (2007) 59(2):297–300. doi: 10.1093/jac/dkl495

87. Nelson RL, Kelsey P, Leeman H, Meardon N, Patel H, Paul K, et al. Antibiotic treatment for clostridium difficile-associated diarrhea in adults. *Cochrane Database Syst Rev* (2011) 9):Cd004610. doi: 10.1002/14651858.CD004610.pub4

88. Rea MC, Sit CS, Clayton E, O'Connor PM, Whittal RM, Zheng J, et al. Thuricin cd, a posttranslationally modified bacteriocin with a narrow spectrum of activity against *Clostridium Difficile*. *Proc Natl Acad Sci* (2010) 107(20):9352–7. doi: 10.1073/pnas.0913554107

89. Mullane K, Lee C, Bressler A, Buitrago M, Weiss K, Dabovic K, et al. Multicenter, randomized clinical trial to compare the safety and efficacy of Lff571 and vancomycin for clostridium difficile infections. *Antimicrob Agents Chemother* (2015) 59(3):1435–40. doi: 10.1128/aac.04251-14

90. Fabbretti A, He CG, Gaspari E, Maffioli S, Brandi L, Spurio R, et al. A derivative of the thiopeptide Ge2270a highly selective against propionibacterium acnes. *Antimicrob Agents Chemother* (2015) 59(8):4560–8. doi: 10.1128/aac.05155-14

91. Donia MS, Cimermancic P, Schulze CJ, Wieland Brown LC, Martin J, Mitreva M, et al. A systematic analysis of biosynthetic gene clusters in the human microbiome reveals a common family of antibiotics. *Cell* (2014) 158(6):1402–14. doi: 10.1016/j.cell.2014.08.032

92. Simons A, Alhanout K, Duval RE. Bacteriocins, antimicrobial peptides from bacterial origin: Overview of their biology and their impact against multidrug-resistant bacteria. *Microorganisms* (2020) 8(5):639. doi: 10.3390/microorganisms8050639

93. O'Sullivan JN, Rea MC, O'Connor PM, Hill C, Ross RP. Human skin microbiota is a rich source of bacteriocin-producing staphylococci that kill human pathogens. *FEMS Microbiol Ecol* (2019) 95(2). doi: 10.1093/femsec/fiy241

94. Claesen J, Spagnolo JB, Ramos SF, Kurita KL, Byrd AL, Aksenov AA, et al. A cutibacterium acnes antibiotic modulates human skin microbiota composition in hair follicles. *Sci Transl Med* (2020) 12(570). doi: 10.1126/scitranslmed.aay5445

95. Oh S, Kim S-H, Ko Y, Sim J-H, Kim KS, Lee S-H, et al. Effect of bacteriocin produced by lactococcus sp. hy 449 on skin-inflammatory bacteria. *Food Chem Toxicol* (2006) 44(8):1184–90. doi: 10.1016/j.fct.2005.08.008

96. Newstead LL, Varjonen K, Nuttall T, Paterson GK. Staphylococcal-produced bacteriocins and antimicrobial peptides: Their potential as alternative treatments for staphylococcus aureus infections. *Antibiotics (Basel)* (2020) 9(2):40. doi: 10.3390/antibiotics9020040

97. Panina I, Taldaev A, Efremov R, Chugunov A. Molecular dynamics insight into the lipid ii recognition by type a lantibiotics: Nisin, epidermin, and gallidermin. *Micromachines (Basel)* (2021) 12(10):1169. doi: 10.3390/mi12101169

98. Kim PI, Sohng JK, Sung C, Joo HS, Kim EM, Yamaguchi T, et al. Characterization and structure identification of an antimicrobial peptide, hominicin, produced by

staphylococcus hominis mbbl 2-9. *Biochem Biophys Res Commun* (2010) 399(2):133–8. doi: 10.1016/j.bbrc.2010.07.024

99. Bitschar K, Sauer B, Focken J, Dehmer H, Moos S, Konnerth M, et al. Lugdunin amplifies innate immune responses in the skin in synergy with host- and microbiota-derived factors. *Nat Commun* (2019) 10(1):2730. doi: 10.1038/s41467-019-10646-7

100. Wladyka B, Piejko M, Bzowska M, Pieta P, Krzysik M, Mazurek L, et al. A peptide factor secreted by staphylococcus pseudintermedius exhibits properties of both bacteriocins and virulence factors. *Sci Rep* (2015) 5:14569. doi: 10.1038/srep14569

101. O'Sullivan JN, O'Connor PM, Rea MC, O'Sullivan O, Walsh CJ, Healy B, et al. A novel natural nisin variant, is produced by staphylococcus capitis sourced from the human skin microbiota. *J Bacteriol* (2020) 202(3). doi: 10.1128/jb.00639-19

102. Lynch D, O'Connor PM, Cotter PD, Hill C, Field D, Begley M. Identification and characterisation of capidermicin, a novel bacteriocin produced by staphylococcus capitis. *PloS One* (2019) 14(10):e0223541. doi: 10.1371/journal.pone.0223541

103. Hernández-González JC, Martínez-Tapia A, Lazcano-Hernández G, García-Pérez BE, Castrejón-Jiménez NS. Bacteriocins from lactic acid bacteria. a powerful alternative as antimicrobials, probiotics, and immunomodulators in veterinary medicine. *Anim (Basel)* (2021) 11(4):979. doi: 10.3390/toxins11060321

104. de Pablo MA, Gaforio JJ, Gallego AM, Ortega E, Gálvez AM, Alvarez de Cienfuegos López G. Evaluation of immunomodulatory effects of nisin-containing diets on mice. *FEMS Immunol Med Microbiol* (1999) 24(1):35–42. doi: 10.1111/j.1574-695X.1999.tb01262.x

105. Begde D, Bundale S, Mashitha P, Rudra J, Nashikkar N, Upadhyay A. Immunomodulatory efficacy of nisin–a bacterial lantibiotic peptide. *J Pept Sci* (2011) 17 (6):438–44. doi: 10.1002/psc.1341

106. Aranha CC, Gupta SM, Reddy KV. Assessment of cervicovaginal cytokine levels following exposure to microbicide nisin gel in rabbits. *Cytokine* (2008) 43(1):63–70. doi: 10.1016/j.cyto.2008.04.005

107. van Hemert S, Meijerink M, Molenaar D, Bron PA, de Vos P, Kleerebezem M, et al. Identification of lactobacillus plantarum genes modulating the cytokine response of human peripheral blood mononuclear cells. *BMC Microbiol* (2010) 10:293–. doi: 10.1186/1471-2180-10-293

108. Lai CY, Yeh DW, Lu CH, Liu YL, Huang LR, Kao CY, et al. Identification of thiostrepton as a novel inhibitor for psoriasis-like inflammation induced by Tlr7-9. *J Immunol* (2015) 195(8):3912–21. doi: 10.4049/jimmunol.1500194

109. Grandclément C, Tannières M, Moréra S, Dessaux Y, Faure D. Quorum quenching: Role in nature and applied developments. *FEMS Microbiol Rev* (2016) 40 (1):86–116. doi: 10.1093/femsre/fuv038

110. Williams MR, Costa SK, Zaramela LS, Khalil S, Todd DA, Winter HL, et al. Quorum sensing between bacterial species on the skin protects against epidermal injury in atopic dermatitis. *Sci Transl Med* (2019) 11(490). doi: 10.1126/scitranslmed.aat8329

111. Brown MM, Kwiecinski JM, Cruz LM, Shahbandi A, Todd DA, Cech NB, et al. Novel peptide from commensal staphylococcus simulans blocks methicillin-resistant staphylococcus aureus quorum sensing and protects host skin from damage. *Antimicrob Agents Chemother* (2020) 64(6):e00172-20. doi: 10.1128/AAC.00172-20

112. Severn MM, Cho YK, Manzer HS, Bunch ZL, Shahbandi A, Todd DA, et al. The commensal staphylococcus warneri makes peptide inhibitors of mrsa quorum sensing that protect skin from atopic or necrotic damage. *J Invest Dermatol* (2022) 142(12):3349–52.e5. doi: 10.1016/j.jid.2022.05.1092

113. Paharik AE, Parlet CP, Chung N, Todd DA, Rodriguez EI, Van Dyke MJ, et al. Coagulase-negative staphylococcal strain prevents staphylococcus aureus colonization and skin infection by blocking quorum sensing. *Cell Host Microbe* (2017) 22(6):746–56.e5. doi: 10.1016/j.chom.2017.11.001

114. Parlet CP, Kavanaugh JS, Crosby HA, Raja HA, El-Elimat T, Todd DA, et al. Apicidin attenuates mrsa virulence through quorum-sensing inhibition and enhanced host defense. *Cell Rep* (2019) 27(1):187–98.e6. doi: 10.1016/j.celrep.2019.03.018

115. Pundir P, Liu R, Vasavda C, Serhan N, Limjunyawong N, Yee R, et al. A connective tissue mast-Cell-Specific receptor detects bacterial quorum-sensing molecules and mediates antibacterial immunity. *Cell Host Microbe* (2019) 26(1):114–22.e8. doi: 10.1016/j.chom.2019.06.003

116. Hwang J, Thompson A, Jaros J, Blackcloud P, Hsiao J, Shi VY. Updated understanding of staphylococcus aureus in atopic dermatitis: From virulence factors to commensals and clonal complexes. *Exp Dermatol* (2021) 30(10):1532–45. doi: 10.1111/exd.14435

117. Eichenfield LF, Tom WL, Berger TG, Krol A, Paller AS, Schwarzenberger K, et al. Guidelines of care for the management of atopic dermatitis: Section 2. management and treatment of atopic dermatitis with topical therapies. *J Am Acad Dermatol* (2014) 71 (1):116–32. doi: 10.1016/j.jaad.2014.03.023

118. Weiss A, Delavenne E, Matias C, Lagler H, Simon D, Li P, et al. Topical niclosamide (Atx201) reduces staphylococcus aureus colonization and increases Shannon diversity of the skin microbiome in atopic dermatitis patients in a randomized, double-blind, placebo-controlled phase 2 trial. *Clin Transl Med* (2022) 12 (5):e790. doi: 10.1002/ctm2.790

119. Chu CY. Targeting the cutaneous microbiota in atopic dermatitis: 'A new hope' or 'Attack of the cons'? *Clin Transl Med* (2022) 12(5):e865. doi: 10.1002/ctm2.865

120. Myles IA, Earland NJ, Anderson ED, Moore IN, Kieh MD, Williams KW, et al. First-in-Human topical microbiome transplantation with roseomonas mucosa for atopic dermatitis. *JCI Insight* (2018) 3(9). doi: 10.1172/jci.insight.120608

121. Nakatsuji T, Hata TR, Tong Y, Cheng JY, Shafiq F, Butcher AM, et al. Development of a human skin commensal microbe for bacteriotherapy of atopic dermatitis and use in a phase 1 randomized clinical trial. *Nat Med* (2021) 27(4):700–9. doi: 10.1038/s41591-021-01256-2

122. de Jong A, van Heel AJ, Kok J, Kuipers OP. Bagel2: Mining for bacteriocins in genomic data. *Nucleic Acids Res* (2010) 38(Web Server issue):W647–51. doi: 10.1093/nar/gkq365

123. Behsaz B, Bode E, Gurevich A, Shi Y-N, Grundmann F, Acharya D, et al. Integrating genomics and metabolomics for scalable non-ribosomal peptide discovery. *Nat Commun* (2021) 12(1):3225. doi: 10.1038/s41467-021-23502-4

124. Foreman RE, George AL, Reimann F, Gribble FM, Kay RG. Peptidomics: A review of clinical applications and methodologies. *J Proteome Res* (2021) 20(8):3782–97. doi: 10.1021/acs.jproteome.1c00295

125. Azkargorta M, Bregón-Villahoz M, Escobes I, Ibáñez-Pérez J, Iloro I, Iglesias M, et al. In-depth proteomics and natural peptidomics analyses reveal antibacterial peptides in human endometrial fluid. *J Proteomics* (2020) 216:103652. doi: 10.1016/j.jprot.2020.103652

126. Oyama LB, Olleik H, Teixeira ACN, Guidini MM, Pickup JA, Hui BYP, et al. In silico identification of two peptides with antibacterial activity against multidrug-resistant staphylococcus aureus. *NPJ Biofilms Microbiomes* (2022) 8(1):58. doi: 10.1038/s41522-022-00320-0

127. Cheung GYC, Fisher EL, McCausland JW, Choi J, Collins JWM, Dickey SW, et al. Antimicrobial peptide resistance mechanism contributes to staphylococcus aureus infection. *J Infect Dis* (2018) 217(7):1153–9. doi: 10.1093/infdis/jiy024

128. Kawada-Matsuo M, Le MN, Komatsuzawa H. Antibacterial peptides resistance in staphylococcus aureus: Various mechanisms and the association with pathogenicity. *Genes (Basel)* (2021) 12(10):1527. doi: 10.3390/genes12101527

129. Ovchinnikov KV, Kranjec C, Thorstensen T, Carlsen H, Diep DB. Bacteriocins revitalize non-effective penicillin G to overcome methicillin-resistant staphylococcus pseudintermedius. *Antibiotics (Basel)* (2022) 11(12):1691. doi: 10.3390/antibiotics11121691

130. Wolska KI, Grześ K, Kurek A. Synergy between novel antimicrobials and conventional antibiotics or bacteriocins. *Pol J Microbiol* (2012) 61(2):95–104. doi: 10.33073/pjm-2012-012

131. Soltani S, Biron E, Ben Said L, Subirade M, Fliss I. Bacteriocin-based synergetic consortia: A promising strategy to enhance antimicrobial activity and broaden the spectrum of inhibition. *Microbiol Spectr* (2022) 10(1):e0040621. doi: 10.1128/spectrum.00406-21

132. Mathur H, Field D, Rea MC, Cotter PD, Hill C, Ross RP. Bacteriocin-antimicrobial synergy: A medical and food perspective. *Front Microbiol* (2017) 8:1205. doi: 10.3389/fmicb.2017.01205

133. Kuo IH, Yoshida T, De Benedetto A, Beck LA. The cutaneous innate immune response in patients with atopic dermatitis. *J Allergy Clin Immunol* (2013) 131(2):266–78. doi: 10.1016/j.jaci.2012.12.1563

134. Duan Y, Llorente C, Lang S, Brandl K, Chu H, Jiang L, et al. Bacteriophage targeting of gut bacterium attenuates alcoholic liver disease. *Nature* (2019) 575 (7783):505–11. doi: 10.1038/s41586-019-1742-x

135. Ting SY, Martínez-García E, Huang S, Bertolli SK, Kelly KA, Cutler KJ, et al. Targeted depletion of bacteria from mixed populations by programmable adhesion with antagonistic competitor cells. *Cell Host Microbe* (2020) 28(2):313–21.e6. doi: 10.1016/j.chom.2020.05.006

136. Riethmuller C, McAleer MA, Koppes SA, Abdayem R, Franz J, Haftek M, et al. Filaggrin breakdown products determine corneocyte conformation in patients with atopic dermatitis. *J Allergy Clin Immunol* (2015) 136(6):1573–80.e2. doi: 10.1016/j.jaci.2015.04.042

137. Callewaert C, Nakatsuji T, Knight R, Kosciolek T, Vrbanac A, Kotol P, et al. Il-4rα blockade by dupilumab decreases staphylococcus aureus colonization and increases microbial diversity in atopic dermatitis. *J Invest Dermatol* (2020) 140(1):191–202.e7. doi: 10.1016/j.jid.2019.05.024

138. Cau L, Williams MR, Butcher AM, Nakatsuji T, Kavanaugh JS, Cheng JY, et al. Staphylococcus epidermidis protease ecpa can be a deleterious component of the skin microbiome in atopic dermatitis. *J Allergy Clin Immunol* (2021) 147(3):955–66.e16. doi: 10.1016/j.jaci.2020.06.024

139. Ochlich D, Rademacher F, Drerup KA, Gläser R, Harder J. The influence of the commensal skin bacterium staphylococcus epidermidis on the epidermal barrier and inflammation: Implications for atopic dermatitis. *Exp Dermatol* (2022). doi: 10.1111/exd.14727

140. Ong PY, Ohtake T, Brandt C, Strickland I, Boguniewicz M, Ganz T, et al. Endogenous antimicrobial peptides and skin infections in atopic dermatitis. *N Engl J Med* (2002) 347(15):1151–60. doi: 10.1056/NEJMoa021481

141. Beck LA, Bieber T, Weidinger S, Tauber M, Saeki H, Irvine AD, et al. Tralokinumab treatment improves the skin microbiota by increasing the microbial diversity in adults with moderate-to-Severe atopic dermatitis: Analysis of microbial diversity in ecztra 1, a randomized controlled trial. *J Am Acad Dermatol* (2022). doi: 10.1016/j.jaad.2022.11.047

frontiers | Frontiers in Immunology

TYPE Original Research
PUBLISHED 20 February 2023
DOI 10.3389/fimmu.2023.1038689

OPEN ACCESS

EDITED BY
Francesca Granucci,
University of Milano-Bicocca, Italy

REVIEWED BY
Liliane Martins Dos Santos,
Federal University of Minas Gerais, Brazil
Barbara Cassani,
University of Milan, Italy

*CORRESPONDENCE
Thomas Schwarz
tschwarz@dermatology.uni-kiel.de

SPECIALTY SECTION
This article was submitted to Molecular Innate Immunity, a section of the journal Frontiers in Immunology

RECEIVED 07 September 2022
ACCEPTED 02 February 2023
PUBLISHED 20 February 2023

CITATION
Schwarz A, Philippsen R, Piticchio SG, Hartmann JN, Häsler R, Rose-John S and Schwarz T (2023) Crosstalk between microbiome, regulatory T cells and HCA2 orchestrates the inflammatory response in a murine psoriasis model.
Front. Immunol. 14:1038689.
doi: 10.3389/fimmu.2023.1038689

Crosstalk between microbiome, regulatory T cells and HCA2 orchestrates the inflammatory response in a murine psoriasis model

Agatha Schwarz[1], Rebecca Philippsen[1], Serena G. Piticchio[2,3], Jan N. Hartmann[1], Robert Häsler[1], Stefan Rose-John[4] and Thomas Schwarz[1]*

[1]Department of Dermatology and Allergology, University Kiel, Kiel, Germany, [2]Institute of Clinical Molecular Biology (IKMB), University Kiel, Kiel, Germany, [3]Facultat de Farmàcia, Universitat de Barcelona, Barcelona, Spain, [4]Institute for Biochemistry, University Kiel, Kiel, Germany

The organ-specific microbiome plays a crucial role in tissue homeostasis, among other things by inducing regulatory T cells (Treg). This applies also to the skin and in this setting short chain fatty acids (SCFA) are relevant. It was demonstrated that topical application of SCFA controls the inflammatory response in the psoriasis-like imiquimod (IMQ)-induced murine skin inflammation model. Since SCFA signal *via* HCA2, a G-protein coupled receptor, and HCA2 expression is reduced in human lesional psoriatic skin, we studied the effect of HCA2 in this model. HCA2 knock-out (HCA2-KO) mice reacted to IMQ with stronger inflammation, presumably due to an impaired function of Treg. Surprisingly, injection of Treg from HCA2-KO mice even enhanced the IMQ reaction, suggesting that in the absence of HCA2 Treg switch from a suppressive into a proinflammatory type. HCA2-KO mice differed in the composition of the skin microbiome from wild type mice. Co-housing reversed the exaggerated response to IMQ and prevented the alteration of Treg, implying that the microbiome dictates the outcome of the inflammatory reaction. The switch of Treg into a proinflammatory type in HCA2-KO mice could be a downstream phenomenon. This opens the opportunity to reduce the inflammatory tendency in psoriasis by altering the skin microbiome.

KEYWORDS

G-protein-coupled receptors, imiquimod, interleukins, microbiome, psoriasis, regulatory T cells, short chain fatty acids

1 Introduction

Psoriasis is a chronic inflammatory dermatosis, with an increasing prevalence, ranging at 0.84% of the population in 2017 (1). The pathogenesis is complex involving several pathways (2). Although psoriasis is assigned to the family of autoimmune dermatoses, a definite autoantigen such as for bullous autoimmune dermatoses has not been detected (3). One

pathomechanism involved appears to be a downregulation of regulatory T cells (Treg) which under normal conditions control inflammatory and immune reactions (4–6). The mechanisms responsible for this alteration of Treg are still unclear.

There is increasing evidence that the microbiome exerts profound effects on Treg, first discovered in the gut. The intestinal microbiome is able to activate Treg (7–10). These effects are partially mediated *via* short chain fatty acids (SCFA), microbiota-derived bacterial fermentation products including butyrate, propionate, and acetate (11, 12). Accordingly, certain alterations of the intestinal microbiome are associated with inflammatory bowel diseases (13–15), It is known that the intestinal microbiome can also modulate inflammatory processes of other organs like the airway system, the central nervous system and even the skin (10, 16, 17),.

Meanwhile it is clear that also other organs including the respiratory and urogenital tract and the oral cavity harbor a certain microbiome milieu which contributes to tissue homeostasis. This applies also to the skin. We demonstrated that topical application of the SCFA sodium butyrate (SB) reduced inflammation in the skin, suggesting that resident skin microbes prevent exaggerated inflammatory responses by exerting a downregulatory function and thereby maintain a stable state under physiologic conditions (18).

Furthermore, we observed that SB exerts a mitigating effect in psoriasis (19). This was primarily demonstrated in the imiquimod (IMQ)-induced inflammation model, an established murine model of psoriasis-like skin inflammation (20). Topically applied SB reduced IMQ-induced inflammation. Treg were definitely involved in this process since the mitigating effect was lost upon depletion of Treg. Furthermore, Treg isolated from the blood of psoriatic patients were reduced in their suppressive activity, which was restored by SB. Additionally, SB restored the fewer numbers of Treg in biopsies of psoriatic lesions and normalized the enhanced expression of IL-17 and IL-6 and the reduced expression of IL-10 and of Foxp3 (19).

SCFA signal *via* G-protein-coupled receptors, including GPR109a/HCA2/NIACR1 (21, 22) and GPR43 (23, 24). SB utilizes primarily HCA2 to mediate its effects. HCA2-activation in the gut exerted antiinflammatory effects, finally inducing Treg and IL-10-producing T cells (8). Accordingly, HCA2-knockout (HCA2-KO) mice showed enhanced susceptibility to colitis (21).

Due to the potential beneficial effect of SB in psoriasis, we quantified the expression of HCA2 in psoriatic skin. Lesional and non-lesional psoriatic skin revealed a decreased expression of HCA2 on keratinocytes in comparison to control skin. Topical application of SB was able to increase the low-level expression of HCA2 (25).

To get more insight into the role of HCA2 in psoriasis, we utilized the IMQ-model and HCA2-KO mice. Here, we show that HCA2-KO mice present with a remarkably increased inflammatory response to IMQ. Adoptive transfer experiments revealed that Treg in HCA2-KO mice were not only impaired in their suppressive activity, but even enhanced the inflammatory response. Obviously, Treg in the absence of HCA2 switch from a regulatory into a proinflammatory type. All these changes appear to be dictated by an altered skin microbiome as a consequence of HCA2-deficiency.

2 Material and methods

2.1 Mice

Eight to nine week old female C57BL/6J mice (WT) (Janvier Labs, stock #U03, Le Genest Saint Isle, France) and HCA2-KO ($Gpr109a^{-/-}$) (26) mice were housed in the animal facilities of the University Clinics Schleswig-Holstein. Mice were kept under SPF conditions (individually ventilated cage, IVC, to keep an animal separated from other animals and possible exposures, including exposure by air). Water and food were autoclaved. Expert personnel in compliance with relevant laws and institutional guidelines utilized animal care. Experiments were approved by the Animal Welfare Commission of Ministry of Energy, Agriculture, the Environment, Nature and Digitalization of the Federal State Schleswig-Holstein. Animals were treated with IMQ-cream (Aldara®) and received 62.5 mg on the shaved backs for 7 days. For all experiments, at least 5 mice per group were used. The clinical response was quantified according to a modified psoriasis area and severity index (PASI) score (27). Skin thickness was quantified with a spring-loaded micrometer. Biopsies were paraffin embedded and sections stained with H&E. Acanthosis was semiquantitatively scored as: - <40 µm; + >40 - <60 µm; ++ >60 - <130 µm; +++ >130 µm; the inflammatory infiltrate was semiquantitatively scored as: sparse: <15 cells/10,000 µm²; moderate: >15 - <35 cells/10,000 µm²; dense: >35 cells/10,000 µm².

2.2 Isolation of Treg

Lymph nodes (LN) and spleens were isolated from donor animals and pooled; single cell suspensions were prepared. The proportion of $CD4^+CD25^+$ cells was more or less the same in the spleens and the LN (Supplementary Figure 1). $CD4^+CD25^+$ T cells were collected with a magnet-activated cell sorter (Miltenyi Biotec, Bergisch Gladbach, Germany) by using the MojoSort™ Mouse $CD4^+CD25^+$ Regulatory T Cell Isolation Kit (BioLegend, Fell, Germany, Cat #480137). $CD4^+CD25^+$ T cells were isolated in a two-step separation process. The cells were first incubated with the biotin conjugated antibody cocktail, followed by the streptavidin nanobeads, to isolate total $CD4^+$ T cells. The second step consisted of a positive enrichment of $CD25^+$ cells using allophycocyanin (APC) conjugated anti-mouse-CD25-antibody and anti-APC nanobeads. The purity of $CD4^+CD25^+$ cells was determined by flow analysis using rat anti-mouse-CD4 conjugated with fluorescein isothiocyanate (FITC; BioLegend; Cat #130308, RRID: AB_1279237) and rat anti-mouse-CD25 labeled with APC (Miltenyi Biotec, Cat #130-102-550, RRID: AB_2660261) and was usually more than 95%. As immunoglobulin controls rat IgG2b FITC and rat IgM APC (both from Santa Cruz Biotechnology, Dallas, USA, Cat #sc-2835, RRID: AB_737268; Cat #sc-2896, RRID: AB_737296) were used. In general, we gained up to 3% $Foxp3^+$ cells of all bulk cells obtained from lymph nodes and spleens which is in accordance with the literature (28). In some experiments Treg were stained with 10 µM carboxyfluorescein succinimidylester (CFSE) (Vybrant® CFDA SE Cell Tracer Kit,

Molecular Probes, Oregon; Cat #V12883). After washing Treg were injected intravenously (i.v.) ($1x10^6$) into recipient animals.

2.3 Suppression assay

$1x10^6$ cells/ml $CD4^+CD25^-$ responder T cells obtained from WT mice were seeded into 96-well plates and mixed with $CD4^+CD25^+$ Treg obtained from WT or HCA2-KO mice at the ratios of 1:1, 2:1 and 4:1. Responder T cells were activated using anti-CD3 and anti-CD28-bound Dynabeads (Dynabeads Mouse T-Activator CD3/CD28, Life technologies, Carlsbad, USA). After 4 days, cell proliferation was measured using Cell Counting Kit-8 (Sigma-Aldrich, Taufkirchen, Germany). Data are presented as percentage of suppression.

2.4 IL-6 experiments

HCA2-KO mice were injected intraperitonealy (i.p.) once with a rat monoclonal anti-IL-6-antibody (clone MP5-20F3; 270 µg; Abcam, Cambridge, England; Cat #ab191194). On day 7 after injection, Treg were isolated from untreated or anti-IL-6-treated HCA2-KO mice and injected i.v. into WT mice.

WT mice were injected i.p. daily for 7 days with 1 µg human recombinant IL-6 expressed in *E. coli* and purified to homogeneity as described (29). We used human IL-6, since it acts both on human and murine cells (30). On day 8 Treg were isolated and injected i.v. into WT animals.

The serum from WT and HCA2-KO mice was collected and the amount of IL-6 was measured using the LEGEND MAX Mouse IL-6 ELISA Kit (BioLegend; #Cat 431307) according to the manufacturer's instructions. Serum samples were assayed in triplicates and absorbance read using the TECAN Infinite M Plex (TECAN, Männedorf, Switzerland) microplate reader at 450 nm and 560 nm.

2.5 Flow cytometry

For intracellular cytokine staining, cell suspension was prepared from pooled LN and spleens and stimulated with PMA and Ionomycin in the presence of Brefeldin A (Cell Activation Cocktail with Brefeldin A; BioLegend; Cat #423303) for 3 hours. After stimulation cells were fixed and permeabilized (Tru-Nuclear Transcription Factor, BioLegend, Cat #424401). Cells were stained for APC-conjugated anti-mouse-Foxp3 (eBioscience, San Diego, USA; Cat #17-5773-82, RRID: AB_469457) and phycoerythrin (PE) conjugated anti-mouse-IL-10 (Cat #505007, RRID: AB_315361, -GARP (Cat #142904, RRID: AB_10962944), -CD25 (Cat #102007, RRID: AB_312857) and -IL-6-antibodies (Cat #504503, RRID: AB_315337; (BioLegend). Furthermore, the following antibodies were used: PE-conjugated anti-mouse CTLA-4 (Cat #106305, RRID: AB_313254, Ki-67 (Cat #151209, RRID: AB_2716014), PD-1 (Cat #109103, RRID: AB_313420), CD73 (Cat #127205, RRID: AB_1089065), FR4 (Cat #125007, RRID: AB_1134202), IL-17A (Cat #506903, RRID: AB_315463), IL-23 (Cat #505203, RRID: AB_315367) and Alexa-488 conjugated anti-mouse Helios (Cat #137213, RRID: AB_10645334; all from BioLegend).

FACS analysis of CFSE-negative and positive cells was conducted using APC-conjugated anti-mouse-IL-6- (Cat # 504507, RRID: AB_10694094), -IL-17A- (Cat #506915, RRID: AB_536017), -IL-23- (Cat # 505205, RRID: AB_315369) and -IL-10- antibodies (Cat # 505009, RRID: AB_315363; all from BioLegend).

Flow analysis after co-housing experiments was performed using rat anti mouse CD4-APC (Miltenyi Biotec, Cat #130-102-597, RRID: AB_2659906) and rat anti mouse Foxp3-PE (eBioscience, Cat #12-5773-80, RRID: AB_465935). As isotype controls the following immunoglobulins: rat IgG2a-APC (Cat #sc-2894, RRID: AB_737246) as control for Foxp3-APC; rat IgG2b-APC (Cat #sc-2895, RRID: AB_737266) as control for IL-10-APC and CD4-APC (both from Santa Cruz); rat IgG2a-PE (Becton Dickinson; Cat #553930, RRID: AB_479719) as control for GARP-PE and Foxp3-PE; rat IgG2b-PE (Cat #556925, RRID: AB_479625) as control for IL-10-PE; rat IgG1-APC (Cat #400411, RRID: AB_326517) as control for IL-6-, IL-17-, IL-23-APC; rat IgG1-PE (Cat #400407, RRID: AB_326513) as control for IL-6-, CD25-, IL-17- and IL-23-PE (both from BioLegend); rat IgG2b-PE (Cat # 556925, RRID: AB_479625) as control for PD-1 and Ki-67-PE (Becton Dickinson); armenian hamster IgG1-PE (Becton Dickinson; Cat #553972, RRID: AB_395172) and Alexa-488 conjugated (BioLegend; Cat #400923; RRID: AB_2814703) as control for CTLA-4-PE, and Helios-A488; rat IgG1-PE (Miltenyi Biotec, Cat # 130-123-746, RRID: AB_2857627) as control for CD73- and FR4-PE. Analysis was performed with a CytoFlex (Beckman Coulter).

2.6 16S rRNA sequencing

Animals were wiped off with wet swabs in both directions (head to tail and tail to head). To generate representative bacteria based on relative abundancies, 16S sequencing was performed as previously described (31). DNA was extracted using the QIAamp UCP Pathogen Mini Kit automated on the QIAcube (Qiagen, Hilden, Germany) following the manufacturer's guidelines.

16S rRNA gene libraries were generated by PCR from purified genomic DNA with primers 27F and 338R, targeting the hypervariable regions V1 and V2 of the 16S rRNA. Amplification and sequencing were performed using a dual-indexing approach (8-nt on forward- and reverse primer) as described by Kozich et al. (32) on the Illumina MiSeq platform (Illumina Inc., San Diego, USA) generating 2x300 bp reads. Demultiplexing after sequencing was based on no mismatches in the indices.

Data processing was performed using the DADA2 version 1.10 workflow for big data sets (33) resulting in abundance tables of amplicon sequence variants (ASVs) according to a workflow adjusted for V1-V2 region, which can be found here: https://github.com/mruehlemann/ikmb_amplicon_processing/blob/master/dada2_16S_workflow_with_AR.R. Resulting ASVs underwent taxonomic annotation using the Bayesian classifier provided in DADA2 and using the Ribosomal Database Project (RDP) version 16 release. One sample with less than 10,000 sequences was not considered for further analysis. ASVs classified as "Chloroplast" were removed. Alpha diversity was estimated with Shannon index and Beta diversity was estimated from Bray-Curtis dissimilarity (*phyloseq* R package). Differential abundance analysis was performed with the linear model

function LinDA (34) in the *MicrobiomeStat* package, which can be found at https://CRAN.R-project.org/package=MicrobiomeStat.

2.7 Statistical analysis

In all experiments except FACS analysis and 16S rRNA sequencing results were analyzed by using the Student t test. For FACS analysis t test with Welch's correction was performed. For multiple comparisons we carried out one-way ANOVA in order to assess whether at least two groups significantly differ. Differences between groups were determined with unpaired two-samples Wilcoxon test for alpha diversity, and PERMANOVA (*adonis2* function of *vegan* R package) for beta diversity. Linear models included confounders (housing, genotype) where applicable. For all analysis p-values <0.05 were considered significant.

3 Results

3.1 HCA2-deficiency enhances the susceptibility to psoriasis-like skin inflammation

To study the role of HCA2 in psoriasis and its impact on Treg, we utilized the IMQ-induced inflammation model and mice which are deficient in the expression of HCA2. C57BL/6J wild type (WT) and HCA2-KO mice received IMQ-cream on the shaved backs daily for 7 days. As described previously (19), IMQ-treated mice developed thickening of the skin, erythema and scales. In HCA2-KO animals the inflammatory response was remarkably stronger (Figure 1A). The clinical response was quantified for this and all following experiments according to a modified PASI score (27). The data of all experiments are summarized in Supplementary Figure 2. Accordingly, measurement of skin thickness revealed swollen skin upon administration of IMQ which was maximally pronounced in IMQ-treated HCA2-KO mice (Figure 1C).

Biopsies were taken and sections stained with H&E. IMQ-treatment induced acanthosis, hyperkeratosis and an inflammatory infiltrate. These changes were stronger pronounced in HCA2-KO mice in comparison to WT animals (Figures 1B, D). Since IMQ, though only topically applied, induces also systemic alterations (20), mice were sacrificed 7 days after initiation of IMQ treatment and spleens were obtained. Spleens of IMQ-treated animals were enlarged and heavier (19). Splenomegaly was stronger pronounced in HCA2-KO mice upon application of IMQ (data not shown).

3.2 HCA2 signaling regulates the suppressive activity and the phenotype of Treg

We previously observed that IMQ-induced inflammation is associated with a decrease/suppression of Treg (19). To analyze whether the enhanced susceptibility of HCA-KO mice to IMQ is due to an impairment of Treg, adoptive transfer experiments were performed. Spleens and LN were isolated from HCA2-KO or WT mice and pooled. Cell suspensions from pooled organs were subjected to FACS analysis. HCA2-KO mice harbored reduced percentage of $CD4^+CD25^+Foxp3^+$ cells (Figure 2A) and also the expression of CD25 on $Foxp3^+$ cells was impaired (Figure 2B). $Foxp3^+$ cells from HCA-KO mice expressed lower levels of IL-10 and glycoprotein A

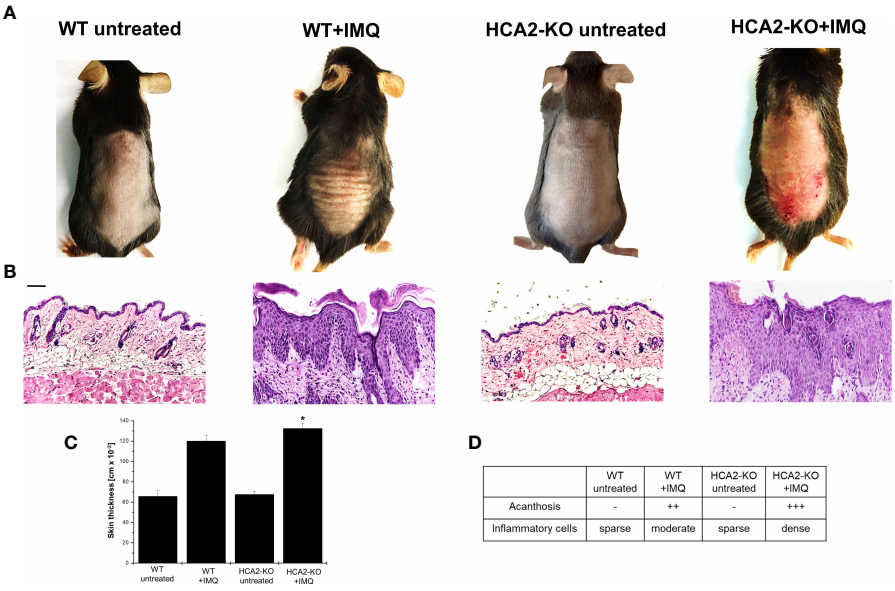

	WT untreated	WT +IMQ	HCA2-KO untreated	HCA2-KO +IMQ
Acanthosis	-	++	-	+++
Inflammatory cells	sparse	moderate	sparse	dense

FIGURE 1
HCA2 deficiency enhances the susceptibility to psoriasis-like skin inflammation. **(A)** WT and HCA2-KO mice were treated topically with 5% IMQ cream on the shaved backs for 7 (d) **(B)** Biopsies were taken, paraffin embedded sections were stained with H&E and analyzed histopathologically. Each group contained 7 animals. Scale bar = 100 µm **(C)** Skin thickness was measured using a spring-loaded micrometer. Student t test and one-way ANOVA was performed. *P < 0.02 WT+IMQ vs HCA2-KO+IMQ; P_{ANOVA} = 1.9 x10^{-10} **(D)** Acanthosis and density of inflammatory infiltrate were scored. Data are presented from one of three independent experiments (n=3).

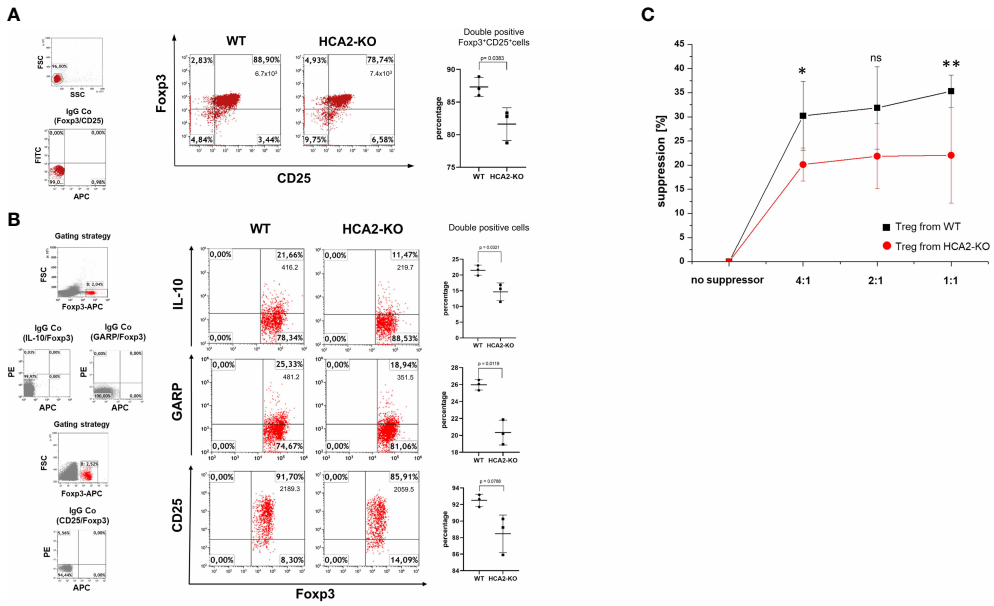

FIGURE 2
HCA2 signaling regulates the suppressive activity *in vitro* and the phenotype of Treg. **(A)** $CD4^+CD25^+$ (Treg) cells were isolated from pooled spleens and lymph nodes (LN) of 7 mice and subjected to FACS analysis. The cell population from both strains was analyzed for double positive CD25/Foxp3 cells and is demonstrated as percentage and total number of double positive cells. As negative control served isotype (IgG Co). FACS analysis is also shown as a scatter graph with mean ± SD. Y axes show percentage of double positive cells. Data were analyzed by using the t test with Welch´s correction. n = 3 **(B)** Pooled LN cells and splenocytes of 4 mice, obtained from both strains were analyzed for double positive Foxp3/IL-10, Foxp3/GARP and Foxp3/CD25 cells and is demonstrated as percentage and total number of double positive cells. FACS analysis is also shown as a scatter graph with mean ± SD. Y axes show percentage of double positive cells. Data were analyzed by using the t test with Welch´s correction. n = 3 Data are presented from one of three independent experiments. **(C)** Pooled LN and spleen cells obtained from WT and HCA2-KO mice (4 for each group) were separated into $CD4^+CD25^-$ (responder cells) and $CD4^+CD25^+$ cells (Treg). Treg and responder cells were mixed at the ratios 1:1, 1:2 and 1:4. Responder cells were activated and after 4 days, cell proliferation was measured using Cell Counting Kit-8. Data are presented as percent suppression from one of three independent experiments. Student t test and one-way ANOVA was performed. *P < 0.03 WT vs HCA2-KO 4:1; P = 0.11504 WT vs HCA2-KO 2:1; ns, not significant; **P < 0.04 WT vs HCA2-KO 1:1; P_{ANOVA} = 0.016; n = 4.

repetitions predominant (GARP), which is specifically expressed on activated Treg (35) (Figure 2B).

To better define Treg obtained from HCA2-KO mice, more markers which are associated with the suppressive activity of Treg were analyzed. $Foxp3^+Helios^+$Treg exert more suppressive characteristics compared to $Foxp3^+Helios^-$ Treg (36). Ki-67 is an activating marker for Treg (37). The ecto-5'-nucleosidase (CD73) contributes to the inhibitory function of Treg by generating adenosine (38). The folate receptor 4 (FR4) is required for the activity of Treg (39). The expression of CTLA-4, CD73, FR4, Helios, Ki-67 was reduced on $Foxp3^+$ cells obtained from HCA2-KO mice in comparison to WT cells (Supplementary Figure 3). Furthermore, the expression of PD-1 which inhibits activation and suppressive capacity of Treg (40, 41) was upregulated in $Foxp3^+$ cells from HCA2-KO mice (Supplementary Figure 3).

To analyze whether this phenotypic alteration is also associated with a functional impact, the suppressive activity of Treg obtained from WT and HCA2-KO mice was evaluated in a suppression assay. $CD4^+CD25^-$ responder cells were coincubated at different ratios with Treg obtained either from WT or HCA2-KO mice and proliferation was measured. The proliferation of $CD4^+CD25^-$ responder cells was reduced upon coincubation with Treg obtained from WT mice. This effect was reduced upon coincubation with Treg obtained from HCA2-KO mice (Figure 2C).

To examine whether the altered phenotype of HCA2-KO Treg also influences their suppressive potency *in vivo*, $CD4^+CD25^+$ cells were isolated from pooled spleens and LN of WT and HCA2-KO mice, respectively. The purity was in the range at least of 95%. Cells were injected i.v. into WT animals which subsequently were treated with IMQ. Injection of Treg obtained from WT mice mitigated IMQ-induced inflammation in WT recipients (Figure 3A). Down-modulation of inflammation by Treg was confirmed histopathologically (Figures 3B, D). Surprisingly, the inflammatory response to IMQ in mice which received Treg from HCA-KO mice was not at all reduced but even remarkably enhanced (Figure 3A). Skin thickness analysis confirmed this observation (Figure 3C). This suggests that HCA2-deficient Treg are not only impaired in their suppressive activity but even enhance inflammation. This phenomenon may contribute to the enhancement of the "psoriatic" response in the absence of HCA2.

3.3 HCA2-deficiency causes defects of Treg at the site of inflammation

Under normal conditions, Treg suppress inflammation, but several publications demonstrated a dysfunction of Treg, particularly in autoimmune diseases (42). To study whether this might also apply for IMQ-induced psoriasis-like inflammation, we stained Treg obtained from WT and HCA2-KO mice with CFSE. Fluorescent Treg were injected i.v. into IMQ-treated WT animals. After 48 hours LN and spleens were obtained from the recipients and FACS analysis of CFSE-negative cells was conducted. This strategy allows to detect the inflammatory status of host cells after injection of Treg. IMQ upregulated the proinflammatory cytokines IL-6, IL-17, and IL-23 in

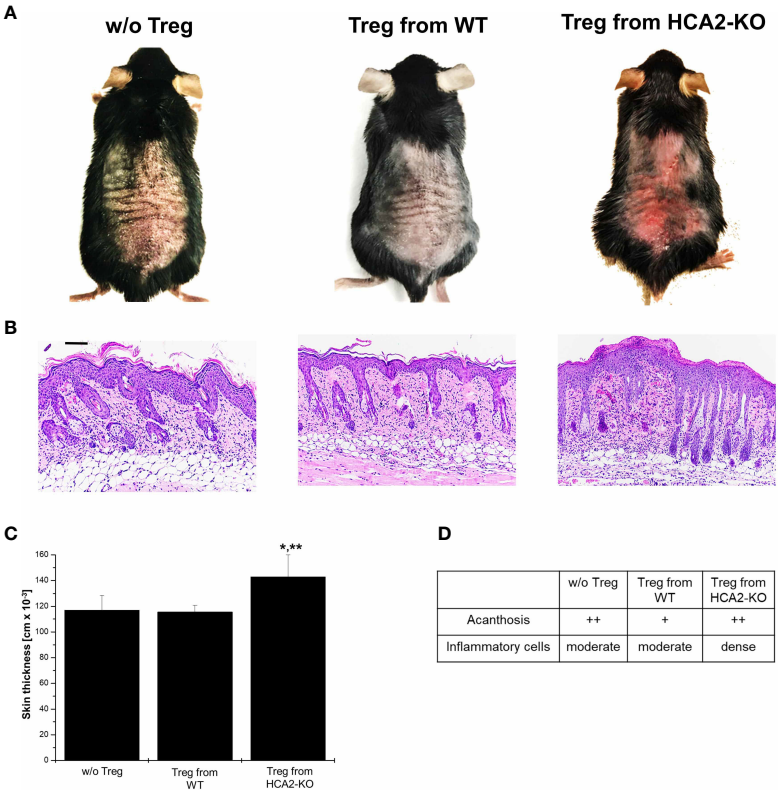

FIGURE 3
HCA2 signaling regulates the suppressive activity *in vivo* **(A)** Treg were isolated from pooled spleens and LN of WT or HCA2-KO mice and injected i.v. into IMQ-treated WT animals. **(B)** Biopsies obtained from IMQ-treated animals were taken. The paraffin embedded sections were stained with H&E and analyzed histopathologically. Each group contained 7 animals. Scale bar = 100 µm **(C)** The skin thickness was measured using a spring-loaded micrometer. Student t test and one-way ANOVA was performed. *P < 0.02 Treg from WT vs Treg from HCA2-KO, **P < 0.02 Treg from HCA2-KO vs w/o Treg; P_{ANOVA} = 0.00872. **(D)** Acanthosis and density of inflammatory infiltrate were scored. Data are presented from one of three independent experiments.

comparison to untreated WT mice (Supplementary Figure 4). The expression of these cytokines was reduced in host cells (CFSE-negative) upon injection of WT-Treg. In contrast, such an effect was not observed upon injection of Treg from HCA2-KO mice. In this case, the expression of the proinflammatory cytokines was even enhanced in the host cells. In turn, the expression of the "suppressive" cytokine IL-10 was induced upon injection of Treg from WT mice in the host cells, but impaired upon injection of Treg from HCA2-KO mice (Figure 4; overlay of red histograms). Statistical analysis was performed after having pooled the data from 3 experiments (Figure 4B).

To gain insight into the production of cytokines by the adoptively transferred cells (CFSE-positive), flow analysis was performed by gating on $CFSE^+$ cells. FACS analysis revealed that injected Treg obtained from HCA2-KO animals expressed enhanced levels of IL-6, IL-17, and IL-23 in comparison to the expression of these cytokines in WT-Treg (Figure 4A; overlay of green histograms). IL-10 was only slightly downregulated in injected Treg from HCA2-KO mice compared to WT Treg. However, those differences were statistically not significant. Statistical analysis was performed after having pooled the data from 3 experiments (Figure 4B). A limitation of this experiment is the low cell number recovered from the recipients. However, this was the maximum yield achieved when injecting $1x10^6$ cells per mouse. Nevertheless, the alteration of the cytokine expression pattern in the recipients upon injection of Treg from different donors appears to correspond to the clinical phenotype (Figure 3A).

3.4 IL-6 is involved in the alteration of Treg in the absence of HCA2

Since IL-6 participates in the pathogenesis of inflammatory and autoimmune diseases by downregulating Treg (43, 44), we studied whether IL-6 plays a role in the alteration of Treg in the absence of HCA2. FACS analysis of Treg revealed higher expression of IL-6 in HCA2-KO than in WT cells (Figure 5A). Epicutaneous application of IMQ induced the expression of IL-6 in Treg in both groups but to a much higher extent in HCA2-KO mice (Figure 5B). To address whether IL-6 is relevant for the functional alteration of Treg, HCA2-KO donors were injected i.p. with a neutralizing monoclonal anti-IL-6-antibody or left untreated. Treg were isolated from both groups and injected i.v. into IMQ-treated WT mice. The inflammatory response was significantly mitigated in the recipients of Treg obtained from anti-IL-6-treated HCA2-KO mice compared to recipients of Treg from untreated HCA2-KO donors (Figure 5C). Histopathological analysis revealed reduced inflammatory and epidermal effects in the skin of recipients of cells from anti-IL-6-treated HCA2-KO donors. We have not yet analyzed the phenotypic alteration of Treg obtained from HCA2-KO mice upon anti-IL-6 treatment. Preliminary data indicate that in the recipients of cells of anti-IL-6-treated donors Treg express enhanced levels of IL-10 and GARP which may contribute to the mitigation of the IMQ-induced inflammatory response (Supplementary Figure 5). In turn, WT Treg

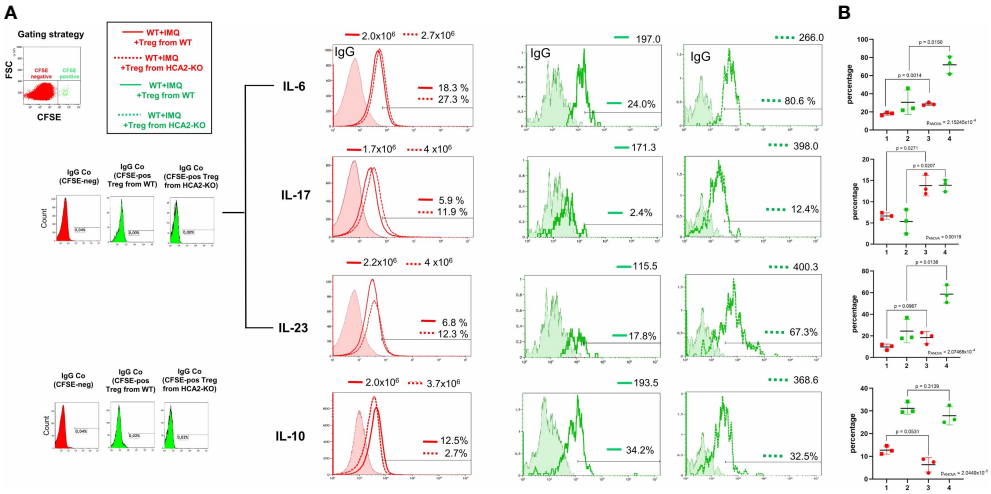

FIGURE 4
HCA2 deficiency causes defects of Treg at the site of inflammation. **(A)** Treg obtained from 7 HCA2-KO and 7 WT mice were stained with CFSE and injected i.v. into IMQ-treated WT animals. After 48 h LN and spleens were obtained from the recipient mice and FACS analysis of CFSE-negative (overlay of red histograms) or CFSE-positive cells (overlay of green histograms) was conducted. The expression of IL-6, IL-17, IL-23 and IL-10 was standardized on isotype controls. For green histograms (Treg from WT and HCA2-KO) two isotype controls were used. For IL-6, IL-17 and IL-23 the same IgG (rat IgG1) control was used. Histograms show fluorescence intensity (x axis) versus cell count (y-axis). The number of cells is displayed in the histograms. **(B)** FACS analysis is also shown as scatter graph with mean ± SD. Y axes show percentage of positive cells. Data were analyzed by using the t test with Welch´s correction. For multiple comparisons we carried out one-way ANOVA in order to assess whether at least two groups significantly differ. 1 WT +IMQ + Treg from WT (red); 2 WT +IMQ + Treg from WT (green); 3 WT +IMQ + Treg from HCA2-KO (red); 4 WT +IMQ + Treg from HCA2-KO (green) n=3.

lost their suppressive activity upon injection of IL-6 into the donors. In this case the inflammatory IMQ-response was not at all reduced in the recipients upon adoptive transfer of Treg (Figure 5D). In addition, IL-6 serum levels were increased upon IMQ administration, this increase was much more pronounced in HCA2-KO than WT mice (Figure 5E).

3.5 Skin dysbiosis in the absence of HCA2 may predispose mice to psoriasis-like inflammation

The skin and mucosal surfaces are colonized by large numbers of microorganisms commonly referred to as the microbiota. A complex interplay between the host immune system and the microbiota is necessary to maintain homeostasis in the gut and the skin (45, 46). Accordingly, interruptions of the relationship between the host and the microbiota can cause autoimmune reactions (47). Since there is a crosstalk between HCAs and the microbiota which involves also SCFA, we studied whether HCA2-KO mice differed in their skin microbiota from WT mice. Skin swab sampling of the back skin was performed. The microbiome of HCA2-KO mice housed under regular conditions in our animal facility was characterized by 16S rRNA sequencing and compared to that of WT mice. We hypothesized that the impaired activity of Treg and the thereby caused enhanced susceptibility to psoriasis-like inflammation upon IMQ-treatment could be explained by the transmission of a disease-predisposing bacterial community. Therefore, we performed co-housing experiments with WT and HCA2-KO mice. WT mice were co-housed with HCA2-KO mice for 1 month. For control purposes strains were housed in a single setting.

The skin microbiome of mice, as a key immunomodulatory player, was analyzed based on swab samples, assessing composition and diversity employing 16S rRNA sequencing methods. A decrease in alpha diversity (Shannon index, quantifying within sample variation) was observed upon co-housing the animals. This effect was more pronounced in WT mice (P = 0.038), while in HCA2-KO mice the observed trend was not significant (Figure 6A). Similarly, assessing the beta diversity (Bray-Curtis dissimilarity, quantifying between sample variation) documented that WT animals and HCA2-KO mice represent to separate groups based on their microbiome when single-housed (P = 0.001), while their differences were reduced when co-housed (Figure 6B). Analysis of the relative abundance of the phyla revealed a higher proportion of *Bacteroidetes* and *Verrucomicrobia* in WT animals than in HCA2-KO mice when single-housed.

In contrast to that, single-housed HCA2-KO mice showed higher proportions of *Proteobacteria*, *Actinobacteria* and *Tenericutes* than WT animals (Figure 6C). In co-housed conditions, these differences were diminished. A detailed differential abundance analysis based on linear models uncovered *Verrucomicrobia* as the only significantly regulated phylum, showing a higher abundance when comparing WT animals versus HCA2-KO mice (p-value (P) = 0.003, Log2FoldChange (LFC) = 4.8) as well as when comparing co-housed vs. single housed scenarios (P = 0.013, LFC = 3.5; Figure 6D). As part of this, *Verrucomicrobia* could not be detected in any of the single housed HCA2-KO mice. Further characterization of differentially abundant genera revealed significantly reduced *Ruminococcus* (P = 0.024, LFC −1,6) and *Faecalibacterium* (P = 0.027, LFC -2.1) genus abundances in WT compared to HCA2-KO mice, whereas *Akkermansia* (P = 0.007, LFC 4.5) and *Catenisphaera* (P = 0.011, LFC 4.8) genus abundances were significantly elevated in WT compared to HCA2-KO mice (Figure 6E).

These changes gave rise to the speculation that the susceptibility to IMQ-induced psoriasis-like inflammation in HCA2-KO mice may be due to a dysbiotic bacterial flora which ultimately alters the function of Treg. Thus, we studied whether the altered skin microbiota is associated

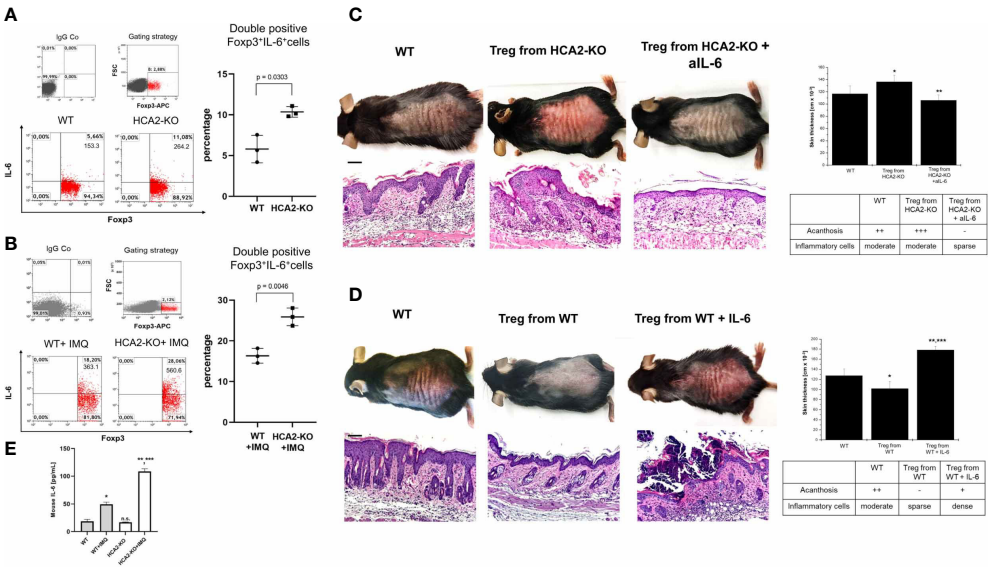

FIGURE 5
IL-6 appears to be involved in the alteration of Treg in the absence of HCA2. Pooled LN cells and splenocytes obtained from 4 naïve mice **(A)** or 4 IMQ-treated **(B)** WT and HCA2-KO mice were analyzed for double positive Foxp3/IL-6 cells and is demonstrated as percentage and total number of double positive cells. FACS analysis is also shown as a scatter graph with mean ± SD. Y axes show percentage of double positive cells. Data were analyzed by using the t test with Welch´s correction. n = 3 **(C)** Treg were obtained from naïve HCA2-KO or from HCA2-KO mice injected i.p. with a rat monoclonal anti-IL-6 antibody. The isolated Treg cells were injected i.v. into IMQ-treated WT mice. Biopsies from IMQ-treated recipients were taken; paraffin embedded sections were stained with H&E and analyzed histopathologically. Scale bar = 100µm. Skin thickness was measured using a spring-loaded micrometer. Student t test and one-way ANOVA was performed. *P < 0.025 WT vs Treg from HCA2-KO, **P < 0.0003 Treg from HCA2-KO vs Treg from HCA2-KO+anti IL-6; $P_{ANOVA} = 9.9x10^{-4}$. Acanthosis and density of inflammatory infiltrate were scored. Each group contained 7 animals. **(D)** Treg were obtained from naïve WT mice or WT mice injected i.p. with IL-6. The isolated Treg cells were injected i.v. into IMQ-treated WT mice. Biopsies from IMQ-treated recipients were taken; paraffin embedded sections were stained with H&E and analyzed histopathologically. Macroscopical and histopathologic pictures of untreated WT mice are not shown for the sake of space. Scale bar = 100 µm. Skin thickness was measured using a spring-loaded micrometer. Student t test and one-way ANOVA was performed. *P < 0.02 WT vs Treg from WT, **P < 0.0002 WT vs Treg from WT+IL-6, ***P < 0.002 Treg from WT vs Treg from WT+IL-6; $P_{ANOVA} = 3.2x10^{-5}$. Acanthosis and density of inflammatory infiltrate were scored. Each group contained 7 animals. Data are presented from one of three independent experiments. **(E)** Serum was obtained from untreated or IMQ-treated WT and HCA2-KO mice, respectively, and IL-6 serum levels were measured using an ELISA. Data were analyzed by using the t test with Welch´s correction and one-way ANOVA. *P = 0.0004 WT vs WT+IMQ; **P = 0.0008 HCA2-KO vs HCA2-KO+IMQ; ***P = 0.0001 WT+IMQ vs HCA2-KO+IMQ; n.s. = 0.4098 WT vs HCA2-KO; $P_{ANOVA} = 3.05815x10^{-11}$; n = 3.

with the outcome of IMQ-induced inflammation in single- and co-housed mice. Therefore, animals were treated for 7 days with IMQ after 1 month of co-housing. As described above, the psoriasis-like skin inflammation was enhanced in single-housed HCA2-KO animals, when compared to single-housed WT mice. The morbidity (skin redness, scaling, hemorrhage and thickness) was significantly enhanced in WT mice upon co-housing with HCA2-KO animals (Figure 7A). This was also observed histopathologically. In contrast, the exaggerated inflammatory response of IMQ-treated HCA2-KO animals co-housed with WT mice was remarkably mitigated (Figure 7A). Together, these changes of the skin microbiota might be responsible for increased susceptibility to psoriasis-like skin inflammation in HCA2-KO animals.

3.6 The skin microbiota may determine the suppressive activity and function of Treg in HCA2-KO mice

Given that the transmissible, modified composition of skin microbiota might be responsible for the increased susceptibility to psoriasis-like skin inflammation in HCA2-KO mice, we hypothesized that a further consequence of the microbiota shift might be an altered activity of Treg. This was addressed by adoptive transfer experiments under co-housing conditions. After 1 month of co-housing Treg were isolated from all groups and injected into WT mice which were treated with IMQ. Treg obtained from single-housed WT mice reduced IMQ-induced inflammation. In contrast, Treg from WT mice co-housed with HCA2-KO mice did not mitigate the IMQ-induced inflammatory response (Figure 7B). The reverse was observed for HCA2-KO mice. As described above, the inflammatory response was significantly stronger pronounced in animals injected with Treg from single-housed HCA2-KO mice. Upon injection of Treg from co-housed HCA2-KO mice, the inflammatory response was not enhanced, as observed upon injection of Treg from single housed HCA2-KO donors, but even reduced. The macroscopic alterations were also reflected by histopathologic analysis of representative skin samples (Figure 7B).

4 Discussion

While the impact of the microbiome on the pathophysiology of psoriasis has been demonstrated in several studies (48), the mechanism by which the microbiome can modulate inflammatory responses in psoriasis remains mostly unclear. Here, we suggest how alteration of the microbiome can impact the inflammatory response in psoriasis.

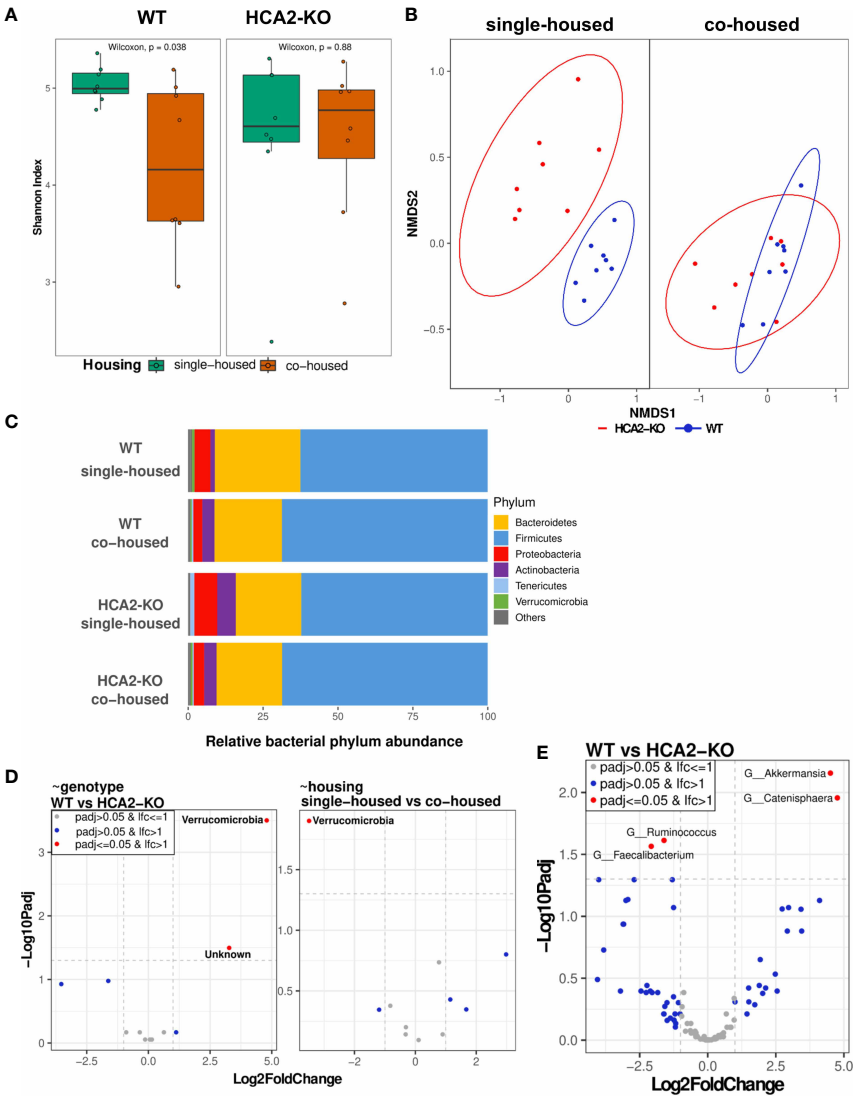

FIGURE 6
Skin dysbiosis in the absence of HCA2 predisposes mice to psoriasis-like inflammation. WT mice were co-housed with HCA2-KO mice for 1 month. 16S rRNA sequencing was performed. **(A)** Alpha diversity (Shannon Index) between WT and HCA2-KO mice, while colors indicate housing conditions. **(B)** Beta diversity calculated with Bray-Curtis dissimilarity and displayed by non-metric multidimensional scaling (NMDS) between single- and co-housed mice, while colors indicate genotype. **(C)** Relative bacterial abundance at phylum level split for the different genotype and housing conditions. **(D)** Differential abundance at phylum level based on linear models by genotype (left) and by housing (right). Volcano plot visualizes −Log10 Benjamini-Hochberg adjusted p-value over Log2FoldChange (LFC). LFC is depicted as relative to HCA2-KO (left) and co-housed (right), i.e. a negative LFC displaying a reduced abundance in WT compared to HCA-KO mice in the left graph and a reduced abundance in single-housed compared to co-housed mice in the right graph. **(E)** Differential abundance at genus level based on linear models by genotype. Volcano plot visualizes −Log10 Benjamini-Hochberg adjusted p-value over Log2FoldChange. A negative LFC shows genera with reduced abundance in WT mice, whereas a positive LFC shows genera more abundant in WT mice. No genus was significantly differentially abundant by housing (data not shown). Each group contained 8 animals. Data are presented from one of three independent experiments.

Dysbiosis of the skin microbiome may shift Treg from a suppressive into a proinflammatory type. Expression and signaling, respectively, of the G-protein-coupled receptor HCA2 appears to be crucially involved.

The rationale for this study was several-fold. It was primarily based on the observation that the SCFA SB can mitigate the inflammatory response in the IMQ-model which is accepted as a suitable model for psoriasis-like skin inflammation (20). There is also evidence that the mitigating effect of SB might also apply to the human system (19). Since SB signals *via* the G-protein-coupled receptor HCA2 and HCA2 expression is reduced in lesional psoriatic skin (25), we were interested to study the effect of HCA2 deficiency in the IMQ-model.

The inflammatory response to IMQ was much stronger pronounced in HCA2-KO mice. This exaggeration was not only confined to the skin but appeared to be also systemic as IMQ-induced splenomegaly was much stronger pronounced in HCA2-KO than in WT mice (data not shown). Since one pathogenetic mechanism in psoriasis is a reduced activity of Treg (4–6), we analyzed whether the same applies to HCA2 deficiency. Adoptive transfer experiments, however, yielded the surprising result that Treg from HCA2-KO mice were not only impaired in their suppressive activity but even enhanced the inflammatory response. Preliminary *in situ* double immunofluorescence analysis for Foxp3 and CD25 revealed a lower number of double positive cells in the skin of mice

10.3389/fimmu.2023.1038689

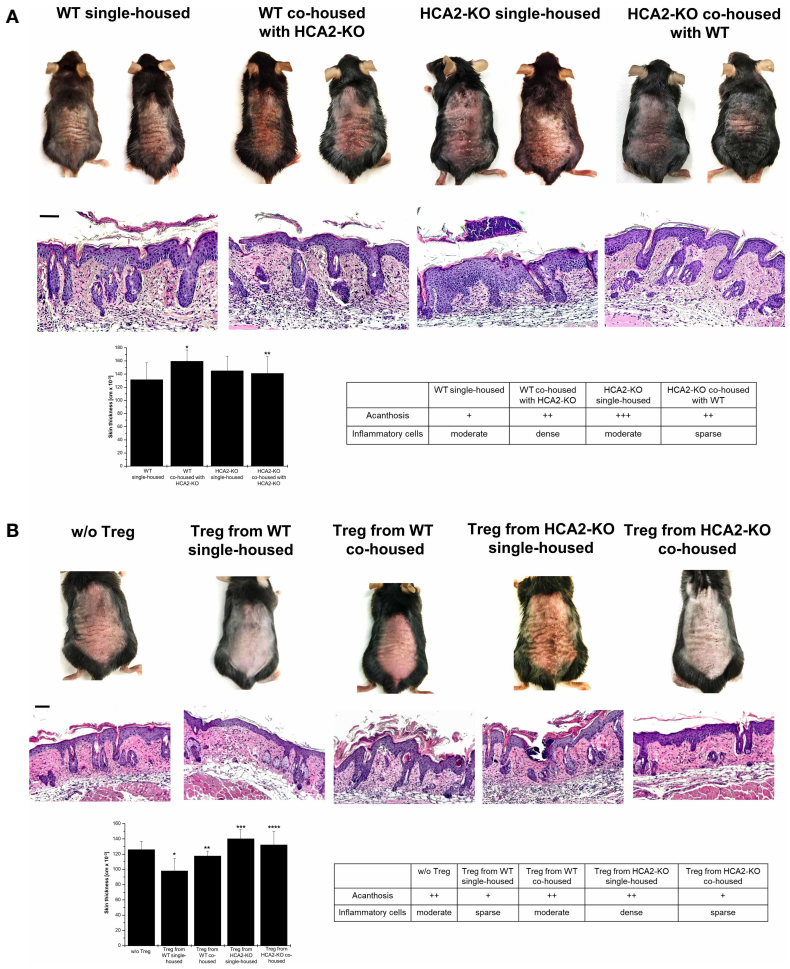

	WT single-housed	WT co-housed with HCA2-KO	HCA2-KO single-housed	HCA2-KO co-housed with WT
Acanthosis	+	++	+++	++
Inflammatory cells	moderate	dense	moderate	sparse

	w/o Treg	Treg from WT single-housed	Treg from WT co-housed	Treg from HCA2-KO single-housed	Treg from HCA2-KO co-housed
Acanthosis	++	+	++	++	+
Inflammatory cells	moderate	sparse	moderate	dense	sparse

FIGURE 7
The skin microbiota determines the suppressive activity and function of Treg in HCA2-KO mice. **(A)** WT mice were co-housed with HCA2-KO mice for 1 month (each group contained 6 animals). Mice were treated topically with 5% IMQ cream on the shaved backs for 7 days. Biopsies were taken, paraffin embedded sections stained with H&E and analyzed histopathologically. Single housed HCA2-KO and WT mice served as controls. Scale bar = 100 µm. The skin thickness was measured using a spring-loaded micrometer. Student t test and one-way ANOVA was performed. *P < 0.015 WT single-housed vs WT co-housed, **P < 0.04 HCA2-KO single-housed vs HCA2-KO co-housed; P_{ANOVA} = 0.00758. The acanthosis and space of inflammatory cells was scored. Data are presented from one of three independent experiments. **(B)** WT mice were co-housed with HCA2-KO mice for 1 month. Treg were obtained either from 6 co-housed HCA2-KO or 6 co-housed WT mice and injected i.v. into IMQ-treated WT mice. As controls, Treg from 6 single-housed HCA2-KO or 6 single-housed WT mice were injected in the same fashion. Biopsies were taken, paraffin embedded sections stained with H&E and analyzed histopathologically. Scale bar = 100 µm. Skin thickness was measured using a spring-loaded micrometer. Student t test and one-way ANOVA were performed. *P < 0.009 w/o Treg vs Treg from WT single-housed, **P < 0.015 Treg from WT single-housed vs Treg from WT co-housed, ***P < 0.0025 Treg WT single-housed vs Treg from HCA2-KO single-housed, ****P < 0.05 Treg from HCA2-KO single-housed vs from HCA2-KO co-housed; P_{ANOVA} = 0.00113. Acanthosis and density of inflammatory infiltrate were scored. Data are presented from one of three independent experiments.

which had received Treg from HCA2-KO mice in comparison to recipients from Treg of WT donors. Upon injection of Treg from HCA2-KO mice, IMQ-treated WT recipients expressed higher levels of IL-17, IL-23 and IL-6 in comparison to the expression of these cytokines in WT-recipients of Treg from WT mice. In contrast, the expression of IL-10 was reduced upon injection of Treg from HCA2–KO mice. We have not analyzed whether the Treg express skin-homing receptors and thus cannot dissect at this stage the contribution of resident Treg versus into the skin immigrating Treg to the modulation of the cutaneous inflammation.

A similar alteration was previously described for several autoimmune disorders which were associated with pathogenic T helper-17 (Th17) cells (49) as well as with dysfunctional Treg (50). Bovenschen et al. (51) demonstrated that psoriatic Treg exhibit a tendency to decrease the expression of the master regulator Foxp3 and develop towards IL-17-producing Treg. Thus, our results imply that Treg in the absence of HCA2 might switch from a regulatory into a proinflammatory type. Soler et al. (52) identified IL-23 as the cytokine primarily responsible for this conversion (51). In concordance with this, we observed that upon inflammatory condition the expression of IL-17 and IL-23 was increased in HCA2-KO mice (Supplementary Figure 6). Furthermore, upon injection of HCA2-KO Treg, the recipients expressed higher levels of IL-23 in comparison to recipients of WT-Treg (Figure 4). The purity of $CD4^+CD25^+$ cells after positive selection was around 95%. This population, however, contained also a minor fraction of Foxp3-

negative cells. Due to the intracellular expression, selection of Foxp3-positive cells for further functional analysis is not possible; which is a limitation of the method. However, since the proinflammatory shift was associated with a decrease of Foxp3 expression, we assume that the $CD4^+CD25^+Foxp3^+$ cells are mostly responsible for this alteration.

This shift appears to be mediated *via* IL-6 since injection of a neutralizing anti-IL-6-antibody into HCA2-KO donors prevented such an alteration of Treg. In turn, a similar modification of Treg was observed when IL-6 was injected into WT donors. In this case, Treg enhanced the IMQ-response upon adoptive transfer. The mechanism for the enhanced expression of IL-6 in the absence of HCA2 remain to be determined as well as the mechanism by which IL-6 alters the status of Treg. In the latter scenario, histone deacetylation appears to play a role. Bovenschen et al. (51) demonstrated that in psoriasis $Foxp3^+$ Treg convert into IL-17-Treg. The histone deacetylase inhibitor trichostatin-A blocked this conversion. Accordingly, we observed that histone acetylation in Treg obtained from psoriasis patients was decreased compared to H3 histones from healthy controls (19). SB upregulated histone acetylation, implying that SB acts as a histone deacetylation inhibitor (18). Whether IL-6 acts as a histone deacetylation inhibitor remains to be determined. Furthermore, IL-6 serum levels were increased upon IMQ administration. This increase was much more pronounced in HCA2-KO than WT mice.

The modification of Treg in the absence of HCA2 could be influenced by the skin microbiome. Since there is a crosstalk between HCAs and the microbiota which involves also SCFA (12, 21, 25, 53–57), we studied the impact of HCA2 on the skin microbiota by comparing WT animals to HCA2-KO mice employing 16S rRNA sequencing of skin swab samples.

Primarily, we observed a microbiome dysbiosis in susceptible animals, similar to what has been described previously for psoriasis as well as for other inflammatory diseases affecting epithelia in humans (58). The exact nature of this dysbiosis is difficult to disentangle, as the bacterial communities often consist of hundreds of species. Nevertheless, in the present scenario, we observed a substantially elevated relative abundance of the genus *Akkermansia*, from the phylum *Verrucomicrobia* in WT mice when compared to the HCA2-KO animals (Figure 6E). Of note, it is known that *Akkermansia (A.) muciniphila* has a protective effect against inflammation because *A. muciniphila* ameliorates chronic colitis of mice through the cross-talk of microbe-derived SCFAs and $Foxp3^+$ Treg (59, 60). Furthermore, *A. muciniphila* supplementation suppressed colon inflammation and increased the frequency of colonic Treg (61). Additionally, previous studies reported that *p.Verrucomicrobia* is negatively correlated with obesity, since reduced abundance of *p.Verrucomicrobia* in the gut resulted in obesity in humans and animals (62, 63). HCA2-KO mice also tend to obesity. Interestingly, the majority of publications analyzed the role of *p.Verrucomicrobia* only in the gut. One of the reasons seems to be that *Akkermansia* was initially described as a strict anaerobe. However, more recently, it was reported that *Akkermansia* tolerates small amounts of oxygen and even benefits from low levels of oxygen (64). Along this line, *Verrucomicrobia* was also detected on the skin. Stehlikova et al. (65) analyzed the microbiota of the skin and of the intestine in Balb/c and C57BL/6 mice and detected also a low amount of *Verrucomicrobia* on the skin. It might be possible that the skin microbiota was not very often searched for *Verrucomicrobia*, because it was anticipated that this phylum is strictly anaerobe.

In our experiments, the microbiome displayed at least partially a causative component. When mice interacted, e.g. by being co-housed, their microbiome was transferred between each other. In the experimental setup presented here, this resulted in the microbiomes becoming more similar to each other. This microbial transfer resulted in transferring phenotypic features. We observed that co-housed HCA2-KO mice showed slightly less inflammation in the IMQ-model than single-housed HCA2-KO mice. This difference seems to be maintained when administering the respective Treg. While we observed that WT mice have an increased inflammatory phenotype in the IMQ-model when co-housed with HCA2-KO mice, our experimental setup does not allow to identify the specific species responsible for this difference. Besides this limitation, it is probable that this is due to the ensemble of additional species that populate WT animals when co-housed with HCA2-KO mice, as observed in the analysis of alpha and beta diversity. This dysbiosis could cause a hyperstimulation of the immune system resulting in increased inflammation. In this context, it has to be noted that our data does not allow to pinpoint a direct molecular effect on the host, such as correlations between alpha diversity and molecular markers (e.g., SCFA receptor mRNA expression). Following this up would require a separate study with an experimental design that specifically aims to elucidate host-microbiome interactions. Couturier-Maillard et al. (66) reported that disturbances of balance state of commensals in the gut directly or indirectly contribute to the pathogenesis of several immune-mediated intestinal illnesses such a Crohn's disease and colitis. They observed that WT mice that were transiently co-housed with Nod2-KO mice, which are more susceptible to an induced colitis, developed an increased susceptibility to colitis. In concordance with this, we demonstrated similar effects in the IMQ-induced psoriasis-like skin inflammation model. We extended co-housing for up to two months. At this point, the phenotypic alterations remained more or less the same. The same seems to apply to the microbiota.

As a final point, it should be mentioned that *A. muciniphila* represents a gut microbiota signature in psoriasis (67). 16S rRNA sequencing revealed that the abundance of *A. muciniphila* was significantly reduced in patients with psoriasis. *A. muciniphila* is believed to have an important function in the pathogenesis of inflammatory bowel diseases and obesity. The authors reported that beside an alteration in the total diversity of microbiota between psoriasis and healthy control, the abundance of *A. muciniphila* is remarkably reduced in patients with psoriasis. This does not only support the validity of the model employed here, but also indicates a potential key-role of *Akkermansia* in this crosstalk, which still requires further studies. These should be focusing on species level classification by advanced methods like metagenomics, additional PCR screening and metabolomics studies to infer causality on molecular level.

Keeping this in mind, our data still illustrates changes in the relative composition of the HCA2-KO skin microbiome. While little

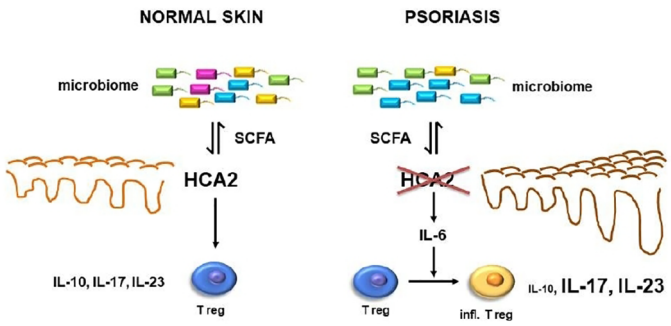

FIGURE 8
In psoriasis, reduced expression of HCA2 which may be mutually influenced by an altered skin microbiome may result in enhanced expression of IL-6 which may switch Treg into a proinflammatory cell type. This appears to be associated with a reduced expression of IL-10 and an enhanced expression of IL-17 and IL-23.

is known about skin microbiota producing SCFA, our data cannot exclude either origin of the SCFA. Further studies will be needed to determine whether SCFA are produced in the skin at significant levels to alter an immune response. Nevertheless, topical application of SB was found to tone down inflammatory responses (18). However, we have not yet tested whether topically applied SB reduces the exaggerated IMQ response in HCA2-KO mice.

The data so far demonstrated the consequences of HCA2-deficiency several-fold: (i) the psoriasis-like inflammation response to IMQ is remarkably enhanced; (ii) Treg may switch from a regulatory into a proinflammatory type; (iii) IL-6 expression is enhanced; (iv) the skin microbiome is altered, which appears to be the most upstream phenomenon in this cascade (Figure 8). This was supported by co-housing experiments. The regulatory activity of Treg in WT mice could be impaired by co-housing of WT mice with HCA2-KO mice, and in turn the proinflammatory activity of Treg in HCA2-KO mice could be reversed by co-housing with WT mice. We have not yet performed detailed phenotypic analysis of the Treg within the co-housing experiments, preliminary data indicate that the enhanced proinflammatory activity appears to be associated with a decreased expression of Foxp3 and vice versa. Since the co-housing was associated with an alteration of the skin microbiome, we surmise that this could be the most upstream event. The *in vivo* response to IMQ was changed accordingly upon co-housing. However, our co-housing experiments cannot rule out changes in the microbiome of the gut or any other organ as well which is a limitation of this *in vivo* model.

While causality of the microbiome and the corresponding molecular effects on the host site are difficult to demonstrate, our findings provide further support for the hypothesis that the microbiome may play a key role in modulating the host's immune response *via* HCA2 and Treg in the murine psoriasis-like inflammation model. These findings may have implications for the development of future strategies to treat psoriasis. Firstly, the altered skin microbiome could be changed with the ultimate aim to modulate the inflammatory psoriatic response, as it has been already demonstrated successfully for atopic dermatitis (68, 69). A second option would be topical application of SB. The effect may be several-fold, firstly a direct modulation of Treg, as demonstrated previously (16), and secondly *via* restoration of the expression of HCA2 (25) which ultimately influences the skin microbiome.

Data availability statement

The datasets presented in this study can be found in online repositories. The names of the repository/repositories and accession number(s) can be found below: https://www.ncbi.nlm.nih.gov/, PRJNA836403.

Ethics statement

The animal study was reviewed and approved by Animal Welfare Commission of Ministry of Energy, Agriculture, the Environment, Nature and Digitalization of the Federal State Schleswig-Holstein.

Author contributions

Conceptualization: AS and TS; Formal Analysis: AS, RH, SR-J, JH, and SP; Funding Acquisition: AS and TS; Investigation: AS and RP; Methodology: AS, RH, SR-J, JH, and SP; Resources: TS and SR-J; Supervision: AS and TS; Validation: AS, RH, SP, and JH; Visualization: AS, RP, and JH; Writing - Original Draft Preparation: AS, RH, and TS; Writing - Review and Editing: TS. All authors contributed to the article and approved the submitted version.

Acknowledgments

This study was supported by a grant from the Deutsche Forschungsgemeinschaft (SCHW 625/10-1). Sequencing, NGS data management and data processing were supported by the CCGA (DFG, INST 257/605-1) as well as by the Cluster of Excellence ExC PMI 2167. RH is supported by Immuniverse (853995), BIOMAP (821511), E:med sysINFLAME (01ZX1306), miTarget (DFG, FOR 5042, P4), and the CRC1182 (DFG, Z3). SP was supported by the "Margarita Salas Grant for the Requalification of the Spanish University System (2021-2023)". The authors are grateful to Corinna Bang for help in processing the raw data of the skin microbiome.

Conflict of interest

SR-J has acted as a consultant and speaker for AbbVie, Chugai, Genentech Roche, Pfizer and Sanofi. He also declares that he is an inventor on patents owned by CONARIS Research Institute, which develops the sgp130Fc protein Olamkicept together with the companies Ferring and I-Mab. He has stock ownership in CONARIS. The remaining authors declare that the research was conducted in the absence of any commercial or financial relationships that could be construed as a potential conflict of interest.

Publisher's note

Supplementary material

The Supplementary Material for this article can be found online at: https://www.frontiersin.org/articles/10.3389/fimmu.2023.1038689/full#supplementary-material

SUPPLEMENTARY FIGURE 1
Cells from LN and spleens obtained from 4 WT and 4 HCA2-KO mice were isolated separately and subjected to FACS analysis. Cells were gated for Foxp3 and double positive cells (Foxp3/CD25) were analyzed. The number of double positive cells is displayed in the histograms. FACS analysis is also shown as scatter graph with mean ± SD. Y axes show percentage of double positive cells. Data were analyzed by using the t test with Welch´s correction (n = 3).

SUPPLEMENTARY FIGURE 2
The clinical response to IMQ was quantified according to a modified PASI score by Wang et al. (24). The data for Figures 1A, 3A, 5C, D, 7A, B are shown.

SUPPLEMENTARY FIGURE 3
Pooled lymph node cells and splenocytes obtained from 4 WT and 4 HCA2-KO mice were gated for Foxp3 and analyzed for the expression of CTLA-4, Helios, Ki-67, PD-1, CD73, FR4. The total cell number of double positive cells is displayed in the histograms. FACS analysis is also shown as scatter graph with mean ± SD. Y axes show percentage of double positive cells. Data were analyzed by using the t test with Welch´s correction (n = 3).

SUPPLEMENTARY FIGURE 4
(A) Treg obtained from 7 HCA2-KO and 7 WT mice were stained with CFSE and injected i.v. into IMQ-treated WT animals. After 48 h LN and spleens were obtained from the recipient mice and FACS analysis of CFSE-negative (overlay of red histograms) was conducted. The expression of IL-6, IL-17, IL-23 and IL-10 was standardized to isotype controls. For IL-6, IL-17 and IL-23 the same IgG (rat IgG1) control was used. Histograms show fluorescence intensity (x axis) versus cell count (y-axis). The number of total cells is displayed in the histograms. **(B)** FACS analysis is also shown as scatter graph with mean ± SD. Y axes show percentage of double positive cells. Data were analyzed by using the t test with Welch´s correction. 1 WT untreated; 2 WT +IMQ + w/o Treg (n = 3).

SUPPLEMENTARY FIGURE 5
Treg were obtained from naïve HCA2-KO or from HCA2-KO mice injected i.p. with a rat monoclonal anti-IL-6 antibody. The isolated Treg were injected i.v. into IMQ-treated WT recipient mice. LN and spleen cells from these recipients were analyzed for double positive Foxp3/IL-10, Foxp3/GARP and Foxp3/CD25 cells and demonstrated as percentage and total number of double positive cells.

SUPPLEMENTARY FIGURE 6
Pooled lymph node cells and splenocytes were obtained from 4 IMQ-treated WT and 4 HCA2-KO mice. Cells were gated for Foxp3 and FACS analysis performed for CD25, IL-17 and IL-23. The number of double positive cells is displayed in the histograms. FACS analysis is also shown as scatter graph with mean ± SD. Y axes show percentage of double positive cells. Data were analyzed by using the t test with Welch´s correction (n = 3).

References

1. AlQassimi S, AlBrashdi S, Galadari H, Hashim MJ. Global burden of psoriasis - comparison of regional and global epidemiology, 1990 to 2017. *Int J Dermatol* (2020) 59:566–71. doi: 10.1111/ijd.14864

2. Rendon A, Schäkel K. Psoriasis pathogenesis and treatment. *Int J Mol Sci* (2019) 20:1475. doi: 10.3390/ijms20061475

3. Prinz JC. Autoimmune aspects of psoriasis: Heritability and autoantigens. *Autoimmun Rev* (2017) 16:970–9. doi: 10.1016/j.autrev.2017.07.011

4. Kanda N, Hoashi T, Saeki H. The defect in regulatory T cells in psoriasis and therapeutic approaches. *J Clin Med* (2021) 10:3880. doi: 10.3390/jcm10173880

5. Owczarczyk-Saczonek A, Czerwińska J, Placek W. The role of regulatory T cells and anti-inflammatory cytokines in psoriasis. *Acta Dermatovenerol Alp Pannonica Adriat* (2018) 27:17–23. doi: 10.15570/actaapa.2018.4

6. Stockenhuber K, Hegazy AN, West NR, Ilott NE, Stockenhuber A, Bullers SJ, et al. Foxp3+ T reg cells control psoriasiform inflammation by restraining an IFN-i-driven CD8 + T cell response. *J Exp Med* (2018) 215:1987–98. doi: 10.1084/jem.20172094

7. Arpaia N, Campbell C, Fan X, Dikiy S, van der Veeken J, deRoos P, et al. Metabolites produced by commensal bacteria promote peripheral regulatory T-cell generation. *Nature* (2013) 504:451–5. doi: 10.1038/nature12726

8. Furusawa Y, Obata Y, Fukuda S, Endo TA, Nakato G, Takahashi D, et al. Commensal microbe-derived butyrate induces the differentiation of colonic regulatory T cells. *Nature* (2013) 504:446–50. doi: 10.1038/nature12721

9. Nagano Y, Itoh K, Honda K. The induction of treg cells by gut-indigenous clostridium. *Curr Opin Immunol* (2012) 24:392–7. doi: 10.1016/j.coi.2012.05.007

10. Trompette A, Gollwitzer ES, Yadava K, Sichelstiel AK, Sprenger N, Ngom-Bru C, et al. Gut microbiota metabolism of dietary fiber influences allergic airway disease and hematopoiesis. *Nat Med* (2014) 20:159–66. doi: 10.1038/nm.3444

11. Maslowski KM, Vieira AT, Ng A, Kranich J, Sierro F, Yu D, et al. Regulation of inflammatory responses by gut microbiota and chemoattractant receptor GPR43. *Nature* (2009) 461:1282–6. doi: 10.1038/nature08530

12. Smith PM, Howitt MR, Panikov N, Michaud M, Gallini CA, Bohlooly-Y M, et al. The microbial metabolites, short-chain fatty acids, regulate colonic treg cell homeostasis. *Science* (2013) 341:569–73. doi: 10.1126/science.1241165

13. Liu YJ, Tang B, Wang FC, Tang L, Lei YY, Luo Y, et al. Parthenolide ameliorates colon inflammation through regulating Treg/Th17 balance in a gut microbiota-dependent manner. *Theranostics* (2020) 10:5225–41. doi: 10.7150/thno.43716

14. Nishida A, Nishino K, Ohno M, Sakai K, Owaki Y, Noda Y, et al. Update on gut microbiota in gastrointestinal diseases. *World J Clin cases* (2022) 10:7653–64. doi: 10.12998/wjcc.v10.i22.7653

15. Zhang Y, Si X, Yang L, Wang H, Sun Y, Liu N. Association between intestinal microbiota and inflammatory bowel disease. *Anim Model Exp Med* (2022) 5:311–22. doi: 10.1002/ame2.12255

16. Belkaid Y, Naik S. Compartmentalized and systemic control of tissue immunity by commensals. *Nat Immunol* (2013) 14:646–53. doi: 10.1038/ni.2604

17. Ochoa-Repáraz J, Mielcarz DW, Ditrio LE, Burroughs AR, Foureau DM, Haque-Begum S, et al. Role of gut commensal microflora in the development of experimental autoimmune encephalomyelitis. *J Immunol* (2009) 183:6041–50. doi: 10.4049/jimmunol.0900747

18. Schwarz A, Bruhs A, Schwarz T. The short-chain fatty acid sodium butyrate functions as a regulator of the skin immune system. *J Invest Dermatol* (2017) 137:855–64. doi: 10.1016/j.jid.2016.11.014

19. Schwarz A, Philippsen R, Schwarz T. Induction of regulatory T cells and correction of cytokine disbalance by short-chain fatty acids: Implications for psoriasis therapy. *J Invest Dermatol* (2021) 141:95–104. doi: 10.1016/j.jid.2020.04.031

20. van der Fits L, Mourits S, Voerman JS, Kant M, Boon L, Laman JD, et al. Imiquimod-induced psoriasis-like skin inflammation in mice is mediated *via* the IL-23/IL-17 axis. *J Immunol* (2009) 182:5836–45. doi: 10.4049/jimmunol.0802999

21. Singh N, Gurav A, Sivaprakasam S, Brady E, Padia R, Shi H, et al. Activation of Gpr109a, receptor for niacin and the commensal metabolite butyrate, suppresses colonic inflammation and carcinogenesis. *Immunity* (2014) 40:128–39. doi: 10.1016/j.immuni.2013.12.007

22. Jobin C. GPR109a: the missing link between microbiome and good health? *Immunity* (2014) 40:8–10. doi: 10.1016/j.immuni.2013.12.009

23. Sivaprakasam S, Gurav A, Paschall AV, Coe GL, Chaudhary K, Cai Y, et al. An essential role of Ffar2 (Gpr43) in dietary fibre-mediated promotion of healthy composition of gut microbiota and suppression of intestinal carcinogenesis. *Oncogenesis* (2016) 5:e238. doi: 10.1038/oncsis.2016.38

24. Tan J, McKenzie C, Potamitis M, Thorburn AN, Mackay CR, Macia L. The role of short-chain fatty acids in health and disease. *Adv Immunol* (2014) 121:91–119. doi: 10.1016/B978-0-12-800100-4.00003-9

25. Krejner A, Bruhs A, Mrowietz U, Wehkamp U, Schwarz T, Schwarz A. Decreased expression of G-protein-coupled receptors GPR43 and GPR109a in psoriatic skin can be restored by topical application of sodium butyrate. *Arch Dermatol Res* (2018) 310:751–8. doi: 10.1007/s00403-018-1865-1

26. Tunaru S, Kero J, Schaub A, Wufka C, Blaukat A, Pfeffer K, et al. PUMA-G and HM74 are receptors for nicotinic acid and mediate its anti-lipolytic effect. *Nat Med* (2003) 9:352–5. doi: 10.1038/nm824

27. Wang Y, Zhao J, Zhang L, Liu X, Lin Y, Di T, et al. Suppressive effect of beta, beta-dimethylacryloyl alkannin on activated dendritic cells in an imiquimod-induced psoriasis mouse model. *Int J Clin Exp Pathol* (2015) 8:6665–73.

28. Rodríguez-Perea AL, Arcia ED, Rueda CM, Velilla PA. Phenotypical characterization of regulatory T cells in humans and rodents. *Clin Exp Immunol* (2016) 185:281–91. doi: 10.1111/cei.12804

29. Ehlers M, Grötzinger J, deHon FD, Müllberg J, Brakenhoff JP, Liu J, et al. Identification of two novel regions of human IL-6 responsible for receptor binding and signal transduction. *J Immunol* (1994) 153:1744–53. doi: 10.4049/jimmunol.153.4.1744

30. Coulie PG, Stevens M, Van Snick J. High- and low-affinity receptors for murine interleukin 6. distinct distribution on b and T cells. *Eur J Immunol* (1989) 19:2107–14. doi: 10.1002/eji.1830191121

31. Thingholm LB, Bang C, Rühlemann MC, Starke A, Sicks F, Kaspari V, et al. Ecology impacts the decrease of spirochaetes and prevotella in the fecal gut microbiota of urban humans. *BMC Microbiol* (2021) 21:276. doi: 10.1186/s12866-021-02337-5

32. Kozich JJ, Westcott SL, Baxter NT, Highlander SK, Schloss PD. Development of a dual-index sequencing strategy and curation pipeline for analyzing amplicon sequence data on the MiSeq illumina sequencing platform. *Appl Environ Microbiol* (2013) 79:5112–20. doi: 10.1128/AEM.01043-13

33. Callahan BJ, McMurdie PJ, Rosen MJ, Han AW, Johnson AJ, Holmes SP. DADA2: High-resolution sample inference from illumina amplicon data. *Nat Methods* (2016) 13:581–3. doi: 10.1038/nmeth.3869

34. Zhou H, He K, Chen J, Zhang X. LinDA: Linear models for differential abundance analysis of microbiome compositional data. *Genome Biol* (2022) 23:95. doi: 10.1186/s13059-022-02655-5

35. Tran DQ, Andersson J, Wang R, Ramsey H, Unutmaz D, Shevach EM. GARP (LRRC32) is essential for the surface expression of latent TGF-beta on platelets and activated FOXP3+ regulatory T cells. *Proc Natl Acad Sci U.S.A.* (2009) 106:13445–50. doi: 10.1073/pnas.0901944106

36. Elkord E, Abd Al Samid M, Chaudhary B. Helios, And not FoxP3, is the marker of activated tregs expressing GARP/LAP. *Oncotarget* (2015) 6:20026–36. doi: 10.18632/oncotarget.4771

37. Santegoets SJ, Dijkgraaf EM, Battaglia A, Beckhove P, Britten CM, Gallimore A, et al. Monitoring regulatory T cells in clinical samples: Consensus on an essential marker set and gating strategy for regulatory T cell analysis by flow cytometry. *Cancer Immunol Immunother* (2015) 64:1271–86. doi: 10.1007/s00262-015-1729-x

38. Ring S, Enk AH, Mahnke K. Regulatory T cells from IL-10-deficient mice fail to suppress contact hypersensitivity reactions due to lack of adenosine production. *J Invest Dermatol* (2011) 131:1494–502. doi: 10.1038/jid.2011.50

39. Kinoshita M, Kayama H, Kusu T, Yamaguchi T, Kunisawa J, Kiyono H, et al. Dietary folic acid promotes survival of Foxp3+ regulatory T cells in the colon. *J Immunol* (2012) 189:2869–78. doi: 10.4049/jimmunol.1200420

40. Kamada T, Togashi Y, Tay C, Ha D, Sasaki A, Nakamura Y, et al. PD-1+ regulatory T cells amplified by PD-1 blockade promote hyperprogression of cancer. *Proc Natl Acad Sci U.S.A.* (2019) 116:9999–10008. doi: 10.1073/pnas.1822001116

41. Tan CL, Kuchroo JR, Sage PT, Liang D, Francisco LM, Buck J, et al. PD-1 restraint of regulatory T cell suppressive activity is critical for immune tolerance. *J Exp Med* (2021) 218:e20182232. doi: 10.1084/jem.20182232

42. Bettini M, Vignali DA. Regulatory T cells and inhibitory cytokines in autoimmunity. *Curr Opin Immunol* (2009) 21:612–8. doi: 10.1016/j.coi.2009.09.011

43. Bettelli E, Carrier Y, Gao W, Korn T, Strom TB, Oukka M, et al. Reciprocal developmental pathways for the generation of pathogenic effector TH17 and regulatory T cells. *Nature* (2006) 441:235–8. doi: 10.1038/nature04753

44. Dominitzki S, Fantini MC, Neufert C, Nikolaev A, Galle PR, Scheller J, et al. Cutting edge: Trans-signaling *via* the soluble IL-6R abrogates the induction of FoxP3 in naive CD4+CD25 T cells. *J Immunol* (2007) 179:2041–5. doi: 10.4049/jimmunol.179.4.2041

45. Coates M, Lee MJ, Norton D, MacLeod AS. The skin and intestinal microbiota and their specific innate immune systems. *Front Immunol* (2019) 10:2950. doi: 10.3389/fimmu.2019.02950

46. Santacroce L, Man A, Charitos IA, Haxhirexha K, Topi S. Current knowledge about the connection between health status and gut microbiota from birth to elderly. A narrative review. *Front Biosci (Landmark Ed)* (2021) 26:135–48. doi: 10.52586/4930

47. Polkowska-Pruszyńska B, Gerkowicz A, Krasowska D. The gut microbiome alterations in allergic and inflammatory skin diseases - an update. *J Eur Acad Dermatol Venereol* (2020) 34:455–64. doi: 10.1111/jdv.15951

48. Liang X, Ou C, Zhuang J, Li J, Zhang F, Zhong Y, et al. Interplay between skin microbiota dysbiosis and the host immune system in psoriasis: Potential pathogenesis. *Front Immunol* (2021) 12:764384. doi: 10.3389/fimmu.2021.764384

49. Tesmer LA, Lundy SK, Sarkar S, Fox DA. Th17 cells in human disease. *Immunol Rev* (2008) 223:87–113. doi: 10.1111/j.1600-065X.2008.00628.x

50. Brusko TM, Putnam AL, Bluestone JA. Human regulatory T cells: role in autoimmune disease and therapeutic opportunities. *Immunol Rev* (2008) 223:371–90. doi: 10.1111/j.1600-065X.2008.00637.x

51. Bovenschen HJ, van de Kerkhof PC, van Erp PE, Woestenenk R, Joosten I, Koenen HJ. Foxp3+ regulatory T cells of psoriasis patients easily differentiate into IL-17A-producing cells and are found in lesional skin. *J Invest Dermatol* (2011) 131:1853–60. doi: 10.1038/jid.2011.139

52. Soler DC, McCormick TS. The dark side of regulatory T cells in psoriasis. *J Invest Dermatol* (2011) 131:1785–6. doi: 10.1038/jid.2011.200

53. Kim MH, Kang SG, Park JH, Yanagisawa M, Kim CH. Short-chain fatty acids activate GPR41 and GPR43 on intestinal epithelial cells to promote inflammatory responses in mice. *Gastroenterology* (2013) 145:396–406.e1-10. doi: 10.1053/j.gastro.2013.04.056

54. Sivaprakasam S, Prasad PD, Singh N. Benefits of short-chain fatty acids and their receptors in inflammation and carcinogenesis. *Pharmacol Ther* (2016) 164:144–51. doi: 10.1016/j.pharmthera.2016.04.007

55. Sun M, Wu W, Liu Z, Cong Y. Microbiota metabolite short chain fatty acids, GPCR, and inflammatory bowel diseases. *J Gastroenterol* (2017) 52:1–8. doi: 10.1007/s00535-016-1242-9

56. Alarcon P, Manosalva C, Carretta MD, Hidalgo AI, Figueroa CD, Taubert A, et al. Fatty and hydroxycarboxylic acid receptors: The missing link of immune response and metabolism in cattle. *Vet Immunol Immunopathol* (2018) 201:77–87. doi: 10.1016/j.vetimm.2018.05.009

57. Carretta MD, Quiroga J, López R, Hidalgo MA, Burgos RA. Participation of short-chain fatty acids and their receptors in gut inflammation and colon cancer. *Front Physiol* (2021) 12:662739. doi: 10.3389/fphys.2021.662739

58. Kapoor B, Gulati M, Rani P, Gupta R. Psoriasis: Interplay between dysbiosis and host immune system. *Autoimmun Rev* (2022) 21:103169. doi: 10.1016/j.autrev.2022.103169

59. Bian X, Wu W, Yang L, Lv L, Wang Q, Li Y, et al. Administration of akkermansia muciniphila ameliorates dextran sulfate sodium-induced ulcerative colitis in mice. *Front Microbiol* (2019) 10:2259. doi: 10.3389/fmicb.2019.02259

60. Hänninen A, Toivonen R, Pöysti S, Belzer C, Plovier H, Ouwerkerk JP, et al. Akkermansia muciniphila induces gut microbiota remodelling and controls islet autoimmunity in NOD mice. *Gut* (2018) 67:1445–53. doi: 10.1136/gutjnl-2017-314508

61. Liu Y, Yang M, Tang L, Wang F, Huang S, Liu S, et al. TLR4 regulates RORγt+ regulatory T-cell responses and susceptibility to colon inflammation through interaction with akkermansia muciniphila. *Microbiome* (2022) 10:98. doi: 10.1186/s40168-022-01296-x

62. Zhong Y, Nyman M, Fåk F. Modulation of gut microbiota in rats fed high-fat diets by processing whole-grain barley to barley malt. *Mol Nutr Food Res* (2015) 59:2066–76. doi: 10.1002/mnfr.201500187

63. Cani PD, Depommier C, Derrien M, Everard A, de Vos WM. Akkermansia muciniphila: paradigm for next-generation beneficial microorganisms. *Nat Rev Gastroenterol Hepatol* (2022) 19:625–37. doi: 10.1038/s41575-022-00631-9

64. Ouwerkerk JP, van der Ark KCH, Davids M, Claassens NJ, Finestra TR, de Vos WM, et al. Adaptation of akkermansia muciniphila to the oxic-anoxic interface of the mucus layer. *Appl Environ Microbiol* (2016) 82:6983–93. doi: 10.1128/AEM.01641-16

65. Stehlikova Z, Kostovcikova K, Kverka M, Rossmann P, Dvorak J, Novosadova I, et al. Crucial role of microbiota in experimental psoriasis revealed by a gnotobiotic mouse model. *Front Microbiol* (2019) 10:236. doi: 10.3389/fmicb.2019.00236

66. Couturier-Maillard A, Secher T, Rehman A, Normand S, De Arcangelis A, Haesler R, et al. NOD2-mediated dysbiosis predisposes mice to transmissible colitis and colorectal cancer. *J Clin Invest* (2013) 123:700–11. doi: 10.1172/JCI62236

67. Tan L, Zhao S, Zhu W, Wu L, Li J, Shen M, et al. The akkermansia muciniphila is a gut microbiota signature in psoriasis. *Exp Dermatol* (2018) 27:144–9. doi: 10.1111/exd.13463

68. Nakatsuji T, Gallo RL, Shafiq F, Tong Y, Chun K, Butcher AM, et al. Use of autologous bacteriotherapy to treat staphylococcus aureus in patients with atopic dermatitis: A randomized double-blind clinical trial. *JAMA Dermatol* (2021) 157:978–82. doi: 10.1001/jamadermatol.2021.1311

69. Williams MR, Costa SK, Zaramela LS, Khalil S, Todd DA, Winter HL, et al. Quorum sensing between bacterial species on the skin protects against epidermal injury in atopic dermatitis. *Sci Transl Med* (2019) 11:eaat8329. doi: 10.1126/scitranslmed.aat8329

frontiers | Frontiers in Immunology

TYPE Original Research
PUBLISHED 22 February 2023
DOI 10.3389/fimmu.2023.1114321

OPEN ACCESS

EDITED BY
Tej Pratap Singh,
University of Pennsylvania, United States

REVIEWED BY
Chao Yuan,
Shanghai Dermatology Hospital, China
Heinz Fischer,
Medical University of Vienna, Austria

*CORRESPONDENCE
Kwang-Hyeon Liu
dstlkh@knu.ac.kr
Chang Ook Park
copark@yuhs.ac

†These authors share first authorship

SPECIALTY SECTION
This article was submitted to Molecular Innate Immunity, a section of the journal Frontiers in Immunology

RECEIVED 02 December 2022
ACCEPTED 07 February 2023
PUBLISHED 22 February 2023

CITATION
Chu H, Kim SM, Zhang K, Wu Z, Lee H, Kim JH, Kim HL, Kim YR, Kim SH, Kim WJ, Lee YW, Lee KH, Liu KH and Park CO (2023) Head and neck dermatitis is exacerbated by *Malassezia furfur* colonization, skin barrier disruption, and immune dysregulation. *Front. Immunol.* 14:1114321. doi: 10.3389/fimmu.2023.1114321

Head and neck dermatitis is exacerbated by *Malassezia furfur* colonization, skin barrier disruption, and immune dysregulation

Howard Chu[1†], Su Min Kim[1†], KeLun Zhang[1,2†], Zhexue Wu[3], Hemin Lee[1], Ji Hye Kim[1], Hye Li Kim[1,2], Yu Ri Kim[1], Seo Hyeong Kim[1], Wan Jin Kim[4], Yang Won Lee[5], Kwang Hoon Lee[1], Kwang-Hyeon Liu[3*] and Chang Ook Park[1,2*]

[1]Department of Dermatology, Severance Hospital, Cutaneous Biology Research Institute, Yonsei University College of Medicine, Seoul, Republic of Korea, [2]Brain Korea 21 PLUS Project for Medical Science, Yonsei University College of Medicine, Seoul, Republic of Korea, [3]Brain Korea 21 FOUR Community Based Intelligent Novel Drug Discovery Education Unit, College of Pharmacy and Research Institute of Pharmaceutical Sciences, Kyungpook National University, Daegu, Republic of Korea, [4]Department of Dermatology, Myongji Hospital, Goyang, Republic of Korea, [5]Department of Dermatology, Konkuk University School of Medicine, Seoul, Republic of Korea

Introduction & objectives: Head and neck dermatitis (HND) is a refractory phenotype of atopic dermatitis (AD) and can be a therapeutic challenge due to lack of responsiveness to conventional treatments. Previous studies have suggested that the microbiome and fungiome may play a role in inducing HND, but the underlying pathogenic mechanisms remain unknown. This study aimed to determine the link between HND and fungiome and to examine the contribution of *Malassezia furfur*.

Materials and methods: To identify the effect of the sensitization status of *M. furfur* on HND, 312 patients diagnosed with AD were enrolled. To elucidate the mechanism underlying the effects of *M. furfur*, human keratinocytes and dermal endothelial cells were cultured with *M. furfur* and treated with Th2 cytokines. The downstream effects of various cytokines, including inflammation and angiogenesis, were investigated by real-time quantitative PCR. To identify the association between changes in lipid composition and *M. furfur* sensitization status, D-squame tape stripping was performed. Lipid composition was evaluated by focusing on ceramide species using liquid chromatography coupled with tandem mass spectrometry.

Results: Increased sensitization to *M. furfur* was observed in patients with HND. Additionally, sensitization to *M. furfur* was associated with increased disease severity in these patients. IL-4 treated human keratinocytes cultured with *M. furfur* produced significantly more VEGF, VEGFR, IL-31, and IL-33. IL-4/*M. furfur* co-cultured dermal endothelial cells exhibited significantly elevated VEGFR, TGF-β, TNF-α, and IL-1β levels. Stratum corneum lipid analysis revealed decreased levels of esterified omega-hydroxyacyl-sphingosine, indicating skin barrier dysfunction in HND. Finally, *M. furfur* growth was inhibited by the addition

of these ceramides to culture media, while the growth of other microbiota, including *Cutibacterium acnes*, were not inhibited.

Conclusions: Under decreased levels of ceramide in AD patients with HND, *M. furfur* would proliferate, which may enhance pro-inflammatory cytokine levels, angiogenesis, and tissue remodeling. Thus, it plays a central role in the pathogenesis of HND in AD.

KEYWORDS

atopic dermatitis, head and neck dermatitis, *Malassezia*, LC-MS/MS, lipid analysis, ceramide, red face syndrome

1 Introduction

Atopic dermatitis (AD) is a chronic relapsing pruritic eczematous skin disorder (1). It is considered a multifactorial disease in which allergen-induced immunoglobulin (Ig) E is thought to be one of the contributing factors, as the levels of these specific IgE antibodies are found to be increased in the sera of patients with AD (2). Head and neck dermatitis (HND) or red face syndrome is one of the features of AD, with characteristic diffuse erythema of the face, which is more commonly observed in infants and adults (3). Due to its chronicity and frequent relapses, patients' quality of life is severely affected.

AD patients with HND have been found to be more sensitized to *Malassezia furfur* (*M. furfur*) and have increased levels of specific IgE compared to AD patients without HND (4–6). In addition, studies have reported that antifungal agents improve symptoms in these patients (3, 7), further supporting the association of *M. furfur* with HND in AD. However, the mechanisms underlying the development of HND and its association with *M. furfur* remain unclear.

M. furfur is a lipophilic yeast that constitutes the normal flora of the skin and produces lipases that break down sebum lipids into unsaturated fatty acids, oleic acid, and arachidonic acid (8). These fatty acids have desquamative effects on keratinocytes and induce the production of pro-inflammatory cytokines (9). *M. furfur* is associated with various cutaneous conditions, such as seborrheic dermatitis and tinea versicolor. Although these conditions may recur and become chronic, they usually respond well to treatment, unlike HND in AD patients. Therefore, we aimed to explore the role of *M. furfur* in the development of HND in AD.

Abbreviations: HND, head and neck dermatitis; HL, healthy control; AD, atopic dermatitis; EASI, eczema area and severity index; VEGF, vascular endothelial growth factor; HMVEC, human microvascular endothelial cells; EO, esterified omegahydroxyacyl; EOP, omega-hydroxyacyl-phytosphingosine; EOS, esterified omega-hydroxyacyl-sphingosine; NP, nonhydroxyacyl-phytosphingosine; AP, α -hydroxyacyl-phytosphingosine; OS, omega-hydroxyacyl-sphingosine; FABP, fatty acid binding protein.

2 Materials and methods

2.1 Ethical approval

This study was approved by the Institutional Review Board of Yonsei University Severance Hospital (IRB no. 4-2018-0334).

2.2 Selection of Patients with HND for basal characteristics analysis

For clinical evaluation of HND patients, a database of approximately 5,007 patients with AD who visited Yonsei University Severance Hospital's Department of Dermatology in 2011 was reviewed retrospectively (10). A query search of patients' electronic medical records with keywords "red face syndrome," "red," "redface," and "Head and Neck Dermatitis" in both English and Korean was also performed.

2.3 Patient selection for the evaluation of *M. furfur* sensitization status

A total of 312 patients were diagnosed with AD at the Department of Dermatology, Severance Hospital, Yonsei University College of Medicine. The diagnosis was made according to the Hanifin and Rajka diagnostic criteria (11). Patients' age and sex were also noted. The severity of AD was assessed using the eczema area and severity index (EASI). Patients with diffuse erythematous patches on the facial skin were categorized into the HND group, whereas the remaining subjects were categorized to the non-HND group. The patients were categorized according to different age groups in which childhood was defined as age less than 12 years, adolescents were aged between 12 and 18 years, and adults were categorized as those older than 18 years. Sensitization to *M. furfur* was assessed using CAP immunoassay. Sensitized status to *M. furfur* was defined by elevation in the levels of IgE specific to *M. furfur* above 0.70 kU/L (Class 2).

2.4 Histological evaluation of facial skin samples

For histological evaluation of HND, a histological database at the Yonsei University Severance Hospital was utilized. A query search of AD patients from 2011 who underwent facial skin biopsy was performed, and five patients were randomly selected from 9 candidates.

Histological analysis of non-HND face specimens was performed through a query search of AD patients who underwent skin biopsy on the face from 2013 for suspected concomitant vitiligo (usually the biopsy is conducted with non-lesional normal skin and lesional skin with vitiligo to compare the melanocyte population). Crude age filtering was performed to age-match AD patients. Among the 10 candidates, five patients were randomly selected for image analysis.

At 200x magnification, the longest distance from the subcorneal level to the basal layer was chosen arbitrarily for epidermal thickness after calibrating the scale bar to pixels. The number of vessels/mm^2 was counted in the dermis of each slide section within a 100 μm distance from the epidermal–dermal junction.

Immunohistochemical staining was performed using paraffin-embedded sections with antibodies against factor VIII-related antigen (1:100, ab236284, Abcam), stromal cell-derived factor-1-alpha (SDF1-α) (1:100, ab25117, Abcam, Cambridge, United Kingdom), Interleukin-1-beta (IL-1-β) (1:100, ab2105, Abcam), tumor necrosis factor-alpha (TNF-α) (1:50, ab1793, Abcam), transforming growth factor-beta (TGF-β) (1:100, ab66043, Abcam), and vascular endothelial growth factor (VEGF) (1:200, ab1316, Abcam). Staining intensity was determined at 400x magnification at a randomly chosen area of the upper dermis. Images were quantified using ImageJ analysis tools (National Institutes of Health, Bethesda, MA).

To calculate the stained area of the antibody, we converted the original image to an 8-bit grayscale image (ImageJ>Image>8-bit), applied a binary threshold, and calculated the percentage positive for the stained part in the standard image. Quantification was performed relative to the entire selected region. The threshold for each staining was set as the average threshold of multiple immunostaining analyses performed by three independent experimenters.

2.5 Co-culture of organisms with human primary cells

Primary normal human epidermal keratinocytes were cultured at 37°C in 5% CO_2 in Epilife medium supplemented with human keratinocyte growth supplement (Gibco, USA). Human microvascular endothelial cells (HMVECs) were cultured at 37°C in 5% CO_2 in EBM-2 basal medium supplemented with EBM-2 growth medium (Lonza, USA).

M. furfur (ATCC 12078) was cultured at 30°C on Difco YM agar supplemented with 1% olive oil. *S. epidermidis* (*Staphylococcus epidermidis*, ATCC 12228) was cultured at 37°C on Difco tryptic soy agar. *C. acnes* (*Cutibacterium acnes*, ATCC 6919) was cultured at 37°C on forced clostridial medium (CM0149; Oxoid) with 2% agar. To induce hypoxia, a BD GasPakTM EZ Pouch was used. All the media were sterilized by autoclaving at 121°C for 15 min.

Organisms were harvested by centrifugation, and the pellet was suspended in the corresponding media. The organisms were heat-killed by incubation at 80°C for 3 min, and then co-cultured with normal human epidermal keratinocytes or human microvascular endothelial cells for 24 h at a density of 1×10^5 cells/mL. To induce allergic environments, recombinant thymic stromal lymphopoietin (TSLP) (50 ng/mL) or IL-4 (50 ng/mL) was used.

2.6 Real-time quantitative PCR

The cells were harvested using trypsin-EDTA (0.25%) and centrifuged. Total RNA was extracted using the RNeasy Plus Mini Kit (Qiagen, Germany), following the manufacturer's instructions. Next, cDNA was generated using a Veriti thermal cycler (Applied Biosystems). Real-time quantitative PCR was performed with cDNA supplemented with the appropriate TaqMan primers using a StepOnePlus PCR system (Applied Biosystems). mRNA expression level was calculated using the 2-ΔΔCT method. The primers used are as follows; VEGF (vascular endothelial growth factor) (Hs00900055_m1), VEGFR (VEGF receptor) (FLT1; Hs01052961_m1), IL-31 (Hs01098710_m1), IL-33 (Hs00369211_m1), TGF-β (Hs00998133_m1), TNF-α (Hs00174128_m1), IL-1β (Hs01555410_m1), and GAPDH (Hs02786624_g1).

2.7 Lipid extraction and quantification of human stratum corneum

The human stratum corneum was collected using D-squame tape (22 mm in diameter; CuDerm, Dallas, Tex) from the facial skin of five subjects from both HND and non-HND groups who provided informed consent. An additional number of five people who did not have any underlying disease history including dermatological conditions were recruited as the control group. Six consecutive D-squame tape strips were collected from each group. The first tape disc was discarded and the remaining tape discs were placed in separate tubes. The tapes were vortexed in 5 mL of methanol for 30 s. The tape debris was removed immediately, and the methanol solution was dried under a nitrogen stream at 30°C.

Total lipid extracts were separated into three fractions using silicic acid column chromatography: neutral lipids (TAG), free fatty acids, and ceramides. Half of the dried extracts were reconstituted in 200 μL of chloroform and loaded into silicic acid columns that were preconditioned with chloroform. After sample loading, each column was washed with 20 mL of chloroform to elute the neutral lipids, 20 mL of chloroform containing 0.2% acetic acid to elute free fatty acids, and 30 mL of methanol to elute the ceramides.

The fatty acid composition of SC lipid fractions was analyzed after derivatization (saponification and methylation) using a gas chromatograph equipped with an SPB-5 capillary column (5% phenol, 30 m, 0.25 mm ID, film thickness: 0.25 μm). The GC operating conditions were as follows: injector temperature, 305°C;

detector temperature, 310°C FID; oven temperature, 175°C; 5°C/min; 300°C (20 min); and carrier gas, He.

The TAG and ceramide fractions of SC lipids were further analyzed using LC-MS/MS for profiling (12). Skin lipids were analyzed using a Nexera2 LC system connected to a triple quadruple mass spectrometer (LCMS 8060; Shimadzu, Kyoto, Japan) with a reversed-phase Kinetex C18 column (100 × 2.1 mm, Phenomenex, Torrance, CA, USA). Mobile phases were water/methanol mixture (1:9, *v*/*v*) with 10 mM ammonium acetate (A) and isopropanol/methanol mixture (5:5, *v*/*v*) with 10 mM ammonium acetate (B). The gradient elution was performed as follows: 0 min (30% of B), 0–15 min (95% of B), 15–20 min (95% of B), and 20–25 min (30% of B). Quantitation was conducted by selected reaction monitoring (SRM) of the $[M + H]^+$ or $[M + NH_4^+]$ ion and related product ion for each lipid species. The concentration of each target lipid species was calculated as the ratio of the target analyte to the internal standard (IS) multiplied by the concentration of the IS. Single-point calibrations of each target lipid species were conducted using a selected IS for each lipid class (NS(d18:1/12:0), NdS(d18:0/12:0), NP(t18:0/8:0), AS(d18:1/18:1), AdS(d18:0/12:0), AP(t18:0/6:0), E(18:2)O(16)S(18), E(18:2)O(16)P(18), A(18:1)NS(d18:1/17:0), A(18:1)NS(d18:1/17:0), sphingosine d_9, OP(t18:0/16:0), OP(t18:0/16:0), OP(t18:0/16:0), and TG 45:0 (15:0/15:0/15:0) for NS, NdS, NP, AS, AdS, AP, EOS, EOP, 1-*O*-Acyl-NS, 1-*O*-Acyl-AS, long chain base (LCB), OS, OP, OH, and TG, respectively).

2.8 Assessment of the effect of ceramide on *M. furfur* colonization

Lyophilized ceramide (esterified omega-hydroxyacyl-sphingosine; EOS) was purchased from Avanti Polar Lipids (USA). EOS was added to sterilized media at 45°C and placed on a magnetic stirrer. *M. furfur* and *C. acnes* were cultured on appropriate culture media discs, and their colonization patterns were observed. The concentrations of ceramide (EOS) were as follows: control (no additional treatment), 2, 5, and 10 μg/mL. Colony area analysis was performed using ImageJ software (13). The observed colony area values were divided by the colony area of the control (no EOS) and compared between different EOS treatments.

Statistical Analysis

The Student's t-test was used for dependent samples, and the nonparametric Mann–Whitney U test was used for comparison of quantitative values between two groups. The Kruskal–Wallis test was used to compare more than two groups. Tukey's multiple comparisons test was used after Kruskal-Wallis test to compare each experimental group against each control group. Quantitative data are described as median and range or as mean ± standard deviation. Statistical differences were considered significant if $p < 0.05$. GraphPad Prism version 9.4.1 for Windows (GraphPad Software, San Diego, CA, USA) and SPSS (version 19.0; SPSS Inc., Chicago, IL, USA) were used to calculate statistical significance.

3 Results

3.1 AD patients with HND exhibited severe clinical/laboratory phenotypes

Among the 5,007 patients with AD, 120 (2.4%) had clinical records indicating HND. The 120 HND and 4,887 non-HND patients were age- and sex-matched using the exact matching method. After eliminating all missing values in the database, 74 HND and 74 non-HND patients were matched for comparison. There were no significant differences in the distribution of age, sex, and disease onset between the HND and non-HND groups (Table 1). Regarding AD phenotypes, there was a higher percentage of extrinsic AD (total serum IgE > 200 IU/mL) in the HND group (Table 1). Interestingly, AD patients with HND showed a higher disease severity, as measured by the EASI score (Table 1. $p<0.0001$) and elevated total IgE (Table 1. p-value<0.0001) during the initial clinic visit.

3.2 Increased sensitization to *M. furfur* in adolescent and adult AD patients with HND

Next, we concentrated on the effect of "fungiome" composition to the HND in AD, especially on *M. furfur*, which has been associated with dandruff (14, 15), HND in AD (4, 16), and AD itself (17). To elucidate the differences in *M. furfur* sensitization status between the HND and non-HND groups, 312 patients were enrolled in the analysis. Of the 312 patients with AD, 75 were in their childhood, 61 were in adolescence, and 176 were adults. The average age of the patients was 24.45 ± 14.56, consisting of 169 male and 143 female AD patients.

The average level of IgE specific to *M. furfur* was 8.57 ± 18.89 kU/L. In the childhood group, the specific IgE level was 1.689 ± 3.46 kU/L, and the levels for the adolescence and adulthood groups were 11.53 ± 22.21 kU/L and 10.48 ± 20.8 kU/L, respectively. The difference between adolescents and adults was not significant, whereas the data were significant for both childhood and adolescence and between childhood and adulthood (Figure 1A; both $p<0.001$) The sex-specific level of specific IgE to *M. furfur* was also assessed, and it was found to be 8.53 ± 19.62 kU/L in males and 8.63 ± 18.05 kU/L in females (Figure 1B). The difference between the two groups was not statistically significant.

3.3 Sensitization to *M. furfur* is associated with increased severity and occurrence of HND

The association between HND and sensitization to *M. furfur* was evaluated. Interestingly, the levels of IgE specific to *M. furfur* was significantly higher in the patients with HND (Figure 1C; 20.61 ± 26.04 vs. 4.07 ± 12.80 kU/L, $p<0.0001$). In addition to laboratory

TABLE 1 Comparison of epidemiological and laboratory characteristics of HND and Non-HND patients.

Characteristics	HND	Non-HND	*p*-value
No. subjects	74	74	
Age, yrs (range)	24 (10-41)	24 (10-41)	>0.9999
Sex			>0.9999
Male, n (%)	48 (64.9)	48 (64.9)	
Female, n (%)	26 (35.14)	26 (35.14)	
Extrinsic AD, n (%)	71 (95.95)	62 (83.78)	0.0038
Onset of AD, yrs			0.4303
Birth~2 years, n (%)	10 (13.51)	11 (14.86)	
3-6 yrs	11 (14.86)	14 (18.92)	
7-12 yrs	10 (13.51)	11 (14.86)	
13-16 yrs	13 (17.57)	10 (13.51)	
16-20 yrs	8 (10.81)	8 (10.81)	
> 20 yrs	20 (27.03)	18 (24.32)	
EASI, score (mean, range)	24.15 (2.00-58.00)	14.64 (0.30-63.40)	<0.0001
Total IgE, IU/mL (mean, range)	3021.3 (39.00-5000.00)	751.9 (9.19-5000.00)	<0.0001

HND, head and neck dermatitis; Non-HND, non-head and neck dermatitis; AD, atopic dermatitis; EASI, Eczema Area and Severity Index.
Paired Student's t-test was done for statistical analysis.

characteristics, the association between the presence of HND and clinical severity, which was measured using the EASI score, revealed that clinical severity was significantly higher in HND patients (Figure 1D; 24.12 ± 15.90 vs. 14.28 ± 11.50, p<0.0001).

The patients were categorized according to their sensitization to *M. furfur*. Of the 312 patients, 142 were sensitized and the remaining 170 were non-sensitized. EASI scores of the *M. furfur* sensitized AD patients were significantly higher than those of the non-sensitized group (Figure 1E; 21.91 ± 14.59 vs. 12.83 ± 11.07, p<0.0001). These data indicate that sensitization to *M. furfur* not only affects the risk of HND in AD but might also contribute to the overall severity of AD.

3.4 Comparison of histopathological characteristics between HND and non-HND subjects

To investigate histological differences between the HND and non-HND groups, skin biopsy specimens were examined by hematoxylin and eosin staining. In HND pathology, a general trend of hyperkeratosis, acanthosis, and parakeratosis was observed, with dense inflammatory cells surrounding the increased vasculature (Figure 2A). The average epidermal thickness in HND group (412.5(292.8–532.1) μm) was significantly higher than that of the non-HND group (179.6 (140.9–205.3) μm) (Figure 2B; p<0.05).

Increased vascularity in HND patients was confirmed by immunohistochemical staining for factor VIII-related antigens (Figure 2C). Average vessel count for HND group was 15 (12–19) with a concurrent average vessel area of 221.4 (159.8–273.4) μm^2. The average vessel count in non-HND histology was 4.5 (3–6) with an average vessel area of 101.0 (78.9–177.3) μm^2. The differences in vessel counts and average vessel sizes were statistically significant (Figures 2D, E; both p<0.05).

Next, immunohistochemical staining of pro-inflammatory cytokines and chemokines was performed to confirm the presence of inflammatory mediators in HND lesions. The evaluated molecules included TNF-α, TGF-β, IL-1β, SDF1-α, and VEGF. As a result of IHC staining, all molecules showed significantly higher signal in HND group, confirming that the HND patients' facial skin show intense inflammatory circumstance than non-HND group. (Figures 3A–F; SDF1-α, p<0.01; IL-1β, p<0.05; TGF-β, p<0.01, TNF-α, p<0.01; VEGF, p<0.001),

3.5 VEGF, VEGFR, IL-31, and IL-33 levels were upregulated in keratinocytes cultured with *M. furfur*

Malassezia spp. colonization/abundance is known to be linked with AD pathogenesis, as AD patients often exhibit hypersensitization to *Malassezia* spp. with higher *Malassezia*-specific IgE levels (18–21). These findings from previous studies indicate the possibility of a positive association between *Malassezia* spp. abundance and hypersensitivity.

Thus, the effects of *M. furfur* colonization on skin were evaluated *in vitro* (Figure 4A). First, keratinocytes (normal human epidermal keratinocytes) were cultured with either *M.*

10.3389/fimmu.2023.1114321

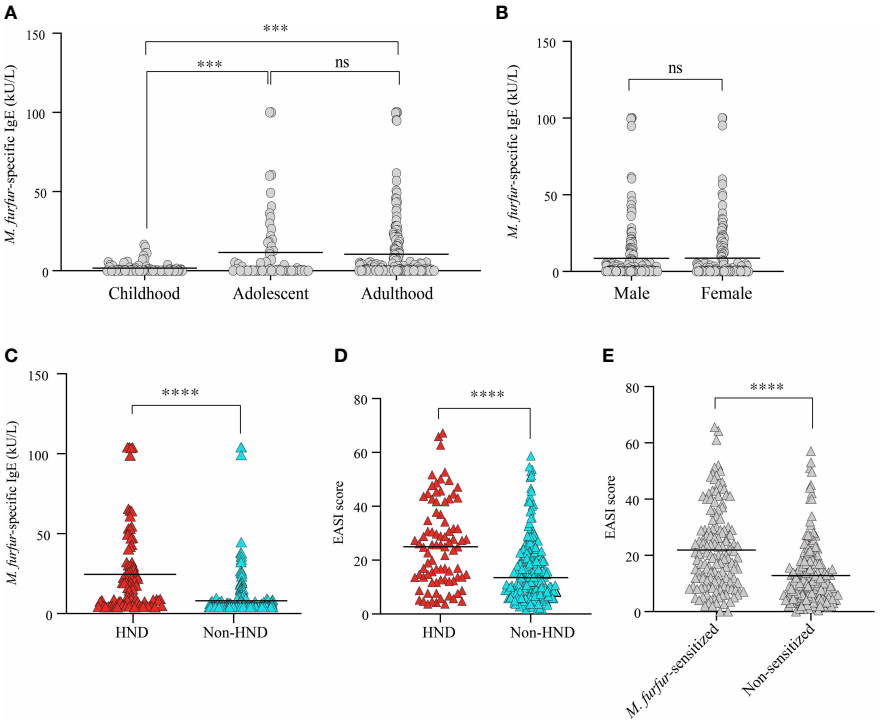

FIGURE 1
Comparison of serum *M. furfur*-specific IgE level according to **(A)** age groups, **(B)** sex, and **(C)** the presence of HND. Clinical severity according to **(D)** the presence of HND, **(E)** *M. furfur* sensitization status. (Unpaired t-test, **(A)** Childhood vs. Adolescent; p = 0.0002, Adulthood vs. Adolescent; p = 0.7392, Adulthood vs. Childhood; p = 0.0003, **(B)** p = 0.9634, **(C)** p< 0.0001 **(D)** p< 0.0001 **(E)** p< 0.0001) HND, Head and neck dermatitis. *** : p<0.001; **** : p<0.0001; ns, Not Significant (p >0.05).

furfur or *S. epidermidis*, and the expression levels of VEGF, VEGFR, IL-31, and IL-33 were evaluated. To create an environment similar to that of AD, TSLP and IL-4 were used. As shown in Figure 4B, the expression levels of VEGF, VEGFR, IL-31, and IL-33 were significantly increased when the cells were co-cultured with *M. furfur* and treated with TSLP (VEGF, p<0.01; VEGFR, p<0.01, IL-31; p<0.05; IL-33, p<0.05). No significant increase in expression was observed in keratinocytes co-cultured with *S. epidermidis*. The

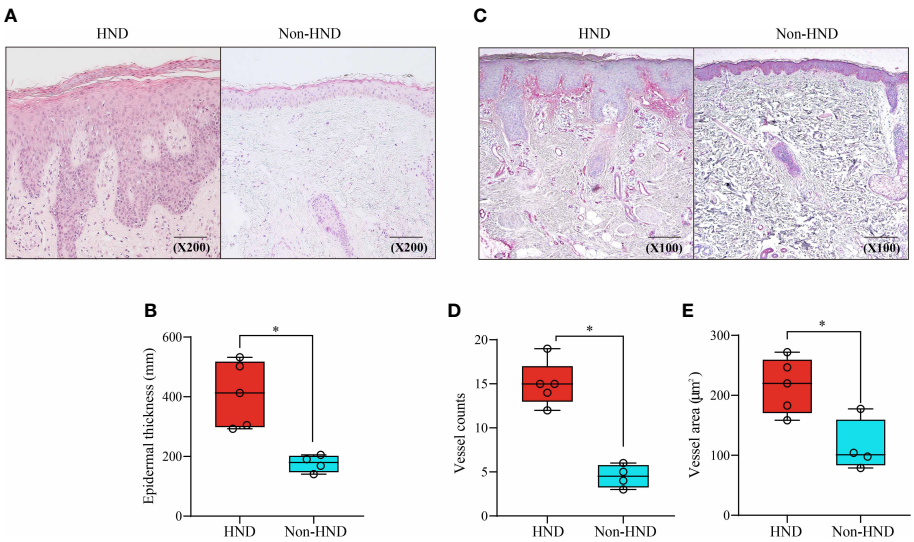

FIGURE 2
Histopathological comparison of facial skin of HND and non-HND subjects. **(A)** Representative image biopsy specimen of HND (left) and non-HND (right) facial pathology. **(B)** Average epidermal thickness of patients with HND was higher than that of non-HND subjects. (200x magnification) **(C)** Immunohistochemistry of the upper dermis for factor VIIIa-related antigen of patients with (left) and without (right) HND. (200x magnification) **(D)** Average vessel count and average vessel area of patients with HND was significantly higher than that of non-HND subjects. (Mann-Whitney U Test, **(B)** p = 0.0159, **(D)** p = 0.0159 **(E)** p = 0.0317) HND, Head and neck dermatitis. * : p<0.05.

10.3389/fimmu.2023.1114321

expression levels did not increase when cells were not treated with TSLP. As shown in Figure 4C, similar results were observed when cells were treated with IL-4, except for VEGF (VEGF, p = 0.1244; VEGFR, p<0.05, IL-31; p<0.05, IL-33; p<0.05). These results suggest that *M. furfur* induces the production of cytokines related to AD, further exacerbating disease severity, and that the expression of VEGF, which induces angiogenesis, may contribute to the erythema observed in HND of AD.

3.6 *M. furfur* induced increased expression levels of VEGFR, TGF-β, TNF-α, and IL-1β in endothelial cells

Figure 4D depicts the effect of *M. furfur* on endothelial cells. Human microvascular endothelial cells were co-cultured with *M. furfur* and treated with IL-4 using the same protocol as that used for keratinocytes. The increase in the expression levels of VEGFR,

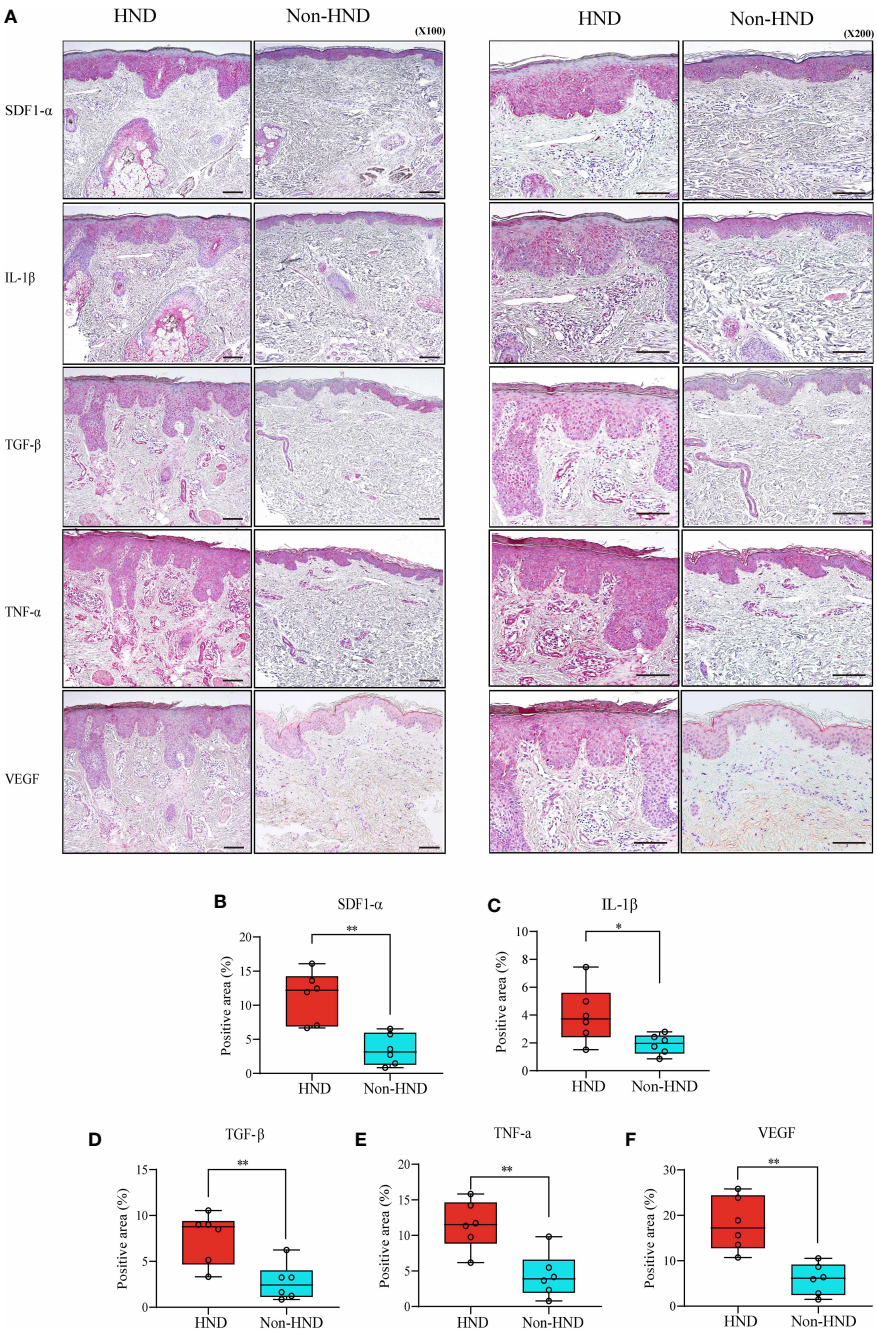

FIGURE 3
Immunohistochemistry of HND and non-HND facial skin specimens. **(A)** Representative histological image at 100x magnification (left) and 200x magnification (right). Quantified staining intensity of **(B)** SDF-1α, **(C)** IL-1β, **(D)** TGF-β, **(E)** TNF-α, and **(F)** VEGF. (Unpaired two-tailed t-test, SDF-1α; p = 0.0014, IL-1β; p = 0.0374, TGF-β; p = 0.0058, TNF-α; p = 0.0035, VEGF; p = 0.0002) HND, head and neck dermatitis; SDF-1 *α*, stromal cell-derived factor-1-alpha; IL-1 *β*, Interleukin-1-beta; TGF- *β*, transforming growth factor-beta; TNF- *α*, tumor necrosis factor-alpha; VEGF, vascular endothelial growth factor. * : p<0.05; ** : p<0.01.

TGF-β, TNF-α, and IL-1β was most significant when the endothelial cells were co-cultured with *M. furfur* and treated with IL-4 (Figure 4D; VEGFR, p<0.05; TGF-β, p<0.001; TNF-α, p<0.001, IL-1β; p<0.001). However, this tendency was not observed in endothelial cells co-cultured with *S. epidermidis*. These results imply that *M. furfur* also affects endothelial cells, inducing the production of pro-inflammatory cytokines, such as TGF-β, TNF-α, and IL-1β, as well as VEGFR, which further promote vascular proliferation.

3.7 Decreased ceramide in AD patients with HND

Malassezia spp. are well known for their ability to produce lipases (22) that break down cutaneous lipid components into unsaturated fatty acids, oleic acid, and arachidonic acid (23, 24). Therefore, we investigated the lipid composition of the stratum corneum, which is essential for the maintenance of skin barrier function.

Tape stripping was performed on the facial skin of patients with HND and those without HND, with five subjects in each group. Five additional subjects without any underlying disease were also tested as controls. Patients with HND had significantly higher erythema index and transepidermal water loss levels in the facial area, which supported the presence of HND (Table 2). Among the various ceramides from the stratum corneum, phytoceramide NP (nonhydroxyacyl-phytosphingosine), AP (α-hydroxyacyl-phytosphingosine), and EO (esterified omegahydroxyacyl) type ceramides (EOS (esterified omega-hydroxyacyl-sphingosine), and EOP (esterified omega-hydroxyacyl-phytosphingosine)) were found to be significantly reduced in the HND group when

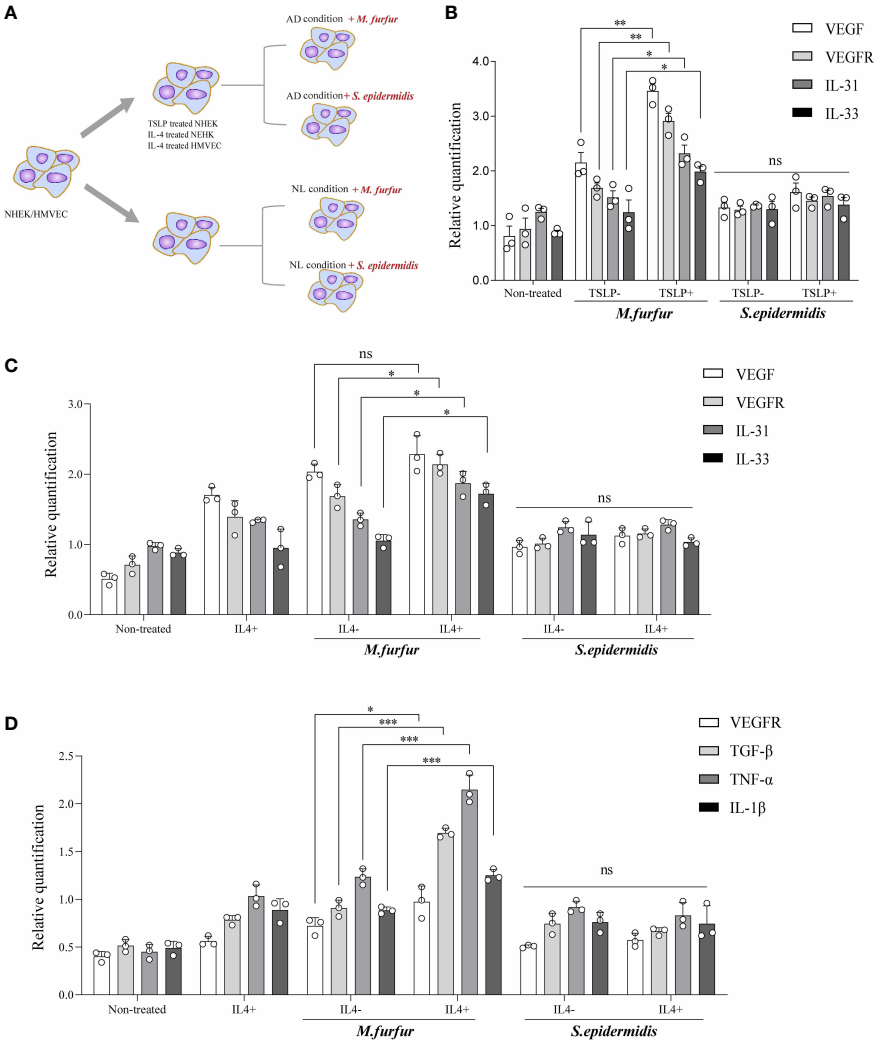

FIGURE 4
In vitro experiments showing **(A)** increased expression levels of VEGF, VEGFR, IL-31, and IL-33 in keratinocytes cultured with *M. furfur*, supplemented with **(B)** TSLP or **(C)** IL-4. *M. furfur* induced increased expression levels of VEGFR, TGF-β, TNF-α, and IL-1β in **(D)** endothelial cells supplemented with IL-4. (three replicates for each column, Unpaired t-test, **(B)** VEGF; p = 0.0044, VEGFR; p = 0.0019, IL-31; p = 0.0145, IL-33; p = 0.0381, **(C)** VEGF; p = 0.1244, VEGFR; p = 0.0244, IL-31; p =0.0382, IL-33; p = 0.0117, **(D)** VEGFR; p-value 0.0266, TGF-β; p-value 0.0002, TNF-α; p-value 0.0009, IL-1β; p-value 0.0009). * : p<0.05; ** : p<0.01; *** : p<0.001; ns, Not Significant (p>0.05).

compared to the non-HND and control groups (Figure 5A, NP; p<0.01, AP; p<0.05, EOS; p<0.01, EOP; p<0.01). However, when the non-HND group was compared to the healthy controls, no significant differences were found. Next, individual lipid components belonging to each ceramide type that varied significantly were compared. In the case of NP- and AP-type ceramides, there was individual lipids with no significant difference between non-HND group and healthy controls. Some individual lipid components showed statistical differences between HND group and non-HND/healthy controls (Figure 5B, t18:0/24:0; p<0.05, t18:0/25:0; p<0.05, t18:0/26:0; p<0.05, t18:0/27:0; p<0.01, t18:0/28:0; p<0.01, Figure 5C, t18:0/24:0; p<0.05, t18:0/25:0; p<0.01, t18:0/26:0; p<0.01). However, all individual lipid components belonging to the EO-type ceramides exhibited statistically significant differences between HND group and non-HND/healthy controls while non-HND group and healthy controls showed no significant difference (Figure 5D, E(18:2)O(28)S(18); p<0.01, E(18:2)O(29)S(18); p<0.01, E(18:2)O(30)S(18); p<0.01, E (18:2)O(31)S(18); p<0.01, E(18:2)O(32)S(18); p<0.01, Figure 5E, E (18:2)O(29)P(18); p<0.05, E(18:2)O(30)P(18); p<0.01, E(18:2)O (31)P(18); p<0.01, E(18:2)O(32)P(18); p<0.001, E(18:2)O(33)P (18); p<0.01, E(18:2)O(34)P(18); p<0.01).

In the above analysis, the decrease ratio between Non-HND/Control to HND group was more prominent in EO type ceramides (EOS, EOP) than that of other types. Among the four EO type ceramides, EOS ceramide is regarded as the main ceramide component of the epidermis (25). In the epidermis, EOS is converted to ω-hydroxyacyl-sphingosine (OS) ceramide. The converted OS is attached to the cornified envelope to maintain the skin barrier function (26–29). Based on the above results and that of previous studies, OS ceramides were analyzed after the extraction of hydrolyzed unbound ceramides. As a result, OS ceramides, which are the most abundant in the stratum corneum, were found to be significantly decreased in the HND group when compared to that in the non-HND and control groups (Figure 6A, OS; p<0.01, OP; p = 0.3833, OH; p = 0.2839). In addition, when the individual lipid components were compared among the three groups, statistically significant differences were found mostly in those belonging to OS-type ceramides (Figure 6B, t18:0/31:0; p = 0.2516, t18:0/32:0; p<0.01, t18:0/34:0; p = 0.538, Figure 6C, t16:1/36:0; p = 0.2839, Figure 6D, d17:1/30:0; p<0.01, d18:1/30:0; p<0.05, d18:1/31:0; p<0.01, d18:1/32:0; p<0.001, d20:1/30:0; p<0.01, d20:1/31:0; p<0.01, d20:1/32:0; p<0.01). These data indicate that ceramide levels, especially EOS-type ceramides, are downregulated in HND. Considering the ability of *Malassezia* spp. to produce lipases, it can be inferred that the *Malassezia* spp. colonization might have been involved in the decreased stratum corneum ceramide levels of HND patients.

3.8 Inhibitory effect of OS-type ceramide on the colonization of M. furfur

Finally, we investigated whether the restoration of OS-type ceramides could reduce the colonization of *Malassezia* spp. *in vitro* (Figure 7A). To assess the effect of ceramide on the growth of *M. furfur*, 0, 2, 5, and 10 μg of EOS (esterified ω-hydroxyacyl-sphingosine) ceramide were added to the growth medium of *M. furfur*. *C. acnes*, the most common bacteria in the normal flora of facial skin, was used as a control, and the same experimental protocol was applied. For *C. acnes*, the total area of colonization did not vary with the concentrations of ceramide (Figure 7B). In contrast, in the case of *M. furfur*, as the concentration of ceramide increased, the total area of colonization of *M. furfur* decreased significantly (Figure 7C, Tukey's multiple comparisons test; control vs. 2μg/mL; p< 0.001, control vs. 5μg/mL; p< 0.001, control vs. 10 μg/mL; p< 0.001). These data indicate that ceramide, especially EOS ceramide, inhibits the growth of *M. furfur*.

4 Discussion

AD is a chronic condition that severely affects patients' quality of life (30), and among its various clinical features, HND may be one of the most deleterious symptoms, as the facial skin is involved. Even after the emergence of biologics, including dupilumab, head and neck dermatitis is often encountered in patients with AD (31–33). Therefore, it is necessary to explore the influence of skin barrier and microbes on the occurrence of HND, in addition to the direct blocking of the Th2 response.

Previous reports have identified a link between *M. furfur* and HND in AD (34–37), as its specific IgE levels were significantly increased in these patients. To verify this relationship further, *M. furfur*-specific IgE levels of 312 patients were analyzed and similar results were obtained. In addition to previous findings, patients sensitized to *M. furfur* were found to have significantly higher

TABLE 2 Basal characteristics, EI, TEWL, and total serum IgE of study subjects.

Characteristics HND	HND	N-HND	NL	*p*-value
Age, yrs (range)	31 (27-51)	26 (19-28)	31 (22-38)	0.0828
Male, n (%)	2 (40)	4 (80)	4 (80)	0.3263
EI, arbitrary unit (range)	574 (373-617)	320 (274-383)	352 (274-393)	0.0172
TEWL, g/m^2/h (range)	45 (30-74)	26 (14-31)	19 (9-26)	0.01
Total IgE, IU/mL (range)	2529 (29.9-5000)	2530 (193-5000)	15.7 (8.52-397)	0.0226

EI, erythema index; TEWL, transepidermal water loss; HND, head and neck dermatitis, N-HND, non-head and neck dermatitis, NL, normal.
Kruskal–Wallis test was done for statistical analysis (significant if p<0.05).

disease severity. In addition, *M. furfur*-specific IgE levels significantly increased in adolescents and adults compared to pediatric patients, correlating with the increase in subjects with HND after adolescence.

Histopathological studies of adult AD patients with recalcitrant facial erythema revealed a mixture of eczematous and steroid-induced rosacea-like changes (38). Similarly, histological observations in our study revealed hyperkeratosis, acanthosis, parakeratosis, and increased vessels in HND lesions. An increase in the number and average area of vessels in the dermis, confirmed with factor VIII-related antigen, most probably underlies the intense redness noted in patients with HND. Along with the increased vessel counts and vessel area, a higher erythema index indicates that the increase in dermal vasculature may be closely associated with the development of HND in AD patients.

Although a possible link between *M. furfur* and HND has been suggested by various clinical/epidemiological/laboratory studies, the specific mechanism underlying its pathogenesis is largely unknown, with few *in vitro* experimental studies. To determine the effect of *M. furfur*, keratinocytes were co-cultured with *M. furfur* and the expression levels of various cytokines were assessed. Furthermore, as AD is Th2-mediated (39), cells were treated with the associated cytokines, TSLP and IL-4, and compared. Keratinocytes co-cultured with *M. furfur* and treated with either TSLP or IL-4 exhibited significantly increased expression levels of VEGF, VEGFR, IL-31, and IL-33. IL-31 is a cytokine involved in AD that is predominantly associated with pruritus (40), and *M. furfur* has been found to enhance its production, which may contribute to augmented pruritic symptoms. IL-33 is mainly produced by keratinocytes and is associated with the pathogenesis of AD, including tissue remodeling and fibrosis in chronic AD (41). In addition, a recent study indicated that the sebum-microbial metabolite-IL-33 axis may play a role in initiating atopic dermatitis (42). *M. furfur* induces the expression of these cytokines in keratinocytes, which is further enhanced by the Th2 milieu in AD, which may contribute to the exacerbation of the disease (43).

To assess whether endothelial cells were also affected by *M. furfur*, a similar experiment was performed on endothelial cells. *M. furfur*, under the influence of Th2 cytokines, enhanced the production of VEGFR, IL-1β, TNF-α, and TGF-β in HMVEC. Increased expression level of VEGFR leads to increased vascular proliferation and expression of pro-inflammatory cytokines, including IL-1β, TNF-α, and TGF-β, leading to increased inflammatory responses. *M. furfur*, under the influence of Th2 cytokines, leads to angiogenesis and an increase in AD-related cytokines as well as other inflammatory cytokines that may contribute to the exacerbation of skin symptoms.

Skin barrier defects are a crucial part of the pathogenesis of AD and are characterized by decreased ceramide levels in the stratum corneum (44). To determine any possible differences in the skin barrier between AD patients with and without HND, tape stripping was performed on facial skin. Our study indicated that the levels of ceramides were reduced, especially those of EOS, and EOP, in patients with HND compared to those without HND. Ceramides, especially EOS ceramides, which link corneocytes and extracellular lipids, form the extracellular lipid envelope in the stratum corneum and are crucial for the repair of the skin barrier (45, 46). This confirms an additional skin barrier defect in AD patients with HND, which may be associated with the development of HND in AD. Also, the decrement of ceramides might lead to the increased fatty acids in epidermis. These free fatty acids from ceramides might be able to induce chronic inflammation with the aids of fatty acid binding proteins (FABPs) which is known to be associated with Th17 inflammation (47), especially in atopic dermatitis and psoriasis (48, 49). Th17 inflammation is well known for their anti-fungal activities (50–52), so the relationship between the decreased ceramides level in the facial skin of HND patients, FABPs, and Th17 immune response might have to be explored in the near future.

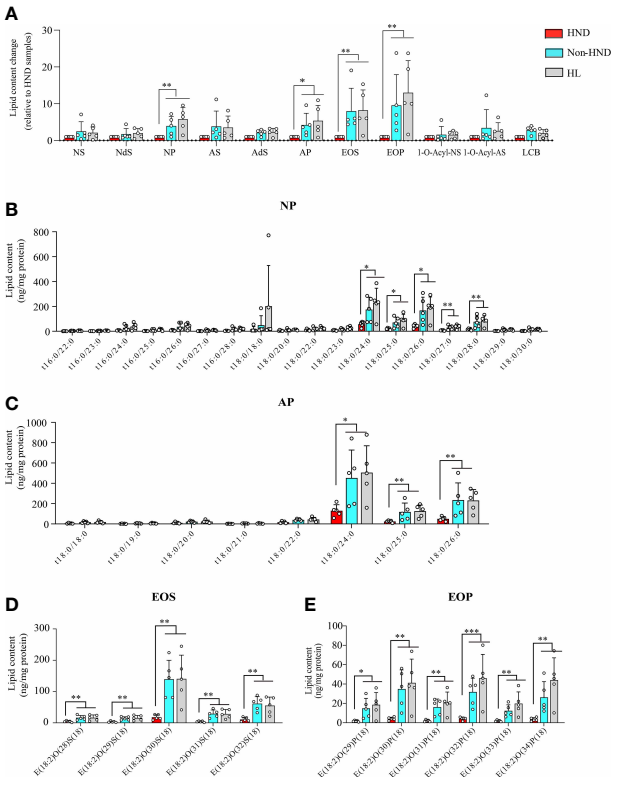

FIGURE 5
Decreased ceramide in AD patients with HND. **(A)** Overall differences in the amounts of various ceramide types according to the presence of HND. Individual ceramide components belonging to ceramide types, which were significantly reduced in HND patients; **(B)** NP, **(C)** AP **(D)** EOS, **(E)** EOP. (five replicates for each column, Mann-Whitney U Test, **(A)** NP; p = 0.0031, AP; p = 0.0111, EOS; p = 0.0029, EOP; p = 0.0012, **(B)** t18:0/24:0; p = 0.0431, t18:0/25:0; p = 0.0272, t18:0/26:0; p = 0.018, t18:0/27:0; p = 0.0035, t18:0/28:0; p = 0.0029, **(C)** t18:0/24:0; p = 0.0176, t18:0/25:0; p = 0.0021, t18:0/26:0; p = 0.0024, **(D)** E(18:2)O(28)S(18); p = 0.0055, E(18:2)O(29)S(18); p = 0.0055, E(18:2)O(30)S(18); p = 0.0029, E(18:2)O(31)S(18); p = 0.0024, E(18:2)O(32)S(18); p = 0.0024, **(E)** E(18:2)O(29)P(18); p = 0.0105, E(18:2)O(30)P(18); p = 0.0024, E(18:2)O(31)P(18); p = 0.0029, E(18:2)O(32)P(18); p = 0.0009, E(18:2)O(33)P(18); p = 0.0012, E(18:2)O(34)P(18); p = 0.0012)
Abbreviations: NP, nonhydroxyacyl phytosphingosine; AP, α-hydroxyacyl-phytosphingosine; EOS, esterified ω-hydroxyacyl sphingosine; EOP, esterified ω-hydroxyacyl phytosphingosine; HND, head and neck dermatitis; Non-HND, non-head and neck dermatitis; HL, healthy control. * : p<0.05; ** : p<0.01; *** : p<0.001.

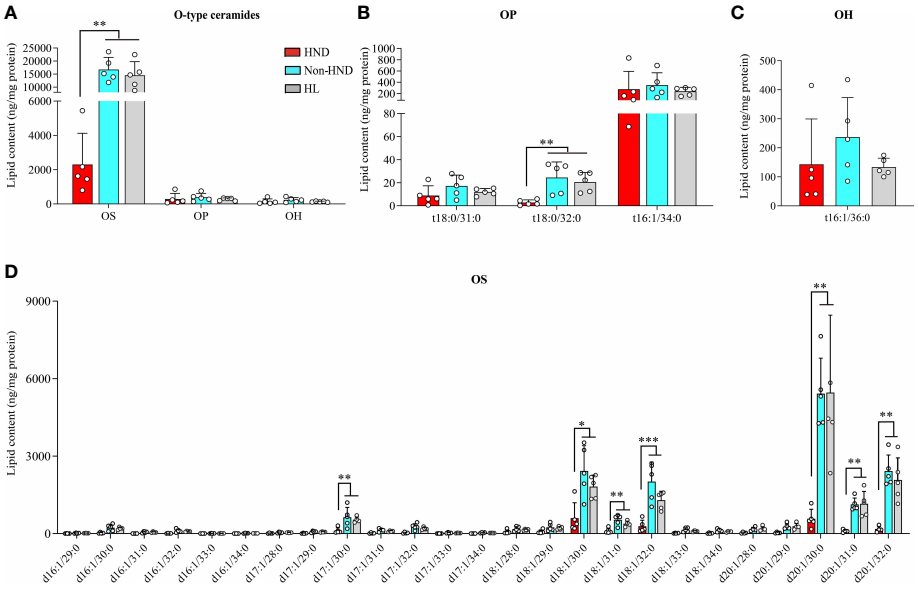

FIGURE 6
ω-Hydroxyceramides (O-type ceramides) contents in human stratum corneum. **(A)** Overall O type ceramides **(B)** OP type ceramides, **(C)** OH (t16:1/36:0) ceramides, and **(D)** OS type ceramides. (five replicates for each column, Mann-Whitney U Test, **(A)** OS; p = 0.0018, OP; p = 0.3833, OH; p = 0.2839, **(B)** t18:0/31:0; p = 0.2516, t18:0/32:0; p = 0.0021, t18:0/34:0; p = 0.538, **(C)** t16:1/36:0; p = 0.2839, **(D)** d17:1/30:0; p = 0.0055, d18:1/30:0; p = 0.0117, d18:1/31:0; p = 0.005, d18:1/32:0; p = 0.0006, d20:1/30:0; p = 0.0029, d20:1/31:0; p = 0.0029, d20:1/32:0; p = 0.0012) Abbreviations: OP, ω-hydroxyacyl phytosphingosine; OH, ω-hydroxyacyl 6-hydroxydsphingosine; OS, ω-hydroxyacyl sphingosine; HND, head and neck dermatitis; Non-HND, non-head and neck dermatitis; HL, healthy control. * : p<0.05; ** : p<0.01; *** : p<0.001.

As the decrease in ceramide levels was confirmed in HND, its possible association with the colonization of *M. furfur* was assessed. The growth of *M. furfur* on the culture medium was evaluated based on the number of colonies formed, and different concentrations of EOS ceramide were added to evaluate whether the growth of *M. furfur* was affected by the addition of ceramide. *C. acnes*, a representative species that constitutes the normal flora of the skin, especially the face, was used as a control. As seen in the results, the number of colonies of *M. furfur* significantly decreased with increasing concentrations of EOS ceramide. However, the

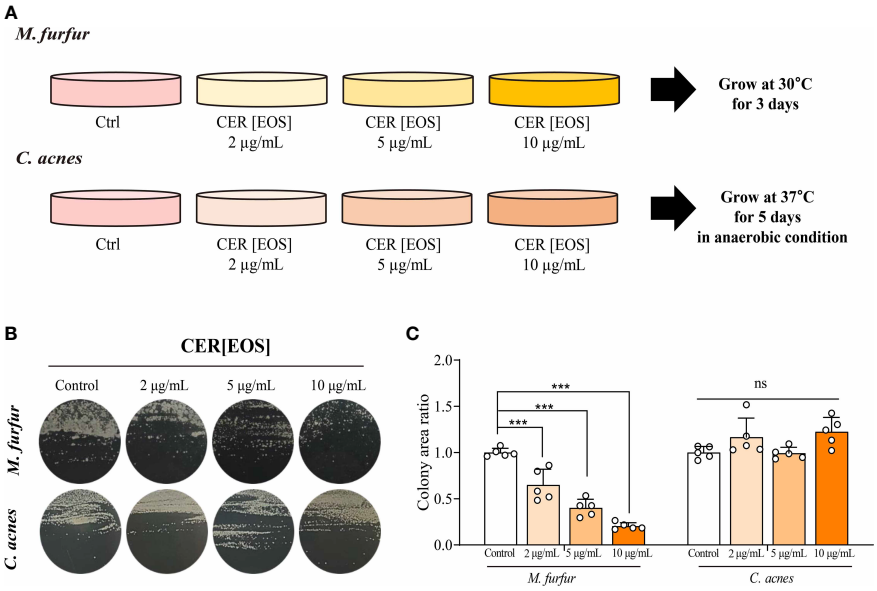

FIGURE 7
Inhibitory effect of OS-type ceramide on the colonization of *M. furfur*. **(A)** Representative image showing the gross morphology of colonies from (up) *M. furfur* and (down) *C. acnes*. **(B)** Quantified area of colonies from (left) *M. furfur* and (right) *C. acnes*. (Five replicates for each column, Tukey's multiple comparisons test; control vs. 2μg/mL; p< 0.001, control vs. 5μg/mL; p< 0.001, control vs. 10 μg/mL; p< 0.001). *** : p<0.001; ns, Not Significant (p>0.05).

growth of *C. acnes* was not altered by ceramide. Ceramide levels are lowered in the facial skin of AD patients with HND, and this decrease may enhance the growth and colonization of *M. furfur*.

Some limitations of our study include the limited number of subjects enrolled in lipid analysis from stratum corneum by LC-MS/MS. The statistical methods did not consider the normality of the data due to the low number of samples; hence, further studies might be needed to confirm these data. Moreover, the effect of ceramide on the colonization of *M. furfur* was verified *in vitro*. Further research might be needed to confirm these findings with an *in vivo* AD mouse model and clinical trials with human subjects. Finally, the effect of the microbiome on the development of HND was not evaluated. Especially, *Staphylococcus* species (including *Staphylococcus aureus* and *Staphylococcus epidermidis*) are well-known skin commensal bacteria engaged in the development/exacerbation of AD. Therefore, the relationship between HND and mycobiome (especially *M. furfur*) from our study needs to be interpreted carefully.

Thus, *M. furfur* proliferates in the facial skin of patients suffering from HND due to decreased levels of ceramide, which inhibits *M. furfur* growth. As *M. furfur* proliferates, it induces keratinocytes to produce various cytokines, which are further enhanced by the Th2 milieu of AD as well as other factors, including VEGF, leading to vascular proliferation. This leads to enhanced production of various pro-inflammatory cytokines and vascular proliferation, resulting in exacerbation of the disease (Figure 8). Therefore, levels of IgE specific to *M. furfur* may be evaluated in AD patients with refractory HND.

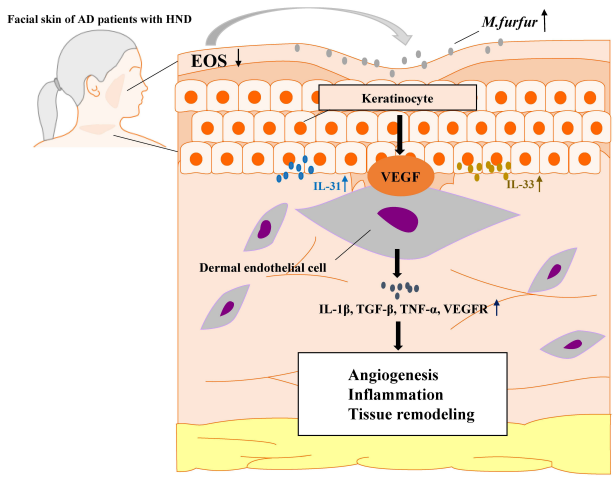

FIGURE 8
A schematic graph of one pathogenetic flow of HND development in AD patients. *M. furfur* proliferates in the facial skin of patients suffering from HND due to decreased levels of ceramide, which induce keratinocytes to secrete Th2 cytokines (IL-31, IL-33) and vascular endothelial growth factor (VEGF), thereby causing dermal endothelial cells to produce various cytokines to induce angiogenesis, exacerbating eczematous inflammation and tissue remodeling.

Data availability statement

The original contributions presented in the study are included in the article/supplementary material. Further inquiries can be directed to the corresponding authors.

Ethics statement

The studies involving human participants were reviewed and approved by Institutional Review Board of Yonsei University Severance Hospital. Written informed consent to participate in this study was provided by the participants' legal guardian/next of kin.

Author contributions

KL, CP, and HC conceived the project and design the study. HC, SMK, KZ, ZW, HL, JK, SHK, HK, WK, and YK collected the data and performed the experiments. HC and SMK wrote the first version of the manuscript. HC, KZ, SMK, and ZW integrated the data and made figures. K-HL supervised a lipid analysis in the skin. YL supervised a mycobiome analysis. CP and K-HL directed the whole experiments and edited the manuscript. All authors contributed to the article and approved the submitted version.

Funding

This study was supported by the National Research Foundation of Korea grants funded by the Korea government (Ministry of Science and ICT) (No. NRF-2020R1A2C1009916 and NRF-2021R1A4A5032185 [to C.O.P.]), grants of the Korea Health Technology R&D Project through the Korea Health Industry Development Institute (KHIDI), funded by the Ministry of Health & Welfare, Republic of Korea (grant HI14C1324 [to C.O.P.] and grant HP20C0018 [to K-H.L.]), and a faculty research grant of Yonsei University College of Medicine (6-2021-0074 [to C.O.P.]).

Acknowledgments

We would like to thank Editage (www.editage.co.kr) for English language editing.

Conflict of interest

The authors declare that the research was conducted in the absence of any commercial or financial relationships that could be construed as a potential conflict of interest.

Publisher's note

References

1. Langan SM, Irvine AD, Weidinger S. Atopic dermatitis. *Lancet (London England)* (2020) 396(10247):345–60. doi: 10.1016/s0140-6736(20)31286-1

2. Park CO, Kim HL, Park JW. Microneedle transdermal drug delivery systems for allergen-specific immunotherapy, skin disease treatment, and vaccine development. *Yonsei Med J* (2022) 63(10):881–91. doi: 10.3349/ymj.2022.0092

3. Guglielmo A, Sechi A, Patrizi A, Gurioli C, Neri I. Head and neck dermatitis, a subtype of atopic dermatitis induced by malassezia spp: Clinical aspects and treatment outcomes in adolescent and adult patients. *Pediatr Dermatol* (2020) 38(1):109–14. doi: 10.1111/pde.14437

4. Zhang E, Tanaka T, Tajima M, Tsuboi R, Kato H, Nishikawa A, et al. Anti-Malassezia-Specific ige antibodies production in Japanese patients with head and neck atopic dermatitis: Relationship between the level of specific ige antibody and the colonization frequency of cutaneous malassezia species and clinical severity. *J Allergy* (2011) 2011:645670. doi: 10.1155/2011/645670

5. Brodska P, Panzner P, Pizinger K, Schmid-Grendelmeier P. Ige-mediated sensitization to malassezia in atopic dermatitis: More common in Male patients and in head and neck type. *Dermatitis Contact Atopic Occupational Drug* (2014) 25(3):120–6. doi: 10.1097/der.0000000000000040

6. Bayrou O, Pecquet C, Flahault A, Artigou C, Abuaf N, Leynadier F. Head and neck atopic dermatitis and malassezia-Furfur-Specific ige antibodies. *Dermatol (Basel Switzerland)* (2005) 211(2):107–13. doi: 10.1159/000086438

7. Kaffenberger BH, Mathis J, Zirwas MJ. A retrospective descriptive study of oral azole antifungal agents in patients with patch test-negative head and neck predominant atopic dermatitis. *J Am Acad Dermatol* (2014) 71(3):480–3. doi: 10.1016/j.jaad.2014.04.045

8. Baroni A, Perfetto B, Paoletti I, Ruocco E, Canozo N, Orlando M, et al. Malassezia furfur invasiveness in a keratinocyte cell line (Hacat): Effects on cytoskeleton and on adhesion molecule and cytokine expression. *Arch Dermatol Res* (2001) 293(8):414–9. doi: 10.1007/s004030100248

9. Grice EA, Dawson TLJ. Host-microbe interactions: Malassezia and human skin. *Curr Opin Microbiol* (2017) 40:81–7. doi: 10.1016/j.mib.2017.10.024

10. Chu H, Shin JU, Park CO, Lee H, Lee J, Lee KH. Clinical diversity of atopic dermatitis: A review of 5,000 patients at a single institute. *Allergy Asthma Immunol Res* (2017) 9(2):158–68. doi: 10.4168/aair.2017.9.2.158

11. Hanifin JM. Diagnostic features of atopic dermatitis. *Acta Derm Venereol* (1980) 92:44–7. doi: 10.2340/00015555924447

12. Lee J-Y, Jeon S, Han S, Liu K-H, Cho Y, Kim K-P. Positive correlation of triacylglycerols with increased chain length and unsaturation with Ω-O-Acylceramide and ceramide-Np as well as acidic ph in the skin surface of healthy Korean adults. *Metabolites* (2023) 13(1):31. doi: 10.3390/metabo13010031

13. Schneider CA, Rasband WS, Eliceiri KW. Nih image to imagej: 25 years of image analysis. *Nat Methods* (2012) 9(7):671–5. doi: 10.1038/nmeth.2089

14. Park M, Cho YJ, Lee YW, Jung WH. Whole genome sequencing analysis of the cutaneous pathogenic yeast malassezia restricta and identification of the major lipase expressed on the scalp of patients with dandruff. *Mycoses* (2017) 60(3):188–97. doi: 10.1111/myc.12586

15. Kim SY, Kim SH, Kim SN, Kim AR, Kim YR, Kim MJ, et al. Isolation and identification of malassezia species from Chinese and Korean patients with seborrheic dermatitis and in vitro studies on their bioactivity on sebaceous lipids and il-8 production. *Mycoses* (2016) 59(5):274–80. doi: 10.1111/myc.12456

16. Kaga M, Sugita T, Nishikawa A, Wada Y, Hiruma M, Ikeda S. Molecular analysis of the cutaneous malassezia microbiota from the skin of patients with atopic dermatitis of different severities. *Mycoses* (2011) 54(4):e24–8. doi: 10.1111/j.1439-0507.2009.01821.x

17. Yim SM, Kim JY, Ko JH, Lee YW, Choe YB, Ahn KJ. Molecular analysis of malassezia microflora on the skin of the patients with atopic dermatitis. *Ann Dermatol* (2010) 22(1):41–7. doi: 10.5021/ad.2010.22.1.41

18. Abdillah A, Ranque S. Chronic diseases associated with malassezia yeast. *J Fungi (Basel)* (2021) 7(10):855. doi: 10.3390/jof7100855

19. Prohic A, Jovovic Sadikovic T, Krupalija-Fazlic M, Kuskunovic-Vlahovljak S. Malassezia species in healthy skin and in dermatological conditions. *Int J Dermatol* (2016) 55(5):494–504. doi: 10.1111/ijd.13116

20. Faergemann J. Atopic dermatitis and fungi. *Clin Microbiol Rev* (2002) 15 (4):545–63. doi: 10.1128/cmr.15.4.545-563.2002

21. Glatz M, Bosshard PP, Hoetzenecker W, Schmid-Grendelmeier P. The role of malassezia spp. in atopic dermatitis. *J Clin Med* (2015) 4(6):1217–28. doi: 10.3390/jcm4061217

22. Park M, Lee JS, Jung WH, Lee YW. Ph-dependent expression, stability, and activity of malassezia restricta Mrlip5 lipase. *Ann Dermatol* (2020) 32(6):473–80. doi: 10.5021/ad.2020.32.6.473

23. Park M, Park S, Jung WH. Skin commensal fungus malassezia and its lipases. *J Microbiol Biotechnol* (2021) 31(5):637–44. doi: 10.4014/jmb.2012.12048

24. Harada K, Saito M, Sugita T, Tsuboi R. Malassezia species and their associated skin diseases. *J Dermatol* (2015) 42(3):250–7. doi: 10.1111/1346-8138.12700

25. Masukawa Y, Narita H, Sato H, Naoe A, Kondo N, Sugai Y, et al. Comprehensive quantification of ceramide species in human stratum corneum. *J Lipid Res* (2009) 50 (8):1708–19. doi: 10.1194/jlr.D800055-JLR200

26. Wertz PW, Downing DT. Covalently bound omega-hydroxyacylsphingosine in the stratum corneum. *Biochim Biophys Acta* (1987) 917(1):108–11. doi: 10.1016/0005-2760(87)90290-6

27. Doering T, Brade H, Sandhoff K. Sphingolipid metabolism during epidermal barrier development in mice. *J Lipid Res* (2002) 43(10):1727–33. doi: 10.1194/jlr.m200208-jlr200

28. Nemes Z, Marekov LN, Fésüs L, Steinert PM. A novel function for transglutaminase 1: Attachment of long-chain omega-hydroxyceramides to involucrin by ester bond formation. *Proc Natl Acad Sci U.S.A.* (1999) 96(15):8402–7. doi: 10.1073/pnas.96.15.8402

29. Chiba T, Nakahara T, Kohda F, Ichiki T, Manabe M, Furue M. Measurement of trihydroxy-linoleic acids in stratum corneum by tape-stripping: Possible biomarker of barrier function in atopic dermatitis. *PloS One* (2019) 14(1):e0210013. doi: 10.1371/journal.pone.0210013

30. Lee MK, Seo JH, Chu H, Kim H, Jang YH, Jeong JW, et al. Current status of patient education in the management of atopic dermatitis in Korea. *Yonsei Med J* (2019) 60(7):694–9. doi: 10.3349/ymj.2019.60.7.694

31. Ahn J, Lee DH, Na CH, Shim DH, Choi YS, Jung HJ, et al. Facial erythema in patients with atopic dermatitis treated with dupilumab - a descriptive study of morphology and aetiology. *J Eur Acad Dermatol Venereol* (2022) 36(11):2140–52. doi: 10.1111/jdv.18327

32. Soria A, Du-Thanh A, Seneschal J, Jachiet M, Staumont-Sallé D, Barbarot S. Development or exacerbation of head and neck dermatitis in patients treated for atopic dermatitis with dupilumab. *JAMA Dermatol* (2019) 155(11):1312–5. doi: 10.1001/jamadermatol.2019.2613

33. de Wijs LEM, Nguyen NT, Kunkeler ACM, Nijsten T, Damman J, Hijnen DJ. Clinical and histopathological characterization of paradoxical head and neck erythema in patients with atopic dermatitis treated with dupilumab: A case series. *Br J Dermatol* (2020) 183(4):745–9. doi: 10.1111/bjd.18730

34. Nowicka D, Nawrot U. Contribution of malassezia spp. to the development of atopic dermatitis. *Mycoses* (2019) 62(7):588–96. doi: 10.1111/myc.12913

35. Darabi K, Hostetler SG, Bechtel MA, Zirwas M. The role of malassezia in atopic dermatitis affecting the head and neck of adults. *J Am Acad Dermatol* (2009) 60(1):125–36. doi: 10.1016/j.jaad.2008.07.058

36. Kozera E, Stewart T, Gill K, de la Vega MA, Frew JW. Dupilumab-associated head and neck dermatitis is associated with elevated pretreatment serum malassezia-specific ige: A multicentre, prospective cohort study. *Br J Dermatol* (2022) 186(6):1050–2. doi: 10.1111/bjd.21019

37. Devos SA, van der Valk PG. The relevance of skin prick tests for pityrosporum ovale in patients with head and neck dermatitis. *Allergy* (2000) 55(11):1056–8. doi: 10.1034/j.1398-9995.2000.00782.x

38. Omoto M, Sugiura H, Uehara M. Histopathological features of recalcitrant erythema of the face in adult patients with atopic dermatitis. *J Dermatol* (1994) 21 (2):87–91. doi: 10.1111/j.1346-8138.1994.tb01420.x

39. Guttman-Yassky E, Waldman A, Ahluwalia J, Ong PY, Eichenfield LF. Atopic dermatitis: Pathogenesis. *Semin cutaneous Med Surg* (2017) 36(3):100–3. doi: 10.12788/j.sder.2017.036

40. Meng J, Moriyama M, Feld M, Buddenkotte J, Buhl T, Szöllösi A, et al. New mechanism underlying il-31-Induced atopic dermatitis. *J Allergy Clin Immunol* (2018) 141(5):1677–89.e8. doi: 10.1016/j.jaci.2017.12.1002

41. Imai Y. Interleukin-33 in atopic dermatitis. *J Dermatol Sci* (2019) 96(1):2–7. doi: 10.1016/j.jdermsci.2019.08.006

42. Qiu Z, Zhu Z, Liu X, Chen B, Yin H, Gu C, et al. A dysregulated sebum-microbial metabolite-Il-33 axis initiates skin inflammation in atopic dermatitis. *J Exp Med* (2022) 219(10). doi: 10.1084/jem.20212397

43. Park HR, Oh JH, Lee YJ, Park SH, Lee YW, Lee S, et al. Inflammasome-mediated inflammation by malassezia in human keratinocytes: A comparative analysis with different strains. *Mycoses* (2021) 64(3):292–9. doi: 10.1111/myc.13214

44. Elias PM, Schmuth M. Abnormal skin barrier in the etiopathogenesis of atopic dermatitis. *Curr Opin Allergy Clin Immunol* (2009) 9(5):437–46. doi: 10.1097/ACI.0b013e32832e7d36

45. Bhattacharya N, Sato WJ, Kelly A, Ganguli-Indra G, Indra AK. Epidermal lipids: Key mediators of atopic dermatitis pathogenesis. *Trends Mol Med* (2019) 25(6):551–62. doi: 10.1016/j.molmed.2019.04.001

46. Li Q, Fang H, Dang E, Wang G. The role of ceramides in skin homeostasis and inflammatory skin diseases. *J Dermatol Sci* (2020) 97(1):2–8. doi: 10.1016/j.jdermsci.2019.12.002

47. Pan Y, Tian T, Park CO, Lofftus SY, Mei S, Liu X, et al. Survival of tissue-resident memory T cells requires exogenous lipid uptake and metabolism. *Nature* (2017) 543 (7644):252–6. doi: 10.1038/nature21379

48. Lee J, Kim B, Chu H, Zhang K, Kim H, Kim JH, et al. Fabp5 as a possible biomarker in atopic march: Fabp5-induced Th17 polarization, both in mouse model and human samples. *EBioMedicine* (2020) 58:102879. doi: 10.1016/j.ebiom.2020.102879

49. Krueger JG, Fretzin S, Suárez-Fariñas M, Haslett PA, Phipps KM, Cameron GS, et al. Il-17a is essential for cell activation and inflammatory gene circuits in subjects with psoriasis. *J Allergy Clin Immunol* (2012) 130(1):145–54.e9. doi: 10.1016/j.jaci.2012.04.024

50. Sparber F, De Gregorio C, Steckholzer S, Ferreira FM, Dolowschiak T, Ruchti F, et al. The skin commensal yeast malassezia triggers a type 17 response that coordinates anti-fungal immunity and exacerbates skin inflammation. *Cell Host Microbe* (2019) 25 (3):389–403.e6. doi: 10.1016/j.chom.2019.02.002

51. Bacher P, Hohnstein T, Beerbaum E, Röcker M, Blango MG, Kaufmann S, et al. Human anti-fungal Th17 immunity and pathology rely on cross-reactivity against candida albicans. *Cell* (2019) 176(6):1340–55.e15. doi: 10.1016/j.cell.2019.01.041

52. Park CO, Fu X, Jiang X, Pan Y, Teague JE, Collins N, et al. Staged development of long-lived T-cell receptor A β T(H)17 resident memory T-cell population to candida albicans after skin infection. *J Allergy Clin Immunol* (2018) 142(2):647–62. doi: 10.1016/j.jaci.2017.09.042

frontiers | Frontiers in Immunology

TYPE Review
PUBLISHED 04 April 2023
DOI 10.3389/fimmu.2023.1151527

OPEN ACCESS

EDITED BY
Tej Pratap Singh,
University of Pennsylvania, United States

REVIEWED BY
Jürgen Harder,
University of Kiel, Germany
Chao Yuan,
Shanghai Dermatology Hospital, China

*CORRESPONDENCE
Richard L. Gallo
rgallo@health.ucsd.edu

SPECIALTY SECTION
This article was submitted to Molecular Innate Immunity, a section of the journal Frontiers in Immunology

RECEIVED 26 January 2023
ACCEPTED 14 March 2023
PUBLISHED 04 April 2023

CITATION
Chen Y, Knight R and Gallo RL (2023) Evolving approaches to profiling the microbiome in skin disease. *Front. Immunol.* 14:1151527. doi: 10.3389/fimmu.2023.1151527

Evolving approaches to profiling the microbiome in skin disease

Yang Chen[1,2,3], Rob Knight[2,4,5,6] and Richard L. Gallo[1,6]*

[1]Department of Dermatology, University of California San Diego, La Jolla, CA, United States, [2]Department of Pediatrics, University of California San Diego, La Jolla, CA, United States, [3]Biomedical Sciences Graduate Program, University of California San Diego, La Jolla, CA, United States, [4]Department of Computer Science and Engineering, University of California San Diego, La Jolla, CA, United States, [5]Department of Bioengineering, University of California San Diego, La Jolla, CA, United States, [6]Center for Microbiome Innovation, University of California San Diego, La Jolla, CA, United States

Despite its harsh and dry environment, human skin is home to diverse microbes, including bacteria, fungi, viruses, and microscopic mites. These microbes form communities that may exist at the skin surface, deeper skin layers, and within microhabitats such as the hair follicle and sweat glands, allowing complex interactions with the host immune system. Imbalances in the skin microbiome, known as dysbiosis, have been linked to various inflammatory skin disorders, including atopic dermatitis, acne, and psoriasis. The roles of abundant commensal bacteria belonging to *Staphylococcus* and *Cutibacterium* taxa and the fungi *Malassezia*, where particular species or strains can benefit the host or cause disease, are increasingly appreciated in skin disorders. Furthermore, recent research suggests that the interactions between microorganisms and the host's immune system on the skin can have distant and systemic effects on the body, such as on the gut and brain, known as the "skin-gut" or "skin-brain" axes. Studies on the microbiome in skin disease have typically relied on 16S rRNA gene sequencing methods, which cannot provide accurate information about species or strains of microorganisms on the skin. However, advancing technologies, including metagenomics and other functional 'omic' approaches, have great potential to provide more comprehensive and detailed information about the skin microbiome in health and disease. Additionally, inter-species and multi-kingdom interactions can cause cascading shifts towards dysbiosis and are crucial but yet-to-be-explored aspects of many skin disorders. Better understanding these complex dynamics will require meta-omic studies complemented with experiments and clinical trials to confirm function. Evolving how we profile the skin microbiome alongside technological advances is essential to exploring such relationships. This review presents the current and emerging methods and their findings for profiling skin microbes to advance our understanding of the microbiome in skin disease.

KEYWORDS

microbiome and dysbiosis, genomics, metagenomics, next-generation sequencing, atopic dermatitis (AD), acne (acne vulgaris), psoriasis

1 Introduction

Human skin acts as a substrate for an ecosystem of diverse life. Serving as our bodies' physical barrier and largest organ, human skin is home to millions of bacteria, fungi, viruses, and microscopic mites, which collectively compose the "skin microbiome." Many studies recognize that the combined genomes from the host and microbes, also known as the "hologenome," determine the complete organism's health and function. Although human skin is colonized mainly by beneficial microorganisms that share in maintaining skin metabolic processes and act as a frontline defense at our body's external interface, they and their host all operate in a delicate balance. Microbial dysbiosis, a general term for the disturbed or abnormal distribution, composition, or relative abundance of microorganisms, can influence various local and systemic disease conditions. For example, in dermal layers of the skin, microbes and their gene products directly interact with the host immune system, thereby modulating general skin health (1, 2). Furthermore, growing evidence suggests that microbes from one barrier tissue can alter the activity of distant organ sites between the skin, gut, and brain (3, 4). Thus, skin microbiome studies have the potential to significantly aid our understanding of inflammatory skin disorders (such as atopic dermatitis and psoriasis) and influence wide-ranging pathologies in the same manner that research on the gut microbiome has advanced scientific knowledge of digestive and digestive-related disorders.

Extrinsic and intrinsic differences in skin anatomy and the activity of local cell types drive the variations of both normal and dysbiotic microbial skin communities. As the external barrier from the body, it is constantly bombarded by harsh environmental forces such as water/sun/pollutant exposure, temperature and pH fluctuations, and behavioral influences resulting from hygiene or beauty practices. These constantly changing variables challenge the skin's ability to adapt and maintain stable and benign/healthy microbiome populations (particularly at the epidermal surface). Additionally, given that skin is our interface, it is important to distinguish the difference between members of the skin microbiome (resident to the skin and holding important functional roles) versus those found on the skin with a transient membership (likely from the environment). Compared to most human microbiomes, the skin's environment is harsh, arid, and of lower nutrient availability. Thus, by nature, the skin's ecological habitat limits colonization to a comparatively less diverse subset of organismal taxa than other human microbiome ecosystems, such as the gut. Yet, despite these factors, human skin is host to distinctly different and commonly found microbes belonging to multiple kingdoms (i.e., bacteria, fungi, viruses, etc.) with complex and dynamic community relationships. These resident microorganisms are well-equipped to adapt to the skin, often settling in their preferred niches.

The complexity of human skin and its innate ability to encourage microbial niche specialization can be considered by two major interlinking features. Firstly, skin exhibits a three-dimensional structure akin to a geographical landscape. The average person's skin surface area is approximately 25 m^2, making it the largest epithelial surface of the human body, with great opportunity for host-microbe interactions (5). Furthermore, skin thickness varies depending on the body site (from approximately 0.5 mm on the eyelids to 1.5-2.0 mm on the face and 4.0 mm on the heels of the feet). Unlike the intestine, where microbes are typically separated from direct interaction with the body by an antimicrobial mucus layer (6), host cells (including those of the immune system) are in direct contact with microbes, especially those that inhabit deeper dermal layers. Secondly, beneath the surface, the skin contains a complex topology of hair follicles and eccrine, apocrine, and sebaceous glands. Similar to the villous epithelium of the human gut, the skin has approximately five million hair follicles (pores) and sweat ducts whose concave structure and depth significantly increase the complexity and diversity of the skin. The densities of these micro-organs make for skin microenvironments to be broadly grouped into three categories: sebaceous/oily (forehead, scalp, chest, and back), moist/humid (skin around nose and mouth, underarms, elbow bend, abdominal, lower buttocks, back of the knee, and foot), and dry (forearms, back of the elbow, buttocks, and front of the knee/legs) (7), although far more fine-scale variation exists on human skin (8). While these features are universal to the skin, their ability to influence temporal and interpersonal variation creates even more microscale diversity and, thus, microbial community membership patterns (9).

Since the introduction of sequencing-based genetic analysis techniques for identifying microorganisms, there has been a significant increase in our understanding of microbial life on the skin. As evolving genomic technologies have been refined to produce richer microbial datasets, so have the accompanying analytical methods appropriate for skin microbiome studies. This review will discuss new and improved practices for analyzing complex microbial communities on human skin. First, we will overview the current status of genomic and metagenomic-based tools and highlight the emerging statistical and computational methods for analyzing microbiome data while discussing their application to healthy and diseased skin research. Next, we will complement our discussion of current profiling practices with the challenges in exploring microbial communities on the skin. The following section will focus on our current knowledge of the healthy skin microbiome from present studies, given our available tools and their known limitations. Finally, we provide perspectives on a few inflammatory skin diseases, summarizing what we know about the skin microbiome's role and suggesting opportunities for future research.

2 Toolbox for surveying microbial skin communities

As recently as twenty years ago, culture-based approaches were the only method of exploring microbial communities on human skin (or in any organ) (Figure 1). Growing microorganisms sampled from the skin provided critical insights into the skin's microbial ecosystem. These early pioneering studies identified the major bacterial genera on the skin, including *Staphylococcus*, *Cutibacterium* (formerly *Propionibacterium*), *Corynebacterium*, and fungi such as *Malassezia*, and built the foundation of skin

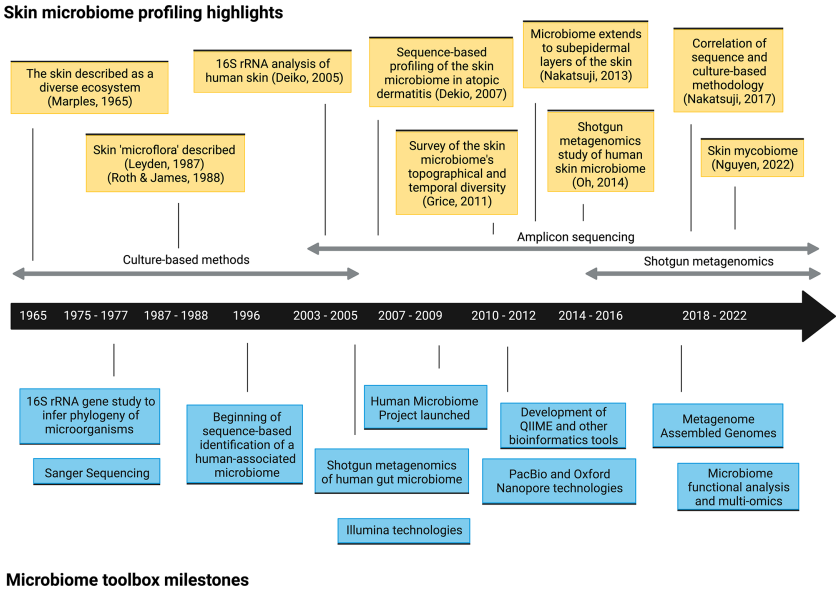

FIGURE 1
Timeline of selected microbiome toolbox milestones and skin microbiome profiling highlights.

microbiome explorations today (4). However, this practice had a significant limitation; culturing microorganisms *in vitro* inevitably provided biased assessments of microbial diversity. Microbes that grow readily in standard growth conditions overwhelmed those with more fastidious growth conditions, which led to a skewed representation of the community. For example, *Staphylococcus* species are more easily cultured, which led to the underestimation of *Cutibacterium* and *Corynebacterium* populations (10). Furthermore, the culture-based approach limited our window to microbes that we knew how to culture or that persistently survived after removal from the skin, meaning that some could be missed and remain functionally invisible. As technologies for DNA sequencing improved and became more accessible, culture-independent methods, including amplicon-based and metagenomic sequencing, have become the conventional practice for profiling the skin microbiome (Figure 1).

2.1 Amplicon-based sequencing and analysis

Many studies that survey bacterial skin communities in healthy and diseased states continue to employ targeted amplification, sequencing, and analysis of sampled genetic material to identify microorganisms. This method involves amplifying and sequencing conserved taxonomic markers within prokaryotic kingdoms to resolve genetic variation and inform the evolutionary relationships between organisms. Most of this work has focused on the 16S ribosomal RNA gene (16S rRNA) in bacteria, which continues to be the *de facto* standard for microbial typing, given its ability to identify bacterial taxa. For fungi, the first internal transcribed spacer (ITS1) is the preferred taxonomic marker, whereas 18S rRNA (while still commonly utilized) is far less precise and offers poor discriminatory ability (11, 12). Unlike bacteria and fungi, viruses do not have a common marker gene and are difficult to characterize by amplicon methods.

Although an important and useful approach, amplicon sequencing techniques require careful methodological choices based on prior assumptions regarding the microorganisms in the sample collection. In order to facilitate sequencing of the full-length 16S gene using shorter-read DNA sequencing technologies, which are often limited in their ability to handle sequences of the gene's full length (~1500 base pairs), most protocols utilize specific locations within the 16S RNA gene known as hypervariable regions (V1-V9). These regions are the most variable between taxa and are situated between conserved regions that can function as PCR primers (13). Because hypervariable areas hold the highest nucleotide variability within 16S, targeting them using specific primers and in different combinations minimizes sequencing cost and effort by capturing the most informative taxon-specific variation in a short sequence (14, 15). Certain specific primer pairs have been more widely employed for different environments, and these primers are most often designed to amplify the V1-V3 or V3-V5 regions. While an "optimal" hypervariable region is not necessarily definitive for different environments, PCR primers designed for different broad-level ecosystems are common, as some regions have been deemed more suitable than others based on microbiome type. For example, the Human Microbiome Project has mainly used primers spanning the V1-V3 and V3-V5 hypervariable regions (16), while the Earth Microbiome Project has traditionally used primers targeting the V4 region (17).

Next, the sequence fragments are read, most popularly on the Illumina platform or using long-read technology *via* the PacBio or Oxford Nanopore platforms. A crucial subsequent step involves a bioinformatics-based process to remove spurious sequencing errors

and merge reads with the same genetic signals. Historically, the most widely employed method was to cluster sequences into Operational Taxonomic Units (OTUs) that share pairwise sequence similarity (often at a 97% probability threshold) into a representative proxy used for downstream analysis (18). However, this method should not be used today. Improved computational methods, known collectively as oligotyping or grouping into Amplicon Sequence Variants (ASVs) or sub-OTUs (sOTUs), provide substantial improvements relative to OTU picking (19). In contrast to OTU clustering, oligotyping includes positional information from sequencing data by making use of the fact that biologically significant variation is more common at specific positions, whereas sequencing errors are randomly distributed. ASVs use a related approach, assuming that rare variants are often sequencing errors of common members in the population. These approaches resolve more biologically relevant groups at higher discriminatory power. Highly cited bioinformatics tools that are OTU-based include QIIME (20) and Mothur (21), while popular ASV-based tools include QIIME2-Deblur (22, 23) and DADA2 (24). Following OTU or ASV-based analysis, a "feature by sample" OTU or ASV table, providing the count of each feature in each sample, is generated and used for taxonomic assignment. QIIME2 and Mothur both support taxonomic profiling, relying on reference databases. Popular taxonomy databases include Silva (25), Greengenes (26), and RDP (27). Finally, functional profiling using PICRUSt (28) or Tax4Fun (29) can link taxonomic data such as that obtained from marker genes to the predicted biological function of taxa within a community. The significant advances in computational methods of 16S and other marker-gene techniques have greatly improved the accuracy of amplicon-based analyses; thus, some of the first conclusions published regarding the identity of bacterial and fungal species on the skin are no longer deemed accurate or of sufficient resolution, underscoring the importance of making the raw data from studies available for periodic re-analyzation with better techniques.

2.2 Shotgun metagenomics and analysis

Shotgun metagenomics, or whole metagenome analysis, attempts to capture and sequence the complete DNA profile of every organism in a sample. This identification method presents an opportunity for a more accurate representation of all microorganisms in a sample and offers multiple advantages over amplicon-based methods regarding the richness of information obtained (30). Multiple systematic comparisons between amplicon sequencing and whole metagenomic sequencing methods have been conducted for the gut microbiome (31–34), although, to the best of our knowledge, none of the skin microbiome. These studies have concluded distinct advantages in using shotgun metagenomics, including identifying a greater diversity of microbial taxa found and enhanced resolution and accuracy of species detection (31, 32), with broad-level biological patterns (such as alpha and beta diversity metrics) being largely consistent (33, 34). Shotgun metagenomics is highly applicable to skin microbiome studies for several reasons. First, this technique can sequence microbes at the whole-genome level, providing a relative abundance of functional genes, not only taxonomic markers. Although marker genes will likely remain an important and efficient way to classify taxa and evaluate microbial communities, shotgun profiling provides a deeper complexity, opening an enhanced window into the microbial dynamics within a skin microbiome sample. Second, because this method is accomplished by randomly fragmenting all DNA within the sample into small pieces, it resolves the sample's complete DNA profile, including bacteria, viruses, microbial eukaryotes, metagenome elements such as plasmids, and the human host. Thus, whole metagenome analyses in the skin microbiome context can obtain multi-kingdom genomic and metagenomic signatures, extending past the phylogenetically limited views of marker gene analyses. Third, because this method resolves whole genomes, shotgun metagenomics provides higher phylogenetic resolution and is better equipped to differentiate species and strains (provided the sequencing is deep enough and the assembly sufficiently successful) (35). As mentioned previously, human skin is preferentially dominated by many different *Staphylococcus* species (*S. epidermidis*, *S. hominis*, and *S. lugdenensis*, to name only a few), which makes short-read amplicon-based genus-level taxonomic resolution limiting, and whole metagenome approaches more capable of discriminating this important taxon.

Illumina platforms are the most popularly employed technology for short-read shotgun metagenomics, followed by Ion Torrent. Long-read machines from Oxford Nanopore MinION and PacBio technologies are scaling rapidly and are likely to see more significant usage. Following sequencing and necessary quality filtering and trimming steps, metagenomics workflows require linking fragmented reads to taxonomic and functional information. Two major approaches carry out this process: reference/read-based and assembly/contig-based workflows (30). Reference-based approaches to identifying microorganisms involve mapping sequences and comparing them to reference genomes from relevant databases. Assembly-based approaches attempt to reconstruct fragmented reads representing the community of microorganisms into contigs and then group or "bin" contigs into species, sometimes referred to as Metagenome-assembled genomes (MAGs) (36). The *de novo* or reference-free approach of MAGs allows for more comprehensive identification of skin microorganisms, including those previously uncharacterized, thus expanding our knowledge and accuracy of the skin's microbial inhabitants (37).

2.3 Integrating other 'omics' technologies for functional studies

For a complete understanding of the composition and function of microbial communities, holistic approaches that go beyond marker gene analysis and metagenomics are necessary to begin inferring the functional roles of different microorganisms. Metatranscriptomics involves sequencing the RNA profile of microorganisms in an environment, thus enabling profiling of which genes are being expressed at a specific time and how they are regulated. Additionally, due to the shorter half-life of RNA,

transcriptomic analysis has some ability to distinguish between live or dead microorganisms and can capture a more dynamic community profile. Combining metatranscriptomics with marker gene analysis or shotgun metagenomics can improve understanding of which microorganisms in a community are actively transcribing and their functional role. Likewise, metaproteomics and metabolomic approaches seek to characterize the proteins and small molecules consumed and produced by the microorganisms to validate profiling findings. For example, 16S sequencing combined with mass spectrometry corroborated the hypothesis that *C. acnes* utilized sebum triglycerides as an energy source by showing their colocalization with fatty acid products (38). A recent study by Roux et al. described the existence of three distinct metabolite-microbe clusters at the skin surface in infants that parallels our current view of the three major environments on human skin; one characterized by *C. acnes* and sebaceous elements at the epidermal barrier, another microbiome network involving *Staphylococcus* spp., moisture and pH regulation at the skin surface, and a third niche with a diverse but unique metabolomic profile which was *Streptococcus*-centered (39). Critically, however, these already complex data sets must be integrated with companion functional data and analysis of the human host to understand how microbes contribute to the health and disease of the "holobiont" (40). Analysis of multi-omics data from the skin microbiome will provide a more complete picture of the behaviors of skin microbes. Furthermore, machine learning and artificial intelligence methods are increasingly being applied to skin microbiome research, including determining changes in abundance or diversity of species and strains, integrating multi-omic microbiome data, and phenotypic prediction (41–43).

2.4 Statistical considerations for microbiome studies

Microbiome data analysis, which typically involves comparing a matrix of features composed of taxa or genes from a simple case to samples of different experimental or phenotypic groups, can be quite complex. Therefore, it is important to use caution when interpreting the results of statistical analyses. Even seemingly basic questions, such as "how does a sample from diseased skin differ from that of healthy skin?" often require complex statistical interpretation. Microbiome data is multi-dimensional, meaning it has a large number of features that can quickly increase with the number of microbes, samples, and time points. Additionally, such data is typically very sparse, with most microbes not present in most of the data, creating a significant skew towards the zeros of the dataset, which represent virtually non-existent microorganisms. Microbiome datasets are also compositional (44), meaning that the sequence counts are heavily influenced by the limitations of the sequencing technology, not just the actual abundance of microbes in the sample (35). These characteristics make it difficult to interpret microbiome data, requiring appropriate and validated techniques.

Microbiome datasets and their broad-level patterns are commonly evaluated using alpha and beta diversity metrics. Alpha diversity measures feature diversity (i.e., taxa or genes) within a single sample and can be compared between different groups of samples. Alpha diversity analyses may describe the diversity of microbial genera or species between skin disease and healthy groups. In contrast, beta diversity measures the difference in composition between two communities. Traditional statistical tests such as Student's t-test or ANOVA should not be used to compare diversity or the relative abundance of taxa across samples because the data often does not follow a normal statistical distribution and/or violates independence assumptions (18). Instead, non-parametric tests should be used to avoid high false discovery rates. Typically, statistical evaluations use the Mann-Whitney U test or Wilcoxon rank-sum test instead of the t-test, Kruskal-Wallis or PERMANOVA instead of ANOVA, and Spearman rank correlation over Pearson correlation. Newer, compositionally aware tools are especially important for differential abundance comparisons. Effect size calculations provide the magnitude of differences between groups and offer a more quantitative understanding of statistical significance beyond p-values (45, 46). For a more extensive review of the quantitative tools and techniques for microbiome data analysis and visualization, we direct the reader to these reviews (18, 47).

3 Special considerations in the sequencing and analysis of skin microbial communities

3.1 Challenges due to low microbial biomass

Whether pursuing culture-based, amplicon, or shotgun genomics methods, there are many challenges involved with analyzing the skin microbiome due to the skin's unique features that can lead to poor-quality genomic data and difficult downstream bioinformatics analysis. Standards and best practices for conducting skin microbiome studies have been described primarily for 16S rRNA gene amplicon sequencing (48) but are largely lacking for metagenomics. Compared to the rich environment inhabited by gut microbes, the skin microbiome holds relatively low microbial biomass (especially at the surface) due to its dry and nutrient-poor conditions (49). Thus, it is critical to note that microbial DNA from skin samples is particularly prone to dilution from human and environmental DNA, and 90% of sequencing reads can be from human DNA when applying metagenomics (50). Furthermore, the issue of low microbial biomass makes it difficult to identify rare or naturally low-abundant taxa that may still have clinical relevance and distinguish these from transient skin microorganisms or possible environmental contaminants. Additionally, characterizing non-bacterial DNA, particularly viruses, whose genomes and microbial biomass are magnitudes smaller than bacteria, presents even greater challenges.

Deeper metagenomic sequencing mitigates issues in low microbial biomass; however, this, in conjunction with appropriate DNA extraction and host/free microbial DNA depletion methodology for skin microbiome samples, is likely the most

ideal and cost-effective. Reduction in human DNA during the DNA extraction and library preparation process for skin samples is possible and seems to be better performed by some commercial kits than others (50). However, to the best of our knowledge, there are no published studies that apply skin-specific methods for a host, bacterial extracellular DNA, or dead bacterial intracellular DNA depletion for the skin microbiome. Chemical digestion or lysing to deplete excessive host DNA after DNA extraction may be necessary before microbial sequencing proceeds from skin samples, as demonstrated for the oral and nasopharynx microbiomes (51, 52). Likewise, a method for depleting both human and free microbial extracellular DNA for metagenomic sequencing *via* selective lysis of eukaryotic cells and endonuclease digestion has been proposed for sputum samples from the Cystic Fibrosis respiratory microbiome (53). Here the authors noted significant increases in microbial sequencing depth and detected taxa and genes compared to commercially available kits. Careful storage procedures of microbial DNA from skin samples are also necessary to prevent further degradation (54). Due to the low abundance of microbial DNA on the skin, the environmental contamination risk is high. Thus, it is crucial to use negative/blank controls throughout all processing steps, from DNA extraction to library preparation and sequencing in parallel with experimental samples. Mock communities (artificial mixtures of known microorganisms) and positive/reference samples are also necessary to benchmark results.

3.2 Challenges due to sampling technique

Human skin represents a vast, multi-layered three-dimensional organ that spans the entire bodily surface. Body-site variation and physiological anatomy create distinct environments, allowing for specialized microbial colonization and unique niche microbiomes. Thus, where you sample on the body is considered to heavily influence results. As the skin contains many layers and species are unevenly distributed, the sampling technique will strongly influence the results (55). Most human skin microbiota studies use swabs as the sampling method; however, this practice is limited to collecting surface and epidermal skin microbes (2). In contrast, a pore strip sample captures mostly microbes in the follicular environment, including the hair follicle and sweat duct. Other sampling methodologies, such as skin biopsies, examine the microbial community within follicular and deeper dermal environments; surface swabs do not always reach those areas. An analysis comparing epidermal and dermal sampling methods suggests the dermal compartment has a greater abundance of microbes with less variability between anatomic locations and between individuals, termed the "universal dermal microbiome" (2). While such observations challenge current research assumptions, this finding may not be surprising as environmental influences (including the individual's hygiene and cosmetic practices) affect the skin microbiome, particularly at the surface. However, so far, fewer studies have performed dermal sampling as it is more invasive. Additionally, performing a skin scrape, biopsy, or other more invasive sampling procedure may capture an even larger proportion of host (human) DNA contamination, posing an additional challenge when choosing this approach.

3.3 Challenges of amplicon methods

Skin microbiome surveys are strongly influenced by the analytical method, including the choice of hypervariable region for 16S-based studies (55). According to Meisel et al., sequencing V1-V3 of skin organisms provides similar results and is more optimal than V4, one of the most commonly employed sequencing targets for investigating the human gut microbiome. Sequencing of the V4 poorly captures *Cutibacterium* and cannot reliably speciate *Staphylococcus* (55). *Cutibacterium acnes* and *Staphylococcus* species are among the most prevalent commensal bacteria, so this presents a significant limitation in the usability of the V4 region for microbes inhabiting the skin. Given that the V4 hypervariable region is shorter and contains more sequence conservation (56), its difficulty in speciating *Staphylococcus* was unsurprising. These findings highlight how the optimal choice of the most useful hypervariable region is ecosystem dependent and can affect results. Improved 16S rRNA V4 gene primers have been designed to specifically improve the capture of underrepresented taxa (57); however, specific benchmarking for skin bacterial communities and identification ability towards *Cutibacterium* and *Staphylococcus* species has not been validated. Importantly, no single hypervariable region nor the whole 16S gene can distinguish all bacterial species for any human microbiome. Only genus-level resolution is typically reliable when using short 16S regions as a marker, although publications often report species-level resolution without checking whether it is even possible for the relevant 16S region and taxa (resolution varies in different parts of the phylogenetic tree). Consolidating OTUs after sequencing is problematic for two major reasons also. Firstly, selecting one OTU sequence as a proxy tends to ignore minor genetic variants and oversimplify the dataset (58). Second, the canonical 97% clustering threshold is outdated and is now believed to be too low for reliable differentiation for most species (59). Originally proposed in 1994, this metric has been based on multiple linking proxies: short-read sequencing of hypervariable regions to approximate full-length sequence identity and full-length sequence identity to approximate whole genome similarity. Thus, reference libraries created by 16S rRNA gene sequencing approaches require systematic re-evaluation now that whole genome sequencing has produced far richer datasets. Barnes et al. investigated the OTU *vs.* ASV method in the atopic dermatitis skin microbiome, particularly those assigned to *Staphylococcus* species (24). Their findings suggested that OTU clustering inflated bacterial richness and concluded the ASV approach with DADA2 managed sequencing errors better. However, the authors stress that when using amplicon sequencing, one should be careful not to overinterpret taxonomic calls at the species level for the *Staphylococcus* community. Genus-level resolution is possible, but attempting to distinguish between species by sequencing only the 16S gene should be treated carefully.

The next step involves taxonomic assignment based on the homology of sequence reads to reference databases. As 16S rRNA sequencing has been widely used, many well-curated databases are available for taxonomic identification. However, careful considerations regarding taxonomic classification are still required. While it has been suggested that ecosystem-specific

databases provide more accurate taxonomic classifications (60), this is likely not true for the skin microbiome. General-purpose microbial taxonomic databases outperform habitat-specific databases in microbiome datasets with significant environmental taxa since these reads may be erroneously assigned if an appropriate reference genome is unavailable (26). Instead, applying environment-specific taxonomic weights within general-purpose databases, such as the Greengenes 16S database with q2-clawback (61), can improve sequence taxonomy classification accuracy from common environments.

3.4 Challenges of whole metagenome methods

Shotgun metagenomics has the potential to yield rich and informative datasets. However, as our technology has advanced, so have the accompanying complexities with data analysis. This technology is still relatively more expensive (though widely becoming more accessible and less costly) than amplicon methods. Producing datasets with sufficiently rich sequencing depths (the number of reads per sample) across the whole genome is crucial relative to other methods, especially when the sample is mostly composed of host DNA reads (50). While shallow- or moderate-depth sequencing has been shown to accurately obtain species-level information, particularly in large-scale studies where deep sequencing is cost-prohibitive, only at deep sequencing depths is the attractive lure of strain-level taxonomic assignment and identification of novel strains and low-abundance taxa with biologically meaningful function within the community possible (35). In skin microbiome studies, the potential to distinguish between *Staphylococcus* species and other commensal strains on the skin is only legitimate if sufficient sequencing depth is achieved. This remains a critical problem because skin sampling typically provides lower biomass of microbes than other body habitats, and low-depth data is common. Contamination from host-derived DNA is a constant challenge, particularly in areas where host DNA dominates microbial DNA, such as the skin. When conducting shotgun metagenomics studies on the human skin microbiome, it is important to filter out sequences from the host. However, the amount of DNA needed for shotgun studies has steadily decreased as the technology has improved, allowing for more efficient sequencing of skin microbiomes.

In contrast, as a newer technology, shotgun metagenome databases currently lack many full reference genomes of microbes and are currently most well-positioned for gut microbiome studies. With the advent of whole metagenomics technology, previous skin microbiome studies observed significant metagenomic reads that did not match those in reference databases suggesting unmapped prokaryotic diversity (62, 63). Thus, the *de novo* (reference-free) approach of MAGs and improved assembly algorithms provide avenues to characterize new and unknown skin species from all domains of life. To address this gap, cultivating microbes to provide high-quality whole-genome sequences, which can then be aligned with MAGs, can provide a more comprehensive catalog of microbial diversity on the skin. This integrated approach has been launched by the Skin Microbial Genome Collection and is expanding our understanding of skin microbes to include new bacterial and eukaryotic species and improved assemblies of viruses and jumbo phages (37).

4 Present knowledge of the healthy skin microbiome

Understanding normal microbiota and typical/benign variations within the skin microbiome in health is necessary to establish a point of reference for investigations into dysbiotic disease states. Human skin contains many resident commensal microorganisms, including bacteria, fungi, viruses, and mites, that utilize skin resources while playing a central role in skin homeostasis and health (Figure 2). However, even commensal bacteria can become pathogenic in specific contexts and contribute to inflammatory skin diseases. The following will summarize current information on this topic. However, it is important to recognize that many reports are subject to the limitations of the sequencing technology employed or the sampling methods used. Thus, some revision of current conclusions will likely occur as better data is developed.

Skin microenvironments are broadly grouped into three categories due to the densities of hair follicles and sweat glands: sebaceous/oily, moist/humid, and dry (7) (although far more fine-scale variation exists on human skin) that is preferentially dominated by commensal organisms. Current data suggests sebaceous body sites, particularly within the follicular microenvironments, are the skin sites showing the least species diversity due to being dominated by *Cutibacterium* species, particularly *C. acnes* (64, 65). Interestingly, a recent study suggests that skin pores spatially segregate *C. acnes* genotypes and that each pore on the face is dominated by a population of *C. acnes* typically differing by < 1 mutation (66). Thus, microenvironments within the skin, such as the hair follicle, represent opportunities for population bottleneck effects. Within most moist areas on the epidermal surface, *Staphylococcus* and *Corynebacterium* species are the most abundant (10, 65). Dry sites have the greatest diversity with a mixed population of *Cutibacterium*, *Staphylococcus*, *Corynebacterium*, and *Streptococcus* species and host more transient microbes (65). *Staphylococcus* commensal species are highly abundant across all skin sites due to the diversity of this genus and their facultative anaerobic abilities; these most commonly include *S. epidermidis*, *S. capitis*, *S. hominis*, *S. lugdengensis*, *S. haemolyticus*, and *S. warneri* (65). Human skin also contains a diverse fungal microbiome (mycobiome) that has only begun to be explored by sequence-based methods (67). *Malassezia* species, particularly *M. restricta*, *M. globosa*, and *M. sympodialis*, are the most prevalent fungal microorganisms on human skin, particularly within the sebaceous sites (65, 67). *Candida* species, including *C. albicans* and *C. auris*, are opportunistic fungal pathogens that frequently colonize the skin (67). The human viral microbiome (virome) is also vastly under-characterized for similar reasons as the human skin mycobiome. Bacteriophages (viruses that infect bacteria) are significant members of the microbial ecosystem on the skin. *Cutibacterium*

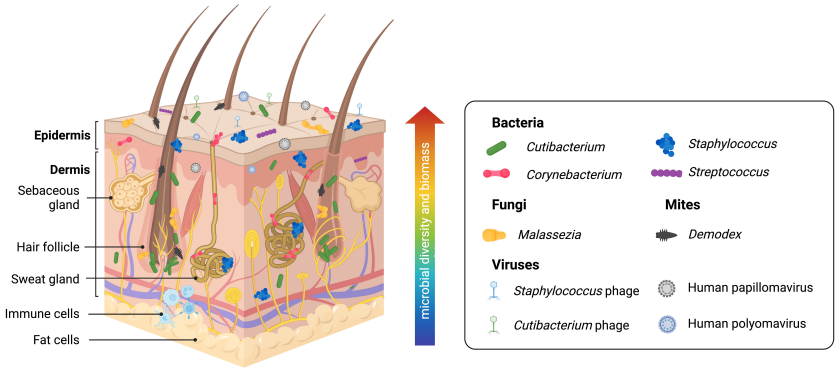

FIGURE 2
Healthy human skin is host to a diverse range of microbes across multiple skin layers and microenvironments. Skin bacteria, many of which belong to the *Cutibacterium*, *Staphylococcus*, *Corynebacterium*, and *Streptococcus* genera, are resident members of the skin microbiome. The skin eukaryome commonly includes fungi and microscopic mites belonging to the *Malassezia* and *Demodex* genera, respectively. Viruses, most notably including *Staphylococcus* phages, *Cutibacterium* phages, human Papillomaviruses, and human Polyomaviruses, are among the dominant members of the skin virome. Archaea (not pictured) has also been identified on the skin microbiome, though likely with a minor or transient presence. Microbial diversity and biomass are typically higher at the skin surface. However, human skin is a three-dimensional space, and microbes form communities that live at the skin surface, deeper skin layers, and within microhabitats such as the hair follicle and sweat glands, allowing complex inter-species relationships and interactions with the host immune system.

and *Staphylococcus* phages are found to be conserved across individuals. However, little is known about the interactions and dynamics between commensal bacteria and bacteriophages on human skin. Eukaryotic viruses, some of which include human papillomaviruses and polyomaviruses (including Merkel cell polyomaviruses associated with skin cancer), have also been found on human skin (62, 65, 68, 69), and they are believed to be more specific to individuals than conserved in certain anatomical sites. Technical limitations with amplicon sequencing and shotgun metagenomics complicate studying the skin virome. Viral genomes lack a taxonomic marker gene like 16S for bacteria or ITS1 for fungi needed for amplicon sequencing and are easily overwhelmed by prokaryotic or eukaryotic genomes (present in populations that are orders of magnitude larger) when shotgun metagenomics is applied (70). Also found on the skin are *Demodex* mites, microscopic arthropods that are a common (and usually benign) part of the commensal skin microbiome (71–73). These mites prefer sebaceous skin sites as their main food source is sebum. Thus, they have been primarily found in the face and scalp, with greater abundance in the pilosebaceous unit. Two *Demodex* species have been identified so far on human skin, *D. follicularum* and *D. brevis*, with imbalances linked to rosacea (71). Though most overlooked, archaea have also been found to be a part of the skin microbiome (74–77). While there is a general lack of consensus on the abundance and role of archaea on the skin, these 16S gene signatures are reported to belong to the *Thermoproteota* (formerly *Thaumarchaeota*), *Methanobacteriota*, and *Halobacteriota* phyla (74–77). Ammonia-oxidizing *Thaumarchaeota* has been suggested to contribute to lowering skin pH and, thus, supporting the skin's barrier against foreign and pathogenic microorganisms (74). In contrast, a recent study profiling skin archaeal communities shows that archaea comprise less than 1% of mammalian skin samples and are more likely to have a minor and transient presence driven by the environment (76). Commonly touched surfaces that interface with the skin, including computer keyboards, phones, and door handles, contained archaea, highlighting how our built environments contribute to microbial inhabitance on the skin (76).

5 The skin microbiome in inflammatory skin diseases

Research in the microbiota of other organs has shown that subtle differences in genetic and metabolic diversity can drive otherwise commensal microbes toward pathogenesis, defining these organisms as pathobionts. These alterations in community composition can have significant implications for disease onset and treatment. While progress has been made in identifying the different types of microbes associated with various skin diseases, whether a dysregulated microbiome causes inflammation or if these associations are a byproduct of the inflammatory environment is unclear (to varying degrees) for different skin diseases. Inflammatory skin disorders have multifactorial etiologies where an intimate balance of host determinants, environmental influences, and microbial composition can influence disease development. Most microbiome studies of inflammatory skin disorders have utilized 16S amplicon sequencing to investigate microbial alterations with specific skin diseases, illuminating important findings. However, deciphering only bacterial genera and their relative abundance has limited usefulness for expanding our current understanding of skin diseases toward improved clinical application. Understanding differences in strain behaviors that could cause them to be pathobionts, commensals, or truly beneficial mutuals may become possible as more comprehensive genomic methods are brought to bear. This is becoming apparent as more studies are applying shotgun metagenomics to the microbiome in skin various diseases (Table 1). Likewise, it is becoming clear that inter-species and inter-kingdom interactions between skin microorganisms play a significant role in skin health as well. Understanding how skin-disease associated microbes interact with the immune system allows opportunities for a deeper understanding of skin microbiota. Such

TABLE 1 Recent studies investigating the microbiome in skin disease utilizing whole metagenomics.

Disease	Whole metagenome studies	Bacterial alterations	Fungal alterations	Other alterations	Key remarks
Atopic Dermatitis	Bjerre et al. (78)	*S. aureus* abundance was higher in all skin sites except from the feet. In the flexures, *S. epidermidis* colonization accompanied *S. aureus* dominance. Decreased *S. hominis* and *C. acnes* was observed where *S. aureus* was highly abundant	Increased *M. osloensis* and *M. luteus* in all AD skin sites except for the neck, where it was absent	Increased abundance of *Cutibacterium* phages PHL041 and PHL092 and *S. epidermidis* phages CNPH82 and PH15 in AD	Dysbiosis in AD is global and site-specific, involving bacteria, fungi, and viruses
	Byrd et al. (79)	↑ *S. aureus* in severe AD ↑ *S. epidermidis* in less severe AD At strain-level, *S. aureus* populations were clonal while *S. epidermidis* were heterogeneous	The authors stated fungal and viral communities were not significantly different in this study likely due to limited reference databases/genomes		Strain-level functional differences contribute to the complexity of AD
Seborrheic Dermatitis	Saxena et al. (80)	↑ *S. epidermidis* ↓ *P. nitroreducens* ↓ *C. acnes*/*S. epidermidis* ratio	↑ *M. restricta*/*M. globosa* ratio ↑ uncultured *Malassezia spp.* ↓ *M. globosa*	Not applicable	The SD scalp microbiome is associated with common bacterial and fungal commensals, and uncharacterized *Malassezia* species
Acne vulgaris	Barnard et al. (81)	↑ *C. acnes*/*C. granulosum* ratio	Not applicable	↓ *C. acnes* phage	A balance of metagenomic elements shapes the skin microbiome in acne and health
Psoriasis	Tett et al. (82)	↑ *Staphylococcus* with no significant differences at species-level	Potentially, *M. restricta*, *M. globosa*, and unknown *Malassezia spp.*	Not applicable	Strain-level variations could be key determinants of the psoriatic microbiome. Uncharacterized *Malassezia* species were also found in the skin mycobiome
Rosacea	None				
Hidradenitis Supprativa	None				
Netherton's Syndrome	Williams et al. (83)	↑ .*S. aureus* ↑ *S. epidermidis*	Not applicable	Not applicable	A monogenic disorder in a protease alters microbial community composition and promotes inflammation

The up arrow means increased, and the down arrow means decreased.

insights will yield powerful and actionable insights into skin disease mechanisms that experiments can validate to confirm function and translate to clinical application. Here, we will focus on areas showing the most progress or best evidence regarding the microbiome's role in inflammatory skin diseases given currently employed methodologies.

5.1 Atopic dermatitis

Atopic dermatitis (AD), also known as eczema, is a chronic inflammatory skin disease characterized by itchy, red, swollen, and cracked skin flares affecting up to 20% of children and 3% of adults (84). Compared to other dermatological disorders, the role of skin microorganisms and dysbiosis in adults with AD is well-documented and exhibits the clearest relationship in which a dysregulated microbiome is causative to skin inflammation. The skin microbiome of adult AD patients typically has reduced biodiversity due to a massive increase in *Staphylococcus aureus* colonization which precedes lesion onset (85, 86). Likewise, skin colonization by *S. aureus* has been found to precede AD diagnosis in infants (87). The dominance and overgrowth of *S. aureus* result in a relative decrease in the proportion of commensal bacteria belonging to the *Cutibacterium*, *Corynebacterium*, and *Streptococcus* genera (85, 88). *S. aureus* commonly presents as a skin pathogen, and colonization by *S. aureus* on healthy skin is rare (89). One recent shotgun metagenomics study by Byrd et al. suggests that not all *S. aureus* strains may be equally pathological (79). This initial work provides insights into *S. aureus* strains from lesional versus non-lesional skin on AD patients. *S. aureus* strains from lesional versus non-lesional sites are phylogenetically clustered separately, suggesting that strain differences may be implicated in AD severity. Multiple studies provide functional evidence of *S. aureus* producing toxins, proteases, phenol-soluble modulins (PSMs), bacteriocins, and other virulence factors exacerbating skin inflammation (90–95).

However, despite a clear link between *S. aureus* and AD, not all AD lesions are colonized by *S. aureus*; many AD patients also have greater colonization of *S. epidermidis* than *S. aureus* (85, 96, 97). These observations are also noted in studies of the AD microbiome where *S. aureus* exclusion leads to greater *S. epidermidis* dominance. Findings from a recent metagenomic study suggest *S. epidermidis* may be a secondary causative agent of AD disease severity as *S. aureus* significantly associates with severe disease, while *S. epidermidis* may be more common with moderate disease (79). Compared to *S. aureus*, *S. epidermidis* is universal on human skin, and some strains exhibit many beneficial properties for skin health, like defense against opportunistic pathogens and enhancing epithelial barrier function (98). For example, *S. epidermidis* induces antimicrobial peptides from keratinocytes and produces phenol-soluble modulins (PSMγ and PSMδ) and other small antimicrobials like lantibiotics to promote colonization by more pathogenic skin bacteria such as Methicillin Resistant Staphylococcus Aureus (MRSA) and *Streptococcus pyogenes* (98–100). Furthermore, *S. epidermidis* strain-level diversity and their functional differences under distinct physiological conditions are increasingly being appreciated (79, 98, 101). For example, it has been suggested that disrupted barrier function (such as that seen in AD skin) can be exacerbated by *S. aureus* and promote the overgrowth of opportunistic *S. epidermidis* strains (98, 102). This hypothesis has been suggested in mouse studies where *S. epidermidis* is resistant to *S. aureus* challenge only in a healthy skin barrier state (103). In AD skin, *S. epidermidis* can injure the epidermis by producing the cysteine protease EcpA that can damage the skin when the organism achieves sufficient density to activate quorum-sensing mechanisms (104). Similarly, *S. epidermidis* cysteine protease EcpA is associated with disease in Netherton's Syndrome and promotes skin damage through a disrupted barrier function (83). Though EcpA is part of the pan-genome of *S. epidermidis*, it is only expressed by some strains, further exemplifying the strain-level functional differences of *S. epidermidis* (104).

The characterization of flare *vs.* non-flare (AD-prone) lesions reveals the potential existence of an AD-susceptible microbiome profile marked by *Streptococcus* and *Gemella* enrichment and *Dermacoccus* depletion (105). Additionally, the function of fungi and viruses and the cross-kingdom interactions of AD microbiomes have yet to be completely investigated, as current studies have mostly concentrated on *S. aureus* and *S. epidermidis*. Differences in fungal and viral communities of the AD skin microbiome have also recently been observed and characterized by body site by Bjerre et al. (78). Increased *M. osloensis* and *M. luteus* were observed in all AD skin sites except the neck, where it was absent. Perhaps unsurprisingly, AD lesions exhibit a higher abundance of *Staphylococcus* phages (78). According to these studies, dysbiosis in AD has global and body-site-specific differences involving bacteria, fungi, and viruses, and strain-level functional differences may contribute to disease complexities (Table 1).

5.2 Seborrheic dermatitis

Seborrheic dermatitis (SD) is another chronic skin disorder that causes a red, itchy rash with flaky skin (106). SD commonly occurs on the body's oily areas like the scalp (where it is known as dandruff), face, and chest. Fungal and bacterial skin microbiome changes are currently implicated in SD, particularly in *Malassezia* and *Staphylococcus* species, with *Malassezia* associated with itchiness and disease severity (106–108). Topical antifungals (ketoconazole) are a common and sometimes effective therapy for SD. However, it is unclear if the mechanism of action occurs on microbes or other effects on the host from this class of drugs (109). To our knowledge, multiple studies have been conducted on the SD scalp microbiome using various 16S regions, and one study employs whole metagenomics. A recent systematic review by Tao et al. of all SD skin microbiome studies (largely conducted on the scalp) suggested an increased *M. restrica* to *M. globosa* and *Staphylococcus* to *Cutibacterium* ratios in SD skin (106). Only one study by Saxena et al. has performed a whole metagenome approach to study the functional pathways of SD and the skin microbiome. According to this study, bacterial alterations are characterized by increased *S. epidermidis*, decreased *P. nitroreducens*, and decreased *C. acnes* to *S. epidermidis* ratio (80). Fungal differences included increased *M. restricta* to *M. globosa* ratio and a significant portion of the mycobiome composed of uncharacterized *Malassezia* species and strains highly associated with dandruff presence (Table 1). Thus, SD represents an important example of how our understanding of the skin mycobiome is severely lacking (67) and how metagenomic assemblies of uncharacterized reads may resolve discoveries of new fungal species and strains.

5.3 Acne vulgaris

Acne is the most common inflammatory skin disease affecting approximately 9% of the population worldwide and 85% of teens and young adults (110). The visible nature of active acne and residual scarring in approximately 1 out of 5 disease cases creates psychosocial impacts through their negative effects on affected patients' physical appearance, social interactions, and self-esteem. The increased incidence of anxiety, depression, and suicide arising from chronic acne, particularly for young adults, is well documented (111). Acne manifests in the pilosebaceous unit, commonly known as the hair follicle or "pore," a lipid-rich niche on the skin with an acidic environment low in oxygen and nutrients that is hostile to most microorganisms (112). The skin microbiota is thought to play a causal role in acne development. In particular, there has been a focus on the role of the commensal skin bacterium *Cutibacterium acnes* (formerly named *Propionibacterium acnes*), an aerotolerant anaerobe that thrives in sebaceous conditions (64, 112). However, the link between *C. acnes* and acne disease has been challenging to pinpoint, even after decades of research and medical practice. The older model of acne implicated *C. acnes* skin "infection" as the disease's cause due to its unique ability to thrive in the same environment where acne develops. This model proposed that increased sebum production in the pores promoted *C. acnes* overgrowth that physically "plugged" the hair follicle and sebaceous gland, thereby inducing inflammation in surrounding skin cells. Other work has suggested that disease in acne can come from cooperation between *C. acnes* and other inhabitants of the follicular microbiome, resulting in cell damage from a Christie, Atkins, Munch-Peterson (CAMP) reaction (113). Multiple studies

have concluded that *C. acnes* is the predominant bacterium within most individuals' skin microbial communities, both in healthy and diseased skin, and can account for nearly 90% of the skin pore microbiota, while its oxygen detoxification abilities allow it also to inhabit the skin surface (67, 79, 86). Nevertheless, topical and systemic antibiotics are a mainstay of acne therapy, and topical bacteriophage therapy has been suggested to have therapeutic potential (112, 114), suggesting that *C. acnes* has an important role in the pathophysiology of this disease.

As a commensal organism with a ubiquitous presence on the skin, the association of acne lesions with *C. acnes* is likely strain-dependent (115, 116). As researchers have attempted to understand how *C. acnes* subgroups are involved in acne disease, several different molecular typing methods have been developed to separate *C. acnes* into strains, making it difficult to cross-compare between studies (117). Genomic analyses concur specific strains of *C. acnes* are more commonly associated with acne (112, 116, 118, 119). However, the functional differences between *C. acnes* strains are generally unknown. It is even less clear if those strains that appear to be associated with acneic skin induce greater skin inflammation (and by what mechanisms). Furthermore, these current strain-typing methods are based on partial amplification and sequencing of conserved genes that likely fail to capture the full extent of *C. acnes* genetic diversity related to pathobiont behavior. For example, the first whole-genome sequencing analysis of *C. acnes* revealed the presence of a novel linear plasmid containing genes encoding potential virulence factors (120).

A greater understanding of the community compositional changes between acne and healthy skin is needed. In healthy skin, *C. acnes* and *S. epidermidis* are among the most prevalent commensals and have been shown to interact frequently with shifts in one species influencing the other. In acne-affected skin, the strain diversity and relative abundance of *S. epidermidis* are increased to inhibit the growth of *C. acnes via* fermentation and other defense mechanisms (112, 117, 121). A deep whole metagenome study by Barnard et al. of acne versus healthy individuals finds a balance of metagenomic elements shapes the skin microbiome in acne and health (81) (Table 1). Compared to healthy individuals, acne patients had a higher diversity of C. acnes populations, more strain types, more virulence-associated factors, and lower metabolic synthesis genes.

Additionally, their analyses suggest the *C. acnes* to *C. granulosum* ratio is important in acne disease, with acne patients having a lower relative *C. granulosum* abundance (81). *C. acnes* and *C. granulosum* have been reported to exist in a potentially competitive relationship, with *C. granulosum* secreting an endogenous extracellular nuclease capable of degrading *C. acnes* biofilm (122). Recently, a published study by Conwill et al. suggests *C. acnes* lineages can coexist across an individual's skin; however, within individual pores, *C. acnes* is nearly clonal (< 1 mutation apart) (66). However, the *C. acnes* diversity at the single-pore level in individuals with acne has yet to be explored using per-pore sampling techniques.

5.4 Psoriasis

Psoriasis occurs in approximately 2% of the population worldwide and has characteristic plaques of red, itchy, and dry skin, most often on the elbows, knees, trunk, and scalp (123, 124). Many studies have shown dysbiotic differences in the psoriasis skin microbiome, especially in healthy and psoriatic individuals' relative bacterial and fungal populations. While these associations are less clear than the previously mentioned diseases, many studies link *Streptococcus* and *Staphylococcus* bacterial species and *Malassezia* and *Candida albicans* fungi. Additionally, a subtype of psoriasis, known as guttate psoriasis, can be systemically triggered by bacterial infections such as "strep throat" from Group A *Streptococcus* (125). Psoriasis lesions have also been reported to have proportionately greater populations of *Staphylococcus. aureus* and *Streptococcus pyogenes* (126), and decreased incidence of *S. epidermidis* and *C. acnes* (82, 127). On psoriatic skin, *Malassezia* diversity decreases as disease severity increases. *M. restricta* and *M. globosa* are predominantly present, and *M. furfur* is reportedly only found on psoriatic skin. Another fungal microbe, *Candida albicans*, is also significantly more common in psoriatic patients and is linked to worsening psoriasis skin lesions (126, 127). In the first whole metagenome study of healthy versus psoriasis skin, Tett et al. suggest psoriatic lesions exhibit an increase in *Staphylococcus*; however, no significant differences were observed at the species level (82). However, their analyses suggest functional differences may lie at the strain level (Table 1). Additionally, similar to findings on the skin mycobiome in seborrheic dermatitis, the psoriasis mycobiome contained uncharacterized *Malassezia* reads, which the authors attributed to limitations in taxonomic databases.

5.5 Rosacea

Rosacea is a skin condition that causes facial flushing and sometimes small, pus-filled bumps on the face (71). The demographic of people most at risk for rosacea are individuals of Caucasian descent and who have fair skin, particularly women over 30 years of age. The skin microbiome is believed to be involved in rosacea; however, the results are inconsistent, likely due to mixed and limited methodologies (128). To the best of our knowledge, all current rosacea studies have used 16S amplicon sequencing and only used the V3 and V4 regions, which has been reported to be an issue in identifying *Staphylococcus* and *Cutibacterium* species (55). Whole metagenomics has not yet been employed to study the rosacea skin microbiome. Multiple studies have reported the skin microbiome of rosacea patients to have increased densities of *Demodex* mites, especially *D. folliculorum* and *D. brevis* (73, 129). (Characterization of *Demodex* mites is based on mitochondrial 16S rDNA partial sequences). While *Demodex* species are considered part of the healthy skin microbiome, in rosacea patients, an increased incidence of *Demodex* is associated with aberrant overactivation of the innate immune system (130). *Bacillus oleronius*, a bacterium carried by *Demodex*, can also independently trigger inflammatory pathways and may play a role in rosacea (73). Multiple studies also report a significant increase in the (normally) commensal bacterium *S. epidermidis* in rosacea patients, particularly within the pus-filled lesions (129, 131). At higher skin temperatures, *S. epidermidis* is known to produce additional proteins that may act as virulence factors (132). In rosacea, increased blood flow on the face leads to

higher temperatures that may allow *S. epidermidis* to behave more opportunistically (129, 131). A decrease in *C. acnes* has also been noted in rosacea patients (133). Both *C. acnes* and *Demodex* mites live in the pilosebaceous unit and utilize sebum as a primary nutrient. Thus, the decrease in *C. acnes* may partly be due to the overgrowth of *Demodex*. However, many of these studies have not seen cross-validation. For a comprehensive review of the skin microbiome studies of rosacea, we direct the reader to the following (128).

5.6 Hidradenitis suppurativa

Also known as acne inversa, hidradenitis suppurativa (HS) is a chronic skin disease with painful nodule-like lesions that presents as abscesses and sinus tracts (tunnel-like wounds) on the skin (134). HS is considered an autoinflammatory disease caused by an aberrant and overactive innate immune system (134, 135). Flares from HS typically occur in body sites with more sweat glands and skin folding, such as the armpits, groin, buttocks, and breasts. Because of its appearance and location, HS can be misdiagnosed as acne, skin infection, herpes, or a sexually transmitted disease (STD). The psychosocial impacts of HS are significant due to its occurrence in private body sites, common misdiagnosis as a contagious STD, and permanent scarring, which is a common outcome. Current therapies are limited for HS, and this disorder is poorly responsive to antibiotics.

Several studies have recently characterized the skin microbiome of HS patients using 16S amplicon sequencing (136–142) (however, none with whole metagenome approaches). Across all studies, an increased abundance of anaerobic bacteria belonging to the *Porphyromonas* and *Prevotella* genera is significantly observed (138–142). Some studies also report an increase in *Corynebacterium* spp., *Moraxella* spp., *Actinomyces* spp., *Peptoniphilus* spp., *Mobiluncus* spp., and *Campylobacter ureolyticus* (138, 140, 142). In contrast, the skin of HS individuals has relatively lower populations of commensal bacteria, including *Cutibacterium* spp., *Staphylococcus epidermidis*, and *Staphylococcus hominis* (138, 142). Furthermore, some studies suggest an increased relative abundance of bacteria within lesional dermal tunnels versus non-lesional or non-dermal tunnel skin (142, 143). These findings demonstrate bacterial dysbiosis is associated with HS and varies with disease severity. Extending current findings with shotgun metagenomics will likely provide new insights into the skin microbiome's role in this disease. Most bacteria currently associated with HS are resolved only at the genus level. An improved genomic analysis of the HS microbiome at the species or strain level will likely elucidate the association between this disease and the skin microbiome. There are currently no whole metagenome studies of the HS skin microbiome. For a comprehensive review of studies investigating the role of the skin microbiome in HS, we recommend the following (144).

5.7 Ichthyoses

Ichthyoses are a family of over 20 genetic skin diseases characterized by widespread, persistent dry, thick, and "fish-scale-like" skin (145). The various types of ichthyoses differ in their genetic inheritance pattern (which may be dominant, recessive, X-linked, or spontaneous), disease symptoms, and onset. Netherton Syndrome (NS) is an autosomal recessive-inherited type of ichthyosis where genetic mutations in the *SPINK5* gene results in the loss of function of lymphoepithelial Kazal-type-related serine protease inhibitor (LEKTI-1) (83). Although NS is a disease linked to germline mutation, its severity, and skin inflammation vary. One recent study investigated how the loss of LEKTI-1 influences resident skin bacteria and contributes to NS (83). Shotgun sequencing of the NS lesional skin microbiome demonstrated a dominance of *S. aureus* and *S. epidermidis*, both able to induce skin inflammation and barrier damage in mice (83). Due to increased proteolytic activity in the LEKTI-1 deficient state, these microbes promote skin inflammation *via S. aureus* phenol-soluble modulin α and increased bacterial proteases staphopain A and B from *S. aureus* or EcpA from *S. epidermidis*. Thus, NS presents an interesting case where a shotgun metagenomic approach plus experimental validation showed how a monogenic disease could influence microbial community shifts (Table 1).

6 Discussion

Just as culture-based studies helped us to discover microbial life on the skin, amplicon sequencing has greatly expanded our knowledge of previously unknown microorganisms. However, as newer technologies and analytical practices have become more refined, our previous goals of describing microbial skin communities at genus-level resolution are no longer a sufficient research aim, particularly when applied to understanding dermatological disorders. Amplicon-based approaches are still valuable tools, but studies employing them should utilize more resolved primer sets and current bioinformatics approaches to generate the most robust datasets possible. There is increasing awareness that sampling and analysis methods can significantly influence results as the skin exhibits multiple forms of variation by body-site-specific niches and between surface, follicular, and dermal layers. Additionally, improved and validated methods of reducing or depleting host DNA in skin samples will greatly improve skin microbial profiling. Thus, future studies should reassess some older conclusions and include further investigation of the subepidermal microbial distribution of specific skin diseases, which may provide new insights into how microbes may be modulating host physiology and immune responses. Additionally, we stress that the relationship between microorganisms and ourselves is often more nuanced than the commonly employed binary descriptions of commensal versus pathogenic. Many skin disorders are influenced by what we typically consider commensal microorganisms that appear to demonstrate pathological differences at the species or strain level. An improved understanding of higher-order taxa disease associations will likely clarify the involvement of microbes and support explaining the multifactorial nature and diverse manifestation of most skin diseases. Furthermore, an under-surveyed non-bacterial community consisting of fungi, viruses, skin mites, and their inter-species community relationships also

appear to play an important role in skin diseases that we are only beginning to uncover.

With the rapid advancement of 'omics' technologies and improved accompanying bioinformatics methodologies, designing research studies to address these questions appropriately are now possible. Whole metagenomics profiling (even at shallow sequencing depths) yields richer datasets than amplicon-based sequencing; however, such studies are currently absent or limited in many skin diseases. Larger scale and systematic studies characterizing the healthy human skin microbiome, such as those aimed at understanding the human gut microbiome, will likely expand as the field progresses. Increasing metagenome-assembled genomes from skin-resident microorganisms (though still limited) are seeing greater development. Other methods, such as functional screening using transcriptomics, proteomics, and metabolomics, combined with profiling efforts, will offer a more comprehensive understanding of the functional potential of skin microbes toward disease and present gateways for clinical applications.

The causative relationship between changes in the skin microbiome and inflammatory skin diseases is a complex issue that remains a subject of debate in the field. While some skin diseases, such as atopic dermatitis, show clear links between microbiome dysregulation and disease onset, the degree of causation is less understood in other skin diseases. In most cases, however, it is likely that both dysregulated microbiome and alterations in the skin's inflammatory environment play a dual role in disease pathogenesis. And whether which comes first may be different for different skin diseases. For example, *S. aureus* colonization has been shown to disrupt the skin barrier and overall skin health, contributing to enhanced colonization of opportunistic *S. epidermidis* strains and decreased overall commensal strains, which also negatively affect disease outcomes. Understanding the underlying mechanisms (as we have most clearly elucidated in atopic dermatitis) is critical to developing effective therapeutic interventions for skin diseases.

Future efforts to uncover the functional impact of microbial dysbiosis in the skin may also support an increased understanding of how the effects extend beyond the skin. We will likely continue to think less about microbiome ecosystems as being only confined to their anatomical location, as crosstalk mechanistic studies support such conclusions. There is increasing evidence for the systemic effects of skin microbiome dysbiosis and disease on distant microbial-related pathologies, termed the 'skin-gut' or 'skin-brain' axes. It is well documented that inflammatory skin disorders are frequently associated with inflammatory bowel disease and that many individuals with a skin disease also have comorbidity with a gut disease. Such relationships between a skin-gut axis have been reported for atopic dermatitis (146), acne (147), psoriasis (148), rosacea (71), and hidradenitis suppurativa (149). Additionally, in psoriasis, a skin-brain axis has been proposed, where skin cells that express neuropeptides and hormones may be directly promoting systemic inflammation and inducing psychological effects in the brain (150). To further explore the role of the skin microbiome in local and systemic health effects, experiments with new and improved clinically applicable models will be necessary to uncover the mechanisms. By continually evolving how we investigate microbes on the skin alongside rapidly advancing technological approaches, new findings push the frontier regarding our scientific knowledge of skin disease and whole-body health, providing opportunities to translate insights into clinical practice.

Author contributions

YC, RK, and RG contributed to researching data and content. YC wrote the manuscript. YC, RK, and RG reviewed and edited the manuscript before submission. All authors contributed to the article and approved the submitted version.

Funding

(NIH) P50AR080594 U01AI152038 R37AI052453 R01DK121760 R01AI153185 R01AR076082.

Acknowledgments

Figures were created using BioRender.com.

Conflict of interest

RG is a co-founder, scientific advisor, consultant, and equity holder in MatriSys Biosciences and is a consultant, receives income, and equity holder in Sente Inc.

The remaining authors declare that the research was conducted in the absence of any commercial or financial relationships that could be construed as a potential conflict of interest.

Publisher's note

References

1. Nakatsuji T, Chiang HI, Jiang SB, Nagarajan H, Zengler K, Gallo RL. The microbiome extends to subepidermal compartments of normal skin. *Nat Commun* (2013) 4(1):1431. doi: 10.1038/ncomms2441

2. Bay L, Barnes CJ, Fritz BG, Thorsen J, Restrup MEM, Rasmussen L, et al. Universal dermal microbiome in human skin. *mBio* (2020) 11(1):e02945–19. doi: 10.1128/mBio.02945-19

3. Arck P, Handjiski B, Hagen E, Pincus M, Bruenahl C, Bienenstock J, et al. Is there a 'gut-brain-skin axis'? *Exp Dermatol* (2010) 19(5):401–5. doi: 10.1111/j.1600-0625.2009.01060.x

4. De Pessemier B, Grine L, Debaere M, Maes A, Paetzold B, Callewaert C. Gut–skin axis: Current knowledge of the interrelationship between microbial dysbiosis and skin conditions. *Microorganisms* (2021) 9(2):353. doi: 10.3390/microorganisms9020353

5. Gallo RL. Human skin is the largest epithelial surface for interaction with microbes. *J Invest Dermatol* (2017) 137(6):1213–4. doi: 10.1016/j.jid.2016.11.045

6. Schroeder BO. Fight them or feed them: How the intestinal mucus layer manages the gut microbiota. *Gastroenterol Rep* (2019) 7(1):3–12. doi: 10.1093/gastro/goy052

7. Cundell AM. Microbial ecology of the human skin. *Microb Ecol* (2018) 76(1):113–20. doi: 10.1007/s00248-016-0789-6

8. Wei Q, Li Z, Gu Z, Liu X, Krutmann J, Wang J, et al. Shotgun metagenomic sequencing reveals skin microbial variability from different facial sites. *Front Microbiol* (2022) 13:933189. doi: 10.3389/fmicb.2022.933189

9. Grice EA, Segre JA. The skin microbiome. *Nat Rev Microbiol* (2011) 9(4):244–53. doi: 10.1038/nrmicro2537

10. Grice EA, Kong HH, Conlan S, Deming CB, Davis J, Young AC, et al. Topographical and temporal diversity of the human skin microbiome. *Science* (2009) 324(5931):1190–2. doi: 10.1126/science.1171700

11. Schoch CL, Seifert KA, Huhndorf S, Robert V, Spouge JL, Levesque CA, et al. Nuclear ribosomal internal transcribed spacer (ITS) region as a universal DNA barcode marker for *Fungi*. *Proc Natl Acad Sci* (2012) 109(16):6241–6. doi: 10.1073/pnas.1117018109

12. Banos S, Lentendu G, Kopf A, Wubet T, Glöckner FO, Reich M. A comprehensive fungi-specific 18S rRNA gene sequence primer toolkit suited for diverse research issues and sequencing platforms. *BMC Microbiol* (2018) 18(1):190. doi: 10.1186/s12866-018-1331-4

13. Kim M, Morrison M, Yu Z. Evaluation of different partial 16S rRNA gene sequence regions for phylogenetic analysis of microbiomes. *J Microbiol Methods* (2011) 84(1):81–7. doi: 10.1016/j.mimet.2010.10.020

14. Liu Z, Lozupone C, Hamady M, Bushman FD, Knight R. Short pyrosequencing reads suffice for accurate microbial community analysis. *Nucleic Acids Res* (2007) 35 (18):e120–0. doi: 10.1093/nar/gkm541

15. Soergel DAW, Dey N, Knight R, Brenner SE. Selection of primers for optimal taxonomic classification of environmental 16S rRNA gene sequences. *ISME J* (2012) 6 (7):1440–4. doi: 10.1038/ismej.2011.208

16. The Human Microbiome Project Consortium. A framework for human microbiome research. *Nature* (2012) 486(7402):215–21. doi: 10.1038/nature11209

17. Thompson LR, Sanders JG, McDonald D, Amir A, Ladau J, Locey KJ, et al. A communal catalogue reveals earth's multiscale microbial diversity. *Nature* (2017) 551 (7681):457–63. doi: 10.1038/nature24621

18. Knight R, Vrbanac A, Taylor BC, Aksenov A, Callewaert C, Debelius J, et al. Best practices for analysing microbiomes. *Nat Rev Microbiol* (2018) 16(7):410–22. doi: 10.1038/s41579-018-0029-9

19. Eren AM, Borisy GG, Huse SM, Mark Welch JL. Oligotyping analysis of the human oral microbiome(2014) (Accessed 2022 Dec 29).

20. Caporaso JG, Kuczynski J, Stombaugh J, Bittinger K, Bushman FD, Costello EK, et al. QIIME allows analysis of high-throughput community sequencing data. *Nat Methods* (2010) 7(5):335–6. doi: 10.1038/nmeth.f.303

21. Schloss PD, Westcott SL, Ryabin T, Hall JR, Hartmann M, Hollister EB, et al. Introducing mothur: Open-source, platform-independent, community-supported software for describing and comparing microbial communities. *Appl Environ Microbiol* (2009) 75(23):7537–41. doi: 10.1128/AEM.01541-09

22. Bolyen E, Rideout JR, Dillon MR, Bokulich NA, Abnet CC, Al-Ghalith GA, et al. Reproducible, interactive, scalable and extensible microbiome data science using QIIME 2. *Nat Biotechnol* (2019) 37(8):852–7. doi: 10.1038/s41587-019-0209-9

23. Amir A, McDonald D, Navas-Molina JA, Kopylova E, Morton JT, Zech Xu Z, et al. Deblur rapidly resolves single-nucleotide community sequence patterns. *Gilbert JA editor. mSystems* (2017) 2(2):e00191–16. doi: 10.1128/mSystems.00191-16

24. Barnes CJ, Rasmussen L, Asplund M, Knudsen SW, Clausen ML, Agner T, et al. Comparing DADA2 and OTU clustering approaches in studying the bacterial communities of atopic dermatitis. *J Med Microbiol* (2020) 69(11):1293–302. doi: 10.1099/jmm.0.001256

25. Silva C, Puente JL, Calva E. Salmonella virulence plasmid: pathogenesis and ecology(2017) (Accessed 2022 Nov 9).

26. McDonald D, Price MN, Goodrich J, Nawrocki EP, DeSantis TZ, Probst A, et al. An improved greengenes taxonomy with explicit ranks for ecological and evolutionary analyses of bacteria and archaea. *ISME J* (2012) 6(3):610–8. doi: 10.1038/ismej.2011.139

27. Cole JR, Wang Q, Cardenas E, Fish J, Chai B, Farris RJ, et al. The ribosomal database project: improved alignments and new tools for rRNA analysis. *Nucleic Acids Res* (2009) 37(Database):D141–5. doi: 10.1093/nar/gkn879

28. Langille MGI, Zaneveld J, Caporaso JG, McDonald D, Knights D, Reyes JA, et al. Predictive functional profiling of microbial communities using 16S rRNA marker gene sequences. *Nat Biotechnol* (2013) 31(9):814–21. doi: 10.1038/nbt.2676

29. Aßhauer KP, Wemheuer B, Daniel R, Meinicke P. Tax4Fun: predicting functional profiles from metagenomic 16S rRNA data: Fig. *1. Bioinf* (2015) 31 (17):2882–4. doi: 10.1093/bioinformatics/btv287

30. Quince C, Walker AW, Simpson JT, Loman NJ, Segata N. Shotgun metagenomics, from sampling to analysis. *Nat Biotechnol* (2017) 35(9):833–44. doi: 10.1038/nbt.3935

31. Ranjan R, Rani A, Metwally A, McGee HS, Perkins DL. Analysis of the microbiome: Advantages of whole genome shotgun versus 16S amplicon sequencing. *Biochem Biophys Res Commun* (2016) 469(4):967–77. doi: 10.1016/j.bbrc.2015.12.083

32. Durazzi F, Sala C, Castellani G, Manfreda G, Remondini D, De Cesare A. Comparison between 16S rRNA and shotgun sequencing data for the taxonomic characterization of the gut microbiota. *Sci Rep* (2021) 11(1):3030. doi: 10.1038/s41598-021-82726-y

33. Rausch P, Rühlemann M, Hermes BM, Doms S, Dagan T, Dierking K, et al. Comparative analysis of amplicon and metagenomic sequencing methods reveals key features in the evolution of animal metaorganisms. *Microbiome* (2019) 7(1):133. doi: 10.1186/s40168-019-0743-1

34. Peterson D, Bonham KS, Rowland S, Pattanayak CW, Consortium RESONANCE, Klepac-Ceraj V. Comparative analysis of 16S rRNA gene and metagenome sequencing in pediatric gut microbiomes. *Front Microbiol* (2021) 512:670336. doi: 10.3389/fmicb.2021.670336

35. Knights D, Beckman KB, Gohl DM, Zhu Q, Shields-Cutler RR, Al-Ghalith GA, et al. Evaluating the information content of shallow shotgun metagenomics. *mSystem* (2018) 3(6):12. doi: 10.1128/mSystems.00069-18

36. Yang C, Chowdhury D, Zhang Z, Cheung WK, Lu A, Bian Z, et al. A review of computational tools for generating metagenome-assembled genomes from metagenomic sequencing data. *Comput Struct Biotechnol J* (2021) 19:6301–14. doi: 10.1016/j.csbj.2021.11.028

37. Saheb Kashaf S, Proctor DM, Deming C, Saary P, Hölzer M, Program NISCCS, et al. Integrating cultivation and metagenomics for a multi-kingdom view of skin microbiome diversity and functions. *Nat Microbiol* (2021) 7(1):169–79. doi: 10.1038/s41564-021-01011-w

38. Bouslimani A, Porto C, Rath CM, Wang M, Guo Y, Gonzalez A, et al. Molecular cartography of the human skin surface in 3D(2015) (Accessed 2023 Jan 16).

39. Roux PF, Oddos T, Stamatas G. Deciphering the role of skin surface microbiome in skin health: An integrative multiomics approach reveals three distinct Metabolite –Microbe clusters. *J Invest Dermatol* (2022) 142(2):469–79. doi: 10.1016/j.jid.2021.07.159

40. Simon JC, Marchesi JR, Mougel C, Selosse MA. Host-microbiota interactions: from holobiont theory to analysis. *Microbiome* (2019) 7(1):5. doi: 10.1186/s40168-019-0619-4

41. Hernández Medina R, Kutuzova S, Nielsen KN, Johansen J, Hansen LH, Nielsen M, et al. Machine learning and deep learning applications in microbiome research. *ISME Commun* (2022) 2(1):98. doi: 10.1038/s43705-022-00182-9

42. Carrieri AP, Haiminen N, Maudsley-Barton S, Gardiner LJ, Murphy B, Mayes AE, et al. Explainable AI reveals changes in skin microbiome composition linked to phenotypic differences. *Sci Rep* (2021) 11(1):4565. doi: 10.1038/s41598-021-83922-6

43. Jaiswal SK, Agarwal SM, Thodum P, Sharma VK. SkinBug: an artificial intelligence approach to predict human skin microbiome-mediated metabolism of biotics and xenobiotics. *iScience* (2021) 24(1):101925. doi: 10.1016/j.isci.2020.101925

44. Gloor GB, Macklaim JM, Pawlowsky-Glahn V, Egozcue JJ. Microbiome datasets are compositional: And this is not optional. *Front Microbiol* (2017) 8:2224. doi: 10.3389/fmicb.2017.02224

45. Sullivan GM, Feinn R. Using effect size–or why the *P* value is not enough. *J Grad Med Educ* (2012) 4(3):279–82. doi: 10.4300/JGME-D-12-00156.1

46. Ferdous T, Jiang L, Dinu I, Groizeleau J, Kozyrskyj AL, Greenwood CMT, et al. The rise to power of the microbiome: Power and sample size calculation for microbiome studies. *Mucosal Immunol* (2022) 15(6):1060–70. doi: 10.1038/s41385-022-00548-1

47. Peeters J, Thas O, Shkedy Z, Kodalci L, Musisi C, Owokotomo OE, et al. Exploring the microbiome analysis and visualization landscape. *Front Bioinforma* (2021) 1:774631. doi: 10.3389/fbinf.2021.774631

48. Kong HH, Andersson B, Clavel T, Common JE, Jackson SA, Olson ND, et al. Performing skin microbiome research: A method to the madness. *J Invest Dermatol* (2017) 137(3):561–8. doi: 10.1016/j.jid.2016.10.033

49. Chen YE, Fischbach MA, Belkaid Y. Skin microbiota–host interactions. *Nature* (2018) 553(7689):427–36. doi: 10.1038/nature25177

50. Bjerre RD, Hugerth LW, Boulund F, Seifert M, Johansen JD, Engstrand L. Effects of sampling strategy and DNA extraction on human skin microbiome investigations. *Sci Rep* (2019) 9(1):17287. doi: 10.1038/s41598-019-53599-z

51. Marotz CA, Sanders JG, Zuniga C, Zaramela LS, Knight R, Zengler K. Improving saliva shotgun metagenomics by chemical host DNA depletion. *Microbiome* (2018) 6 (1):42. doi: 10.1186/s40168-018-0426-3

52. Rajar P, Dhariwal A, Salvadori G, Junges R, Åmdal HA, Berild D, et al. Microbial DNA extraction of high-host content and low biomass samples: Optimized protocol for nasopharynx metagenomic studies. *Front Microbiol* (2022) 13:1038120. doi: 10.3389/fmicb.2022.1038120

53. Nelson MT, Pope CE, Marsh RL, Wolter DJ, Weiss EJ, Hager KR, et al. Human and extracellular DNA depletion for metagenomic analysis of complex clinical infection samples yields optimized viable microbiome profiles. *Cell Rep* (2019) 26 (8):2227–2240.e5. doi: 10.1016/j.celrep.2019.01.091

54. Marotz C, Cavagnero KJ, Song SJ, McDonald D, Wandro S, Humphrey G, et al. Evaluation of the effect of storage methods on fecal, saliva, and skin microbiome composition. *Beiko RG editor. mSystems* (2021) 6(2):e01329–20. doi: 10.1128/mSystems.01329-20

55. Meisel JS, Hannigan GD, Tyldsley AS, SanMiguel AJ, Hodkinson BP, Zheng Q, et al. Skin microbiome surveys are strongly influenced by experimental design. *J Invest Dermatol* (2016) 136(5):947–56. doi: 10.1016/j.jid.2016.01.016

56. Chakravorty S, Helb D, Burday M, Connell N, Alland D. A detailed analysis of 16S ribosomal RNA gene segments for the diagnosis of pathogenic bacteria. *J Microbiol Methods* (2007) 69(2):330–9. doi: 10.1016/j.mimet.2007.02.005

57. Walters W, Hyde ER, Berg-Lyons D, Ackermann G, Humphrey G, Parada A, et al. Improved bacterial 16S rRNA gene (V4 and V4-5) and fungal internal transcribed spacer marker gene primers for microbial community surveys. *Bik H editor. mSystems* (2016) 1(1):e00009–15. doi: 10.1128/mSystems.00009-15

58. Callahan BJ, McMurdie PJ, Rosen MJ, Han AW, Johnson AJA, Holmes SP. DADA2: High-resolution sample inference from illumina amplicon data. *Nat Methods* (2016) 13(7):581–3. doi: 10.1038/nmeth.3869

59. Edgar RC. Updating the 97% identity threshold for 16S ribosomal RNA OTUs. *Bioinformatics* (2018) 34(14):2371–5. doi: 10.1093/bioinformatics/bty113

60. Lobanov V, Gobet A, Joyce A. Ecosystem-specific microbiota and microbiome databases in the era of big data. *Environ Microbiome* (2022) 17(1):37. doi: 10.1186/s40793-022-00433-1

61. Kaehler BD, Bokulich NA, McDonald D, Knight R, Caporaso JG, Huttley GA. Species abundance information improves sequence taxonomy classification accuracy. *Nat Commun* (2019) 10(1):4643. doi: 10.1038/s41467-019-12669-6

62. Comparative Sequencing Program NISC, Oh J, Byrd AL, Deming C, Conlan S, Kong HH, et al. Biogeography and individuality shape function in the human skin metagenome. *Nature* (2014) 514(7520):59–64. doi: 10.1038/nature13786

63. Oh J, Byrd AL, Park M, Kong HH, Segre JA. Temporal stability of the human skin microbiome. *Cell* (2016) 165(4):854–66. doi: 10.1016/j.cell.2016.04.008

64. Scholz CFP, Kilian M. The natural history of cutaneous propionibacteria, and reclassification of selected species within the genus propionibacterium to the proposed novel genera acidipropionibacterium gen. nov., cutibacterium gen. nov. and pseudopropionibacterium gen. nov. *Int J Syst Evol Microbiol* (2016) 66(11):4422–32. doi: 10.1099/ijsem.0.001367

65. Byrd AL, Belkaid Y, Segre JA. The human skin microbiome. *Nat Rev Microbiol* (2018) 16(3):143–55. doi: 10.1038/nrmicro.2017.157

66. Conwill A, Kuan AC, Damerla R, Poret AJ, Baker JS, Tripp AD, et al. Anatomy promotes neutral coexistence of strains in the human skin microbiome. *Cell Host Microbe* (2022) 30(2):171–82.e7. doi: 10.1016/j.chom.2021.12.007

67. Nguyen UT, Kalan LR. Forgotten fungi: the importance of the skin mycobiome. *Curr Opin Microbiol* (2022) 70:102235. doi: 10.1016/j.mib.2022.102235

68. Foulongne V, Sauvage V, Hebert C, Dereure O, Cheval J, Gouilh MA, et al. Human skin microbiota: High diversity of DNA viruses identified on the human skin by high throughput sequencing. *PloS One* (2012) 7(6):e38499. doi: 10.1371/journal.pone.0038499

69. Wylie KM, Mihindukulasuriya KA, Zhou Y, Sodergren E, Storch GA, Weinstock GM. Metagenomic analysis of double-stranded DNA viruses in healthy adults. *BMC Biol* (2014) 12:71. doi: 10.1186/s12915-014-0071-7

70. Grice EA. The intersection of microbiome and host at the skin interface: Genomic- and metagenomic-based insights. *Genome Res* (2015) 25(10):1514–20. doi: 10.1101/gr.191320.115

71. Daou H, Paradiso M, Hennessy K, Seminario-Vidal L. Rosacea and the microbiome: A systematic review. *Dermatol Ther* (2021) 11(1):1–12. doi: 10.1007/s13555-020-00460-1

72. Chen W, Plewig G. Human demodicosis: revisit and a proposed classification. *Br J Dermatol* (2014) 170(6):1219–25. doi: 10.1111/bjd.12850

73. O'Reilly N, Menezes N, Kavanagh K. Positive correlation between serum immunoreactivity to *Demodex* -associated *Bacillus* proteins and erythematotelangiectatic rosacea: Correlation between *Bacillus* proteins from *Demodex* and erythematotelangiectatic rosacea. *Br J Dermatol* (2012) 167(5):1032–6. doi: 10.1111/j.1365-2133.2012.11114.x

74. Moissl-Eichinger C, Probst AJ, Birarda G, Auerbach A, Koskinen K, Wolf P, et al. Human age and skin physiology shape diversity and abundance of archaea on skin. *Sci Rep* (2017) 7(1):4039. doi: 10.1038/s41598-017-04197-4

75. Probst AJ, Auerbach AK, Moissl-Eichinger C. Archaea on human skin. *PloS One* (2013) 8(6):e65388. doi: 10.1371/journal.pone.0065388

76. Umbach AK, Stegelmeier AA, Neufeld JD. Archaea are rare and uncommon members of the mammalian skin microbiome. *mSystems* (2021) 6(4):e00642–21. doi: 10.1128/mSystems.00642-21

77. Koskinen K, Pausan MR, Perras AK, Beck M, Bang C, Mora M, et al. First insights into the diverse human archaeome: Specific detection of archaea in the gastrointestinal tract, lung, and nose and on skin. *mBio* (2017) 8(6):e00824–17. doi: 10.1128/mBio.00824-17

78. Bjerre RD, Holm JB, Palleja A, Sølberg J, Skov L, Johansen JD. Skin dysbiosis in the microbiome in atopic dermatitis is site-specific and involves bacteria, fungus and virus. *BMC Microbiol* (2021) 21(1):256. doi: 10.1186/s12866-021-02302-2

79. Byrd AL, Deming C, Cassidy SKB, Harrison OJ, Ng WI, Conlan S, et al. *Staphylococcus aureus* and *Staphylococcus epidermidis* strain diversity underlying pediatric atopic dermatitis. *Sci Transl Med* (2017) 9(397):eaal4651. doi: 10.1126/scitranslmed.aal4651

80. Saxena R, Mittal P, Clavaud C, Dhakan DB, Hegde P, Veeranagaiah MM, et al. Comparison of healthy and dandruff scalp microbiome reveals the role of commensals in scalp health. *Front Cell Infect Microbiol* (2018) 8:346. doi: 10.3389/fcimb.2018.00346

81. Barnard E, Shi B, Kang D, Craft N, Li H. The balance of metagenomic elements shapes the skin microbiome in acne and health. *Sci Rep* (2016) 6(1):39491. doi: 10.1038/srep39491

82. Tett A, Pasolli E, Farina S, Truong DT, Asnicar F, Zolfo M, et al. Unexplored diversity and strain-level structure of the skin microbiome associated with psoriasis. *NPJ Biofilms Microbiomes* (2017) 3(1):14. doi: 10.1038/s41522-017-0022-5

83. Williams MR, Cau L, Wang Y, Kaul D, Sanford JA, Zaramela LS, et al. Interplay of staphylococcal and host proteases promotes skin barrier disruption in netherton syndrome. *Cell Rep* (2020) 30(9):2923–2933.e7. doi: 10.1016/j.celrep.2020.02.021

84. Nutten S. Atopic dermatitis: Global epidemiology and risk factors. *Ann Nutr Metab* (2015) 66(Suppl. 1):8–16. doi: 10.1159/000370220

85. Kong HH, Oh J, Deming C, Conlan S, Grice EA, Beatson MA, et al. Temporal shifts in the skin microbiome associated with disease flares and treatment in children with atopic dermatitis. *Genome Res* (2012) 22(5):850–9. doi: 10.1101/gr.131029.111

86. Leyden JJ, Marples RR, Kligman AM. Staphylococcus aureus in the lesions of atopic dermatitis. *Br J Dermatol* (1974) 90(5):525–5. doi: 10.1111/j.1365-2133.1974.tb06447.x

87. Meylan P, Lang C, Mermoud S, Johannsen A, Norrenberg S, Hohl D, et al. Skin colonization by staphylococcus aureus precedes the clinical diagnosis of atopic dermatitis in infancy. *J Invest Dermatol* (2017) 137(12):2497–504. doi: 10.1016/j.jid.2017.07.834

88. Shi B, Bangayan NJ, Curd E, Taylor PA, Gallo RL, Leung DYM, et al. The skin microbiome is different in pediatric versus adult atopic dermatitis. *J Allergy Clin Immunol* (2016) 138(4):1233–6. doi: 10.1016/j.jaci.2016.04.053

89. Di Domenico EG, Cavallo I, Capitanio B, Ascenzioni F, Pimpinelli F, Morrone A, et al. Staphylococcus aureus and the cutaneous microbiota biofilms in the pathogenesis of atopic dermatitis. *Microorganisms* (2019) 7(9):301. doi: 10.3390/microorganisms7090301

90. Bekeredjian-Ding I, Inamura S, Giese T, Moll H, Endres S, Sing A, et al. *Staphylococcus aureus* protein a triggers T cell-independent b cell proliferation by sensitizing b cells for TLR2 ligands. *J Immunol* (2007) 178(5):2803–12. doi: 10.4049/jimmunol.178.5.2803

91. Spaulding AR, Salgado-Pabón W, Kohler PL, Horswill AR, Leung DYM, Schlievert PM. Staphylococcal and streptococcal superantigen exotoxins. *Clin Microbiol Rev* (2013) 26(3):422–47. doi: 10.1128/CMR.00104-12

92. Nakagawa S, Matsumoto M, Katayama Y, Oguma R, Wakabayashi S, Nygaard T, et al. Staphylococcus aureus virulent PSMα peptides induce keratinocyte alarmin release to orchestrate IL-17-Dependent skin inflammation. *Cell Host Microbe* (2017) 22 (5):667–677.e5. doi: 10.1016/j.chom.2017.10.008

93. Vu AT, Baba T, Chen X, Le TA, Kinoshita H, Xie Y, et al. Staphylococcus aureus membrane and diacylated lipopeptide induce thymic stromal lymphopoietin in keratinocytes through the toll-like receptor 2–toll-like receptor 6 pathway. *J Allergy Clin Immunol* (2010) 126(5):985–93.e3. doi: 10.1016/j.jaci.2010.09.002

94. Nakamura Y, Oscherwitz J, Cease KB, Chan SM, Muñoz-Planillo R, Hasegawa M, et al. Staphylococcus δ-toxin induces allergic skin disease by activating mast cells. *Nature* (2013) 503(7476):397–401. doi: 10.1038/nature12655

95. Shaw L, Golonka E, Potempa J, Foster SJ. The role and regulation of the extracellular proteases of staphylococcus aureus. *Microbiology* (2004) 150(1):217–28. doi: 10.1099/mic.0.26634-0

96. Seite S, Flores G, Henley J, Martin R, Zelenkova H, Luc A. Microbiome of affected and unaffected skin of patients with atopic dermatitis before and after emollient treatment. *J Drugs Dermatol* (2014) 13(11):1365–72.

97. Hon KL, Tsang YCK, Pong NH, Leung TF, Ip M. Exploring staphylococcus epidermidis in atopic eczema: Friend or foe? *Clin Exp Dermatol* (2016) 41(6):659–63. doi: 10.1111/ced.12866

98. Brown MM, Horswill AR. Staphylococcus epidermidis–skin friend or foe? *PloS Pathog* (2020) 16(11):e1009026. doi: 10.1371/journal.ppat.1009026

99. Wanke I, Steffen H, Christ C, Krismer B, Götz F, Peschel A, et al. Skin commensals amplify the innate immune response to pathogens by activation of distinct signaling pathways. *J Invest Dermatol* (2011) 131(2):382–90. doi: 10.1038/jid.2010.328

100. Cogen AL, Yamasaki K, Muto J, Sanchez KM, Crotty Alexander L, Tanios J, et al. Staphylococcus epidermidis antimicrobial δ-toxin (Phenol-soluble modulin-γ) cooperates with host antimicrobial peptides to kill group a streptococcus. *PloS One* (2010) 55(1):e8557. doi: 10.1371/journal.pone.0008557

101. Conlan S, Mijares LA NISCComparative Sequencing Program, , Becker J, RW B, GG B, et al. Staphylococcus epidermidis pan-genome sequence analysis reveals diversity of skin commensal and hospital infection-associated isolates. *Genome Biol* (2012) 13(7):R64. doi: 10.1186/gb-2012-13-7-r64

102. Ochlich D, Rademacher F, Drerup KA, Gläser R, Harder J. The influence of the commensal skin bacterium staphylococcus epidermidis on the epidermal barrier and inflammation: Implications for atopic dermatitis. *Exp Dermatol* (2022) 20:exd.14727. doi: 10.1111/exd.14727

103. Burian M, Bitschar K, Dylus B, Peschel A, Schittek B. The protective effect of microbiota on s. aureus skin colonization depends on the integrity of the epithelial barrier. *J Invest Dermatol* (2017) 137(4):976–9. doi: 10.1016/j.jid.2016.11.024

104. Cau L, Williams MR, Butcher AM, Nakatsuji T, Kavanaugh JS, Cheng JY, et al. Staphylococcus epidermidis protease EcpA can be a deleterious component of the skin microbiome in atopic dermatitis. *J Allergy Clin Immunol* (2021) 147(3):955–966.e16. doi: 10.1016/j.jaci.2020.06.024

105. Chng KR, Tay ASL, Li C, Ng AHQ, Wang J, Suri BK, et al. Whole metagenome profiling reveals skin microbiome-dependent susceptibility to atopic dermatitis flare. *Nat Microbiol* (2016) 1(9):16106. doi: 10.1038/nmicrobiol.2016.106

106. Tao R, Li R, Wang R. Skin microbiome alterations in seborrheic dermatitis and dandruff: A systematic review. *Exp Dermatol* (2021) 30(10):1546–53. doi: 10.1111/exd.14450

107. Lin Q, Panchamukhi A, Li P, Shan W, Zhou H, Hou L, et al. Malassezia and staphylococcus dominate scalp microbiome for seborrheic dermatitis. *Bioprocess Biosyst Eng* (2021) 44(5):965–75. doi: 10.1007/s00449-020-02333-5

108. Carmona-Cruz S, Orozco-Covarrubias L, Sáez-de-Ocariz M. The human skin microbiome in selected cutaneous diseases. *Front Cell Infect Microbiol* (2022) 12:834135. doi: 10.3389/fcimb.2022.834135

109. Goularte-Silva V, Paulino LC. Ketoconazole beyond antifungal activity: Bioinformatics-based hypothesis on lipid metabolism in dandruff and seborrheic dermatitis. *Exp Dermatol* (2022) 31(5):821–2. doi: 10.1111/exd.14505

110. Tan JKL, Bhate K. A global perspective on the epidemiology of acne. *Br J Dermatol* (2015) 172:3–12. doi: 10.1111/bjd.13462

111. Vallerand IA, Lewinson RT, Parsons LM, Lowerison MW, Frolkis AD, Kaplan GG, et al. Risk of depression among patients with acne in the U.K.: A population-based cohort study. *Br J Dermatol* (2018) 178(3):e194–5. doi: 10.1111/bjd.16099

112. O'Neill AM, Gallo RL. Host-microbiome interactions and recent progress into understanding the biology of acne vulgaris. *Microbiome* (2018) 6(1):177. doi: 10.1186/s40168-018-0558-5

113. Nakatsuji T, Tang D chu C, Zhang L, Gallo RL, Huang CM. Propionibacterium acnes CAMP factor and host acid sphingomyelinase contribute to bacterial virulence: Potential targets for inflammatory acne treatment. *Horsburgh MJ editor. PloS One* (2011) 6(4):e14797. doi: 10.1371/journal.pone.0014797

114. Rimon A, Rakov C, Lerer V, Sheffer-Levi S, Oren SA, Shlomov T, et al. Topical phage therapy in a mouse model of cutibacterium acnes-induced acne-like lesions. *Nat Commun* (2023) 14(1):1005. doi: 10.1038/s41467-023-36694-8

115. Jahns AC, Lundskog B, Ganceviciene R, Palmer RH, Golovleva I, Zouboulis CC, et al. An increased incidence of propionibacterium acnes biofilms in acne vulgaris: a case-control study: Increased incidence of p. acnes biofilms in acne vulgaris. *Br J Dermatol* (2012) 167(1):50–8. doi: 10.1111/j.1365-2133.2012.10897.x

116. Fitz-Gibbon S, Tomida S, Chiu BH, Nguyen L, Du C, Liu M, et al. Propionibacterium acnes strain populations in the human skin microbiome associated with acne. *J Investigate Derma* (2013) 133:2152–60. doi: 10.1038/jid.2013.21

117. Dagnelie MA, Khammari A, Dréno B, Corvec S. Cutibacterium acnes molecular typing: time to standardize the method. *Clin Microbiol Infect* (2018) 24(11):1149–55. doi: 10.1016/j.cmi.2018.03.010

118. Salar-Vidal L, Achermann Y, Aguilera-Correa JJ, Poehlein A, Esteban J, Brüggemann H, et al. Genomic analysis of cutibacterium acnes strains isolated from prosthetic joint infections. *Microorganisms* (2021) 9(7):1500. doi: 10.3390/microorganisms9071500

119. Spittaels KJ, Coenye T. Developing an *in vitro* artificial sebum model to study propionibacterium acnes biofilms. *Anaerobe* (2018) 49:21–9. doi: 10.1016/j.anaerobe.2017.11.002

120. Kasimatis G, Fitz-Gibbon S, Tomida S, Wong M, Li H. Analysis of complete genomes of *Propionibacterium acnes* reveals a novel plasmid and increased pseudogenes in an acne associated strain. *BioMed Res Int* (2013) 2013:1–11. doi: 10.1155/2013/918320

121. Dreno B, Martin R, Moyal D, Henley JB, Khammari A, Seité S. Skin microbiome and *acne vulgarisStaphylococcus*, a new actor in acne. *Exp Dermatol* (2017) 26(9):798–803. doi: 10.1111/exd.13296

122. Bronnec V, Eilers H, Jahns AC, Omer H, Alexeyev OA. Propionibacterium (Cutibacterium) granulosum extracellular DNase BmdE targeting propionibacterium (Cutibacterium) acnes biofilm matrix, a novel inter-species competition mechanism. *Front Cell Infect Microbiol* (2022) 11:809792. doi: 10.3389/fcimb.2021.809792

123. Greb JE, Goldminz AM, Elder JT, Lebwohl MG, Gladman DD, Wu JJ, et al. Psoriasis. *Nat Rev Dis Primer* (2016) 2(1):16082. doi: 10.1038/nrdp.2016.82

124. Hugh JM, Weinberg JM. Update on the pathophysiology of psoriasis. *Cutis* (2018) 102(5S):6–12.

125. Weisenseel P. Streptococcal infection distinguishes different types of psoriasis. *J Med Genet* (2002) 39(10):767–8. doi: 10.1136/jmg.39.10.767

126. Lewis DJ, Chan WH, Hinojosa T, Hsu S, Feldman SR. Mechanisms of microbial pathogenesis and the role of the skin microbiome in psoriasis: A review. *Clin Dermatol* (2019) 37(2):160–6. doi: 10.1016/j.clindermatol.2019.01.011

127. Chang HW, Yan D, Singh R, Liu J, Lu X, Ucmak D, et al. Alteration of the cutaneous microbiome in psoriasis and potential role in Th17 polarization. *Microbiome* (2018) 6(1):154. doi: 10.1186/s40168-018-0533-1

128. Tutka K, Żychowska M, Reich A. Diversity and composition of the skin, blood and gut microbiome in rosacea–a systematic review of the literature. *Microorganisms* (2020) 8(11):1756. doi: 10.3390/microorganisms8111756

129. Holmes AD. Potential role of microorganisms in the pathogenesis of rosacea. *J Am Acad Dermatol* (2013) 69(6):1025–32. doi: 10.1016/j.jaad.2013.08.006

130. Casas C, Paul C, Lahfa M, Livideanu B, Lejeune O, Alvarez-Georges S, et al. Quantification of *Demodex folliculorum* by PCR in rosacea and its relationship to skin innate immune activation. *Exp Dermatol* (2012) 21(12):906–10. doi: 10.1111/exd.12030

131. Whitfeld M, Gunasingam N, Leow LJ, Shirato K, Preda V. Staphylococcus epidermidis: A possible role in the pustules of rosacea. *J Am Acad Dermatol* (2011) 64(1):49–52. doi: 10.1016/j.jaad.2009.12.036

132. Dahl MV, Ross AJ, Schlievert PM. Temperature regulates bacterial protein production: possible role in rosacea. *J Am Acad Dermatol* (2004) 50(2):266–72. doi: 10.1016/j.jaad.2003.05.005

133. Wang R, Farhat M, Na J, Li R, Wu Y. Bacterial and fungal microbiome characterization in patients with rosacea and healthy controls. *Br J Dermatol* (2020) 183(6):1112–4. doi: 10.1111/bjd.19315

134. Chopra D, Arens RA, Amornpairoj W, Lowes MA, Tomic-Canic M, Strbo N, et al. Innate immunity and microbial dysbiosis in hidradenitis suppurativa – vicious cycle of chronic inflammation. *Front Immunol* (2022) 13:960488. doi: 10.3389/fimmu.2022.960488

135. Nomura T. Hidradenitis suppurativa as a potential subtype of autoinflammatory keratinization disease. *Front Immunol* (2020) 11:847. doi: 10.3389/fimmu.2020.00847

136. Goldburg SR, Strober BE, Payette MJ. Hidradenitis suppurativa. *J Am Acad Dermatol* (2020) 82(5):1045–58. doi: 10.1016/j.jaad.2019.08.090

137. Mintoff D, Borg I, Pace NP. The clinical relevance of the microbiome in hidradenitis suppurativa: A systematic review. *Vaccines* (2021) 9(10):1076. doi: 10.3390/vaccines9101076

138. Riverain-Gillet É, Guet-Revillet H, Jais JP, Ungeheuer MN, Duchatelet S, Delage M, et al. The surface microbiome of clinically unaffected skinfolds in hidradenitis suppurativa: A cross-sectional culture-based and 16S rRNA gene amplicon sequencing study in 60 patients. *J Invest Dermatol* (2020) 140(9):1847–1855.e6. doi: 10.1016/j.jid.2020.02.046

139. Ring HC, Sigsgaard V, Thorsen J, Fuursted K, Fabricius S, Saunte DM, et al. The microbiome of tunnels in hidradenitis suppurativa patients. *J Eur Acad Dermatol Venereol* (2019) 33(9):1775–80. doi: 10.1111/jdv.15597

140. Ring HC, Thorsen J, Saunte DM, Lilje B, Bay L, Riis PT, et al. The follicular skin microbiome in patients with hidradenitis suppurativa and healthy controls. *JAMA Dermatol* (2017) 153(9):897. doi: 10.1001/jamadermatol.2017.0904

141. Guet-Revillet H, Jais JP, Ungeheuer MN, Coignard-Biehler H, Duchatelet S, Delage M, et al. The microbiological landscape of anaerobic infections in hidradenitis suppurativa: A prospective metagenomic study. *Clin Infect Dis* (2017) 65(2):282–91. doi: 10.1093/cid/cix285

142. Naik HB, Jo JH, Paul M, Kong HH. Skin microbiota perturbations are distinct and disease severity–dependent in hidradenitis suppurativa. *J Invest Dermatol* (2020) 140(4):922–5.e3. doi: 10.1016/j.jid.2019.08.445

143. Ring HC, Thorsen J, Jørgensen AH, Bay L, Bjarnsholt T, Fuursted K, et al. Predictive metagenomic analysis reveals a role of cutaneous dysbiosis in the development of hidradenitis suppurativa. *J Invest Dermatol* (2020) 140(7):1473–6. doi: 10.1016/j.jid.2019.11.011

144. Świerczewska Z, Lewandowski M, Surowiecka A, Barańska-Rybak W. Microbiome in hidradenitis suppurativa–what we know and where we are heading. *Int J Mol Sci* (2022) 23(19):11280. doi: 10.3390/ijms231911280

145. Gutiérrez-Cerrajero C, Sprecher E, Paller AS, Akiyama M, Mazereeuw-Hautier J, Hernández-Martín A, et al. Ichthyosis. *Nat Rev Dis Primers* (2023) 9:2. doi: 10.1038/s41572-022-00412-3

146. Lee SY, Lee E, Park YM, Hong SJ. Microbiome in the gut-skin axis in atopic dermatitis. *Allergy Asthma Immunol Res* (2018) 10(4):354. doi: 10.4168/aair.2018.10.4.354

147. Siddiqui R, Makhlouf Z, Khan NA. The increasing importance of the gut microbiome in acne vulgaris. *Folia Microbiol (Praha)* (2022) 67(6):825–35. doi: 10.1007/s12223-022-00982-5

148. Chen L, Li J, Zhu W, Kuang Y, Liu T, Zhang W, et al. Skin and gut microbiome in psoriasis: Gaining insight into the pathophysiology of it and finding novel therapeutic strategies. *Front Microbiol* (2020) 11:589726. doi: 10.3389/fmicb.2020.589726

149. Luck ME, Tao J, Lake EP. The skin and gut microbiome in hidradenitis suppurativa: Current understanding and future considerations for research and treatment. *Am J Clin Dermatol* (2022) 23(6):841–52. doi: 10.1007/s40257-022-00724-w

150. Marek-Jozefowicz L, Czajkowski R, Borkowska A, Nedoszytko B, Żmijewski MA, WJ Cubała, et al. The brain–skin axis in psoriasis–psychological, psychiatric, hormonal, and dermatological aspects. *Int J Mol Sci* (2022) 23(2):669. doi: 10.3390/ijms23020669

frontiers | Frontiers in Immunology

TYPE Original Research
PUBLISHED 14 April 2023
DOI 10.3389/fimmu.2023.1114586

OPEN ACCESS

EDITED BY
Eun Jeong Park,
Mie University, Japan

REVIEWED BY
James Alexander Pearson,
Cardiff University, United Kingdom
Yuhao Jiao,
Peking Union Medical College Hospital (CAMS), China

*CORRESPONDENCE
Heng Xu
xuheng81916@scu.edu.cn
Wei Li
liweihx_hxyy@scu.edu.cn

†These authors have contributed equally to this work and share first authorship

SPECIALTY SECTION
This article was submitted to Molecular Innate Immunity, a section of the journal Frontiers in Immunology

RECEIVED 02 December 2022
ACCEPTED 28 March 2023
PUBLISHED 14 April 2023

CITATION
Wang Y, Xia X, Zhou X, Zhan T, Dai Q, Zhang Y, Zhang W, Shu Y, Li W and Xu H (2023) Association of gut microbiome and metabolites with onset and treatment response of patients with pemphigus vulgaris. *Front. Immunol.* 14:1114586. doi: 10.3389/fimmu.2023.1114586

Association of gut microbiome and metabolites with onset and treatment response of patients with pemphigus vulgaris

Yiyi Wang[1†], Xuyang Xia[2†], Xingli Zhou[1], Tongying Zhan[1], Qinghong Dai[3], Yan Zhang[4], Wei Zhang[3], Yang Shu[2], Wei Li[1*] and Heng Xu[2,5*]

[1]Department of Dermatology & Rare Disease Center, West China Hospital, Sichuan University, Chengdu, China, [2]State Key Laboratory of Biotherapy and Cancer Center, West China Hospital, Chengdu, China, [3]Department of Clinical Pharmacology, Hunan Key Laboratory of Pharmacogenetics, Xiangya Hospital, Central South University, Changsha, China, [4]Lung Cancer Center, West China Hospital, Sichuan University, Chengdu, China, [5]Department of Laboratory Medicine, Research Center of Clinical Laboratory Medicine, West China Hospital, Sichuan University, Chengdu, China

Background: Gut dysbiosis and gut microbiome-derived metabolites have been implicated in both disease onset and treatment response, but this has been rarely demonstrated in pemphigus vulgaris (PV). Here, we aim to systematically characterize the gut microbiome to assess the specific microbial species and metabolites associated with PV.

Methods: We enrolled 60 PV patients and 19 matched healthy family members, and collected 100 fecal samples (60 treatment-naïve, 21 matched post-treatment, and 19 controls). Metagenomic shotgun sequencing and subsequent quality control/alignment/annotation were performed to assess the composition and microbial species, in order to establish the association between gut microbiome with PV onset and treatment response. In addition, we evaluated short-chain fatty acids (SCFAs) in PV patients through targeted metabolomics analysis.

Results: The diversity of the gut microbiome in PV patients deviates from the healthy family members but not between responder and non-responder, or before and after glucocorticoid treatment. However, the relative abundance of several microbial species, including the pathogenic bacteria (e.g., *Escherichia coli*) and some SCFA-producing probiotics (e.g., *Eubacterium ventriosum*), consistently differed between the two groups in each comparison. *Escherichia coli* was enriched in PV patients and significantly decreased after treatment in responders. In contrast, *Eubacterium ventriosum* was enriched in healthy family members and significantly increased particularly in responders after treatment. Consistently, several gut microbiome-derived SCFAs were enriched in healthy family members and significantly increased after treatment (e.g., butyric acid and valeric acid).

Conclusions: This study supports the association between the gut microbiome and PV onset, possibly through disrupting the balance of gut pathogenic bacteria and probiotics and influencing the level of gut microbiome-derived SCFAs. Furthermore, we revealed the potential relationship between specific microbial species and glucocorticoid treatment.

KEYWORDS

pemphigus vulgaris, microbiome, glucocorticoid, short-chain fatty acids, metagemonic

Introduction

Pemphigus is a severe, recurrent, potentially fatal autoimmune bullous disease characterized by the formation of flaccid blisters and erosive lesions on the skin or mucous membranes (1). Multiple pemphigus subtypes were identified, with pemphigus vulgaris (PV) ranking at the top in terms of incidence. The production of pathogenic autoantibodies against the desmosomal adhesion glycoproteins desmoglein (Dsg)1 and Dsg3 is considered the direct cause of pemphigus (1–3). Nevertheless, the molecular mechanisms underlying the onset of pemphigus remain poorly understood. Diverse risk factors have been explored, including several HLA haplotypes as inherited predispositions and environmental factors such as adverse drug reactions, viral infections, diet, and stress (1, 2, 4–6)

Environmental factors are believed to be key determinants of gut microbial composition and function, and dysbiosis of the gut microbiome can induce local and systemic immune responses in the host, thereby influencing the onset of autoimmune diseases (7). Indeed, numerous studies have identified significant differences in the gut microbiome between healthy controls and patients with autoimmune diseases (e.g., rheumatoid arthritis, systemic lupus erythematosus, and ankylosing spondylitis) (8–10). Their immunologic process might be influenced by the disturbed gut microbiome through several hypothesized pathways, including oxidative phosphorylation and biosynthesis of branched-chain amino acids (8, 11, 12). Similarly, the association between the gut microbiome and PV onset has also been revealed (13), which suggested a few specific PV-associated microbial species due to the limitation of sample size and 16S rRNA sequencing technical. Therefore, larger sample sizes and higher-resolution approaches are required for a more comprehensive analysis. In contrast to 16S rRNA sequencing, metagenomic sequencing can locate the differential bacteria at the species level and obtain more comprehensive information on detailed functional genes and pathways (14–16).

Moreover, complex bidirectional interactions between the gut microbiome and drugs/treatment outcomes were also revealed (17). Multiple non-antibiotic drugs can alter the composition viability of the gut microbiome, while the gut microbiome may in turn regulate the therapeutic effects and toxicities of drugs (17–22). Recently, *in vitro* screening of the extensive impact of non-antibiotic drugs on human gut bacteria has revealed that approximately a quarter of the marketed non-antibiotic drugs exhibit an inhibitory effect on the representative gut microbial strains (23). Not surprisingly, the association between the gut microbiome and individualized drug response (e.g., anti-TNFα) has been investigated in autoimmune diseases (24–26). For PV treatment, although most patients remit and recover after receiving typical conventional treatment, some cases remain refractory and resistant to conventional therapy, which may be attributed to the individualized microbiome.

Gut microbiome-derived metabolites are small molecules produced as intermediate or final products of microbial metabolism. They are one of the primary mechanisms by which the gut microbiome interacts with the host, and exhibit an important and diverse effect on host physiology (27, 28). Specific classes of gut microbiome-derived metabolites, such as short-chain fatty acids (SCFAs), have been implicated to act on numerous cell types to regulate many biological processes, including host metabolism and immune function (29), thus contributing to the onset of diseases and treatment response (30–32). It is worthwhile to investigate whether gut microbiome-derived metabolites play a role in the underlying mechanism of PV.

In this study, we systematically explored the gut microbiome and metabolites in PV patients through metagenomic shotgun sequencing and a targeted metabolomics approach, shedding light on their potential roles in PV onset and treatment response.

Material and methods

Study cohort and patient information

Patients in this study were derived from the autoimmune blister disease cohort in the Department of Dermatology, West China Hospital of Sichuan University. All samples were collected from November 2017 to April 2019. The study was approved by the local ethics committee [West China Hospital, Sichuan University, approval no. 2017 (241)], and all participants signed informed consent forms.

The PV group comprised glucocorticoid-naïve patients with clinically confirmed PV between the ages of 18 and 80 years. PV was diagnosed strictly by the accepted standard (10): patients must have typical clinical manifestations of pemphigus vulgaris,

intraepidermal blistering and acantholysis on histopathology, net-like immunoglobulin G (IgG), and complement component 3 (C3) deposition on mucosa and/or skin membranes detected by direct immunofluorescence and increased anti-Dsg3 antibody with or without anti-Dsg1 antibody in serum. Controls were healthy family members of some patients in the PV group who were free of skin diseases and live together with their matched pemphigus patients. The healthy controls also have similar eating habits, lifestyles, and living environments with PV patients and are generally comparable to PV patients in terms of sex, age, and body mass index (BMI) (Table S1). Individuals were excluded if they had a medication history within three months before sampling (including antibiotics, probiotics, immunosuppressors, etc.) or any other diseases (including other autoimmune diseases, metabolic diseases, malignant tumors, visceral organ dysfunction, etc.). Pregnant or lactating women were also excluded.

Detailed demographic and clinical information of all subjects was collected and presented in Table S1, including sex, age, BMI, affected skin/mucosa, pemphigus disease area index (PDAI), anti-Dsg1 antibody titers, and anti-Dsg3 antibody titers. PDAI was evaluated by two experienced dermatologists, while laboratory indexes were measured by the Department of Laboratory Medicine in our hospital according to standard procedures.

At the time of sampling, PDAI scores were evaluated for patients in the PV group. Subsequently, following the British guidelines for the management of pemphigus (33), the certain treatment option was applied for one patient based on disease severity (mild, moderate, or severe), disease stage (acute progressive or stable stage), relative restriction of large-dose GC, etc. In this cohort, 46 of them received glucocorticoid-alone therapy and 14 of them who are not suitable for large-dose glucocorticoid (e.g., elder patients) or at disease acute progressive stage received glucocorticoid combined with azathioprine/cyclosporine therapy. The PDAI scores were reassessed after one month. PDAI improvement rate (ΔPDAI) referred to the percentage of reduction in PDAI scores after one month of conventional treatment. Patients were defined as the responder group if their ΔPDAI were more than or equal to 50%, whereas refractory pemphigus vulgaris, namely the non-responder group, had PDAI scores that decreased by less than 50%. Furthermore, after one month of glucocorticoid-alone therapy, 21 patients were resampled and separated into the responder and non-responder groups to explore the gut microbial changes after glucocorticoid treatment.

Sample collection and DNA extraction

Fresh stool samples were collected in the hospital and then immediately transported to the laboratory in an ice bag. In the laboratory, the samples were divided into four 15 mL centrifuge tubes containing 1 g of stool each and stored at -80°C for further processing. DNA extraction was performed using the CTAB method. The DNA concentration was measured using a Qubit® dsDNA Assay Kit in a Qubit® 2.0 fluorometer, and its degradation degree was monitored on 1% agarose gels.

DNA library construction and sequencing

A total amount of 1 μg DNA per sample was used as input material for the DNA sample preparations. Utilizing the NEBNext® UltraTM DNA Library Prep Kit for Illumina (NEB, USA) following the manufacturer's instructions, sequencing libraries were created, and index codes were added to assign sequences to specific samples. Briefly, after being sonicated to a fragment size of 350 bp, the DNA sample was end-polished, A-tailed, and ligated with the full-length adaptor for Illumina sequencing with further PCR amplification. Finally, libraries were evaluated for size distribution using an Agilent2100 Bioanalyzer, and quantities were determined using real-time PCR after PCR products had been purified (AMPure XP system). On a cBot Cluster Generation System, the index-coded samples were clustered in accordance with the manufacturer's recommendations. Following cluster creation, the library preparations were sequenced on an Illumina HiSeq platform, resulting in the production of paired-end reads.

Gene catalog construction

Following quality control, the sequencing reads were *de novo* assembled into contigs using Megahit v1.2.9 (11). Gene prediction from the assembled contigs was performed using Prokka v1.13 (12). Using CD-hit (13), redundant genes with 90% coverage and 95% similarity were eliminated. Finally, we used Salmon v1.4.0 (14) to quantify the relative abundances of the genes and obtained a nonredundant gene catalog comprising 4045593 genes.

Taxonomical annotation

For the accuracy of taxonomical annotation, we used MetaPhlAn2 (15) for alignment and annotation based on bacterial marker genes. After obtaining a taxonomical relative abundance profile, we used the Galaxy online platform (http://huttenhower.sph.harvard.edu/galaxy) to perform the linear discriminant analysis effect size (LEFSe) and visualized the result using boxplots (R v3.6.1, ggplot2 package).

Rarefaction curve analysis, diversity analyses, and enterotypes

To evaluate the gene richness in PV patients and healthy controls, a rarefaction curve was created. By randomly subsampling the cohort 30 times with replacement, we were able to calculate the gene richness from a given number of samples. We discovered that the gene richness progressively increased and leveled out as the sample size increased, demonstrating that the sample size was adequate. The process was implemented using the vegan package in R v3.6.1. α-Diversity was calculated based on the taxonomical abundance profile of each sample according to the Shannon index, while β-diversity was calculated using the Bray–

Curtis distance. Furthermore, the genus abundance profile of the samples was subjected to permutational multivariate analysis of variance (PERMANOVA) (16) in order to compare the group of PV with healthy controls. We used Bray–Curtis distance and 9,999 permutations (R v3.6.1, vegan package). The enterotypes of each sample were analyzed by the Dirichlet multinomial mixture model-based method (17) using the DirichletMultinomial package in R v3.6.1.

Co-occurrence network

Spearman's rank correlation coefficient between differential species was calculated based on the species abundance profile. A network was then constructed by using the method implemented in Cytoscape v3.8.2. In the network, the edges indicate the correlation between two species, following the standard that Spearman's rank correlation coefficient > 0.25 (blue line of the edge) or < -0.25 (red line of the edge).

Random forest classifier

The random forest model with 10-fold cross-validation was established (R v3.6.1, randomForest package) using the differential species abundance profile. The average error curves from five trials of the 10-fold cross-validation were calculated. The cutoff was determined using the average curve's smallest error plus the standard deviation at that point. We compiled a list of all species marker sets with errors lower than the cutoff value, and the set with the fewest species was chosen as the optimal set (18). The receiver operating characteristic curves were drawn using the pROC3 package in R v3.6.1.

Functional analysis

For KEGG analysis, we first determined the KEGG Orthologs (KO) name of each gene by aligning the gene catalog to the eggNOG database using Diamond v2.0.5 (19) to expedite the protein sequence alignment procedure. By adding up the identical KOs, the relative abundance profile of KOs was obtained (a KO name contains multiple genes). Next, we downloaded the latest KEGG pathway list from the KEGG database (https://www.kegg.jp/keggbin/show_brite?ko00001.keg), enriched the KOs to the KEGG pathways, and screened the B- and C-level differential KEGG pathways between the PV and healthy control groups. The detailed screening method was as follows: 1) the KOs only expressed in less than 5 samples were removed, 2) different KOs were identified between the PV and healthy control groups (Benjamin–Hochberg q-value < 0.2, two-tail Wilcoxon sum-rank test), 3) the percentages of KO markers belonging to each KEGG category out of the total PV-enriched or control-enriched KO markers were calculated, and 4) Fisher's exact test was used to calculate the significance level (20). Finally, KEGG with a P value < 0.05 was considered a different KEGG pathway between the PV and healthy control groups. Furthermore, we obtained significant MetaCyc pathways based on HUMAnN2 pipeline (34) and showed the contribution of specific microbial species to these pathways using the ggplot2 package in R v3.6.1.

Detection of short-chain fatty acids

First, a 2 mL EP tube was filled with a 20 mg fecal sample that had been precisely weighed. The EP tube was filled with a milliliter of phosphoric acid solution (0.5% v/v) and a tiny steel ball. The mixture was three times ground for 10 seconds each, vortexed for 10 minutes, and ultrasonically heated for 5 minutes. The mixture was then centrifuged at 12000 rpm for 10 min at 4°C before being put into a 1.5 mL centrifuge tube with 0.1 mL of the supernatant. The centrifuge tube was filled with 0.5 mL of MTBE solution (including internal standard). The combination underwent 3 minutes of vortexing and 5 minutes of ultrasonication. The mixture was then centrifuged for 10 minutes at 4°C at a speed of 12000 rpm. GC-MS/MS analysis was performed using the supernatant that was obtained (21).

Then, an Agilent 7890B gas chromatograph coupled to a 7000D mass spectrometer with a DB-FFAP column (30 m length × 0.25 mm i.d. × 0.25 μm film thickness, J&W Scientific, USA) was employed for GC–MS/MS analysis of short-chain fatty acids (SCFAs). Helium was used as a carrier gas at a flow rate of 1.2 mL/min. The injection volume was 2 L, and the injection was performed in split mode. The oven temperature was kept at 90°C for one minute, then increased by 25°C every minute to 100°C, 20°C every minute to 150°C, held for 0.6 minutes, and then increased by 25°C every minute to 200°C, and held for 0.5 minutes after running for 3 minutes. All samples underwent numerous modalities of reaction monitoring analysis. The transfer line and injector inlet temperatures were 200 and 230 degrees Celsius, respectively (21, 22).

Finally, SCFA contents were detected by MetWare (http://www.metware.cn/) based on the Agilent 7890B-7000D GC–MS/MS platform.

Statistical analysis

A significant difference in the study was determined if the P value was less than 0.05 (different KOs were identified based on the adjusted P value was less than 0.2 using the Benjamin-Hochberg method). The P value of α- and β-diversities were calculated by two-tail Wilcoxon sum-rank test and PERMANOVA, respectively. The two-tail Wilcoxon sum-rank test was also used to compare species and SCFAs in PV-healthy control groups and responder-non-responder groups, while paired t-test was performed to compare the pre- and post-treatment groups. We utilized the Kruskal-Wallis test for comparisons involving more than two groups. The difference in KEGG pathways between PV and healthy controls was determined using Fisher's exact test. All correlation analyses were performed by using Spearman's correlation analysis.

Results

Gut microbial dysbiosis in pemphigus vulgaris

We enrolled 60 PV patients and 19 healthy controls, who were comparable in age, sex, and body mass index (BMI) (Table 1). In addition, the patients and healthy controls shared their eating habits, lifestyles, and living environments to minimize the influence of non-PV-related factors. The characteristics of PV patients were summarized, including anti-Dsg 1/3 antibodies and affected skin/mucosa (Table 1). A total of 100 fecal samples were prospectively collected for metagenomic shotgun sequencing (treatment-naïve, n=60; post-treatment, n=21; healthy control, n = 19). The high-quality sequencing reads were aligned to a taxonomical database and then assembled *de novo*, and the identified genes were compiled into a nonredundant catalog of 4045593 genes for further functional analysis. Rarefaction analysis based on the 60 treatment-naïve PV patients and 19 healthy controls revealed that the gene richness approached saturation in each group, implying that the sample size of each group was adequate (Figure S1A).

Next, we investigated the microbial community differences between PV and controls in terms of microbiome diversity. Differences were not observed for α-diversity (P=0.77, Wilcoxon sum-rank test, Figure 1A), whereas β-diversity reached statistical significance (P=0.002, PERMANOVA, Figure 1B), suggesting that the compositions of the gut microbiome rather than the species richness of microbial communities were altered in PV patients compared to healthy family members. We also performed enterotype analysis to assess the global alterations of the gut microbiome, dividing these participants into three different enterotype groups: (i.e., E1, E2, and E3) (Figures 1C, S1B). Despite all three enterotypes being present in both PV patients and healthy controls, E2 and E3 were significantly enriched in PV patients and controls, respectively (P = 0.02, Chi-squared test) (Figure 1D). Specifically, these three enterotypes were attributed to the relative abundance of different microbial species, such as *Faecalibacterium* (predominant in E1), *Escherichia* (predominant in E2), and *Bacteroides* (predominant in E3) (Figure 1E), confirming that the composition of the gut microbiome in PV deviated from that of healthy controls.

To further elucidate the specific bacteria that differed between PV patients and healthy controls, we performed LEfSe analysis and identified PV- and control-enriched bacteria at each level (Figures 1F, G; Table S2). For instance, at the phylum level, *Actinobacteria* and *Bacteroidetes* were more abundant in the PV patients and healthy controls, respectively (Figures S1C, E; Table S2). At the genus level, *Bacteroides* was enriched in the healthy control whereas *Escherichia* was enriched in the PV patients, which is consistent with a previous report on the gut microbiome of PV (13) (Figures S1D, F; Table S2). Finally, at the species level, we found a significant decrease in the relative abundance of probiotics in PV patients compared to healthy controls, including *Bacteroides ovatus*, *Bacteroides uniformis*, and some SCFA-producing bacteria, such as *Eubacterium rectale*, *Eubacterium ventriosum*, *Roseburia intestinalis*, and *Roseburia inulinivorans* (Figure 1H; Table S2), whereas the number of enriched bacteria in PV patients were

TABLE 1 Demographic and clinical information of patients with PV and healthy controls.

	PV (n=60)	Healthy controls (n=19)	*P* value
Sex			
Female, n (%)	33 (55.00)	9 (47.37)	0.75
Male, n (%)	27 (45.00)	10 (52.63)	
Age, years, mean (S.D.)	47.38 (12.82)	41.00 (14.81)	0.10
BMI, kg/m^2, mean (S.D.)	22.52 (2.81)	23.44 (3.28)	0.28
Mocosa affected			
Yes, n (%)	53 (88.33)	\	\
No, n (%)	7 (11.67)	\	
Skin affected			
Yes, n (%)	57 (95.00)	\	\
No, n (%)	3 (5.00)	\	
PDAI			
Before treatment, mean (S.D.)	20.09 (14.43)	\	\
After treatment, mean (S.D.)	8.65 (8.67)	\	\
Anti-Dsg1 antibody, μ/mL, mean (S.D.)	108.85 (66.56)	\	\
Anti-Dsg3 antibody, μ/mL, mean (S.D.)	123.8 (63.72)	\	\

PV, pemphigus vulgaris; BMI, body mass index; PDAI, pemphigus disease area index; Dsg, desmoglein. The symbol "\" means healthy controls did not have these PV related features.

10.3389/fimmu.2023.1114586

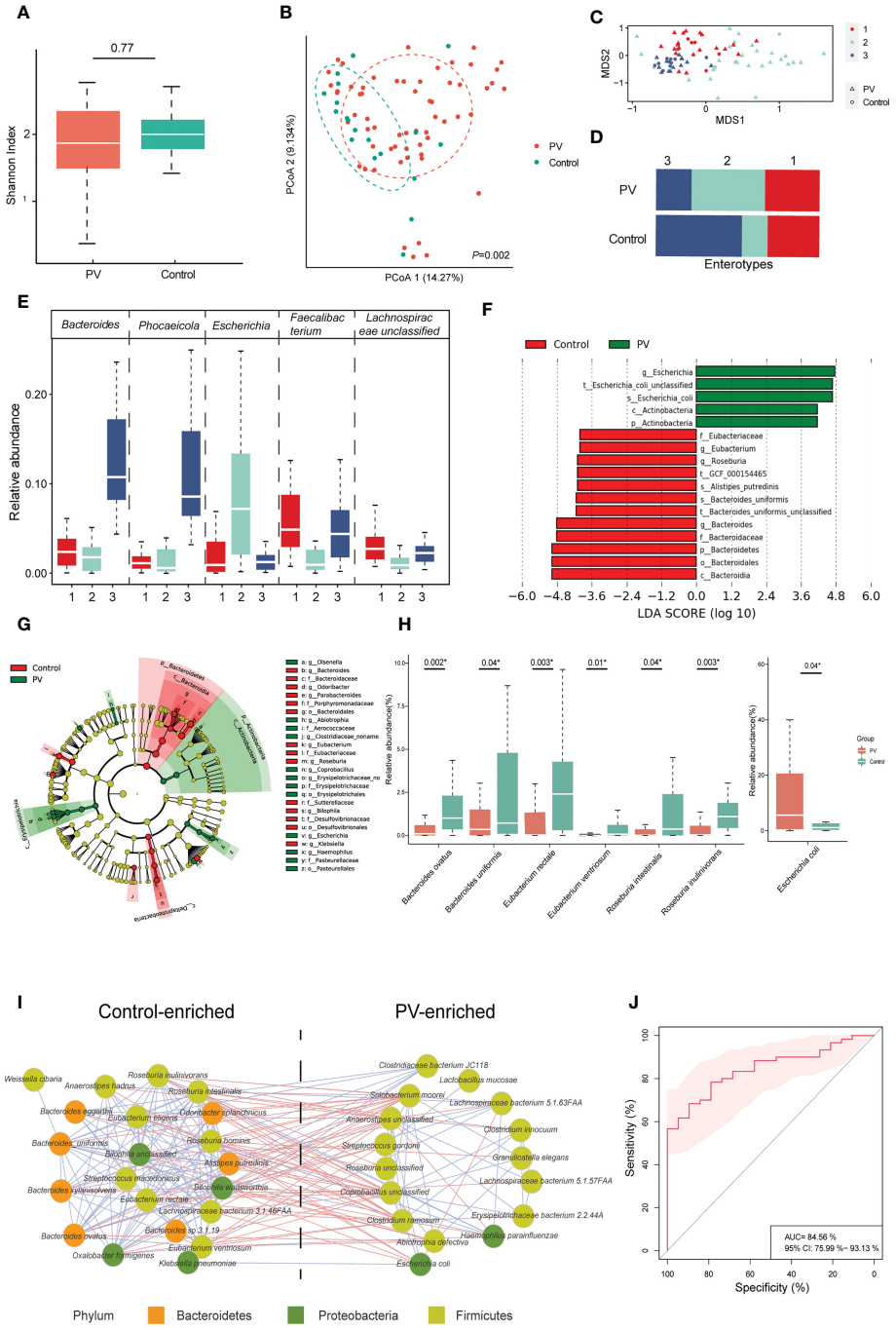

FIGURE 1
Diversities, enterotypes and differential microbial species between PV and healthy controls. **(A, B)** The α-diversity and β-diversity of the gut microbiome in the PV and healthy control groups; **(C)** The distribution of the three enterotypes is shown in descending order using non-metric multidimensional scaling; Red, green and blue represent enterotype1, enterotype2, and enterotype3 respectively, while the triangle represents patients with PV and the circle represents healthy controls; **(D)** Proportion of enterotypes distribution in PV and healthy controls; **(E)** The dominant genus of each enterotype; **(F, G)** Results of differential bacteria between PV and healthy controls by LEFse analysis; **(H)** Main differential species between the healthy control and PV groups (* represents statistical significance with the *P* value <0.05 using Wilcoxon sum-rank test); **(I)** The interaction of differential species between patients with PV and healthy controls, with the red line representing negative correlations and the blue line representing positive correlations; only species with absolute values of correlation coefficients greater than 0.25 are shown; **(J)** Species-based identification of pemphigus vulgaris; ROC curve for the set with an AUC of 84.56% and the 95% CI of 75.99% to 93.13%. PV, pemphigus vulgaris; PCoA, principal coordinates analysis; LEFse, LDA effect size analysis; LDA, linear discriminant analysis; ROC, receiver operating characteristic curve; AUC, the area under the receiver operating curve; CI, confidence interval.

small, mainly including *Escherichia coli* (Figure 1H and Table S2). Moreover, the control/PV-enriched microbial species exhibited positive internal correlations with each other, whereas they tended to have negative correlations between the two groups (Figure 1I), suggesting an antagonistic or mutually exclusive relationship. Finally, we constructed a random forest classifier to demonstrate the diagnostic potential of the gut microbiome for PV. Five repeats of 10-fold cross-validation on the training set led to the optimal selection of 28 species markers with an area under the receiver operating curve (AUC) of 84.56% (Figure 1J, S1G).

Noteworthy, we obtained consistent results in the subgroup analysis specifically with PV and their matched family member controls, as shown by the fact that the gut microbiome between the two groups revealed substantial variations in β-diversity (P=0.01, PERMANOVA, Figure S2A) but not in α-diversity (P=0.78, Wilcoxon sum-rank test, Figure S2A). Moreover, the different species between the two groups were consistent with those indicated above between the PV and healthy control groups (Figures S2B, C), including *Escherichia coli*, *Bacteroides ovatus*, *Eubacterium rectale*, *Eubacterium ventriosum*, *Roseburia intestinalis*, and *Roseburia inulinivorans*. This consistent finding demonstrates the accuracy of the analysis results and eliminates the possible association of these specific bacteria with characteristics unrelated to disease, such as sample size, eating habits, lifestyles, and living environments.

Correlation of gut microbiome with clinical features of PV

Since disease severity in PV patients positively correlates with PDAI scores and anti-Dsg antibody titers, we estimated the correlation of differential species with clinical indexes of PV (Figure 2A). Only a few of the varied microbial species exhibited significant association, including a positive correlation of *Lachnospiraceae bacterium 5.1.57FAA* abundance with anti-Dsg3 antibodies (R = 0.35, P = 0.005, Spearman) and PDAI scores (R = 0.32, P=0.02, Spearman), and negative correlation of PDAI scores with the abundance of *Eubacterium rectale* (R = -0.26, P = 0.04, Spearman) and *Roseburia inulinivorans* (R = -0.36, P = 0.01, Spearman) (Figure 2A), which also exhibited the same trend with categorical division (Figure 2B). Therefore, these findings demonstrated the possible link between the gut microbiome and PV severity.

Given that the response to conventional glucocorticoid-based treatment can be reflected by the ΔPDAI (Figure 2C), we estimated the correlation between ΔPDAI and each microbiota component to evaluate the potential prognostic value of the microbial species with response outcomes. In the linear model, *Eubacterium ventriosum* exhibited the strongest positive correlation with the ΔPDAI (R=0.36, P=0.01, Spearman) (Figure 2A), consistent with the categorical division (Figure 2D). With LEfSe analysis in a categorical model, *Escherichia coli* was found to be the predominant microbial species in the responder group, compared to the non-responder group (Figures 2E, F). Paradoxically, *Escherichia coli* is a pathogenic bacterium that is enriched in PV patients compared to healthy controls and showed higher abundance in responders than non-responders, suggesting its possible bi-directional role in PV onset and treatment response.

Glucocorticoid partially altered the gut microbiome in PV patients

To examine the effect of glucocorticoid treatment on the gut microbiome in PV patients, we compared the gut microbiome of 21 pairs of matched fecal samples collected before and after one month of treatment, particularly focusing on the relative abundance of PV-related bacteria. Both α-diversity and β-diversity did not differ significantly between pre-and post-treatment samples (Figures 3A, B), suggesting the weak overall interaction of glucocorticoid treatment and microbiome. However, some PV-related bacteria were altered after treatment, particularly in responders. For instance, the relative abundance of *Escherichia coli* decreased in responders after treatment (P=0.05, paired t-test, Figure 3C), whereas the probiotics abundance (e.g., *Eubacterium ventriosum*) was specifically elevated in responders (P=0.01, paired t-test, Figure 3D), implying that glucocorticoid treatment might help inhibit *Escherichia coli* and reestablish a healthy gut microbiome in responders. However, such an impact might not be achievable in non-responders because they were resistant to glucocorticoid medication. The precise mechanisms underlying resistance to glucocorticoid therapy in these patients remain to be further explored in the future.

Functional changes in the gut microbiome

We conducted KEGG analysis and found that PV-enriched KO markers were typically involved in the KEGG B-level categories of membrane transport and protein families involving signaling/cellular processes, whereas healthy control-enriched KO markers were frequently involved in translation and protein families involved in metabolism (Figure 4A). At the level of KEGG class C, 13 and 6 pathways were enriched in the healthy family members and PV patients, respectively (Figure 4B). Intriguingly, the phosphotransferase system (PTS) pathway, which can regulate the virulence of pathogenic bacteria, was highly presented in PV patients, and had the strongest correlation with *Escherichia coli* (R=0.59, P=1.58e-10, Spearman, Figure 4C), whereas fatty acid biosynthesis pathway was enriched in healthy controls and had the strongest correlation with *Bacteroides ovatus* (R=0.41, P= 2.67e-05, Spearman, Figure 4C), suggesting the two functional pathways attributed to *Escherichia coli*/*Bacteroidetes* dominant effects. Furthermore, among MetaCyc pathways, we also found *Bacteroidetes* mainly contributed to the fatty acid biosynthesis pathway, and apart from PTS, *Escherichia coli* had predominance in enterobactin biosynthesis pathways (Figures S3A, B). We further performed SCFA-targeted metabolomics analysis to investigate the relationship between SCFA components and PV onset and treatment outcomes. With available leftover fecal samples from metagenomic sequencing (treatment-naïve, n = 59; post-treatment, n = 20, healthy relatives, n = 13) (Figure 4D), healthy controls had

10.3389/fimmu.2023.1114586

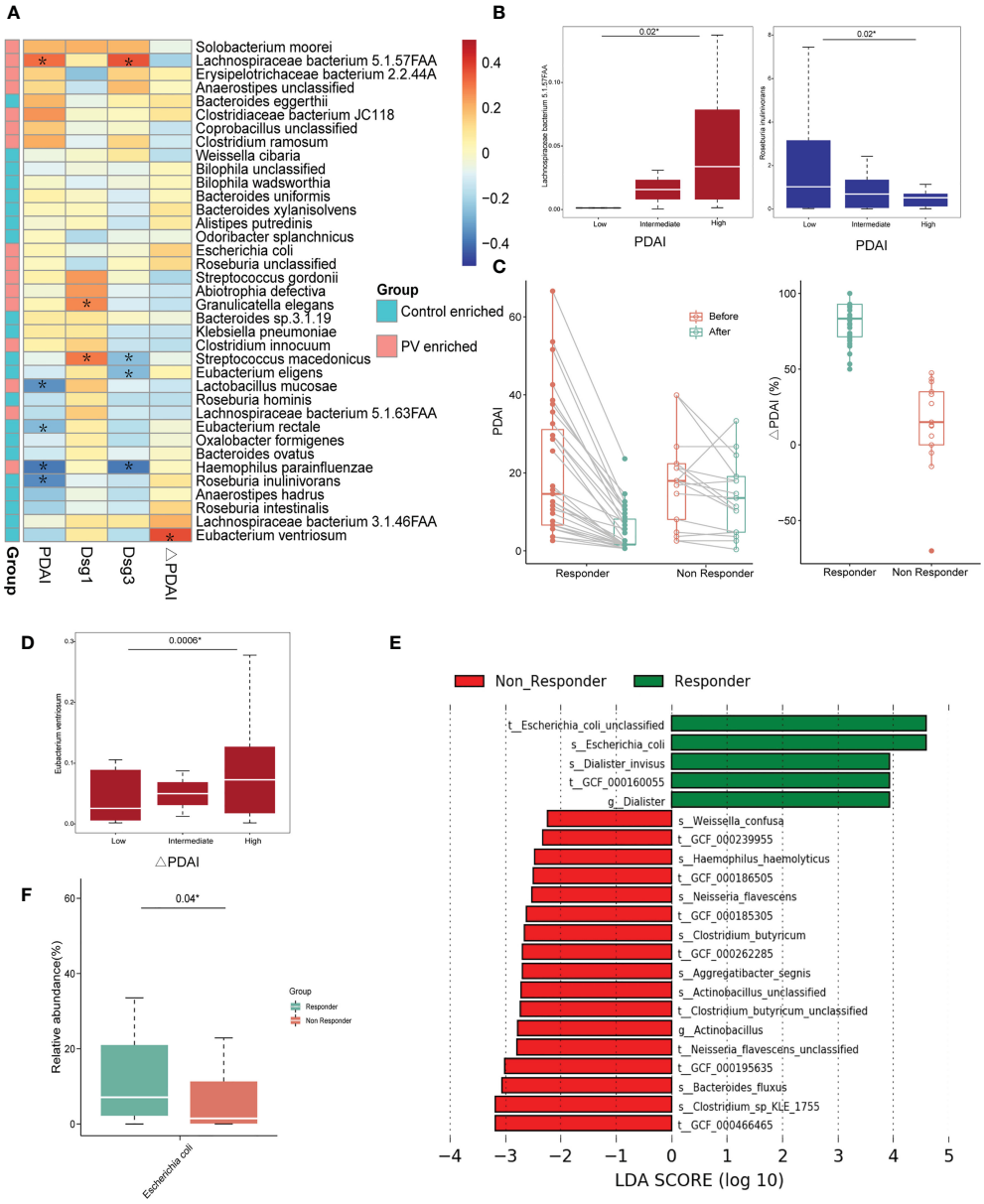

FIGURE 2
The correlation between differential microbial species and clinical indexes. **(A)** Heatmap of correlation coefficients between differential microbial species and PDAI, anti-Dsg1 antibody titers, anti-Dsg3 antibody titers, and ΔPDAI; The *means the *P* value is less than 0.05 using Spearman's correlation analysis; **(B)** Positive correlation between PV-enriched gut microbiome and PDAI scores and negative correlation between the healthy control-enriched gut microbiome and PDAI scores (*represents statistical significance with the *P* value <0.05 using Kruskal-Wallis test); **(C)** The graph on the left shows the change in PDAI scores before and after treatments in the responder and non-responder groups; The graph on the right shows the ΔPDAI for the responder and non-responder groups; **(D)** The positive correlation between the relative abundance of *Eubacterium ventriosum* and ΔPDAI (*represents statistical significance with the *P* value <0.05 using Kruskal-Wallis test); **(E–G)** Results of differential bacteria between the responder and non-responder groups by LEFse analysis; **(F)** Boxplots of the relative abundance of *Escherichia coli* in the responder and non-responder groups (*represents statistical significance with the *P* value <0.05 using Wilcoxon sum-rank test). PV, pemphigus vulgaris; PDAI, pemphigus disease area index; Dsg: desmoglein; ΔPDAI: PDAI improvement rates; LEFse, LDA effect size analysis; LDA, linear discriminant analysis.

higher or comparable SCFA levels compared to PV patients (Figure 4E). Particularly, butyric acid (P = 0.02, paired t-test) and valeric acid (P = 0.05, paired t-test) rebounded significantly after one month of glucocorticoid treatment in PV patients (Figure 4F). However, there were no significant differences in any SCFA levels between the responder and non-responder of PV patients (Figure 4G). It is worth mentioning that healthy control-enriched probiotics had significant correlations with SCFA levels (Figure 4H), which suggests that the vital function of these probiotics might to produce SCFA.

Discussion

In this study, we explored the PV-related gut microbiome alteration that are associated with both onset and treatment

10.3389/fimmu.2023.1114586

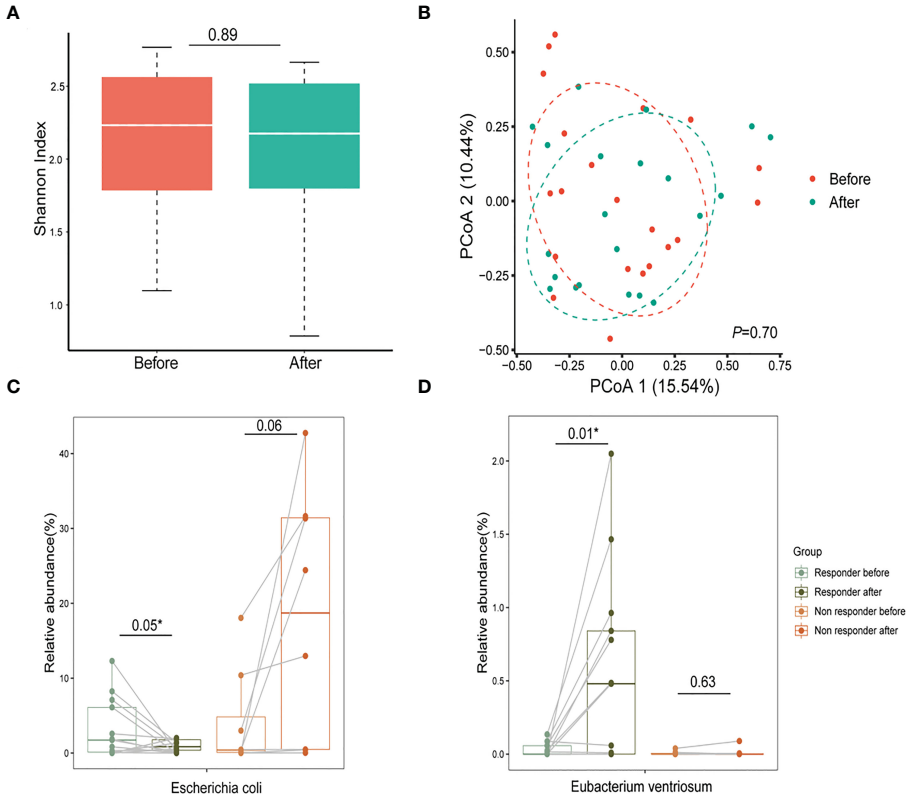

FIGURE 3
Glucocorticoids aid in reestablishing a healthy gut microbiome in patients with PV. **(A, B)** The α-diversity and β-diversity of the gut microbiome in the pre-treatment and post-treatment groups; **(C)** After one month of glucocorticoid therapy, *Escherichia coli* decreased in relative abundance in the responder group and increased in the non-responder group (* represents statistical significance with the *P* value <0.05 using paired t-test); **(D)** The relative abundance of probiotics (*Eubacterium ventriosum*) reduced in the PV group increased after treatment with glucocorticoids (*represents statistical significance with the *P* value <0.05 using paired t-test). PV, pemphigus vulgaris; PCoA, principal coordinates analysis.

response. Moreover, the decreased SCFA level revealed by targeted metabolomics is strongly correlated with decreased SCFA-producing probiotics in fecal samples from PV patients. To the best of our knowledge, this is the first comprehensive investigation of the gut microbiome and microbiome-derived metabolites of PV, which provide a basis for the possible noninvasive diagnostic approach and interventions for the risk reduction and treatment of PV.

Among all differential gut microbial species, *Escherichia coli* tends to play the most significant role in PV, as it was not only abundant in PV patients and decreased after conventional treatment, but also enriched in responders compared to non-responders, suggesting that PV onset in some patients may be attributed to *Escherichia coli* and sensitive to glucocorticoid treatment. *Escherichia coli* is a member of the *Proteobacteria* phylum, *gamma-Proteobacteria* class, and *Escherichia* genus, the level of which has been consistently linked to PV onset in a previous study (13). As a gram-negative bacterium, the outer membrane surface of *Escherichia coli* is coated with lipopolysaccharide (LPS), a complex glycolipid that is a major bacterial virulence factor. LPS can induce a robust proinflammatory response and the secretion of proinflammatory cytokines, which may lead to the disruption of the intestinal barrier. The impaired intestinal barrier allows the passage of toxins, antigens, and bacteria to pass into the lumen and enter the bloodstream, triggering the onset and progression of autoimmune disease (35–37). Moreover, we observed that *Escherichia coli* played a dominant contribution role in the enrichment of PTS pathway in PV patients. The PTS pathway has been proved to modulate the expression of virulence genes in pathogenic bacteria, such as *Vibrio cholerae* (38) and *Bacillus anthracis* (39). Therefore, we speculated that PTS may also increase the virulence gene expression of *Escherichia coli*, which increases its pathogenicity and then exacerbates the disruption of the intestinal barrier in PV patients. Given that glucocorticoid (e.g., prednisolone) does not exhibit direct *in vitro* antibacterial activity against *Escherichia coli* (23), the decrease of gut *Escherichia coli* after glucocorticoid treatment are more likely to be influenced by its regulatory role in the immune system, but the mechanism remains to be elucidated.

On the other hand, we observed a consistent decrease in the relative abundance of multiple probiotics, including *Bacteroides* (e.g., *Bacteroides uniformis*, *Bacteroides ovatus*) and several SCFA-producing bacteria (e.g., *Eubacterium ventriosum*), which might be due to the inhibitory effect of *Escherichia coli*. Our results demonstrated that these probiotics had a mutually exclusive relationship with *Escherichia coli*, which could be explained by the speculation that *Escherichia coli*-dominated enterobactin biosynthesis pathway was enriched in PV patients and the production of which could promote the own growth of

10.3389/fimmu.2023.1114586

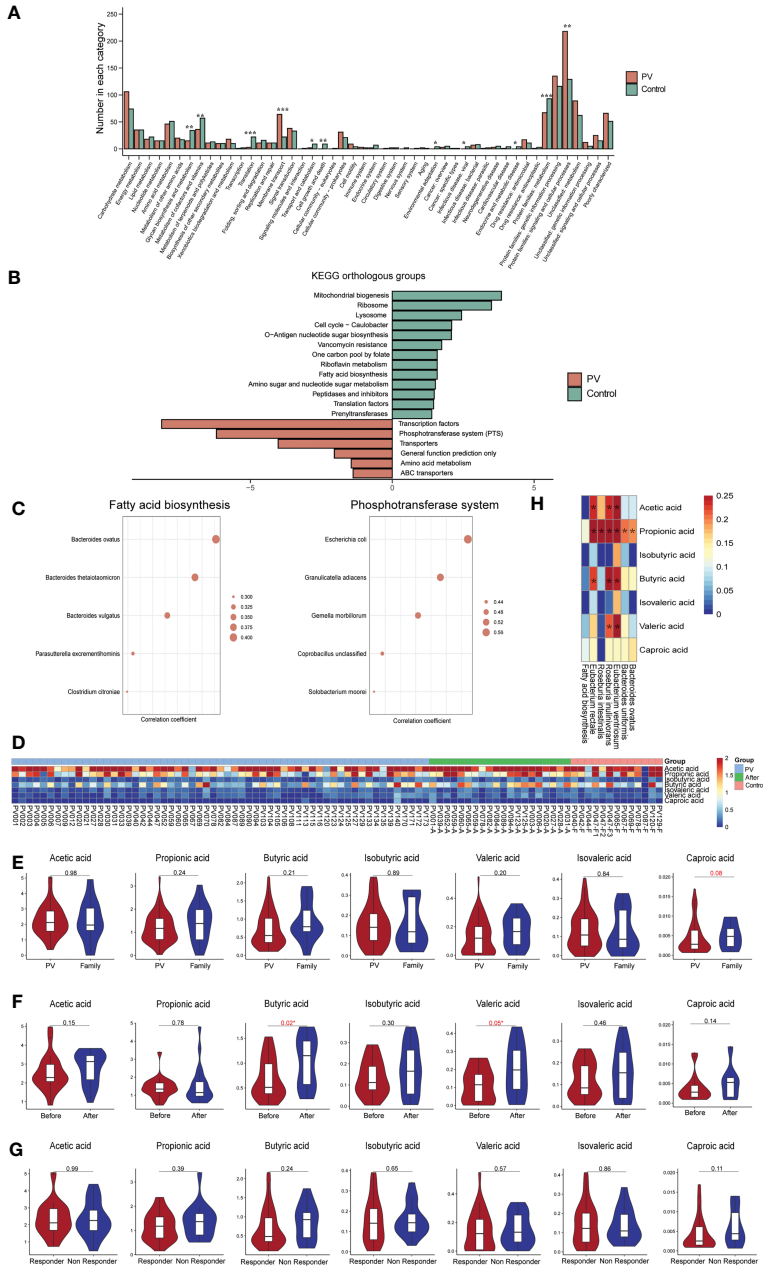

FIGURE 4
Functional changes in the gut microbiome. **(A)** Level B differential KEGG pathways, horizontal coordinates represent pathway names, vertical coordinates represent the number of differential KOs involved in each pathway (*represents a *P* value less than 0.05, **represents a *P* value less than 0.005, ***represents a *P* value less than 0.0005); **(B)** C-level difference KEGG pathway between PV patients and healthy controls, horizontal coordinate represents the *P* value of -log10; **(C)** The top five microbial species with the strongest association with fatty acid biosynthesis and phosphotransferase system pathways; **(D)** Heatmap of short fatty acids contents in each sample; **(E–G)** SCFA levels in the **(E)** PV and healthy control groups, **(F)** pre-treatment and post-treatment groups, and **(G)** responder and non-responder groups; **(H)** Heatmap of correlation coefficients between healthy control-enriched probiotics and SCFA levels; The *means the *P* value is less than 0.05 using Spearman's correlation analysis. PV, pemphigus vulgaris; KEGG, Kyoto encyclopedia of genes and genomes; KO, KEGG Orthology; SCFA, short chain fatty acid.

Escherichia coli by ingesting iron while inhibiting the growth of other bacteria (40). Previous studies have shown that many species of *Bacteroides* can alleviate LPS-induced inflammation and improve gut barrier function (37, 41, 42). Therefore, a lack of *Bacteroides* can exacerbate the inflammation induced by LPS in *Escherichia coli*, resulting in a worsening of intestinal barrier disruption and an increase in intestinal inflammation levels. Meanwhile, we noted a decline of SCFAs in PV patients, which was significantly correlated with the decreased abundance of healthy control-enriched probiotics. The important roles of SCFA have been established in modulating immune/inflammatory responses and intestinal barrier function (29). Particularly, butyric acid can act as an anti-inflammatory agent and maintain the balance of tolerance to commensals and immunity to pathogenic bacteria in the intestinal immune system (43). The decline of SCFA levels in PV patients could further impair intestinal barrier function and

promote the disease progression, while glucocorticoids can partially restore the SCFA-producing bacteria and the SCFA level (e.g., butyric acid) in responders. Our results suggested that glucocorticoids may effectively improve microbial and metabolite dysbiosis and strengthen the intestinal barrier, thereby aiding in the restoration of intestinal homeostasis in PV patients. Also, it is worth determining whether supplementing SCFAs can render refractory PV patients responsive to conventional treatment in the future.

This is the first study to combine the use of metagenomic and metabolomic technologies to investigate the relationship between the gut microbiome/metabolites and onset/treatment response of PV. We concluded a potential mechanism for PV onset: increased pathogenic *Escherichia coli* secreting toxins and enterobactin could disrupt the intestinal barrier and inhibit numerous probiotics. As a result, the gut microbiome is imbalanced and SCFA levels significantly decrease in PV patients, which further impairs the intestinal barrier function. We speculated that pathogenic bacteria/toxins might then pass through the damaged intestinal barrier and trigger the initiation and development of PV through antigen mimicry, inducing immune responses, etc. However, our study still has several limitations. First, since the research is cross-sectional, we were only able to determine the correlation, not the causality of the gut microbiome. Second, as a single-center study with relatively small sample sizes, our findings need further support and verifications by independent studies. Thirdly, due to the lack of a control group for other autoimmune diseases in this study, the differential species identified in this study may be shared by other autoimmune diseases but not unique to PV. Finally, the mechanisms by which *Escherichia coli* and toxins subsequently trigger the immune process of PV and the implications of SCFA supplementation for PV treatment will need to be further explored in subsequent studies.

In conclusion, our comprehensive investigation of the gut microbiome in PV patients suggests an association of PV onset with the enrichment of pathogenic bacteria and a lack of probiotics (e.g., SCFA-producing bacteria), which can be partially restored towards healthy individuals after glucocorticoid treatment. Future *in vivo* and *in vitro* experiments are required to elucidate the causal relationship between the gut microbiome and PV, as well as possible mechanisms.

Data availability statement

The data presented in the study are deposited in the database (https://bigd.big.ac.cn/gsa-human/browse/), accession number HRA004017.

Ethics statement

The studies involving human participants were reviewed and approved by Ethics committee of the West China Hospital, Sichuan University, approval no. 2017 (241)). The patients/participants provided their written informed consent to participate in this study.

Author contributions

Conception and design: YW, XX, WL, and HX; Administrative support: WL and HX; Collection of study materials or patient samples: YW, XZ, TZ, YZ, and WL. Collection and assembly of data: YW, XX, WL, and YS; Data analysis and interpretation: YW, XX, QD, and WZ; Funding acquisition: WZ, WL, and HX; All authors contributed to the article and approved the submitted version.

Funding

This work was supported by grants from the National Key R&D Program of China (No. 2021YFA1301203), the National Natural Science Foundation of China (No. 81973408 and 81903735), the Sichuan Science & Technology Program (No. 2022YFS0202), and 1.3.5 Project for Disciplines of Excellence, West China Hospital, Sichuan University (No. ZYYC20003, ZYJC21024, ZYJC18004, ZYYC20007, ZYGD20006, and ZYJC21006)

Acknowledgments

All authors of this paper fulfilled the criteria of authorship. The authors thank the participants for this study.

Conflict of interest

The authors declare that the research was conducted in the absence of any commercial or financial relationships that could be construed as a potential conflict of interest.

Publisher's note

Supplementary material

The Supplementary Material for this article can be found online at: https://www.frontiersin.org/articles/10.3389/fimmu.2023.1114586/full#supplementary-material

SUPPLEMENTARY FIGURE 1
Diversities, enterotypes, and differential species between the PV and healthy control groups. **(A)** The rarefaction curve showed that the gene richness approached saturation in each group with red representing PV and green representing healthy control; **(B)** Three enterotypes were clustered using the DMM model; **(C, E)** Differential phylum between the healthy control and PV

groups; **(D, F)** Differential genus between the healthy control and PV groups; **(G)** Contribution of each species to the random forest model in the optimal set. PV, pemphigus vulgaris; DMM, Dirichlet Multinomial Mixture Model.

SUPPLEMENTARY FIGURE 2

Subgroup analysis specifically with PV and their matched family member controls. **(A)** The α-diversity (left) and β-diversity (right) of the gut microbiome in the PV patients and their matched family members; **(B)** Results of differential bacteria between PV and family members by LEFse analysis; **(C)** Main differential species between PV patients and their family members (* represents statistical significance with the P value <0.05 using Wilcoxon sum-rank test); **(D)** C-level difference KEGG pathway between PV patients and their matched family members, horizontal coordinate represents the P value of -log10. PV, pemphigus vulgaris; PCoA, principal coordinates analysis; LEFse, LDA effect size analysis; LDA, linear discriminant analysis; KEGG, Kyoto encyclopedia of genes and genomes.

SUPPLEMENTARY FIGURE 3

Different MetaCyc pathways between PV patients and healthy controls. **(A)** Contribution of the microbial genus to the fatty acid biosynthesis pathway; **(B)** Contribution of the microbial species to the enterobactin biosynthesis pathway.

SUPPLEMENTARY TABLE 1

Clinical information for all samples.

SUPPLEMENTARY TABLE 2

Microbial phylum, genus, and species associated with pemphigus vulgaris.

References

1. Schmidt E, Kasperkiewicz M, Joly P. Pemphigus. *Lancet* (2019) 394(10201):882–94. doi: 10.1016/s0140-6736(19)31778-7

2. Kasperkiewicz M, Ellebrecht CT, Takahashi H, Yamagami J, Zillikens D, Payne AS, et al. Pemphigus. *Nat Rev Dis Primers* (2017) 3:17026. doi: 10.1038/nrdp.2017.26

3. Stanley JR, Amagai M. Pemphigus, bullous impetigo, and the staphylococcal scalded-skin syndrome. *N Engl J Med* (2006) 355(17):1800–10. doi: 10.1056/NEJMra061111

4. Gao J, Zhu C, Zhang Y, Sheng Y, Yang F, Wang W, et al. Association study and fine-mapping major histocompatibility complex analysis of pemphigus vulgaris in a han chinese population. *J Invest Dermatol* (2018) 138(11):2307–14. doi: 10.1016/j.jid.2018.05.011

5. Zhang SY, Zhou XY, Zhou XL, Zhang Y, Deng Y, Liao F, et al. Subtype-specific inherited predisposition to pemphigus in the Chinese population. *Br J Dermatol* (2019) 180(4):828–35. doi: 10.1111/bjd.17191

6. Sinha AA. The genetics of pemphigus. *Dermatol Clin* (2011) 29(3):381–91. doi: 10.1016/j.det.2011.03.020

7. Khan MF, Wang H. Environmental exposures and autoimmune diseases: Contribution of gut microbiome. *Front Immunol* (2019) 10:3094. doi: 10.3389/fimmu.2019.03094

8. Zhang X, Chen BD, Zhao LD, Li H. The gut microbiota: Emerging evidence in autoimmune diseases. *Trends Mol Med* (2020) 26(9):862–73. doi: 10.1016/j.molmed.2020.04.001

9. Alpizar-Rodriguez D, Lesker TR, Gronow A, Gilbert B, Raemy E, Lamacchia C, et al. Prevotella copri in individuals at risk for rheumatoid arthritis. *Ann Rheum Dis* (2019) 78(5):590–3. doi: 10.1136/annrheumdis-2018-214514

10. Azzouz D, Omarbekova A, Heguy A, Schwudke D, Gisch N, Rovin BH, et al. Lupus nephritis is linked to disease-activity associated expansions and immunity to a gut commensal. *Ann Rheum Dis* (2019) 78(7):947–56. doi: 10.1136/annrheumdis-2018-214856

11. Chen BD, Jia XM, Xu JY, Zhao LD, Ji JY, Wu BX, et al. An autoimmunogenic and proinflammatory profile defined by the gut microbiota of patients with untreated systemic lupus erythematosus. *Arthritis Rheumatol* (2021) 73(2):232–43. doi: 10.1002/art.41511

12. Zhou C, Zhao H, Xiao XY, Chen BD, Guo RJ, Wang Q, et al. Metagenomic profiling of the pro-inflammatory gut microbiota in ankylosing spondylitis. *J Autoimmun* (2020) 107:102360. doi: 10.1016/j.jaut.2019.102360

13. Huang S, Mao J, Zhou L, Xiong X, Deng Y. The imbalance of gut microbiota and its correlation with plasma inflammatory cytokines in pemphigus vulgaris patients. *Scand J Immunol* (2019) 90(3):e12799. doi: 10.1111/sji.12799

14. Han D, Gao P, Li R, Tan P, Xie J, Zhang R, et al. Multicenter assessment of microbial community profiling using 16s rrna gene sequencing and shotgun metagenomic sequencing. *J Adv Res* (2020) 26:111–21. doi: 10.1016/j.jare.2020.07.010

15. Durazzi F, Sala C, Castellani G, Manfreda G, Remondini D, De Cesare A. Comparison between 16s rrna and shotgun sequencing data for the taxonomic characterization of the gut microbiota. *Sci Rep* (2021) 11(1):3030. doi: 10.1038/s41598-021-82726-y

16. Mallick H, Ma S, Franzosa EA, Vatanen T, Morgan XC, Huttenhower C. Experimental design and quantitative analysis of microbial community multiomics. *Genome Biol* (2017) 18(1):228. doi: 10.1186/s13059-017-1359-z

17. Weersma RK, Zhernakova A, Fu J. Interaction between drugs and the gut microbiome. *Gut* (2020) 69(8):1510–9. doi: 10.1136/gutjnl-2019-320204

18. Zhou B, Xia X, Wang P, Chen S, Yu C, Huang R, et al. Induction and amelioration of methotrexate-induced gastrointestinal toxicity are related to immune response and gut microbiota. *EBioMedicine* (2018) 33:122–33. doi: 10.1016/j.ebiom.2018.06.029

19. Yu C, Zhou B, Xia X, Chen S, Deng Y, Wang Y, et al. Prevotella copri is associated with carboplatin-induced gut toxicity. *Cell Death Dis* (2019) 10(10):714. doi: 10.1038/s41419-019-1963-9

20. Gopalakrishnan V, Spencer CN, Nezi L, Reuben A, Andrews MC, Karpinets TV, et al. Gut microbiome modulates response to anti-Pd-1 immunotherapy in melanoma patients. *Science* (2018) 359(6371):97–103. doi: 10.1126/science.aan4236

21. Dubin K, Callahan MK, Ren B, Khanin R, Viale A, Ling L, et al. Intestinal microbiome analyses identify melanoma patients at risk for checkpoint-Blockade-Induced colitis. *Nat Commun* (2016) 7:10391. doi: 10.1038/ncomms10391

22. Yan X, Zhang S, Deng Y, Wang P, Hou Q, Xu H. Prognostic factors for checkpoint inhibitor based immunotherapy: An update with new evidences. *Front Pharmacol* (2018) 9:1050. doi: 10.3389/fphar.2018.01050

23. Maier L, Pruteanu M, Kuhn M, Zeller G, Telzerow A, Anderson EE, et al. Extensive impact of non-antibiotic drugs on human gut bacteria. *Nature* (2018) 555(7698):623–8. doi: 10.1038/nature25979

24. Dai Q, Xia X, He C, Huang Y, Chen Y, Wu Y, et al. Association of anti-Tnf-α treatment with gut microbiota of patients with ankylosing spondylitis. *Pharmacogenet Genomics* (2022) 32(7):247–56. doi: 10.1097/fpc.0000000000000468

25. Yin J, Sternes PR, Wang M, Song J, Morrison M, Li T, et al. Shotgun metagenomics reveals an enrichment of potentially cross-reactive bacterial epitopes in ankylosing spondylitis patients, as well as the effects of tnfi therapy upon microbiome composition. *Ann Rheum Dis* (2020) 79(1):132–40. doi: 10.1136/annrheumdis-2019-215763

26. Chen Z, Zheng X, Wu X, Wu J, Li X, Wei Q, et al. Adalimumab therapy restores the gut microbiota in patients with ankylosing spondylitis. *Front Immunol* (2021) 12:700570. doi: 10.3389/fimmu.2021.700570

27. Holmes E, Li JV, Athanasiou T, Ashrafian H, Nicholson JK. Understanding the role of gut microbiome-host metabolic signal disruption in health and disease. *Trends Microbiol* (2011) 19(7):349–59. doi: 10.1016/j.tim.2011.05.006

28. Chang AE, Golob JL, Schmidt TM, Peltier DC, Lao CD, Tewari M. Targeting the gut microbiome to mitigate immunotherapy-induced colitis in cancer. *Trends Cancer* (2021) 7(7):583–93. doi: 10.1016/j.trecan.2021.02.005

29. Kim CH. Control of lymphocyte functions by gut microbiota-derived short-chain fatty acids. *Cell Mol Immunol* (2021) 18(5):1161–71. doi: 10.1038/s41423-020-00625-0

30. Lu Y, Yuan X, Wang M, He Z, Li H, Wang J, et al. Gut microbiota influence immunotherapy responses: Mechanisms and therapeutic strategies. *J Hematol Oncol* (2022) 15(1):47. doi: 10.1186/s13045-022-01273-9

31. Agus A, Clément K, Sokol H. Gut microbiota-derived metabolites as central regulators in metabolic disorders. *Gut* (2021) 70(6):1174–82. doi: 10.1136/gutjnl-2020-323071

32. Lavelle A, Sokol H. Gut microbiota-derived metabolites as key actors in inflammatory bowel disease. *Nat Rev Gastroenterol Hepatol* (2020) 17(4):223–37. doi: 10.1038/s41575-019-0258-z

33. Harman KE, Brown D, Exton LS, Groves RW, Hampton PJ, Mohd Mustapa MF, et al. British Association of dermatologists' guidelines for the management of pemphigus vulgaris 2017. *Br J Dermatol* (2017) 177(5):1170–201. doi: 10.1111/bjd.15930

34. Franzosa EA, McIver LJ, Rahnavard G, Thompson LR, Schirmer M, Weingart G, et al. Species-level functional profiling of metagenomes and metatranscriptomes. *Nat Methods* (2018) 15(11):962–8. doi: 10.1038/s41592-018-0176-y

35. Mu Q, Kirby J, Reilly CM, Luo XM. Leaky gut as a danger signal for autoimmune diseases. *Front Immunol* (2017) 8:598. doi: 10.3389/fimmu.2017.00598

36. Petta I, Fraussen J, Somers V, Kleinewietfeld M. Interrelation of diet, gut microbiome, and autoantibody production. *Front Immunol* (2018) 9:439. doi: 10.3389/fimmu.2018.00439

37. Hiippala K, Jouhten H, Ronkainen A, Hartikainen A, Kainulainen V, Jalanka J, et al. The potential of gut commensals in reinforcing intestinal barrier function and alleviating inflammation. *Nutrients* (2018) 10(8):988. doi: 10.3390/nu10080988

38. Wang Q, Millet YA, Chao MC, Sasabe J, Davis BM, Waldor MK. A genome-wide screen reveals that the vibrio cholerae phosphoenolpyruvate phosphotransferase system modulates virulence gene expression. *Infect Immun* (2015) 83(9):3381–95. doi: 10.1128/iai.00411-15

39. Stülke J. Regulation of virulence in bacillus anthracis: The phosphotransferase system transmits the signals. *Mol Microbiol* (2007) 63(3):626–8. doi: 10.1111/j.1365-2958.2006.05556.x

40. Raymond KN, Dertz EA, Kim SS. Enterobactin: An archetype for microbial iron transport. *PNAS* (2003) 100(7):5. doi: 10.1073/pnas.0630018100

41. Tan H, Zhao J, Zhang H, Zhai Q, Chen W. Novel strains of bacteroides fragilis and bacteroides ovatus alleviate the lps-induced inflammation in mice. *Appl Microbiol Biotechnol* (2019) 103(5):2353–65. doi: 10.1007/s00253-019-09617-1

42. Hiippala K, Kainulainen V, Suutarinen M, Heini T, Bowers JR, Jasso-Selles D, et al. Isolation of anti-inflammatory and epithelium reinforcing bacteroides and parabacteroides spp. from a healthy fecal donor. *Nutrients* (2020) 12(4):935. doi: 10.3390/nu12040935

43. Fu X, Liu Z, Zhu C, Mou H, Kong Q. Nondigestible carbohydrates, butyrate, and butyrate-producing bacteria. *Crit Rev Food Sci Nutr* (2019) 59(sup1):S130–s52. doi: 10.1080/10408398.2018.1542587

frontiers | Frontiers in Immunology

TYPE Original Research
PUBLISHED 16 May 2023
DOI 10.3389/fimmu.2023.1114699

OPEN ACCESS

EDITED BY
Tej Pratap Singh,
University of Pennsylvania, United States

REVIEWED BY
Frank A. Redegeld,
Utrecht University, Netherlands
Ritobrata Goswami,
Indian Institute of Technology
Kharagpur, India

*CORRESPONDENCE
Alan Chuan-Ying Lai
alanlai320@gmail.com
Ya-Jen Chang
yajchang@ibms.sinica.edu.tw

SPECIALTY SECTION
RECEIVED 02 December 2022
ACCEPTED 28 April 2023
PUBLISHED 16 May 2023

CITATION
Luo C-H, Lai AC-Y and Chang Y-J (2023) Butyrate inhibits *Staphylococcus aureus*-aggravated dermal IL-33 expression and skin inflammation through histone deacetylase inhibition.
Front. Immunol. 14:1114699.
doi: 10.3389/fimmu.2023.1114699

Butyrate inhibits *Staphylococcus aureus*-aggravated dermal IL-33 expression and skin inflammation through histone deacetylase inhibition

Chia-Hui Luo[1,2], Alan Chuan-Ying Lai[1,3]* and Ya-Jen Chang[1,4]*

[1]Institute of Biomedical Sciences, Academia Sinica, Taipei, Taiwan, [2]Taiwan International Graduate Program in Molecular Medicine, National Yang Ming Chiao Tung University and Academia Sinica, Taipei, Taiwan, [3]Department of Pharmaceutical Sciences, School of Pharmacy, College of Pharmacy, Taipei Medical University, Taipei, Taiwan, [4]Institute of Translational Medicine and New Drug Development, China Medical University, Taichung, Taiwan

Atopic dermatitis (AD) is an inflammatory skin disease caused by the disruption of skin barrier, and is dominated by the type 2 immune responses. Patients with AD have a high risk of developing *Staphylococcus aureus* infection. Interleukin-33 (IL-33), an alarmin, has been implicated in the pathophysiology of AD development. Butyrate, a short chain fatty acid known to be produced from the fermentation of glycerol by the commensal skin bacterium, *Staphylococcus epidermidis*, has been reported to possess antimicrobial and anti-inflammatory properties that suppress inflammatory dermatoses. However, little is known about the effects of butyrate on dermal IL-33 expression and associated immune response in *S. aureus*-aggravated skin inflammation in the context of AD. To decipher the underlying mechanism, we established an AD-like mouse model with epidermal barrier disruption by delipidizing the dorsal skin to induce AD-like pathophysiology, followed by the epicutaneous application of *S. aureus* and butyrate. We discovered that *S. aureus* infection exacerbated IL-33 release from keratinocytes and aggravated dermal leukocyte infiltration and IL-13 expression. Moreover, we showed that butyrate could attenuate *S. aureus*-aggravated skin inflammation with decreased IL-33, IL-13, and leukocyte infiltration in the skin. Mechanistically, we demonstrated that butyrate suppressed IL-33 expression and ameliorated skin inflammation through histone deacetylase 3 (HDAC3) inhibition. Overall, our findings revealed the potential positive effect of butyrate in controlling inflammatory skin conditions in AD aggravated by *S. aureus* infection.

KEYWORDS

atopic dermatitis, butyrate, histone deacetylase, interleukin 33, keratinocytes, S. aureus, S. epidermidis

Abbreviations: AD, atopic dermatitis; AEW, acetone and ether followed by water; HDAC, histone deacetylase; SCFAs, short-chain fatty acids; TSA, trichostatin A; WT, wild-type; 4-CMTB, 4-chloro-α-(1-methylethyl)-N-2-thiazolyl-benzeneacetamide.

Introduction

AD is a chronic, relapsing, and inflammatory skin condition with a complex etiology. It is characterized by epidermal thickening and dermal leukocyte infiltration and is mediated by epithelial-derived IL-33 and Th2 cytokines, including IL-4, IL-5, and IL-13 (1, 2). Studies have reported that secretion of IL-33 by epithelial cells during cellular injury or damage activates type 2 innate lymphoid cells (ILC2), T helper 2 cells (Th2), macrophages, and eosinophils to generate a Th2-skewed microenvironment (3), leading to the development of Th2 inflammation. To study the disease mechanisms of AD, the establishment of an AD-like mouse model is essential. Recent studies have suggested that skin delipidized by organic solvent mixture (AEW, acetone/ether, and water washing protocol) results in hyper-proliferation of keratinocytes in the basal layer and scratching, the cardinal feature of AD (4, 5).

The human skin microbiota harbors a plethora of resident microorganisms of different species. These microorganisms can interact with host cells, as well as the host immune system (3). One such microbe is *S. aureus*, which is a gram-positive bacterium residing in skin and mucosa. The superficial skin is a major site for *S. aureus* colonization, which normally resides in 10-20% of healthy individuals (6). Moreover, studies have reported that 80-100% of AD patients are colonized with *S. aureus*, which is strongly associated with disease severity (7, 8). *S. aureus* is capable of secreting virulence factors, including biofilm, enterotoxins, and superantigens that are considered as important elements of the vicious cycle of AD (9). Importantly, a disrupted skin barrier increases the susceptibility to *S. aureus* infection in skin lesions, which is associated with the overexpression of Th2 cytokines in AD patients (8, 10).

Short-chain fatty acids (SCFAs) are microbiota-derived metabolites composed of a carboxylic acid moiety and a hydrocarbon tail. SCFAs are produced by microbes in the gut and by skin-commensal bacteria on the skin at low concentrations (11, 12). Studies have shown that SCFAs derived from skin-commensal bacterium *S. epidermidis* inhibit the overgrowth of an opportunistic pathogen on the skin, *Propionibacterium acnes* (13, 14). Moreover, the products of *S. epidermidis* can suppress cutaneous inflammation through a mechanism depending on the toll-like receptor TLR2 (15). SCFAs reportedly also influenced inflammatory disease symptoms. For example, SCFAs could mediate cytokine and chemokine production by leukocytes and epithelial cells through the activation of G-protein-coupled receptors GPR41 and GPR43 and the inhibition of histone deacetylases (HDACs) (16). However, the regulatory role of SCFAs on IL-33 expression and skin inflammation in the context of *S. aureus* infection remains poorly understood.

As a previous study has demonstrated that SCFA butyrate, produced from the glycerol fermentation of *S. epidermidis* in the skin microbiome, could inhibit *S. aureus* growth (17), and our own previous study on butyrate alone has demonstrated its ability to regulate type 2 innate lymphoid cell function in the context of airway inflammation and hyperreactivity (18), we choose to focus on butyrate to investigate its regulatory role in *S. aureus*-aggravated skin inflammation.

Materials and methods

Mice

Three-week-old C57BL/6 mice were purchased from National Laboratory Animal Center (Taipei, Taiwan) and housed under specific pathogen-free conditions.

Bacterial strains

S. epidermidis (ATCC 12228) and AD patients-isolated *S. aureus* were kindly provided by Prof. Chun-Ming Huang (University of California, San Diego, USA) (17). The bacteria were cultured in tryptic soy broth (TSB, Sigma-Aldrich) at 37 °C with 250 rpm shaking overnight. Aliquots of *S. aureus* culture were centrifuged at 2200 ×*g*, and the pellets were washed with phosphate-buffered saline (PBS) and adjusted to an optical density of 1 at 600 nm, corresponding to approximately 1×10^9 *S. aureus* cells/mL.

Cell lines

KERTr cells were purchased from the American Type Culture Collection (Manassas, VA, USA) and cultured in antibiotic-free keratinocyte-SFM medium (Thermo Fisher).

Establishment of an AD-like mouse model, infection with *S. aureus*, and butyrate treatment

Hair from the dorsal skin (1.0×1.0 cm^2) of C57BL/6 mice was shaved prior to the start of the experiment. To perform the delipidization treatment, the organic solvent of acetone and ether mixture (1:1) was applied to the shaved area twice daily for two days (4, 5). For epicutaneous *S. aureus* infection, 5×10^8 colony-forming units (CFU) of *S. aureus* was suspended in 0.1 mL of TSB and applied to a cotton pad (1.0×1.0 cm^2), which was then applied onto the dorsal skin of mice for 24 h following delipidization. For intradermal *S. aureus* infection, C57BL/6 mice were intradermally (*i.d.*) inoculated into their backs with 10^7 colony-forming units (CFU) of *S. aureus* suspended in 0.1 mL of PBS and were sacrificed three days after *S. aureus* inoculation. For butyrate treatment on *S. aureus*-infected skin, after delipidization treatment, the dorsal skin of C57BL/6 mice was treated with a cotton pad (1.0×1.0 cm^2) for 24 h with 5×10^8 CFU of *S. aureus* that was suspended in 0.1 mL of 1 mM butyrate.

Treatment of *S. epidermidis* glycerol ferment on mouse skin

Glycerol fermentation by *S. epidermidis* was performed using a method described in a previous study (17). In brief, C57BL/6 mice subjected to AEW treatment were treated with 50 ul of *S. epidermidis*

or *S. aureus* (5×10^8 CFU) individually or simultaneously, in the presence or absence of 2% glycerol, using a cotton pad (1.0×1.0 cm^2). After 24 h of infection, the dorsal skin of the mice was excised and cut into smaller pieces for cytokine detection.

Mouse skin thickness measurement and histology

Mice dorsal skin was excised and fixed with 4% formaldehyde (Merck) for 24 h, and gradually dehydrated with 50%, 70%, and 90% ethanol (J.T. Baker) for 15 minutes each. The skin samples were embedded in paraffin for further histological analysis. For epidermal thickness, the skin sections were stained with hematoxylin and eosin (H&E) and measured using an Olympus CX31 microscope (Olympus Corp, Tokyo, Japan).

Processing of mouse skin and preparation of single-cell suspension

Dorsal skin (1.0×1.0 cm^2) was excised from delipidized mice, cut into smaller pieces, and incubated in 5 mL DMEM containing 1 mg/mL DNase I (Worthington Biochemicals), 0.5 mg/mL collagenase type I (Worthington Biochemicals), and 0.2 mg/mL collagenase type II (Worthington Biochemicals) for 60 min at 37°C. The digested tissue suspension was then filtered through a 70-µm mesh to obtain a single-cell suspension. The red blood cells in the single-cell suspension were lysed using ACK lysing buffer (Thermo Fisher) before the cells were resuspended in the appropriate buffer for further processing.

Isolation and culturing of murine primary keratinocytes

The murine primary keratinocytes were isolated following an established protocol (19). Briefly, neonates from C57B/6 mice aged 0-2 days were sacrificed, and the limbs removed just above the wrist and ankle joints. The whole skin was then peeled off and incubated in 4.3 mg/mL neutral protease at 4 ˚C overnight. The next day, forceps were used to separate the epidermis from the dermis, which was then further digested using 0.25 mg/mL trypsin/EDTA to obtain a single suspension of keratinocytes. Freshly isolated keratinocytes were cultured in antibiotic-free progenitor cell targeted medium (CELLnTEC) in 96-well plates at a density of 1×10^5 cells in 0.2 mL/well for further experimentation.

In vitro infection with S. aureus

Cells were cultured at 1×10^5 cells/mL in 96-well plates and infected with *S. aureus* at 10 MOI (multiplicity of infection) for 24 h. The culture supernatant was then collected for ELISA measurement. For mRNA detection, cells were cultured in antibiotic-free medium at 5×10^5 cells/mL in 12-well plates and infected with *S. aureus* at 10 MOI prior to mRNA isolation.

Determination of SCFA bactericidal activity

S. aureus (2×10^7 CFU/mL) was incubated with PBS (control) or 1 mM of acetate, butyrate or propionate for 24 h. After incubation, a 10-fold serial dilution from 10^{-1} to 10^{-5} was prepared from the treated bacteria, and 5 µl of each dilution was spotted on an agar plate. The bactericidal activity of SCFA was then determined in CFU from the highest dilution that showed bacterial growth.

Cytotoxicity analysis

KERTr cells (10^5 cells/well) were treated with butyrate for 24 h, and the cytotoxicity of butyrate was evaluated using the MTT assay (Supplementary Table 2) according to the manufacturer's instructions.

Flow cytometry

Single cell suspensions were washed once with PBS and stained with 100 µL FVD (eBioscience) diluted in PBS for 30 min at 4°C. Cells were washed with equal volume of PBS/2% FCS, followed by Fc blocking with 100 µL anti-human TruStain FcX (BioLegend) in PBS/2% FCS for 10 min at 4°C. Cells were then stained with the PerCP/Cy5.5 anti-CD45 (Biolegend) for 30 min at 4°C and were washed with equal volume of PBS/2% FCS and resuspended in 200 µL PBS/2% FCS for FACS analysis. Data were acquired using an LSR II (BD Biosciences) and analyzed using FlowJo v.10.1 software (TreeStar).

ELISA

The dorsal skin (1.0×1.0 cm^2) was cut into smaller pieces and transferred to 1 mL of DMEM. The explants were then incubated at room temperature with gentle shaking for 30 min. After incubation, the supernatant from the organ culture was collected and assayed for cytokines using ELISA kits according to the manufacturer's instructions. The ELISA kits used for cytokine detection are listed in Supplementary Table 1.

Immunoblotting

KERTr cells (2×10^6 cells/well) were lysed in protein lysis buffer, sonicated, and centrifuged at 13,000 ×*g* for 10 min at 4 ˚C to remove cell debris. Protein concentration was determined using the micro-

BCA protein assay kit (ThermoFisher). Equal amounts of protein (12 μg/sample) were separated using SDS-PAGE and transferred to PVDF membranes (PALL Corporation). Membranes were blocked with Tris-buffered saline and Tween 20 containing 5% bovine serum albumin. The primary antibodies for immunoblotting are listed in Supplementary Table 2. The primary antibodies were detected with peroxidase-conjugated anti-rabbit IgG or anti-mouse IgG, followed by detection with Western Lightning ECL pro reagent (PerkinElmer) according to the manufacturer's recommendations.

Immunofluorescence staining of skin tissue sections

Mouse dorsal skin was harvested, fixed with 4% formaldehyde (Merck), and gradually dehydrated with 50%, 70%, and 90% ethanol (J.T. Baker) for 15 min each. Paraffin-embedded skin sections were stained with streptavidin Alexa Fluor 488-conjugated anti mouse K14 antibody, Alexa Fluor 568-conjugated anti mouse HDAC2 antibody, and Alexa Fluor 568-conjugated anti mouse HDAC3 antibody (Supplementary Table 1), followed by the Alexa Fluor-conjugated secondary antibody (Thermo Fisher). Tissue auto-fluorescence was reduced by incubating slides with 1% Sudan black (Sigma-Aldrich) for 20 min before mounting. Image acquisition was performed using an Olympus BX51 microscope.

Quantitative real-time-PCR

Total RNA was isolated from skin tissue or cultured cells and extracted using the Quick-RNA^{TM} MicroPrep (Zymo Research) according to the manufacturer's instructions. A total of 1-2 μg of cDNA was synthesized using the high-capacity cDNA reverse transcription kit (Applied Biosystems), and real-time PCR was conducted using an Optical 96 real-time PCR thermal cycler (Biometra). Reactions were run in triplicate, and samples were normalized to *GAPDH* expression and quantities determined according to the $2^{-\Delta\Delta Ct}$ method. The primers used for qRT-PCR are listed in Supplementary Table 3.

Statistical analysis

Statistical analyses were performed using Prism 6 (GraphPad Prism). Student's unpaired *t*-test or one-way ANOVA were used to determine statistical significance between groups; values of $p < 0.05$ were considered significant.

Results

S. aureus infection induces the expression of epithelial cell-derived IL-33 *in vitro*

S. aureus is a common opportunistic pathogen associated with chronic inflammation in patients with skin disorders such as AD (20); however, its effect on the function of keratinocytes remains unclear. Therefore, to elucidate the potential role of *S. aureus* in contributing to the exacerbation of allergic responses during AD, we tested the ability of a *S. aureus* strain isolated from an AD patient to induce IL-33, as well as two other epithelial cell-derived cytokines, IL-25 and thymic stromal lymphopoietin (TSLP), in the human keratinocyte cell line, KERTr cell. We found that the *S. aureus* clinical isolate triggered the release of IL-33 in an infection dose- and time-dependent manner (Figures 1A, B). Moreover, IL-25 also increased in *S. aureus*-infected KERTr cells (Figure 1C). However, TSLP was undetectable in *S. aureus* infected KERTr cells (Figure 1D). A similar effect was observed in primary mouse keratinocytes infected with *S. aureus*, in which increased IL-33 and IL-25 expression was observed, along with positive TSLP expression (Figures 1E–G).

Epicutaneous exposure of *S. aureus* aggravates IL-33 release and skin inflammation

To determine whether *S. aureus* infection could induce IL-33 expression *in vivo*, we infected C57BL/6 mice with *S. aureus* by intradermal injection (*i.d.*). We observed an increase in IL-33 and IL-6 production from *S. aureus*-infected mice (Figures 2A, B). As a recent study has reported that *S. aureus* could penetrate through the epidermis into the dermis and trigger the expression of Th2 cytokines (21), we established an AD-like mouse model to mimic the natural route of *S. aureus* infection in AD patients with skin barrier disruption. This involved applying AEW treatment to mice, followed by epicutaneously challenging them with *S. aureus*. We discovered that *S. aureus* infection exacerbated AEW-induced IL-33 and IL-6 expressions in the skin (Figures 2C, D). Furthermore, the mRNA levels of *Il6* and *Il33*, as well as the Th2 cytokine *Il13*, increased substantially in *S. aureus*-infected skin (Figures 2E–G). However, the level of Th17 cytokine *Il17a* mRNA was undetectable (Figure 2H), and the level of Th1 cytokine *Ifng* mRNA did not change significantly during *S. aureus* infection (Figure 2I). Overall, these results suggest that *S. aureus* infection enhances IL-33 induction and aggravates Th2 inflammation in the skin of mice.

S. epidermidis glycerol ferment suppresses *S. aureus*-aggravated IL-33

Previous studies have reported that SCFAs possess antimicrobial and anti-inflammatory properties, suggesting immunomodulatory roles (17, 22). Therefore, we examined whether *S. epidermidis* grown in 2% glycerol could suppress *S. aureus*-induced IL-33 and IL-6 *in vivo*. C57BL/6 mice subjected first to AEW treatment were epicutaneously challenged with *S. epidermidis* or *S. aureus* (5×10^8 CFU), individually or simultaneously, with or without 2% glycerol. We found that the IL-33 level was reduced when the skin was treated with the two bacteria in the presence of glycerol compared with the treatment

10.3389/fimmu.2023.1114699

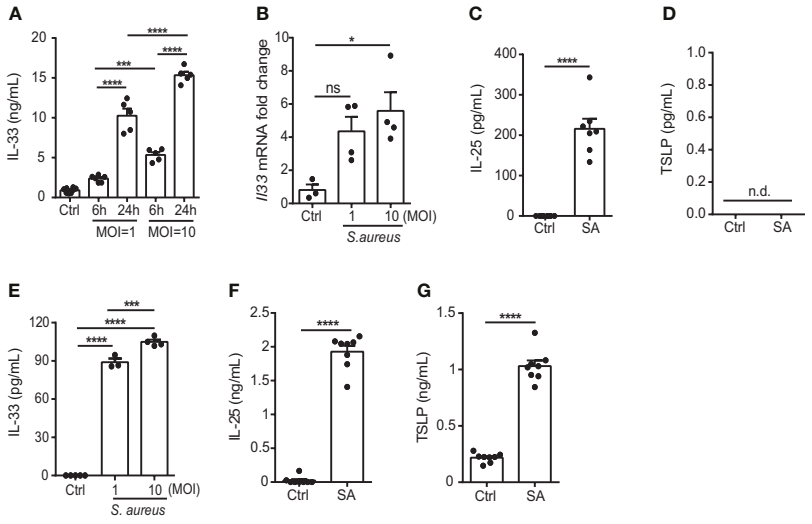

FIGURE 1
S. aureus infection induces the expression of epithelial cell-derived IL-33 *in vitro*. **(A)** IL-33 protein levels in KERTr cells infected with *S. aureus* at multiplicity of infection (MOI) of 1 and 10 for 6 h and 24 h. **(B)** IL-33 mRNA levels in KERTr cells infected with *S. aureus* at MOI of 1 and 10 for 6 h. **(C, D)**. Protein levels of **(C)** IL-25 and **(D)** TSLP secreted by KERTr cell under *S. aureus* infection at MOI of 10. **(E–G)**. Protein levels of **(E)** IL-33, **(F)** IL-25, and **(G)** TSLP secreted by mouse primary keratinocytes under *S. aureus* infection at MOI of 10. Data are shown as mean ± SEM from 3 independent experiments (n=3-8 per group). Statistical analysis was performed using one-way ANOVA **(A, B, E)** or an unpaired two-tailed t test **(C, D, F, G)**. *n.d,* Not detectable; *n.s,* Not significant. **p<0.05, ***p<0.001, ****p<0.0001.*

with the two bacteria without glycerol (Figure 3A). However, the expression of IL-6 was not significantly altered by the addition of 2% glycerol (Figure 3B).

Three SCFAs, acetate, butyrate, and propionate, are known to be produced by the fermentation of glycerol by *S. epidermidis* (23). Consequently, we investigated the effect of all three SCFAs on cultured keratinocytes following *S. aureus* infection. We found that all three SCFAs could inhibit IL-33 expression in the KERTr cells (Figure 3C), as well as in the mouse primary keratinocytes (Figure 3D). Since butyrate treatment in KERTr cells at 1mM demonstrated a trend of stronger IL-33 suppression compared to the other two SCFAs, we further examined the dose-response of butyrate treatment on IL-33 expression. We found that butyrate suppressed IL-33 expression in *S. aureus*-infected KERTr cells in a dose-dependent manner (Figure 3E), with the IL-33 suppression effect plateauing at 1 mM butyrate. We also assessed the toxicity effect of butyrate treatment on KERTr cells and observed no reduction in viability in butyrate-treated KERTr cell at the concentrations we examined, even at a high concentration of 100 mM (Figure 3F). Although all three SCFAs could inhibit IL-33 expression in *S. aureus*-infected keratinocytes, they did not suppress the growth of *S. aureus* (Figures 3G, H). This suggests that the inhibition of IL-33 in *S. aureus*-infected keratinocytes was not due to a reduction of *S. aureus* viability, but rather resulted from the regulatory effect of SCFAs on IL-33 expression.

Butyrate suppresses IL-33 production and attenuates skin inflammation

Encouraged by the results of our previous study on using butyrate as an immunomodulatory agent (18), we turned our focus to assess the effects of butyrate on *S. aureus*-induced skin inflammation. We concurrently applied *S. aureus* and butyrate to the dorsal skin after AEW treatment, and the expression levels of *Il33*, *Il13*, and *Il6* mRNA were diminished by butyrate co-treatment (Figures 4A–C). Simultaneously, we found that butyrate decreased the number of dermal infiltrating leukocytes in *S. aureus*-infected mice (Figure 4D; Supplemental Figure 1). However, the epidermal thickening was not influenced by butyrate treatment (Figure 4E). Collectively, these results demonstrated that butyrate could inhibit *S. aureus*-exacerbated skin inflammation by suppressing IL-33 release from keratinocytes.

Butyrate suppresses IL-33 expression in *S. aureus*-infected KERTr cell through HDAC3 inhibition

Previous studies have shown that SCFAs exert modulatory functions either by binding to free fatty acid receptors FFAR2 and FFAR3 to activate downstream signaling pathways (24, 25) or by inducing histone acetylation through HDAC inhibitory activity (26–28). To determine the involvement of FFAR2, FFAR3, and HDACs in response to butyrate in *S. aureus* infection, we first treated *S. aureus*-infected KERTr cells in the absence of butyrate with FFAR2 agonist 4-chloro-α-(1-methylethyl)-N-2-thiazolyl-benzeneacetamide (4-CMTB), the FFAR3 agonist AR420626, or the pan-HDAC inhibitor trichostatin A (TSA). We found that both receptor agonists and the pan-HDAC inhibitor suppressed *S. aureus*-induced IL-33 production (Figure 5A). Next, to clarify the mechanism underlying IL-33 release, KERTr cells were infected with *S. aureus* and treated with butyrate alone or co-treated with

10.3389/fimmu.2023.1114699

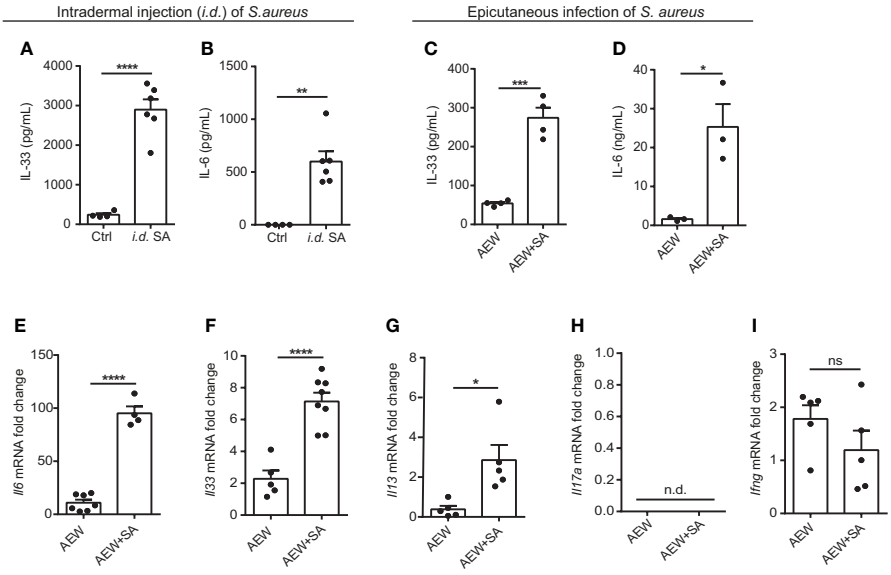

FIGURE 2
Epicutaneous exposure of *S. aureus* aggravates IL-33 release and skin inflammation. **(A, B)** Three-week old C57BL/6 mice were intradermally (*i.d.*) inoculated with 10^7 colony-forming units (CFU) of *S. aureus* and sacrificed 3 days after *S. aureus* infection. **(A)** IL-33 protein level in the skin. **(B)** IL-6 protein level in the skin. **(C–I).** Three-week old C57BL/6 mice were treated with the AEW protocol daily for 2 days, followed by the epicutaneous *S. aureus* infection at 5×10^8 CFU for 24 h. **(C)** IL-33 protein level in the skin. **(D)** IL-6 protein level in the skin. **(E–I).** mRNA levels of **(E)** *Il6*, **(F)** *Il33*, **(G)** *Il13*, **(H)** *Il17a*, and **(I)** *Ifng* in the skin. Data are shown as mean ± SEM from 3 independent experiments (n=3-8 per group). Statistical analysis was performed using an unpaired two-tailed t test **(A–I)**. *n.d.* Not detectable. *n.s.* Not significant. **p<0.05, **p<0.01, ***p<0.001, ****p<0.0001.*

butyrate in the presence of 4-CMTB, AR420626, or TSA. As expected, the results showed that both FFAR2 and FFAR3 agonists synergized with butyrate to inhibit IL-33 expression (Figure 5B). However, the effect of butyrate and TSA co-treatment on the level of IL-33 level did not differ significantly from either treatment on their own (Figure 5B).

The expression of HDAC3, a member of the class I HDAC family, is known to correlate with the expression of IL-33 (29). Therefore, we assessed the possible involvement of HDAC3 in IL-33 expression in *S. aureus*-infected keratinocytes. We found that the class I HDAC inhibitor MS-275 alone suppressed *S. aureus*-induced IL-33 production in KERTr cells, and the co-treatment of butyrate and MS-275 did not further downregulate IL-33 expression in comparison to either treatment alone (Figure 5C), suggesting that butyrate might act as a HDAC inhibitor and lead to increased histone acetylation and regulated gene transcription. We went on to measure the level of histone 3 acetylation (AC-H3) using western blot and found that butyrate treatment caused an increase in histone 3 acetylation in KERTr cells in a dose-dependent manner (Figures 5D, E).

We next investigated whether butyrate acted on HDAC targets similarly to MS-275 in *S. aureus*-infected KERTr cells. Western blot analysis for class I HDACs HDAC1, 2, 3, and 8 revealed that only HDAC3 levels were reduced by butyrate treatment (Figures 5F, G; Supplemental Figures 2A–C). To further determine the involvement of HDAC3 in IL-33 expression, we treated *S. aureus*-infected KERTr cells with HDAC3 antagonist RGFP966. We found that co-treatment with butyrate and RGFP966 did not further suppress IL-33 expression compared to either treatment alone (Figure 5H). Collectively, our data suggest that butyrate can inhibit IL-33 expression in *S. aureus*-infected KERTr cells by blocking HDAC3 action.

Butyrate ameliorates skin inflammation induced by *S. aureus* through HDAC3 inhibition

We performed additional analysis on the protein expression of IL-33 in the skin of WT mice using immunofluorescence staining. Our results revealed that *S. aureus* infection led to increased IL-33 expression in the delipidized skin. Nevertheless, treatment with butyrate significantly reduced *S. aureus*-aggravated IL-33 expression in the skin (Figures 6A, B). To investigate the effect of butyrate on HDAC3 expression, we found that butyrate treatment significantly reduced *S. aureus*-exacerbated HDAC3 expression in the skin (Figures 6C, D). However, we did not observe a significant difference in the expression of other members of the HDAC class I, such as HDAC2, between the groups (Supplemental Figures 3A, B). We also observed a reduction in the co-localization of HDAC3 and IL-33 in butyrate-treated skin (Figure 6E). This suggests that butyrate inhibits keratinocyte-derived IL-33 expression in *S. aureus*-infected skin cells through HDAC3 inhibition.

10.3389/fimmu.2023.1114699

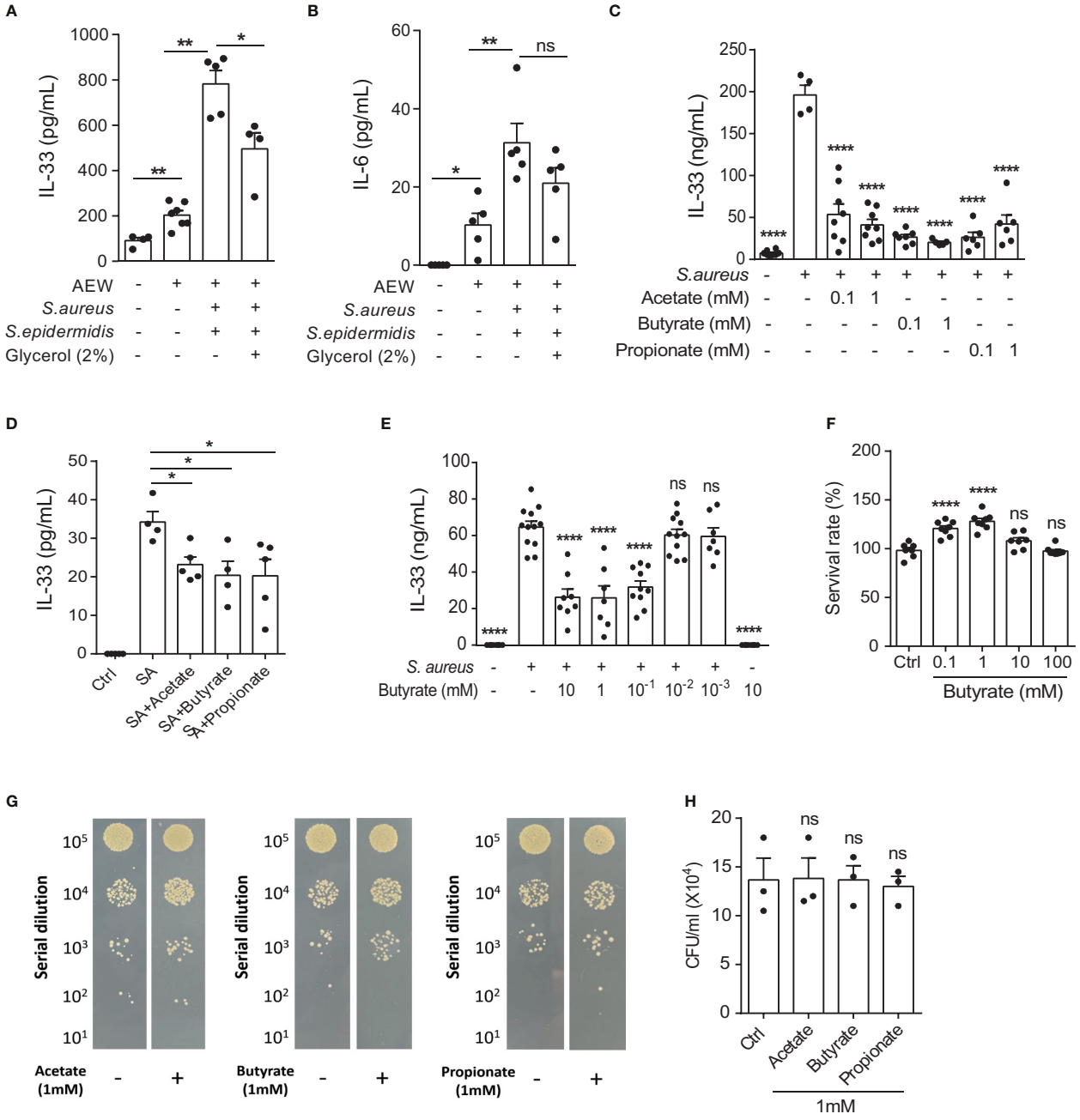

FIGURE 3
S. epidermidis glycerol ferment suppresses *S. aureus*-aggravated IL-33. **(A, B)**. Three-week old C57BL/6 mice were first subjected to AEW treatment twice daily for 2 days, and were then epicutaneously challenged with *S. epidermidis* or *S. aureus* (5×10^8 CFU) individually or simultaneously, with or without 2% glycerol. Mice were sacrificed the next day following the epicutaneous challenges **(A)** IL-33 level in the skin. **(B)** IL-6 level in the skin. **(C, D)**. IL-33 secreted by **(C)** KERTr cells and **(D)** mouse primary keratinocytes infected with *S. aureus* and treated concurrently with acetate, butyrate, or propionate for 24 h. **(E)** Level of IL-33 from KERTr cell infected with *S. aureus* and treated with butyrate for 24 h. **(F)** Survival rate of KERTr cells after 24 h of butyrate treatment. **(G, H)**. The evaluation *S. aureus* (2×10^7 CFU/ml) growth after incubation with 1 mM of acetate, butyrate, or propionate for 24 h. Data are shown as mean ± SEM from 3 independent experiments (n=3-8 per group). Statistical analysis was performed using one-way ANOVA (A-F and H). *n.s,* Not significant. **p<0.05, **p<0.01, ****p<0.0001.*

Discussion

Our study utilized both *in vitro* experiments and *in vivo* mouse models to simulate *S. aureus* infection in dry skin condition experienced by AD patients. We demonstrated that *S. aureus* infection could worsen skin inflammation by increasing IL-33 release from keratinocyte and exacerbate dermal leukocyte infiltration. Furthermore, we elucidated the regulatory role of

10.3389/fimmu.2023.1114699

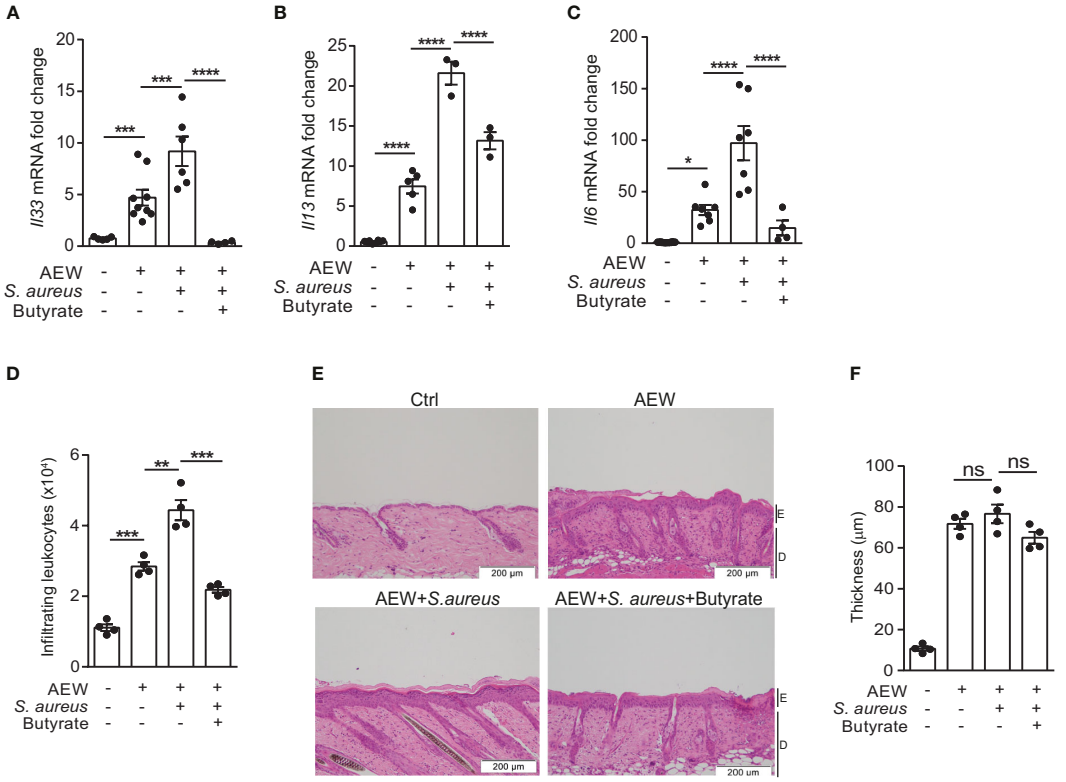

FIGURE 4
Butyrate suppresses IL-33 production and attenuates skin inflammation. **(A–F)**. *S. aureus* (5×10^8 CFU) was applied onto the dorsal skin of mice with or without butyrate (1 mM) after the last AEW treatment. Mice were sacrificed the next day for further experimentation. **(A–C)**. Levels of **(A)** *Il33*, **(B)** *Il13*, and **(C)** *Il6* mRNAs in the skin. **(D)** Mean numbers of total $CD45^+$ leukocytes in the skin. **(E)** Hematoxylin and eosin (H&E) stained skin sections. (Scale bars: 200 μm, Magnification: 10X; E, epidermidis; D, dermal). **(F)** Measurement of skin thickness. Data are shown as mean ± SEM from 3 independent experiments (n=3-9 per group). Statistical analysis was performed using one-way ANOVA **(A–C, E–F)**. *n.s*, Not significant. **p<0.05, **p<0.01, ***p<0.001, ****p<0.0001.*

butyrate, a metabolite of skin commensal bacterium *S. epidermidis*, which can attenuate skin inflammation resulting from *S. aureus* infection. Mechanistically, we found that butyrate could suppress keratinocyte-derived IL-33 expression in *S. aureus*-infected KERTr cells by inhibiting HDAC3. Overall, our findings, illustrated in Figure 7, suggest that butyrate may serve as a therapeutic agent for treating inflammatory skin conditions in AD patients with *S. aureus* infection.

Skin commensal bacteria are known to produce the SCFA butyrate, which has been shown to prevent skin inflammatory response by activating skin resident regulatory T cells (30). SCFAs also inhibit Th2 responses and interact with other immune cells (31). In our prior study, we have demonstrated that butyrate, but not acetate or propionate, inhibits the Th2 response mediated by murine ILC2s in the lungs (18). Thus, based on our previous experience with SCFAs, we selected butyrate to investigate its effect on *S. aureus*-aggravated inflammation in the skin. Our results show that butyrate attenuates skin inflammatory responses, as evidenced by decreased infiltrating leukocytes and IL-33 expression both *in vitro* and *in vivo*. Although a previous study has reported that a high concentration of 50 mM butyrate is required to suppresses the growth of *S. aureus* (17),, we indirectly confirmed this by demonstrating that no suppression of *S. aureus* growth was observed at the high dosage of 1 mM SCFAs (Figures 3G, H). Therefore, directly using butyrate to suppress *S. aureus* growth on the skin of AD patients may not be feasible. However, our data also showed that as little as 0.1 mM of butyrate was enough to inhibit *S. aureus*-aggravated IL-33 expression *in vitro* (Figures 3C, E), suggesting butyrate as a potential therapeutic agent for *S. aureus*-exacerbated skin inflammation.

In addition, our *in vitro* experiment also shows that acetate and propionate, likewise produced by the *S. epidermidis* glycerol fermentation (23), can inhibit IL-33 release from *S. aureus*-infected keratinocytes (Figures 3C, D). Therefore, we cannot exclude the possibility that acetate and propionate can also suppress IL-33 expression to ameliorate skin inflammation. Further investigation is needed to determine whether acetate or propionate has a similar inhibitory effect as butyrate on *S. aureus*-exacerbated skin inflammation *in vivo*. In short, our results suggest that microbial metabolites can positively influence *S. aureus*-exacerbated skin inflammation.

SCFAs produced by microbes have been reported to alter gene expression and cell proliferation by inhibiting the chromatin-remodeling activity of HDACs (26). In allergic skin inflammation,

10.3389/fimmu.2023.1114699

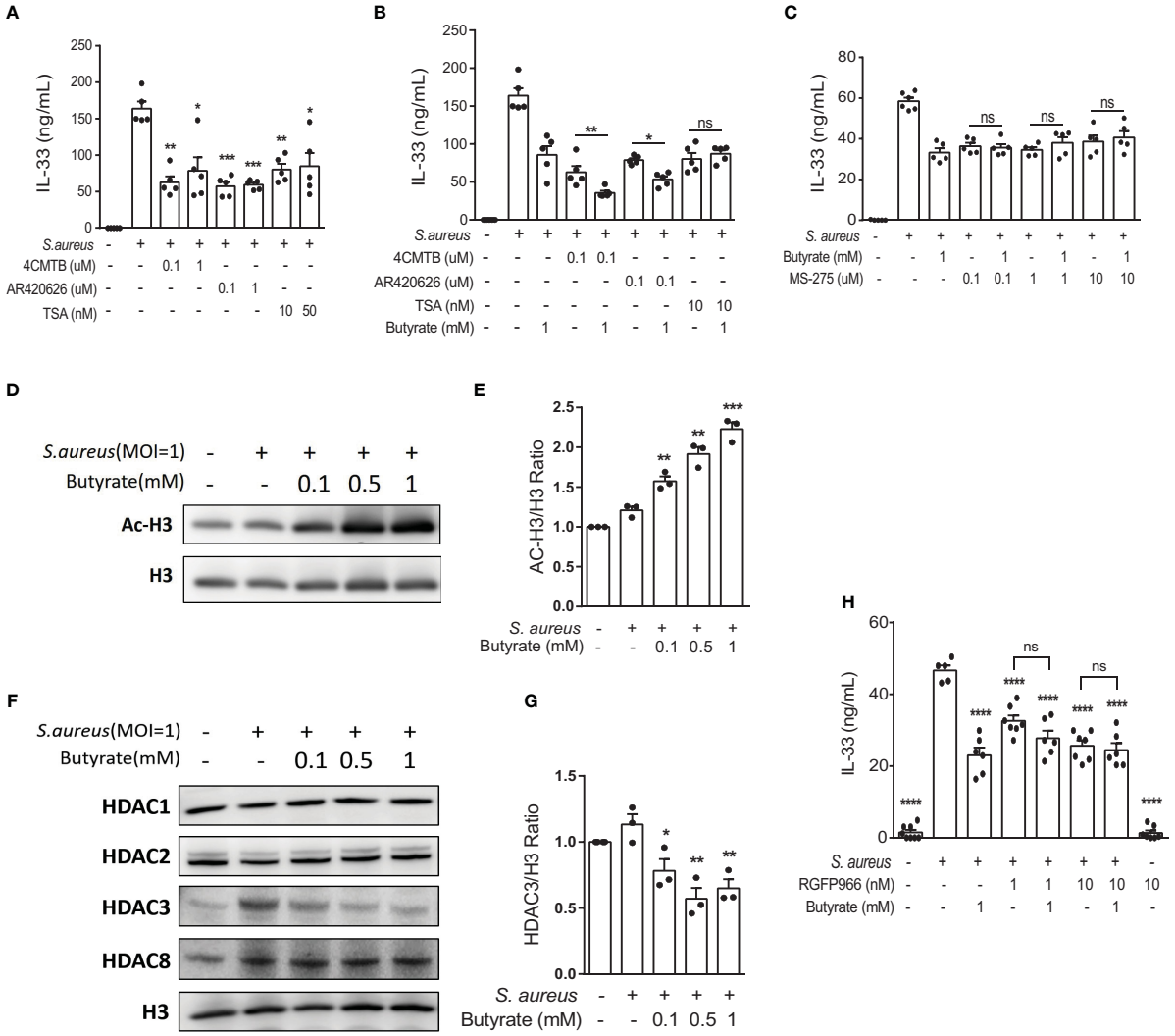

FIGURE 5
Butyrate suppresses IL-33 expression in *S. aureus*-infected KERTr cells through HDAC3 inhibition. **(A)** IL-33 level in the culture supernatant of KERTr cells infected with *S. aureus* in conjunction with the treatment of 4-CMTB (0.1 and 1 μM), AR420626 (0.1 and 1 μM), or TSA (10 and 50 nM). **(B)** IL-33 level in the culture supernatant of KERTr cells infected with *S. aureus* in conjunction with the treatment of 4-CMTB (0.1 μM), AR420626 (0.1 μM), or TSA (10 nM), and in the presence or absence of butyrate (1 mM). **(C)** IL-33 level in the culture supernatant of KERTr cells infected with *S. aureus* in conjunction with the treatment of MS-275 (0.1, 1, and 10 μM), and in the presence or absence of butyrate (1 mM). **(D–G)**. KERTr cells infected with *S. aureus* were treated with butyrate (0.1, 0.5, and 1 mM) for 6 h. **(D)** Representative western blot of acetylated histone 3 (Ac-H3) and total histone 3 (H3). **(E)** Quantification of Ac-H3 normalized to H3. **(F)** Representative western blot of class I HDACs (HDAC1, 2, 3, and 8) and H3. **(G)** Quantification of HDAC3 normalized to H3. **(H)** IL-33 level in the culture supernatant of KERTr cells infected with *S. aureus* and treated RGFP966 (1 and 10 nM) in the presence or absence of butyrate (1 mM) 24 h. Data are shown as mean ± SEM from 3 independent experiments (n=3-7 per group). Statistical analysis was performed using one-way ANOVA **(A–C, E, G, H)**. *n.s,* Not significant. **p<0.05, **p<0.01, ***p<0.001, ****p<0.0001,* compared to *S. aureus* infection alone groups.

HDAC3 inhibition by TSA suppresses MCP1 expression, alleviating mast cell-mediated passive cutaneous anaphylaxis (32). Furthermore, butyrate-induced HDAC3 inhibition in the intestine leads to metabolic changes and the induction of the bactericidal function of macrophages, promoting gut homeostasis (33). In our investigation, we first established that butyrate could inhibit IL-33 expression in *S. aureus*-infected human keratinocyte KERTr cells through HDAC inhibition, especially of the class I HDAC. Subsequently, we demonstrated that butyrate upregulated histone 3 acetylation and downregulated HDAC3 expression. We also used a HDAC3-specific inhibitor in *S. aureus*-infected KERTr cells to clarify the role of HDAC3 in IL-33 regulation and determine the inhibitory function of butyrate on HDAC3 activity. In the *S. aureus*-infected skin, we found that butyrate treatment significantly reduced the co-expression of IL-33 and HDAC3-expressing cells, further suggesting the regulation of butyrate in HADC3 and IL-33 expression.

Our data suggest that butyrate acts as an inhibitor of the class I HDACs in *S. aureus*-infected KERTr cells, and the downregulation of HDAC3 by butyrate attenuated IL-33 expression. However, the

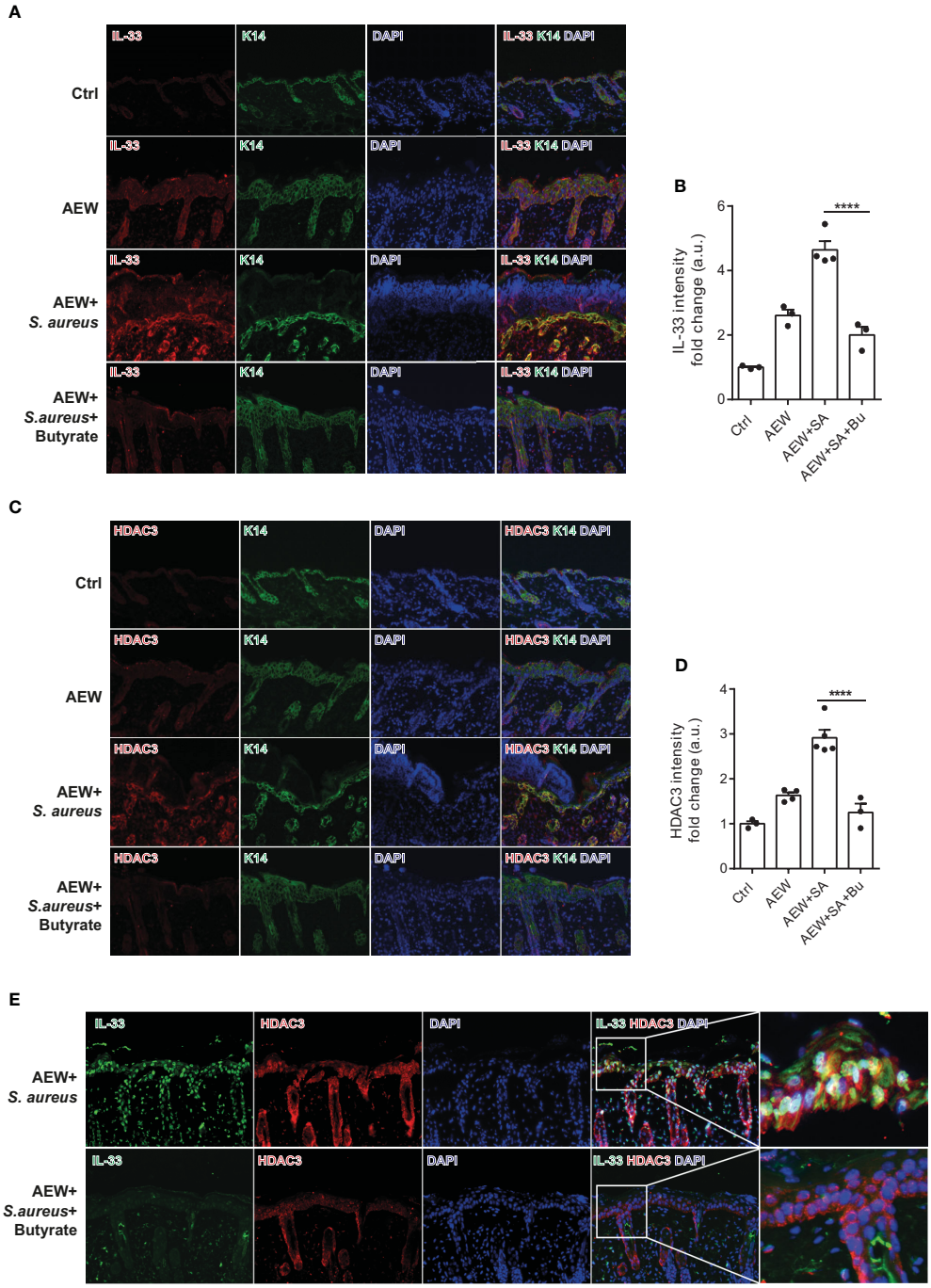

FIGURE 6
Butyrate ameliorates skin inflammation induced by *S. aureus* through HDAC3 inhibition. **(A)** Immunofluorescence staining of IL-33 (red), K14 (green), and DAPI (blue) in the skin of WT mice. (Magnification: 40X). **(B)** Densitometry analysis for IL-33 in the mouse skin. **(C)** Immunofluorescence staining of HDAC3 (red), K14 (green), and DAPI (blue) in the skin of WT mice. (Magnification: 40X). **(D)** Densitometry analysis for HDAC3 in the mouse skin. **(E)** Immunofluorescence staining of IL-33 (green), HDAC3 (red), and DAPI (blue) in the skin of WT mice. (Magnification: 40X). Data are shown as mean ± SEM from 3 independent experiments (n=3-5 per group). Statistical analysis was performed using one-way ANOVA **(B, D)**. *****p<0.0001.*

downstream effects of HDAC inhibition remain to be elucidated. Although HDAC3 can act as a transcriptional repressor to influence IL-33 expression in many diseases, including multiple sclerosis and allergic asthma (29), it is still unclear whether the inhibitory effect of butyrate is due to the direct acetylation of the *Il33* gene or indirectly through the transcriptional activation/suppression of other targets that can alter the IL-33 expression. Further investigation is needed to understand the mechanism of butyrate's inhibitory effect on IL-33 expression.

In summary, our model of epicutaneous application of *S. aureus* to delipidized skin mimicked the natural route of *S. aureus* infection in patients with AD. We demonstrated the regulatory role of butyrate, produced by the skin commensal bacterium *S. epidermidis*, in suppressing HDAC3 activity and attenuating skin

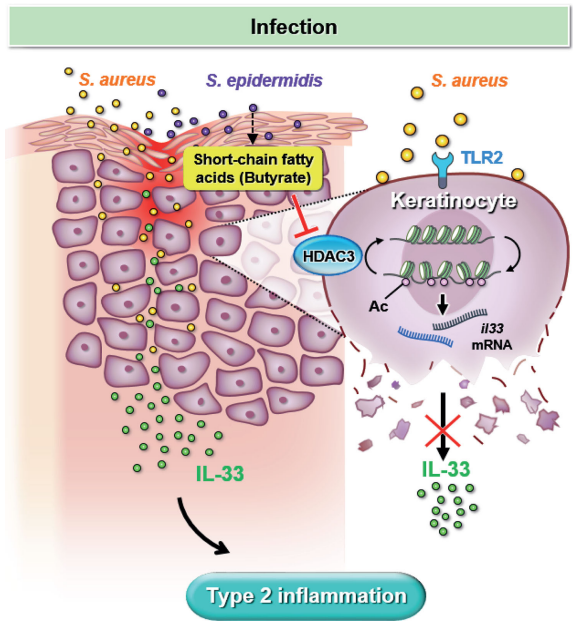

FIGURE 7
Butyrate attenuates *S. aureus*-aggravated dermal IL-33 and skin inflammation through histone deacetylase 3 inhibition. *S. aureus* infection exacerbates keratinocyte-derived IL-33 expression and contributes to skin inflammation. Butyrate suppresses *S. aureus*-aggravated dermal IL-33 expression to ameliorate skin inflammation through HDAC3 inhibition.

inflammation caused by *S. aureus* infection. Additionally, we revealed the underlying mechanism of butyrate in regulating IL-33 and provided evidences supporting butyrate as a potential therapeutic agent for controlling inflammatory skin conditions exacerbated by *S. aureus* infection in AD patients.

Data availability statement

The original contributions presented in the study are included in the article/Supplementary Material. Further inquiries can be directed to the corresponding authors.

Ethics statement

The animal study was reviewed and approved by Academia Sinica Institutional Animal Care and Use Committee.

Author contributions

Conceptualization, writing – original draft, and writing – review and editing, C-HL, AL, Y-JC. Methodology and visualization, C-HL. Investigation, C-HL and AL. Funding acquisition, project administration, and supervision, Y-JC. All authors contributed to the article and approved the submitted version.

Funding

This work was supported by the National Health Research Institutes [NHRI-EX110-10836SI], Ministry of Science and Technology [104-2320-B-001-022; 111-2320-B-001-025-MY3] and by the Academia Sinica [AS-IA-110-L04 and AS-GC-110-05 to Y-JC] in Taiwan.

Acknowledgments

We would like to thank Prof. Chun-Ming Huang for giving us Staphylococcus bacteria and advices on culturing them. We would also like to thank the staff of the IBMS Flow Cytometry Core Facility [AS-CFII-111-212] for services and facilities provided.

Conflict of interest

The authors declare that the research was conducted in the absence of any commercial or financial relationships that could be construed as a potential conflict of interest.

Publisher's note

Supplementary material

The Supplementary Material for this article can be found online at: https://www.frontiersin.org/articles/10.3389/fimmu.2023.1114699/full#supplementary-material

SUPPLEMENTARY FIGURE 1
Butyrate reduces infiltrating dermal leukocytes in *S. aureus*-infected mice. Representative flow cytometry plot showing dermal leukocytes (FVD^+ $CD45^+$), assessed by FACS.

SUPPLEMENTARY FIGURE 2
Butyrate does not alter HDAC1, HDAC2, and HDAC8 expressions in KERTr cells under *S. aureus* infection. KERTr cells infected with *S. aureus* were treated with butyrate (0.1, 0.5, and 1 mM) for 6 h, and the ratios of **(A)** HDAC1, **(B)** HDAC2, and **(C)** HDAC8 normalized to total histone 3 were determined. Data are shown as mean ± SEM from 3 independent experiments (n=3-7 per group). Statistical analysis was performed using one-way ANOVA. *n.s.* Not significant, compared to *S. aureus* infection alone groups.

SUPPLEMENTARY FIGURE 3
Butyrate does not alter HDAC2 expression in the skin of mice with tested conditions under *S. aureus* infection. **(A)**. Immunofluorescence staining of HDAC2 (red), K14 (green), and DAPI (blue) in the skin of mice. (Magnification: 40X) **(B)**. Densitometry analysis for HDAC2 in the mouse skin. Data are shown as mean ± SEM from 3 independent experiments (n=3-7 per group). Statistical analysis was performed using one-way ANOVA **(B)**. *n.s.* Not significant, compared to *S. aureus* infection alone groups.

References

1. Hill DA, Spergel JM. The atopic march: critical evidence and clinical relevance. *Ann Allergy Asthma Immunol* (2018) 120(2):131–7. doi: 10.1016/j.anai.2017.10.037

2. Bantz SK, Zhu Z, Zheng T. The atopic march: progression from atopic dermatitis to allergic rhinitis and asthma. *J Clin Cell Immunol* (2014) 5(2):202. doi: 10.4172/2155-9899.1000202

3. Tamagawa-Mineoka R, Okuzawa Y, Masuda K, Katoh N. Increased serum levels of interleukin 33 in patients with atopic dermatitis. *J Am Acad Dermatol* (2014) 70 (5):882–8. doi: 10.1016/j.jaad.2014.01.867

4. Wilson SR, Nelson AM, Batia L, Morita T, Estandian D, Owens DM, et al. The ion channel TRPA1 is required for chronic itch. *J Neurosci* (2013) 33(22):9283–94. doi: 10.1523/JNEUROSCI.5318-12.2013

5. Miyamoto T, Nojima H, Shinkado T, Nakahashi T, Kuraishi Y. Itch-associated response induced by experimental dry skin in mice. *Jpn J Pharmacol* (2002) 88(3):285–92. doi: 10.1254/jjp.88.285

6. Lowy FD. Staphylococcus aureus infections. *N Engl J Med* (1998) 339(8):520–32. doi: 10.1056/NEJM199808203390806

7. Spergel JM, Paller AS. Atopic dermatitis and the atopic march. *J Allergy Clin Immunol* (2003) 112(6 Suppl):S118–27. doi: 10.1016/j.jaci.2003.09.033

8. Tauber M, Balica S, Hsu CY, Jean-Decoster C, Lauze C, Redoules D, et al. Staphylococcus aureus density on lesional and nonlesional skin is strongly associated with disease severity in atopic dermatitis. *J Allergy Clin Immunol* (2016) 137(4):1272–1274 e3. doi: 10.1016/j.jaci.2015.07.052

9. Blicharz L, Rudnicka L, Samochocki Z. Staphylococcus aureus: an underestimated factor in the pathogenesis of atopic dermatitis? *Postepy Dermatol Alergol* (2019) 36 (1):11–7. doi: 10.5114/ada.2019.82821

10. Berdyshev E, Goleva E, Bronova I, Dyjack N, Rios C, Jung J, et al. Lipid abnormalities in atopic skin are driven by type 2 cytokines. *JCI Insight* (2018) 3(4): e98006. doi: 10.1172/jci.insight.98006

11. Furusawa Y, Obata Y, Fukuda S, Endo TA, Nakato G, Takahashi D, et al. Commensal microbe-derived butyrate induces the differentiation of colonic regulatory T cells. *Nature* (2013) 504(7480):446–50. doi: 10.1038/nature12721

12. Smith PM, Howitt MR, Panikov N, Michaud M, Gallini CA, Bohlooly YM, et al. The microbial metabolites, short-chain fatty acids, regulate colonic treg cell homeostasis. *Science* (2013) 341(6145):569–73. doi: 10.1126/science.1241165

13. Burtenshaw JM. The mechanism of self-disinfection of the human skin and its appendages. *J Hyg (Lond)* (1942) 42(2):184–210. doi: 10.1017/S0022172400035373

14. Christensen GJ, Bruggemann H. Bacterial skin commensals and their role as host guardians. *Benef Microbes* (2014) 5(2):201–15. doi: 10.3920/BM2012.0062

15. Lai Y, Cogen AL, Radek KA, Park HJ, Macleod DT, Leichtle A, et al. Activation of TLR2 by a small molecule produced by staphylococcus epidermidis increases antimicrobial defense against bacterial skin infections. *J Invest Dermatol* (2010) 130 (9):2211–21. doi: 10.1038/jid.2010.123

16. Vinolo MA, Rodrigues HG, Nachbar RT, Curi R. Regulation of inflammation by short chain fatty acids. *Nutrients* (2011) 3(10):858–76. doi: 10.3390/nu3100858

17. Traisaeng S, Herr DR, Kao HJ, Chuang TH, Huang CM. A derivative of butyric acid, the fermentation metabolite of staphylococcus epidermidis, inhibits the growth of a staphylococcus aureus strain isolated from atopic dermatitis patients. *Toxins (Basel)* (2019) 11(6):311. doi: 10.3390/toxins11060311

18. Thio CL, Chi PY, Lai AC, Chang YJ. Regulation of type 2 innate lymphoid cell-dependent airway hyperreactivity by butyrate. *J Allergy Clin Immunol* (2018) 142 (6):1867–1883 e12. doi: 10.1016/j.jaci.2018.02.032

19. Li F, Adase CA, Zhang LJ. Isolation and culture of primary mouse keratinocytes from neonatal and adult mouse skin. *J Vis Exp* (2017) 125:56027. doi: 10.3791/56027

20. Sator PG, Schmidt JB, Honigsmann H. Comparison of epidermal hydration and skin surface lipids in healthy individuals and in patients with atopic dermatitis. *J Am Acad Dermatol* (2003) 48(3):352–8. doi: 10.1067/mjd.2003.105

21. Nakatsuji T, Chen TH, Two AM, Chun KA, Narala S, Geha RS, et al. Staphylococcus aureus exploits epidermal barrier defects in atopic dermatitis to trigger cytokine expression. *J Invest Dermatol* (2016) 136(11):2192–200. doi: 10.1016/j.jid.2016.05.127

22. Lamas A, Regal P, Vazquez B, Cepeda A, Franco CM. Short chain fatty acids commonly produced by gut microbiota influence salmonella enterica motility, biofilm formation, and gene expression. *Antibiotics (Basel)* (2019) 8(4):265. doi: 10.3390/antibiotics8040265

23. Kao MS, Huang S, Chang WL, Hsieh MF, Huang CJ, Gallo RL, et al. Microbiome precision editing: using PEG as a selective fermentation initiator against methicillin-resistant staphylococcus aureus. *Biotechnol J* (2017) 12(4). doi: 10.1002/biot.201600399

24. Tazoe H, Otomo Y, Kaji I, Tanaka R, Karaki SI, Kuwahara A. Roles of short-chain fatty acids receptors, GPR41 and GPR43 on colonic functions. *J Physiol Pharmacol* (2008) 59(Suppl 2):251–62.

25. Lu Y, Fan C, Li P, Lu Y, Chang X, Qi K. Short chain fatty acids prevent high-fat-diet-induced obesity in mice by regulating G protein-coupled receptors and gut microbiota. *Sci Rep* (2016) 6:37589. doi: 10.1038/srep37589

26. Davie JR. Inhibition of histone deacetylase activity by butyrate. *J Nutr* (2003) 133 (7 Suppl):2485S–93S. doi: 10.1093/jn/133.7.2485S

27. Nguyen NH, Morland C, Gonzalez SV, Rise F, Storm-Mathisen J, Gundersen V, et al. Propionate increases neuronal histone acetylation, but is metabolized oxidatively by glia. relevance for propionic acidemia. *J Neurochem* (2007) 101(3):806–14. doi: 10.1111/j.1471-4159.2006.04397.x

28. Gao X, Lin SH, Ren F, Li JT, Chen JJ, Yao CB, et al. Acetate functions as an epigenetic metabolite to promote lipid synthesis under hypoxia. *Nat Commun* (2016) 7:11960. doi: 10.1038/ncomms11960

29. Zhang F, Tossberg JT, Spurlock CF, Yao SY, Aune TM, Sriram S. Expression of IL-33 and its epigenetic regulation in multiple sclerosis. *Ann Clin Transl Neurol* (2014) 1(5):307–18. doi: 10.1002/acn3.47

30. Schwarz A, Bruhs A, Schwarz T. The short-chain fatty acid sodium butyrate functions as a regulator of the skin immune system. *J Invest Dermatol* (2017) 137 (4):855–64. doi: 10.1016/j.jid.2016.11.014

31. Trompette A, Gollwitzer ES, Yadava K, Sichelstiel AK, Sprenger N, Ngom-Bru C, et al. Gut microbiota metabolism of dietary fiber influences allergic airway disease and hematopoiesis. *Nat Med* (2014) 20(2):159–66. doi: 10.1038/nm.3444

32. Kim M, Kwon Y, Jung HS, Kim Y, Jeoung D. FcepsilonRI-HDAC3-MCP1 signaling axis promotes passive anaphylaxis mediated by cellular interactions. *Int J Mol Sci* (2019) 20(19):4964. doi: 10.3390/ijms20194964

33. Schulthess J, Pandey S, Capitani M, Rue-Albrecht KC, Arnold I, Franchini F, et al. The short chain fatty acid butyrate imprints an antimicrobial program in macrophages. *Immunity* (2019) 50(2):432–445 e7. doi: 10.1016/j.immuni.2018.12.018

frontiers | Frontiers in Immunology

TYPE Original Research
PUBLISHED 26 May 2023
DOI 10.3389/fimmu.2023.1098160

OPEN ACCESS

EDITED BY
Tej Pratap Singh,
University of Pennsylvania, United States

REVIEWED BY
Juan Carlos Cancino-Diaz,
National Polytechnic Institute (IPN), Mexico
Aayushi Uberoi,
University of Pennsylvania, United States

*CORRESPONDENCE
Cecile Clavaud
cecile.clavaud@loreal.com
Mathias L. Richard
mathias.richard@inrae.fr

†These authors have contributed equally to this work

RECEIVED 14 November 2022
ACCEPTED 04 May 2023
PUBLISHED 26 May 2023

CITATION
Landemaine L, Da Costa G, Fissier E, Francis C, Morand S, Verbeke J, Michel M-L, Briandet R, Sokol H, Gueniche A, Bernard D, Chatel J-M, Aguilar L, Langella P, Clavaud C and Richard ML (2023) *Staphylococcus epidermidis* isolates from atopic or healthy skin have opposite effect on skin cells: potential implication of the AHR pathway modulation.
Front. Immunol. 14:1098160.
doi: 10.3389/fimmu.2023.1098160

Staphylococcus epidermidis isolates from atopic or healthy skin have opposite effect on skin cells: potential implication of the AHR pathway modulation

Leslie Landemaine[1,2], Gregory Da Costa[1,3], Elsa Fissier[1,3], Carine Francis[2], Stanislas Morand[2], Jonathan Verbeke[4], Marie-Laure Michel[1,3], Romain Briandet[1], Harry Sokol[3,5], Audrey Gueniche[6], Dominique Bernard[2], Jean-Marc Chatel[1,3], Luc Aguilar[2], Philippe Langella[1,3], Cecile Clavaud[2*†] and Mathias L. Richard[1,3*†]

[1]Université Paris-Saclay, INRAE, AgroParisTech, Micalis Institute, Jouy-en-Josas, France, [2]L'Oréal Research and Innovation, Aulnay-sous-Bois, France, [3]Paris Center for Microbiome Medicine (PaCeMM), Fédération Hospitalo-Universitaire, Paris, France, [4]iMEAN, Toulouse, France, [5]Sorbonne Université, INSERM UMRS-938, Centre de Recherche Saint-Antoine, Assistance Publique - Hôpitaux de Paris (AP-HP), Paris, France, [6]L'Oréal Research and Innovation, Chevilly-Larue, France

Introduction: *Staphylococcus epidermidis* is a commensal bacterium ubiquitously present on human skin. This species is considered as a key member of the healthy skin microbiota, involved in the defense against pathogens, modulating the immune system, and involved in wound repair. Simultaneously, *S. epidermidis* is the second cause of nosocomial infections and an overgrowth of *S. epidermidis* has been described in skin disorders such as atopic dermatitis. Diverse isolates of *S. epidermidis* co-exist on the skin. Elucidating the genetic and phenotypic specificities of these species in skin health and disease is key to better understand their role in various skin conditions. Additionally, the exact mechanisms by which commensals interact with host cells is partially understood. We hypothesized that *S. epidermidis* isolates identified from different skin origins could play distinct roles on skin differentiation and that these effects could be mediated by the aryl hydrocarbon receptor (AhR) pathway.

Methods: For this purpose, a library of 12 strains originated from healthy skin (non-hyperseborrheic (NH) and hyperseborrheic (H) skin types) and disease skin (atopic (AD) skin type) was characterized at the genomic and phenotypic levels.

Results and discussion: Here we showed that strains from atopic lesional skin alter the epidermis structure of a 3D reconstructed skin model whereas strains from NH healthy skin do not. All strains from NH healthy skin induced AhR/OVOL1 path and produced high quantities of indole metabolites in co-culture with NHEK; especially indole-3-aldehyde (IAld) and indole-3-lactic acid (ILA); while AD strains did not induce AhR/OVOL1 path but its inhibitor STAT6 and produced the lowest levels of indoles as compared to the other strains. As a

consequence, strains from AD skin altered the differentiation markers FLG and DSG1. The results presented here, on a library of 12 strains, showed that *S. epidermidis* originated from NH healthy skin and atopic skin have opposite effects on the epidermal cohesion and structure and that these differences could be linked to their capacity to produce metabolites, which in turn could activate AHR pathway. Our results on a specific library of strains provide new insights into how *S. epidermidis* may interact with the skin to promote health or disease.

KEYWORDS

***S. epidermidis*, aryl hydrocarbon receptor, indoles, inflammation, biofilms, proteases, skin microbiome, skin type**

1 Background

Staphylococcus epidermidis is a coagulase negative commensal bacterium ubiquitously present on human skin and mucous membranes (1, 2). It is the most commonly cultured bacteria in clinical microbiology laboratories and of almost all body sites of healthy individuals (3, 4). *S. epidermidis* presents opposite roles. Its ability to form biofilms on medical devices when implanted and its antibiotic resistance places *S. epidermidis* as the second cause of nosocomial infections (5, 6). On the skin an overgrowth of *S. epidermidis* has been correlated to the severity of dermatological disorders such as atopic dermatitis (AD) (7), Netherton syndrome (NS) (8) and scalp seborrheic dermatitis/dandruff (9, 10). In particular, the pathogenicity of *S. epidermidis* strains from AD lesional skin has been related to the expression of an exocellular protease EcpA under the control of the regulator Agr, a pathogenic trait shared with its related species *Staphylococcus aureus* (11). Simultaneously, *S. epidermidis* is considered as a key member of the healthy skin microbiota. Recent studies have shown its role in the maintenance of an effective skin barrier *in vitro* (12, 13), in the wound healing (14), protection against the colonization by skin pathogens (15–17) and modulation of the immune system (18–20). Recent developments in the field have provided insights into how *S. epidermidis* strains have benefits for the skin. Specifically, particular commensal strains of *S. epidermidis* can produce the exocellular serine protease (Esp) which inhibits *S. aureus* biofilm formation (19); lantibiotics like epidermin and Pep-S which inhibit the growth of *S. aureus* (20) and 6-N-hydroxyaminopurine (6-HAP) which has an anti-proliferative activity against cancer cells and could protect against skin cancer (21).

While the hypothesis has been proposed of a shift in the behavior of *S. epidermidis* from a commensal to a pathogenic bacterium (21), in last years, a new model showing the diversity of strains has been proposed based on large scale comparative genomics studies comparing healthy and infectious strains (22–24). On the skin, genetically diverse strains of *S. epidermidis* co-exist (22). First report on the genetic difference between *S. epidermidis* isolated from healthy and acne skin identified various functions including biofilm formation and antimicrobials production, suggesting isolates specific effects (25). In the case of AD, *S. epidermidis* isolates have shown phenotypic specificities in terms of antimicrobial and protease activities compared to healthy skin isolates. However, the functional study of *S. epidermidis* isolates from pathological and healthy skin remains limited to particular cases and on a limited number of isolates (11, 20, 25). Moreover, in healthy skin, the exact mechanisms by which commensals *S. epidermidis* interact with host cells and specific receptors remain poorly understood and is likely to be multifaceted.

Two main skin receptors to *S. epidermidis* have been reported to date, with limited information on the molecular effectors involved (26). The immune modulatory molecules such as lipoteichoic acid (LTA), cell wall polysaccharides, peptidoglycan and aldehyde dipeptides constituent or produced by *S. epidermidis* can be sensed by TLRs receptors contributing to the relationship between the bacteria and keratinocyte. For example, a *S. epidermidis* LTA suppresses inflammation by binding to TLR2, limiting tissue damage in mice and promoting wound healing (27). A small molecule of <10 kDa secreted from *S. epidermidis* increases the expression of antimicrobial peptides (in particular β-defensins) through TLR2 signaling (15). *S. epidermidis*-conditioned media could even sensitize human keratinocytes toward *S. aureus* and amplifies the innate immune response against *S. aureus* (28). A second pathway reported to be involved in mediating epidermal response upon *S. epidermidis* stimulation is the aryl hydrocarbon receptor (AHR) (29). *S. epidermidis* could even activate AHR by secreted molecules <2kDa. AHR is a receptor to environmental pollutants including polycyclic aromatic hydrocarbons, tryptophan derivatives such as the photoproduct 6-formylindolo[3,2-b] carbazole (FICZ), the microbial metabolite Indole-3-Aldehyde (IAld); and xenobiotics (30, 31). Whereas AHR has been involved in various skin disorders such as accelerated aging, skin carcinogenesis and inflammation (30–33) AHR is also essential for skin barrier integrity (34) and its activation has been reported to improve the skin barrier in atopic dermatitis (35). Moreover, Uberoi et al. showed that commensal bacteria isolated from human skin can restore skin barrier function via AHR activation

in a mouse model (36). Thus, while TLR2 pathway is associated to the skin innate immune response in general, AHR seems to be more related to skin barrier integrity. Considering the diversity of strains on the skin, it raises questions about the effect of *S. epidermidis* strains from different skin origins on this pathway, and how such strains may affect skin barrier components.

Our aim in this study was to determine if the phenotypic characteristics of the *S. epidermidis* strains isolated from skin was correlated to the type of the skin, healthy or atopic. A large phenotypic characterization was conducted to answer this question and showed: (i) that skin origin can be correlated to a specific phenotype of the *S. epidermidis* isolates; (ii) that the AHR pathway might be responsible for part of the differences in behavior observed; and (iii) it also showed that the AHR ligands production from these strains was strongly influenced by the environmental conditions, especially by the interaction with skin cells.

2 Methods

2.1 Bacterial strains: subjects skin type and sample collection

S. epidermidis isolates used in this study were isolated from skin swabs from individuals belonging to two different cohorts. The studies protocols complied with the World Medical Association Declaration of Helsinki, national and EU regulations and L'Oréal Research and Innovation's procedures based on ICH guidelines for Good Clinical Practice. All volunteers received verbal and written information concerning the study in accordance with the applicable local regulations, guidelines and the current SOP. The volunteer's written informed consent to participate in the study was obtained prior to any study related procedure being carried out. All data was analyzed anonymously and steps were taken to protect the identities of all participants.

The first cohort (ARC/COPEG/1125; 2013, France) involved 31 healthy women (18 to 45 years old) with different sebum levels on forehead. The non hyperseborrheic (NH) and hyperseborrheic (H) skin status have been determined by measuring the sebum level with Sebumeter (SM810 Courage & Khazaka, Cologne, Germany) by following manufacturer's instruction on the middle of one half-forehead; sebum levels ranging from 80 - 120 µg/cm² and greater than 150 µg/cm², were assigned to the NH and H status respectively.

Participants were asked to wash their face with the provided neutral soap without anti-bacterial compounds for 3 days (once per day) prior to sampling. Last shampoo and soap were applied 48 and 24 h respectively before sampling. No other products were allowed on the face until sampling was performed.

Participants did not have acute cutaneous disorders, did not receive antibiotics nor had used topical treatments (including anti-acne and anti-seborrhea treatments) or exfoliating products 1 month prior to sampling, or had intense UV-exposure 3 weeks before the study starts.

The sampling for bacterial isolation was conducted as described earlier (37, 38) in a climate-controlled room (22 °C; 60% humidity). The samples were collected by using sterile cotton-tipped swabs pre-moistened with ST solution (0.15 M NaCl with 0.1% Tween 20). Swabs were rubbed firmly on the forehead for 60 sec to cover a surface area of 2 cm². After sampling, each cotton swab was placed into ST solution, vortexed and the suspension were plated on TSA (Tryptic Soy agar) medium to provide the isolates clones.

The second cohort [2012, France (39)] involved patients with moderate atopic dermatitis (AD) (3 to 39 years old). Disease severity was clinically assessed by the dermatologist using the SCORAD (SCORing Atopic Dermatitis) index and clinical signs of erythema, dryness, desquamation at one or more typical lesional (affected) skin areas and a close non-lesional (unaffected) area. Individuals presenting a SCORAD between 25 and 40 were included in the study. Skin microbiome samples were collected using sterile cotton-tipped swabs pre-moistened as described above at the inclusion visit, prior to any treatment, on adult patients. Sampling was conducted in lesional and the closest non-lesional skin sites of 1 cm^2 by rubbing firmly for 20 sec. over a 1cm^2 areas as previously reported. Individual bacteria were isolated from the swabs after plating on TSA medium, identified by 16S rRNA gene amplicon sequencing and stored at -80°C.

In the present study, we have included 12 isolates (Table 1) and one public strain ATCC 12228. Eight isolates were originated from healthy subjects, with either H (n=4) or NH (n=3); and one additional bacteria isolated from axillary sweat of a healthy subject to reinforce our conclusion with another healthy skin site. Four isolates were originated from 4 different AD patients, which were sampled in either lesional (n=3) or non lesional (n=1) area.

2.2 Bacterial genome sequencing

High molecular weight genomic DNA was extracted from an overnight culture grown in Trytic Soy Broth at 37°C using the Nucleospin tissue kit (Macherey-Nagel). Genomic DNA sequencing was performed on a HiSeq 2500 system (Illumina, 2-kb Nextera XT library, 2x100b paired-end). Short-reads raw data quality was analyzed with FastQC v0.11.8 (40) and reads cleaned with cutadapt v1.18 (41) and Prinseq v0.20.4 (42) in order to remove adapters in 3' of the sequences the first 15 bases of each read; reads with low quality bases (phred score < 30) at the end of the reads; reads with undetermined nucleotides and sequences whose mean phred score was less than 30. The genomic DNA was also sequenced on a MinION system (Oxford Nanopore Technologies, R9.4.1 flowcell, Rapid Sequencing SQK-RAD004 library, basecalling with Guppy v4.2.2 in 450bps_fast configuration). A hybrid *de novo* reads assembly approach was used as previously described (43). Read remapping rate was verified using Bowtie v2.3.4.3 (44) by calculating the Reads Mapped Back to Contigs (RMBC) index. Each assembly was annotated using PROKKA v1.13.3 (45). The annotated sequences and raw reads were deposited in the NCBI and SRA databases under the accession numbers listed in Supplementary Table T1.

2.3 Comparative genome analysis

The core genome was generated following the method described by Christensen et al. (23). Briefly, the ATCC 12228 reference *S. epidermidis* genome was split into 200b non-overlapping fragments

TABLE 1 Bacterial isolates used in this study.

Skin type	Isolate Name	Sampling area		Cohort
NC	ATCC 12228	NC	NC	(Winslow and Winslow 1908)
Hyperseborrheic	R10C	forehead	Healthy	ARC/COPEG/1125
	11H	forehead	Healthy	ARC/COPEG/1125
	50D	forehead	Healthy	ARC/COPEG/1125
	492 (PH1-28)	forehead	Healthy	ARC/COPEG/1125
Atopic	44	buttock	Atopic (lesion)	Flores et al, 2014
	45A5	left leg	Atopic (lesion)	Flores et al., 2014
	45A6	right arm	Atopic (lesion)	Flores et al., 2014
	48	knee	Atopic (non-lesional)	Flores et al., 2014
Non- hyperseborrheic	52B	forehead	Healthy	ARC/COPEG/1125
	1190	forehead	Healthy	ARC/COPEG/1125
	1191	forehead	Healthy	ARC/COPEG/1125
	45	Right arm	Healthy (sweat)	ARC/COPEG/1125

NC, Strain isolated on skin but body site has not been communicated by ATCC.

and used as Blast query on the 11 *S. epidermidis* genomes sequenced in this study. Each common hit was kept and aligned with MUSCLE v3.8.31 (46) in order to obtain gapped multiple alignments. All the gapped alignments were then concatenated to generate each isolate core genome. Another comparative method used the FastANI v1.31 (47) by calculating the Average Nucleotide Index for each genome pair. Either the core genomes alignment or the ANI distance matrix were used to generate phylogenic trees with FastTree v2.1.11 (48). Phage sequences were identified from the genomes using PHASTER (49). Accumulation-associated protein (*aap*) sequence search was conducted using a Blast query with the 492 isolate *aap* gene (REF). Antimicrobial resistance (ABR) genes were identified using Abricate v1.0.1 tool (50). Default parameters were used for all software unless otherwise specified.

Genome sequences from 811 *S. epidermidis* strains were available from Larson et al. (51). Genomes from each strain described in this study have been sequenced and phylogenic trees were generated using PhyloMEAN by iMEAN, based on phylonium (52) and PHYLIP (53) with default parameters. Isolates described in this study were assigned into the primarily described clades (51) based on their primary branch from an unrooted tree. The cladogram was visualized with Dendroscope (54, 55). Blast analyses were performed on each genome to identify presence of genes implicated in indole metabolites biosynthesis pathway (see Supplementary Table T7).

2.4 Biofilms analysis

Biofilm analysis was conducted as described earlier (56, 57). Briefly, bacteria were pre-cultured in TSB 3% w/v overnight at 37°C, 170 RPM. 200 µL of each bacteria was deposited at OD=1 (optical density) in duplicate on 96 well plates of black polystyrene with transparent bottom (µClear Greiner Bio-one, France) according to Christensen et al. (58), incubated 1 hour at 37°C aerobically. Then medium was refreshed in order to remove non-adherent microorganisms, and plates were further incubated for 3 days at 37°C, the medium was refreshed every day. Negative controls, comprising wells containing 200 µL of TSB without microbial suspension, were also prepared under the same conditions. At the end of the incubation period, the microorganisms were stained by SYTO^{TM}9 (Invitrogen) (diluted 1:350 in TSB from a stock solution at 5 mM in DMSO), a green fluorescent nucleic acid stain that is permeant to bacteria cell membrane, for 45 min at room temperature in the dark. Biofilms were defined as the presence of adherent and cohesive bacteria in the plate after 5 washes. Stained biofilms were examined at the MIMA2 imaging platform with a confocal laser microscope (Leica model HCS SP8; Leica Microsystems CMS GmbH, Mannheim, Germany) using a 40× objective (HC PL FLUOTAR). In order to minimize the air contact and maintain constant sample moisture condition, a coverslip was used on the specimen. A 488 nm argon laser was used to excite SYTO^{TM}9, and the emitted green fluorescence was collected in the range 500 to 540 nm using a hybrid detector. 512x512 pixels images from four randomly selected areas of raw biofilms, and two after five manual successive washes with sterile water, were acquired for each well. For each of them, sequential optical sections of 1 µm were collected along the z axis over the complete thickness of the sample to be subsequently analyzed. Biofilm biovolume (in µm^3) was extracted from image series using the Fiji software (Fiji, ImageJ, Wayne Rasband National Institutes of Health) and rendered into 3D mode using Imaris software (Bitplane AG).

2.5 Proteases activity assay

The protease activity assays were performed by using the EnzChek Elastase Assay Kit and EnzChek Gelatinase/Collagenase

Assay Kit (Thermo Fisher Scientific) according to the manufacturer's instructions. Briefly, 10 µL of each bacterial supernatant (12 *S. epidermidis* (Table 1) and ATCC 12228) cultivated in 2 mL medium for 24h at 37°C, were incubated with 1 µg of DQelastin or DQgelatin (Thermo Fisher Scientific) diluted in the supplied reaction buffer (qsp 200 µL) in 96-well black plates (Corning, NY) for 20 hours. Relative fluorescent intensity was analyzed with a Fluorometer Infinite® M200 PRO (Tecan system; excitation wavelength, 485 nm; emission wavelength, 538 nm).

2.6 Keratinocytes culture and treatments

Normal neonatal human primary epidermal keratinocytes (NHEKs) (CellnTec) were cultured in CnT-57 supplemented medium (CellnTec) containing bovine pituitary extract (BPE) at 37°C and 5% CO_2. NHEKs were used only for experiments between passages 3 to 5. NHEKs were seeded at 10,000 cells/well in 12 wells plates and then grown to about 80% confluency in keratinocyte-SFM (Gibco, Life Tech. Corp., Grand Island, USA) supplemented with EGF 0,035 µg/µL and BPE 12,4 mg/mL (Gibco) 24 hours before treatments. For bacterial supernatant treatments, NHEKs were treated for 14h with sterile-filtered bacterial supernatant at 50% (vol) (prepared in KSFM medium for 14 hours) and then harvested for RNA extraction. For the treatment with live bacteria, *S. epidermidis* were pre-cultured in keratinocytes culture medium (KSFM) overnight until exponential phase. Bacterial suspensions concentrations were then adjusted to 10^8 CFU/mL (corresponding to Optical Density = 0.18) by adding KSFM and added to the NHEKs at a MOI = 10:1. After 14h of this co-culture, at 37°C and 5% CO_2 conditioned media (supernatants) were collected and analyzed for IL-8 quantification (IL-8 DuoSet ELISA, R&D systems), cytotoxicity assay (CyQuant™ LDH cytotoxicity assay, Thermo Fisher) following manufacturer's instruction, while NHEK cells were harvested for RNA extraction for quantitative real-time PCR (qRT-PCR) assays.

2.7 3D skin treatments

The human skin equivalent model (HSE) LabSkin (Innovenn, York, UK) (full thickness human skin equivalent incorporating fully-differentiated dermal and epidermal components), are received at day 13 after air-liquid interface exposure and placed in deep wells plates with the medium provided by the manufacturer, overnight at 37°C, 5% CO_2. HSEs were then treated with 20 µl of a suspension containing 10^3 UFC of a single *S. epidermidis* isolate [*S. epidermidis* ATCC 12228, or clinical isolates from NH (BC1191, 52B), H (50D) or AD skin (45A6, 44)]. Each strain was pre-cultured in TSB 3% and then resuspended in LabSkin medium before topical application using a sterile loop as described previously (59). Application of 20 µL sterile Labskin medium was inoculated as control. HSEs were then incubated at 37°C, 5% CO_2 for 2, 5 and 7 days. Medium was refreshed every 2 days. At day 5 and 7, skin conditioned media were collected and submitted to IL-8 quantification, and HSEs were cut in half for quantitative real-time PCR assay and histology analysis (hematoxylin eosin safran HES staining).

2.8 Quantitative RT-qPCR

Total RNA was extracted from keratinocytes by using the RNeasy Micro kit (Qiagen, Hilden, Germany) according to the manufacturer's protocol with an additional DNAse treatment (Rnase-Free Dnase Set, Qiagen). RNA concentration was determined using a Nanodrop™ (Nanodrop 1000, Thermo Scientific). iScript cDNA Synthesis (Biorad) was used to synthesize cDNA. mRNA levels were measured with the StepOnePlus™ Real-Time PCR System (Applied Biosystems™) and SYBR Green Master Mix (Biorad). Quantitative PCR (qPCR) data were analyzed using the $2^{-\Delta\Delta Ct}$ quantification method with GAPDH (glyceraldehyde-3-phosphate deshydrogenase) for eukaryotes cells and GyrB (DNA gyrase subunit B) for *Staphylococcus* as the endogenous control. Primers for FLG, IVL, KLK7, DSG1, CDSN, Ki67, DEFB4, STAT6, OVOL1, OVOL2 were provided by Biorad, the other primers sequences are shown in Table 2.

2.9 Metabolites quantification

Internal standards were purchased from Santa Cruz Biotechnology (5-Hydroxyindole acetic acid-d5, Serotonin-d4, Indole-3-acetic acid-d4, Kynurenic acid-d5, Melatonin-d4, Piconilic acid-d3, Tryptamine-d4, and Xanthurenic acid-d4) and Toronto Research Chemicals (3-Hydroxyanthranilic acid-d4, 3-Hydroxykynurenine-13C2–15N, 5-Hydroxytryptophan-d4, Indole-3-acetamide-d5, Kynurenine-d4, and Tryptophan-d5). Stock solutions of labeled analytes were prepared in water with 0.1% of formic acid and final concentrations have been chosen to match estimated endogenous metabolites concentrations. Metabolites were extracted from 50 µL of bacteria supernatant or co-culture medium. After addition of the internal standards (100 µL) and 300 µL of MeOH, the samples were vortexed for 15 s and homogenized at -20°C, for 30 min. After centrifugation at 5 000

TABLE 2 qPCR primers used in this study.

Gene target	Forward primer 5'-3'	Reverse primer 5'-3'	Reference
CYP1A1	CAG CTC AGC TCA GTA CCT CA	CTT GAG GCC CTG ATT ACC CA	This study
EcpA *Se*	TGT GCT TAA AAC GCC ACG TA	GTA TAG CCG GCA CAC CAA CT	Cau, 2020 (11)
GyrB *Se*	GTT GTA ATT GAG AAA GAC AAT TG	TAC AGT TAA GAT AAC TTC GAC AG	This study

rpm 10 min at -4°C, 350 µL of supernatant were collected and concentrated under N2 flux. The residues were reconstituted in 100 µL of MeOH/H2O (1:9) and transferred to a 96-well plate for LC-HRMS analysis. Analyses were performed as described previously (60) with some adaptations. Briefly, 2 µL were injected into the LC-MS (XEVO-TQ-XS, Waters®). A Kinetex C18 xb column (1.7 µm x 150 mmx 2.1 mm, temperature 55°C) associated with a gradient of two mobile phases (Phase A: Water + 0.5% formic acid; Phase B: MeOH + 0.5% formic acid) at a flow rate of 0.4 mL/min were used. The solvent gradient, the parameters of the Unispray® ion source along with the parameters for fragmentation and analysis of the metabolites and internal standards are given in supplementary data (Supplementary Table T8 and Supplementary File_F1). For each metabolite, a calibration curve was created by calculating the intensity ratio obtained between the metabolite and its internal standard. These calibration curves were then used to determine the concentrations of each metabolite in samples (61).

2.10 Statistical analysis

All experiments were performed with at least three biological replicates. GraphPad Prism version 7 (San Diego, CA, USA) was used for all analyses and preparation of graphs. For all data displayed in graphs, the results are expressed as the mean ± SEM. The D'Agostino and Pearson test of normality was applied to all data sets, and in cases where the data did not demonstrate a normal distribution, non-parametric tests were used to analyze statistical differences. For comparisons between two groups, Student's t test for unpaired data or non-parametric Mann–Whitney test was used. For comparisons between more than two groups, one-way analysis of variance (ANOVA) and *post hoc* Tukey test or nonparametric Kruskal–Wallis test followed by a *post hoc* Dunn's test was used. For all statistical tests, differences with a p value less than 0.05 were considered statistically significant: *p <0.05, **p <0.01, ***p<0.005, ****p<0.001.

3 Results

3.1 Genome sequence comparisons show cluster of strains isolated from atopic skin

Twelve *S. epidermidis* were isolated from different subjects depending on the skin type and the disease status (Table 1). As it is reported that *S. epidermidis* subtypes differ significantly between skin microenvironment (moist, sebaceous, dry), we selected healthy skin isolates from two skin types: NH and H (1). Three groups were created: healthy skin comprising NH and H skin isolates and AD skin isolates. For comparison the reference strain ATCC 12228, not associated with any type of skin, was used as control strain. The genome sequencing of 11 isolates was completed with Illumina and Nanopore technology, a long read sequencing to improve the genome quality. The sequences were assembled using SPAdes algorithm and automatically annotated using Prokka algorithm. Genome sizes were oscillating between 2,300,583 bp and 2,598,183 bp with a GC content between 31.97% and 32.05% (Supplementary Table T1). Two global genomic comparisons were carried out using these assembled genomes, one based on the core genomes alignment as described by Christensen et al. (25), the other based on whole genome sequences using the FastANI algorithm. Using both methods we confirmed that all isolates were *S. epidermidis*.

Observation of the phylogenic trees obtained by both methods revealed that the S. epidermidis bacteria isolated from atopic skin were clustering genetically, while others from the two others types of skin were not (Figure 1 and Supplementary Figure S1). Interestingly, the isolate 48 isolated from a non-lesional skin of a subject with atopic dermatitis was genetically different from the AD cluster, using both methods. These data suggest that even if all isolates are *S. epidermidis*, those from atopic skin might have genetic differences.

We then inspected characteristics of *S. epidermidis* genomes associated with their genetic diversity on skin and differentially observed on body sites (24). PHASTER analysis revealed the presence of intact StB20-like prophage in 7 genomes associated to the 3 skin types (NH n= 2; H n=3; AD n= 2) and StB12 prophage in 1 genome associated to AD lesion (Supplementary Table T2). Comparison of the 7 StB20-like phage sequences did not show major differences among their genomic structure (Supplementary Figure S2A). Search for antimicrobial resistance genes using Abricate v1.0.1 tool, showed differences in the gene patterns (Supplementary Table T3), for example isolates 45A5 (AD lesional), 48 (AD non lesional), 492 (H) and 52B (NH) did not carry the *blaZ* beta-lactamase gene present in the reference strain ATCC 12228 strain. However, the differences in antimicrobial resistance (*abr*) genes content did not match with the skin type. Finally, the presence of the accumulation-associated protein (Aap) CDS, coding for a megaprotein protein involved in skin corneocytes adhesion (62) and biofilm formation in commensal *S. epidermidis*

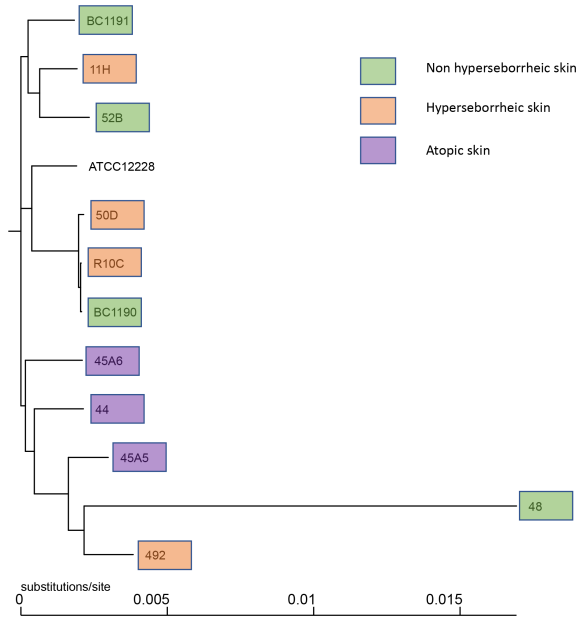

FIGURE 1
Phylogenetic tree of the 11 core genomes of *S. epidermidis* using strain core genome. The tree was generated using FastTree v2.1.11 (43).

strains (63), has been investigated. Additionally, a particular organization of this gene has been reported, regarding the absence of C-terminal collagen triple helix domain (43). Here we confirmed the presence of an Aap CDS in the majority of the genomes (9/11), and 8/9 aap CDS contained- a C-terminal collagen triple helix domain, independently of the skin type of origin (Supplementary Figure S2B). This first analysis suggests that genetic specificities of the strains from atopic skin are not related to the presence of prophage, *abr* genes or *aap* CDS.

3.2 *S. epidermidis* isolated from patients with atopic skin lesions form smaller biofilms

Biofilm formation is a unique feature developed by microorganisms that permits colonizing various types of biotic or abiotic niches and resists environmental factors allowing the persistence of microorganisms. Biofilm formation of *S. epidermidis* has been studied for many years due to various nosocomial infections caused by biofilm formation on indwelling devices (64, 65) even if not all isolates of *S. epidermidis* form a biofilm (66). There are controversial data concerning the capacity of the model strain *S. epidermidis* ATCC 12228 to form or not biofilms, since originally this strain was described as incapable of forming a biofilm (67). However, it seems from the literature that it depends on the growth conditions as several publications reported a biofilm formed by this strain (68–70).

To date a few reports have described the variation of biofilm formation among commensal *S. epidermidis* isolates (71). We characterized the biofilm phenotype of the 11 *S. epidermidis* isolates and ATCC 12228, using confocal laser scanning microscopy (CLSM) and image analysis of biofilms in 96 well plates. Confocal microscopic images showed that all tested isolates of *S. epidermidis* were able to form a biofilm in the conditions of our experiment (Figure 2A). The capacity of *S. epidermidis* ATCC 12228 strain to form a biofilm has been also verified on the 3D reconstructed skin LabSkin using scanning electron microscopy (Figure 2B).

Using confocal microscopy, the 3D structure of each biofilm formed in the 96 wells was reconstructed before and after five washes with sterile water, thus allowing to describe biofilm cohesion and resistance to mechanical shear stress (Figure 2A for images and Figure 2C for the associated biovolumes). Before wash, the biovolumes were homogenous (average range: 6 to 8.6 μm^3) for all the bacteria. The isolates from atopic skins origin were producing significantly less biofilms (p val = 0.0015) than the ones formed by bacteria from NH skins. The biovolume of the biofilm formed by the H strains and the ATCC 12228 were intermediate. After 5 washes, the cohesive behavior of each bacteria was different and was not related to the initial biovolume before wash. Three isolates (45, 52B from NH healthy skin and 45A5 from AD skin) formed particularly cohesive biofilms with high resistance to rinses compared to ATCC 12228, while other isolates were almost completely removed (biovolume < 1 μm^3 after rinses). Altogether these data suggest that the skin origin is associated with a different capacity to form a thick biofilm and isolates from atopic skin seem to have thinner biofilms. However, skins origin cannot help to predict the resistance of the biofilm.

3.3 Proteases activities of *S. epidermidis* isolates correlates with skin origin

The production of proteases by *S. epidermidis* has been recently highlighted as a potential virulence factor. More specifically EcpA, a cysteine protease, was shown to alter skin integrity, triggering inflammation and disrupting the skin physical barrier (8) (11). We first identified the presence of EcpA active domain sequence in the genomes of the isolates (Supplementary Figure S2C). Then we determined for each isolate the protease activity using collagenases and gelatinase *in vitro* assays. The average protease activity of the isolates pertaining to each of the three groups of bacteria (NH, H and AD) is presented (Figures 3A, B). As isolate 48, from a non lesional AD skin, showed low protease activities, it was included in the group of NH healthy strains. isolates from atopic lesional skins showed the highest protease activities. While isolates from healthy NH and H skins showed low gelatinase or elastase activity. Quantification of EcpA gene expression on all isolates co-cultured with keratinocytes were in accordance with the *in vitro* assays on protease activity. The level of EcpA expression in isolates from AD skins was significantly higher than the expression of EcpA in isolates from healthy NH and H skins (Figure 3C). Combination of *in vitro* assays and RT-qPCR showed that *S. epidermidis* isolates from atopic lesional skins had stronger protease activities compared to all other isolates tested and might have a higher potential to alter skin structure (11).

3.4 IL-8 secretion and tissue structure maintenance depend on the skin type origin of the bacteria

In order to characterize further the interactions of theses isolates with the skin, *S. epidermidis* isolates were co-cultured for 14 hours with primary normal human epidermal keratinocytes (NHEK) and the effect of these isolates on cell viability and inflammatory cytokine IL-8 were analyzed. Observation of the cytotoxic effect of the bacteria, on the NHEK, showed a significant difference in association with the isolates' origin. Bacteria isolated from NH healthy skins were significantly more cytotoxic than the ones isolated from H or AD skins (Figure 4A). For IL-8 production, co-culture with the bacteria isolated from NH skin leads to a significantly higher IL-8 release compared to the two others groups of isolates (Figure 4B), IL-6 and TNF-α were also quantified showing no significant modification between isolates but only a high level of TNF-α production in presence of the ATCC12228 strain (Supplementary Figure S3).

A test on reconstructed 3D skin model was then performed to characterize the effects on a skin tissue, using representative isolates of each group chosen based on their capacity to induce cytotoxicity and IL-8 production on NHEK: NH skin (1191, 52B), H skin (50D) and lesional AD skin (45A6, 44) as well as the reference strain

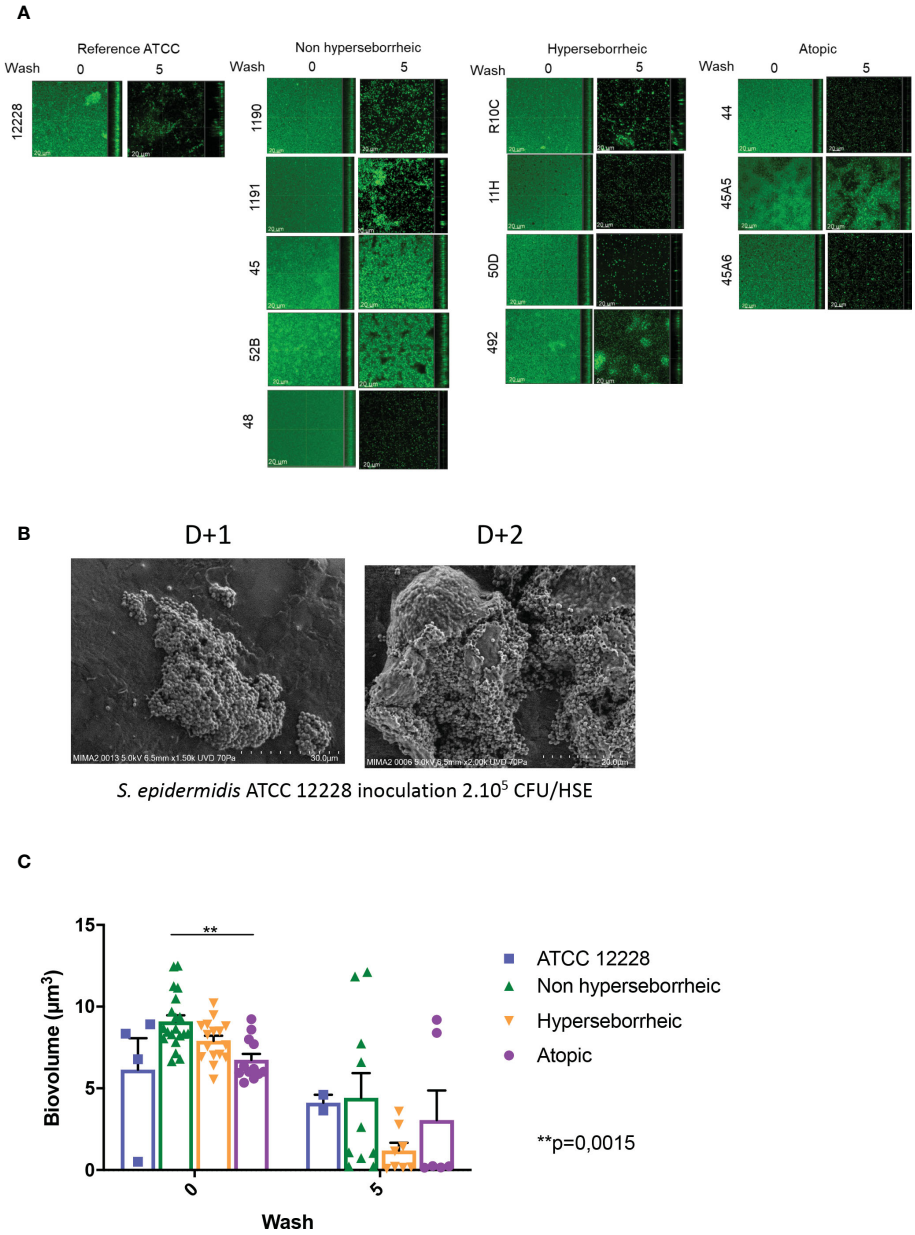

FIGURE 2
All *S. epidermidis* strains tested have the capacity to form biofilm. The biofilms formed on polystyrene were observed after 3 days of culture by confocal microscopy, before and after 5 washes **(A)** and their biovolumes were measured **(C)**. Moreover, the ATCC 12228 can form biofilm on 3D reconstructed skin 2 days after inoculation of 2.10^5 CFU/HSE **(B)**. For statistical comparisons, (*) indicates comparison of all versus all samples grouped by number of washes, $^{**}p < 0.01$.

ATCC 12228. Growth levels of the *S. epidermidis* bacteria on the model were quantified and presented similar ranges of CFU, except the reference strain that is slightly lower (Supplementary Figure S4). There was an increase in IL-8 secretion, from 5 days of colonization, with the clinical isolates; which was significantly higher than the reference strain ATCC 12228. Interestingly, the levels of IL-8 secretion measured were similar between the clinical isolates at each timepoint (Figure 4C). In contrast, histological observation of the colonized and non-colonized tissues showed remarkable differences between isolates (Figure 4D and Supplementary Figure S5). Specifically, colonization with isolates 45A6 and 44 from atopic lesional skin leads to a visible degradation of the viable epidermis and impacted the skin integrity, with the presence of bacteria in the dermal layer. Isolates from NH and H healthy skins had no visible impact on the epidermal morphology. It is important to note that these differences could not be linked to differences in growth levels on the model (Supplementary Figure S4). Altogether the data presented here showed distinct behavior of the *S. epidermidis* isolates depending on their skin origin and the type of the skin model. More particularly a higher cytotoxicity and IL-8 secretion were observed in the NHEK in co-culture with the bacteria isolated from NH skin, while they behave like the reference strain on the 3D differentiated model (Supplementary Figure S5). In contrast, bacteria isolated from AD lesional skin seemed to express

10.3389/fimmu.2023.1098160

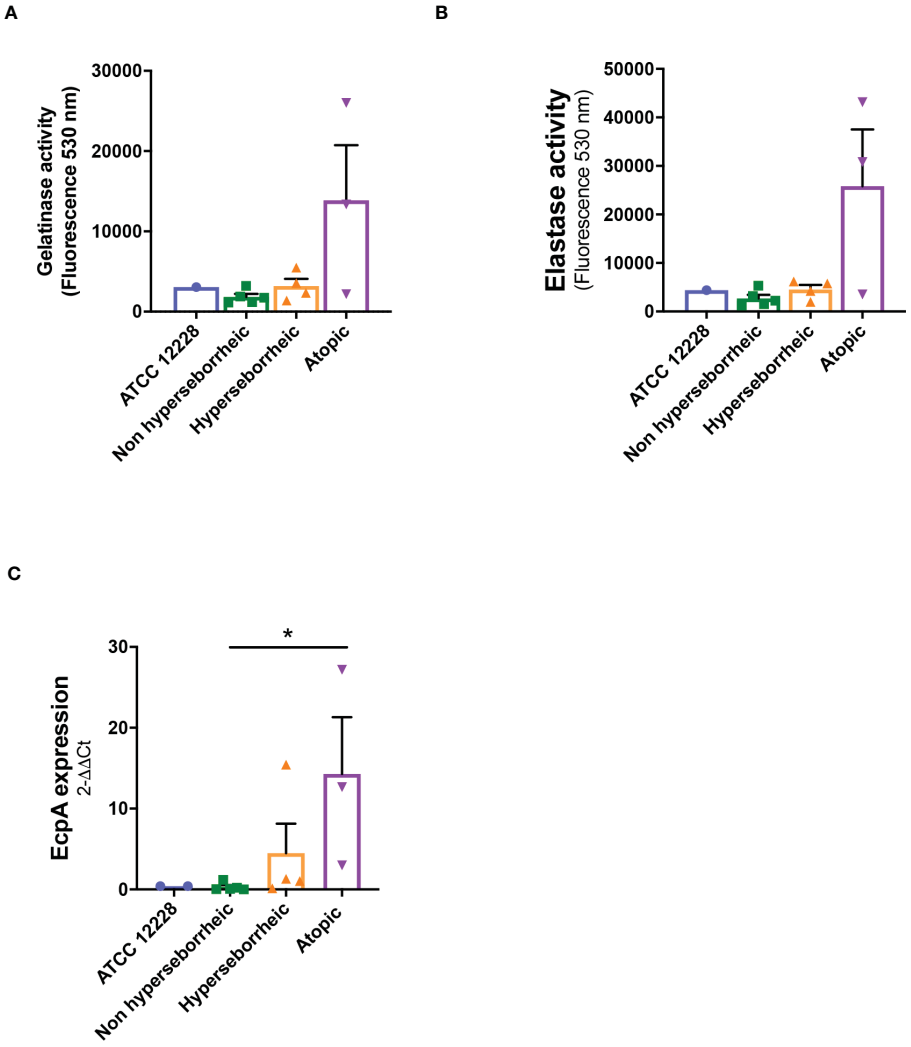

FIGURE 3
Live *S. epidermidis* from atopic skin can have a strong protease activity compared to strains from normal and hyperseborrheic skin. Average protease activity of the 3 groups of strains against gelatin-like **(A)** and elastase-like **(B)** measured in the supernatant of *S. epidermidis* cultured for 20h. **(C)** Average, for each skin type group, of the protease *EcpA* mRNA levels (normalized to *GyrB*) expressed after a co-culture of *S. epidermidis and* keratinocytes for 14h. For statistical comparisons, (*) indicates comparison of all versus all samples, *p <0.05.

pathogenic traits only on the more differentiated 3D model. As the reconstructed 3D model is more representative of the human skin as compared to NHK alone, we did not investigate further on the high cytotoxicity and IL-8 secretion in the 2D model.

3.5 Induction of AHR response pathway during interaction with *S. epidermidis* strains depends on the skin type origin of the bacteria

The AHR pathway has been described as implicated in several processes related to the skin immunomodulation and differentiation, through tryptophan derived ligands produced by UV light (FICZ) or microbial metabolism (indoles). Considering the potential of *S. epidermidis* to activate AHR, and the differential impact of the 12 isolates on skin cell cytotoxicity and inflammation, we investigated the effect of *S. epidermidis* isolates from different skin origins on this pathway. In order to follow *AHR* gene regulation in NHEK in co-culture with *S. epidermidis* strains, we quantified by qRT-PCR the expression of four genes: *CYP1A1, OVOL1, OVOL2* and *STAT6*. *CYP1A1* expression level is usually monitored to account for AHR induction in several cellular models. However, in keratinocytes other effectors are implicated like the couple OVOL1 and OVOL2; OVOL1 being linked to keratinocytes differentiation and OVOL2 keratinocytes proliferation, thus the balance between those two transcription factors may partially orient the cell maturation (72). STAT6, another transcription factor may be also involved in cell maturation through its inhibition of *OVOL1* expression (35).

Results showed that *CYP1A1* was slightly induced, although not significantly, with the bacteria isolated from NH skin and that bacteria from AD or H skins had no effect on *CYP1A1* expression (Figure 5A). For NH skin associated strains, *OVOL1* expression

10.3389/fimmu.2023.1098160

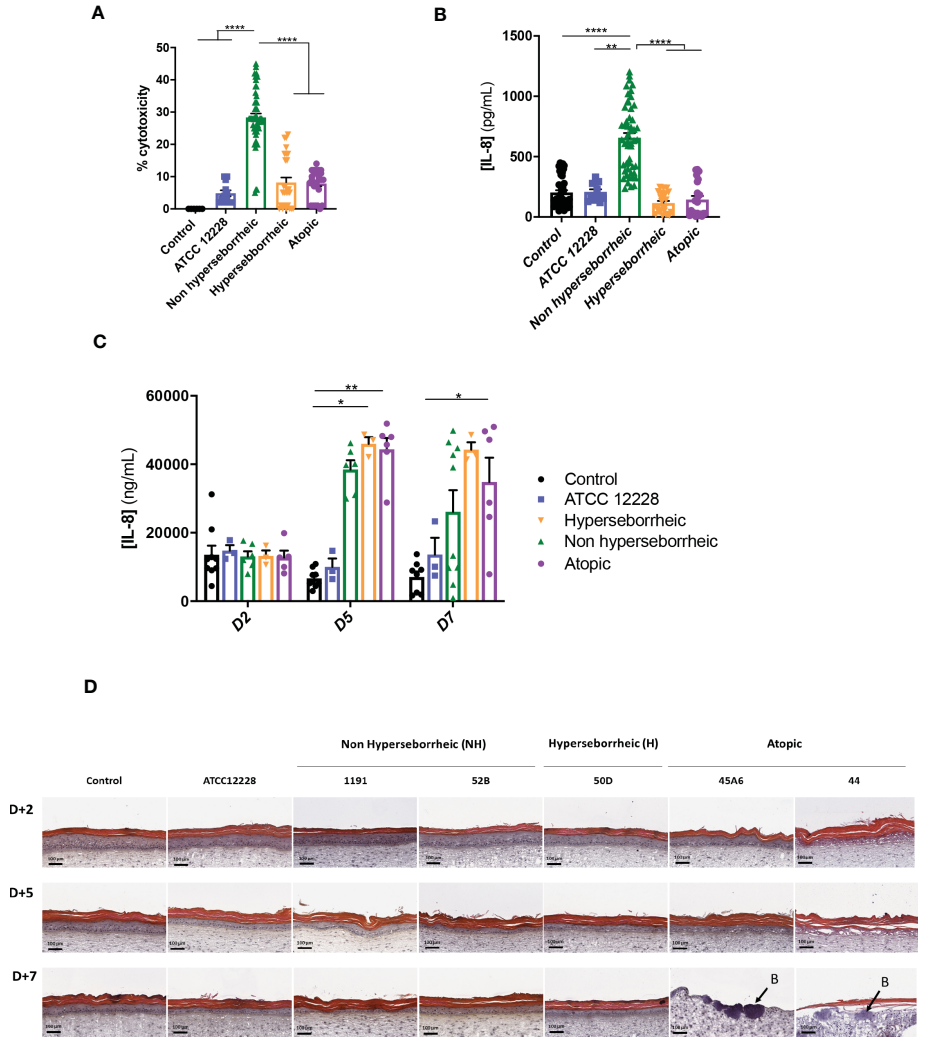

FIGURE 4
Live *S. epidermidis* effect on keratinocytes depends on skin type origin. **(A)** Average, for each skin type group of *S. epidermidis*, of the cytotoxicity and **(B)** IL-8 secretion in NHEK 2D co-culture and **(C)** IL-8 secretion in 3D reconstructed skin model after colonization. **(D)** HES images of tissues colonized with representative strains of the three skin types origins. Arrows indicate bacteria **(B)**. For statistical comparisons, (*) indicates comparison of all versus all samples, *p <0.05, **p<0.01, ****p<0.001.

followed the same pattern as *CYP1A1* as expected, knowing the regulation in the AHR but here the differences were statistically significant (Figure 5B). Isolates from H skin increased also significantly *OVOL1* expression. Interestingly, *STAT6* was inversely modulated compared to *CYP1A1* and *OVOL1* (Figure 5C) which follows the model of gene regulation described to date (35, 73). *OVOL2* expression was slightly decrease for all the bacteria (Supplementary Figure S6A). We also quantified filaggrin (*FLG*) expression, which is related to AHR/OVOL1 activation. Filaggrin is also a major protein involved in late differentiation of the epidermis (74). *FLG* expression levels obtained here did not allowed us to confirm a link with AHR pathway modulation for most of the *S. epidermidis* isolates tested. All the isolates maintained the same expression levels as the control (Figure 5D) except ATCC 12228 that showed a significant inhibition of *FLG* mRNA level. To address the skin integrity modifications observed in the 3D models, we also investigate Desmoglein 1 (*DSG1*) expression. Interestingly, *DSG1* expression followed the same pattern as *CYP1A1* (Figure 5E).

Following the expression of various effectors of the AHR regulation we showed a differential modulation of the AHR pathway depending on the skin origin of the *S. epidermidis* isolates. More particularly *S. epidermidis* bacteria isolated from NH healthy skin had an opposite effect on skin cell compared to those isolated from lesional AD skin, clear up-regulation of the AHR pathway in presence of isolates from NH healthy skin.

3.6 AHR ligands metabolites produced by *S. epidermidis* when interacting with NHEK

To better understand the interaction between *S. epidermidis* and AHR, we investigated the capacity of the 12 *S. epidermidis* isolates

10.3389/fimmu.2023.1098160

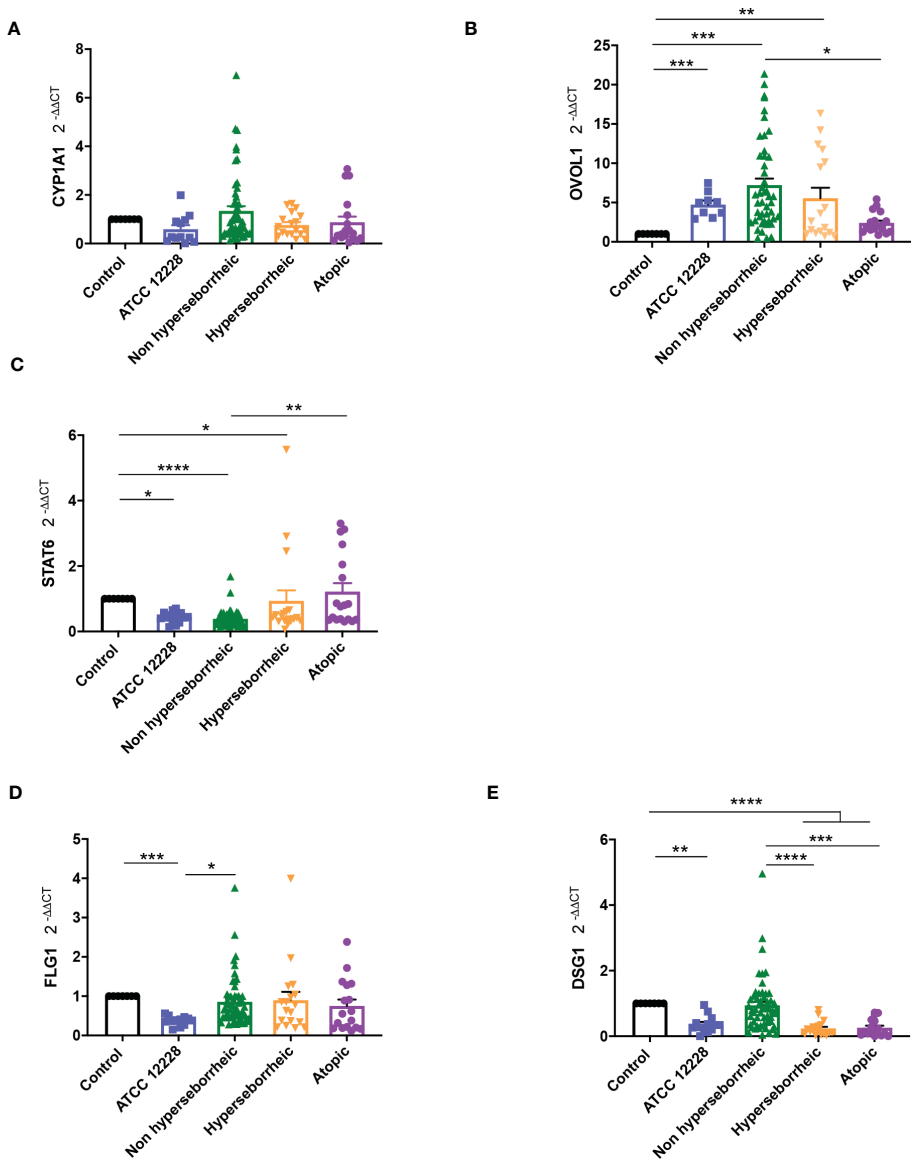

FIGURE 5
Live *S. epidermidis* can induce AhR pathway depending on skin type origin. Average of mRNA levels of AhR pathway genes CYP1A1 **(A)**, OVOL1 **(B)**, STAT6 **(C)** and average of mRNA levels of FLG1 **(D)** and DSG1 **(E)**, for each skin type group of *S. epidermidis*. For statistical comparisons, (*) indicates comparison of all versus all samples, *p <0.05, **p<0.01, ***p<0.005, ****p<0.001.

tryptophan derived metabolites. Moreover, a recent study demonstrated that AD patients have significantly lower level of indole-3-aldéhyde (IAld) than healthy subjects (31) on their skin. Tryptophan is the main precursor of AHR ligands produced by micro-organisms, allowing the biosynthesis of indoles ligands like indole-3-aldehyde (IAld), tryptamine, indole-3-lactic acid (ILA) or indole -3-acetic acid (IAA). In order to further understand the AHR regulation we analyzed the different AHR ligands produced by these bacteria cultivated alone or in co-culture with NHEK. We first quantified the total indoles produced by the bacteria cultivated in the same culture medium as for co-culture (KSFM) (Supplementary Table T4). This analysis showed that all *S. epidermidis* have the capacity to produce indoles and that isolates from atopic skins seemed to produce slightly lower quantities of indoles compared to the other two groups although the differences were not significant when looking at the sum of all indoles (tryptamine + IAld + ILA + IAA) (Figure 6A). Quantification of specific AHR ligands revealed that IAld and ILA, which is a precursor of IA, were following the same pattern as the total Indole with a lower production of these molecules in bacteria isolated from AD skins (Figures 6B, C). Higher levels of ligands (mainly IAld) were obtained with bacteria isolated from H skin. As *S. epidermidis* bacteria might not have the same metabolism when they are cultivated alone, or in co-culture with keratinocytes, we have quantified AHR ligands and precursors in the culture medium, after co-culture of *S. epidermidis* bacteria with NHEK (Supplementary Table T5). We observed again a lower production of indoles when we analyzed the supernatants of the co-culture of *S. epidermidis* bacteria isolated from AD skin with NHEK,

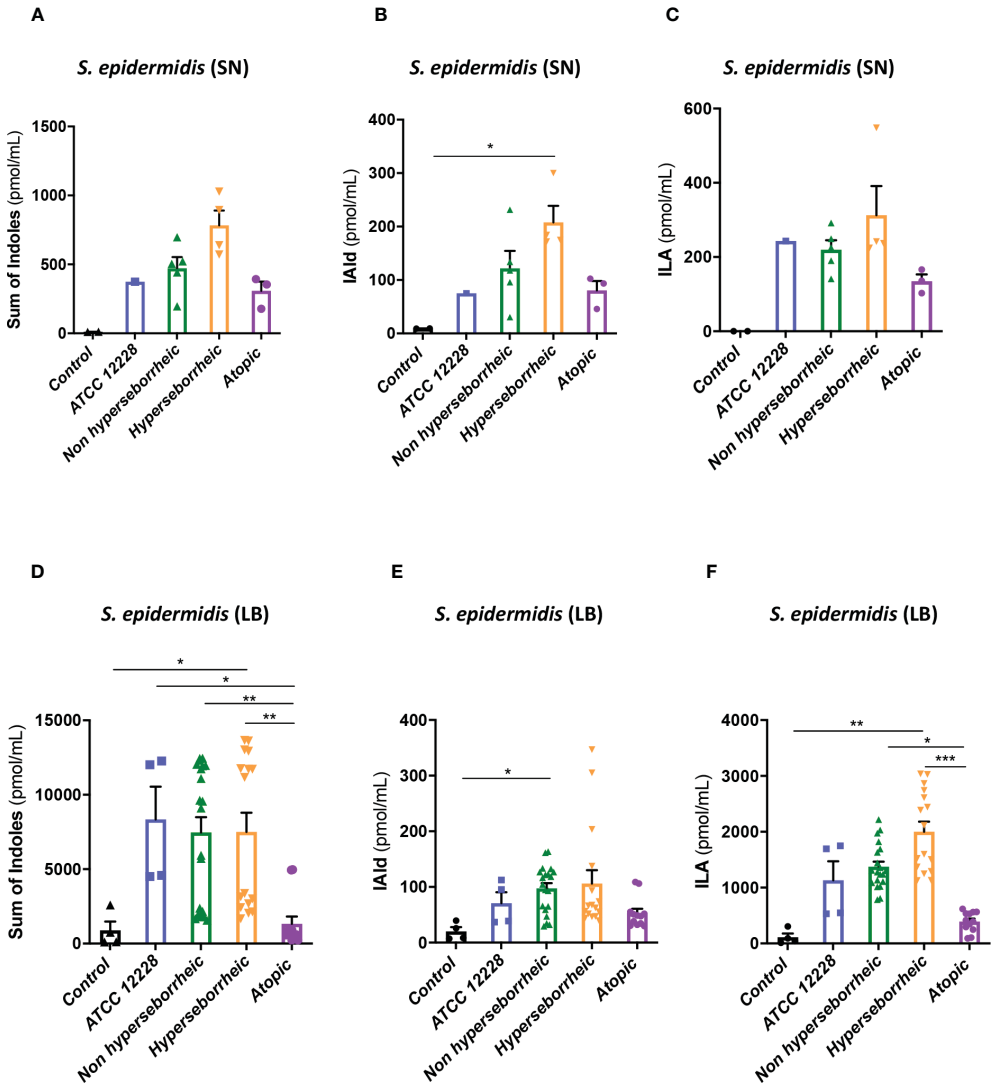

FIGURE 6
S. epidermidis produce indoles depending on skin type origin. **(A)** Sum of indoles (tryptamine + IAld + ILA + IAA) measured in the supernatant of *S. epidermidis* ATCC 12228, *S. epidermidis* from normal, hyperseborrheic or atopic skin type; quantification of Iald **(B)** and ILA **(C)** released in the culture medium. **(D)** Sum of indoles measured in the co-culture medium of NHEK and *S. epidermidis* ATCC 12228, *S. epidermidis* from normal, hyperseborrheic or atopic skin type; quantification of Iald **(E)** and ILA **(F)**. LB, Live bacteria; SN, supernatant. For statistical comparisons, (*) indicates comparison of all versus all samples, *p <0.05, **p<0.01, ***p<0.005.

as compared to the other two groups of isolates (Figures 6D–F). We explored the link between the differences in metabolites levels measured between the group of isolates, and the presence of predicted proteins in the indoles biosynthetic pathway of the *S. epidermidis* isolates (Figure 7A). Specifically, the enzyme Tdc (Aromatic-L-amino-acid decarboxylase; UNIPROT Q5HKV0) which converts tryptophan into tryptamine, a precursor of IA and IAld, is absent from the four genomes of AD isolates (lesional and non lesional), while this protein was predicted to be present in isolates from NH (52B, 1190) and H skin (R10C, 50D), supporting the lower levels of indoles quantified. Interestingly, kynurenine, a compound mainly produced by host cells through the IDO pathway, was significantly more produced when bacteria isolated from AD skin were incubated with NHEK, compared to other isolates (Figure 7B) while bacteria alone did not show differences on kynurenine production (Figure 7C).

In a tentative way of generalizing our results to more *S. epidermidis* isolates we used the public curated genomes sequences available in the literature in order to characterize them regarding the different genes implicated in the tryptophan metabolic pathways. 811 strains from the study by Zhou et al. were used as references: in their work Zhou and co-workers defined 10 clades using the genomes sequences. From these data, we constructed a heatmap of positive isolates in each clade for each gene implicated in indole metabolites biosynthesis pathway (Supplementary Figure 7A) and we rebuild a cladogram of these isolates to localize each of our isolates within these clades (Supplementary Figure 7B). From these data we were only able to

10.3389/fimmu.2023.1098160

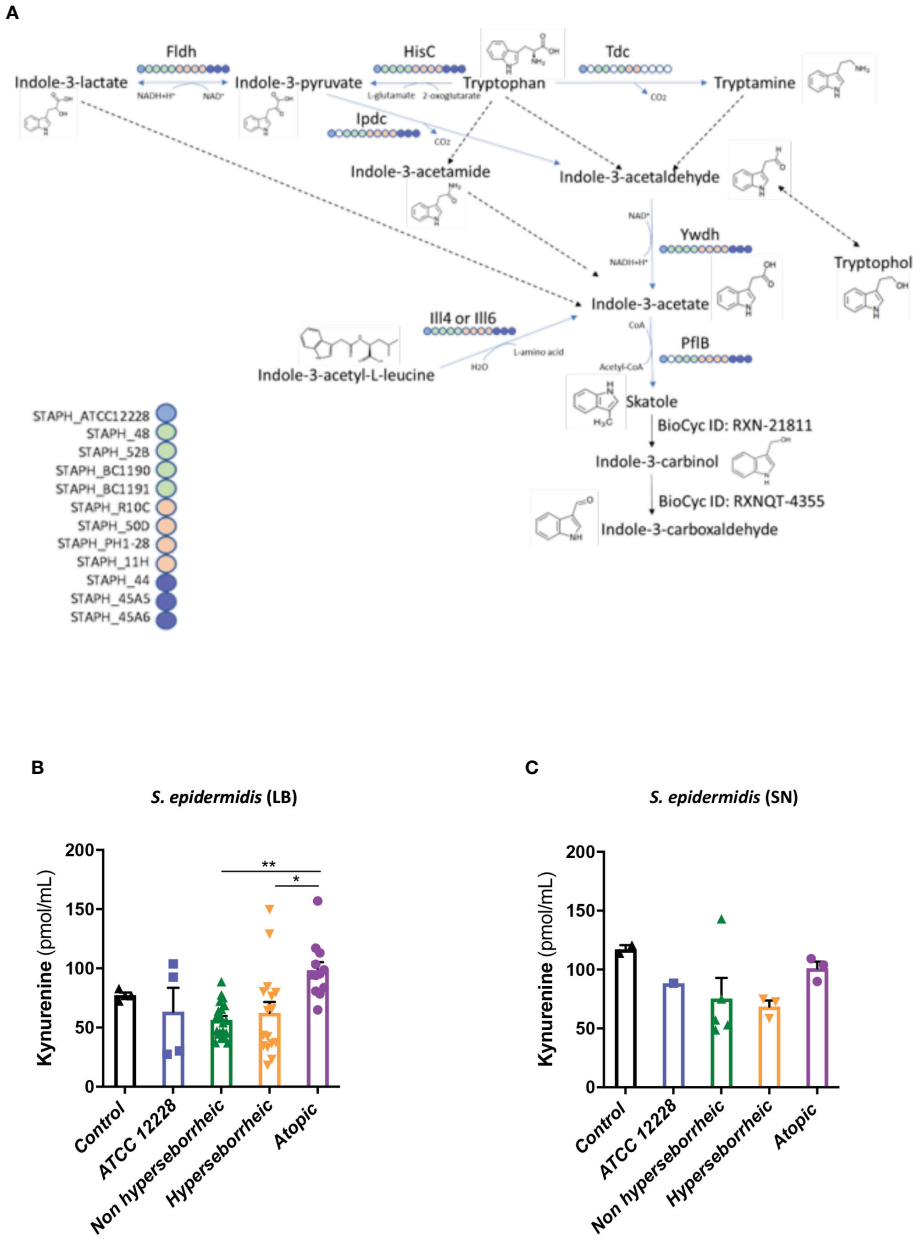

FIGURE 7
(A): Reconstruction of tryptophan metabolic pathway in the 11 *S. epidermidis and* ATCC 12228, based on the genome sequences. Circles represent each strains: light blue ATCC 12228; green: non hyperseborrheic skin; orange: hyperseborrheic skin; dark blue: AD strains. Open circle means that the protein is not found. IAA, Indole Acetic Acid; IA, Indole-3-acetate; IAld, Indole-3-aldehyde; ILA, Indole-3-Lactic Acid. **(B, C)** Kynurenine metabolite quantification in the 11 S. epidermidis and the reference strain ATCC 12228 culture supernatant, after NHEK treatments with either living bacteria (LB) or bacterial supernatant (SN). Quantities are presented per group of skin type. For statistical comparisons, (*) indicates comparison of all versus all samples, *p <0.05, **p<0.01.

confirm that concerning the *tdc* gene, which was absent in all AD isolates, the comparative genomic analysis supported in part these results, showing that most of the healthy isolates from our study are phylogenetically close to clade C which is enriched in *tdc* (59% of the isolates).

In order to confirm the link between AHR ligand production and AHR activation in NHEK, we used an inhibitor of AHR during the co-culture. The presence of AHR inhibitor had a deleterious effect on keratinocytes viability making impossible the analysis of keratinocytes gene expression. Finally, the data presented here showed that the 12 isolates have the capacity to produce AHR ligands in various ranges. Bacteria isolated from AD skin produce the lowest levels of indoles, which might explain the modulation of AHR pathway genes expression.

4 Discussion

Variations in the diversity of the microbiota and predominance of specific strains in disease is well documented (19, 75–83), but the

variability of the same species, in our case *S. epidermidis* isolated from different skin types (NH, H and AD) remains to be described. In this study, we demonstrated that isolates from NH and H healthy skins differed from AD skin. First at the genetic level, the genomes of the AD isolates clustered distinctly from bacteria isolated from NH and H skin. A more thorough analysis will be needed in order to identify whether these global differences could be pinpointed to specific genes or operons. At the phenotypic level, isolates from NH and AD skin presented contrasted proteases activities, AHR activation and indoles secretions, which were associated with the maintenance or not of the epidermis structure (Figure 8). Isolates from H skin had main characteristics in common with isolates from NH skin, however there were some minor differences at the level of indole secretion (ILA and IAld) and *DSG1* expression maintenance.

4.1 Biofilm thickness production is correlated to the origin skin type

Because previous studies comparing bacteria from different skin types (acne and healthy) have identified genetic variations in genes implicated in biofilm formation (25), we tested the ability of 12 different isolates of *S. epidermidis* to form a biofilm. Although *S. epidermidis* ATCC 12228 is independently described as a biofilm- or a non-biofilm-forming strain (67), we verified this capacity in our conditions and observed the formation of a thick biofilm both on a plastic support in a culture plate and on the LabSkin model emphasizing the importance of culture conditions for *S. epidermidis* biofilm formation (temperature, carbon sources, iron availability) (84, 85). All clinical isolates formed a biofilm *in vitro*, thus our results confirmed the capacity of *S. epidermidis* to form biofilms. This capacity is generally described in a pathogenic context (64, 86, 87), in contrast, here we demonstrated that isolates from NH skin form significantly bigger biofilms than isolates from AD skin. As a tentative way of explaining these differences between isolates, we tried to correlate with the presence/absence of genes known to be involved in biofilm formation (n = 28 as reported by Otto [6]) with the skin origin. The genes were retrieved in a very similar pattern among the isolates, and we did not observed differences based on the skin origin (Supplementary Table T6). In addition, when the gene was present in the *S. epidermidis* genome annotation (11/12 genomes), we compared the CDS organization of the accumulation-associated protein (*aap*), a protein involved in adhesion and biofilm formation [6] (88). However, all isolates harbored an *aap* gene coding for very similar proteins (Supplementary Figure S2B) and the differences in

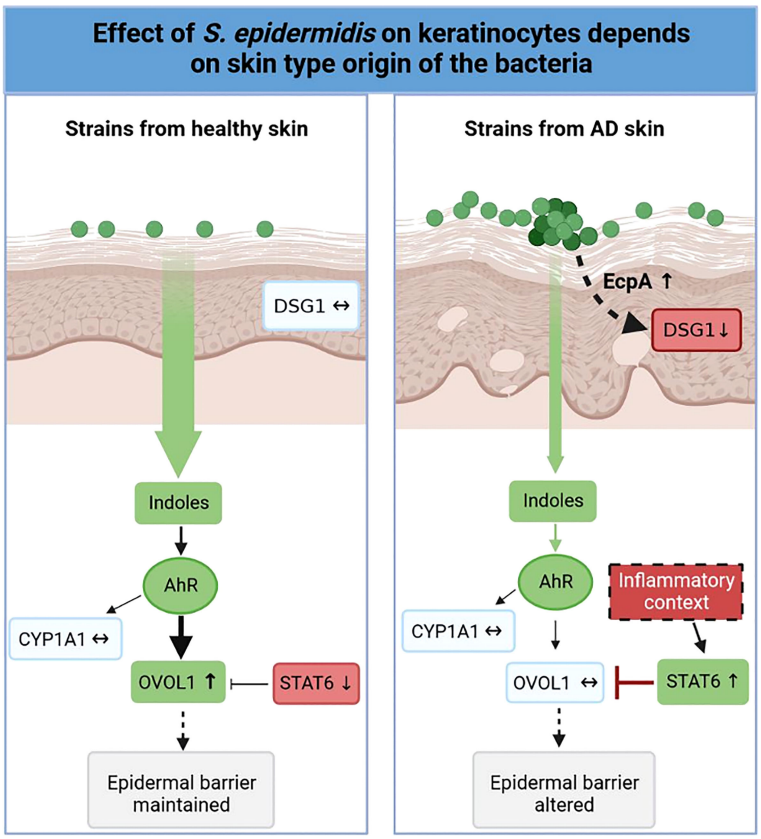

FIGURE 8
Graphical abstract. Effect of *S. epidermidis on* keratinocytes depends on skin type of origin of the bacteria. Strains from normal skin induce AhR/OVOL1 pathway via production of indoles while atopic strains produce low amounts of indoles and an overexpression of STAT6 resulting in a strong decrease of OVOL1 expression compared to normal and hyperseborrheic strains inductions. Moreover, strains from atopic skin induce tissue structure damages correlated with a strong protease activity and a decrease of DSG1. The thickness of the arrows represents the intensity of the induced signal, the dotted arrows represent links previously described in the literature but not verified in this study.

the CDS organization did not correlate with the skin origin. This suggested that the genes reported to be responsible for biofilm formation in *S. epidermidis* and specifically Aap may not be the reason of the phenotypic differences.

These data would need further investigation in 3D model in order to correlate immersed biofilm on plastic to biofilm growth on 3D reconstituted skin. It would help us understand whether this biofilm feature could be of biological importance for protection of the skin against other bacteria or environmental assaults as described in other contexts (detoxification in human gut (89); bioremediation (90)), and thus if this trait of isolates from NH skin might be of importance in skin physiology.

4.2 Proteases production is a key element to define *S. epidermis* effect on the skin

A recent study has shown that in the context of AD, the overgrowth of *S. epidermidis* could induce skin damage via protease EcpA that can disrupt the skin barrier and degrades desmoglein 1 (DSG-1) a key protein for physical barrier integrity (11). The same authors reported that this effect was dependent on the bacterial load. Here we add that EcpA expression is also dependent on the skin type origin of the isolate. Using a 3D reconstructed skin model, we characterized the isolates phenotype and compared it to the data obtained in 2D keratinocytes co-culture model. This allowed us to show that keratinocytes from the 3D model reacted very differently compared to the ones in 2D, with a more homogenous production of IL-8 among the isolates and no cytotoxicity induced by the bacteria from healthy skin (NH and H). Interestingly, the ATCC 12228 strain behaved in a very different way suggesting that this model strain is phenotypically far from the clinical isolates tested. This result needs to be considered when interpreting experiments done with bacterial strains in general in different *in vitro* models (59, 85–88, 91, 92). Additionally, the study of the histology pictures showed that the isolates from AD skin were not only producing more elastase-like, collagenase-like and EcpA proteases but their growth on the skin was much more deleterious than the 2 other type of strains with a clear degradation of the skin structure after one week of colonization. It can be hypothesized that this higher proteolytic activity is likely to explain in part why these isolates have such an effect on skin structures. Specific extraction of mRNA of these isolates under these conditions or the use of antiproteases could help us investigate this possibility. This suggests that bacteria isolated from AD skin, even if they belong to the same species as *S. epidermidis* from healthy skin, present specific phenotypic traits, which were captured using a differentiated human skin equivalent model.

4.3 AHR pathway and skin differentiation

S. epidermidis was described to active AHR pathway to mediate immune defenses (29) and activation of the AHR pathway is known to accelerate terminal differentiation by inducing an increase in the production of epidermal barrier proteins *in vitro* (keratinocytes from mice and humans) and *in vivo* (mice model) (93–94). Here, we have shown that AHR pathway could be induced by *S. epidermidis* as demonstrated by the *OVOL1* induction by strains from healthy skin. Additionally, *CYP1A1* and *DSG1* expression showed the same expression profile. A correlation between AHR activation, using chemical compound or bacterial indoles, and junctions proteins (Zonuline *ZO*, Claudine, Desmoglein 1 *DSG1*) over-expression, has been described in other cell types such as primary mammary epithelial cells (MECs) and enterocyte cells, however this link remains to be investigated in detail in skin cells (95, 96).

Once again, the effects were dependent on the skin type origin of the isolate, those from NH healthy skin induce *OVOL1* whereas strains from atopic skin induce *STAT6*. In the context of AD, it was recently shown that the high level of IL-4 and IL-13 induce the decrease of FLG-1 via induction of STAT6 (73). Thus, we can speculate that isolates from AD skin could inhibit the epidermal differentiation induced by AHR by activating the inhibitor STAT6 whereas isolates from NH healthy skin participate in epidermal differentiation by activating the OVOL1 axis, but there is still need of experimental data to fully confirm such work hypothesis.

When following the product of AHR pathway it was remarkable to show that levels of ligands produced by the isolates from H skin did not correlate with any expression markers or production compared to the other isolates suggesting a lack of knowledge on the AHR regulation is still important. Additionally, it was clear that the AHR ligands secreted when the bacteria were alone in the medium or in interaction with keratinocytes were different in quantities but also the pattern between isolates were different. Interestingly a strong correlation was observed when we compared the pattern of ligands production in co-culture with the OVOL1 axis. This suggest that another level of complexity is added to the comprehension of AHR pathway regulation since the bacterial environment seems to affect strongly the ligands secretion. This result suggests the need of an interaction between the bacteria and the keratinocytes, but the mechanism is not clear. The bacteria could secrete AHR ligands, with different capacity to induce AHR pathway, depending on its environment and interactions with cells. For example, the indole production in *E.coli* depends on pH, temperature and the presence of antibiotics in the medium (97). Considering a study showing that co-culture of bacteria (*Pseudomonas* sp. and *Streptomyces* sp.) led to the upregulation of indoles that were not previously observed in the monocultures of each bacteria (98), the ability of *S. epidermidis* from healthy skin to produce indoles might be potentiated by the addition of other bacteria or fungi from healthy skin microbiota. For instance, it could be interesting to mix *S. epidermidis* with *Malassezia* which can induce AHR pathway by secreting malassezin (99) and observe the expression of differentiation markers by keratinocytes. Additionally, the role of the keratinocytes themselves is open to question, would they consume some AHR ligands more than other? The complexity of the events that can occur when *S. epidermidis* and keratinocytes are co-cultured plead for further experiments in order to disconnect

each event of this interaction and how such modulation of AHR pathway may impact on skin maturation.

Genomics analysis using public genome databases on 811 genomes of *S. epidermidis* strains and targeting the genes involved in the AHR pathway showed that the very heterogenous pattern of *tdc* gene presence/absence between the different clades suggested that this gene might be an interesting target to define *S. epidermidis* isolates diversity.

5 Conclusions

In conclusion, this study first confirmed that the role of *S. epidermidis* in epidermal differentiation could be partly mediated by its ability to regulate AHR signaling but also led us to postulate that the capacity of the isolates to secrete indoles which in turn activate the AHR pathway might be dependent of the skin type of origin of the bacteria. These results are consistent with current understanding of the interactions between microbiota and healthy skin or the pathogenesis of AD (7, 35, 100). However, the AHR pathway is differently regulated by many ligands with synergic or opposite effects and further work, involving a larger number of isolates and full bacterial communities, is needed to understand the modulation of this pathway in health and disease by the microbiota.

Data availability statement

The datasets presented in this study can be found in online repositories. The names of the repository/repositories and accession number(s) can be found below: https://www.ncbi.nlm.nih.gov/, PRJNA721837 https://www.ncbi.nlm.nih.gov/, PRJNA721841 https://www.ncbi.nlm.nih.gov/, PRJNA721842 https://www.ncbi.nlm.nih.gov/, PRJNA721843 https://www.ncbi.nlm.nih.gov/, PRJNA721840 https://www.ncbi.nlm.nih.gov/, PRJNA662445 https://www.ncbi.nlm.nih.gov/, PRJNA721839 https://www.ncbi.nlm.nih.gov/, PRJNA721845 https://www.ncbi.nlm.nih.gov/, PRJNA721847 https://www.ncbi.nlm.nih.gov/, PRJNA721846 https://www.ncbi.nlm.nih.gov/, PRJNA721836.

Ethics statement

The studies were conducted in compliance with the 1975 World Medical Association Declaration of Helsinki, national and EU regulations and L'Oréal Research and Innovation's procedures based on ICH guidelines for Good Clinical Practice. For study ACR/COPEG/1125 (2013, France), according to the national "Arrêté du 11 mai 2009 relatif aux définitions de certaines catégories de recherches biomédicales", this non-interventional study without tested product nor invasive assessment method did not require Regulatory Approval. However, this study has been approved by L'Oréal's Ethic's Group. For the cohort 2 (2012, France), the study was approved by the DOST ethical committee. All volunteers received verbal and written information concerning the study in accordance with the applicable local regulations, guidelines and the current SOP. This information explained the nature, purpose and risks of the study and emphasized that participation in the study was voluntary and that the volunteer might withdraw from the study at any time and for any reason. The volunteer's written informed consent to participate in the study was obtained prior to any study related procedure being carried out. All data was analyzed anonymously and steps were taken to protect the identities of all participants, according to national law "Informatique et liberté" dated January 6th 1978, modified by law No 94–548 dated July 1st 1994, and law n° 2004–801 dated August 6th 2004, applicable at the time of the study.

Author contributions

LL performed lab work, analyzed data, statistical analyses, and wrote the manuscript. GC, EF, CF performed lab work. JV and SM performed sequencing, bioinformatics and statistical analyses. MR conceive and supervised the study, performed bioinformatics analyses, statistical analyses, contribute to and wrote the manuscript. CC conceived and supervised the study, contribute to analyze the data and wrote the paper. RB, HS, M-LM, AG, DB, J-MC, LA and PL provided input on the analyses and writing of the manuscript. All authors contributed to the revision of the manuscript and have approved the final version of the manuscript.

Funding

This project was co-funded by L'Oréal Research and innovation and INRAE. PhD salary was granted by the French Association Nationale de la Recherche et de la Technologie (ANRT) grant n° CIFRE 2017/1768.

Acknowledgments

We thank Lionel Breton (L'Oréal Research and Innovation) for his support in conceiving the project; Stephanie Nouveau (L'Oréal Research and Innovation) for the clinical support, Pascal Hilaire and Olivier Da Cruz (L'Oréal Research and Innovation) for sharing the *Staphylococcus epidermidis* isolates; and Samira Tamoutounour (L'Oréal Research and Innovation) for her help in interpreting the data; Sandy Contreras (Genoscreen, France) for her help in Illumina sequencing and genome analysis; Remi Peyraud and Lucas Marmiesse (iMEAN, France) for their support in metabolic reconstruction and genomic analysis. We acknowledge Thierry Meylheuc from the platform Microscopy and Imaging Facility for Microbes, Animals and Foods (MIMA2, INRAE) and Julien Deschamps for their support in microscopy analysis.

Conflict of interest

Authors LL, CC, CF, SM, AG, DB and LA were employed by the company L'Oréal Research and Innovation, Aulnay-sous-Bois. JV was employed by iMEAN, Toulouse, France.

L'Oréal Research and Innovation, as funder, has been involved in the decision to submit the study for publication.

Publisher's note

Supplementary material

The Supplementary Material for this article can be found online at: https://www.frontiersin.org/articles/10.3389/fimmu.2023.1098160/full#supplementary-material

SUPPLEMENTARY FIGURE 1
Phylogenetic tree of the 11 complete draft genomes of *S. epidermidis* using FastANI v1.31 (42) by calculating the Average Nucleotide Index for each genome pair. The tree was generated using FastTree v2.1.11 (43).

SUPPLEMENTARY FIGURE 2
(A) Comparison of the genomic structure of Stb20 and STB20-like phage loci identified in seven *S. epidermidis* strains. **(B)**: Accumulation-associated protein (aap) CDS organization in the 10 *S. epidermidis* strains. **(C)**: EcpA active domain comparison. Alignment of active amino acid sequences for the 12 *S. epidermidis* strains. *S. epidermidis* cysteine protease EcpA (UniProtKB/Swiss-Prot: P0C0Q0.1) were aligned using MAFFT multiple alignment tool.

SUPPLEMENTARY FIGURE 3
Live *S. epidermidis* effect on keratinocytes depends on skin type origin. **(A)** Average, for each skin type group of *S. epidermidis*, of IL-6 and TNF-alpha secretion in NHEK 2D co-culture. For statistical comparisons, (*) indicates comparison of all versus all samples, *p <0.05, **p<0.01, ***p<0.005.

SUPPLEMENTARY FIGURE 4
S. epidermidis growth on LabSkin HSE model from D0 (inoculation) to D7 post inoculum. The reference strain ATCC 12228 is in blue, the strains from non hyperseborrheic skin in green (1191, 52B), the strain from hyperseborrheic skin in orange (50D) and the strains from atopic skin in purple (44, 45A6).

SUPPLEMENTARY FIGURE 5
Live *S. epidermidis* effect on keratinocytes depends on skin type origin. Magnification part of HES images of tissues colonized with representative strains of the three skin types origins.

SUPPLEMENTARY FIGURE 6
Average, per group of skin type, of OVOL2 mRNA expression *in* NHEK co-cultivated with one of the 11 *S. epidermidis* isolates or the reference strain ATCC 12228.

SUPPLEMENTARY FIGURE 7
(A): Heatmap of positive isolates in each clade for each gene implicated in indole metabolites biosynthesis pathway; **(B)** cladogram to localize each of the 11 isolates within the previous described clades.

References

1. Oh J, Byrd AL, Park MNISC Comparative Sequencing Program, , HH K, Segre JA. Temporal stability of the human skin microbiome. *Cell* (2016) 165:854–66. doi: 10.1016/j.cell.2016.04.008

2. Oh J, Byrd AL, Deming C, Conlan S, Kong HH, Segre JA. Biogeography and individuality shape function in the human skin metagenome. *Nature* (2014) 514:59–64. doi: 10.1038/nature13786

3. Chen YE, Tsao H. The skin microbiome: Current perspectives and future challenges. *J Am Acad Dermatol* (2013) 69:143–155.e3. doi: 10.1016/j.jaad.2013.01.016

4. Cogen AL, Nizet V, Gallo RL. Skin microbiota: a source of disease or defence? *Br J Dermatol* (2008) 158:442–55. doi: 10.1111/j.1365-2133.2008.08437.x

5. Le KY, Otto M. Quorum-sensing regulation in staphylococci-an overview. *Front Microbiol* (2015) 6:1174. doi: 10.3389/fmicb.2015.01174

6. Otto M. Staphylococcus epidermidis – the "accidental" pathogen. *Nat Rev Microbiol* (2009) 7:555–67. doi: 10.1038/nrmicro2182

7. Byrd AL, Deming C, Cassidy SKB, Harrison OJ, Ng W-I, Conlan S, et al. Staphylococcus aureus and s. epidermidis strain diversity underlying human atopic dermatitis. *Sci Transl Med* (2017) 9. doi: 10.1126/scitranslmed.aal4651

8. Williams MR, Cau L, Wang Y, Kaul D, Sanford JA, Zaramela LS, et al. Interplay of staphylococcal and host proteases promotes skin barrier disruption in netherton syndrome. *Cell Rep* (2020) 30:2923–2933.e7. doi: 10.1016/j.celrep.2020.02.021

9. Clavaud C, Jourdain R, Bar-Hen A, Tichit M, Bouchier C, Pouradier F, et al. Dandruff is associated with disequilibrium in the proportion of the major bacterial and fungal populations colonizing the scalp. *PloS One* (2013) 8:e58203. doi: 10.1371/journal.pone.0058203

10. Park HK, Ha M-H, Park S-G, Kim MN, Kim BJ, Kim W. Characterization of the fungal microbiota (mycobiome) in healthy and dandruff-afflicted human scalps. *PloS One* (2012) 7:e32847. doi: 10.1371/journal.pone.0032847

11. Cau L, Williams MR, Butcher AM, Nakatsuji T, Kavanaugh JS, Cheng JY, et al. Staphylococcus epidermidis protease EcpA can be a deleterious component of the skin microbiome in atopic dermatitis. *J Allergy Clin Immunol* (2021) 147:955–966.e16. doi: 10.1016/j.jaci.2020.06.024

12. Kuo I-H, Carpenter-Mendini A, Yoshida T, McGirt LY, Ivanov AI, Barnes KC, et al. Activation of epidermal toll-like receptor 2 enhances tight junction function: implications for atopic dermatitis and skin barrier repair. *J Invest Dermatol* (2013) 133:988–98. doi: 10.1038/jid.2012.437

13. Ohnemus U, Kohrmeyer K, Houdek P, Rohde H, Wladykowski E, Vidal S, et al. Regulation of epidermal tight-junctions (TJ) during infection with exfoliative toxin-negative staphylococcus strains. *J Invest Dermatol* (2008) 128:906–16. doi: 10.1038/sj.jid.5701070

14. Linehan JL, Harrison OJ, Han S-J, Byrd AL, Vujkovic-Cvijin I, Villarino AV, et al. Non-classical immunity controls microbiota impact on skin immunity and tissue repair. *Cell* (2018) 172:784–796.e18. doi: 10.1016/j.cell.2017.12.033

15. Lai Y, Cogen AL, Radek KA, Park HJ, Macleod DT, Leichtle A, et al. Activation of TLR2 by a small molecule produced by staphylococcus epidermidis increases antimicrobial defense against bacterial skin infections. *J Invest Dermatol* (2010) 130:2211–21. doi: 10.1038/jid.2010.123

16. Cogen AL, Yamasaki K, Muto J, Sanchez KM, Alexander LC, Tanios J, et al. Staphylococcus epidermidis antimicrobial δ-toxin (Phenol-soluble modulin-γ) cooperates with host antimicrobial peptides to kill group a streptococcus. *PloS One* (2010) 5:e8557. doi: 10.1371/journal.pone.0008557

17. Lai Y, Gallo RL. AMPed up immunity: how antimicrobial peptides have multiple roles in immune defense. *Trends Immunol* (2009) 30:131–41. doi: 10.1016/j.it.2008.12.003

18. Scharschmidt TC, Vasquez KS, Truong H-A, Gearty SV, Pauli ML, Nosbaum A, et al. A wave of regulatory t cells into neonatal skin mediates tolerance to commensal microbes. *Immunity* (2015) 43:1011–21. doi: 10.1016/j.immuni.2015.10.016

19. Williams MR, Gallo RL. The role of the skin microbiome in atopic dermatitis. *Curr Allergy Asthma Rep* (2015) 15:65. doi: 10.1007/s11882-015-0567-4

20. Nakatsuji T, Chen TH, Narala S, Chun KA, Two AM, Yun T, et al. Antimicrobials from human skin commensal bacteria protect against staphylococcus aureus and are deficient in atopic dermatitis. *Sci Transl Med* (2017) 9. doi: 10.1126/scitranslmed.aah4680

21. Nakatsuji T, Chen TH, Butcher AM, Trzoss LL, Nam S-J, Shirakawa KT, et al. A commensal strain of staphylococcus epidermidis protects against skin neoplasia. *Sci Adv* (2018) 4:eaao4502. doi: 10.1126/sciadv.aao4502

22. Méric G, Mageiros L, Pensar J, Laabei M, Yahara K, Pascoe B, et al. Disease-associated genotypes of the commensal skin bacterium staphylococcus epidermidis. *Nat Commun* (2018) 9. doi: 10.1038/s41467-018-07368-7

23. Dib RW, Numan Y, Li X, Kalia A, Raad I, Shelburne SA. Invasive staphylococcus epidermidis isolates are highly clonal and distinct from commensal strains: Time for a new paradigm in infection control? *Open Forum Infect Dis* (2017) 4(suppl_1):S564–4. doi: 10.1093/ofid/ofx163.1475

24. Zhou W, Spoto M, Hardy R, Guan C, Fleming E, Larson PJ, et al. Host-specific evolutionary and transmission dynamics shape the functional diversification of staphylococcus epidermidis in human skin. *Cell* (2020) 180:454–470.e18. doi: 10.1016/j.cell.2020.01.006

25. Christensen GJM, Scholz CFP, Enghild J, Rohde H, Kilian M, Thürmer A, et al. Antagonism between staphylococcus epidermidis and propionibacterium acnes and its genomic basis. *BMC Genomics* (2016) 17:152. doi: 10.1186/s12864-016-2489-5

26. Swaney MH, Kalan LR. Living in your skin: Microbes, molecules, and mechanisms. *Infect Immun* (2021) 89:e00695–20. doi: 10.1128/IAI.00695-20

27. Lai Y, Di Nardo A, Nakatsuji T, Leichtle A, Yang Y, Cogen AL, et al. Commensal bacteria regulate TLR3-dependent inflammation following skin injury. *Nat Med* (2009) 15:1377–82. doi: 10.1038/nm.2062

28. Wanke I, Steffen H, Christ C, Krismer B, Götz F, Peschel A, et al. Skin commensals amplify the innate immune response to pathogens by activation of distinct signaling pathways. *J Invest Dermatol* (2011) 131:382–90. doi: 10.1038/jid.2010.328

29. Rademacher F, Simanski M, Hesse B, Dombrowsky G, Vent N, Gläser R, et al. Staphylococcus epidermidis activates aryl hydrocarbon receptor signaling in human keratinocytes: Implications for cutaneous defense. *J Innate Immun* (2019) 11:125–35. doi: 10.1159/000492162

30. Marrot L. Pollution and sun exposure: A deleterious synergy. *Mech Opportunities Skin Protection. Curr Med Chem* (2018) 25:5469–86. doi: 10.2174/0929867324666170918123907

31. Yu J, Luo Y, Zhu Z, Zhou Y, Sun L, Gao J, et al. A tryptophan metabolite of the skin microbiota attenuates inflammation in patients with atopic dermatitis through the aryl hydrocarbon receptor. *J Allergy Clin Immunol* (2019) 143:2108–2119.e12. doi: 10.1016/j.jaci.2018.11.036

32. Parrado C, Mercado-Saenz S, Perez-Davo A, Gilaberte Y, Gonzalez S, Juarranz A. Environmental stressors on skin aging. *Mechanistic Insights Front Pharmacol* (2019) 10:759.

33. Stockinger B, Meglio PD, Gialitakis M, Duarte JH. The aryl hydrocarbon receptor: Multitasking in the immune system. *Annu Rev Immunol* (2014) 32:403–32. doi: 10.1146/annurev-immunol-032713-120245

34. Haas K, Weighardt H, Deenen R, Köhrer K, Clausen B, Zahner S, et al. Aryl hydrocarbon receptor in keratinocytes is essential for murine skin barrier integrity. *J Invest Dermatol* (2016) 136:2260–9. doi: 10.1016/j.jid.2016.06.627

35. Furue M, Hashimoto-Hachiya A, Tsuji G. Aryl hydrocarbon receptor in atopic dermatitis and psoriasis. *Int J Mol Sci* (2019) 20:5424. doi: 10.3390/ijms20215424

36. Uberoi A, Bartow-McKenney C, Zheng Q, Flowers L, Campbell A, Knight SAB, et al. Commensal microbiota regulates skin barrier function and repair *via* signaling through the aryl hydrocarbon receptor. *Cell Host Microbe* (2021) 29:1235–1248.e8. doi: 10.1016/j.chom.2021.05.011

37. Camera E, Ludovici M, Tortorella S, Sinagra J-L, Capitanio B, Goracci L, et al. Use of lipidomics to investigate sebum dysfunction in juvenile acne. *J Lipid Res* (2016) 57:1051–8. doi: 10.1194/jlr.M067942

38. Shibagaki N, Suda W, Clavaud C, Bastien P, Takayasu L, Iioka E, et al. Aging-related changes in the diversity of women's skin microbiomes associated with oral bacteria. *Sci Rep* (2017) 7. doi: 10.1038/s41598-017-10834-9

39. Seite S, Flores GE, Henley JB, Martin R, Zelenkova H, Aguilar L, et al. Microbiome of affected and unaffected skin of patients with atopic dermatitis before and after emollient treatment. *J Drugs Dermatol JDD.* (2014) 13:1365–72.

40. Brown J, Pirrung M, McCue LA. FQC dashboard: integrates FastQC results into a web-based, interactive, and extensible FASTQ quality control tool. *Bioinformatics* (2017) 33:3137–9. doi: 10.1093/bioinformatics/btx373

41. Martin M. Cutadapt removes adapter sequences from high-throughput sequencing reads. *EMBnet.journal* (2011) 17:10–2.

42. Schmieder R, Edwards R. Quality control and preprocessing of metagenomic datasets. *Bioinformatics* (2011) 27:863–4. doi: 10.1093/bioinformatics/btr026

43. Hilaire P, Landemaine L, Contreras S, Blanquart-Goudezeune H, Siguier P, Cornet F, et al. Complete genome sequence of staphylococcus epidermidis PH1-28, isolated from the forehead of a hyperseborrheic donor. *Microbiol Resour Announc* (2021) 10. doi: 10.1128/MRA.00165-21

44. Langmead B, Salzberg SL. Fast gapped-read alignment with bowtie 2. *Nat Methods* (2012) 9:357–9. doi: 10.1038/nmeth.1923

45. Seemann T. Prokka: rapid prokaryotic genome annotation. *Bioinformatics* (2014) 30:2068–9. doi: 10.1093/bioinformatics/btu153

46. Edgar RC. MUSCLE: multiple sequence alignment with high accuracy and high throughput. *Nucleic Acids Res* (2004) 32:1792–7. doi: 10.1093/nar/gkh340

47. Jain C, Rodriguez-R LM, Phillippy AM, Konstantinidis KT, Aluru S. High throughput ANI analysis of 90K prokaryotic genomes reveals clear species boundaries. *Nat Commun* (2018) 9:5114. doi: 10.1038/s41467-018-07641-9

48. Price MN, Dehal PS, Arkin AP. FastTree 2 – approximately maximum-likelihood trees for large alignments. *PloS One* (2010) 5:e9490. doi: 10.1371/journal.pone.0009490

49. Arndt D, Grant JR, Marcu A, Sajed T, Pon A, Liang Y, et al. PHASTER: a better, faster version of the PHAST phage search tool. *Nucleic Acids Res* (2016) 44:W16–21. doi: 10.1093/nar/gkw387

50. Seemann T. Tseemann/abricate. *Perl* (2021).

51. Larson PJ, Zhou W, Santiago A, Driscoll S, Fleming E, Voigt AY, et al. Associations of the skin, oral and gut microbiome with aging, frailty and infection risk reservoirs in older adults. *Nat Aging.* (2022) 2:941–55. doi: 10.1038/s43587-022-00287-9

52. Klötzl F, Haubold B. Phylonium: fast estimation of evolutionary distances from large samples of similar genomes. *Bioinforma Oxf Engl* (2020) 36:2040–6. doi: 10.1093/bioinformatics/btz903

53. Felsenstein J. *PHYLIP - phylogeny inference package.* (1989).

54. Huson DH, Scornavacca C. Dendroscope 3: an interactive tool for rooted phylogenetic trees and networks. *Syst Biol* (2012) 61:1061–7. doi: 10.1093/sysbio/sys062

55. Huson DH, Richter DC, Rausch C, Dezulian T, Franz M, Rupp R. Dendroscope: An interactive viewer for large phylogenetic trees. *BMC Bioinf* (2007) 8:460. doi: 10.1186/1471-2105-8-460

56. Bridier A, Tischenko E, Dubois-Brissonnet F, Herry J-M, Thomas V, Daddi-Oubekka S, et al. Deciphering biofilm structure and reactivity by multiscale time-resolved fluorescence analysis. In: Linke D, Goldman A, editors. *Bacterial adhesion: Chemistry, biology and physics*. Dordrecht: Springer Netherlands (2011). p. 333–49.

57. Đapa T, Leuzzi R, Ng YK, Baban ST, Adamo R, Kuehne SA, et al. Multiple factors modulate biofilm formation by the anaerobic pathogen clostridium difficile. *J Bacteriol* (2013) 195:545–55. doi: 10.1128/JB.01980-12

58. Christensen GD, Simpson WA, Younger JJ, Baddour LM, Barrett FF, Melton DM, et al. Adherence of coagulase-negative staphylococci to plastic tissue culture plates: a quantitative model for the adherence of staphylococci to medical devices. *J Clin Microbiol* (1985) 22:996–1006. doi: 10.1128/jcm.22.6.996-1006.1985

59. Landemaine L, Cenizo V, Lemaire G, Portes P. *Colonization of a 3D skin model with a complete microbiota by L'Occitane research. skinobs* (2019). Available at: https://www.skinobs.com/news/en/non-classe-en/colonization-of-a-3d-skin-model-with-a-complete-microbiota/ (Accessed 30 Dec 2020).

60. Lefèvre A, Mavel S, Nadal-Desbarats L, Galineau L, Attucci S, Dufour D, et al. Validation of a global quantitative analysis methodology of tryptophan metabolites in mice using LC-MS. *Talanta* (2019) 195:593–8. doi: 10.1016/j.talanta.2018.11.094

61. Alarcan H, Chaumond R, Emond P, Benz-De Bretagne I, Lefèvre A, Bakkouche S-E, et al. Some CSF kynurenine pathway intermediates associated with disease evolution in amyotrophic lateral sclerosis. *Biomolecules* (2021) 11:691. doi: 10.3390/biom11050691

62. Macintosh RL, Brittan JL, Bhattacharya R, Jenkinson HF, Derrick J, Upton M, et al. The terminal a domain of the fibrillar accumulation-associated protein (Aap) of staphylococcus epidermidis mediates adhesion to human corneocytes. *J Bacteriol* (2009) 191:7007–16. doi: 10.1128/JB.00764-09

63. Wu Y, Liu J, Jiang J, Hu J, Xu T, Wang J, et al. Role of the two-component regulatory system arlRS in ica operon and aap positive but non-biofilm-forming staphylococcus epidermidis isolates from hospitalized patients. *Microb Pathog* (2014) 76:89–98. doi: 10.1016/j.micpath.2014.09.013

64. Nguyen TH, Park MD, Otto M. Host response to staphylococcus epidermidis colonization and infections. *Front Cell Infect Microbiol* (2017) 7. doi: 10.3389/fcimb.2017.00090

65. Fey PD, Olson ME. Current concepts in biofilm formation of staphylococcus epidermidis. *Future Microbiol* (2010) 5:917–33. doi: 10.2217/fmb.10.56

66. Ribič U, Klančnik A, Jeršek B. Characterization of staphylococcus epidermidis strains isolated from industrial cleanrooms under regular routine disinfection. *J Appl Microbiol* (2017) 122:1186–96. doi: 10.1111/jam.13424

67. Zhang Y-Q, Ren S-X, Li H-L, Wang Y-X, Fu G, Yang J, et al. Genome-based analysis of virulence genes in a non-biofilm-forming staphylococcus epidermidis strain (ATCC 12228). *Mol Microbiol* (2003) 49:1577–93. doi: 10.1046/j.1365-2958.2003.03671.x

68. Okajima Y, Kobayakawa S, Tsuji A, Tochikubo T. Biofilm formation by staphylococcus epidermidis on intraocular lens material. *Invest Ophthalmol Vis Sci* (2006) 47:2971–5. doi: 10.1167/iovs.05-1172

69. Uribe-Alvarez C, Chiquete-Félix N, Contreras-Zentella M, Guerrero-Castillo S, Peña A, Uribe-Carvajal S. Staphylococcus epidermidis: metabolic adaptation and biofilm formation in response to different oxygen concentrations. *Pathog Dis* (2016) 74:ftv111. doi: 10.1093/femspd/ftv111

70. Büttner H, Mack D, Rohde H. Structural basis of staphylococcus epidermidis biofilm formation: mechanisms and molecular interactions. *Front Cell Infect Microbiol* (2015) 5:14. doi: 10.3389/fcimb.2015.00014

71. Harris LG, Murray S, Pascoe B, Bray J, Meric G, Magerios L, et al. Biofilm morphotypes and population structure among staphylococcus epidermidis from commensal and clinical samples. *PloS One* (2016) 11:e0151240.

72. Tsuji G, Ito T, Chiba T, Mitoma C, Nakahara T, Uchi H, et al. The role of the OVOL1-OVOL2 axis in normal and diseased human skin. *J Dermatol Sci* (2018) 90:227–31. doi: 10.1016/j.jdermsci.2018.02.005

73. Furue M. Regulation of filaggrin, loricrin, and involucrin by IL-4, IL-13, IL-17A, IL-22, AHR, and NRF2: Pathogenic implications in atopic dermatitis. *Int J Mol Sci* (2020) 21:5382. doi: 10.3390/ijms21155382

74. McAleer MA, Irvine AD. The multifunctional role of filaggrin in allergic skin disease. *J Allergy Clin Immunol* (2013) 131:280–91. doi: 10.1016/j.jaci.2012.12.668

75. Dréno B, Pécastaings S, Corvec S, Veraldi S, Khammari A, Roques C. Cutibacterium acnes (Propionibacterium acnes) and acne vulgaris: a brief look at the

latest updates. *J Eur Acad Dermatol Venereol JEADV* (2018) 32(Suppl 2):5–14. doi: 10.1111/jdv.15043

76. Fyhrquist N, Muirhead G, Prast-Nielsen S, Jeanmougin M, Olah P, Skoog T, et al. Microbe-host interplay in atopic dermatitis and psoriasis. *Nat Commun* (2019) 10:4703. doi: 10.1038/s41467-019-12253-y

77. Conlan S, Mijares LA, NISC Comparative Sequencing Program, Becker J, Blakesley RW, Bouffard GG, et al. Staphylococcus epidermidis pan-genome sequence analysis reveals diversity of skin commensal and hospital infection-associated isolates. *Genome Biol* (2012) 13:R64. doi: 10.1186/gb-2012-13-7-r64

78. Ganju P, Nagpal S, Mohammed MH, Nishal Kumar P, Pandey R, Natarajan VT, et al. Microbial community profiling shows dysbiosis in the lesional skin of vitiligo subjects. *Sci Rep* (2016) 6:18761. doi: 10.1038/srep18761

79. Kong HH, Oh J, Deming C, Conlan S, Grice EA, Beatson MA, et al. Temporal shifts in the skin microbiome associated with disease flares and treatment in children with atopic dermatitis. *Genome Res* (2012) 22:850–9. doi: 10.1101/gr.131029.111

80. Nakatsuji T, Gallo RL. The role of the skin microbiome in atopic dermatitis. *Ann Allergy Asthma Immunol Off Publ Am Coll Allergy Asthma Immunol* (2019) 122:263–9. doi: 10.1016/j.anai.2018.12.003

81. Paller AS, Kong HH, Seed P, Naik S, Scharschmidt TC, Gallo RL, et al. The microbiome in patients with atopic dermatitis. *J Allergy Clin Immunol* (2019) 143:26–35. doi: 10.1016/j.jaci.2018.11.015

82. Picardo M, Ottaviani M. Skin microbiome and skin disease: The example of rosacea. *J Clin Gastroenterol* (2014) 48:S85. doi: 10.1097/MCG.0000000000000241

83. Gaitanis G, Magiatis P, Hantschke M, Bassukas ID, Velegraki A. The malassezia genus in skin and systemic diseases. *Clin Microbiol Rev* (2012) 25:106–41. doi: 10.1128/CMR.00021-11

84. Oliveira F, França Â, Cerca N. Staphylococcus epidermidis is largely dependent on iron availability to form biofilms. *Int J Med Microbiol* (2017) 307:552–63. doi: 10.1016/j.ijmm.2017.08.009

85. Zou M, Liu D. Effects of carbon sources and temperature on the formation and structural characteristics of food-related staphylococcus epidermidis biofilms. *Food Sci Hum Wellness* (2020) 9:370–6. doi: 10.1016/j.fshw.2020.05.007

86. Hoyle BD, Costerton JW. Bacterial resistance to antibiotics: the role of biofilms. *Prog Drug Res Fortschr Arzneimittelforschung Progres Rech Pharm* (1991) 37:91–105. doi: 10.1007/978-3-0348-7139-6_2

87. Mack D, Rohde H, Harris LG, Davies AP, Horstkotte MA, Knobloch JK-M. Biofilm formation in medical device-related infection. *Int J Artif Organs* (2006) 29:343–59. doi: 10.1177/039139880602900404

88. Speziale P, Pietrocola G, Foster TJ, Geoghegan JA. Protein-based biofilm matrices in staphylococci. *Front Cell Infect Microbiol* (2014) 4:171. doi: 10.3389/fcimb.2014.00171

89. de Vos WM. Microbial biofilms and the human intestinal microbiome. *NPJ Biofilms Microbiomes* (2015) 1:1–3.

90. Muhammad MH, Idris AL, Fan X, Guo Y, Yu Y, Jin X, et al. Beyond risk: Bacterial biofilms and their regulating approaches. *Front Microbiol* (2020) 11. doi: 10.3389/fmicb.2020.00928

91. Duckney P, Wong HK, Serrano J, Yaradou D, Oddos T, Stamatas GN. The role of the skin barrier in modulating the effects of common skin microbial species on the inflammation, differentiation and proliferation status of epidermal keratinocytes. *BMC Res Notes* (2013) 6:474. doi: 10.1186/1756-0500-6-474

92. Williams MR, Nakatsuji T, Sanford JA, Vrbanac AF, Gallo RL. Staphylococcus aureus induces increased serine protease activity in keratinocytes. *J Invest Dermatol* (2017) 137:377–84. doi: 10.1016/j.jid.2016.10.008

93. Loertscher JA, Lin T-M, Peterson RE, Allen-Hoffmann BL. *In utero* exposure to 2,3,7,8-tetrachlorodibenzo-p-dioxin causes accelerated terminal differentiation in fetal mouse skin. *Toxicol Sci* (2002) 68:465–72. doi: 10.1093/toxsci/68.2.465

94. Sutter CH, Bodreddigari S, Campion C, Wible RS, Sutter TR. 2,3,7,8-tetrachlorodibenzo-p-dioxin increases the expression of genes in the human epidermal differentiation complex and accelerates epidermal barrier formation. *Toxicol Sci Off J Soc Toxicol* (2011) 124:128–37. doi: 10.1093/toxsci/kfr205

95. Bansal T, Alaniz RC, Wood TK, Jayaraman A. The bacterial signal indole increases epithelial-cell tight-junction resistance and attenuates indicators of inflammation. *Proc Natl Acad Sci* (2010) 107:228–33. doi: 10.1073/pnas.0906112107

96. Basham KJ, Kieffer C, Shelton DN, Leonard CJ, Bhonde VR, Vankayalapati H, et al. Chemical genetic screen reveals a role for desmosomal adhesion in mammary branching morphogenesis *. *J Biol Chem* (2013) 288:2261–70. doi: 10.1074/jbc.M112.411033

97. Han TH, Lee J-H, Cho MH, Wood TK, Lee J. Environmental factors affecting indole production in escherichia coli. *Res Microbiol* (2011) 162:108–16. doi: 10.1016/j.resmic.2010.11.005

98. Maglangit F, Fang Q, Kyeremeh K, Sternberg JM, Ebel R, Deng H. A co-culturing approach enables discovery and biosynthesis of a bioactive indole alkaloid metabolite. *Molecules* (2020) 25:256. doi: 10.3390/molecules25020256

99. Gaitanis G, Magiatis P, Stathopoulou K, Bassukas ID, Alexopoulos EC, Velegraki A, et al. AhR ligands, malassezin, and indolo[3,2-b]carbazole are selectively produced by malassezia furfur strains isolated from seborrheic dermatitis. *J Invest Dermatol* (2008) 128:1620–5. doi: 10.1038/sj.jid.5701252

100. Hon KL, Tsang YCK, Pong NH, Leung TF, Ip M. Exploring staphylococcus epidermidis in atopic eczema: friend or foe? *Clin Exp Dermatol* (2016) 41:659–63. doi: 10.1111/ced.12866

Frontiers in Immunology

Explores novel approaches and diagnoses to treat immune disorders.

The official journal of the International Union of Immunological Societies (IUIS) and the most cited in its field, leading the way for research across basic, translational and clinical immunology.

Discover the latest Research Topics

See more →

Frontiers

Avenue du Tribunal-Fédéral 34
1005 Lausanne, Switzerland
frontiersin.org

Contact us

+41 (0)21 510 17 00
frontiersin.org/about/contact